LIVER REGENERATION BY HEPATIC PROGENITOR CELLS

By

Thomas Graham Bird

PhD

The University of Edinburgh

2011

Declaration

This thesis has been written by myself and represents my own work. The experiments described herein were performed by myself alone or in collaboration with researchers named in the text. This work has not been submitted for any other degree or professional qualification.

Thomas Graham Bird

Acknowledgements

Firstly I would like to thank Stuart, John and Owen for all of their invaluable support and continuous patience during this PhD. Stuart, a special thank you, for your discussions and original ideas which led to the Fellowship and for putting up with my inane schemes and for keeping me as focused as best you could.

Thank you also to Luke, Bex and Anto in the lab for laughing at my bad jokes and talking me round and making me see reality when the project seemed to be falling apart. Also thanks to Alicia and Trevor for their major contributions to the transgenic work.

Mostly, thanks go to my wife Kate. You have stuck with me through all the tough times of this work. I am incredibly grateful for your help and support in all things.

Abstract

The liver is the largest solid organ in the body and is frequently the site of injury. During disease, liver injury is usually compensated for by exceptionally efficient regeneration which occurs both from differentiated epithelia and also from an undifferentiated cell population with stem cell like qualities known as hepatic progenitor cells (HPCs). HPCs are particularly active during massive or chronic liver injury and therefore are an attractive target for much needed novel therapies to enhance regeneration in patients for whom the only current effective therapy is liver transplantation.

Stem cells in other organs systems are believed to reside in a specialised microenvironment or niche which supports their maintenance and function. To investigate the hypothesis that HPCs are supported by a functional niche and are capable of regenerating hepatocytes, we commenced by establishing a number of murine *in vivo* models. Having shown a stereotypical niche, consisting of macrophages, myofibroblasts and laminin exists in both animal models and human disease, we investigated the active recruitment of extrahepatic cells into this niche and showed that macrophages are actively recruited from the bone marrow during liver injury. Macrophages were shown to influence HPC behaviour during injury. Furthermore using macrophages as a cellular therapy, induced HPC activation with corresponding changes to liver structure and function. Investigation of signalling pathways revealed and confirmed a TWEAK dependent activation of HPCs following macrophage transfer.

Having demonstrated the potential for macrophage therapy via HPC activation, we aimed to study the ability of HPCs to regenerate the hepatic parenchyma. To do so we developed and characterised a novel model of hepatocellular injury and HPC activation. Using the genetic labeling of hepatocytes in this model we were able to show rapid and large scale repopulation of hepatocytes from a precursor source with HPCs being the critical precursor source of hepatocellular regeneration. In addition this process is again dependent on TWEAK signalling, without which HPC mediated regeneration fails resulting in mortality. Therefore HPCs are an attractive biological target for regenerative medicine, and both TWEAK signalling and autologous macrophage infusion offer genuine potential to manipulate these cells as future therapies.

Table of Contents

Declaration 1

Acknowledgements 2

Abstract 3

Table of Contents 4

Table of Figures and Tables 11

Abbreviations 16

Chapter 1: Introduction 19

1.1 The need for new therapies for Liver Disease 19

1.2 Liver architecture and function 20

1.3 Liver regeneration in the context of tissue regeneration and stem cells 23

1.31 Hepatocyte mediated regeneration 25

1.32 Hepatic progenitor cells and liver regeneration 27

1.33 The role of bone marrow in liver regeneration 60

1.34 HPCs and cancer 62

1.4 The liver stem/progenitor cell niche 63

1.41 Introduction to the stem cell niche 63

1.42 Cellular candidates in the HPC niche 65

1.5 Functions of BM derived stem cells during human liver disease 68

Chapter 2: Methods 72

2.1 In vivo experimental models 72

2.11 HPC models 72

2.12 Cell manipulation models 74

2.13 Hepatocellular mitogen administration 78

2.14 Tissue harvesting and preparation 79

2.2 In vitro work 79

2.21 HPC and NPC purification 79

2.22 Culture of the BMOL Progenitor Line 80

2.23 Hepatocyte purification 80

2.24 Macrophage differentiation 81

2.25 Bone marrow colony culture in nitrocellulose 82

2.3 Tissue and cellular analysis 82

2.31 Immunohistochemistry and immunocytochemistry 82

2.32 β-Galactosidase detection 85

2.33 EdU detection 86

2.34 FISH 86

2.35 TUNEL 87

2.36 FACS 87

2.37 Cell counting and image analysis 88

2.4 Serum Analysis 92

2.41 Serum Albumin 92

2.42 Alanine Aminotransferase 93

2.43 Aspartate Aminotransferase 93

2.44 Serum Alkaline Phosphatase 93

2.45 γ-Glutamyltransferase 94

2.46 Total Bilirubin 94

2.5 DNA and RNA analysis 94

2.51 DNA preparation 94

2.52 RNA extraction and reverse transcription 95

2.53 qPCR 96

2.54 Southern blotting 98

2.55 Genotyping 101

2.56 Sequencing 103

2.6 Statistics 103

Chapter 3: Establishment and characterisation of in HPC induction models 104

3.1 Hypothesis 104

3.2 Aims 104

3.3 HPCs in healthy mice 104

3.4 The CDE dietary model of HPC activation 105

3.41 Trial using 100% choline deficiency and 0.165% ethionine resulted in excess morbidity and mortality 105

3.42 Optimisation of the CDE 106

3.43 Recovery from the CDE diet 113

3.5 DDC diet establishment 115

3.6 Paracetamol overdose model 115

3.7 Characterisation of the composition of the HPC niche 117

3.71 HPC activation in human liver disease 117

3.72 Identification of a stereotypical HPC niche composed of myofibroblasts, macrophages and endothelial cells 118

3.73 Laminin is universally present in the HPC niche 127

3.8 Discussion 127

3.81 HPCs in normal mammals 129

3.82 Optimisation of the CDE diet for use as a model of HPC activation 130

3.83 HPC and niche characterisation in the CDE diet 132

3.84 Characterisation of the cellular HPC niche 134

3.9 Conclusions 139

Chapter 4: Cellular recruitment to the HPC niche 140

4.1 Hypothesis 140

4.2 Aims 140

4.3 Proliferation of niche cells during HPC activation 140

4.4 Cell tracking demonstrates macrophage recruitment to the HPC niche 142

4.5 Discussion 145

4.6 Conclusions 150

Chapter 5: Macrophages as functional cells within the HPC niche 151

5.1 Hypothesis 151

5.2 Aims 151

5.3 Introduction to models of macrophage manipulation 151

5.4 Macrophages are not required for HPC expansion but influence HPC cell fate 157

5.5 Macrophage derived Wnt as the potential mechanism for influencing cell fate 162

5.6 Niche engraftment by macrophages is sufficient for HPC activation in the absence of injury 169

5.61 Background to experimental methods 169

5.62 Transfer of syngeneic BMCs to healthy mice results in HPC activation in healthy recipient mice 170

5.63 Bone marrow transfer results in transient liver engraftment by donor-derived macrophages 174

5.64 Macrophages are themselves capable of activating an HPC response 179

5.7 HPC activation following BMC transfer is dependent on TWEAK-Fn14 signalling 181

5.8 Discussion 188

5.81 Macrophage depletion during the CDE diet 188

5.82 The role of macrophages in stimulating HPC expansion in the absence of injury 197

5.83 The use of macrophages as therapy for liver disease 202

5.9 Conclusions 205

Chapter 6: Hepatocyte MDM2 deletion reveals the potential of HPC mediated regeneration 206

6.1 Hypothesis 206

6.2 Aims 206

6.3 Background to p53 function and the AhCre MDM2^{flox} model 206

6.4 Highly efficient inducible hepatocyte specific recombination in the AhCre MDM2^{flox} model.....212

6.5 Hepatic phenotype following hepatocyte specific MDM2 gene deletion.....213

6.51 Induced hepatocyte senescence in the AhCre MDM2^{flox} model.....213

6.52 Induced hepatocellular injury in the AhCre MDM^{flox} model.....217

6.53 Induced massive HPC activation in the AhCre MDM2^{flox} model 218

6.6 Characterisation of hepatic phenotype in alternative models of transgenic MDM2 deletion in AhCre MDM2^{flox} models.....221

6.61 Hepatic parenchymal repopulation in the AhCre^{+} MDM2$^{flox/-}$ model.....225

6.7 In vitro hepatocyte differentiation of HPCs isolated from actively regenerating AhCre MDM2^{flox} livers.....229

6.8 Relationship of HPCs to hepatocyte regeneration in vivo in the AhCre MDM2flox model.....232

6.9 Absence of long term sequelae following complete hepatic parenchymal regeneration in the AhCre MDM2$^{flox/-}$ model.....233

6.10 Manipulation of HPC results in altered regeneration in the AhCre MDM2^{flox} model.....236

6.11 Discussion.....239

6.11A Efficiency of transgenic induction in AhCre MDM2^{flox} model 239

6.11B Induced hepatocyte senescence in the AhCre MDM2^{flox} model 241

6.11C Liver injury and associated HPC activation in the AhCre MDM2^{flox} model 242

6.11D Examination of the product precursor relationship between HPCs and hepatocytes in the AhCre MDM2^{flox} model 247

6.11E Implications and future directions 251

6.12 Conclusion 255

Thesis Conclusions 256

References 257

Appendix 1 Publications arising from this thesis 287

Appendix 2 Wnt pathway array data (whole liver) 316

Table of Figures and Tables

CHAPTER 1

Figure 1.1 The requirement for alternative therapies for liver disease 20

Figure 1.2 The microscopic structure of the mammalian liver. 21

Figure 1.3 The two tiers of adult hepatocellular regeneration 29

Table 1.1 Markers of adult HPCs in humans and rodents.....31

Figure 1.4 HPC activation in the CDE diet model.....33

Table 1.2 Functional studies in HPC activation.....42

Figure 1.5 Signal transduction in the Wnt pathway.....51

CHAPTER 2

Figure 2.1 Assessment of GFP protein expression in skin and bone marrow 76

Figure 2.2 Typical efficiency of macrophage differentiation 81

Table 2.1 Antibodies and antigen retrieval used.....84

Figure 2.3 Validation of cellular quantification methods 90

Figure 2.4 Utility of immunohistochemical identification of hepatocytes by CYP2D6..92

Table 2.2 Primers used for qRT-PCR.....97

Table 2.3 In house primers used for PCR.....99

Table 2.4 PCR conditions for in house PCR.....99

Figure 2.5 Generation of southern blot probe for MDM2 100

Figure 2.6 Representative examples of PCR based mouse genotyping.....102

CHAPTER 3

Figure 3.1 HPCs in healthy liver with varying age 105

Figure 3.2 Mortality and morbidity in the CDE diet with 0.165% ethionine 107

Figure 3.3. Increased tolerance of CDE diet without HPC activation with reduced dietary ethionine 108

Figure 3.4 HPC expansion in the optimised CDE diet 110

Figure 3.5 HPC characterisation in the CDE diet 112

Figure 3.6 Resolution of injury and loss of HPCs following CDE diet reversal 114

Figure 3.7 HPC expansion in the DDC diet 116

Figure 3.8 HPC expansion in paracetamol toxicity model 117

Figure 3.9 Expansion of HPC in human liver 118

Figure 3.10 Myofibroblast association with activated HPCs 121

Figure 3.11 Macrophage association with activated HPC 123

Figure 3.12 Association between macrophages and myofibroblasts in murine HPC models 125

Figure 3.13 Association between macrophages, myofibroblasts and HPCs in human disease 126

Figure 3.14 Laminin associates with and encases activated HPCs 128

CHAPTER 4

Figure 4.1 *In situ* proliferation of macrophages and myofibroblasts 141

Figure 4.2 Scheme of bone marrow cell tracking and HPC activation 143

Figure 4.3 HPC associated niche cells are frequently BM derived 144

Figure 4.4 Hepatic myofibroblasts and macrophages may be bone marrow derived 146

Figure 4.5 Niche macrophages are the recruited element in the CDE diet.....147

CHAPTER 5

Figure 5.1 Transgenic DTR mouse mediated deletion of hepatic macrophages.....154

Figure 5.2 Liposomal clodronate mediated deletion of hepatic macrophages.....156

Figure 5.3 Efficient depletion of macrophages during CDE diet using Liposomal clodronate.....158

Figure 5.4 Relationship of altered phenotype following macrophage depletion to Numb expression.....161

Figure 5.5 Macrophage depletion results in loss of Numb expression and a change in HPC fate.....164

Figure 5.6 Wnt activity in models of HPC activation.....167

Figure 5.7 Wnt activity in CDE diet and failure of BATgal reporter system.....168

Figure 5.8 Whole BM transfer results in HPC activation in healthy liver.....172

Figure 5.9 Functional consequences of whole bone marrow transfer.....173

Figure 5.10 Absence of injury or inflammation following BMC transfer.....175

Figure 5.11 Absence of long term side effects following BMC transfer.....176

Figure 5.12 Localised engraftment to the HPC niche following BMC transfer.....177

Figure 5.13 Transient cellular engraftment following BMC transfer.....178

Figure 5.14 Macrophages from whole BMC engraft following transfer.....179

Figure 5.15 Macrophage transfer recapitulates whole BMC transfer.....180

Figure 5.16 Fate of HPCs following macrophage transfer.....182

Figure 5.17 Screening cytokines reveals TWEAK as a potential signal for HPC activation 183

Figure 5.18 Engrafted macrophages produce TWEAK with in the liver 184

Figure 5.19 BMC mediated HPC activation is dependent on TWEAK signalling 185

Figure 5.20 Effect of aged BMC on HPC expansion 187

CHAPTER 6

Figure 6.1 Introduction to the AhCre MDM2 flox model 210

Figure 6.2 Highly efficient recombination following B-naphthoflavone induction 214

Figure 6.3 Hepatocyte specific MDM2 deletion results in hepatocyte senescence 215

Figure 6.4 Hepatocyte specific MDM2 deletion results in hepatocellular injury 219

Figure 6.5 Progressive activation of HPC following induction in the AhCre MDM2 model 222

Figure 6.6 Reduced recombination and HPC activation in female mice 223

Figure 6.7 Efficient recombination but delayed hepatic injury in AhCre MDM2$^{-/flox}$ mice 224

Figure 6.8 Hepatocellular injury and apoptosis in the AhCre^{+} MDM2$^{flox/-}$ model 226

Figure 6.9 Regeneration of hepatocytes from a precursor source 228

Figure 6.10 HPCs are not phenotypically affected by induction in the AhCre MDM2^{flox} model 230

Figure 6.11 *In vitro* evidence for HPC mediated regeneration 231

Figure 6.12 Gene analysis following *in vitro* differentiation of HPCs 232

Figure 6.13 Product precursor relationship from HPCs to hepatocytes *in vivo* 234

Figure 6.14 Generation of proliferating hepatocytes from HPCs 236

Figure 6.15 Absence of fibrosis following complete hepatic repopulation by HPCs....237

Figure 6.16 TWEAK dependent regeneration in the AhCre MDM2^{flox} model 238

Abbreviations

^{3}H,	Tritiated Thymidine
αFP,	Alphafetoprotein
αSMA,	α Smooth Muscle Actin
AAF,	2-N-acetylaminofluorene
Ah,	aryl hydrocarbon
AhR,	aryl hydrocarbon receptor
Alk Phos,	Alkaline Phosphatase
ALT,	Alanine Aminotransferase
AST,	Aspartate Aminotransferase
BCG,	bromocresol green
BDL,	Bile duct ligation
BM,	Bone marrow
BMC,	Bone marrow cell
BMSC,	bone marrow stem cell
βNF	β-Napthoflavone
BrdU,	5-bromo-2-deoxyuridine
CCl_4,	Carbon tetrachloride
CDE,	Choline deficient ethionine supplemented
cDNA,	complementary DNA
CK,	Cytokeratin
CT-1,	Cardiotrophin 1
CTGF,	Connective Tissue Growth Factor
CYP,	Cytochrome
DAB,	Diaminobenzidine
DAPI,	4',6-diamidino-2-phenylindole
DDC,	Diethyl 1,4-dihydro-2,4,6-trimethyl-3,5-pyridinedicarboxylate
Dlk,	Delta Like Kinase CK, Cytokeratin
DMSO,	Dimethyl sulfoxide
DPPIV,	Dipeptidyl Peptidase IV

EdU,	5-ethynyl-2'-deoxyuridine
ECM,	extracellular matrix
EGF,	Epidermal Growth Factor
EpCAM,	Epithelial Cell Adhesion Molecule
Epo,	Erythropoietin
ES,	Embryonic Stem
FACS,	Fluorescence Activated Cell Sorting
$FAH^{-/-}$,	Fumarylacetoacetate Hydrolase knockout
FCS,	Feotal Calf Serum
FGF,	Fibroblast growth factor
FISH,	Fluorescent In-Situ Hybridisation
FITC,	Fluorescein isothiocyanate
Flp,	Flippase recombinase
Fn14,	Fibroblast growth factor-inducible 14
FRT,	Flippase Recognition Target
Fz,	Frizzled
gDNA,	genomic DNA
G-CSF,	Granulocyte Colony Stimulating Factor
GFP,	Green Fluorescent Protein
gGT,	γ-Glutamyltransferase
HBV,	Hepatitis B Virus
HCC,	Hepatocellular carcinoma
HCV,	Hepatitis C Virus
HGF,	Hepatocyte Growth Factor
Hh,	Hegdehog
HPC,	Hepatic Progenitor Cell
HRP,	Horseradish Peroxidase
HSP,	Heat shock protein
IFN,	Interferon
IL,	Interleukin
i.p.,	intraperitoneal
iPS,	induced Pluripotent Stem
i.v.,	intravenous

LIF,	Leukaemia Inhibitory Factor
LIFR,	LIF receptor
LT,	Lymphotoxin
MDM2,	murine double minute 2
MMP,	metalloproteinase
NPC,	Non Parenchymal Cell
OC,	Oval Cell
OSM,	Oncostatin M
PanCK,	Pancytokeratin
PBS,	Phosphate Buffered Saline
PCR,	Polymerase Chain Reaction
PH,	Partial hepatectomy
PhB,	Phenobarbitol
PPIA,	peptidylprolyl isomerase A
qPCR	Quantitative PCR
rh,	recombinant human
rm,	recombinant mouse
RT-PCR,	Reverse Transcription PCR
SCF,	Stem cell factor
SDF-1,	Stromal cell derived factor 1
SEM,	Standard Error of the Mean
SgIGSF,	Spermatogenic immunoglobulin superfamily
SSC,	Sodium Chloride-Sodium Phosphate
T3,	triodothyronine
TGF,	Transforming Growth Factor
TIMP,	Tissue Inhibitor of Metalloproteinase
TNF,	Tumour Necrosis Factor
TUNEL,	Terminal deoxynucleotidyl transferase dUTP nick end labeling
TWEAK,	TNF-like weak inducer of apoptosis
uPA,	urokinase-type plasminogen activator
Wnt,	Wingless-int
WT,	Wild Type

Chapter 1: Introduction

1.1 The need for new therapies for Liver Disease

Chronic liver disease represents one of the major health burdens worldwide. In the UK it is the 5th most common cause of death. Liver fibrosis currently kills more men than Parkinson's disease and more women than cervical cancer, and these numbers are increasing. Over the last decade rates of cirrhosis in Scotland have more than doubled (Leon and McCambridge, 2006). Liver disease continues to rise in the UK as a whole at approximately 5% per year on year to 2008. Furthermore it is the only major cause of death still increasing year-on-year (Baker *et al.*, 2008). Liver transplant is the only life-prolonging treatment in liver failure, and yet while organ donation rates are static, waiting list numbers and mortality continues to increase (Carpentier *et al.*, 2009). Therefore there is an urgent need for alternative therapies for liver disease (Figure 1.1).

Liver failure results from inadequate function of the liver and excess scar formation. A major clinical need exists for therapy to improve liver function when the liver's regenerative capacity is overwhelmed. This is required for both acute massive liver injury, and more commonly with minor but sustained damage during chronic liver disease. During both these situations a second regenerative compartment composed of liver stem cells and progenitor cells is activated to regenerate the liver. In order to address our current shortfalls in therapy there is a great interest in characterising the stem cell mediated regenerative capacity of the liver to uncover ways in which these processes may be manipulated therapeutically. There is also strong evidence pointing towards the liver stem cells and their progeny, in the formation of hepatocellular carcinoma (HCC). Therefore an understanding of the process controlling hepatic stem cell function may offer the opportunity of maximising liver function while preventing the formation of HCC. Stem cells also provide a potential precursor source of cells for extracorporeal liver support devices (Carpentier *et al.*, 2009).

Figure 1.1 The requirement for alternative therapies for liver disease

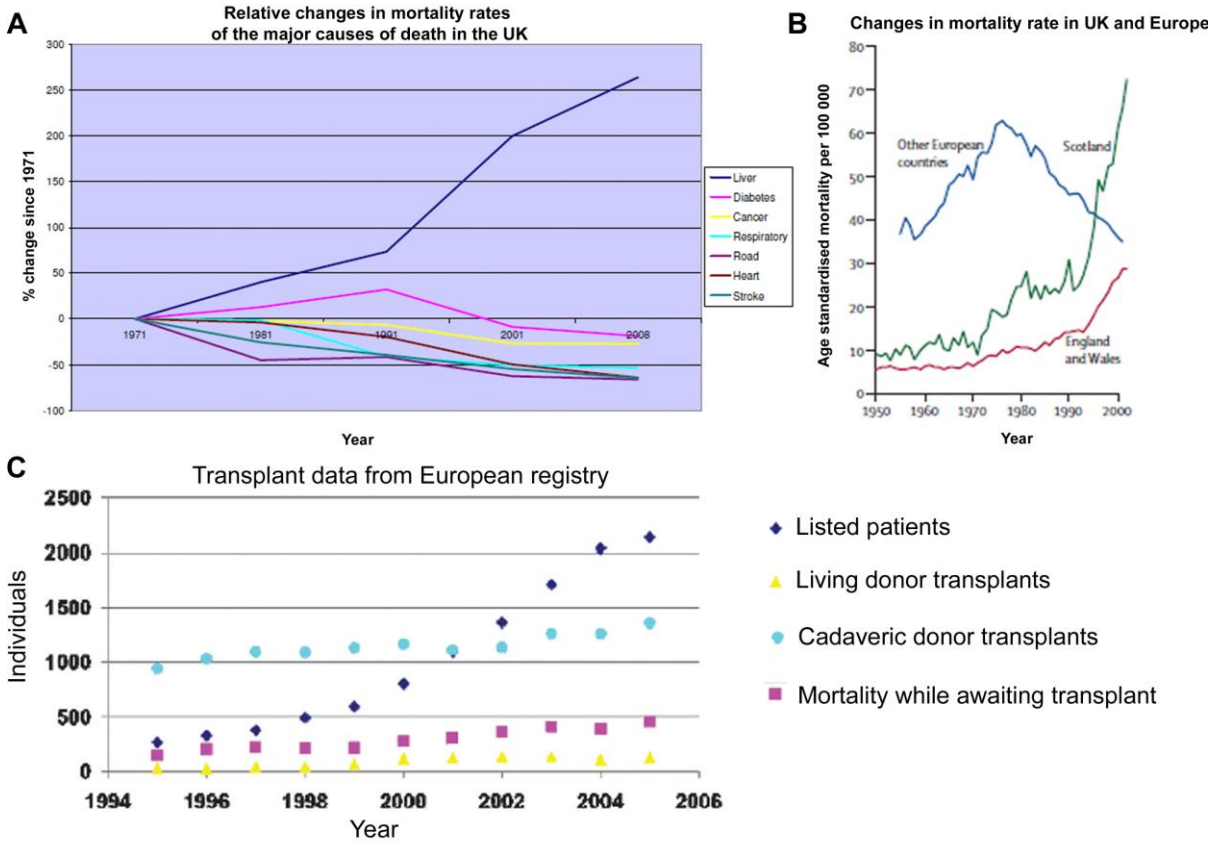

(A) Of the major causes of mortality in the UK liver disease is to continually increase over time (adapted from Baker *et al.*, 2008). (B) Rates of cirrhosis and mortality in the UK and Europe in men aged 45-65 (adapted from Leon and McCambridge, 2006). (C) Statistics for 1995 to 2005 from the European transplant registry, (adapted from Carpentier *et al.*, 2009).

1.2 Liver architecture and function

The liver is the largest internal organ in the body. Functionally it is divided into the right and left lobes. The right is larger and contains the caudate and quadrate lobes. Each lobe is then further divided subdivided into a total of eight segments each receiving its own portal pedicle containing branches of the portal vein, hepatic artery, hepatic vein and biliary tree.

The blood supply to the liver constitutes approximately 25% of cardiac output and is provided predominantly (75%) via the hepatic portal vein which drains most of the gastrointestinal tract and spleen. The other 25% of hepatic vascular supply is provided by arterialised blood from the hepatic artery. Blood from these vessels is distributed to the segments and passes into the sinusoids via the portal tracts (Figure 1.2). After passing along the sinusoid blood leaves the liver by entering branches of the portal vein before passing to the inferior vena cava. Lymph is formed predominantly in the perisinusoidal space and in collected in lymphatic vessels present in the portal tracts.

Figure 1.2 The microscopic structure of the mammalian liver.

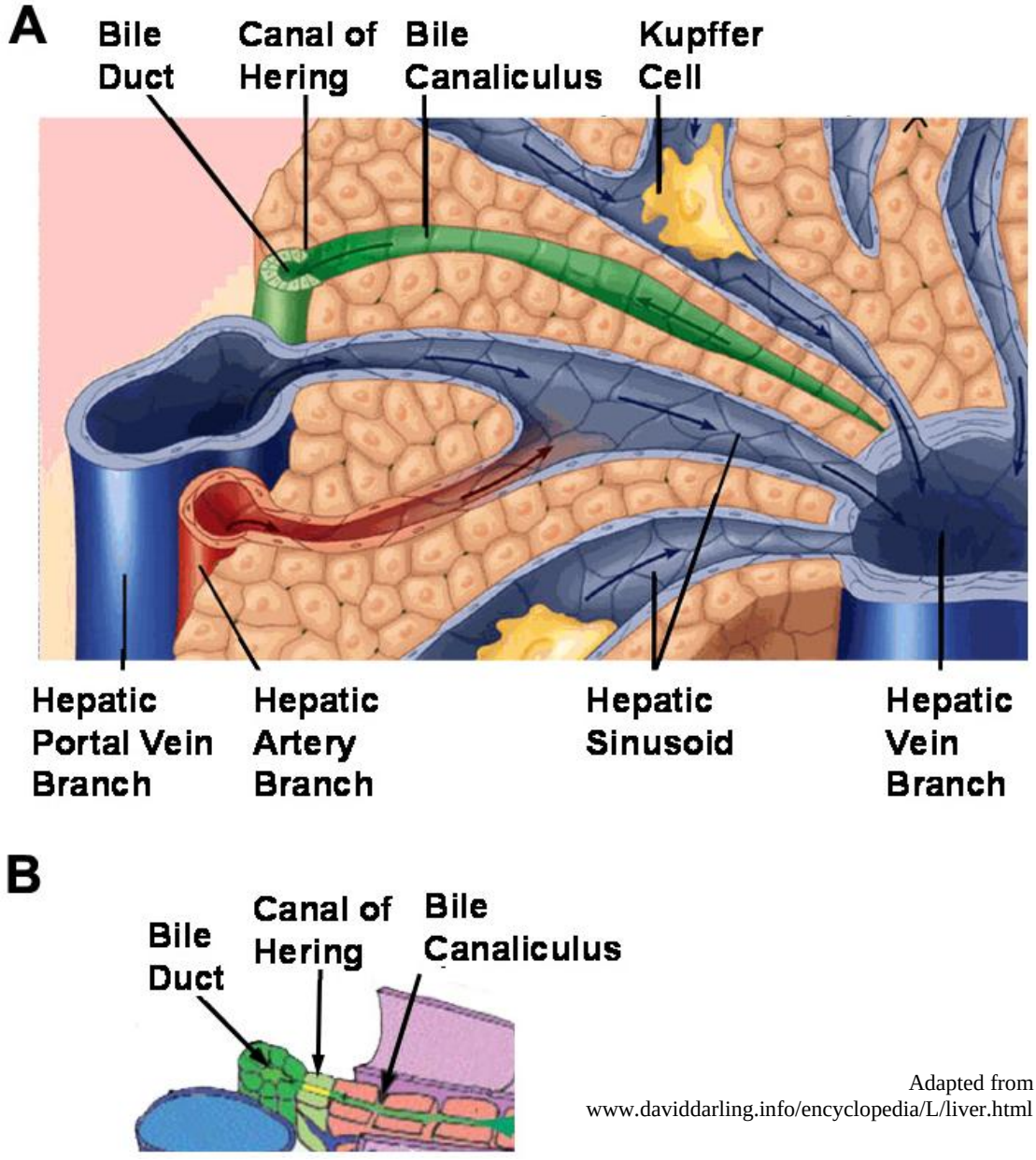

Adapted from www.daviddarling.info/encyclopedia/L/liver.html

The hepatic sinusoids lack a basement membrane and are loosely surrounded by a specialised fenestrated endothelium along with phagocytic, monocyte derived, Kupffer cells. The sinusoids are separated from the plates of hepatocytes by the space of Dissé which contains a matrix of basement membrane constituents and stellate cells. Stellate cells in the normal liver store retinoids in their resting state and contain the intermediate filament desmin and glial fibrillary acidic protein (GFAP). When activated they become the contractile cells, called myofibroblasts, which are characterised by their expression of α-smooth muscle actin (αSMA). Following activation myofibroblasts play a major role in controlling sinusoidal blood flow and the deposition of extra-cellular matrix (Friedman, 2008).

The functional unit of the liver is the acinus, which consists of parenchyma supplied by portal tracts containing portal vein radicals, hepatic arterioles, and bile ductules. The hepatocytes in this vicinity are well supplied with oxygenated blood and are generally the most resistant to damage. In contrast the hepatocytes nearer the central terminal hepatic venule branch of the hepatic vein are less well oxygenated and are more susceptible to damage. These periportal and perivenular zones are referred to as zones 1 and 3 respectively with a central area of intermediate hepatocytes lying in an area referred to as zone 2. Specific enzymatic and metabolic activities, i.e. carbohydrate metabolism, ammonia detoxification, bile formation/transport/secretion and drug biotransformation, are confined to the perivenular zone 3 or periportal zone 1 (Gebhardt, 1992). Intriguingly, inversion of the blood flow direction changes the enzymatic gradients reverses much of the liver metabolism zonation, implying an influence exerted by the oxygen and circulating molecules on this phenomenon (Kinugasa and Thurman, 1986). For the bloodstream independent gradients, cell-cell and cell-extracellular matrix interactions have been suggested as crucial determinants of liver zonation together with paracrine signalling particularly by Wnt (Burke and Tosh, 2006).

The biliary system comprises the collection of ducts extend from the bile canaliculi formed between hepatocytes, to the ampulla of Vater which opens into the duodenum. Bile is produced principally by hepatocytes and is initially excreted into a fine network of channels formed between the cell membranes of hepatocytes known as bile canaliculi. These canaliculi then join to form thin bile ductules near the portal tract. The smallest bile ductules which join the bile canaliculi to the specialised cholangiocyte lined tree of the biliary system are known as the canal of Hering (Figure 1.2B).

1.3 Liver regeneration in the context of tissue regeneration and stem cells

The liver is a site of frequent injury. The liver's anatomical position, together with its role in the metabolism and excretion of toxins, make it particularly susceptible to toxic injury. In addition, a variety of infectious and autoimmune diseases frequently result in liver injury. It is likely that frequent injury from these varied factors, have imposed upon the liver its remarkable regenerative capacity.

Like most organs of the body, the liver has the potential to regenerate following cellular loss or injury. Mammals, for example, can survive surgical removal of up to 75% of the total liver mass. Here within 1 week after liver resection, the total number of liver cells is restored (Michalopoulos and DeFrances, 1997). Indeed this ability to maintain a constant size, following injury, transplantation of a size mismatched organ or even induced hypertrophy (Forbes *et al.*, 2000), is one of the liver's defining characteristics. This potential to grow or even shrink clearly demonstrates the liver's delicate balances of cellular regeneration and loss.

Regeneration, while differing substantially between organs, retains many common features across the body as a whole. While some tissues constantly shed large numbers of cells and are therefore in a constant state of highly active regeneration (e.g. intestine,

skin or testis), others remain relatively quiescent throughout adult life (e.g. brain). With its relatively low rate of turnover, the liver lies somewhere between these two extremes. Within the uninjured mammalian liver approximately 0.5% of hepatocytes are in cell cycle at any one time in keeping with an average life span of adult hepatocytes of 200-300 days (Duncan *et al.*, 2009). None-the-less, as is clear from the massive regeneration occurring following liver resection, the liver is capable of regeneration as impressive as any other organ when required.

Tissue regeneration in most organs is thought to be principally from tissue stem cells. The concept of a stem cell implies that this cell possesses the potential for longevity in an unchanged state whilst continuing to producing a fresh source of progeny capable of differentiating into multiple cell types. In other words, the key characteristics a cell must possess in order to be called a stem cell are multipotentiality combined with ongoing self renewal. These two fundamental characteristics give rise to the key feature of a stem cell which is long term tissue reconstitution. In practice these attributes are tested via a number of means. Serial transplantation is able to test the self renewal of a stem cell in addition to multipotentiality. Clonal assays utilise the assessment of a single cell to form colonies which can then be tested for multipotentiality. This provides an improved assessment of the multipotentiality than transplantation of mixed cell populations. Lineage tracing is used to demonstrate product precursor relationships between freshly generated cells of one phenotype from those of another and essentially provides a test of multipotentiality but also using well selected markers may demonstrate longevity within a tissue (Barker *et al.*, 2007). While the best and most obvious example of a stem cell remains as the fertilised egg, recent work has identified cells with stem cell characteristics in adult organs including the bone marrow (BM) and intestine (Taoudi *et al.*, 2008; Barker *et al.*, 2007; Rock *et al.*, 2009; Barker *et al.*; Wagers, 2005).

The extent to which liver regeneration relies on stem cells remains hotly debated. The reasons for interest in this field are clear, particularly from a clinical perspective. Chronic liver disease is common and has severe clinical consequences that arise from

loss of functional hepatocytes together with excess scar formation. Currently therapies are insufficient to treat these disorders effectively. There is therefore a great interest in characterising the regenerative capacity of the liver in order to manipulate this process therapeutically.

1.31 Hepatocyte mediated regeneration

Acute liver injury, for example the removal of a number of liver segments by partial hepatectomy (PH), results in rapid and effective regeneration with hepatocytes undergoing mitosis leading to subsequent restoration of liver mass and function by compensatory hypertrophy within two cycles of hepatocyte division (Fausto *et al.*, 2006). Naturally the question has been raised as to whether hepatocytes themselves function as stem cells. Early work using retroviral mediated incorporation of beta-galactosidase (Bralet *et al.*, 1994) showed clonal patches of hepatocytes following regeneration scattered throughout the liver and argued strongly against a zonal source of liver regeneration in these models. More recent landmark transplantation studies in fumarylacetoacetate hydrolase knockout (FAH $^{-/-}$) and urokinase plasminogen activator (uPA) transgenic mice have demonstrated that hepatocytes possess a virtually unlimited proliferative potential. They are capable of a least 69 cell divisions and can restore normal architecture and impaired function in the injured liver (Overturf *et al.*, 1997; Rhim *et al.*, 1994). Furthermore, Grompe and coworkers have shown in the FAH$^{-/-}$ mouse that adult hepatocytes expand clonally (Overturf *et al.*, 1999) and may be serially transplanted (Overturf *et al.*, 1997). By the use of wild type hepatocytes in an environment of otherwise metabolically defective hepatocytes, these models do however rely on a strong selection advantage against native hepatocytes. Additionally in alternative model of hepatocyte transplantation wild type hepatocytes appear to show multipotentiality when transplanted into the livers of Dipeptidyl Peptidase IV (DPPIV) knockout rats followed by PH and retrorsine treatment. DPPIV is an exopeptidase expressed on the bile canalicular surface of hepatocytes in addition to diffuse

cytoplasmic expression by bile duct epithelia. Using this model transplanted $DPPIV^+$ cells reconstitute bile ducts following bile duct ligation (BDL; Michalopoulos *et al.*, 2005). The authors of this work have previously described the hepatocyte population used for this infusion to be a mixed population, therefore definitive multipotentiality at the level of single cells has not been confirmed (Michalopoulos *et al.*, 2001). None-the-less, this study raises the possibility that hepatocytes may, in specific circumstances, display multipotentiality. Under certain conditions therefore, hepatocytes may show many of the characteristics of stem cells. However the many models demonstrating self renewal share a continual selection pressure for transplanted hepatocytes versus indigenous parenchyma in the context of persistent liver injury. Whether human hepatocytes are capable of acting as true stem cells remains unclear.

As implied above, hepatocytes posses the ability to remain quiescent for extended periods and yet re-enter cell cycle rapidly if required. This feature is bestowed upon them by their propensity to remain in the G_0 stage of the cell cycle. The G_0 phase is a period in the cell cycle where cells exist in a quiescent state. G_0 phase may be viewed as an extended G_1 phase where the cell is neither dividing nor preparing to divide (Loyer *et al.*, 1996). Unlike many cells in the G_0 phase hepatocytes may survive for long periods in this state, in which they may remain until stimulated to re-enter the cell cycle. This quiescent state is in contrast to cellular senescence, which is a state that may be induced by tissue injury or degradation which could make a cell's progeny non-viable. Senescence then, unlike quiescence, is often a biochemical alternative to the self-destruction of such a damaged cell by apoptosis and implies a failure to respond to normal mitotic stimuli. Senescence is an important feature of hepatocytes during liver pathology, occurring frequently during chronic injury (Marshall *et al.*, 2005; Paradis *et al.*, 2001; Wiemann *et al.*, 2002). When hepatocyte senescence occurs, regeneration does not fail, implying that there is an alternative source of hepatocyte regeneration. The reasons for, and mechanisms of, hepatocytic senescence remain poorly understood, however they appear to involve telomerase shortening (Wege *et al.*, 2007) and p53, p21 and p16 activation (Ozturk *et al.*, 2009; Shay *et al.*, 1991; Teoh *et al.*, 2010) along with

β-galactosidase expression which is used as a marker of senescence (Paradis *et al.*, 2001).

1.32 Hepatic progenitor cells and liver regeneration

While the liver's ability to utilise hepatocytes for regeneration is well described, it is clear that regeneration may occur even when proliferation of hepatocytes is prevented and hepatocytes may be generated from precursor cells other than hepatocytes (Bird *et al.*, 2008). These precursors may in time be demonstrated to reliably fulfill the characteristics of true stem cells, however whilst this remains to be demonstrated reliably I will refer to these precursors as Hepatic Progenitor Cells (HPCs); for clarity this population is identical to oval cells, which is frequently used pseudonym for this population in rodent models.

The concept that regeneration may occur both from differentiated parenchyma and from precursors in the liver is perhaps not surprising. Intuitively, hepatocytes are themselves derived from a primitive precursor during development. Additionally regeneration in all other organs occurs from undifferentiated precursors. Much of what is understood regarding adult HPCs shares strong similarities with what is known of the hepatic stem cells which are active during development. HPCs in adults are described as facultative as they only participate in hepatocyte replacement when regeneration by mature hepatocytes is overwhelmed or impaired (Figure 1.3). This population can be demonstrated by preventing hepatocellular proliferation using agents such as AAF or retrorsine, which are activated into toxic metabolites by mature hepatocytes. When applied, in the context of simultaneous liver injury, these agents result in the expansion of HPCs from portal areas.

The first description of HPCs as candidate hepatic stem-like cells was made in 1937 (Kinosita, 1937) with the subsequent naming of oval cells in rodents following a report by Farber in 1956 (Farber, 1956). Whilst described in a variety of models and diseases,

these cells are thought to possess the characteristics of a transit amplifying population or progenitor cells, and are characteristically not seen in the uninjured mammalian parenchyma. These cells were described morphologically as 'small ovoid cells with scant lightly basophilic cytoplasm and pale blue-staining nuclei'.

Investigation of HPCs has made remarkable progress since seminal work by Thorgeirsson and coworkers who used rats treated with AAF followed by PH (AAF/PH) and showed HPC proliferation beginning in the periportal region (Evarts *et al.*, 1987; Evarts *et al.*, 1989). At later time points in these models, label retaining basophilic hepatocytes were seen in the mid parenchyma suggesting, but not definitely proving, a precursor/product relationship. Detailed analysis of cells during regeneration has shown cells with a number of intermediate phenotypes between HPCs and fully differentiated hepatocytes (De Vos and Desmet, 1992; Mandache *et al.*, 2002; Alison *et al.*, 1996), and has shown that HPCs migrate into regenerative nodules (Vig *et al.*, 2006). Tracing tritiated thymidine transfer from HPCs to parenchymal cells in combination with differentiation markers demonstrates bipotentiality of HPCs, showing them capable of forming either hepatocytes or cholangiocytes (Evarts *et al.*, 1989; Holic *et al.*, 2000). More recent work using HPCs, either as primary cell culture or as cell lines has shown their bipotentiality during *in vitro* culture (Conigliaro *et al.*, 2008; Lazaro *et al.*, 1998; Lorenzini *et al.*, 2010; Okabe *et al.*, 2009; Rountree *et al.*, 2007). Indeed, even in their undifferentiated form, HPCs themselves may express mature hepatocyte or biliary duct markers such as CK18 or CK19 (Table 1.1). In addition these cells are also capable of engrafting following transplantation and expanding in the recipient liver (Faris and Hixson, 1989; Wang *et al.*, 2003a; Yasui *et al.*, 1997). Therefore HPCs, in rodents at least, appear to possess the characteristics of progenitor cells in addition to possessing a variety of markers implying stem cell function (e.g. c-kit, CD34, flt3 and CD133). Further studies analogous to those in the BM or intestine demonstrating long term tissue repopulation will require suitable lineage tracing or transplantation models (Barker *et al.*, 2007; Taoudi *et al.*, 2008).

Figure 1.3 The two tiers of adult hepatocellular regeneration

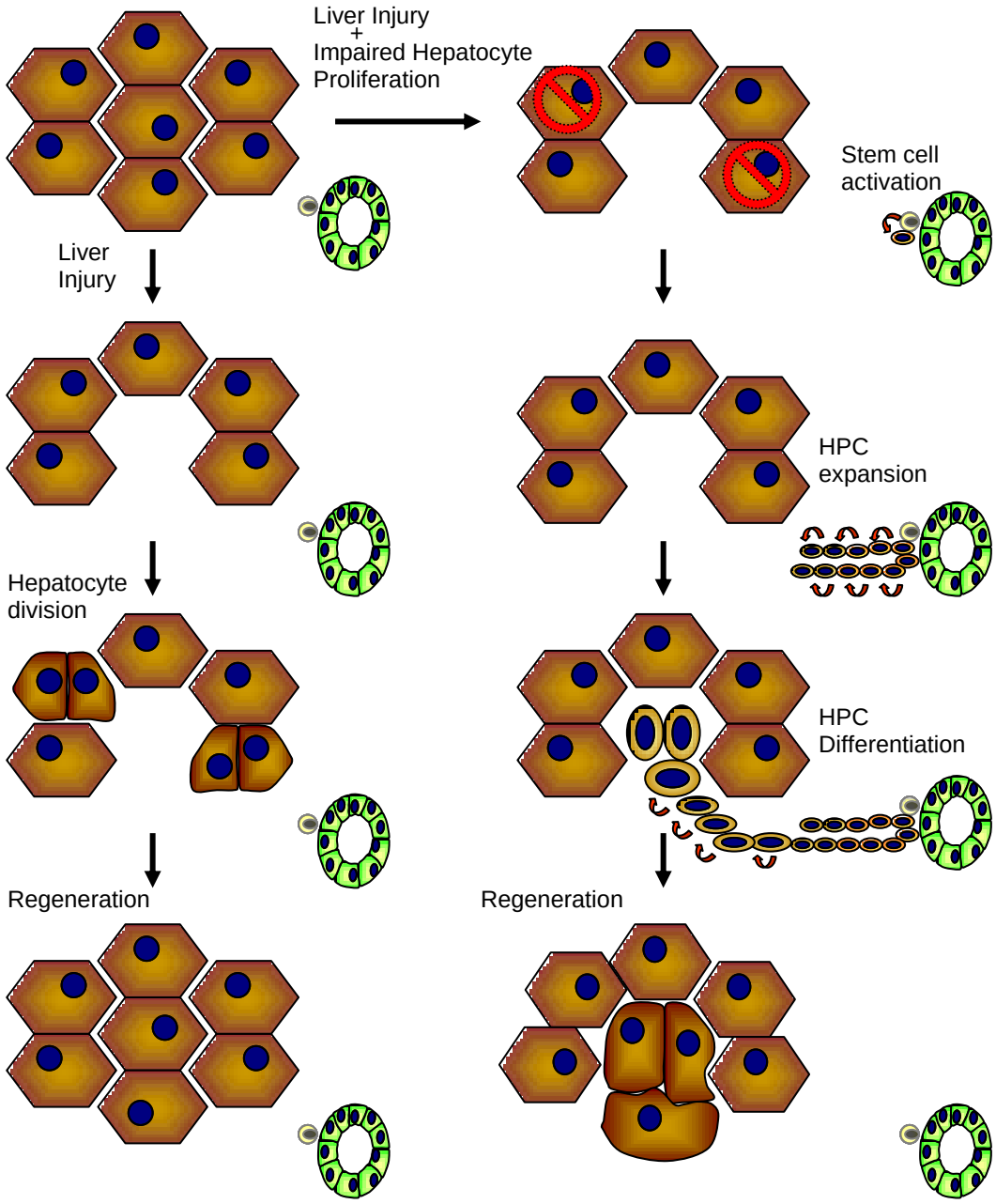

Regeneration of the mammalian liver may occur from two sources. If hepatocytes are able to divide then they do so quickly and efficiently to fully restore the parenchyma without the expansion of HPCs (left hand panels). If hepatocyte injury occurs in the context of impaired hepatocyte proliferation (right hand panels) then stem cells located in the terminal biliary tree are activated leading to the generation of HPCs which spread into the liver parenchyma and are able to differentiate into functional parenchyma. Adapted from Bird *et al.* 2008.

Meticulous studies in rodents and humans are consistent with an origin of HPCs from the terminal ducts of the biliary tree known as the canals of Hering (Theise *et al.*, 1999; Saxena *et al.*, 1999; Paku *et al.*, 2001; De Alwis *et al.*, 2009; Fellous *et al.*, 2009). Following activation they expand, forming ductular structures extending between the biliary tree and hepatocytes (Paku *et al.*, 2001). This anatomical position, at the interface between the parenchyma and the portal tract mesenchyme, is also the site of bipotential hepatoblasts during hepatic organogenesis.

HPC models

A crucial tool for the investigation of HPC biology has been their description in a variety of animal models. The most common rodent HPC activation model to date utilises the mitogenic stimulus of PH in combination with inhibitors, such as 2-N-acetylaminofluorene (AAF) or retrorsine, which are activated by hepatocyte cytochromes P-450s and subsequently inhibit the proliferation of these mature hepatocytes. These inhibitors can alternatively be combined with other forms of hepatic injury e.g. carbon tetrachloride (CCl_4) or allyl alcohol. These models are principally employed in rats. For many reasons, including their smaller size, reduced cost, breeding characteristics, and particularly their increasing genetic manipulation, mouse models have many advantages over those in other species, including the rat. For these reasons focus will be given to the two most frequently utilised murine models, the Choline Deficient Ethionine supplemented (CDE) diet and the 3,5-diethoxycarbonlyl-1,4-dihydrocollidine supplemented (DDC) diet (See Chapter 3). Whilst these models have provided important breakthroughs in our understandings of HPCs they remain with some significant disadvantages. In particular, neither operates via a characterised mechanism and both induce significant toxicity with only relatively modest HPC activation in comparison to models described in other species.

Table 1.1 Markers of adult HPCs in humans and rodents

Hepatic progenitor cell marker	References
Adult biliary marker	
Cytokeratin 19 (CK19)	Bisgaard et al. 1993
PanCK	Kofman et al. 2005
CK7	Paku et al. 2005
CK14	Bisgaard et al. 1993
γ-Glutamyl transpeptidase (γGT)	Cameron et al. 1978
Glutathione-S-transferase P (GST-P)	Tee et al. 1992
Muscle pyruvate kinase (MPK)	Akhurst et al. 2005
OV-6 (recognises CK14 and CK19)	Bisgaard et al. 1993
OV1	Sanchez et al. 2004
A6	Engelhardt et al. 1993
OC.2 and OC.3	Hixson and Allison 1985
Connexin 43	Zhang and Thorgeirsson 1994
CX3Cl1	Yovchev et al. 2007
CD24	Yovchev et al. 2007
MUC1	Yovchev et al. 2007
Deleted in malignant brain tumour 1 (DMBT1)	Bisgaard et al. 2002
Adult hepatocyte markers	
Albumin	Tian et al. 1997
CK8	Libbrecht et al. 2000b
CK18	Libbrecht et al. 2000b
α1-Antitrypsin	Gauldie et al. 1980
Hepatocyte nuclear factor 4 (HNF4)	Nagy et al. 1994
HBD.1	Faris et al. 1991
c-Met	Hu et al. 1993
Fetal hepatocyte markers	
Delta-like protein (Dlk 1)	Yovchev et al. 2007
Epitheliam Cell Adhesion Molecule (EpCAM)	de Beor et al. 1999
α-Fetoprotein (αFP)	Evarts et al. 1987
Aldolase A and C	Lamas et al. 1987
c-Met	Hu et al. 1993
Cadherin 22	Yovchev et al. 2007
CD24	Yovchev et al. 2007
CD44	Kon et al. 2006
Others including adult haematopoietic markers	
c-kit	Fujio et al. 1994
Alanine aminopeptidase (CD13)	Kakinuma et al. 2009
CXCR4	Zheng et al. 2006
CD34	Omori et al. 1997
TROP 2	Okabe et al. 2009
Sca-1	Petersen et al. 2003

The CDE diet

The CDE diet is, to date, the most frequently studied murine model of HPC activation. It was originally developed in rats following the opportunistic observation this combination resulted in HPC expansion (Shinozuka *et al.*, 1978; Yaswen *et al.*, 1984). Initially, the carcinogen ethionine was used as a rat model of Hepatocellular Carcinoma (HCC) development. Ethionine is the S-ethyl analogue of the essential amino acid methionine and is believed to act principally by inhibiting the SAM (S-adenosyl-L methionine) synthetase enzymes. Consistent with this is the reversal of most of ethionine's biochemical and morphological effects by the administration of methionine or adenine (Alix, 1982). Ethionine is, therefore, believed to block one or more of the essential functions of methionine in cells. However, the precise mechanism by which this combination stimulates HPC activation remains far from clear. When choline deficiency was added to ethionine treatment pronounced HPC proliferation was noted. This model was developed as choline is both a methionine precursor and ethionine, as an antagonist of methionine, is also an inhibitor of choline biosynthesis via the transsulfuration pathway (Figure 1.4A). Interestingly, neither choline deficiency alone nor administration of ethionine results in HPC activation. Choline deficiency in humans was in the past, a not infrequent consequence of total parenteral nutrition and resulted in liver injury and steatosis (Buchman *et al.*, 2001). When applied to mice the CDE diet induces HPC activation analogous to that seen in the CDE diet in rats. However in mice the HPCs infiltrate the injured parenchyma as thinner columns of cells often in single file, as opposed to the ductular morphology seen in rats (Akhurst *et al.*, 2001; Tee *et al.*, 1996). In mice the expansion of HPCs has been described to be progressive over approximately 2 weeks followed by a continuous but stable HPC activation (Figure 1.4B). In addition to inducing a maintained HPC activation the CDE diet also results in HCC in mice when given continuously over six to twelve months in a chronic injury model (Akhurst *et al.*, 2001; Knight *et al.*, 2008; Knight *et al.*, 2000).

Figure 1.4 HPC activation in the CDE diet model

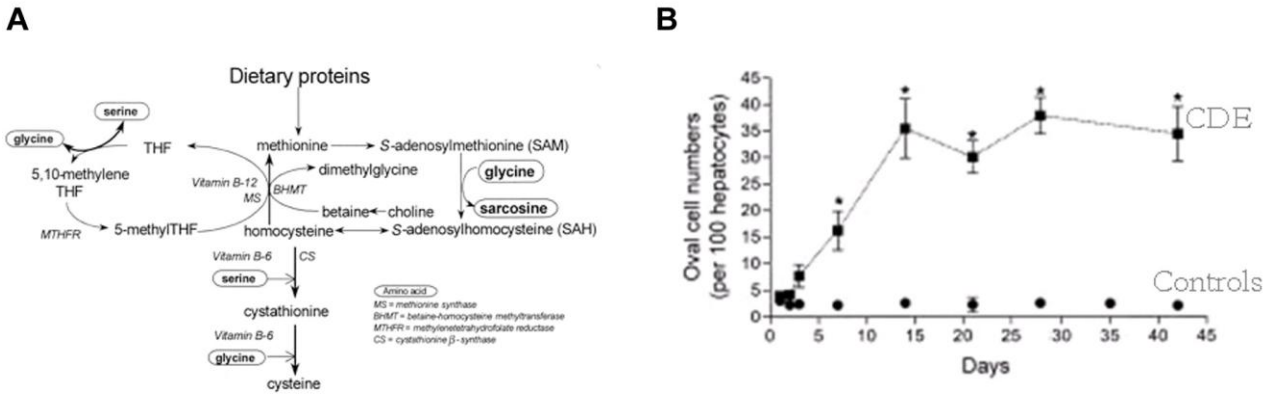

(A) The transsulfuration pathway in eukaryotes enables the creation of the amino acid cysteine from the essential amino acid methionine. Ethionine blocks the conversion of methionine to homocystiene. (B) Published data examining $A6^{+}$ HPCs following CDE diet in a murine model of HPC expansion. Data is presented as mean±SEM (adapted from Akhurst *et al.*, 2001)

The DDC diet

The DDC diet is an alternative model of HPC activation in the mouse (Preisegger *et al.*, 1999). Unlike the CDE diet it results in persistent proliferation of primitive ductules with poorly defined lumens. These ductules accumulate in the periportal regions and while the cells of the ductules maintain many of the cellular markers of the HPCs in the CDE diet they are clearly morphologically distinct (Jelnes *et al.*, 2007). Once again, the mechanism of action resulting in HPC activation in this model is not known. What is clear is that, as with the CDE diet, hepatocellular injury is seen both by raised serum transaminases, and architecturally. In the recent past the DDC diet has been used in many published HPC studies. Crucially HPCs extracted from DDC induced mice have been shown to be capable of hepatocyte repopulation in a transplantation model (Wang *et al.*, 2003a).

<u>HPCs in human liver disease</u>

In humans, HPC activation is believed to take the form of a ductular reaction. This is morphologically and immunohistochemically analogous to the rodent HPC response. The clinical relevance of the HPC reaction is implied by its frequency in the full spectrum of human liver diseases including fulminant hepatic failure, chronic viral hepatitis, alcoholic disease and non alcoholic fatty liver disease, immune cholangiopathies, and hereditary liver disorders (Falkowski *et al.*, 2003; Roskams, 2003; Roskams *et al.*, 1991; Roskams *et al.*, 2003a; Roskams *et al.*, 2003b). During acute liver injury HPC regeneration may be seen occurring synchronously with a degree of hepatocyte replication. The presence of HPC activation during chronic liver disease appears, however, to be a feature of eventual exhaustion of hepatocyte proliferation by senescence over many years or decades (Wiemann *et al.*, 2002). Characteristically the magnitude of HPC activation corresponds to the severity of liver fibrosis and inflammation (Libbrecht *et al.*, 2000; Lowes *et al.*, 1999; Roskams *et al.*, 2003a) as is also observed in rodents (Pritchard and Nagy, 2010). In addition the more aggressive a hepatocellular injury in humans, the higher the proportion of observed HPCs that resemble intermediate hepatocytes. This implies that an escalating hepatocyte deficiency promotes a greater degree of differentiation down the progenitor cell–hepatocyte axis (Roskams *et al.*, 2003b). A particular disease condition in which dramatic HPC activation and expansion is fibrosing cholestatic hepatitis, an aggressive and usually fatal form of viral hepatitis (Dixon and Crawford, 2007).

Aside from histological and immunohistochemical demonstration of HPCs in a wide range of human diseases, other observations from human livers supports the role of HPC mediated regeneration. Sequential biopsies, taken from patients with liver disease, have shown HPC proliferation and suggests their differentiation by observing a progressive increase in intermediate hepatocytes in association with their progressive extension into the liver lobule over time (Demetris *et al.*, 1996; Falkowski *et al.*, 2003; Roskams *et al.*, 1991). These observations are in keeping with clonal analysis performed using mitochondrial mutations in both normal and injured liver which suggests that the portal tract, is likely to be a crucial origin of clonal hepatocytes in the adult human (Lin *et al.*,

2010; Fellous *et al.*, 2009). Rodent HPCs are similarly described to arise from the Canal of Hering. Finally proliferating cells, analogous to those in animal models, have been isolated from foetal and adult human liver and are capable of hepatocyte-like differentiation (Herrera *et al.*, 2006; Porretti *et al.*, 2010; Schmelzer *et al.*, 2007).

HPC markers and their relevance

In order to aid the accurate and consistent identification of HPC in the wide variety of models and species they have been described an increasingly large number of cell markers have been ascribed to this population. By their nature, HPCs are heterogeneous, consisting of a spectrum of cells ranging from an immature phenotype to mature cholangiocytes and intermediate hepatocytes. Although markers for the most immature progenitor cells have not been identified, there are currently a variety of established markers for constituents of the HPC compartment (Table 1.1). Many HPC markers are also expressed by mature cholangiocytes or hepatocytes. No universal HPC marker, specific to this compartment, has been identified to date, with most of the frequently used HPC markers also identifying mature cholangiocytes. This cross reactivity between mature and immature cell populations is likely to be a feature of the progressive differentiation of HPCs during which they vary their marker expression. Currently there is a genuine requirement for a thorough understanding of the stepwise marker expression in HPCs, akin to that described for the haematopoietic stem cell development (Bird *et al.*, 2008). A small number of these markers have been used to enrich HPCs which, as a population, have shown transplantability and hepatocellular reconstitution from either foetal (Dlk^+ - Oertel *et al.*, 2008 or $EpCAM^+$ - Schmelzer *et al.*, 2007), $CD13^+$ (Kakinuma *et al.*, 2009) or adult donors ($cKit^+$ - Wang *et al.*, 2003a).

Early HPC markers described to date include c-kit, Sca-1, NCAM, SgIGSF and multidrug resistance transporters which denote a Side Population (SP) phenotype. The SP phenotype was originally described in the haematopoietic system and relates to the

ability to efflux the dye Hoechst 33342. It appears to identify cells with immature characteristics particularly in hepatic embryogenesis (Tsuchiya *et al.*, 2005) and carcinogenesis (Chiba *et al.*, 2006). Another feature of immature cells is the absence of cytokeratin 7 (CK7) expression. CK7 is expressed as HPCs acquire a mature phenotype (Paku *et al.*, 2005). Alphafetoprotein (αFP) is an HPC marker which is expressed also during hepatic embryogenesis and carcinogenesis. It appears to be present in intermediate ducts (Theise *et al.*, 1999) with prolonged expression for over 3 weeks following partial hepatectomy (PH) with retrorsine treatment (Gordon *et al.*, 2000) and is also expressed by more differentiated hepatocyte like cells (Evarts *et al.*, 1989). αFP is however difficult to detect histologically in murine HPC models (Jelnes *et al.*, 2007). CD133, also known as prominin-1, is recognised as a marker for other stem cell populations (Shmelkov *et al.*, 2005). In the adult liver it appears to be marker of biliary cells consistent with HPCs in the Canal of Hering (Shmelkov *et al.*, 2008). Furthermore adult liver derived $CD133^+$ cells have recently shown bipotentiality in clonogenic assays (Porretti *et al.*, 2010 ; Suzuki *et al.*, 2008).

The cytokeratins and panCK

The most frequently used markers for HPCs across all species and models of HPC activation utilise specific cytokeratins by HPCs (Santoni-Rugiu *et al.*, 2005). Cytokeratins (CKs) form the intermediate filaments between the nucleus and the cell membrane of epithelial cells and, due to their many forms, a cell's CK expression may be used as a signature its epithelial tissue origin. Briefly CKs are usually found in pairs comprising one basic or neutral type I CK (CK1-9) and one acidic type II cytokeratin (CK10-20). Many CKs are used for HPC identification with other specific HPC identifying antibodies (e.g. OV6 and A6) known to recongnise epitopes within specific CKs (Table 1.1). A polyclonal antibody to panCK recognises multiple cytokeratin epitopes and has been described to show near identical recognition pattern to the HPC marker A6 in mice, and additionally has the significant advantage of its effective use in

formalin fixed tissues (Kofman *et al.*, 2005). This commercially available antibody has become one of the most frequently used HPC markers in the field. For historical reasons the work presented here uses PanCK as the default HPC marker. Where appropriate, cross reference to other HPC markers particularly Dlk1 and EpCAM will be made.

Dlk1

The now accepted cell surface marker of hepatoblasts in the developing liver Dlk1 has more recently been described in adult HPCs (Jensen *et al.*, 2004; Oikawa *et al.*, 2009; Tanimizu *et al.*, 2003). While Dlk1 (also known as Pref1) is readily recognised in a variety of rat HPC models it has also been shown in low levels in murine models (Jelnes *et al.*, 2007). Functionally it is known to interact with the Notch receptor on the cell surface (Bray, 2006). It is therefore of use also as a potential target for cell sorting of the HPC population (Tanimizu *et al.*, 2004). Furthermore its interaction with the Notch signalling pathway places it with the potential to influence cell fate choice (see Notch section Chapter 1)

EpCAM

A widely accepted marker of HPCs which has recently gained increasing credence is the cell surface antigen EpCAM (Epithelial cell adhesion molecule) or CD326. EpCAM is a Type 1 transmembrane glycoprotein and is expressed on the basolateral membrane of cells by the majority of epithelial tissues. Functional EpCAM is a Ca^{2+}-independent cell-cell adhesion molecule and is known to be intricately linked with the Cadherin-Catenin pathway and hence the Wnt pathway (see Wnt section Chapter 1).

A key advantage to the use of EpCAM as an HPC marker is that it is not expressed by many differentiated epithelia including adult squamous epithelium and crucially hepatocytes (de Boer *et al.*, 1999). EpCAM expression has been reported to be a

possible marker of early malignancy, with expression being increased in tumour cells and almost all carcinomas, with de novo expression being seen in dysplastic squamous epithelium.

The evidence for EpCAM as a marker of HPCs is many fold. Following an early description of ductular reaction being $EpCAM^+$ (de Boer *et al.*, 1999) it has emerged as a marker with perhaps the strongest evidence for containing primordial HPCs. Firstly adult mouse $EpCAM^+$ cells are bipotential with colonies forming both hepatocytes and cholangiocytes (Okabe *et al.*, 2009). Furthermore adult rat $EpCAM^+$ HPCs are transplantable and can differentiate into hepatocytes *in vivo*. The $EpCAM^+$ HPC population also exists in human liver constituting approximately 2% of the hepatocyte depleted fraction from normal adults but increasing to over 10% in adults with chronic liver disease (Porretti *et al.*, 2010). Additionally, human derived $EpCAM^+$ cells are bipotential and transplantable forming hepatocytes in a NOD/SCID mouse transplant model (Schmelzer *et al.*, 2007). EpCAM is also recognised not only as a marker of a cholangiocarcinoma and a subset of HCC (de Boer *et al.*, 1999), but additionally provides prognostic information in HCC (Yamashita *et al.*, 2008). Interesting the $EpCAM^+$ population within HCCs contains a transplantable cancer stem cell (Yamashita *et al.*, 2009) adding further weight to its use as an HPC marker.

More recently alternative approaches such as profiling HPC like cells during development (Ochsner *et al.*, 2007) or immunising rabbits with cells isolated from adult HPC models (Dorrell *et al.*, 2008) have been used to generate other novel HPC markers. While monoclonal antibodies which appear to recognise specific populations both of HPCs and their associated cells have been produced, their utility remains to be shown. In the future, these antibodies or their target molecules may permit more specific recognition of primitive HPCs or even hepatic stem cells as well as the various stages

during differentiation. A thorough description of the stage of HPC differentiation from stem cell to fully differentiated hepatocyte will greatly benefit our understanding of hepatic regeneration.

Despite the apparently stereotyped HPC response seen across a wide range of human diseases there is heterogeneity both between species and injury models (Jelnes *et al.*, 2007). For example, the expression of αFP which is characteristically seen in rat HPC models, is rare in the human ductular reaction and difficult to detect in many murine HPC models. Differing characteristics are seen between models, for example the expression of DMBT1 is seen following hepatocellular injury but is not seen during human cholestatic liver disease or following BDL in rodents (Bisgaard *et al.*, 2002). Consistent with the atypical HPC response observed in the BDL model, dexamethasone does not affect ductule formation following BDL in rats but inhibits HPC activation following AAF/PH (Nagy *et al.*, 1998).

Other potential hepatocyte precursor populations

Lineage tracing experiments in the mouse have provided some information regarding alternative potential origins of hepatocytes during liver regeneration. Using a constitutively active Foxl1-Cre mouse, a small number of labelled hepatocytes (0.5% max) were seen following biliary injury in this lineage tracing system. Interestingly while this occurs in an injury model the proportion of hepatocytes derived from $Foxl1^+$ precursors during development and physiological liver homeostasis is extremely low suggesting that while $Foxl1^+$ cells may have the potential to become hepatocytes, but in reality even during injury their propensity to support liver function is very low indeed (Sackett *et al.*, 2009).

Another constitutively active lineage tracing system, this time under the control of a GFAP promoter has also been used to track precursors of hepatocytes (Yang *et al.*, 2008). In this model larger numbers of labelled hepatocytes are seen following exposure

to a dietary injury model. However, once again the low level of labelled hepatocytes prior to dietary initiation calls into question how relevant $GFAP^+$ precursor are during development and adult homeostasis. Furthermore it is apparent that while GFAP is classically a marker of hepatic stellate cells, it is also a marker of HPCs and cholangiocytes (Yang *et al.*, 2008). Therefore, the role of hepatic stellate cells in the formation of hepatocytes remains in doubt. It seems more plausible that these findings represent the differentiation of HPCs into hepatocytes as HPCs have been described to express GFAP, at least transiently. Whether all HPCs express GFAP and at what point in their differentiation this occurs is a question that requires further investigation. This in my opinion makes the assumption that hepatic stellate cells are HPCs, unreliable and currently unfounded.

Mechanisms of HPC activation

The mechanisms controlling the HPC response remain under intensive investigation. Many of the signals that control liver regeneration from hepatocytes themselves are also involved in HPC mediated regeneration. None-the-less minor injury to a normal liver results in no evidence of activation of the HPC compartment and yet causes effective hepatocyte proliferation. Therefore significant additional factors appear to be crucial in determining whether or not HPC activation occurs. The most common contexts in which the HPC reaction is observed is when the hepatocyte's cell cycle is blocked either by toxins or replicative senescence. Nevertheless these two modes of liver regeneration are not entirely mutually exclusive. HPC and hepatocyte replication can be observed simultaneously in some injury models (Rosenberg *et al.*, 2000; Wang *et al.*, 2003a). This may simply be a function of the location, duration and/or magnitude of these specific signals in response to injury or the failure of sufficient regeneration. However other factors such as the cellular environment are likely to be highly relevant in generating the HPC response. Certainly the wide range of candidate signals, with many

showing only modest effects, suggests that there is a significant signal redundancy in HPC control.

Observational studies show a correlation between the severity of liver disease and the magnitude of the HPC response (Libbrecht *et al.*, 2000; Lowes *et al.*, 1999). A central role of inflammatory cytokines has been suggested in rodents also (Knight, Matthews *et al.* 2005). These observations are consistent with the dramatic inhibition of HPC responses noted upon treatment with anti-inflammatory agents (Davies, Knight *et al.* 2006; Nagy *et al.*, 1998). In terms of specific signals, many have been studied directly during HPC activation *in vitro* and *in vivo* (for overview see Table 1.2). Many of these signals are also seen during PH; however they are often different in either intensity or duration of signal.

TNF superfamily

Members of the pro-inflammatory TNF superfamily include TNFα, and TWEAK (TNF-like weak inducer of apoptosis) both of which appear to play pivotal roles in HPC activation. TWEAK is upregulated during hepatic injury both in rodents and a variety of human diseases and mediates pro-proliferative effects directly on HPCs via its monogamous Fn14 receptor (Jakubowski *et al.*, 2005; Winkles, 2008; Tirnitz-Parker *et al.*, 2010; Burkly *et al.*, 2007). TWEAK is sufficient, although not necessary, to induce a modest HPC response, whilst its inhibition results in an attenuated murine HPC response to both the DDC and CDE diets (Jakubowski *et al.*, 2005; Tirnitz-Parker *et al.*, 2010)). This therefore positions TWEAK as arguably the most important paracrine signal inducing the hepatic HPC response. Interestingly in a more detailed examination over time using Fn14 knockout mice treated with the CDE diet, a delayed, rather than prolonged loss of HPC expansion was observed. This feature suggests a degree of redundancy in the control of HPC behaviour with compensation by other pathways of activation.

Table 1.2 Functional studies in HPC activation

Signal	Oval Cell Model M=mouse, R=rat	Effect on OCs	Reference
TNF			
↓ In vivo	50% CDE diet (M)	↓ expansion	(Knight et al. 2000)
↑ In vitro	LE6 cells IV (R)	↑ proliferation	(Kirillova et al. 1999)
↑ In vitro	LE6 cells IV (R)	↑ mitogenesis	(Brooling et al. 2005)
TWEAK			
↑ In vivo	Uninjured (M)	↑ expansion	(Jakubowski et al. 2005)
↑ In vivo	Uninjured adults (M)	↑ expansion	
↓ In vivo	DDC diet (M)	↓ expansion	
↑ In vitro	NRC line (R)	↑ mitogenesis	
LTα			
↓ In vivo	CDE diet (M)	↓ expansion	(Knight and Yeoh 2005)
LTβ			
↓ In vivo	CDE diet (M)	↓ expansion	(Akhurst et al. 2005)
STAT3			
↑ In vivo	None (M)	↑ expansion	(Subrata et al. 2005)
↑ In vivo	CDE diet (M)	↑ expansion, migration	(Subrata et al. 2005)
IL6			
↓ In vivo	50% CDE diet (M)	↓ proliferation	(Knight et al. 2000)
↑ In vitro	PIL2/PIL4 lines (M)	↑ proliferation	(Matthews et al. 2004)
↑ In vivo	CDE diet (M)	↑ expansion, proliferation	(Subrata et al. 2005)
↓ In vivo	AAF/PH (R)	↓ expansion	(Nagy et al. 1998)
OSM			
↑ In vitro	PIL2/PIL4 lines (M)	↓ growth	(Matthews et al. 2005)
↑ In vitro	Primary OCs (M)	No effect on growth	(Matthews et al. 2005)
IFNγ			
↑ In vivo	Uninjured (M)	OC like expansion	(Toyonaga et al. 1994)
↑ In vitro	LE6 cells (R)	↑ mitogenesis	(Brooling et al. 2005)
↑ In vitro	LE2 cells (R)	Possible ↓ mitogenesis	(Brooling et al. 2005)
↓ In vivo	CDE diet (M)	↓ expansion	(Akhurst et al. 2005)
↑ In vivo	2/3 PH (M)	↑ expansion	(Brooling et al. 2005)
IFNα			
↑ In vitro	PIL2/PIL4 lines (M)	↓ proliferation	(Lim et al. 2006)
↑ In vivo	CDE diet (M)	↓ expansion, proliferation	
HGF			
↑ In vivo	AAF (R)	↑ proliferation	(Nagy et al. 1996)
↑ In vivo	AAF/PH (R)	↑ early expansion	(Hasuike et al. 2005)
↑ In vivo	AAF/PH (R)	↑ expansion	(Oe et al. 2005)
EGF			
↑ In vivo	AAF (R)	↑ proliferation	(Nagy et al. 1996)
↑ In vitro	MOC lines (M)	↑ proliferation	(Isfort et al. 1997)
TGFβ			
↑ In vivo	DDC diet (M)	↓ expansion	(Preisegger et al. 1999)
↑ In vitro	LE2/LE6 cells (R)	↓ proliferation	(Nguyen et al. 2007)
SCF			
↓ In vivo	AAF/PH (R)	↓ expansion	(Matsusaka et al. 1999)
Sympathetic nervous system			
↓ In vivo	50% CDE diet (M)	↓ expansion (CK)	(Oben et al. 2003)
Parasympathetic nervous system			
↓ In vivo	Galactosamine (R)	↓ expansion (OV6)	(Cassiman et al. 2002)

Artificial manipulation of target signal is shown by arrows, ↑ indicates upregulation and ↓ indicates inhibition of signalling. References are cited for each study. For HPC models M and R denote murine and rat studies respectively.

The source of TWEAK in these models remains an important question. In other situations TWEAK is produced predominantly by monocytes particularly following IFNγ stimulation (Nakayama *et al.*, 2000) and is initially expressed as a membrane bound molecule which can also be released in a soluble form. TWEAK activates NFκB (Tirnitz-Parker *et al.*, 2010) which is described as pro-proliferative to HPCs (Kirillova *et al.*, 1999). TWEAK may also play a role in the proliferation of other mesenchymal progenitors (Girgenrath *et al.*, 2006) including promoting angiogenesis (Jakubowski *et al.*, 2002) and contributes to hepatic embryogenesis and carcinogenesis (Kawakita *et al.*, 2005). Examination of the source of TWEAK within the liver during the CDE diet suggests that macrophages and NK cells may be principal sources although other sources including myofibroblasts remain possible (Tirnitz-Parker *et al.*, 2010).

TNFα production is increased during chronic human liver disease (Tilg *et al.*, 1992). It too is described as being predominantly produced by macrophages, but also by other cells types including lymphocytes and fibroblasts (Locksley *et al.*, 2001). Hepatic TNFα is upregulated during the rodent HPC response (Akhurst *et al.*, 2005; Knight *et al.*, 2000). The cellular activity of TNFα is mediated via the TNF R1 and TNF R2 receptors. Administration of TNFα to HPC lines *in vitro* results in proliferation (Kirillova *et al.*, 1999). Furthermore TNF R1 knockout mice show a markedly impaired HPC response (Knight *et al.*, 2000). To date no study, including that with TNFα/Lymphotoxin α (LTα) knockout mice (Knight and Yeoh, 2005), has shown an absolute requirement for TNFα for HPC activation. However is appears that TNFα is required for an optimal HPC response. Unlike TWEAK, raised TNF alone has not been described to be sufficient for HPC activation.

LT-α, LT-β and LIGHT are further members of the TNF superfamily and are well described in other organs to be involved in a variety of processes including influencing cell survival and proliferation (Tumanov *et al.*, 2007). Production of LT-α, LT-β and LIGHT is principally by lymphocyte populations. LT-α in similarity with TNFα binds

TNF R1 which, as previously described, plays an important role in the control of the HPC response. This receptor's role in HPC activation is suggested but not confirmed by the demonstration that LT-α/TNFα double knockout mice develop an attenuated HPC response following the CDE diet (Knight and Yeoh, 2005). LT-α may also act in combination with LT-β via the formation of a heterotrimer (LTα1β2) which is the ligand for a separate receptor; LT-β Receptor (LT-βR). LT-β expression is upregulated both during rodent HPC activation and during chronic human liver disease. Both LT-β knockout and LT-βR knockout mice show an partially impaired HPC response (Akhurst *et al.*, 2005). A further ligand for LT-βR called LIGHT is therefore also implicated in HPC function via LT-βR mediated signal transduction. LIGHT is predominantly expressed by lymphocytes (Hansson, 2007) and although its effects on HPCs have not been directly investigated it is known to signal to hepatocytes via LT-βR (Lo *et al.*, 2007).

GP130 activators

A variety of cytokines, including IL6, Oncostatin M (OSM) and Leukaemia Inhibitor Factor (LIF), act through the gp130 signalling pathway. Activation of this pathway results from the homodimerisation of gp130, which in turn activates the JAK/STAT and ERK pathways. STAT 3 and its targets are up regulated during the rodent HPC response and during human chronic liver disease (Sanchez *et al.*, 2004; Subrata *et al.*, 2005).

Aside from TWEAK, gp130 is the only signal demonstrated to date capable of initiating an HPC response alone. This was demonstrated in uninjured $gp130^{Y757F}$ mice with constitutively active gp130 (Subrata *et al.*, 2005; Yeoh *et al.*, 2007) in which an expansion of $A6^{+}$ HPCs is observed in the absence of other interventions. Another of gp130's downstream targets, the ERK-1/2 pathway, was shown by the same investigators to be a negative regulator of HPC expansion (Yeoh *et al.*, 2007). Therefore gp130 is potentially a key element in the activation and expansion of hepatic HPCs.

Using hepatocyte specific knockout, gp130 has also been demonstrated to play a key role in protection from injury in the DDC diet with knockout resulting in greater hepatocellular injury and corresponding increased HPC activation (Plum *et al.* 2010).

IL-6 is the best characterised of gp130's activators (Santoni-Rugiu *et al.*, 2005). It is produced by a variety of cell types including macrophages and Kupffer cells (Naugler *et al.*, 2007), in addition to fibroblasts, and endothelia. Recent studies have demonstrated that IL-6 is pro-proliferative to the HPC response and that IL-6 knockout mice demonstrate an attenuated HPC response (Fischer *et al.*, 1997; Knight *et al.*, 2000; Yeoh *et al.*, 2007). Treatment of HPC lines with IL-6 results in proliferation and migration (Matthews *et al.*, 2004; Yeoh *et al.*, 2007).

IL-6 functions as the ligand to the type I cytokine receptor CD126 (IL-6Rα) along with the signal transducing gp130 homodimer principally activating STAT3 (Yeoh *et al.*, 2007). IL-6 expression increases in both acute and chronic human disease and rodent liver injury models (Akhurst *et al.*, 2005; Fausto *et al.*, 2006; Streetz *et al.*, 2003). IL-6 is a key signal in hepatocyte proliferation but is not in itself capable of inducing an HPC response (Yeoh *et al.*, 2007). The source of IL-6 during liver injury is likely to arise from activated leukocytes including Kupffer cells and lymphocytes (Streetz *et al.*, 2003), however IL6 production has also been described from HPCs themselves, raising the possibility of autocrine stimulation (Matthews *et al.*, 2004). In further support for a role of IL6 in HPC function, IL6 appears to be a central player in the development of HCC (Naugler *et al.*, 2007; Wands, 2007), which as discussed is a process which shares many similarities to the expansion of HPCs during regeneration (see section 1.34 HPCs and Cancer).

LIF and OSM both participate in a variety of processes including regulation of growth and differentiation. LIF's action is mediated via the LIF receptor (LIFR), which is composed of LIFRβ and gp130. Its downstream action in HPCs is predominantly via STAT1 (Kirillova *et al.*, 1999). Both LIF and LIFR are upregulated during the HPC

reaction in the rat (Omori *et al.*, 1996) and in human cirrhotic livers, with LIFRβ localising to proliferating $CK7^+$ intermediate hepatobiliary cells (Znoyko *et al.*, 2005). Although the effects of LIF on HPC proliferation are not clear it does have stimulatory effects on progenitor cells in other organs, including murine haematopoietic progenitors (Metcalf and Gearing, 1989). LIF has also been described to have effects of hepatocyte differentiation. Murine embryonic bodies when cultured with LIF are maintained in a undifferentiated state but differentiate into hepatocyte like cells upon its removal (Chinzei *et al.*, 2002).

OSM also activates gp130, either via its own OSM receptor (OSMRβ) subunit or via the LIFR (Heinrich *et al.*, 2003). OSM influences extrahepatic progenitor cell activity and extracellular matrix (ECM) deposition in addition to inducing an acute phase response and therefore may influence HPC behaviour via a number of distinct pathways (Knight *et al.*, 2005a). It is produced by hepatic macrophages in humans and is upregulated both during cirrhotic human liver disease (Znoyko *et al.*, 2005) and the rodent HPC reaction (Matthews *et al.*, 2005). Both murine HPCs and human intermediate hepatobiliary cells express OSMRβ which induces activation of STAT3 (Matthews *et al.*, 2005; Znoyko *et al.*, 2005). OSM has been described to promote proliferation and differentiation of foetal hepatoblasts (Kinoshita *et al.*, 1999) and HPCs lines respectively (Yin *et al.*, 1999; Yin *et al.*, 2002). Conflicting data however has come from an immortalised p53 deficient HPC line (Matthews *et al.*, 2005). Further investigation is required to clarify the role of OSM in HPC activation.

IFNγ

Unlike the previous examples of signalling via gp130, IFNγ activates the JAK-STAT pathway via STAT1 rather than STAT3 (Croker *et al.*, 2003). There is strong evidence for a role of the inflammatory cytokine IFNγ in HPC activation. It is characteristically expressed by T lymphocytes and NK cells. IFNγ's role in HPC activation was initially

examined using a transgenic mouse with constitutive hepatic IFNγ expression using a serum amyloid P component gene promoter. These mice demonstrated cords of small cells morphologically similar to HPCs in the context of progressive liver inflammation (Toyonaga *et al.*, 1994). Since then HPCs have been found to possess functional IFNγ receptors and IFNγ expression have been shown during the HPC reaction (Bisgaard *et al.*, 1999). Varying effects, including proliferation, are seen when IFNγ is administered to HPC lines (Brooling, Campbell *et al.* 2005). More consistent effects have been seen using *in vivo* manipulation with a reduced HPC expansion seen in IFNγ knockout mice (Akhurst *et al.*, 2005) and IFNγ treatment stimulated an HPC response following PH in mice (Brooling *et al.*, 2005). These observations are consistent with the impaired HPC response seen in BALB/c mice which lack Th1 signalling, of which IFNγ is a key component (Knight *et al.*, 2007). Caution however should be noted as reduced HPC expansion has also been noted *in vitro* (Brooling *et al.*, 2005) and it is possible that IFNγ may have indirect effects upon the HPC response via inhibition of hepatocyte proliferation (Fausto *et al.*, 2006). IFNγ has been proposed to be a factor in determining hepatocyte versus HPC mediated regeneration although convincing data to support this hypothesis is lacking.

Type I Interferons

The effects of the type 1 interferons (IFNα and IFNβ) on HPCs appear to differ significantly from that of IFNγ. IFNα signals predominantly through STAT3 in murine liver (Lim *et al.*, 2006). Analysis of paired biopsies in human liver biopsies reveals that either successful or unsuccessful IFNα treatment of Hepatitis C virus is associated with a reduced number of HPCs (Lim *et al.*, 2006; Tsamandas *et al.*, 2006). This effect is not reliant on Hepatitis C as IFNα reduces HPC proliferation both *in vitro* and *in vivo* in the absence of Hepatitis C infection (Lim *et al.*, 2006). Furthermore IFNα appears to promote differentiation particularly into hepatocyte like cells. The effects of IFNβ on HPCs are unknown although in similarity to IFNα it impairs regeneration following PH

(Theocharis *et al.*, 1997; Wong *et al.*, 1995). Its role in HPC activation therefore warrants further investigation.

Primary growth factors

The role of Hepatocyte Growth Factor (HGF) in stimulating hepatocyte proliferation in the primed liver is well described (Fausto *et al.*, 2006). HPCs, in similarity to hepatocytes, also express the HGF receptor c-Met (Hu *et al.*, 1993; Muller *et al.*, 2002). The expression of HGF is increased following PH/AAF in the rat (Evarts *et al.*, 1993; Hu *et al.*, 1993), as is urokinase plasminogen (uPA) which can release HGF stored in its bound form on ECM(Nagy *et al.*, 1996). HGF levels are also increased in the serum of patients with chronic liver disease, and those experiencing acute injury, compared to healthy controls (Shiota *et al.*, 1995). HGF is both mitogenic to, and promotes differentiation of, HPCs *in vivo* (Hasuike *et al.*, 2005; Nagy *et al.*, 1996). This is in concordance with similar effects on embryonic hepatic stem cells (Suzuki *et al.*, 2003). There is therefore strong evidence for a role of HGF in influencing HPC behaviour; however it should be noted that elevations of HGF in the context of PH alone are insufficient to stimulate HPC expansion.

Transforming Growth Factor α (TGFα) and Epidermal Growth Factors (EGF) are structurally related membrane bound growth factors which bind the EGF receptor (EGFR) of adjacent cells, in turn initiating a variety of effects including upregulation of the EGFR and cell proliferation (Leahy, 2004). Membrane bound pro-TGFα may also be cleaved to release a soluble signal capable of autocrine and paracrine signalling. In rodents TGFα and EGF are produced predominantly by stellate cells which are known to line HPC ductules (Paku *et al.*, 2001) whist the EGFR is expressed by HPCs (Evarts *et al.*, 1992). TGFα is upregulated following AAF/PH injury in rodents (Evarts *et al.*, 1993) and both EGF and TGFα localise to ductular reactions in human chronic liver

disease (Hsia *et al.*, 1994; Komuves *et al.*, 2000). EGF is mitogenic to HPCs *in vitro* suggesting a role of both growth factors in HPC activation.

FGFs

The fibroblasts growth factors (FGFs) are a family of growth factors which bind their FGF receptors (FGFR) with the aid of heparin sulfate proteoglycans (Pellegrini, 2001). FGFs are involved in hepatic embryogenesis (Jung *et al.*, 1999) and are up regulated in both the rats AAF/PH model (Marsden *et al.*, 1992) and during human chronic liver disease (Jin-no *et al.*, 1997). While FGFR2 is upregulated both in a variety of liver injuries and is expressed by numerous cells types, FGFR1 in adult rats is upregulated specifically during HPC inducing injury and is expressed by HPCs (Hu *et al.*, 1995). In keeping with their role in organogenesis FGFs induce a hepatocyte like phenotype in BM derived 'multipotent adult progenitor cells' *in vitro* (Schwartz *et al.*, 2002).

TGF-β

TGF-β is well recognised to limit hepatocyte mediated regeneration by inhibiting hepatocyte proliferation while inducing apoptosis (Fausto *et al.*, 2006). TGF-β is actively expressed by myofibroblasts following HPC inducing injury (Park and Suh, 1999). Active expression of TGF-β in a transgenic mouse fed on the DDC diet results in a reduced HPC response (Preisegger *et al.*, 1999), and concordantly TGF-β is inhibitory to HPC lines *in vitro* (Nguyen *et al.*, 2007) although TGF-β is less inhibitory of mitosis in HPCs than hepatocytes.

SDF-1

The chemokine, Stromal Cell Derived factor 1 (SDF-1) uniquely binds to the CXCR4 receptor, and plays a variety of roles including cell trafficking, proliferation, and organogenesis. CXCR4 is expressed by a variety of progenitor cells and SDF-1 is

upregulated during human chronic liver disease (Terada *et al.*, 2003). There is however some disagreement over the source of SDF during the hepatic HPC response with reports suggesting either hepatocytes or periportal production (Hatch *et al.*, 2002; Mavier *et al.*, 2004; Zheng *et al.*, 2006). However, it is clear that SDF is upregulated in following HPC inducing rodent injury. SDF has been shown to be both pro-proliferative (Pi *et al.*, 2005) and chemotactic (Hatch *et al.*, 2002) to HPCs.

Wnt

Metazoan development is controlled by a defined group of signalling pathways including but not limited to Hedgehog (Hh), Wnt/Wingless (Wnt), and Receptor Tyrosine Kinase (RTK) (Hayward *et al.*, 2008; Ma *et al.*, 2008; Pownall *et al.*, 1996). All of these pathways are now appreciated to influence adult tissue stem cell behaviour in many organs including the liver.

The name Wnt was coined after the combination of wingless (Wg) and int-1 (Rijsewijk *et al.*, 1987). Wnts are secreted cell signals and are now believed to have a central role in both liver development and regeneration. Having been originally described in Drosophila melanogaster, there are currently 19 Wnts described in the human and mouse, constituting a family of highly conserved secreted signalling molecules that regulate cell-to-cell interactions during embryogenesis, regeneration, aging and carcinogenesis (Brack *et al.*, 2007; Micsenyi *et al.*, 2004; Ober *et al.*, 2006; Kirstetter *et al.*, 2006). In keeping with this Wnt has been described to play a central role in stem cell niches out with the liver (Fleming *et al.*, 2008; Voog and Jones).

The mechanism of Wnt signal transduction is summarised in Figure 1.5. In general secreted Wnts bind to their receptors called Frizzled (Fz). In the absence of Wnts, β-catenin is phosphorylated by a destruction complex constituted by APC, axins, GSK3β and CK1, and then ubiquitinated, promoting its degradation by the proteasome. Binding of soluble Wnts to the Frizzled receptors activates Wnt/β-catenin signalling (de La Coste

et al., 1998). This results in the stabilisation of β-catenin by the inhibition the its destruction complex and subsequent β-catenin translocation into the nucleus where, in conjunction with members of LEF1/TCF transcription factor family, it activates the transcription of several target genes including cMyc, Axin2 and Cyclin D. The effects of stablisation of β-catenin and resultant target gene activation, induces general effects such as cellular proliferation, and maintenance of stem cells. However, the mechanism by which Wnt achieves its effects varies from cell type to cell type and organ to organ (Reed *et al.*, 2008).

Figure 1.5 Signal transduction in the Wnt pathway

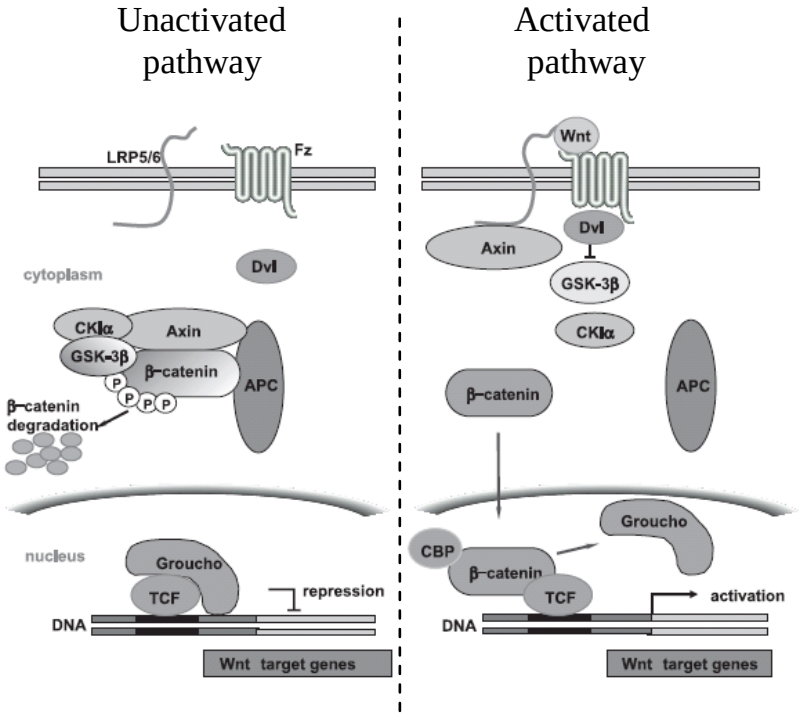

In the absence of Wnt the degradation of β-catenin renders the Wnt signalling transduction pathway inactive by the inhibition of target gene transcription by TCF-Groucho interactions. In this instance, the destruction complex including APC, axins, GSK3β and CK1 promotes β-catenin's destruction by the proteasome. In the presence of Wnt, and signal transduction by Fz/LRP at the level of the cell membrane the activity of the destruction complex is inhibited resulting in accumulation of β-catenin and its transfer to the nucleus. Here β-catenin replaces Groucho, resulting in Wnt target gene activation via its association with TCF. Adapted from Nusse, 2005).

Many other pathways interact with Wnt/ β-catenin signalling. Wnt may also activate so called non-canonical (β-catenin independent signalling), and β-catenin may be stablised in a Wnt independent manner (He, 2006). For example HGF signalling is intricately coupled to β-catenin mediated signalling via the c-Met receptor (Apte *et al.*, 2006; Monga *et al.*, 2002); TGFβ signalling promotes the nuclear localisation of β-catenin (Jian *et al.*, 2006). Furthermore the association of cytosolic β-catenin with E-cadherin, exposes it to cell-ECM interactions also.

Characterisation of the Wnt gene expression signature of the resting and injured liver has been performed, revealing that in the resting state a large number of Wnts are produced by a variety of cell populations within the liver (Zeng *et al.*, 2007). While Wnt has been shown to play roles in a variety of hepatic processes including fibrosis and hepatic stellate cell activation (Cheng *et al.*, 2008; Kordes *et al.*, 2008; Myung *et al.*, 2007), Wnt appears to be a central signalling molecule influencing HPC behaviour, differentiation and specifying zonation of hepatocellular function (Gebhardt and Hovhannisyan, 2010).

With regard to liver regeneration, Wnt signalling plays a role in the predominantly hepatocellular regeneration which occurs following partial hepatectomy (Sekine *et al.*, 2007; Sodhi *et al.*, 2005). Accordingly over expression of stable β-catenin results in hepatomegaly (Cadoret *et al.*, 2001; Tan *et al.*, 2005) while hepatocytic β-catenin knockdown results a reduction in liver size (Sekine *et al.*, 2006).

In the rat, following PH/AAF, nuclear β-catenin is observed in HPCs (Apte *et al.*, 2007). In this study HPCs were shown to express the Wnt receptor Frizzled 2, in addition to dynamic changes in Wnt1 and WIF expression, consistent with an environment promoting Frizzled activation. Nuclear β-catenin is also seen in HPCs in mice exposed to the DDC diet (Hu *et al.*, 2007), with target gene activation confirmed in

these cells using a reporter transgenic mouse line (Hu *et al.*, 2007). In the same model when β-catenin is knocked out in a mature HPC/hepatocyte population a reduction in HPCs ($A6^+$) is seen in the DDC diet (Apte *et al.*, 2007). *In vitro* work also supports a pro-proliferative role for Wnt in HPCs (Hu *et al.*, 2007).

The effects of Wnt in the development and behaviour of HCC also supports its role in modulating HPC behaviour. Increased canonical Wnt signalling has been demonstrated in metastatic vs. non-metastatic HCC (Qin *et al.*, 2007) and the tendency of hepatic adenoma to progress to HCC is strongly dependent on their β-catenin status (Bioulac-Sage *et al.*, 2007). None-the-less, mutations of APC are relatively rare in HCC in comparison to their prevalence in intestinal cancer.

HPC fate also appears to be strongly influenced by Wnts. During development the fate decisions of hepatoblast are Wnt dependent (Monga *et al.*, 2003; Nejak-Bowen and Monga, 2008). Similarly Wnt appears to influence hepatocyte phenotype across the lobule in the adult mammal. Here Wnt signalling follows a stable gradient within the hepatic lobule with a reduction in active Wnt signal transduction observed in periportal zone 1 (Burke and Tosh, 2006). The source of Wnt within the normal adult liver is not elucidated but may arise at least in part from endothelia. High Wnt signalling exists in the relative absence of APC in zone 3 while the opposite occurs in zone 1 (low active β-catenin and high APC; Benhamouche *et al.*, 2006). These changes act directly with HNF4α to promote the differences in hepatocytic phenotype observed across the liver lobule (Colletti *et al.*, 2009). HNF4α plays a similar role in promoting a zone 1 hepatocellular phenotype (Stanulovic *et al.*, 2007).

While not directly analogous the increasing use of Wnts, in particular Wnt 3, in the *in vitro* differentiation of pluripotent stem cell populations (both ES and iPS) supports the central role of applied Wnts in promoting hepatocellular differentiation from their precursors (Ober *et al.*, 2006). In these instances the use of Wnts following endodermal differentiation and immediately prior to the generation of hepatocytes implies their

particular role in controlling stem/progenitor cell fate at an analogous stage to that of HPC differentiation (Hay *et al.*, 2008).

Notch

In vertebrates the Notch signalling pathway consists of four Notch receptors (Notch 1-4). These receptors are large multi-domain, single pass, membrane receptors and receive signals from the DSL family of membrane associated ligands. These DSL ligands fall into two distinct classes: Delta and Jagged comprised of 3 and 2 homologues respectively (Artavanis-Tsakonas *et al.*, 1999). During intracellular production the notch receptor is cleaved to form its active isoform in the endoplasmic reticulum by a furin-like convertase (S1 cleavage), and is then trafficked to the cell surface as an inactive receptor (Logeat *et al.*, 1998). Upon ligand binding this functional receptor is cleaved by a membrane bound ADAM-family metalloproteinase (S2 cleavage). This cleavage event permits Notch signalling with the aid of further proteolytic cleavage by γ-secretase (S3) which facilitates subsequent liberation of the cytoplasmic domain of Notch receptor (N^{icd} domain) from its membrane anchor and allows it to translocate into the nucleus.

Once within the nucleus the N^{icd} domain interacts with RBP-Jκ. As Notch target genes are normally repressed by RBP-Jκ along with a series of co-repressors upon interaction with N^{icd} this transcriptional repressor is converted to a transcriptional activator. This switch from repression to activation facilitates the expression of the Hairy/Enhancer of split (Hes) genes in mammals which themselves regulate further gene transduction (Bray, 2006). One critical function of Notch described to date of Notch in variety of systems is its control of cell differentiation. Using cell-cell contact signalling between Notch and Notch ligand and a process of lateral inhibition cells receiving Notch signalling remain in a dedifferentiated state while promoting the differentiation of their neighbours (Chitnis, 1995).

The HPC marker Dlk1 (also known as Pref-1) is a recently described atypical Notch ligand, which is structurally related to both Notch and Delta but is not involved in the facilitating the classical Notch cleavage events. Instead Dlk-1 can bind via the EGF repeats on both itself and Notch receptor can negatively regulate the normal action of Notch (Bray *et al.*, 2008).

There are multiple lines of evidence suggesting and important role for the Notch signalling pathways in HPC biology. Firstly Notch signalling has been heavily implicated in both the development of the foetal liver and certain conditions which involve aberrant signalling. During development the ductal plate is located between the portal mesenchyme and the hepatic parenchyma as a continuous layer which undergoes focal dilations and gives rise to epithelial bile ducts some of which are incorporated into the portal mesenchyme (Lozier *et al.*, 2008). At this time Delta-like1 (Dlk1) is a known marker of hepatoblasts in the developing liver (Tanimizu *et al.*, 2003). These cells are the developmental corollary of adult HPCs. Indeed Dlk1 is an accepted marker of adult HPCs (Jensen *et al.*, 2004). As these cells express a negative regulator of Notch signalling, it feasible to suggest that these cells are also expressing the Notch receptor and that Notch signalling may play a key role in the differentiation and development of these cells.

Functional evidence for the role of Notch signalling in the developing liver has been shown by a number of means. Firstly over embryonic over-expression of N^{icd} was shown to down regulate hepatocyte differentiation genes and protein suggesting Notch inhibits hepatocellular differentiation from precursor cells (Tanimizu *et al.*, 2004). When cultured in contact with laminin cells upregulate known cholangiocyte markers such as CK7, CK19 and HNF1β implying a synergy between activated Notch and the Integrin signalling pathway in defining cholangiocyte and hepatocyte differentiation (Tanimizu *et al.*, 2004). The link between Notch signalling and hepatic development in the developing liver is mediated by a plethora or liver-enriched transcription factors such as HNF and C/EBP (Tanimizu *et al.*, 2004). Most crucially, a human condition known

as Alagilles syndrome results in the aberrant development of multiple organs including the liver, heart, and eye together with cranio-facial malformations (Kodama *et al.*, 2004). A key hepatic feature of Alagilles is bile duct retardation, with sufferers often requiring a liver transplant as a result of liver failure (Kasahara *et al.*, 2003). Alagilles syndrome results from aberant Notch signalling during development and is classically associated with a mutation in the *jag1* gene, which typically encodes the Notch ligand Jagged1 (Yuan *et al.* 2006). Multiple mutations in this gene are implicated in an altered transcript which fails to function as the WT (wild type) protein. It is this haplo-insufficiency which results in attenuated Jagged1 activation of Notch (McCright *et al.*, 2002). There are multiple cases of Alagilles patients who have normal Jagged1 but who phenotypically appear to suffer from Alagilles. Current lines of study are also focusing on the presence of mutations in the Notch receptor. In a mouse model of Alagilles, mutations or heterozygous knock outs of *jag1* do not result in the typical hepatic and cardiac deficiencies commonly associated with Alagilles (McDaniell *et al.*, 2006). It is only when a hypomorphic allele of Notch (in this case N2) is introduced that the typical Alagilles phenotype is observed, suggesting that Alagilles is a heterogeneous disorder of the Notch signalling pathway.

Gene knockout studies in mice have also revealed the importance of Notch signalling in both development and adult liver homeostasis. Conditional knockouts of Notch1 and/or 2 and Jagged 1 have been investigated when Cre is expressed under an Albumin (*Alb*) promoter (Geisler *et al.*, 2008; Loomes *et al.*, 2007). These studies imply that certain Notch homologues are required for correct hepatobiliary specification. Conditional Notch2 resulted in delayed and impaired development of the biliary network with cells rarely forming any organised tubular structures. Notch 1 appears to play a less crucial role (Loomes *et al.*, 2007). In keeping with a key role of Notch 2 in differentiation, knocking out its ligand Jagged 1, results in marked bile duct proliferation in the adult (Geisler *et al.*, 2008). In the context of hepatocyte mediated regeneration, changes in Notch signalling have been described in the adult mammal. In a partial hepatectomy model of liver injury and regeneration in the rat, Jagged levels increase

dramatically in the early period following resection (Kohler *et al.*, 2004). During this time, and in spite of reduced expression of Notch 1 there is a considerable increase in nuclear N^{icd}. Interesting in the early phase of regeneration the Jagged 1 target, Notch 2, is upregulated in periportal hepatocytes where early proliferation is known to occur (Michalopoulos and DeFrances, 1997).

Hedgehog

Hedgehog (Hh) signalling is recognised as a fundamental pathway in regulation and patterning in embryogenesis. More recently the description of Hedgehog's involvement in the remodeling of adult tissues following injury in combination with its activation in HPC has highlighted its potential in affecting HPC mediated liver regeneration (Sicklick *et al.*, 2006). Liver injury may induce Sonic Hedgehog ligand and several downstream targets such as patched (Jung *et al.*, 2008). To my knowledge no detailed functional studies have been performed examining the effects of Hh manipulation on adult HPC biology either in *in vitro* or *in vivo*, however work with foetal hepatoblasts suggests that Hh acts to maintain an undifferentiated phenotype of hepatocyte precursors (Hirose *et al.*, 2009).

Hippo

Hippo has been described as a key factor in control of the specification of organ and tissue size during development in Drosophila. Its mammalian homologues Mst1 and Mst2 have more recently been identified in controlling liver size during both development and regeneration. In addition to developing HCC (Zhou *et al.*, 2009) when Mst1 and Mst2 are deleted under an albumin-Cre promoter system, large scale HPC activation is observed (Lu *et al.*, 2009; Song *et al.*, 2009).

Thyroid hormones

The thyroid hormone tri-iodothyronine (T3) is a known mitogen for hepatocytes which has been used experimentally for a number of years, both alone (Forbes *et al.*, 1998) or in combination with other mitogens (e.g. HGF) with which it acts synergistically (Forbes *et al.*, 2000). HPC express T3 receptors and following PH/AAF model show enhanced incorporation of BrdU (Laszlo *et al.*, 2008) following T3 administration. Additionally BrdU pulse-chase in this model has suggested that laminin encased HPCs become small hepatocytes with hepatocellular function, therefore implying a role for T3 in promoting differentiation of this transit amplifying population.

Neural input

Fewer intermediate hepatobiliary cells are seen in liver transplant graft livers which develop recurrent disease than matched liver biopsies taken from untransplanted patients. This provocative observation lead to hypothesis that denervation as result of transplantation directly affects the HPC response. Expression of both adrenoreceptors and muscarinic receptors corresponding to the sympathetic and parasympathetic nervous system respectively has been described by HPCs. Inhibition of the sympathetic or parasympathetic nervous systems in rodents results in expansion or contraction of the HPC response respectively (Cassiman *et al.*, 2002; Oben *et al.*, 2003). The mechanism of action of neurotransmitters upon HPCs, together with a demonstration that neurons make direct functional contract with these cells are questions that remain to be answered.

Extracellular matrix

Laminins

Laminins are a family of ECM proteins, composed of 3 different polypeptide chains, termed α, β and γ (Aumailley *et al.*, 2005). At present, 5α, 4β and 3γ chains are described in mouse and human (Miner and Yurchenco, 2004), which can combine to

form at least 15 different trimers. Expression of different laminins varies between organs and at different stages of development (Yurchenco *et al.*, 2004). Each laminin trimer contains binding sites for several receptors, which are predominantly but not exclusively integrins (Yurchenco *et al.*, 2004).

The integrin receptor is a heterodimer, composed of α and β subunits. 18α and 8β chains have been described in mammals, forming at least 21 different dimers. Integrins that bind laminin include $\alpha_1\beta_1$, $\alpha_2\beta_1$, $\alpha_3\beta_1$, $\alpha_6\beta_1$ and $\alpha_6\beta_4$. Non-integrin laminin-binding receptors also exist and include syndecan, dystroglycan and lutheran.

Laminin is associated with the stem cell niche in other organs (Lathia *et al.*, 2007; Schlotzer-Schrehardt *et al.*, 2007) and is present within the liver in contact with HPCs (Dudas *et al.*, 2006; Paku *et al.*, 2001). Stem cells in other systems have been described to express many integrins particular the $\alpha_6\beta_1$ integrin (Nagato *et al.*, 2005; Tate *et al.*, 2004), blockade of which disrupts stem cell behaviour (Shen *et al.*, 2008). Work in hepatocytes suggests that integrin linked kinases play a key role in regulating liver regeneration (Apte *et al.*, 2009). In human liver disease, increases in laminin and integrins have been noted consistently across a variety of disease states (Volpes *et al.*, 1991) with corresponding changes observed in both HCC and cholangiocarcinoma (Volpes *et al.*, 1993). When integrin linked kinase function is lost, dysregulation of liver regeneration is observed, with ongoing regeneration resulting in excessive liver growth. Increased expression of hepatic $\alpha_6\beta_2$ integrin has been observed concurrently with HPC activation in the DDC diet along with laminin and ICAM1 a further integrin ligand (Wu *et al.*, 2005).

Fibronectin

Fibronectin is a heterodimeric extracellular matrix glycoprotein which also binds to cells via integrins. In addition to integrins, fibronectin also binds extracellular matrix components such as collagen, fibrin and heparin sulfate proteoglycans (e.g. syndecans).

While produced from a single gene alternative mRNA splicing leads to the creation of several isoforms which may be either soluble or insoluble. Insoluble fibronectin is a major component of the extracellular matrix and is secreted by a variety of cells including fibroblasts and myofibroblasts. Fibronectin plays a major role in cell adhesion, growth, migration and differentiation, and is important for processes such as wound healing and embryonic development. Within the liver, fibronectin localises to HPCs during regeneration (Zhang *et al.*, 2009). During embryogenesis fibronectin in an *in vitro* system appears to promote the differentiation of hepatocyte precursors into functional hepatocytes (Sanchez *et al.*, 2000), implying that fibronectin may also promote hepatocellular differentiation of HPCs in the adult liver.

1.33 The role of bone marrow in liver regeneration

Hepatic parenchymal regeneration by the BM

Over the last decade it has become apparent that HPCs express a variety of markers such as c-kit and sca-1 that have been previously thought of as haematopoietic (Petersen *et al.*, 2003), see Table 1.1. Furthermore BM derived stem cells could be shown to differentiate into hepatocyte-like cells *in vitro* (Yamada *et al.*, 2006; Yamazaki *et al.*, 2003). When hepatocytes were identified that expressed extrahepatic markers in both rodent (Petersen *et al.*, 1999) and human liver (Alison *et al.*, 2000; Theise *et al.*, 2000) the exciting possibility that BM derived cells were transdifferentiating into hepatocytes was raised. Examination using Y chromosome tracking in human liver specimens from either female patients with previous BM transplant from male donors, or male patients who had received a liver transplant from female donors, demonstrated that a number (varying from 0-40% depending upon the study) of hepatocytes possessed a Y chromosome (Thorgeirsson and Grisham, 2006). The implication was, therefore, that BM derived cells were crossing lineage boundaries via transdifferentiation to form hepatocytes. This was investigated in detail in rodents included the $FAH^{-/-}$ mouse. This

murine system is a model for human hereditary type I tyrosinaemia in which the hepatic injury may be inhibited at will by the administration of a protective chemical (NTBC). NTBC prevents hepatotoxicity by blocking the formation of fumarylacetoacetate. When $FAH^{-/-}$ mice were given BM and the protection of NTBC was gradually withdrawn, hepatocytes expressing markers of the transplanted BM were seen to reconstitute the mouse liver (Lagasse *et al.*, 2000). Subsequent work however has convincingly shown that instead of plasticity, monocyte-hepatocyte fusion was the mechanism by which BM cells were rescuing a genetically deficient phenotype in the $FAH^{-/-}$ mice (Alvarez-Dolado *et al.*, 2003; Camargo *et al.*, 2004; Vassilopoulos *et al.*, 2003; Wang *et al.*, 2003b; Willenbring *et al.*, 2004). These monocyte-hepatocyte fusion events are rare, but rescue in the $FAH^{-/-}$ model is due to proliferation of these fusion cells (Wang *et al.*, 2002). This occurs as selective pressure is applied against native hepatocytes lacking the correcting wild-type genes. In the absence of such selective pressure however, significant hepatocytes replacement is rarely seen and at most occurs at a level far below that of native hepatocytes turnover (Thorgeirsson and Grisham, 2006; Yannaki *et al.*, 2005). Despite initial reports that HPCs may be in part BM derived (Petersen *et al.*, 1999), more recent studies suggest that this does not occur to any significant degree (Menthena *et al.*, 2004; Vig *et al.*, 2006; Wang *et al.*, 2003a). HPCs from BM transplanted mice neither express the BM tracking marker to any significant degree nor show clustering suggestive of expansion of BM derived HPCs. Importantly transplantation of an HPC fraction into the $FAH^{-/-}$ mouse in one study showed that transplantable cells were not BM derived (Wang *et al.*, 2003a). There is some ongoing uncertainty in this area however as a recent report suggests that HPCs may be BM derived (Oh *et al.*, 2007). This study investigated $DPPIV^{+}$ cells after DPPIV deficient rats were transplanted with wild type BM. AAF/PH was used in these animals to induce an HPC response and resulted in $DPPIV^{+}$ cells within the liver. DPPIV is however not a specific hepatocyte marker and is expressed by sinusoidal endothelia (Koivisto *et al.*, 2001) and T lymphocytes (Vivier *et al.*, 1991).

Similar questions regarding the origin of HPCs have also been raised. The majority of work in this field is consistent demonstrating that HPCs defined by a variety of markers and in a variety of models are not BM derived (Wang *et al.*, 2003a; Kubota *et al.*, 2008; Tonkin *et al.*, 2008; Vig *et al.*, 2006). Alternatively a report, in other another less commonly used HPCs model (again using DPPIV mismatch), has suggested that HPCs may be BM derived (Oh *et al.*, 2007). While this seems unlikely, a compelling recent study in the rat using whole liver transplantation suggests that HPCs may be BM derived under certain circumstances (Sun *et al.*, 2009). While liver transplantation is well tolerated in this circumstance, it may well be that the presence of a minor histocompatability mismatch between donor and recipient in this model drives the selection of donor derived HPCs. Whether the source of HPCs in this case may be out with the BM transplantable population remains a distinct possibility. Nonetheless it seems that in the absence of selection, the BM does not generate HPCs to a physiologically relevant degree.

The role of extrahepatic stem cells activation during liver disease

Over the last decade the importance of BM stem cell (BMSC) activation during liver disease has become apparent. $CD34^+$ and $CD133^+$ cells appear to be upregulated following liver transplantation or PH in the diseased liver (De Silvestro *et al.*, 2004; Gehling *et al.*, 2005; Lemoli *et al.*, 2006). Similarly cells with haematopoietic stem cell markers are mobilised following liver injury in rodents (Fujii *et al.*, 2002) and in this context are recruited to the liver (Kollet *et al.*, 2003). There has been considerable interest in the possibility that the BM contributes to liver parenchymal and non-parenchymal cells. Furthermore current data points towards a role in modulating hepatic fibrosis in addition to the control of HPC behaviour outlined above.

1.34 HPCs and cancer

An important consideration regarding the activation of stem cells during liver disease relates to their potential role in carcinogenesis (Alison *et al.*, 2008). The chronic activation of hepatic progenitor cells occurs at a time when liver cancer develops. Inhibition of the rodent HPC response during long term CDE diet was associated with a reduction in the incidence of cancerous lesions (Knight *et al.*, 2000). The occurrence of mixed forms of liver cancer with features of both hepatocellular carcinoma and cholangiocarcinoma is consistent with a bipotential HPC origin (Alison, 2005; Roskams, 2006). Furthermore, a proof of concept study, has demonstrated that inhibition of HPCs via the c-Kit receptor not only reduces HPC expansion but inhibits the formation of HCC in the chronic CDE diet model (Knight *et al.*, 2008). Clearly these observations not only link HPC to carcinogenesis but also have implications for the use of HPC directed therapies in the development of HCC.

1.4 The liver stem/progenitor cell niche

1.41 Introduction to the stem cell niche

Whilst there has been a large amount of work published on the molecular signals which may influence the behaviour of HPCs, much less is known regarding the cellular source of such signals. While some of the signalling environment sampled by HPC may have originated from distant cells either within or out-with the liver. Some of the signals discussed to date take the form of direct cell-cell signalling necessitating cellular contact. It is probably the case that the major proportion of the paracrine signalling milieu provided to HPCs is produced locally.

Such a local environment is in keeping with the concept of a stem cell niche. A stem cell niche is the restricted compartment in a tissue that maintains and regulates stem cell behaviour, supporting self-renewal and maintaining the balance between quiescence, proliferation and differentiation required in response to injury (Fuchs *et al.*, 2004; Ohlstein *et al.*, 2004; Spradling *et al.*, 2001). Stem cells niches have now been

described in all of most studied stem cell systems (Voog and Jones, 2010). A highly provocative study recently demonstrates that stem cell niches not only provide the environment for adult tissue stem cells but can also integrate circulating signals, including the age of organism, to influence stem cells contained within the niche (Mayack *et al.*, 2010).

If such a niche exists in the liver for hepatic stem cells and HPCs remarkably little is known regarding its composition and function. Early work in the description of HPCs suggested that certain cell populations (mesenchymal desmin^{+} cells) and matrix proteins (laminin) are found in close proximity to HPCs (Paku *et al.*, 2001). Recently work in the field suggest HPCs exist in the context of a particular environment, both spatially (Sawitza *et al.*, 2009; Yovchev *et al.*, 2009) and temporally (Van Hul *et al.*, 2009). However, the consistency of this environment between the various models studied and whether or not the presence of such a milieu imposes any functional significance upon HPC behaviour remains a key question. Clearly until hepatic stem cells themselves can be specifically identified then the existence and nature of the hepatic stem cell niche will remain elusive.

An important observation from the work in the intestinal stem cell field that single intestinal stem cells may be cultured into distinctive three dimensional organoids suggests that stem cells do not require a specialised niche; at least not in the form of living cells (Sato *et al.*, 2009). These findings are consistent with the ability of iPS or ES cells to be differentiated into hepatocyte-like cells in cell free media (Hay *et al.*, 2008; Si-Tayeb *et al.*, 2010; Sullivan *et al., 2010*). While there is no absolute requirement in this system for a cellular niche, albeit in the context of a specialised matrix and growth factor rich environment, this does not mean that the niche does not play a crucial physiological role in influencing both stem cells and the transit amplifying compartment.

1.42 Cellular candidates in the HPC niche

Mesenchyme

While approximately 80% of the liver mass is comprised of parenchymal epithelial cells, a number of other non-parenchymal cell types play a variety of key physiological roles within the liver. Of these the most frequently referred to are Kupffer cells (KCs), sinusoidal endothelial cells (SEC) and hepatic stellate cells.

Mesenchyme appears to play an important role in hepatic development. While as previously discussed mesenchyme is not essential for stem cell differentiation, mesenchyme has the ability affect stem cell behaviour. For example liver mesenchyme imposes an hepatic cord phenotype on epithelial lung buds, which may also be instructed to form not only bronchial epithelia, but also gastric glands in the presence of stomach mesenchyme or intestinal villus epithelia by intestinal mesenchyme (Birchmeier and Birchmeier, 1993). The main mesenchymal element of the adult liver is comprised of hepatic stellate cells, and their activated counterparts myofibroblasts. These cells are central in the deposition and remodelling of collagen and other components of the ECM (Henderson and Iredale, 2007). Studies in rodent models using labeled BM transplantation (Baba *et al.*, 2004; Russo *et al.*, 2006) or human studies following sex mismatched liver or BM transplants (Forbes *et al.*, 2004) have shown a significant BM contribution to both hepatic stellate cell and myofibroblast populations, and this process does not appear to occur through cell fusion. Other studies using the BDL model have reported that only a small proportion (5-10%) of collagen producing cells were BM derived (Kisseleva *et al.*, 2006). In addition to their effects on the ECM, hepatic stellate cells and myofibroblasts may produce a number of secreted and cell surface bound signals including Wnts (Zeng *et al.*, 2007), Notch (Kordes *et al.*, 2009; Oakley *et al.*, 2003), HGF, IL6, TNF and TGFβ (Friedman, 2008).

Kupffer cells/Macrophages

Originally described by von Kupffer in 1876, Kupffer cells (KCs) constitute approximately 80% of the tissue macrophages in the reticuloendothelial system and approximately 15% of the total liver cell population (Bouwens *et al.*, 1986). They are mainly found in the periportal area of the lobule (approximately 45%), but exist throughout the hepatic lobule. Despite the view that KCs are fixed tissue macrophages of the liver, there is good evidence that they have the ability to migrate along sinusoidal walls with a mean speed of approximately 5 microns/minute. Transplantation studies suggest that KCs are mostly, if not all, BM derived (Paradis *et al.*,1989; Abe *et al.*, 2003; Higashiyama *et al.*, 2007), although a significant proportion may be capable of limited intra-hepatic self renewal (Naito *et al.*, 2004; Klein *et al.*, 2007). Perhaps as a feature of this transition between circulating precursor macrophages and tissue resident KCs a precise definition of each population is somewhat arbitrary. In the rat cell surface markers ED1 and ED2 (CD163) are associated with monocytes and resident tissue macrophage respectively (Bilzer *et al.*, 2006). For the purposes of clarity and given the continuum between monocytes and Kupffer cells this population will for brevity's sake be dealt with as a whole under the title macrophages for the remainder of this work (unless otherwise stated).

Macrophages are implicated in a variety of processes during hepatic disease including inflammation, regeneration, fibrosis, and ECM remodeling (Henderson and Iredale, 2007; Martinez *et al.*, 2009; Boulton *et al.*, 1998; Fausto *et al.*, 2006). Administration of Gadolinium Chloride, which inhibits macrophages, prevents MPK-positive HPC expansion in response to BDL in rats (Olynyk *et al.*, 1998). This is consistent with the intimate spatial relationship between Kupffer cells and HPCs (Yin *et al.*, 1999). Similarly Gadolinium Chloride treatment is also able to reduce fibrosis in thioacetamide treated rats (Ide *et al.*, 2005) consistent with the putative role of macrophages in the process of hepatic fibrosis and ECM remodeling. This role has been corroborated using an inducible, macrophage specific depletion model (DTR) in mice during or following

CCl_4 injury. This work demonstrated that both the generation and resolution of fibrosis are macrophage dependent (Duffield *et al.*, 2005). The mechanism of tissue remodeling may include expression of the matrix remodeling metalloproteinase MMP-9 by BM derived F4/80$^+$ macrophages during the resolution of fibrosis following CCl_4 injury (Fallowfield *et al.*, 2007; Higashiyama *et al.*, 2007).

Macrophages (and related populations) have recently been described to play a role in the influence of stem cells in other organs. It appears that macrophages in the intestine (Pull *et al.*, 2005; Seno *et al.*, 2009), mammary gland (Gyorki *et al.*, 2009) and osteoclasts in the BM (Kiel and Morrison, 2008) play roles in their respective stem cell niches, while evidence against a role for macrophages comes from an alternative model of macrophage deficiency in the skin (Martin *et al.*, 2003). Experimentally, alternatively activated macrophages are thought to be particularly important in such roles (Stappenbeck and Miyoshi, 2009) with a recent report suggesting that M2 macrophages are critical in the regenerative response in skeletal muscle (Ruffell *et al*., 2009).

Other leukocyte populations, in particular T cells and NK cells, appear to play a role in HPC biology. Work using mice with a variety of leukocyte population deficiencies, has demonstrated impaired expansion of the HPC population in response to the CDE diet (Strick-Marchand *et al.*, 2008). Lymphocytes (both CD4+ and CD8+) localise in proximity to HPCs, possibly in direct contact, however whether such cells act directly via the production of stimulatory cytokines or cell-cell signalling or whether they act indirectly via other niche cells remains to be elucidated.

Vascular endothelium

A final cellular population which is an attractive candidate as a constituent of the HPC niche is the vascular endothelium. These cells are known to be involved in other stem

cell niches (Kiel and Morrison, 2008). The vascular endothelium is involved in liver organogenesis (Matsumoto *et al.*, 2001).

1.5 Functions of BM derived stem cells during human liver disease

As all of the candidates of the HPC niche discussed above may be BM derived (Paradis *et al.*,1989; Miyata *et al.*, 2007; Russo *et al.*, 2006; Gao *et al.*, 2001), it is important to assess the role the BM is known to have on liver regeneration aside from its contribution the regenerating epithelial cells directly. To date a handful of clinical trials have investigated the role of stem cell mobilisation therapy or stem cell infusion in adults. G-CSF (Granulocyte colony stimulating factor) has been used to induce haematopoietic stem cell mobilisation to the peripheral blood of patients with cirrhosis (Gaia *et al.*, 2006). Although the mobilisation of $CD34^+$ and $CD133^+$ cells was observed, only 2 of 8 patients showed moderate improvement in liver function. Clearly further studies are warranted investigating the effects of G-CSF upon cellular mobilisation and hepatic engraftment during human liver disease to investigate this potential therapeutic modality.

In addition to mobilisation strategies, autologous BM has been examined in a number of studies (Houlihan and Newsome, 2008). These studies include a cohort of patients with liver cancer in whom portal vein embolisation was used to induce compensatory hypertrophy in the contralateral liver lobe prior to surgical resection. Thirteen patients underwent portal vein embolisation, six of whom received an infusion of autologous $CD133^+$ Bone Marrow Cells (BMCs). This non randomised trial demonstrated a marginal but significant increase in liver volume and reduced time to surgery in patients receiving autologous BMC infusions (Furst *et al.*, 2007). Another uncontrolled study in five patients with cirrhosis investigated the effects of autologous $CD34^+$ BMCs. Three of these patients showed transient improvements in biochemical markers, such as bilirubin and albumin, over the following 2 months (Gordon *et al.*, 2006). A case report

describes clinical improvement following infusion of autologous G-CSF mobilised $CD34^+$ BMCs in a single patient with hepatic failure (Gasbarrini *et al.*, 2006). Autologous monocyte therapy has also been attempted using a larger number of unsorted cells extracted from the BM of cirrhotic patients. In the nine patients receiving BMCs there was an improvement in Child-Pugh score with an increase in intrahepatic cell proliferation in the patients biopsied after treatment (Terai *et al.*, 2006). Despite these encouraging reports caution must be noted. Only one of these trials was used controls, and in none were patients randomised. These studies were, understandably for preliminary reports, performed in a small number of patients. Engraftment or colonisation of infused cells was not investigated in any of the studies, nor has the mechanism by which an improvement in liver function is derived been examined in detail.

Should therapeutic manipulation of HPCs be achievable it may provide a mechanism to promote regeneration of the severely damaged liver without recourse to liver transplantation (Alison *et al.*, 2009). Although HPC transplantation studies in rodents HPCs have provided some success (Schmelzer *et al.*, 2007; Wang *et al.*, 2003a), the isolation of human HPCs is currently not a practical therapeutic option, particularly on an individual patient basis. Furthermore this therapeutic strategy offers little advantage over mature hepatocyte transplantation. Therefore the manipulation a patient's own endogenous HPCs currently represents both a more realistic approach and, crucially, one likely to yield more immediate success (Knight *et al.*, 2008; Spahr *et al.*, 2008).

The recent studies using intravenous delivery of whole (BMCs) in patients with liver injury have suggested various possible beneficial effects, including improved liver function and regeneration (Houlihan and Newsome, 2008). BMC therapy is clinically attractive from several perspectives. Firstly, BM is accessible via a minimally invasive procedure and provides an autologous source of cells with associated immunological advantages. Furthermore, the donor BMC population may be expanded and manipulated *in vitro*, either through culture, selection, or modification, to potentially enrich for

beneficial characteristics of these cells. A large body of evidence shows that BMCs do track to the liver and will engraft without exogenous manipulation, and do not themselves form hepatic parenchyma as discussed previously. The effects of BMC on hepatic regeneration therefore may be via paracrine signalling to indigenous liver cell populations. If a greater understanding of the mechanism by which BMCs are able to influence liver regeneration can be achieved, it may be possible to manipulate these processes to enable effective regenerative therapy.

1.6 Hypotheses and Aims

The hypotheses for this work were that

- HPCs are surrounded by a stereotypical and functional niche consisting of macrophages and myofibroblasts

- Extrahepatic, bone marrow derived cells, are recruited into this niche and influence HPC behaviour

To test these hypotheses I aimed

- To study the characteristics of the HPC niche by analysing candidate cell populations and extracellular matrix in a variety of animal models in analogy to human disease.

- To investigate the role of recruitment of cells into the HPC niche during liver injury

- To study whether any of these niche cell populations may functionally influence HPC behaviour

- To explore the possibility of using niche manipulation as a form of regenerative therapy

Chapter 2: Methods

2.1 In vivo experimental models

Animals were housed in a specific pathogen free environment and kept under standard conditions with a 12-hour day/night cycle and access to food and water *ad libitum.* All animal experiments were carried out under procedural guidelines and with ethical permission from the Home Office (UK).

2.11 HPC models

In order analyse the hepatic progenitor cell response and its niche, comparison was made across a number of model systems and in different species. In order to assess tracking BM derived cells or to measure the effects of cellular depletion during HPC activation the models below were combined with cellular manipulation strategies outlined later. Furthermore in order to label or track proliferating cells in such models BrdU (Cell Proliferation Labeling Reagent, Amersham UK; delivered at 50µg/g) or EdU (Invitrogen, UK, delivered at 50µg/g) were administered by intraperitoneal (i.p.) injection.

2.11A Mouse models

The CDE dietary model

The Choline Deficient Ethionine supplemented (CDE) dietary protocol used C57Bl/6 mice which were fed a diet composed of powdered choline deficient chow (MP biomed) with sweetened water containing 0.15% (working concentration) DL-ethionine (Sigma, UK) unless otherwise stated. Water was sweetened with orange squash (Robinsons) in a

1:5 ratio with ethionine supplemented water. A modified version of the CDE diet, called the 50% CDE diet, was used in BM transplantation studies to reduce mouse morbidity. The 50% CDE diet contained choline deficient chow (MP biomed) mixed in a 1:1 ratio with normal powdered chow supplemented with DL-ethionine at 0.15% in sweetened water.

The DDC dietary model

A further dietary model using Diethyl 1,4-dihydro-2,4,6-trimethyl-3,5-pyridinedicarboxylate (DDC) to induce a liver injury was also utilised. DDC (Sigma, UK, 0.1% w:w) was added to normal chow (DBM Scotland) and fed *ad libitum* to 8 week old, initially C57Bl/6 and latterly S129S2 mice. Mice had access to normal drinking water and were assessed daily.

HBsAg Retrorsine model

Twenty-six–week old female mice, transgenic for the hepatitis B surface antigen (HBsAg) were used. These mice have hepatocyte specific expression of the HBV BgIII-A fragment and develop hepatocellular injury. To induce HPC proliferation animals were treated with the pyrolizidine alkaloid, retrorsine, (70mg/kg i.p, Sigma-Aldrich, UK) with a further injection 2 weeks later. Liver tissue was analysed 6 months later. Liver from age matched C57/B6 animals was used as control. Blocks of animal tissue were kindly provided by Dr Pamela Vig.

AhCre MDM2^{flox}

6-8 week old AhCre^{+} MDM2$^{flox/flox}$ mice were used along with AhCre^{-} MDM2$^{flox/flox}$ and AhCre^{+} MDM2$^{flox/+}$ littermates as controls and performed in collaboration with Professor Owen Sansom (Beatson Institute, Glasgow). Induction of genetic deletion used the intraperitoneal injection of β-Napthoflavone at 40-80mg/kg. β-Napthoflavone

was prepared previously under sterile conditions at 1% (w:v) in corn oil. $AhCre^{+}$ $MDM2^{flox/-}$ work was performed in collaboration with Professor Alan Clarke and Trevor Hay (School of Biosciences, Cardiff). $MDM2^{flox}$ and $MDM2^{-}$ mice were generously provided by Professor Gigi Lozano, Department of Cancer Genetics, University of Texas.

2.11B Rat AAF/PH model

Male Fischer rats weighing 200g were treated with 2-acetylaminofluorene and subsequent partial hepatectomy (2-AAF/PH model) as previously described (Vig *et al.*, 2006). Livers were analysed from 3 to 13 days after PH. Livers from normal rats were used as controls.

2.11C Human tissue

Human tissue was provided by the pathology department Edinburgh Royal Infirmary with informed patient consent and under the approval of the local ethical committee. The human tissue analysed belonged to one of the following categories: 1. control liver tissue obtained from a pre-perfusion liver biopsy (n=1); 2. hepatitis C virus (HCV) related chronic hepatitis (n=10); 3. hepatitis B virus (HBV) chronic hepatitis (n=10); 3. biopsies performed from 0-6 months after liver transplant in a patient who received a liver transplant for hepatitis C and developed recurrent fibrosing cholestatic hepatitis post-transplant (n=1).

2.12 Cell manipulation models

2.12A Bone Marrow Transplantation

To enable BM tracking, 6 week old female mice were irradiated with whole-body gamma irradiation (10.5 Gray) followed by i.v. injection with $1x10^{7}$ BM cells extracted

from 6 week old male femurs. Mice were allowed to reconstitute for 6 weeks and then started the 50% CDE diet for 2 weeks prior to tissue analysis. Mice were treated for one week prior to and for 4 weeks following BM transplantation with Baytril antibiotics (W&J Dunlopes Ltd. Veterinary Wholesalers).

When BM transplantation was combined with the CDE dietary model of HPC activation modifications were made to the CDE diet. These modifications were made due to increased morbidity observed upon use of the 100% choline deficient diet and 0.15% ethionine which were observed in the context of excessive growth of incisors in BM transplanted recipients. This incisor growth limited the ability of experimental animals to eat even normal chow and resulted in weight loss. As a result significant concern was raised when a trial of CDE diet was used in these mice resulting in further significant weight loss and morbidity. As a result a modified 50% CDE diet where choline deficient chow was delivered as a mashed diet to recipients. Such a diet has been used by other groups in the past as a successful means of HPC induction (Akhurst *et al.*, 2001). In keeping with this, I observed HPC induction in this diet, albeit to a lesser extent than the full CDE diet used in other models this study (see Figure 4.3).

Whilst other reports of similar lethal irradiation followed by BM transplantation have not observed or reported the side effects observed in this study (Tonkin *et al.*, 2008; Vig *et al.*, 2006) multiple reports of dose dependent irradiation induced incisor injury have been previously reported (Coady *et al.*, 1967; Larsen *et al.*, 2006; Pearson and Phelps, 1981; Upton *et al.*, 1956). None-the-less previous studies have used lower irradiation doses (e.g. 8G in divided doses in Balb/c mice) to achieve BM reconstitution (Russo *et al.*, 2006) and therefore if further studies were to be performed in mice the efficacy of reconstitution in C57Bl/6 mice with lower doses of irradiation should be assessed.

2.12B Bone Marrow Transfer

BMC transfer

Male and female C56Bl/6 mice, 6 weeks of age, were purchased from Harlan (UK), female Fn14$^{-/-}$ (Jakubowski *et al.*, 2005) and female TgTP6.3 tauGFP (MacKay *et al.*, 2005) and respective female wild type littermates were from internal colonies. Fn14$^{-/-}$ work was performed in collaboration with Owen Sansom (Beatson Institute, Glasgow) and were generously provided by Biogen Idec. In addition to genotyping GFP protein expression was assessed in skin and BM of GFP^{+} animals (Figure 2.1). Donor BMCs were extracted from the femurs and tibias of mice with PBS and a single cell suspension prepared by passing the cells through a 21-guage needle prior to a 40μm filter (BD Falcon), after which the cells were pooled and centrifuged at 400g for 5 minutes, washed with PBS, and resuspended in PBS for injection at 5x10^{7} cells/ml following quantification using Turks medium in a haemocytometer. Healthy female recipient mice received 1x10^{7} BMC via tail vein injection. Prior to injection recipient mice had no intervention such as irradiation. For irradiated cell controls, cells were exposed to 30 gray from a GammaCell 40E (MDS Nordian, Fleuvus, Belgium) with a Caesium 137 source. BrdU (50μg/g w/w: Cell proliferation reagent, Amersham UK) was administered by i.p. injection as stated in figure legends.

Figure 2.1 Assessment of GFP protein expression in skin and bone marrow

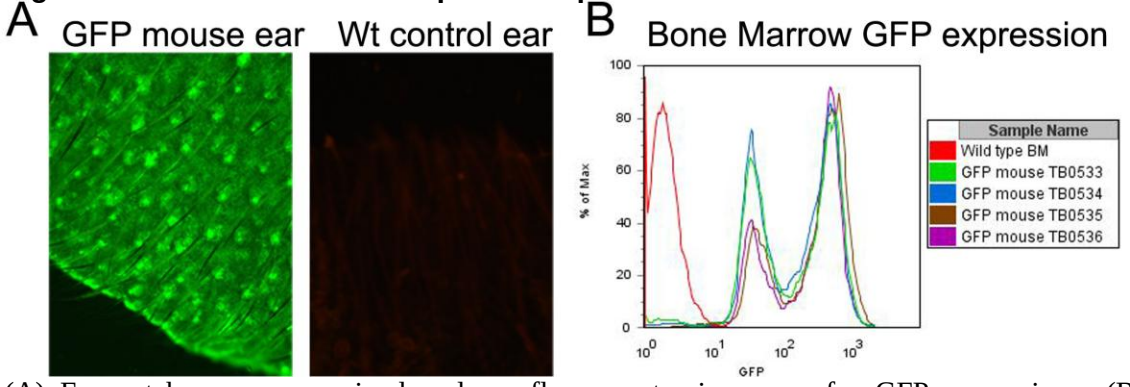

(A) Ear notches were examined under a fluorescent microscope for GFP expression. (B) Histogram of extracted BMCs from 4 representative animals was assessed by flow cytometry for GFP expression (>99% GFP^{+} in each sample vs. 0% in Wt control).

Macrophage transfer

Pure F4/80^{+} macrophage cultures were generated from BMC *in vitro* as described (Macrophage Differentiation). Following filtering through a 40µm filter they were injected via tail vein into healthy recipient mice. For irradiated macrophage controls, cells were exposed to 30 gray irradiation prior to injection as previously described. Purity of culture was assessed by immunocytochemistry and was routinely >99% (Figure 2.2)

2.12C Myofibroblast depletion

Gliotoxin myofibroblast depletion

The fungal toxin gliotoxin was used as previously described (Douglass *et al.*, 2008a; Plumpe *et al.*, 2000) to deplete/inhibit myofibroblasts *in vivo* in combination with HPC induction models. Briefly gliotoxin (Sigma) was dissolved to 2mg/ml in DMSO. A working solution was then produced by dissolving DMSO in sterile PBS to a final gliotoxin concentration of 60µg/ml. Mice undergoing the CDE diet were then administered 0.6µg/g gliotoxin by i.p. injection every 72 hours. Control animals received vehicle control of DMSO in PBS.

C13-G myofibroblast depletion

C13-G (Douglass *et al.*, 2008a; Douglass *et al.*, 2008b) was generously provided by Dr Matthew Wright, Newcastle University, UK and was administered at 0.04 mg/g body weight (from a 1 mg/ml PBS stock) by *i.p.* injection after 9 days of CDE diet. Mice were analysed 3 days subsequently alongside mice receiving vehicle control.

2.12D Macrophage depletion

Liposomal Clodronate

Clodronate Liposomes were kindly supplied by Nico van Rooijen [nvanrooijen@clodronateliposomes.org] (Van Rooijen *et al.*, 1990; Van Rooijen and Sanders, 1996). Clodronate Liposomes were shaken and warmed to room temperature before 200µl was injected via tail vein injection. Volume matched PBS Liposomes and PBS injections were used as controls.

DTR transgenic mouse depletion model

An independent model of macrophage depletion was also trialed for use in depleting hepatic macrophages as previously described (Duffield *et al.*, 2005). Briefly 8 weeks old DTR mice and wild type littermates were tail bled prior to administration of 5-20ng Diptheria Toxin by i.p. injection. Mice were killed by CO_2 inhalation and peripheral blood and liver analysis performed.

2.13 Hepatocellular mitogen administration

Whilst capable of acting individually, HGF (Takayama *et al.*, 1996) and T3 (Tri-iodothyrodine; Forbes *et al.*, 1998) have been described to play a synergistic role as hepatocellular mitogens in rodents (Forbes *et al.*, 2000). Sterile hrHGF (R and D technologies) was dissolved in sterile PBS at 0.05µg/µl and stored at -20°C. HGF (250µg/kg) was administered via tail vein injection. T3 (Sigma) was dissolved in solution (0.01M NaOH, 0.9M NaCl) at 0.4mg/ml. This solution was then neutralised with 2M HCl to just prior to T3 precipitation and stored at -20°C. T3 was administered at 4mg/kg to mice via subcutaneous (s.c.) injection.

2.14 Tissue harvesting and preparation

Mice were killed by CO_2 inhalation or cervical dislocation. Unless livers were perfused, blood was harvested by cardiac puncture. Organs were harvested and stored following fixation in 10% formalin (in PBS) for 6 hours or methacarn (60% methanol 30% chloroform 10% glacial acetic acid) for 24 hours prior to embedding in paraffin blocks. Samples of liver were taken and snap frozen in an ethanol bath in dry ice in OCT media, RNAlater or directly for later analysis.

2.2 In vitro work

2.21 HPC and NPC purification

Mice were euthanised using CO_2 for 5 minutes. The livers were excised and minced in Leibovitz-15 medium containing Collagenase B and DNase I for 45 minutes at 37°C. Digested liver was passed through a 40µm cell strainer and spun at 50xG for 5 minutes. Supernatant was removed to a clean tube and the 50xG spin was repeated twice more. The final supernatant was spun for 10 minutes at 120xG. This cell pellet was resuspended in Ammonium Chloride red cell lysis buffer (160mM NH_4Cl 10mM $KHCO_3$ containing 0.01% EDTA) on ice for 5 minutes. Erythrocyte depleted cells were then pelleted and resuspended in HPC medium (50% Dulbecco's Modified Eagles Medium 50% Hams-F12 Nutrient Mix, 10% FCS, Insulin, Hydrocortisone, Sodium Pyruvate Gentamicin). Resuspended cells were underlaid with a discontinuous layers of 20% and then 50% percoll (Sigma), diluted in PBS. Cells were then spun at 1400xG for 20 minutes at 4°C.

Cells were collected from the 20%/50% percoll interface and washed twice using culture medium. The resulting cells were sorted either by FACS or using magnetic beads. For magnetic bead purifications, cells were first pelleted by centrifuging at 120xG for 5 minutes and resuspended with CD45R iMag magnetic beads (BD

Biosciences), which were incubated for 20 minutes at 4°C. Bead labelled cells were removed using an iMag magnet for 15 minutes at room temperature. CD45 depleted cells were resuspended in culture medium containing 10% FCS. These cells were plated at $5x10^4$ cm^2 on tissue culture plastic which had been incubated with laminin for 2 hours at 37°C. Non-adherent cells were washed off 12 hours after initial plating with PBS and fed with medium containing 10% FCS for 48 hours after which the amount of FCS was reduced to 5% for the remainder of time in culture to remove endothelial contamination. Typically HPCs were cultured for 7-14 days to remove contaminating hepatocytes and endothelia. HPC differentiation into hepatocytes was induced by transfer to a differentiation media of Williams E with 5% FCS, 50ng/ml EGF, 2% matrigel, 1% Pen/Strep for 5 days.

2.22 Culture of the BMOL Progenitor Line

Cryopreserved BMOL (Tirnitz-Parker *et al.*, 2007) cells were resuscitated into BMOL culture media (Williams E Medium containing 5% Foetal Bovine Serum, 2mM L-Glutamine, 2.5µg/ml Fungizone, 10U/ml Penicillin; 100µg/ml Streptomycin, 30ng/ml IGF2, 20ng/ml EGF and 10µg/ml insulin). These cells were grown until 70% confluency and were then trypsinised and either passaged or replated for use.

2.23 Hepatocyte purification

Animals were sacrificed by CO_2 inhalation and their livers digested *in situ* using a modified retrograde perfusion technique (Tirnitz-Parker *et al.*, 2007) consisting of: 1) Liver Perfusion Medium (Gibco) for 5 minutes; 2) Liver Digest Medium (Gibco) for 10 minutes. The liver was then excised and the capsule disrupted to yield a cell suspension which was collected in Liver perfusion medium (Gibco) and passed through a 50µm filter (BD Bioscences). Hepatocytes were pelleted by centrifugation at 135xG for 1 minute followed by resuspension in Williams Medium. The cell suspension was then

purified as described previously (Goncalves *et al.*, 2007). Briefly cells were underlayered with 1.06, 1.08 and 1.12g/ml Percoll in PBS. The 1.08mg/ml layer was spiked with phenol red to aid visualisation. Cells were then spun at 750xG for 20 minutes at 20°C without the brake. The cell layer collected between the 1.08 and 1.12mg/ml percoll layers was harvested, and resuspended in Williams Medium. This suspension was then purified a further 2 times using percoll layers as previously described. Finally cells were quantified using a haemocytometer and prepared for cytospins and future DNA, RNA and protein analysis via resuspension in TriSOL reagent (Invitrogen).

2.24 Macrophage differentiation

Macrophage differentiation was performed using $2x10^7$ isolated BMC cultured for 7 days in Teflon pots (Roland Vetter Labs) in DMEM containing penicillin and streptomycin, 10% FCS and 20% L929 media as previously described (Boltz-Nitulescu *et al.*, 1987). Purity was assessed by F4/80 immunocytochemical analysis and was consistently >99% (Figure 2.2).

Figure 2.2 Typical efficiency of macrophage differentiation

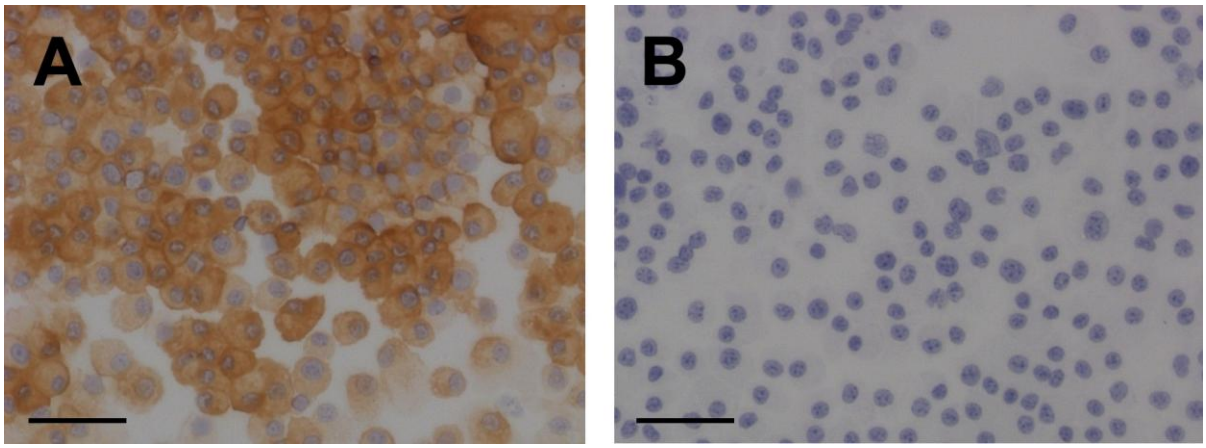

Immunocytochemistry for the F4/80 antigen performed on cytospin of cells following macrophage differentiation. (A) shows typical expression of F4/80 by all cells, (B) isotype control. Scale bar denotes 50μm.

2.25 Bone marrow colony culture in nitrocellulose

To assess the colony forming capacity and nature of Haematopoietic Stem Cells a whole BMC was cultured in a methylcellulose based medium containing rmSCF, rmIL3, rhIL6, and rhEpo (Methocult® M3434, Stem Cell Technologies) according to manufacturer's instructions. Briefly between $3x10^5$ and $1.25x10^6$ BMC extracted as previously described from mouse femurs were added to 1.5ml Methocult® media and cultured for 7 days at 37°C. Colonies were identified depending on morphology and counted and the number of discrete colonies per culture. Results were normalised to input cell number.

2.3 Tissue and cellular analysis

2.31 Immunohistochemistry and immunocytochemistry

Paraffin embedded sections (3μm thick), were dewaxed in xylene for 10 minutes at room temperature and sequentially rehydrated through sequential ethanols (100%, 75%, 60%) for 5 minutes each, and then finally rehydrated in water for 10 minutes. Antigen retrieval where required was performed, see Table 2.2. Sections were then washed in PBS containing 0.05% Tween 20 for 5 minutes. All further washes were performed using PBS alone. Endogenous peroxidase activity was blocked by incubating in 1% H_2O_2 for 10 minutes. Sections were then washed and mounted in Sequenza racks using PBS. Endogenous avadin and biotin were blocked using an avadin and biotin blocking kit (DAKO) for 15 minutes each; sections were thoroughly washed between blocks. Non-specific binding of the secondary antibody was prevented using 20% species specific serum to block sections for 30 minutes at room temperature. Sections were then incubated with primary antibody diluted in 20% species specific serum for 1 hour or

overnight at 4°C. Prior to incubating with secondary antibody for 30 minutes, sections were washed with PBSx3. If required, following a further 3 PBS washes a tertiary reagent was added. For DAB development this consisted of incubation for 30 minutes with Vector RTU following which after a further 3 PBS washes visualisation used DAB chromagen (DAKO) for 3-5 minutes. Development was stopped by washing with PBS. Subsequently slides were counterstained with Harris Haematoxylin by 10 seconds of immersion in Haematoxylin followed by 10 seconds in Scotts Tap Water. Following dehydration through graduated ethanols slides were washed with Xylene and mounted using Portex hard set mounting medium and stored in the dark at room temperature. For immunohistochemistry using fluorescent detection slides were mounted in DAPI containing Vectashield mountant (Vector, UK) to aid identification of cell nuceli; or where DAPI was not required, Aqueous mountant (DAKO).

Table 2.1 Antibodies and antigen retrieval used

Antibody list						
	Antigen	**Source Species**	**Supplier**	**Ref no.**	**Dilution**	**Antigen retrieval**
HPC markers	panCK	Rabbit	DAKO	Z0622	1:300	5mins * 5mins ***
	Dlk1	Rabbit	Abcam	Ab21682	1:150	5mins *
	EpCAM	Rabbit	Abcam	Ab32392	1:200	10mins *
	Cytokeratin 7	Mouse	DAKO	M7018	1:200	5mins *
Proliferation	BrdU	Rat	Abcam	Ab6326	1:100	10mins *
	BrdU	Mouse	Exalpha	X1028	1:200	10mins *
	Ki67	Rabbit	Novocastra	301112	1:500	10mins *
	MCM2	Rabbit	Cell Signalling Tech	#4007	1:300	5mins*
Hepatocyte markers	CYP2D6	Sheep	Prof R Wolfe		1:400	10mins *
	CYP1A2	Mouse	Prof R Wolfe		1:200	10mins *
	CYP2C	Rabbit	Prof R Wolfe		1:200	10mins *
	HNF4a	Rabbit	Santa Cruz	SC8987	1:100	5mins * 5mins ***
	Asialoglycoprotein	Rabbit				
Other cell populations	αSMA	Mouse	Sigma	A6228	1:6000	10mins *
	CD45	Rat	R and D systems	MAB114	1:100	10mins **
	CD11c	Rat	Serotec	MCA1369GA	1:100	15mins *****
	CD11b	Hamster	Serotec	MCA711G	1:100	15mins *****
	F4/80	Rat	Abcam	AB6640	1:200	Nil
	vWF	Rabbit	DAKO	A0082	1:50	15mins *
Other antigens	Laminin	Rabbit	DAKO	Z0097	1:50	10mins * 5mins ***
	Caspase 3	Rabbit	Abcam	Ab13847	1:50	10mins *
	Notch1		Abcam	Ab27526		
	Numb		Abcam			
	p53	Mouse	Lab Vision	MS-104 - P1	1:25	10mins **
	p21	Rabbit	Santa Cruz	BMK-2202	1:500	20mins *
	anti Rabbit biotinylated	Swine	DAKO	E0353	1:200	NA
	anti Rabbit HRP	Swine	DAKO	P0399	1:200	NA
	anti Rat biotinylated	Rabbit	DAKO	E0468	1:200	NA
	anti Sheep Alexa 350	Donkey	Invitrogen	A21097	1:200	NA
	anti Rabbit Alexa 488	Goat	Invitrogen	A11008	1:200	NA
	anti Rabbit Alexa 488	Donkey	Invitrogen	A21206	1:200	NA
	anti Rat Alexa 488	Donkey	Invitrogen	A21208	1:200	NA
	Alexa 488	strepatividin	Invitrogen	S32354	1:200	NA
	anti Rat Alexa 546	Goat	Invitrogen	A11081	1:200	NA
	anti Hamster 546	Goat	Invitrogen	A21111	1:200	NA
	anti Rabbit Alexa 555	Goat	Invitrogen	A21425	1:200	NA
	Alexa 555	strepatividin	Invitrogen	S32355	1:200	NA
	anti Sheep Alexa 650	Donkey	Invitrogen	A21448	1:200	NA

* Microwave at 800W in 0.1M NaCitrate pH6.0
** Heated under pressure in Borg decloaker RTU solution
*** Proteinase K 0.0125% (w/v) in PBS
**** Microwave at 800W in 0.1M EDTA
***** Paraformaldehyde 4%

For frozen sections liver tissue was excised and mounted in OCT fixative. These samples were embedded in OCT and frozen in an 100% ethanol bath on dry ice. Samples were stored at -80°C. Frozen sections were cut at 10µm thickness. Cytospins were prepared by spinning 1000-5000 cells at 300rpm for 3 minutes onto superfrost plus

slides using a Cytospin2 centrifuge (Shandon) prior to fixing for 5 minutes in methanol followed by air drying overnight and storing at -20°C. Cytospins and frozen sections were initially rehydrated in PBS followed by processing for immunocyto/histochemistry as outlined in Table 2.1.

Where dual staining involving multiple primary antibodies from the same source species, tyramide deposition was used to amplify an antibody signal prior to stripping of the antibody complexes. In these cases an HRP conjugated secondary antibody was introduced instead of a biotinylated secondary for 30 minutes. Sections were incubated with Cy5 or Flourescin conjugated tyramide for 10 minutes. Antibody complexes were then stripped by boiling in 0.01M NaCitrate for 3 minutes followed by resting for 30 minutes prior to repeat staining with further antibodies. Appropriate no primary, and isotype controls were performed to ensure no cross reactivity between antibody complexes.

2.32 β-Galactosidase detection

Lac-Z staining was performed on 10μm thick frozen sections which were initially fixed for 5 minutes (0.5M NaH_2PO_4, 0.5M Na_2HPO_4, 25% (w/v) gluteraldehyde, 100mM EGTA (pH 7.3), 1M $MgCl_2$) followed by 3x5 minute washes in wash solution (0.5M NaH_2PO_4, 0.5M Na_2HPO_4 1M $MgCl_2$). Sections were then incubated at 37°C overnight in X-gal staining solution (0.5M NaH_2PO_4, 0.5M Na_2HPO_4, 25mg/ml X-gal in dimethyl formamide, potassium ferrocyanide, potassium ferricyanide, 1% (w/v) deoxycholate, 2% (v/v) nonidet-P40, 1M $MgCl_2$). Slides were then rinsed in wash buffer and allowed to stand in wash buffer for a further 6 hours at 4°C. Sections were then counterstained with Eosin prior to dehydration using graded ethanols and mounting with pertex hard set media.

2.33 EdU detection

Following initial antigen detection, using standard immunohistochemistry and directly fluorophore conjugated secondary antibody, slides were washed in PBS with 0.5% Triton X for 20 minutes and a further 3x5 minute PBS washes. Slides were then removed from sequenza racks and prior to placing in a dark box, the sections were outlined using a hydrophobic pen. 100µl of fixative buffer was then added. 5 minutes later a further 100µl of reaction cocktail was added (1 vial of alexa labelled click-it reagent, 200µl of 1x reaction buffer, 200µl of reaction buffer additive, and 600µl of 13.3mM $CuSO_4$ (8mM final concentration) and left for 30 minutes for detection. Sections were then washed 3 times in PBS before mounting with DAPI containing mountant (Vector, UK).

2.34 FISH

Donor derived cells in sex mismatched (male to female) transfer experiments were confirmed by FISH for the Y chromosome (STARFISH 1189-YMF; Cambio, UK) according to the manufacturer's instructions. Briefly immunohistochemistry was performed followed by detection using 1:200 Streptavidin-AP and VectorRed (Vector UK) following manufacturers instructions. Following IHC, sections were washed in PBS and incubated in 1M sodium thiocyanate in distilled water for 10 minutes at 80°C, then washed in PBS, and digested in 0.4% w/v pepsin in 0.1M HCl at 37ºC for 5 minutes, followed by quenching in 0.2% glycine in double 2x PBS for 2 minutes. Samples were post-fixed in 4% paraformaldehyde for 2 minutes, and then dehydrated through graded alcohols before air drying. A FITC-labeled Y chromosome paint (Star-FISH, Cambio® no. 1189-YMF) was added to sections, sealed under a glass cover slip, denatured at 60°C for 10 minutes before overnight incubation in a 37°C water bath. Slides were then washed in formamide (50%w/v)/2x saline sodium citrate (SSC) at 37°C, then washed with 2x SSC, then washed with 4x SSC/Tween-20 (0.05% w/v) at

37°C. The slides were rinsed in 0.5x SSC at 37°C, then PBS before mounting with DAPI containing mounting media (Vector Labs®, UK).

2.35 TUNEL

Apoptosis was assessed using the DeadEnd™ Colorimetric or Fluorometric (Alexa 488) TUNEL System (Promega #TB199) according to manufacturer's instructions. Briefly formalin fixed tissue sections were deparaffinised in xylene and rehydrated through graded alcohols before washing in 0.85% NaCl for 5 minutes. They were then washed 3 times in PBS before fixing in 10% buffered formalin for 15 minutes. Following a PBS wash sections were digested for 5 minutes in 20µg/ml Proteinase K prior to 3 further PBS washes before further fixation in 10% buffered formalin for 5 minutes. Slides were washed prior to the addition of equilibration buffer for 10 minutes. Biotinylated Nucleotide mix containing rTdT Enzyme and biotinylated nucleotides was prepared and added to the sections followed by incubating at 37°C for 60 minutes to allow nucleotide incorporation to 3'-OH DNA ends. Slides were washed with 2xSSC for 15 minutes and then PBS prior to peroxidase blocking with 1% H_2O_2. After further PBS washes development used Streptavidin-HRP and DAB following which slides were counterstained with Harris Haematoxylin and mounted using pertex mounting media. Positive control slides used DNase1 treatment (7units DNaseI in 100ml 40mM Tris HCl (pH 7.9), 10mM NaCl, 6mM $MgCl_2$, 10mM $CaCl_2$). Negative controls were performed using a biotinylated nucleotide mix without rTdT enzyme.

2.36 FACS

Analysis and sorting was performed using a FACSVantage, equipped with a Coherent INNOVA Enterprise II laser (Becton and Dickinson, Oxford, UK). Propidium Iodide (PI) (Sigma Aldrich, Dorset, UK) was added to the cells prior to sorting at a final concentration of 2µg/ml to distinguish and exclude dead cells in the BM population.

Cells were also immunophenotyped using PE conjugated CD45 (BD Biosciences, Pharmingen, Oxford, UK).

2.37 Cell counting and image analysis

2.37A HPCs

Images were obtained on a Zeiss Axiovert 200 microscope using a Zeiss Axiocam MRc camera. Cell counts were performed on blinded and randomised slides by manually counting panCK positive progenitor cells in 30 consecutive non overlapping fields with liver parenchyma at all boundaries at x200 magnification. Fields were included that contained vascular structures or bile ducts in the field. Small (approximately 10μm) $panCK^+$ cell with oval/cuboidal morphology with high nuclear to cytoplasmic ratio were counted. Cells with hepatocyte like morphology e.g. larger (over 20μm) with low nuclear to cytoplasmic ratio were not counted even if they have weak staining for panCK as they were considered morphologically typical for intermediate hepatocyte-like cells. Interlobular bile ducts, defined as small panCK positive cells directly abutting a lumen, were excluded as previously described (Oben *et al.*, 2003). Results are expressed as mean number of HPCs per high powered field.

Validation of the method of quantification of the HPC compartment is a vital prerequisite to further HPC quantification. Variation in the number of HPCs is noted based on the choice of HPC markers used (panCK, Dlk1, and EpCAM), in addition to variation between liver lobes and between peripheral and hilar regions. Therefore it was necessary to sample a larger area than is used in a number of published studies. It is also vital to assess a number of lobes so that an accurate representation is achieved.

To assess the area of liver that should be assessed a preliminary study was performed in which 120 fields (40 from each of 3 lobes) was performed. Analysis was performed taking the first 10, 15, 20, 25, 30, 35 and 40 fields, which were compared to next group

of an equal number. When this was performed on multiple mice (n=3) it was seen that at least 30 fields are required to be analysed in order to provide a representative sample (Figure 2.3). As a result of such preliminary study a total of 30 fields were chosen to provide a representative sample for quantification.

To validate this method of quantification the intra and inter-observer error was assessed by the counting of a blinded sample twice by the same and different individuals (Figure 2.3).

2.37B Niche myofibroblasts

In order to analyse changes in the myofibroblasts within the HPC niche, quantification of niche myofibroblasts was performed in contrast to whole liver myofibroblasts. Here dual immunohistochemistry for αSMA and panCK was performed using Alexa 555 and Alexa 488 respectively for visualisation. Images of 20 non-overlapping x200 fields containing HPCs were taken from at least 3 lobes. These images were then assessed for the number of αSMA^+ myofibroblasts in direct contact with $panCK^+$ HPCs. Results are expressed as mean number of niche myofibroblasts per field.

2.37C Macrophages

To quantify the number of hepatic $F4/80^+$ macrophages a total of 10 x200 magnification fields were analysed corresponding to >1300 macrophages in non-depleted animals. If <1300 macrophages were seen then a total of 10 fields were counted. Results are expressed as mean number of $F4/80^+$ macrophages per x200 magnification field.

Figure 2.3 Validation of cellular quantification methods

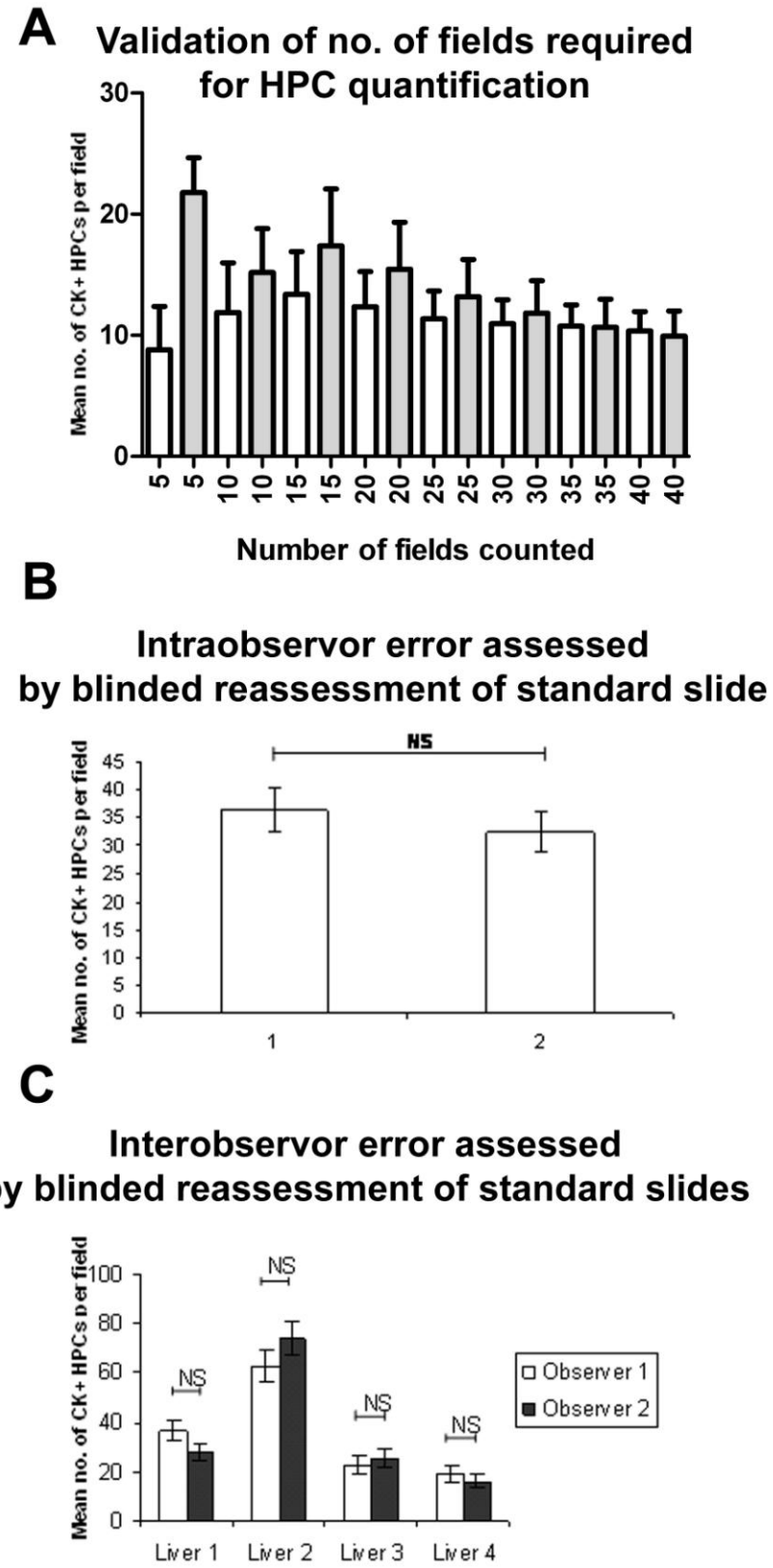

(A) To quantify the number of fields required to accurately assess HPC number following immunohistochemistry a series of field numbers were assessed from two separate and independent counts of separate areas of the liver, 1st and 2nd counts are shown as white and shaded bars respectively. Whilst at lower numbers of fields non-significant changes in results were obtained it is clear that for accurate assessment of cell number counts in excess of 25 fields are required. To assess intraobservor error and interobservor error and series of slides were assessed by either the same observer multiple times or different observers respectively. HPC counts were consistent upon repeated assessment by either the same (B) or different observers (C)). All data is presented as mean±SEM.

2.37D Hepatocytes

While many previous studies have often relied upon a morphological criteria of hepatocytes, in these studies an immunohistochemical definition of hepatocytes has been used. The rationale for this approach is that whilst using counterstained tissue, hepatocytes may be identified (due to their and their nuclei's characteristic shape), when immunofluorescence is used alone large nuclei can often be seen which upon further investigation are clearly not hepatocytes. These cells represent other large cells within the sinusoids (Figure 2.4).

Due to its panlobular distribution, (Figure 2.4), CYP2D6 positivity was used to identify hepatocytes. In order to quantify the status of hepatocytes Image J was used incorporating its cell counter feature and colour channel control. Hepatocytes were counted manually with the independent characteristic channel (eg p53 status) removed. Then once hepatocytes had been identified this latter channel was returned and the hepatocyte status assessed.

2.37E Image analysis

Sections were stained in a single batch with picro-sirius red. At least 22 images were taken at x200 magnification under standardised conditions (up to 40 images were taken, tissue permitting). Images were analysed using Adobe Photoshop choosing a single colour and fuzziness permitting accurate identification of collagen staining. Results are expressed as mean percentage of positive pixels per field.

Figure 2.4 Utility of immunohistochemical identification of hepatocytes by CYP2D6

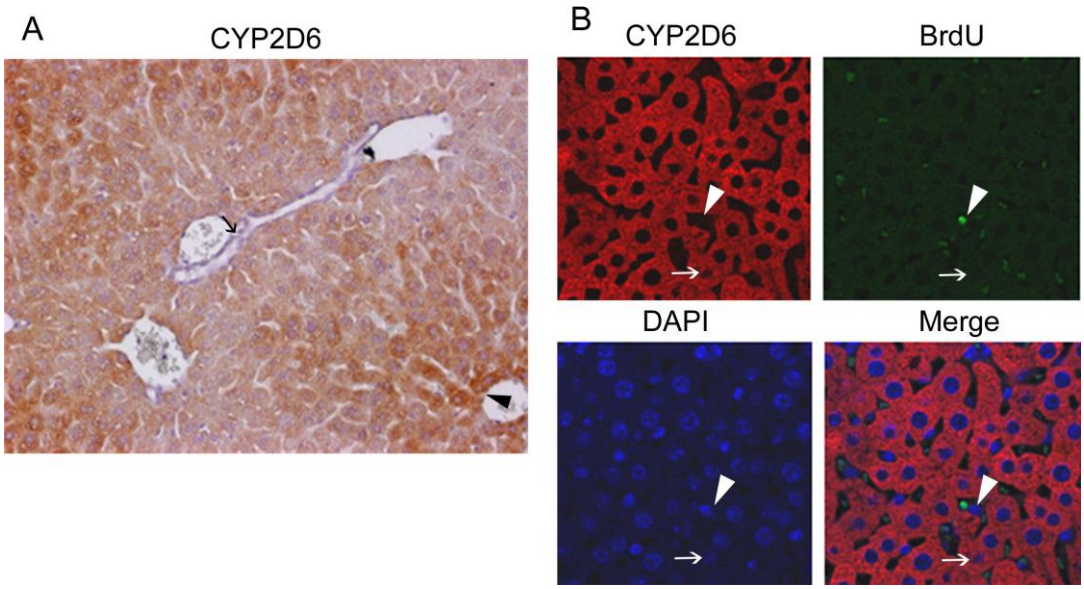

(A) CYP2D6 is expressed throughout the hepatic lobule with expression extending to the central vein (arrowhead) and limiting plate (arrow). The use of cell and nuclear morphology alone (DAPI channel) is helpful for definition of hepatocytes but is greatly added by addition of a specific marker such as CYP2D6. (B) Confocal analysis of DAPI CYP2D6 shows that nuclear morphology may produce false positive (arrowhead) and negative (arrow) identification of hepatocytes.

2.4 Serum Analysis

Blood was collected by cardiac puncture and left overnight at 4°C to clot. The following day blood was centrifuged at 5 minutes at 8,000xG and serum removed. Haemolysed samples were identified visually and excluded from analysis. Specific biochemical analysis was performed as follows:

2.41 Serum Albumin

Mouse or rat serum albumin measurements were determined using a commercial serum albumin kit (Alpha Laboratories Ltd., Eastleigh, UK) adapted for use on a Cobas

Fara centrifugal analyser (Roche Diagnostics Ltd, Welwyn Garden City, UK). The measurement of serum albumin is based on its quantitative binding to bromocresol green (BCG). The albumin-BCG-complex absorbs maximally at 578nm, the absorbance being directly proportional to the concentration in the sample. Within run precision was CV < 2.5% while intra-batch precision was CV < 4%.

2.42 Alanine Aminotransferase

ALT was measured using the method described by Bergmeyer *et al.* (1), utilising a commercial kit (Alpha Laboratories Ltd., Eastleigh, UK) adapted for use on a Cobas Fara centrifugal analyser (Roche Diagnostics Ltd, Welwyn Garden City, UK). Within run precision was CV < 4% while intra-batch precision was CV < 5%. (Bergmeyer *et al.*, 1978)

2.43 Aspartate Aminotransferase

AST was determined by a commercial kit (Randox Laboratories, UK) adapted for use on a Cobas Fara centrifugal analyser (Roche Diagnostics Ltd, Welwyn Garden City, UK). γ-oxogluterate reacts with L-aspartate in the presence of AST to form L-glutamate plus oxaloacetate. The indicator reaction utilises the oxaloacetate for a kinetic determination of NADH consumption. Within run precision was CV < 4% while intra-batch precision was CV < 5%.

2.44 Serum Alkaline Phosphatase

ALP was determined by a commercial kit (Randox Laboratories, UK) adapted for use on a Cobas Fara centrifugal analyser (Roche Diagnostics Ltd, Welwyn Garden City, UK). The substrate p-nitriphenyl phosphate is hydrolysed by ALP from the sample, in the presence of magnesium ions, to form p-nitophenol which is yellow in colour and its

production can be monitored at 405nm. Within run precision was CV < 4% while intra-batch precision was CV < 5%.

2.45 γ-Glutamyltransferase

γGT was determined by a commercial kit (Randox Laboratories, UK) adapted for use on a Cobas Fara centrifugal analyser (Roche Diagnostics Ltd, Welwyn Garden City, UK). The substrate L-γ-glutamyl-3-carboxy-4-nitroanilide, in the presence of glycylglycerine is converted by γGT, in the sample, to 5-amino-2-nitrobenzoate which can be measured at 405nm. Within run precision was CV < 4% while intra-batch precision was CV < 5%.

2.46 Total Bilirubin

Total bilirubin was determined by the acid diazo method described by Pearlman and Lee (Clinical Chemistry 1974; 20:447-453) using a commercial kit (Alpha Laboratories Ltd., Eastleigh, UK) adapted for use on a Cobas Fara centrifugal analyser (Roche Diagnostics Ltd, Welwyn Garden City, UK). In this method a surfactant is used as a solubiliser. Conjugated and solubilised unconjugated bilirubin react with diazotised sulphanilic acid to produce an acid azobilirubin, the absorbance of which is proportional to the concentration of bilirubin in the sample and can be measured at 550nm. Within run precision was CV < 4% while intra-batch precision was CV < 5%.

2.5 DNA and RNA analysis

2.51 DNA preparation

Genomic DNA was extracted from perfused whole liver using DNA Blood Mini Kit (Qiagen UK). DNA resulting from PCR or restriction digests was processed using the Qiagen Gel Extraction Kit according to the manufacturer's instructions. Typically DNA was eluted in 30µl TE buffer.

Genomic DNA from mouse ear notches or tail snips to be used for genotyping only was extracted by incubating the fresh tissue in 100µl of 50mM Tris (pH 8.5) containing 12mM $MgCl_2$ and 50µg proteinase K (Sigma, UK) at 60°C overnight. The following morning samples were vortexed and centrifuged at 8000xG for 10 minutes and the supernatant containing DNA removed to a fresh Eppendorf tube and stored at -20°C.

2.52 RNA extraction and reverse transcription

RNA derived from whole liver was extracted from liver frozen after harvesting in RNAlater (Sigma) according to manufacturer's instructions. 30-50mg liver tissue was then added to 300µl of TRIsol reagent (Invitrogen) in a 1.5ml Eppendorf and mixed thoroughly and homogenised using a pestle. RNA derived from cell populations was processed from up to 10^7 cells which were added to 300µl TRIsol reagent. Once in TRIsol RNA could be stored, or further processed for extraction by adding 60µl of chloroform and the solution centrifuged at 12 000xG for 15 minutes at 4°C. The aqueous phase was removed and the RNA purified using RNAeasy mini columns (Qiagen) according to manufacturer's instructions. RNA was eluted in 30µl ddH_20 and analysed using a nanodrop spectrophotometer (ThermoScientific) for RNA concentration and purity (260/280 and 260/230 ratios). Yield was typically approximately 500ng/µl and purity >2 and >1.8 for 260/280 and 260/230 ratios respectively.

Reverse transcription was performed on 1µg RNA using Qiagen QuantiTect® Reverse Transcription Kit according to manufacturer's instructions, including a DNA degradation

step prior to reverse transcription. No RT, and no RNA template controls were performed as standard.

2.53 qPCR

Real time PCR was performed using either gDNA or cDNA. Real time RT-PCR and melt curve analysis was performed in a ABI Prism 7500 fast cycler using SYBR green detection and Qiagen primers (Table 2.1) and QuantiFast SYBR Green PCR reagents (Qiagen UK). Y chromosome analysis used SRY primers and β-actin control primers (ABI). Generation of standard curves for qPCR: cDNA from each sample was combined and this was diluted 1:10 with RNAse free water. Serial 1:1-4 dilutions were produced giving a final range of concentrations. Samples of cDNA were diluted 1:100 for analysis of gene expression. Data were managed and analysed using the LightCycler® system and Microsoft Excel following normalisation to PPIA mRNA content and a calibrator. All samples were run in triplicate alongside positive murine controls of adult liver, spleen, thymus or E15 liver.

Wnt Pathway focused gene expression profiling was performed using the RT^2 Profiler™ PCR array system (SAB Bioscience; Cat no. PAMM-043A), according to the manufacturer's instructions. Briefly RNA was prepared using a Trizol based extraction and purification as previously followed by further clean-up using RNeasy columns (Qiagen) and elution in 30μl RNase free water. Samples were used only if the A260:280 and A260:230 were >2.0 and 1.8 respectively. Reverse transcription including gDNA elimination was performed from 1.5μg RNA using SuperArray's RT^2 First Strand Kit (SAB Bioscience; Cat no. C-03). cDNA was then stored at -20°C until further use within 1 week. Mouse Wnt Signalling Pathway PCR plates were run on an ABI Prism 7900HT thermal cycler including a melt curve analysis. Data was analysed using software provided by SAB Bioscience.

Table 2.2 Primers used for qRT-PCR

Group	Gene target	Product no.
Notch		
	NUMB	QT00097328
	HES1	QT00268044
	HES5	QT00313537
Cell tracking		
	SRY	QT01038555
Integrins and matrix		
	Integrin b1	QT00155855
	Integrin a6	QT00144354
Cyotkines and mitogens		
	IFNg	QT01038821
	TNF	QT00104006
	TWEAK	QT01743252
	IL6	QT00098875
	HGF	QT00158046
	Lymphotoxin a	QT01046206
	Lymphotoxin b	QT00107443
	Oncostatin M	QT00263193
p53 targets		
	Bax	QT00102536
	p21	QT00137053
	PUMA	QT01657432
	p16	QT00252595
HPC markers		
	CK19	QT00156667
	EpCAM	QT00248276
	Dlk-1	QT00134344
	Fn14	QT00255038
	c-kit	QT00124887
	CK7	QT00173649
	AFP	QT00174020
	M2-PK	QT01763811
	CD133	QT01065162
	CD44	QT00173404
	LGR5	QT00123195
	e-cadherin (cadherin-1)	QT00121163
Other cell markers		
	CSF1-R (macrophage)	QT01055810
	GFAP (myofib)	QT00101143
	CD45 (common leukocyte antigen; ptprc)	QT00139405
	HNF1a	QT00170975
	HNF1b	QT00103320
	C/EBPa	QT00311731
	HNF4a	QT00144739
	HNF6 (OneCut)	QT00297815
	GGT-1	QT00104209
	Albumin	QT00115570
	Transferrin Receptor 1	QT00122745
	Tyrosine Aminotransferase	QT00112833
	CK8	QT01775795
	Asialoglycoprotein	QT00100520
	CYP7A1	QT00121569
	Aquaporin 1	QT00109242
Control		
	PPIA	QT00247707

2.54 Southern blotting

2.54A Probe generation

A 353bp probe from the Murine MDM2 exon 7 was amplified by PCR using in house primers Exon 7 F1 and R1 to amplify a region of murine MDM2 Exon 7 (Table 2.3 and Figures 2.5 and 6.1). The resulting product was excised from a 1% agarose gel and purified using the Qiagen Gel Extraction Kit (Qiagen no 28704) according to manufacturer's instructions. 25ng of DNA was then inserted into the pGEM®-T Easy plasmid at a 2:1 ratio using T4 DNA Ligase (Promega), concurrent positive and negative ligation controls were used. Following overnight ligation at 4°C One Shot® MAX Efficiency® DH5α™ -T1® Competent cells (Invitrogen) were transformed with 10µl of plasmid using Heat Shock at 42°C for 45 seconds following by culture in SOC medium (Invitrogen) for 90 minutes at 37°C. Transformed bacteria were then plated onto LB Agar containing 100µg/ml Ampicillin for overnight incubation at 37°C and resistant colonies selected. Colonies containing the desired 353bp insert were assessed by PCR using primers F1 and R1 and subsequently grown in LB broth for DNA purification using Midi prep columns (Qiagen) according to manufacturer's instructions. DNA was digested using NotI and SacII restriction enzymes (New England Biolabs). The resulting products were separated on a 2% agarose gel and the 353bp bands removed and purified using the Qiagen Gel Extraction Kit. PCR using primers F1 and R1 in addition to DNA sequencing was performed to confirm probe sequence (Figure 2.5).

The probe was labelled with ^{32}P dCTP using Ready to Go™ labelling beads (Amersham) according to manufacturer's instructions. Briefly the probe was initially denatured by boiling for 3 minutes prior to the addition of DNA labelling bead and 5µl of [α-^{32}P] dCTP (3000Ci/mmol) and the final 50µl mixture incubated at 37°C for 15 minutes.

Table 2.3 In house primers used for PCR

No.	Name	Species	Direction	Sequence	Size	Tm	Combines with	Product size
1	LacZ F	Mouse	F	CGGTGATGGTGCTGCGTTGGA	21	68	LacZ R	385
2	LacZ R	Mouse	R	ACCACCGCACGATAGAGATTC	21	66		
3	YFP common	Mouse	F	AAAGTCGCTCTGAGTTGTTAT	21			
4	YFP mutant	Mouse	R	AAGACCGCGAAGAGTTTGTC	20		YFP common	320
5	YFP wild type	Mouse	R	GGAGCGGGAGAAATGGATATG	21		YFP common	600
6	AhC	Mouse	F	CCTGACTAGCATGGCGATAC	20		Cre B	1000
7	Cre A	Mouse	F	TGACCGTACACCAAAATTTG	20		Cre B	1000
8	Cre B	Mouse	R	ATTGCCCCTGTTTCACTATC	20			
9	Gigi F1	Mouse	F	TGTGGAGAAACAGTTACTTC	20	20		
10	Gigi R2	Mouse	R	CTGTGCTCCTTCACAGAG	18		Gigi F1	342/474
11	Gigi R3	Mouse	R	TGAGATGAGTCAAAGCCTGG	20		Gigi F1	2314
12	Mdm Exon 7 F1	Mouse	F	CTTCAGACTCTGGCACATCG	20		Mdm Exon 7	353
13	Mdm Exon 7 R	Mouse	R	AACATTGGCTGTTCCACACC	20			
14	Mdm Exon 7 F2	Mouse	F	CATCGCTGAGTGAGAGCAGA	20		Mdm Exon 7	338
15	Mdm Exon 5	Mouse	F	ACGAGAAGCAGCAGCACATTG	21		Mdm Exon 5 R	113
16	Mdm Exon 5	Mouse	R	TTATAACCCACCACGCACAAGG	22			
17	Mdm Exon 2	Mouse	F	AACCTGGATTATCGCACAGTCG	22		Mdm Exon 2 R	90
18	Mdm Exon 2	Mouse	R	TCGCAGTGACCACTCTCTAATGC	23			

Table 2.4 PCR conditions for in house PCR

Reaction	AC Genotyping AhCre	MF Genotyping Mdm2 flox/wt	Exon 7 Making Southern probe	YFP mut Genotyping R26YFP + alleles	YFP wt Genotyping R26YFP - alleles	BATgal Genotyping BATgal mice	Mdm2 Exon 2 Testing Mdm2 control	Mdm2 Exon 5 Testing Mdm2 flox
Buffer x10	2.5	2.5	2.5	2.5	2.5	2.5	2.5	2.5
dNTPs (10um)	0.4	1	0.2	0.2	0.2	1	1	1
Taq	0.4	0.2	0.2	0.2	0.2	0.2	0.2	0.2
Primer (100uM)	0.05	0.5	0.2	0.24	0.24	0.5	0.5	0.5
MgCl (50mM)	0	0.5	0	0.25	0.25	2	2	1
H2O	18.6	16.8	18.7	18.37	18.37	17.3	15.3	16.3
DNA template (ON Prot K from ear notch)	3	3	3	3	3	1	3	3
Total volume	25	25	25	25	25	25	25	25
Forward primer	AhCre	Gigi1	Mdm Exon 7 F1	YFP common	YFP common	LacZ F	Mdm Exon 2F	Mdm Exon 5F
Reverse primer	Cre B	Gigi2R	Mdm Exon 7 R	YFP mutant	YFP wild type	LacZ R	Mdm Exon 2R	Mdm Exon 5R

2.54B Southern blotting

Whole liver or purified cell population DNA was prepared using DNA Blood Mini Kit (Qiagen UK). 10µg DNA was restricted overnight at 37°C with 50U Pst1 (New England Biolabs) according to manufacturer's instructions. The following morning a further 10U Pst1 was added to ensure complete DNA restriction. The resulting fragments were run for 5 hours on a 1% agarose gel. The gel was then washed in 0.25M HCl for 10 minutes to fragment DNA following by washing for 2x20 minutes in denaturation solution (1.5M NaCl, 0.5M NaOH) and subsequently a further 20 minutes in neutralising solution (1.5M NaCl, 0.5M Tris HCl, 1mM EDTA @ pH 7.2).

Following this the gel was loaded onto 3mm Watman paper wicks above a 20xSSC solution. The gel was covered in positively charged nylon membrane which was previously soaked in 2xSSC. A further layer of Watman paper was placed above this and layers of absorbent tissue; and the stack left overnight to transfer the DNA to the nylon membrane.

Figure 2.5 Generation of southern blot probe for MDM2

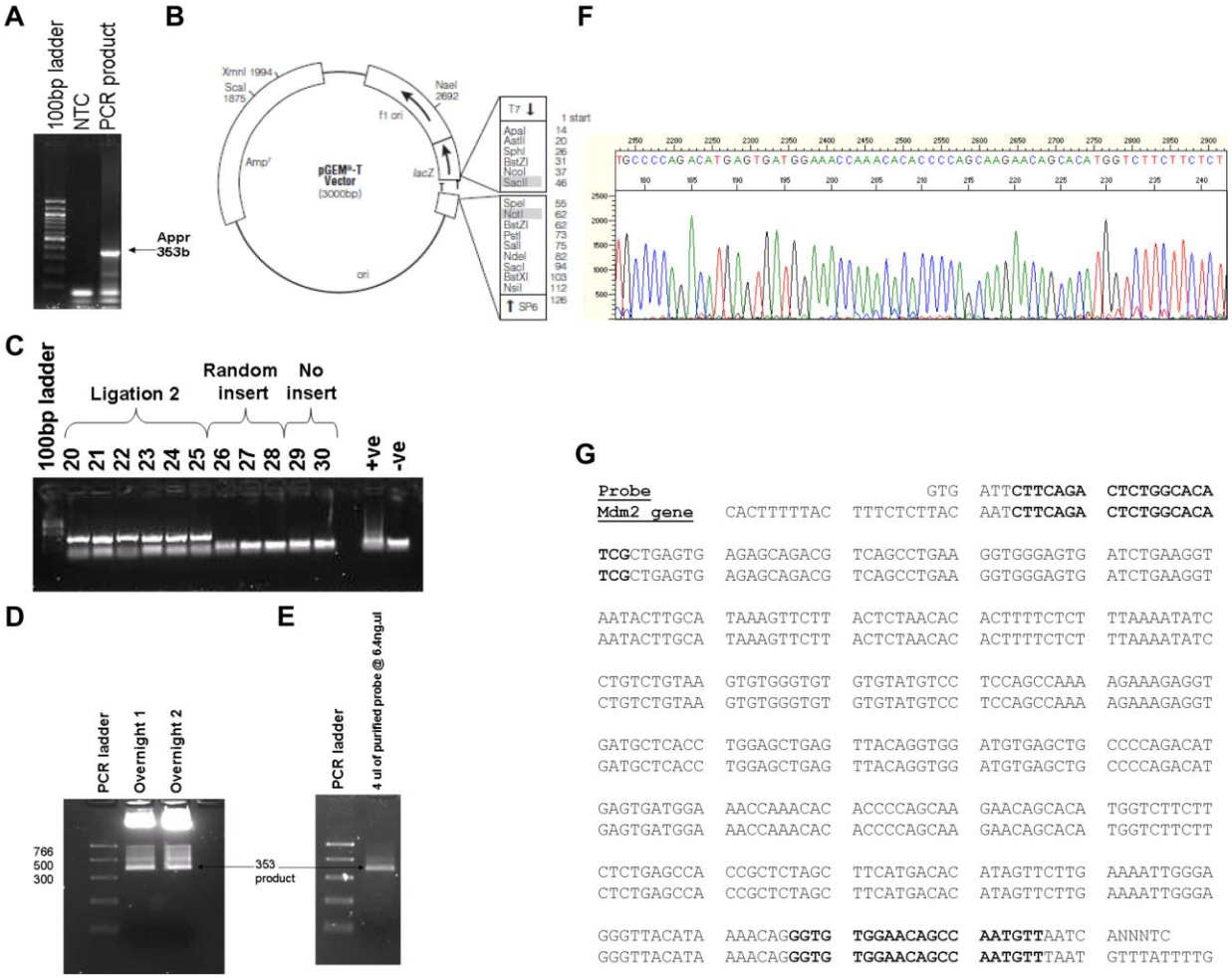

A DNA probe for Southern Blotting was produced by amplifying a segment of Exon 7 of the murine MDM2 gene using primers MDM2 Exon 7F and MDM2 Exon 7R to yield a 353bp fragment (A). This fragment was then inserted into the pGEM®-T Easy vector (B). Colonies were expanded and the presence of the insert tested by PCR (C). A colony containing the specified insert was then used to generate DNA which was restricted using NotIHF and SacII (D). This fragment was then purified by size to yield a final probe of approximately 353bp(E). This probe was sequenced (F) and the sequence compared to known MDM2 exon 7 sequence confirming 100% homology (G) within the probe sequence (G). Primer sites are marked in bold.

The following day the nylon membrane was removed and baked at 80°C for 2 hours prior to hybridisation. The membrane was then incubated for 3 hours at 65°C in 25mls of hybridisation buffer (0.5M phosphate buffer pH7.2, 7% (w/v) SDS, 10mM EDTA) containing 100µl of ssDNA. The labelled probe was then added in hybridisation buffer and left to incubate overnight at 65°C. After washing with wash buffer 1 (20mM Na_2HPO_4 ph7.2, 1mM EDTA, 5% SDS) at 65°C for 15 minutes, the membrane was washed with wash buffer 2 (20mM Na_2HPO_4 ph7.2, 1Mm EDTA, 1% SDS) 3 times for 10 minutes each. The film was then developed for 72 hours using radiographic film.

Stripping membranes prior to rehybridisation was performed using 3x15 minute washes at 65°C in pre-boiled stripping solution (0.2M NaOH, 0.1% (w/v) SDS). Following this the membrane was washed for 15 minutes in 2xSCC before returning to the prehybridisation step above.

2.55 Genotyping

All transgenic mice were genotyped using standard qualitative PCR (Tables 2.3 and 2.4). Genomic DNA was extracted from ear or tail samples as described previously. PCR utilised DNA Taq polymerase (New England Biolabs, UK) with 5x PCR buffer, dNTPs (10µM working concentration: New England Biolabs, UK) and $MgCl_2$ (50µM). PCR products were assessed on a 2% agarose gel in 1xTBE (0.089M Tris Base, 0.089M Boric Acid, 2mM EDTA, pH 8.3), containing Gel Red (Biotium) for visualisation and run for 30 minutes at 80mV. Images were obtained using VersaDoc imaging system. Reactions for genotyping AhCre, MDM2, R26YFP, and BATgal (Figures 2.6A-D respectively).

Figure 2.6 Representative examples of PCR based mouse genotyping

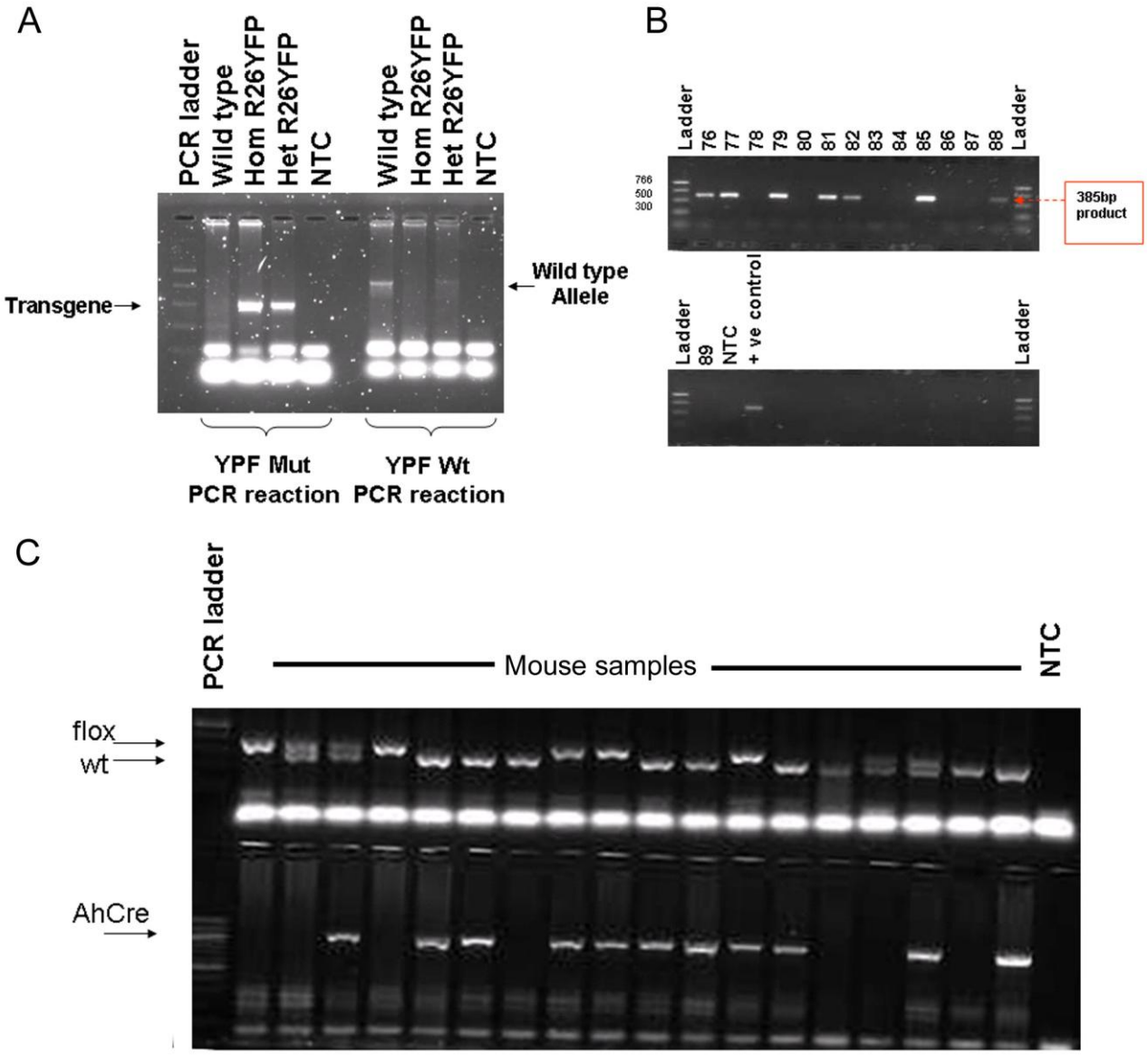

Examples are given for gel electrophoresis of products of PCR based genotyping of R26R-YPF (A), BATgal (B), AhCre and MDM2^{flox} (C) transgene constructs. The transgenic (mut) and wild-type loci for the R26R-YFP gene amplify 320bp and 600bp fragments respectively. The BATgal transgene results in a 385bp product. AhCre results in a 1kp product. The amplification of both wild type and MDM2flox loci may result in detection of heterozygotes by a single primer set amplifying fragments of 342bp and 474bp respectively.

2.56 Sequencing

DNA sequencing was performed using BigDye® Terminator Sequencing Kit (ABI biosystems, UK) and run on an ABI3730 capillary analyser. Briefly, approximately 5ng of template DNA was added to 3.2pmol primer in a final volume of 6µl. Forward and reverse sequence primers were used. Data analysis was performed using Vector NTI Advance 11 software (Invitrogen) following extraction using ABI sequence scanner v1.0.

2.6 Statistics

Prism software (GraphPad Software, Inc) was used for all statistical analysis. Mean HPCs per field from 30 fields for each mouse were compared. For comparison of parametric data sets where previous data had shown a consistent directional trend the one tailed Student's t test was used, otherwise direct comparison used a two tailed Student's t test. Parametric distribution was assessed using D'Agostina and Pearson omnibus testing ($p<0.05$). Comparison between multiple groups was performed using one-way analysis of variance with parametrically distributed data being sub-analysed using Bonferroni testing. Comparison between multiple groups of non-parametrically distributed data was performed using Kruskal-Wallis testing with Dunn analysis performed between individual data points. In all cases *, ** and *** denote $p<0.05$, <0.01, and <0.001 respectively.

Chapter 3: Establishment and characterisation of in HPC induction models

3.1 Hypothesis

- During liver regeneration HPCs are surrounded by a stereotypical niche comprised of a specialised cellular and extracellular environment

3.2 Aims

- To develop, optimise and characterise HPC activation and their surrounding environment in an in-house murine model of HPC activation

- To compare HPC activation and its associated niche in multiple models of HPC activation in rodent and humans

3.3 HPCs in healthy mice

Prior to commencing work on HPC induction, it is important to appreciate HPCs in the uninjured liver. Examination of healthy livers from C75/Bl6 mice revealed that in young mice there is very little evidence of HPC activation with portal tracts containing usually one and occasionally more intralobular bile ducts (Figure 3.1A). Occasional HPCs were seen infiltrating away from the intralobular bile ducts and into the adjacent hepatic parenchyma. When mice of varying ages was examined a striking increase in HPCs was observed in elderly mice beginning at approximately 4-6 months of age and increasing dramatically over the subsequent 12 months (Figure 3.1B). In light of these observations all subsequent work was carried out with contemporaneous age matched controls unless otherwise stated.

Figure 3.1 HPCs in healthy liver with varying age

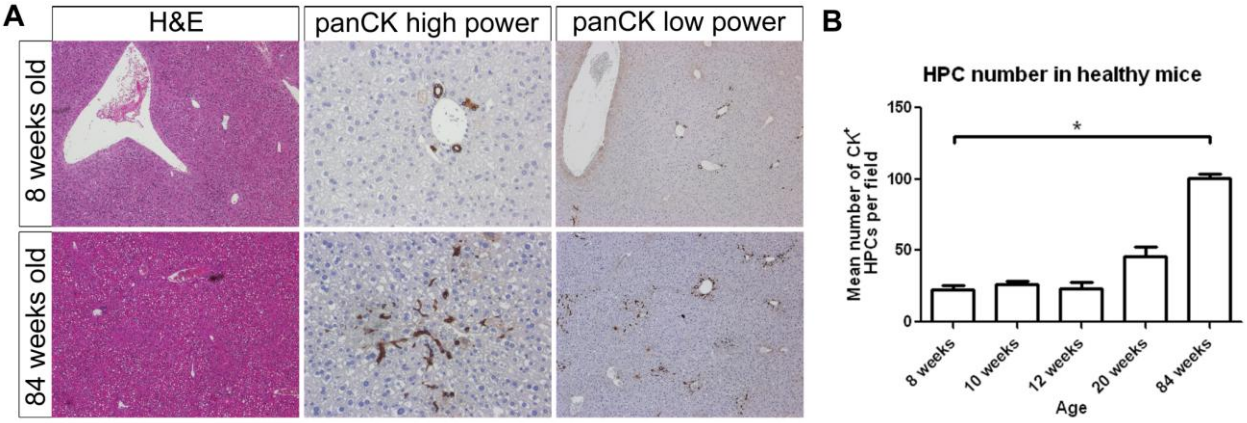

Comparison between healthy C57Bl/6 mice of 8 weeks ranging to 84 weeks demonstrates a progressive expansion of HPC both morphologically (A) and when quantified (B). *p<0.05 by T test.

3.4 The CDE dietary model of HPC activation

3.41 Trial using 100% choline deficiency and 0.165% ethionine resulted in excess morbidity and mortality.

Following on from multiple previous reports using the CDE diet with 100% choline deficient diet and 0.165% ethionine in water, age and sex matched mice C57Bl6 mice were initially trialed with this CDE diet. From as early as 36 hours after commencing the diet significant weight loss was observed, together with other associated adverse clinical effects including hunching, social withdrawal and piloerection. Two days after diet initiation, mortality was first noted despite careful monitoring. With ongoing monitoring a careful regime of humane euthanasia was instituted when morbidity was excessive. This resulted in either the death or culling of the entire cohort by day 6 (Figure 3.2A). Variation in weight loss was noted within the group with some mice undergoing dramatic (>20%) weight loss in as little as 2 days, while others lost virtually no weight (Figure 3.2B). Microscopic analysis of the mice revealed, even as early as 6 days, extensive liver injury along with expansion of HPCs (Figure 3.2C-E).

Additionally the development of an HPC-associated, panCK$^-$ non-parenchymal cell 'niche' became apparent (Figure 3.2C).

3.42 Optimisation of the CDE

In order to create a diet which, in my hands, resulted in the required HPC activation and expansion without the adverse side effects a series of diets were tested in male C57Bl6 mice of >6 weeks age. Initially, the effects of ethionine alone were tested at 0.075% and 0.15% in combination with water which was sweetened with orange juice. No adverse effects were noted either by clinical status or weight loss in either group (Figure 3.3A). Histological analysis demonstrated no changes in portal areas compatible with HPC activation (Figure 3.3B).

Following this, a preparation of a choline sparse diet was prepared and used in combination with ethionine administration. When given either 0.12% or 0.15% ethionine alongside the choline sparse diet, mice did not lose weight (Figure 3.3C), nor was any significant panCK$^+$ HPC activation observed (Figure 3.3D and E respectively).

Using fully choline deficient chow, either in combination with 0.15% or 0.165% ethionine in 8 week old male C57Bl6 mice, weight loss was once again observed (Figure 3.3F). This time in the older mice there was no spontaneous mortality in either group, however 2/12 in the 0.165% group required euthanasia on clinical grounds between days 2 and 7. In contrast to mice treated with CDE diet initially (with 0.165% ethionine), mice in these groups were not only 2 weeks older at diet initiation but also were maintained on sweetened water throughout the diet. Sweetening the water improves mouse fluid intake of water alone, but also appears prevent the reduction of intake seen upon addition of ethionine to the drinking water (Figure 3.3H).

Figure 3.2 Mortality and morbidity with the CDE diet with 0.165% ethionine

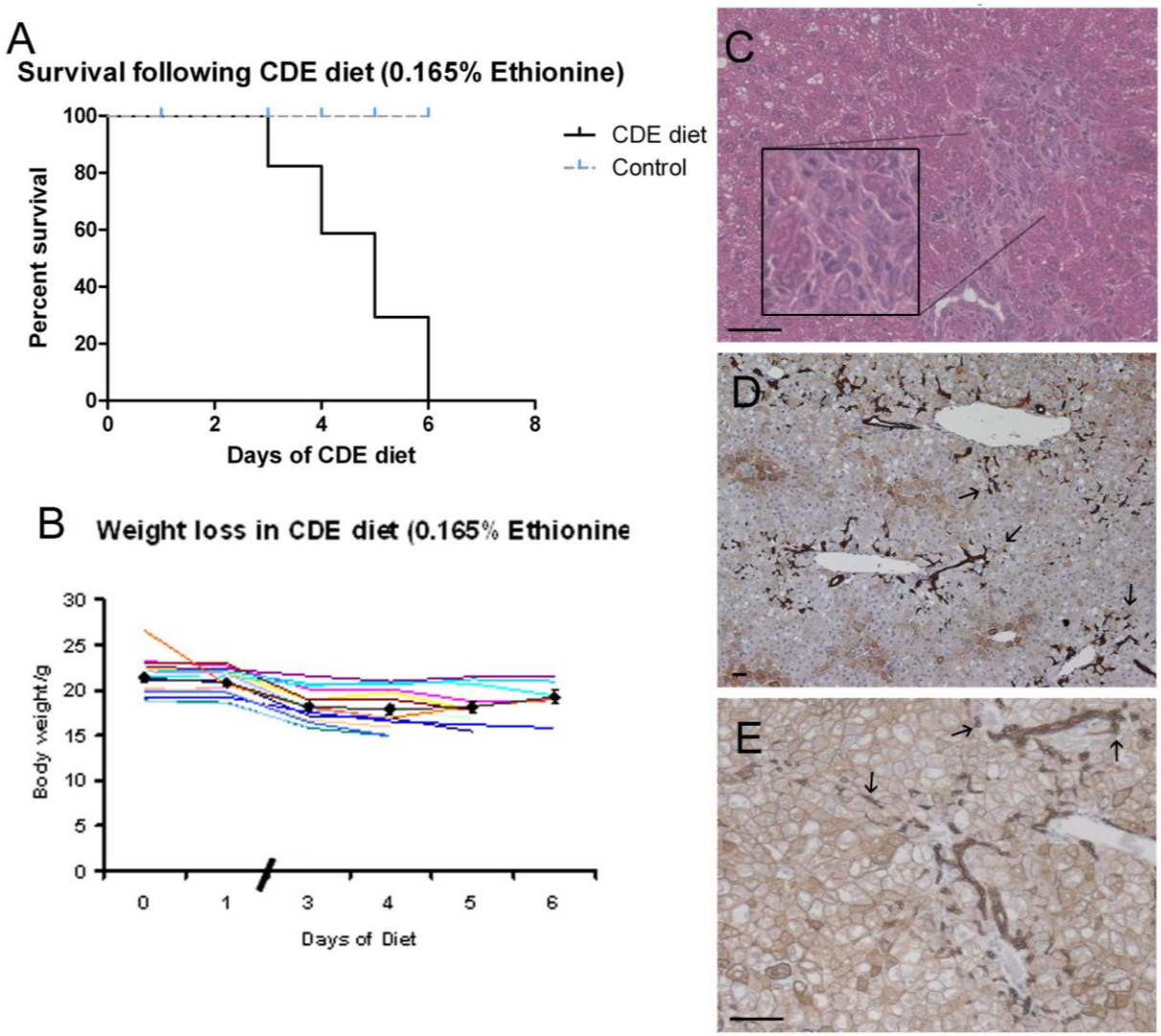

(A) Survival in a group (n=18) of 6 week old male C57Bl6 mice following commencing CDE diet (0.165% ethionine). Of these mice 2 died spontaneously while other mice with clinical signs of significant morbidity were euthanised. (B) Significant weight loss in this group of mice from baseline, individual weights are shown along with mean±SEM for the group (black line). Liver analysis by H&E (C; with magnified insert) panCK (D and E) showed significant expansion of small cells (arrows) consistent with published reports of HPCs. Whilst HPCs extend predominantly in single file columns into the parenchyma, H&E reveals an association of $panCK^-$ NPCs adjacent to the $panCK^+$ HPC.

Figure 3.3 Increased tolerance of CDE diet without HPC activation with reduced dietary ethionine

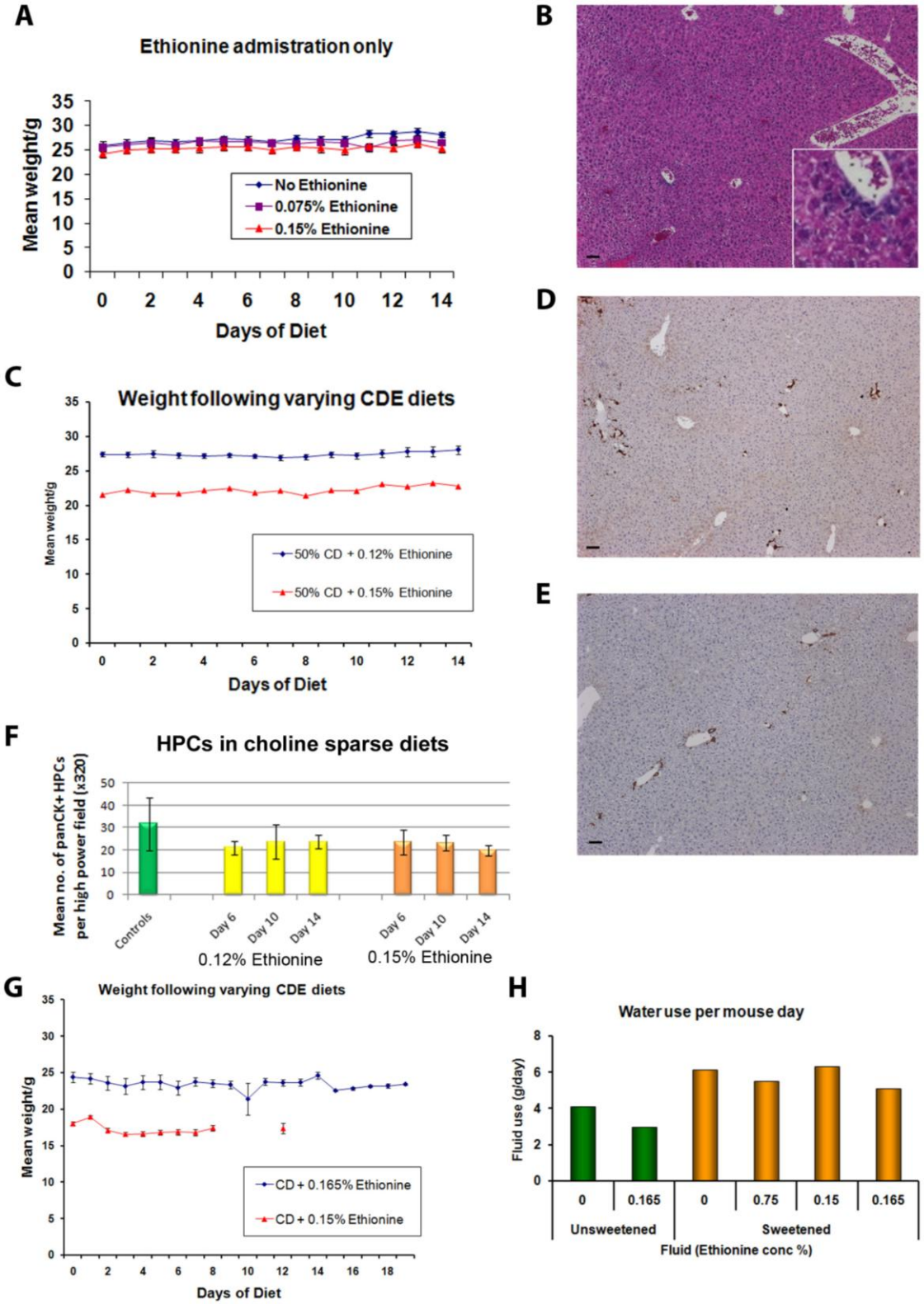

Normal weight gain (A) but an absence of HPC expansion (B) followed administration of ethionine only to 6 week old male C57Bl6 mice (n=5 each group). Following combination of a choline sparse deficient diet with either 0.12% or 0.15% ethionine normal weight gain (C) and only minor HPC activation (D and E respectively) were seen or quantified (F) at up to 14 days (n=5 each group). (G) In 8 week old male C57Bl6 mice, the combination of choline deficient diet and either with sweetened 0.15% or 0.165% ethionine resulted in early weight loss and a failure of weight gain over 2-4 weeks (n<4 each group). (H) Mouse fluid usage per day compared between various fluid preparations. Usage calculated by reduction of weight of cage bottles and extrapolated on a per mouse per day basis. All scale bars denote 50μm. Data points represent mean ±SEM.

In both groups treated with CDE diet with sweetened water hepatic effects were observed both macroscopically and microscopically. Macroscopically livers appeared pale (Figure 3.4A) and were larger than controls. A corresponding increase in liver weight was observed after 3 weeks of the CDE diet (Figure 3.4B). Microscopic analysis of liver revealed prominent microvesicular steatosis. Small isolated areas of hepatocyte necrosis were noted intermittently but no generalised hepatitis was present. Minor portal inflammatory infiltrate was present, predominantly formed by lymphocytes and monocytes. A progressive expansion of small cells, morphologically consistent with HPCs, was observed extending from portal tracts and confirmed as HPCs by $panCK^+$ expression. Consistent with previous observations in the CDE diet, a $panCK^-$ non parenchymal cell (NPC) expansion is seen alongside the HPCs (Figure 3.4D). HPC expansion was observed over a two week period beyond which the number of HPCs plateaus but remains elevated (Figures 3.4D and E). A strong correlation is seen between the extent of hepatic injury (serum Alt) and the degree of HPC expansion in mice within the cohort (Figure 3.4F).

Figure 3.4 HPC expansion in the optimised CDE diet

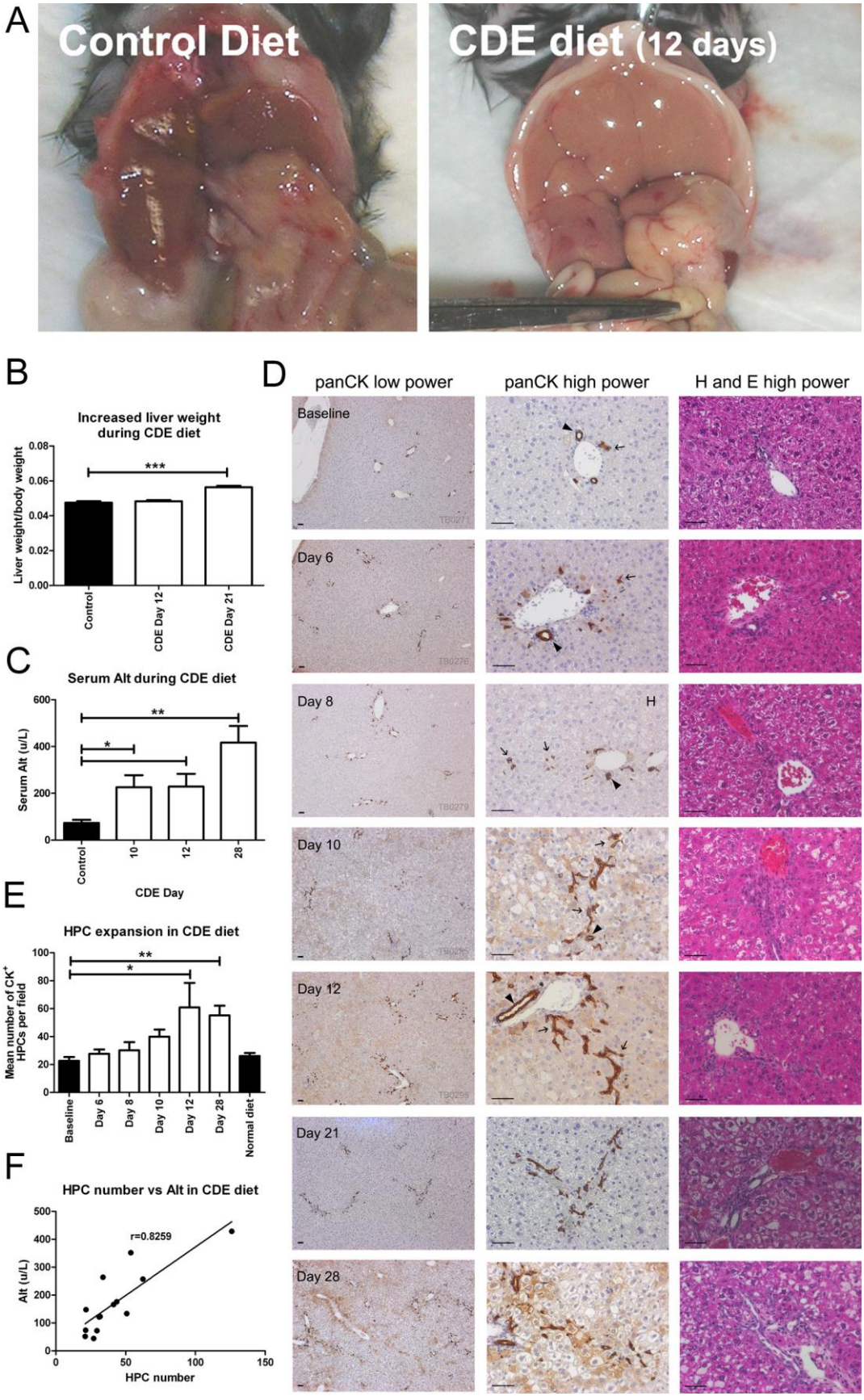

8 week old male mice were fed choline deficient chow with sweetened water containing 0.15% ethionine. At post mortem mice livers were pale in colour (A) and were enlarged in size and weight (B). Liver weight is presented as liver/body weight n<5 each group. Serum Alt is raised during the CDE diet (C), n<4 each group. A progressive expansion of panCK$^+$ HPCs (arrows) is observed from the portal tracts (arrowheads) of treated animals (D and E), (n<4 each group). Furthermore on an individualised analysis there is strong correlation between liver injury (F) and HPC expansion. Injury was assessed at post mortem assessed by serum Alt and compared to HPC activation using a Pearson's correlation coefficient (r). All graphs represent mean±SEM and scale bars 50μm.

Further examination of the cell characteristics during the CDE diet revealed ongoing proliferation of HPCs during the period of HPC expansion with large number of proliferating panCK$^+$ HPCs identified at 10 days following diet initiation (Figure 3.5A). Other cellular proliferation is identified alongside the HPCs, including hepatocytes and non-parenchymal cells. Notably non-parenchymal cells adjacent to the HPCs are frequently Ki-67$^+$ (Figure 3.5A). Other recognised HPC markers (see Chapter 1) were also assessed by immunohistochemistry. Expansion of both Dlk1 and EpCAM$^+$ HPCs was also observed in the CDE diet (Figure 3.5B and C respectively). TUNEL and activated Caspase 3 expression (Figure 3.5D and E respectively) also revealed marked apoptosis in the hepatic parenchyma and in the periportal regions during CDE diet compared to control mice.

Figure 3.5 HPC characterisation in the CDE diet

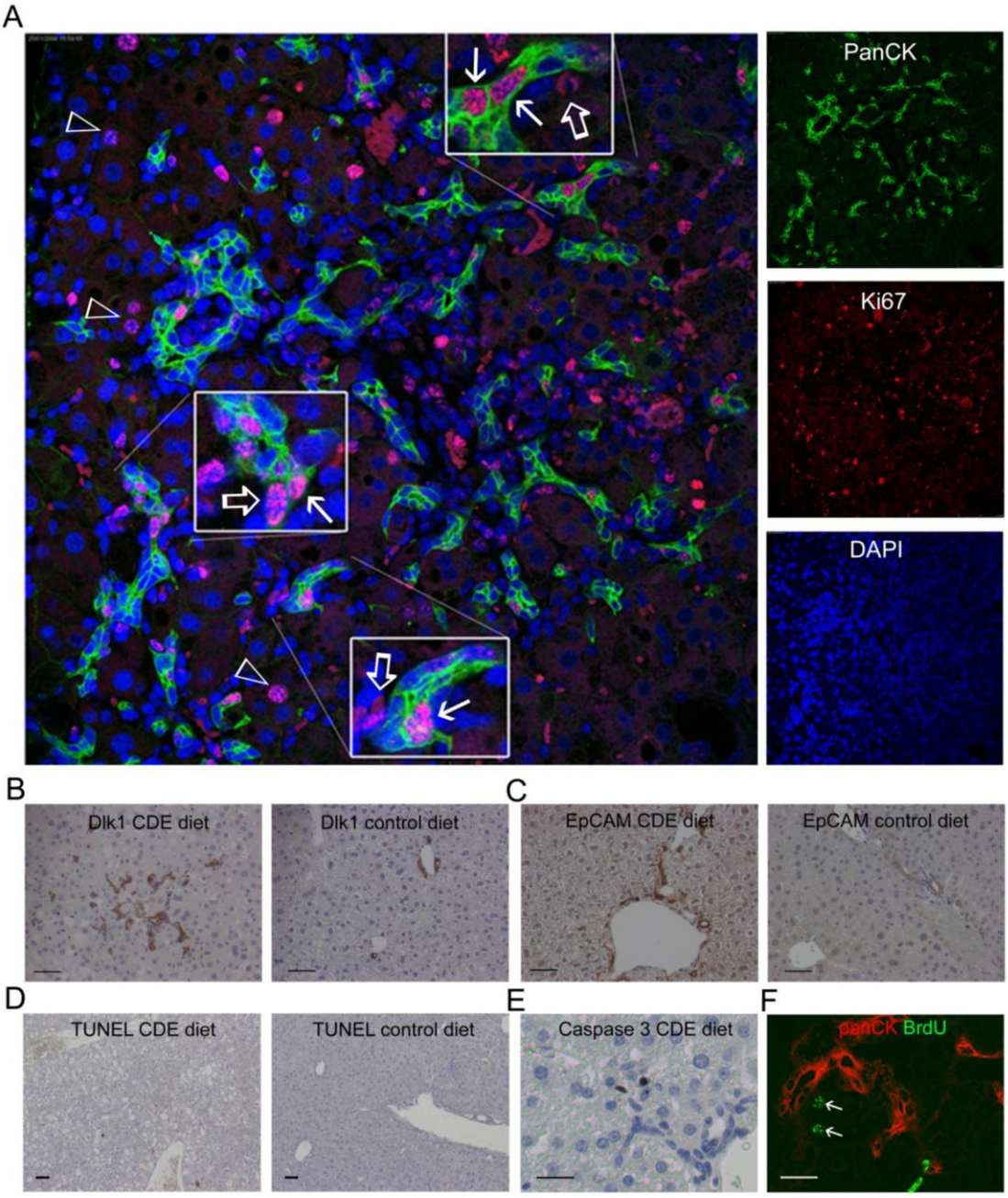

(A) During this expansion of HPCs (Day 10) ongoing proliferation (Ki-67 red) is seen within the HPC population (panCK green; Solid Arrows) as well as proliferation of hepatocytes (Arrowheads) and other non-parenchymal cells (Hollow Arrows). Expansion of $Dlk1^{+}$ HPCs (B) and $EpCAM^{+}$ HPCs (C) is also observed during the CDE diet. Increased apoptosis is observed throughout the hepatic parenchyma by TUNEL (D) and also associated with cells in the portal tract by Caspase 3 (E). (F) $BrdU^{+}$ hepatocytes adjacent to $panCK^{+}$ HPCs after 12 days of CDE diet when 50µg/g i.p. BrdU is given at day 9. All scale bars denote 50µm.

3.43 Recovery from the CDE diet

Having demonstrated that a reproducible expansion of HPC may be seen upon exposure to the CDE diet, I then asked whether return to a normal diet would result in reversal of liver injury and resolution of HPC expansion. Age, weight and sex matched mice were then exposed to 12 days of the CDE diet followed by return to normal chow and drinking water for a varying period of time prior to tissue analysis. Surprisingly rapid resolution of hepatocellular injury is observed within 3 days with a loss of steatosis (Figure 3.6). Furthermore identification of HPC reveals a remarkably rapid loss of HPC expansion with complete reversal seen within 1 day or return to a normal diet (Figure 3.6B). Consistent with a resolution of injury serum Alt levels fall back to baseline by 3 days recovery (Figure 3.6C). Serum Alkaline Phosphatase however remains elevated for greater than 1 week following CDE diet cessation (Figure 3.6D).

Figure 3.6 Resolution of injury and loss of HPCs following CDE diet reversal

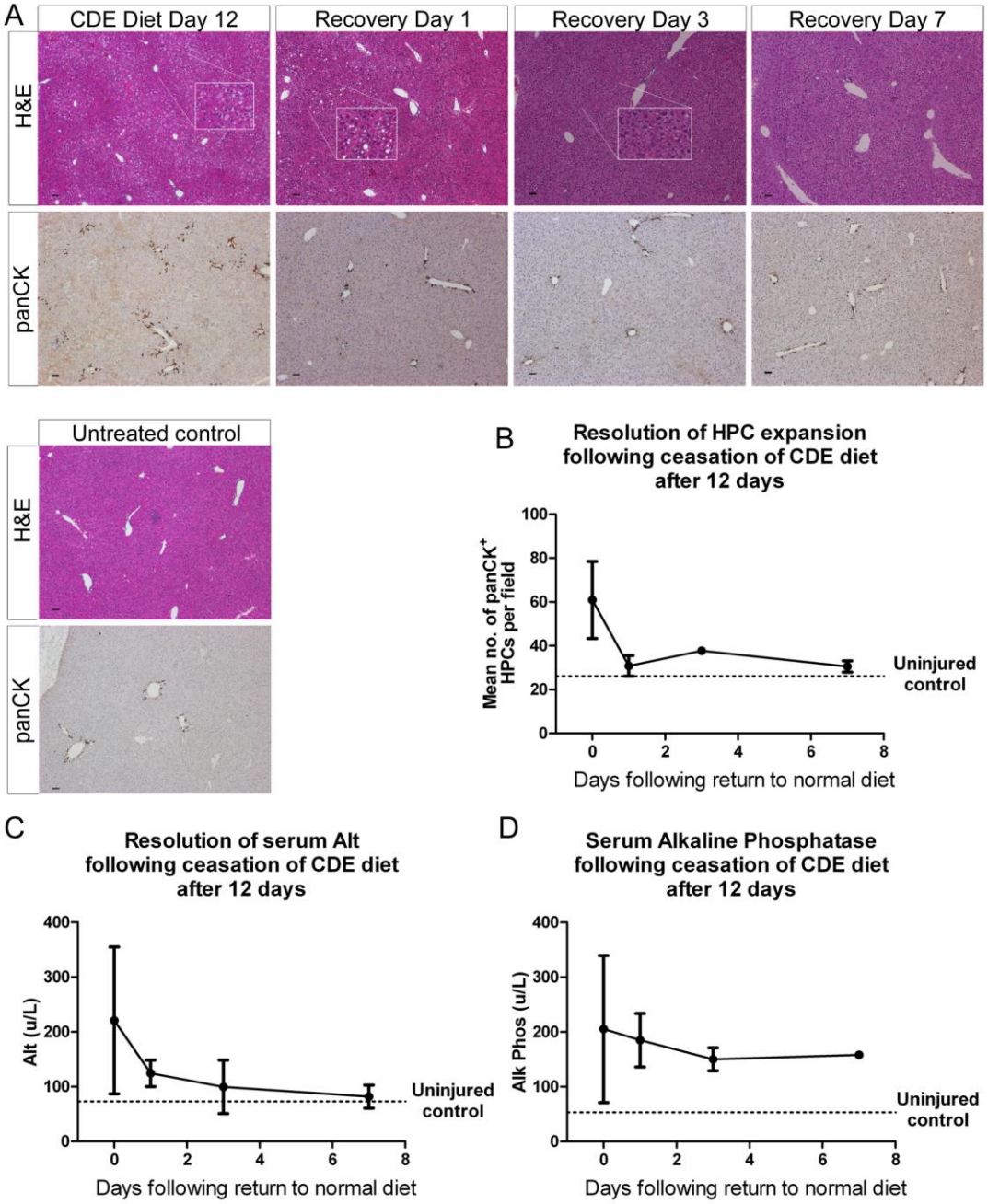

Following 12 days of CDE diet, mice were returned to normal chow to investigate the resolution of injury and HPC expansion following CDE diet cessation. (A) Histologically there is resolution of steatosis within three days of return to a normal diet and panCK$^+$ HPCs are quickly lost. (B) Quantification of HPC numbers demonstrates their return to normal within 1 day of return to normal diet. Serum Alt also returns to normal (C), however resolution of raised Alk Phos is considerably slower (D). Each mouse group n≥3. All scale bars denote 50μm.

3.5 DDC diet establishment

A further model discussed previously which has gained increasing use over the last decade is the DDC diet (see Section 1.32). To test this method of HPC activation, normal chow containing 0.1% DDC was fed to C57Bl/6 mice for up to 2 weeks. During this period universal weight loss of between 3-30% was observed together with clinical side effects requiring humane euthanasia of the experimental cohort. Subsequent work performed using the 0.1% DDC was performed with S129 mice and whilst resulting in weight loss did not lead to adverse side effects nor the requirement for humane euthanasia. Analysis of livers taken following 6-18 days of the DDC diet revealed a periportal ductular proliferation of cells expressing HPC markers panCK$^+$, EpCAM$^+$ and Dlk1$^+$ (Figure 3.7).

3.6 Paracetamol overdose model

Paracetamol is a frequent modality of fulminant hepatic failure in humans and has also been used in a variety of animal models of acute liver injury. HPCs have been described in human paracetamol overdose and also in a murine model of liver injury (Kofman *et al.*, 2005). Mice injured with varying doses of paracetamol (courtesy of Dr N Henderson and Dr K Simpson) were assessed for HPC activation. Immunohistochemical staining for HPCs using panCK revealed no significant HPC activation even in lethal doses of paracetamol in this model (Figure 3.8). Resolution of injury with near complete restoration of liver architecture is achieved in 1 week post paracetamol administration.

Figure 3.7 HPC expansion in the DDC diet

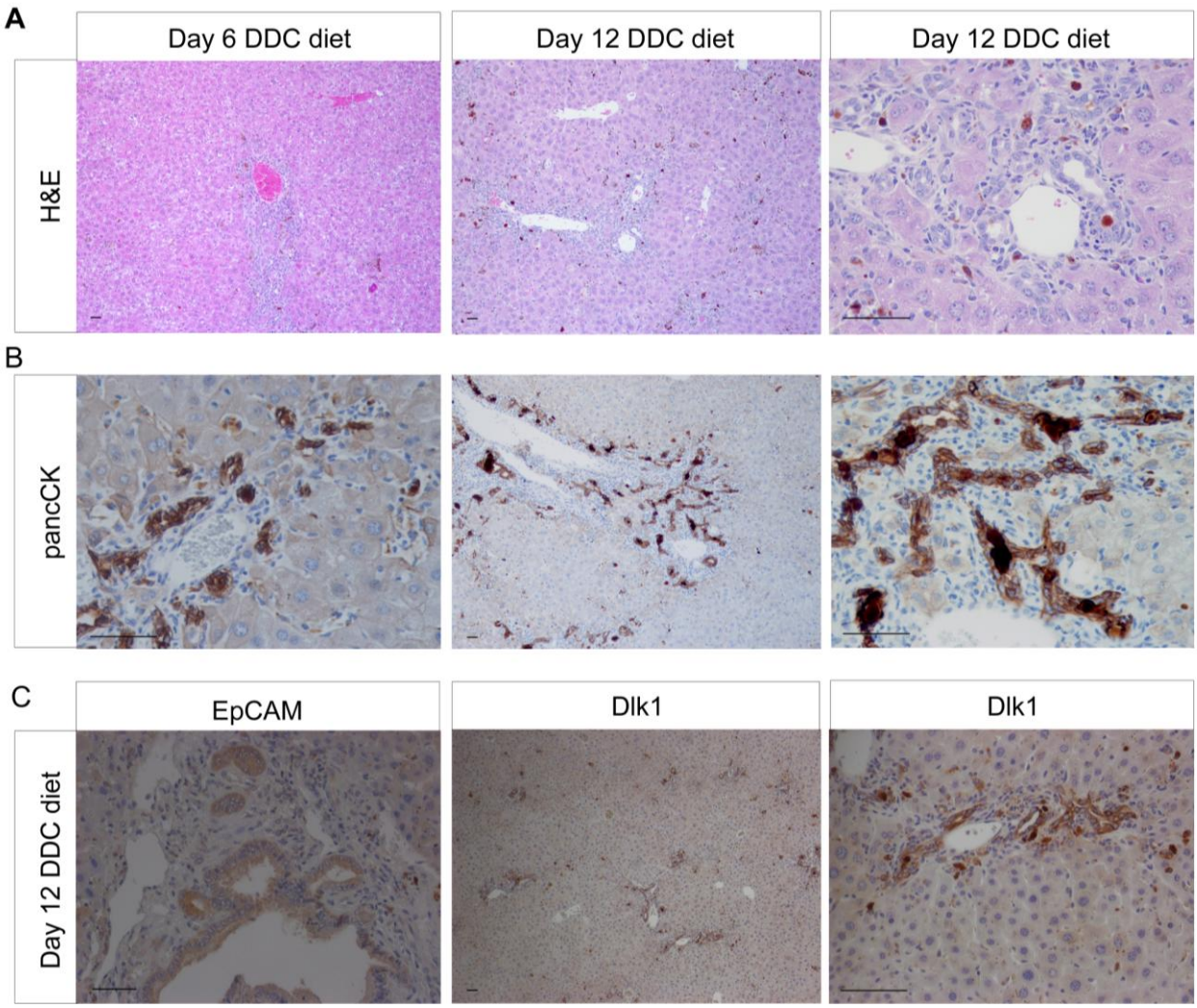

Following exposure to the DDC diet for upto 18 days, an expansion of biliary ducts is noted on H&E (A). Cells on the luminal surface of these ducts express the HPC markers panCK (B), EpCAM and Dlk1 (C). All scale bars denote 50μm.

Figure 3.8 HPC expansion in paracetamol toxicity model

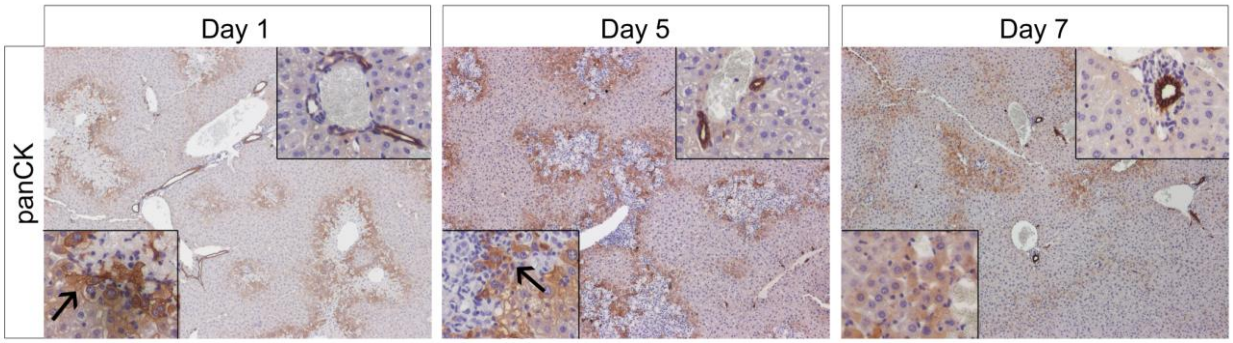

Inbred S129 were administered 350mg/kg paracetamol via i.p. injection. Immunohistochemistry for panCK in livers over time following paracetamol administration reveals no significant periportal panCK$^+$ HPC activation in this model despite overt liver injury particularly in zone 3 (Arrows). Onset of injury begins at approximately 1 day after paracetamol administration with peak hepatocellular injury at 5 days following by gradual resolution by day 7. Insets highlight high power images of areas of liver injury (bottom left) and the portal tract (top right) where an absence of panCK$^+$ HPCs is observed throughout injury and recovery.

3.7 Characterisation of the composition of the HPC niche

3.71 HPC activation in human liver disease

Having therefore established a number of models in which to study HPC biology, I wanted to address the question of whether a stereotypical niche existed around HPCs in these models and whether this was consistent not only with other rodent models but also and most importantly to human disease.

I therefore sought to examine a variety of human liver specimens taken either at protocol biopsy or at explant of the liver during liver transplantation. In the example of Hepatitis C Virus (HCV) infection, a profound HPC expansion was observed (Figure 3.9). Here, HPC cords are identified extending from the portal tract into the hepatic parenchyma analogous to those seen in the murine CDE (Figure 3.4) and DDC diets (Figure 3.7).

3.72 Identification of a stereotypical HPC niche composed of myofibroblasts, macrophages and endothelial cells

I therefore set out to investigate whether myofibroblasts, macrophages and endothelial cells are seen in colocalisation with HPCs in the various models described above. These cellular associations, observed in these models, were compared to alternative rodent models of HPC activation (both rat and mouse). These were also compared to examples of human chronic liver disease in order to assess the stereotypical nature of this environment between these different examples of liver regeneration.

Figure 3.9 Expansion of HPC in human liver

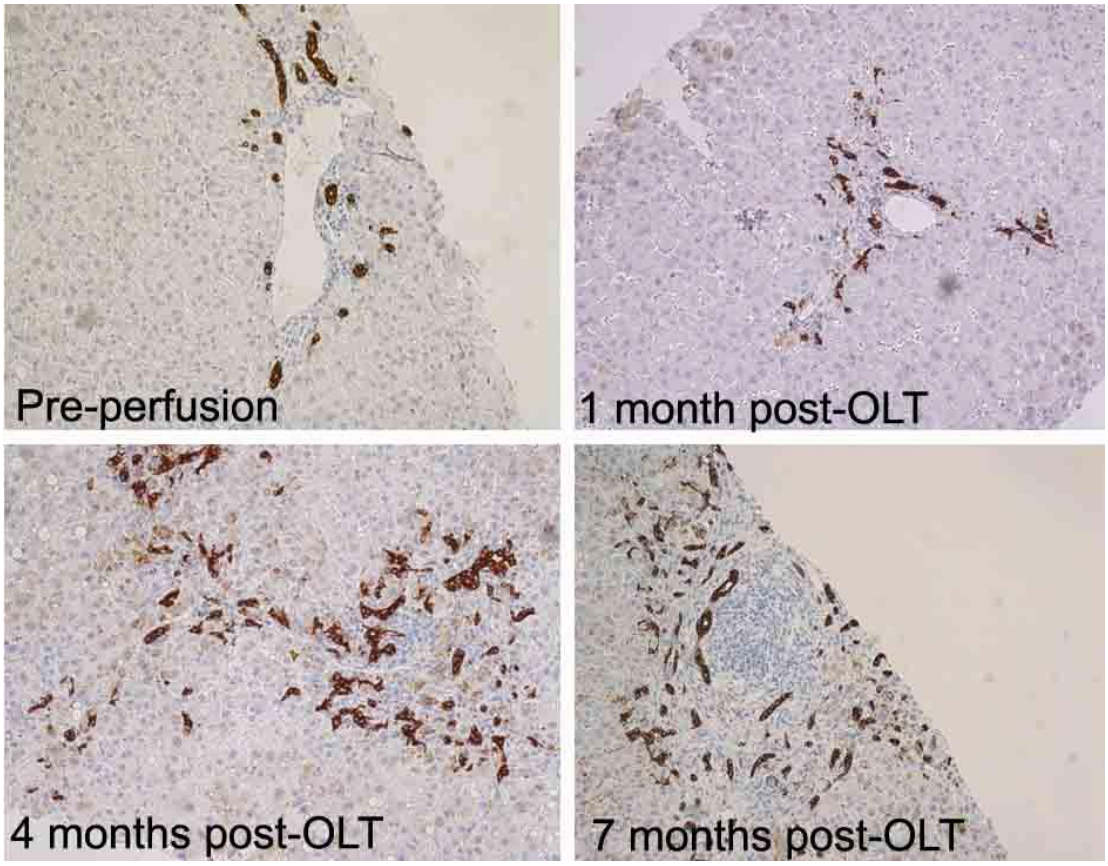

Human $CK7^{+}$ HPC expansion also known as ductular reaction observed in a patient with recurrent HCV infection following cadaveric transplantation. Pre-perfusion biopsy taken of the donor liver prior to surgical implantation and HCV infection with normal bile duct expression of CK7. Biopsies of the same liver at 1 and 4 and 7 months respectively post transplantation show marked and progressive expansion of HPC cords extending from the portal tract into the liver parenchyma.

3.72A Myofibroblasts in the HPC niche

In the normal liver tissue from healthy humans and uninjured rats and mice no expansion of HPCs is observed and while myofibroblasts are present, particularly in association with the vasculature, there is no apparent association between any HPC and myofibroblasts (Figure 3.10A-C). Upon HPC activation in the various models or human disease, a close association between myofibroblasts and HPCs is observed in each model, including the murine CDE and DDC dietary models developed as part of work presented earlier in this chapter (Figure 3.10D-H). It is striking how many of the HPCs are in direct contact with myofibroblasts which in many instances form a near continuous lining to the HPC cords.

3.72B Macrophages in the HPC niche

In healthy liver, hepatic macrophages are scattered throughout the parenchyma. Once again in this instance there is no discernable association between these cells and bile ducts or HPCs (Figure 3.11A-C). In contrast, in each species and model examined, upon HPC activation macrophages are seen in close proximity to HPCs. In most cases macrophages frequently make direct contact with HPCs (Figure 3.11D-G).

Given the close association observed between both myofibroblasts and macrophages to HPCs I set out to investigate the relationship of these two cell populations to one another. In murine models a close association is observed between the macrophages and myofibroblasts (Figure 3.12). This association between myofibroblasts and macrophages is also observed in the context of HPC activation during human liver disease. When examination of macrophages and myofibroblasts was performed on serial 3μm sections taken either side of a section stained for HPCs, this close association is observed between all three cellular populations with a tendency of each to associate with each other (Figure 3.13). This frequent association of all three cell populations was

however by no means exclusive and areas were easily identifiable where any two of the three populations was in close association at the exclusion of the other.

Following the observation that macrophages are found in the HPC niche over time in the CDE diet, I sought to examine whether a corresponding increase in hepatic macrophages is observed in the whole liver over this period. Unexpectedly quantification of total hepatic macrophages during HPC expansion in the CDE diet revealed a significant reduction in the number of hepatic macrophages over the period of HPC expansion in this model (Figure 3.11C). Further examination of the sections reveals the explanation for the apparently discordant results with a relative paucity of hepatic macrophages in zone 2 of the liver during HPC expansion compensating for the accumulation of macrophages observed in the periportal area (Figure 3.11B).

Figure 3.10 Myofibroblast association with activated HPCs

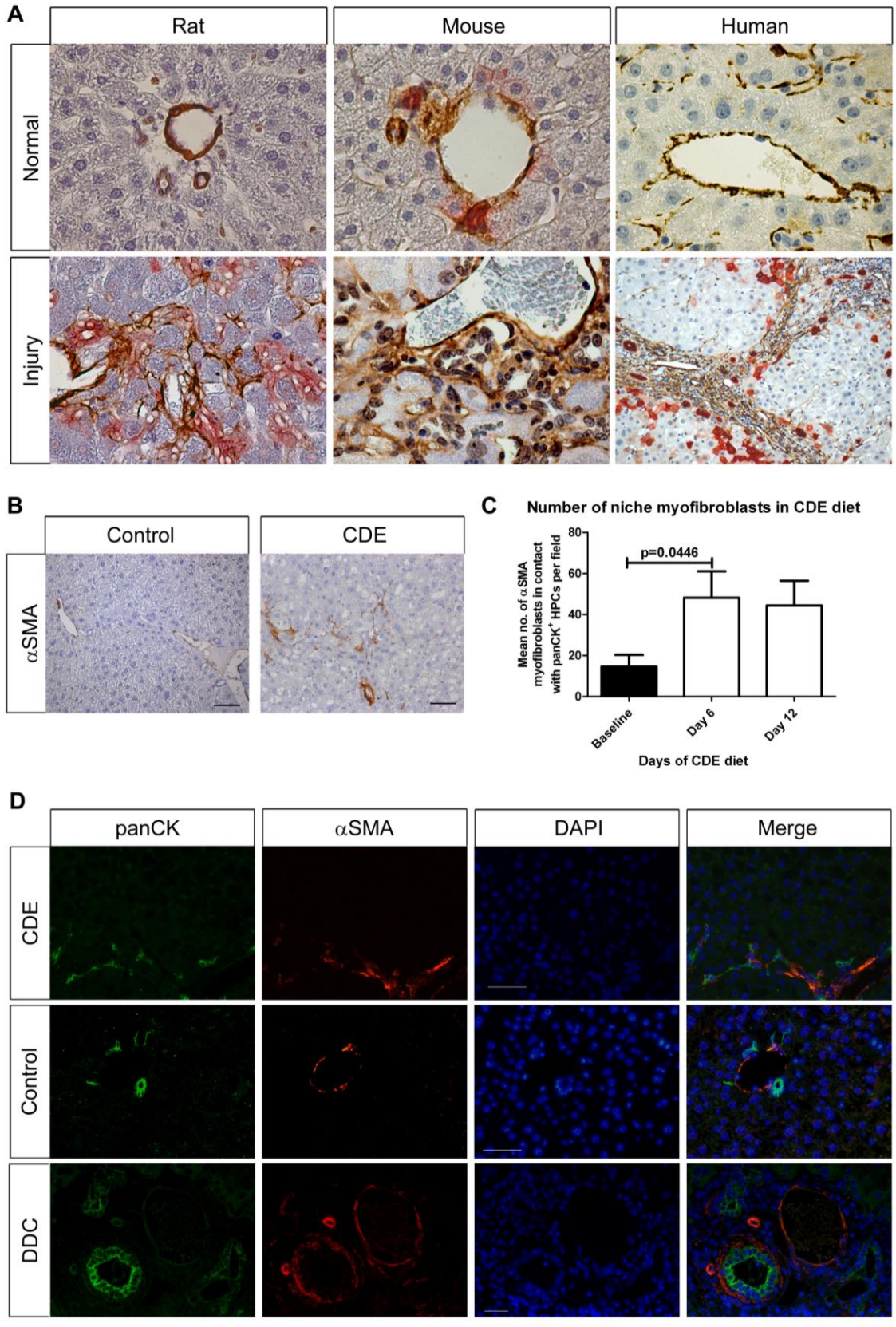

Identification of myofibroblasts using αSMA immunohistochemistry. (A) In normal control liver from rat, mouse and human (pre-perfusion biopsy from donor without liver disease) only small numbers of myofibroblasts are seen in periportal areas but no identifiable association with HPCs (red). In contrast in each species, upon injury and during HPC induction, intimate contact between HPCs and myofibroblasts is observed (HPC are identified by CK19, panCK and CK7 in rat, mouse and human respectively; Staining performed by Dr S Lorenzini; rat day 9 following PH in 2AAF/PH model, mouse HBsAg-tg/retrorsine model, human HCV related cirrhosis. (B) In the CDE diet there is again portal expansion of myofibroblasts. (C) Quantification of niche myofibroblasts in the CDE diet reveals a significant increase in the number of myofibroblasts in contact with HPCs per field (n=5 each group, p value denotes Mann Whitney test). (D) Comparison between the spatial localisation of myofibroblasts in CDE diet and DDC diet to normal control reveals that myofibroblasts contact panCK$^+$ HPC in the CDE model but a thicker layer of myofibroblasts surround panCK$^+$ HPC ductules in the DDC diet. All scale bars denote 50μm.

Figure 3.11 Macrophage association with activated HPC

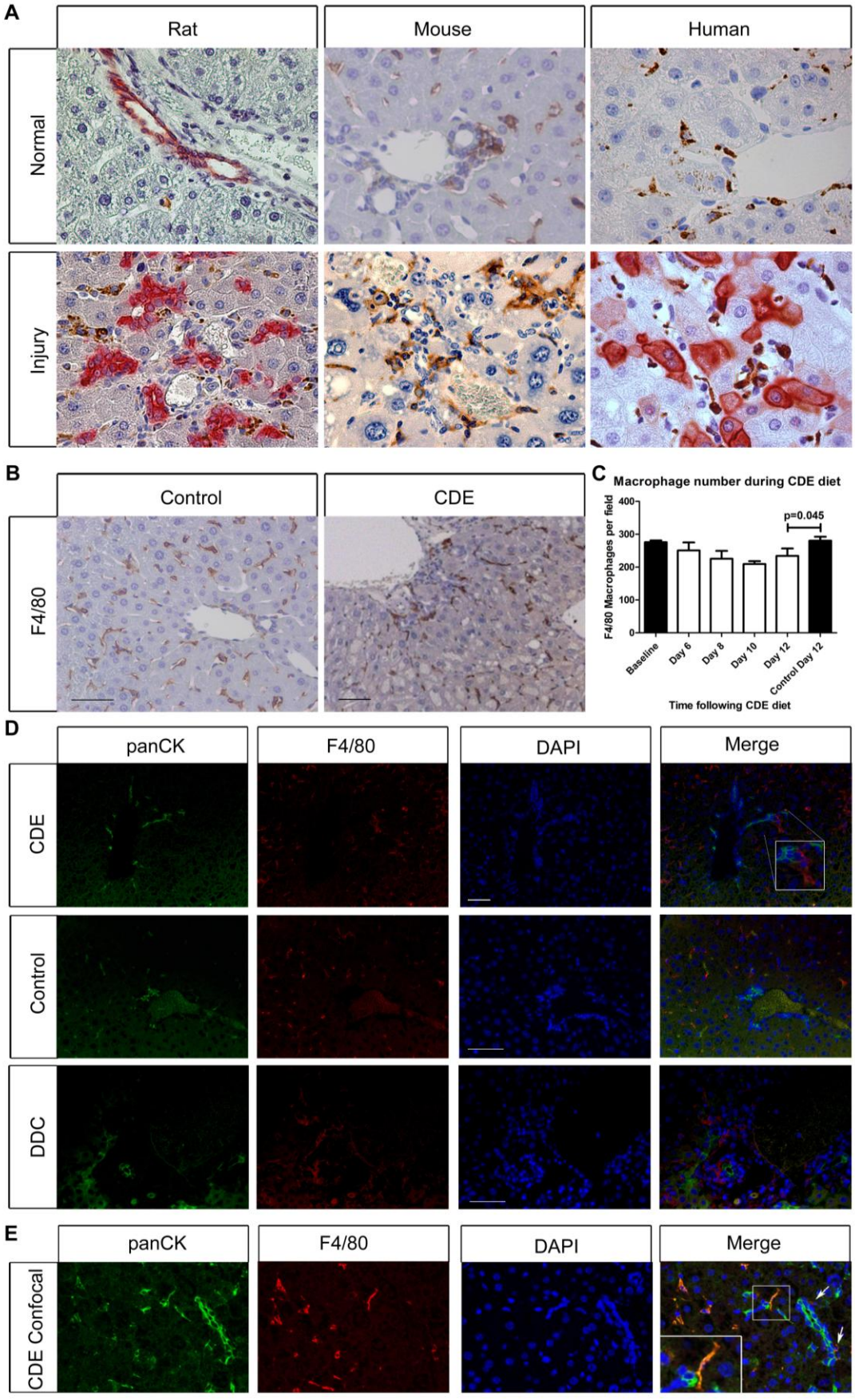

Identification of macrophages using immunohistochemistry (mouse-F4/80, rat-ED1, and human-CD68). (A) In normal control liver from rat, mouse and human (preperfusion biopsy from donor without liver disease) only small numbers of macrophages (brown) are seen in scattered within the periportal area with no identifiable association with HPCs (red). In contrast in each species, upon injury and during HPC induction, intimate contact between HPCs and myofibroblasts is observed. HPC are identified by CK19, panCK and CK7 in rat, mouse and human respectively; Staining performed by Dr S Lorenzini (rat day 9 following PH in 2AAF/PH model, mouse HBsAg-tg/retrorsine model, HCV related cirrhosis). (B) In the CDE diet models macrophages are seen in close proximity to HPC in the periportal region. (C) Quantification of total hepatic macrophages over time in the CDE diet. Results are expressed as mean numbers of cells per field ($n \geq 4$ each group; p value denotes T test). (D) Dual immunodetection of $F4/80^+$ macrophages and $panCK^+$ HPC reveals their close association in the CDE and DDC diets but not uninjured control. (E) Confocal microscopy reveals contact between macrophages and HPCs in the CDE diet. All scale bars denote 50μm.

Figure 3.12 Association between macrophages and myofibroblasts in murine HPC models

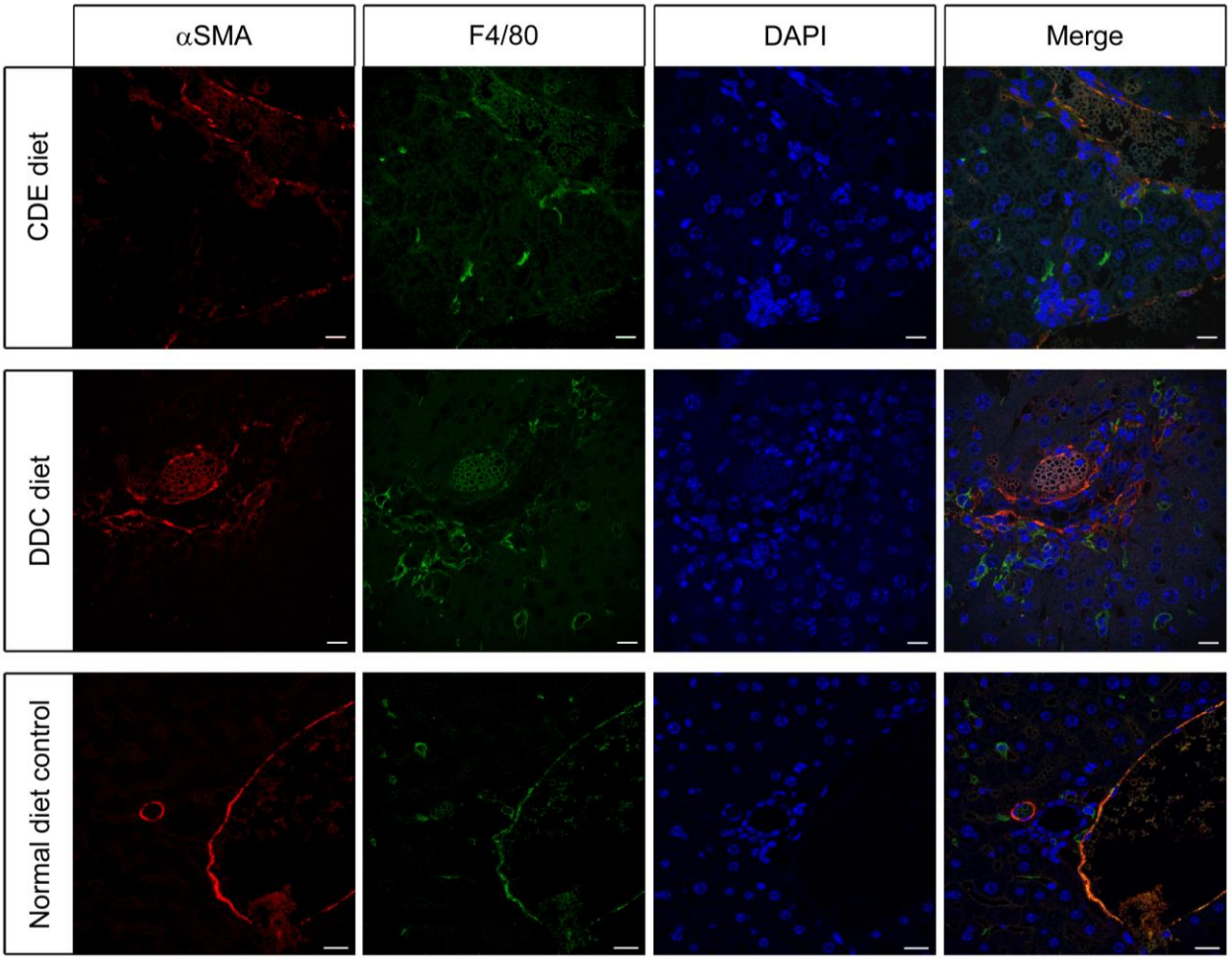

Dual immunohistochemistry for myofibroblasts (αSMA;red) and macrophages (F4/80;green) in the CDE and DDC dietary models of HPC activation in the mouse (12 and 18 days respectively). All scale bars denote 50μm.

Figure 3.13 Association between macrophages, myofibroblasts and HPCs in human disease

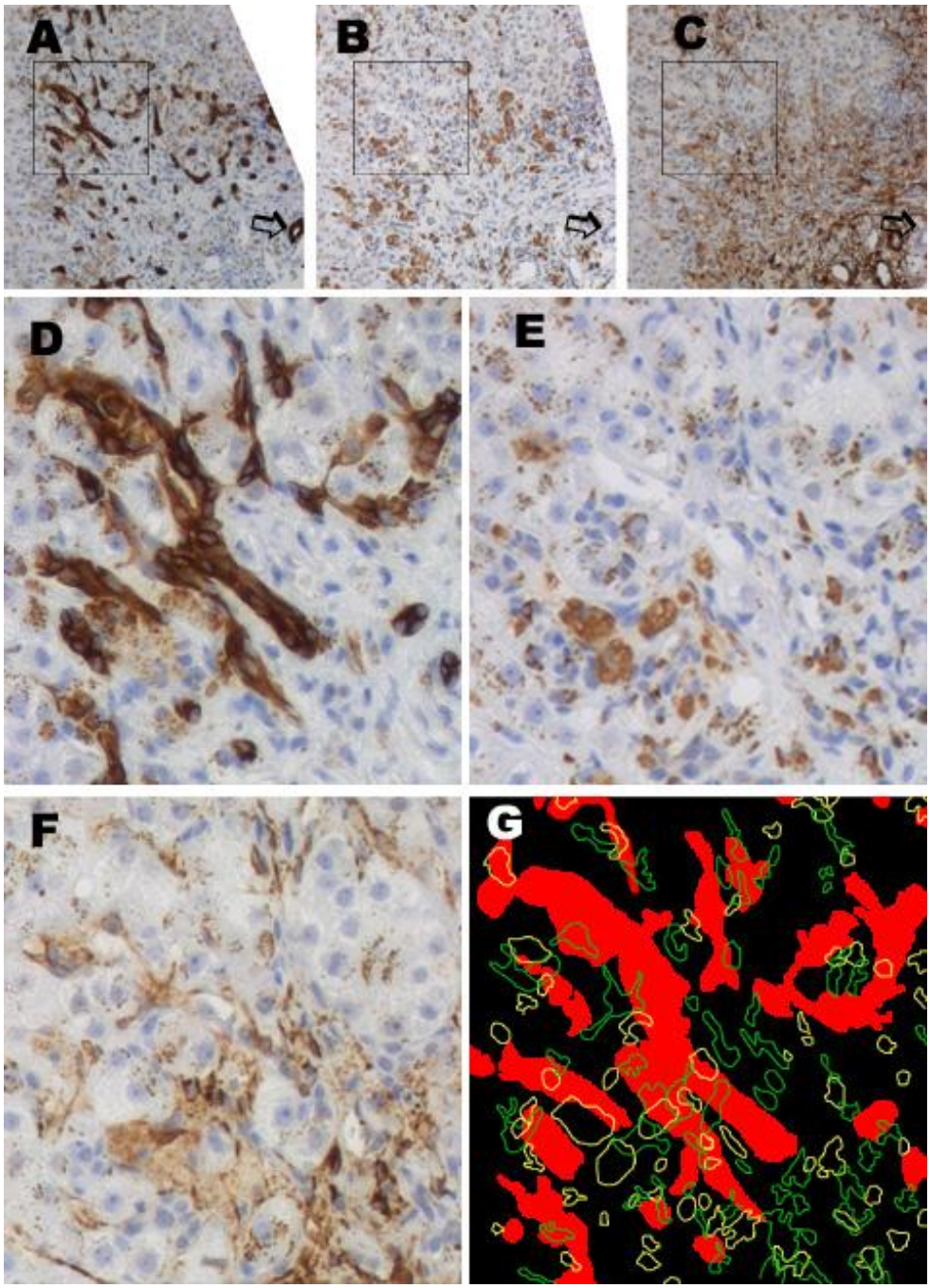

Examination of serial sections from a 6 month biopsy of a patient with aggressive post-transplant recurrent HCV infection reveal the intimate co-localisation of HPCs (A; CK7), macrophages (B; CD68) and myofibroblasts (C; αSMA) at low power and high power (D, E and F respectively) . Sections were aligned using a series of architectural structures included the bile ducts (arrow). (G) False colouring of HPCs (red) macrophages (yellow) and myofibroblasts (green) revealed the association of all three cell types in relation to expanding HPCs.

3.73 Laminin is universally present in the HPC niche

In addition to examination of the cellular component of the HPC niche, I also wished to examine the role of specialised extracellular matrix components within the niche. Laminins, as previously discussed, are ECM components which are not only described to play a crucial role in stem cell biology (Domogatskaya *et al.*, 2008) but are also described in certain rodent HPC models to be localised with HPCs (Paku *et al.*, 2001). Given the striking findings described by Paku *et al.* of a near complete laminin sheath around the HPCs in the PH/AAF model, I wished to exam whether a similar relationship is observed in the CDE diet. Using immunohistochemistry this strikingly consistent association of laminin and HPCs is preserved in the CDE diet (Figure 3.14). Further examination in other models also demonstrated consistent association across models and species between HPCs and a juxtaposed laminin rich basement membrane.

3.8 Discussion

The activation of HPCs has been described in previous work by many groups in a variety of human diseases and animal models (Roskams *et al.*, 2003b; Alison *et al.*, 1996; Arends *et al.*, 2009; Preisegger *et al.*, 1999). In order to examine the relationship of HPCs to candidate cells within the stem cell niche I first examined the HPC response in a variety of models and compared this to the HPC reaction observed in human disease.

Figure 3.14 Laminin associates with and encases activated HPCs

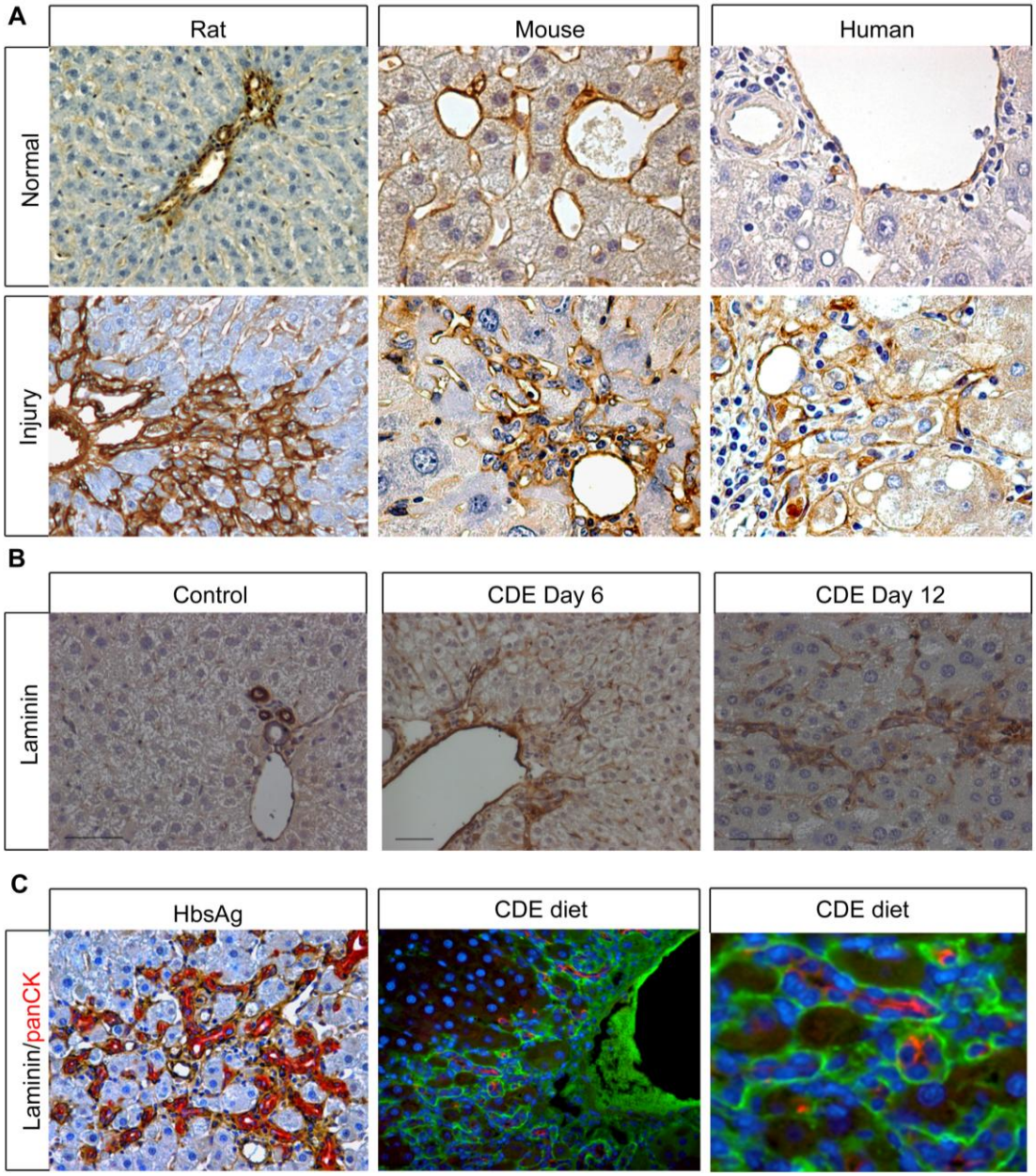

Identification of laminin by immunohistochemistry. (A) In normal control liver from rat, mouse and human (pre-perfusion biopsy from donor without liver disease) laminin is observed particularly associated with the vessels in the periportal tract. During HPC induction laminin extends from the portal tract and surrounds cells with an HPC morphology. Staining performed by Dr S Lorenzini. Injury models and disease: rat day 9 following PH in 2AAF/PH model, mouse HBsAg-tg/retrorsine model, HCV related cirrhosis. (B) In the CDE diet model a progressive expansion of laminin is observed from the portal tracts mirroring the expansion of HPCs. (C) Dual immunohistochemistry for panCK^{+} HPCs and laminin in the HBsAg/retrorsine and CDE diet models reveals intimate association between the two in both murine injury models. All scale bars denote 50μm.

3.81 HPCs in normal mammals

An important initial consideration with regard to the examination HPCs in all studies is the accurate identification of these cells. As previously discussed (Chapter 1) many markers have been identified in numerous models. It is important to note that while many 'stem cell like' attributes have been ascribed to individual (and often impure) populations based on these markers, no current consensus regarding HPC markers exists with many studies using a 'strength in depth' approach by examining multiple markers (Jelnes *et al.*, 2007; Wang *et al.*, 2003a). In this work I have principally used panCK as a marker of HPCs on the basis of historical acceptance of this marker (Kofman *et al.*, 2005). In this work I demonstrate that, in the widely used CDE diet, that there is a numerical expansion of panCK$^+$ HPCs and that this population is actively expanding *in vivo* rather than arising through a dedifferentiation event.

A complicating factor for the identification of HPCs, using any of the currently ascribed HPC markers, is the issue of concurrent identification of cholangiocytes. When immunohistochemical analysis is used, this only represents a modest problem, as intralobular or larger bile ducts are easily identifiable by eye. However when examining cells by immunocytochemical methods, the contamination of the HPC population by cholangiocytes becomes a significant problem which may interfere dramatically with the interpretation of results. Accordingly I have used immunohistochemistry as the cornerstone of identification of HPCs in this work and when HPCs are quantified the methodology has been designed to minimise this problem of false positive cholangiocytes. Additionally in this study examination of HPC with multiple markers was performed in each model to validate the identity of HPCs as accurately as possible.

This work has confirmed the presence of the EpCAM and panCK as HPC markers in the mouse but also is to my knowledge the first description of reproducible Dlk1 immunohistochemistry in murine HPC models. My work has also shown that these markers to not identify identical populations and while some cells simultaneously

express multiple markers there are discrete differences between panCK$^+$, EpCAM$^+$ and Dlk1$^+$ populations.

While very little evidence is seen of any HPCs in young adult mice, it is interesting to note the reproducible and consistent expansion of HPCs which occurs as mice age. This observation is the first report of this effect. It is well described that the regenerative capacity of most organs including the liver is impaired with increasing age (Kirkwood, 2005). In the liver, specifically in the context of partial hepatectomy, regeneration is impaired (Timchenko *et al.*, 1998) and this process appears to be mediated through inhibition of c-Myc by C/EBPα in elderly mice (Iakova *et al.*, 2003). It is not known whether similar changes in C/EBPα occur with age in the HPC population; however it is likely that a reduction in hepatocyte turnover related to such inhibition may be a stimulus for HPC expansion in elderly mice even in the absence of specific injury.

3.82 Optimisation of the CDE diet for use as a model of HPC activation

Optimisation of the CDE diet aimed to generate a dietary model which reproducibly activates HPCs but does not result in the intolerable morbidity or mortality as observed using higher concentrations of ethionine (>0.15%). Initially, it was necessary to optimise the CDE diet due to considerable weight loss and even unexpected mortality in male mice on the original CDE diet (with 0.165% ethionine). The reason the apparent discrepancy between the morbidity/mortality observed in our unit versus that of other units worldwide remains unclear. Certainly many other investigators use this higher concentration of ethionine in C57Bl6 male mice, even without the additional benefits of sweetened water, and yet do not report the toxicity I have observed in this work. The most probable explanation for this discrepancy is variability between strains of C57Bl6 mice although I cannot rule out alterations between preparations of the CDE diet; although the supplier remained consistent between ourselves and other research groups.

The demonstration here of a failure for ethionine to expand HPCs over 2 weeks at concentrations up to 0.15% demonstrates the necessity of inclusion of ethionine to choline deficiency in order to stimulate HPCs and is in keeping with a report in rats when the CDE diet was initially developed; even over a ten week period (Shinozuka *et al.*, 1978).

The rapid weight loss seen in the initial trial of the CDE diet (0.165% ethionine) was presumed to be principally due to poor oral intake of water due, the dramatic weight loss and apparent dehydration of the experimental animals. Reduced oral intake may have also played a role. Whilst large daily weight fluctuation are not seen in larger mammals, small animals are required to eat a much larger proportion of their body weight per day. In my experience a 25g C57Bl6 mouse will eat approximately 3.5g of chow per day. This therefore raises the possibility of poor intake of food played a significant part in animal weight loss and morbidity. None-the-less the attenuation of weight loss with reducing ethionine concentration implies that higher doses of ethionine are the principle factor causing the observed side effects.

Consistently upon commencing the CDE diet, the greatest predicting factor for development of clinical side effects or mortality was significant weight loss (>20%). In no instance did mice die or develop clinical signs (hunching, pilo-erection, or social withdrawal) in the absence of >20% weight loss. As a result changes were instituted to the Animal Project License permitting weight loss >20% in the absence of clinical signs, provided that twice daily assessment revealed no clinical deterioration and that mouse weight improved to <20% loss within 72 hours. If at any time mouse weight fell below >30% mice were euthanised.

As a result of optimisation of the CDE diet the working concentration of ethionine was reduced from the frequently published 0.165% to 0.15%. In addition water was sweetened with orange squash which was demonstrated to improve animal oral intake. Following these changes, consistent HPC activation was achieved in combination with

hepatocellular injury. These changes along with the infiltrating morphology of HPC migration was analogous to that previously reported with the CDE diet (Akhurst *et al.*, 2001).

Measurement of oral intake in mice is for many reasons fraught with difficulty making such analysis difficult. Intake is measured on the basis of reduced weight in cage bottles and thus reflects cage rather than individual mouse use. Furthermore losses from bottles during cage handling make this inaccurate although attention was paid to monitor each cage identically to minimise any cage/cage variation in these measurements.

Due to the addition of orange squash it is not possible to guarantee complete choline deficiency was achieved. Unfortunately no data was available regarding choline content of this. Nonetheless choline is typically found in oranges although only at 2mg/100g and therefore the choline content in added artificial orange squash is likely to be negligible (typically 1μg/day; recommended daily amount approximately 100μg/day; Zeisel and Blusztajn, 1994). As previously discussed, the addition of ethionine in rodents results in only very minimal HPC expansion (Shinozuka *et al.*, 1978). Therefore the HPC expansion in our CDE diet model is consistent with functional choline deficiency.

3.83 HPC and niche characterisation in the CDE diet

Having characterised the limited toxicity and HPC response to fully choline deficient chow in combination with 0.15% ethionine, this diet was used to investigate a variety of features of HPC activation in the mouse. This optimised diet did not result in any unexpected mortality and only a very small number of mice (<1%) required euthanasia due to poor clinical status.

Examination of the HPC response in the CDE diet demonstrates an expansion of HPCs identified by either panCK, Dlk1 or EpCAM. The panCK population actively expands

by proliferation in response to the CDE diet. The mode of action of the CDE remains uncharacterised, however in line with previous studies, HPCs in the CDE diet expand alongside widespread liver injury as demonstrated by raised serum transaminases, histological evidence of damage and widespread hepatocyte apoptosis (Figures 3.3 and 3.4; Knight *et al.*, 2005a). Additionally, when mice are individually analysed there is a strong correlation between the degree of liver injury and HPC activation; again supporting the role of HPC mediated regeneration in injury (Figure 3.4). Other reports using alternative analyses have demonstrated links between severity of injury and degree of HPC activation in humans disease (Libbrecht *et al.*, 2000; Lowes *et al.*, 1999; Roskams *et al.*, 2003a).

The recovery from withdrawal of the CDE diet and return to normal diet in this work is striking. Previous observations in this field have looked over longer periods (>7 days recover) and have shown resolution of HPC response and serum transaminases (Knight *et al.*, 2005a). In this report, the authors conclude that the disappearance of HPCs together with a lack of HPC apoptosis is evidence for differentiation into parenchyma. The rapidity with which both fall has, to date, not previously been reported. Additional examination during in the immediate time following CDE diet withdrawal may provide further insight into whether early HPC apoptosis occurs. Furthermore whether HPCs number reduction is due to differentiation into hepatocytes could be investigated during this time using lineage tracing, either with transgenic reporter activation or more crudely through BrdU pulse-chase labelling. Initial study in this area in this work using BrdU administered at day 9 to mice during the CDE diet followed by examination 3 days later showed many BrdU labelled hepatocytes are observed in periportal regions (Figure 3.5F). However as hepatocytes are also labelled during the BrdU pulse no definitive statement linking HPCs and the periportal $BrdU^+$ hepatocytes observed at day 12 may be made from this work at this time.

Examination of archival tissue from mice treated with paracetamol was performed given the recent description of marked $panCK^+$ HPC expansion in this model (Kofman

et al., 2005). I was unable to reproduce this effect. I believe this contrast between my findings and those published by Kofman *et al.* are due to the lower doses of paracetamol administered in our study (350mg/g vs. ≤1000mg/g). The use of 350mg/g still resulted in severe hepatocellular injury and even a mortality rate of approximately 20%. For this reason further experimentation with higher doses of paracetamol was not performed.

An interesting observation to come to light from the examination of the tissue from paracetamol treated mice is the presence of a number of intermediate-like small hepatocytes observed at the front of hepatocellular necrosis during injury. These cells often express high levels of panCK. There are however geographically distinct from the portal tract and there is no expansion of panCK$^+$ HPC connecting the two regions. For this reason, I believe that panCK expression is seen in injured hepatocytes and therefore panCK expression alone is not a definitive marker of an HPC. Again the methodology of HPC identification in this work has been developed to exclude such false identification.

3.84 Characterisation of the cellular HPC niche

While a large literature exists regarding HPC biology there is little data regarding their surrounding environment which is likely to act as a niche and therefore strongly influence HPC behaviour. The work presented in this chapter describes the systematic examination of HPC reactions in multiple rodent models and human liver disease. Here I demonstrate that HPCs are closely accompanied by a cellular niche composed of myofibroblasts, and macrophages throughout the progenitor cell response. These associations remain consistent throughout a range of diverse rodent models and human disease. The description of HPCs with mesenchymal cells expressing desmin or vimentin has been previously reported (Paku *et al.*, 2001). Myofibroblasts are known to express these intermediate filaments, and therefore the work presented here regarding

niche myofibroblasts contributes to this previous work by describing their mesenchymal phenotype.

The work presented up to this point demonstrates the association of macrophages, and myofibroblasts with HPCs but clearly does not address the functional importance of these cells. Nevertheless the consistence of this stereotypical niche implies that its formation is not a random event and argues for a functional role of these cells. The exact role of these progenitor-associated macrophages and myofibroblasts is unknown. However, it is tempting to speculate that these NPCs may act as a link between tissue injury and progenitor cell activation. Indeed, hepatic macrophages and myofibroblasts can express a variety of signals critical for controlling liver development and hepatic stem/progenitor cell behaviour (Bird *et al.*, 2008). Recent inhibition of myofibroblast activation in the PH/AAF model has implied a functional role of the niche myofibroblasts promoting HPC activation (Pintilie *et al.*, 2010). In addition, myofibroblasts make and macrophages remodel ECM and therefore these cells may be necessary for the extension and resolution of the HPC response through effects on the stereotypical basement membrane observed with HPC activation (Duffield *et al.*, 2005; Fallowfield *et al.*, 2007; Henderson and Iredale, 2007).

In addition, or as an alternative, to the niche provide signalling to the HPCs there may also be reciprocal passage of signals from the HPCs to the niche cells. It is possible that the profound activation of HPCs in diseases such as fibrosing cholestatic hepatitis may account for the local activation of myofibroblasts and macrophages and thus provide a link between the dramatic HPC activation and the rapidity and severity of hepatic fibrosis observed in this condition. This hypothesis would require further examination to establish a direct and causative link between HPC activation and fibrosis.

The work presented here, has focused on the role of the intrahepatic macrophages (including Kupffer cells). The monocyte-macrophage lineage is a complex and heterogeneous population and is characterised by expression of a variety of cellular

markers. I chose the accepted macrophage/Kupffer cell marker F4/80 to identify macrophages/Kupffer cells in this system. The $F4/80^+$ antigen (which is also recognised by the BM8 monoclonal antibody) is observed on all known macrophage populations ,including Kupffer cells (Hashimoto *et al.*, 1996) and bronchoalveolar macrophages; and is absent from any cell types that are definitely not mononuclear phagocytes (Hume *et al.*, 1984). F4/80 is a member of the EGF seven transmembrane-spanning family of hormone receptors, little is currently known regarding its ligands and biological function although it appears to play a role in the generation of efferent $CD8^+$ regulatory T cells (van den Berg and Kraal, 2005). F4/80 is not crucial to macrophage formation as demonstrated by the development of macrophages in the absence of F4/80 in transgenic studies (Schaller *et al.*, 2002).

The observation that macrophages associate with HPCs in injury models is particularly intriguing. Work in the field of hepatocyte mediated regeneration has demonstrated many roles for macrophages in the regenerative process, particularly the production of multiple stimulatory cytokines such as TNF and IL6 (Fausto *et al.*, 2006). None-the-less depletion of macrophages in such models has shown varying effects depending on the model system investigated. In either the normal liver or following partial hepatectomy in the rat, depletion of macrophages results increased hepatocyte proliferation (Boulton *et al.*, 1998). However, in other studies depletion by the same method resulted in delayed regeneration following partial hepatectomy (Takeishi *et al.*, 1999). The conflicts in these results are likely to lie in differences in the depletion protocols used. However the observation that constitutively macrophage deplete mice display impaired liver regeneration compared to wild type mice suggests a stimulatory role for macrophages in hepatocyte regeneration. This observation therefore supports a role for macrophages in hepatocyte mediated liver regeneration (Amemiya *et al.*, 2009). It is likely that macrophages may not simply play a stimulatory role but may be capable of both up and down regulation of hepatocyte mediated regeneration, possibly depending on different stimuli, and the presence or absence of different macrophage subsets.

A particularly important question relating to the observations reported in this work is why macrophages fail to associate with HPCs in the DDC model and does this lack of association result in alteration of HPC behaviour? The failure of macrophages to associate may be an active process which blocks their association, such as the exclusion of macrophages by another cell population which fails to grant entry of macrophages to the newly formed HPCs. Alternatively macrophage homing to HPCs which appears to be an active process in other model may be inhibited in some fashion, whether this may occur by a failure of production of chemotactic ligands or the absence of chemotactic receptors or inhibition of their downstream signalling a very interesting potential question for the future.

It is possible that macrophage chemotaxis is at least in part mediated by the CXCR4/SDF-1 axis, itself implicated in HPC function (see Chapter 1). SDF-1 is known to be produced in the periportal area and appears to play a role in guiding $CXCR4^{+}$ cells to this area (Kollet *et al.*, 2003). SDF is known to be upregulated following liver injury (Terada *et al.*, 2003). Macrophages which are well characterised to express CXCR4 and may in part be attracted to HPCs by this axis.

Similarly an important question, which is not fully addressed by this work, is what is the nature of the cells which lie between the macrophages and the HPCs in the DDC model and do they differ in identity or function to the cells of the HPC niche in other models where macrophages contact HPCs? Certainly a large proportion of cells sandwiched between the macrophages and the HPCs in the DDC model are myofibroblasts (Figure 3.10G) as they lie in direct juxtaposition to the HPCs. Further characterisation of this model is required to assess whether these are the only cells in this layer or indeed whether they are functionally analogous to the myofibroblasts seen in the niche in other models where macrophages penetrate this layer.

While in this study I have investigated the associations of macrophages, myofibroblasts and HPCs, other cell populations may occur in association with HPCs.

Work by Dr Stefania Lorenzini in collaboration with this work has shown that both B and T lymphocytes are also found in association with HPCs (Lorenzini *et al.*, 2010), and is in keeping with the previous description of expansion of lymphocytes in the CDE diet (Knight *et al.*, 2005a). This work is further supported by the observations of others that lymphocytes and in NK cells may play an influential role in manipulating HPC biology *in vivo* (Strick-Marchand *et al.*, 2008).

The association of laminin with HPCs has been previously reported in the rat AAF/PH model (Paku *et al.*, 2001). Detailed confocal analysis in this study demonstrated the appearance of a laminin rich basement membrane encasing cytokeratin^{+} HPCs. Whilst this membrane surrounded these cells, small holes were present in the membrane through which the HPCs make contact with non-parenchymal cells, which themsleves typically were desmin^{+}. The work presented here in the rat is consistent with the laminin encasement of HPCs in the rat PH/AAF model, but extends this observation to other murine models and human disease. A recent publication has also corroborated this work and has implied, although not definitely shown, that the expansion of laminin in the CDE diet model precedes the expansion of HPCs (Van Hul *et al.*, 2009). This report is consistent with work presented here, and also from others in the Forbes Group, which demonstrates a beneficial effect of laminin in maintaining a dedifferentiated state in HPCs *in vitro* (Lorenzini *et al.*, 2010).

3.9 Conclusions

In summary this work has established and characterised local model of mouse HPC activation and compared them to archival tissue from human disease and other rodent models of HPC activation. I show that the CDE and DDC dietary models reproducibly activate HPCs and do so with alternative phenotypes; the CDE with invasive cord-like structures, while the DDC does so with a periportal ductular expansion.

Upon characterising these models, there is a consistent association of myofibroblasts and laminin in direct contact with HPCs. While macrophages are in most instances found in direct contact with HPCs they are closely associated but excluded from direct contact in the ductular DDC model of HPC activation.

Chapter 4: Cellular recruitment to the HPC niche

4.1 Hypothesis

- The macrophages and myofibroblasts in the HPC niche are in part derived from bone marrow derived cells recruited to the HPC niche during liver injury

4.2 Aims

Having demonstrated that the cellular niche is stereotyped across a wide variety of species, diseases and animal models, I sought to answer the question of how this niche forms. To do this I aimed to:

- Examine the intrahepatic proliferation of cells of the HPC niche
- Examine the recruitment of BM derived cells to the HPC niche

4.3 Proliferation of niche cells during HPC activation

Having previously demonstrated reproducible HPC activation using the CDE diet I sought to investigate whether there was evidence of in-situ proliferation of the niche components. Previous work in this study has demonstrated that a large number of cells associated with the panCK^{+} HPCs are proliferating (Ki-67^{+}) in-situ (Figure 3.5). Utilising the benefits of EdU as a nucleoside analogue, in that it can be used with minimal antigen retrieval unlike BrdU or other markers of proliferation such as MCM2

or Ki-67, I investigated whether there was any evidence of proliferation of myofibroblasts and macrophages during CDE diet induced HPC activation by delivering EdU during the early phase of HPC expansion. Along with proliferation of HPCs proliferation of intrahepatic myofibroblasts and macrophages was observed (Figure 4.1). In a small proportion of instances these proliferating cells appeared to be in contact with cells morphologically compatible with HPCs. Therefore, there appears to be a role for active expansion of the HPC niche along with expansion of HPCs themselves.

Figure 4.1 *In situ* proliferation of macrophages and myofibroblasts

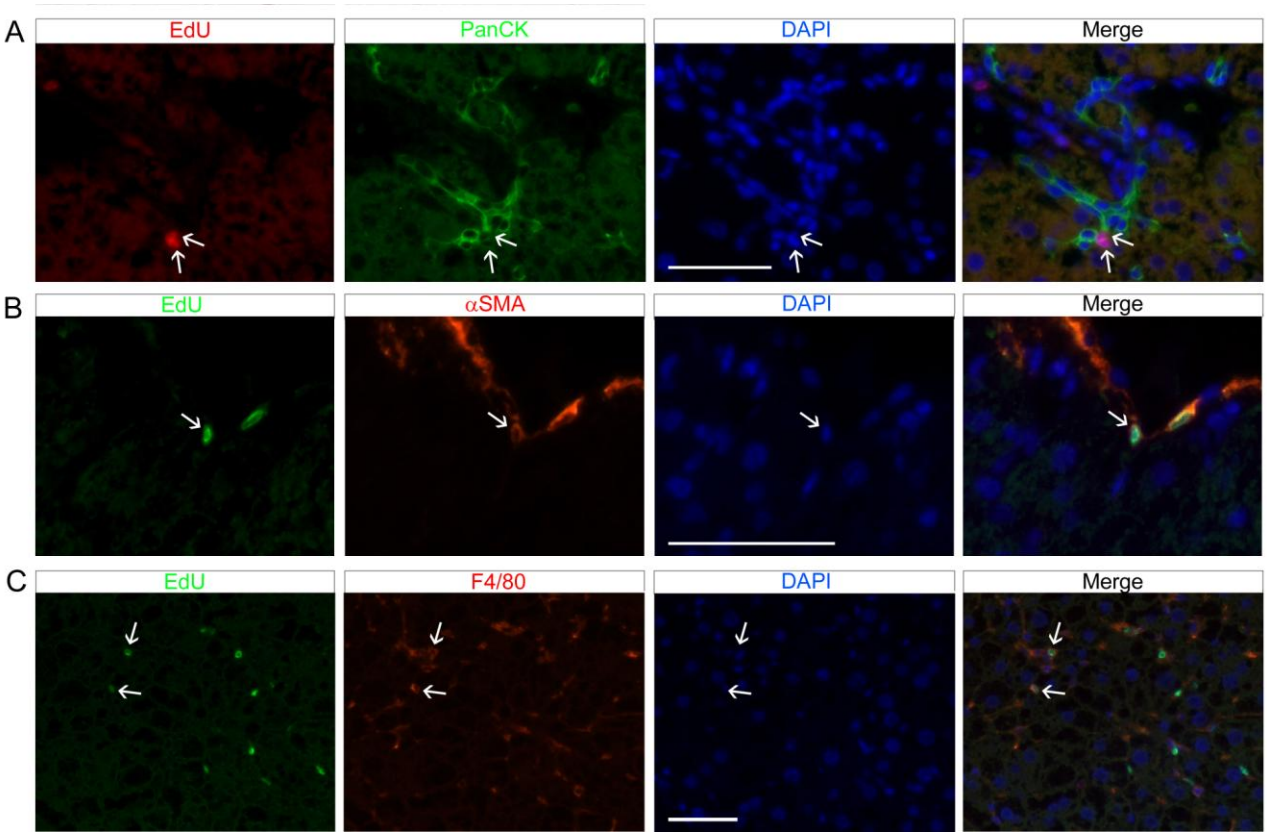

Mice were fed the CDE diet to induce liver injury and regeneration resulting in expansion of panCK$^+$ HPCs. Labeling of proliferating cells was assessed by administering EdU 2 hours prior to tissue harvest at 3 days. Colocalisation of cellular markers PanCK (A), αSMA (B) and F4/80 (C) was performed along with EdU detection showing active proliferation within each of these cell populations. All scale bars denote 50μm.

4.4 Cell tracking demonstrates macrophage recruitment to the HPC niche

As the BM is a source of both macrophages and hepatic myofibroblasts I chose to use a sex-mismatched BM transplantation model as a method of tracking the contribution of the BM to the HPC niche. The transplantation of BM in mice is well established and relies on the ablation of endogenous haematopoietic stem cells by a lethal dose of irradiation. An infusion of donor derived cells including haematopoietic stem cells is then delivered, and these donor derived cells are then able to engraft within the BM and reconstitute the haematopoietic system. This therefore affords the possibility of using antigens or markers in the donor haematopoietic stem cells which are not present in the recipient as a method of tracking BM derived cells from the point of haematopoietic reconstitution. The methodology I employed used whole BM from inbred C57Bl6 male mice to reconstitute inbred female C57Bl6 mice. Therefore the only antigenic difference between donor and recipient is the presence of the Y chromosome and its associated proteins. Following a period of recovery sex-mismatched BM transplanted mice were given either the CDE diet or control diet (Figure 4.2). Efficacy of reconstitution was assessed by examining the spleen of transplanted animals to ensure repopulation with male derived BM by using fluorescence in-situ hybridisation (FISH) directed again the Y-chromosome.

Examination of livers from mice following the CDE diet once again demonstrated expansion of HPCs. Using dual analysis of HPCs and BM derived cells it is apparent that HPCs themselves are not BM derived. No convincing evidence of a BM derived panCK$^+$ HPC was observed in any of the mice at confocal microscopy (Figure 4.3). It is also apparent from these images that a large number of BM derived cells have been recruited to lie around the HPCs (Figure 4.3 arrows).

Figure 4.2 Scheme of bone marrow cell tracking and HPC activation

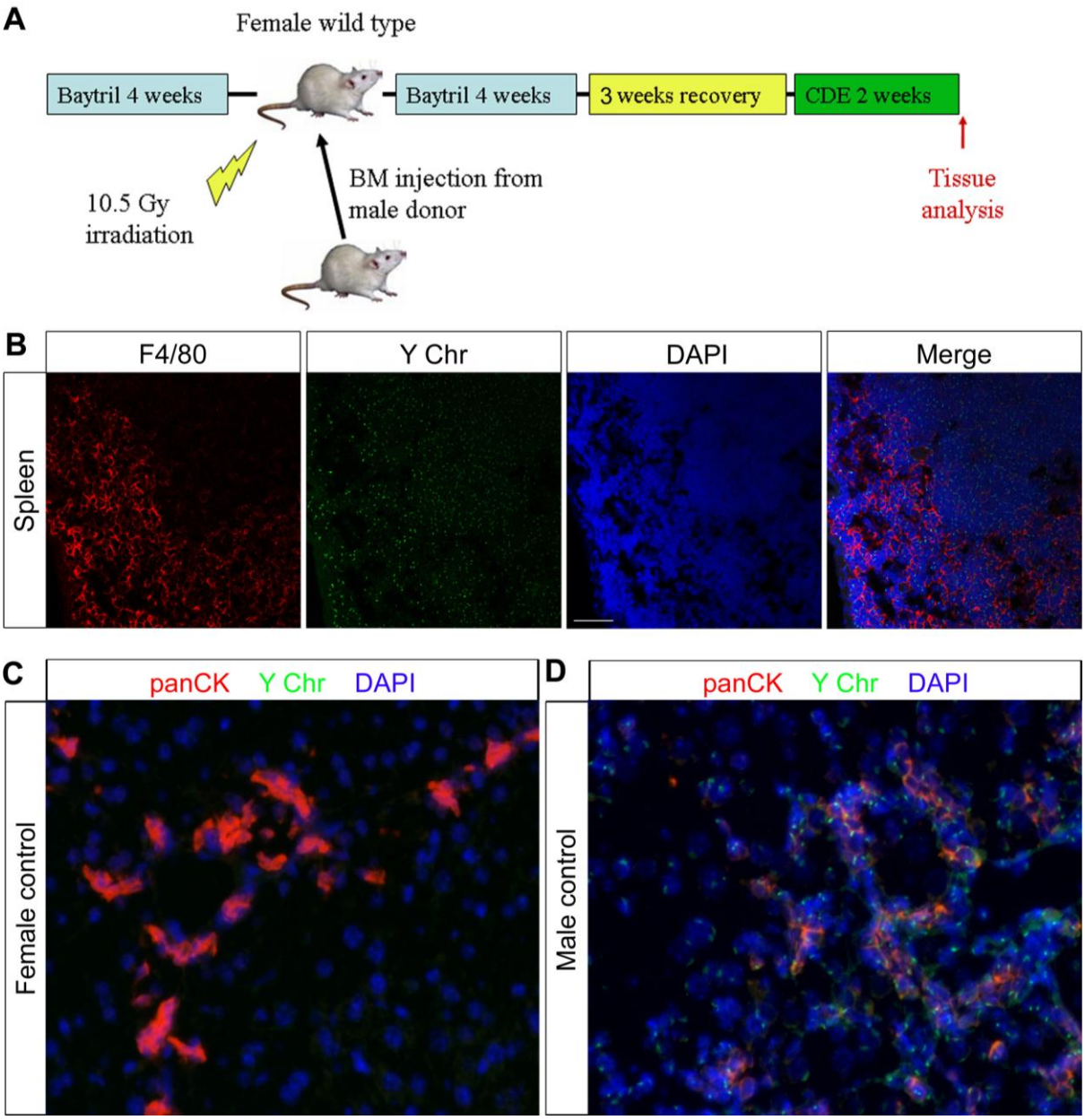

Following BM transplantation with male BM and a period of recovery HPCs were induced in female mice using the 50% CDE diet (A). To assess the degree of reconstitution the spleen was assessed in each animal to confirm repopulation with cells possessing the Y chromosome by FISH and confocal microscopy (B). To assess specificity of Y chromosome detection male and female mice which had not undergone BM transplantation were assessed in each instance. Representative Y chromosome analysis by confocal microscopy using FISH (FITC) combined with immunohistochemistry for panCK (Vector Red) in female (C) and male (D) controls demonstrates that intrahepatic cells are either Y chromosome negative or positive respectively. Scale bars denote 50μm.

Figure 4.3 HPC associated niche cells are frequently BM derived

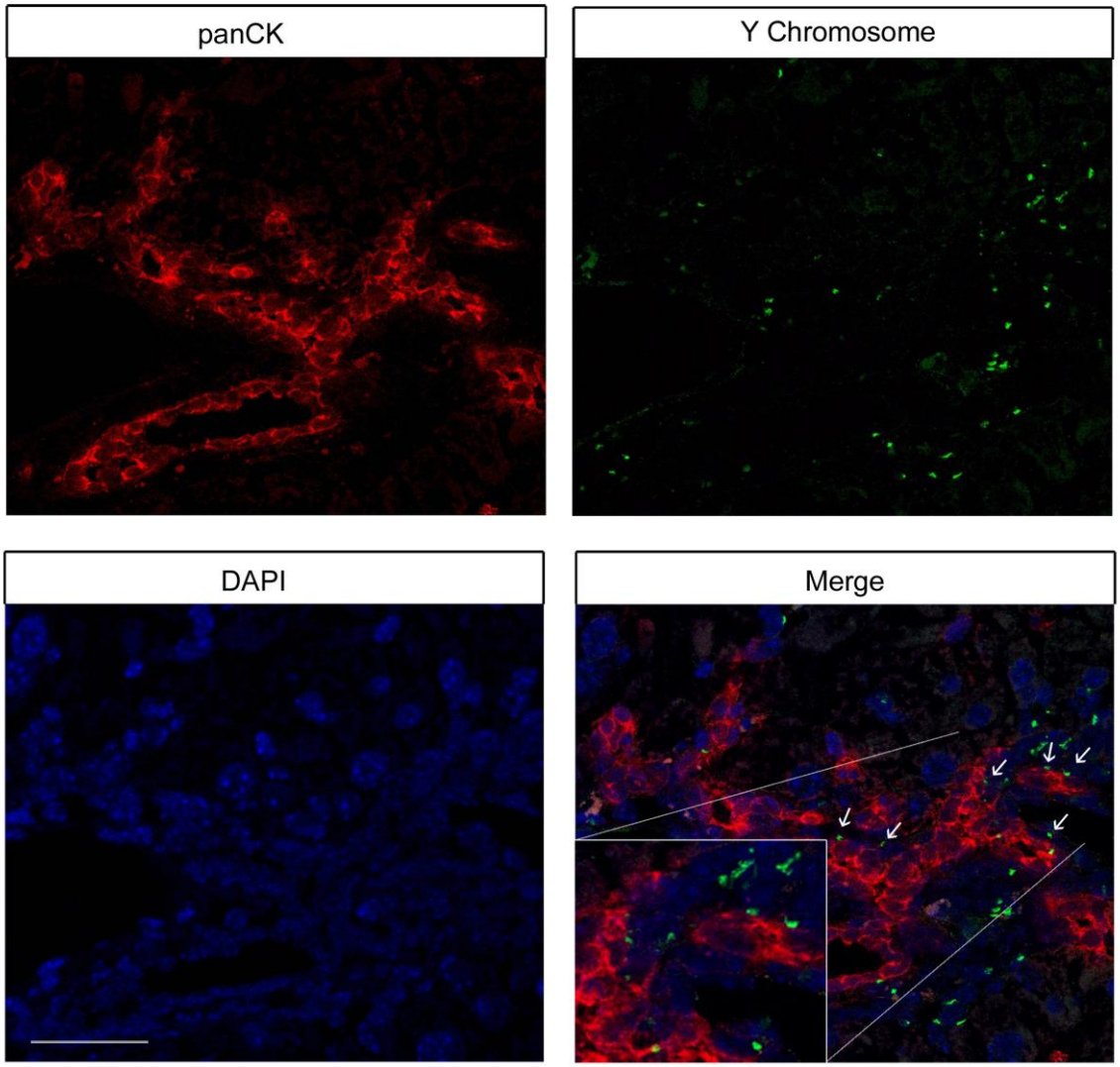

Dual analysis of panCK+ HPCs by immunofluorescence (Vector Red, red) and Y-chromosome^{+} BM derived cells by FISH (FITC, green). Arrows mark BM derived cells lying in direct contact with panCK^{+} HPCs. Inset demonstrates this association in high magnification. Scale bar denotes 50μm.

Having demonstrated that BM derived cells are recruited to the stem cell niche I then sought to identify the nature of these cells. To do this candidate BM derived cell populations were analysed along with FISH for the Y-chromosome. The majority of intrahepatic macrophages were identified as BM derived following 2 weeks of CDE diet (Figure 4.4A). Smaller numbers of myofibroblast were BM derived (Figure 4.4B),

while hepatic stellate cells were not (Figure 4.4C). A significant number of intrahepatic endothelial cells were BM derived; particularly those within the hepatic parenchyma (Figure 4.4D).

The identity of the BM derived niche component identified previously was examined using analysis of serial sections for the markers of non-parenchymal cell populations in combination with identification of HPCs and BM derived cells. In all instances BM derived macrophages could be identified in contact with panCK^{+} HPCs, however there was no evidence of BM derived myofibroblasts, hepatic stellate cells, or endothelia in direct contact with HPCs (Figure 4.5). Therefore macrophages are actively recruited to the HPC niche during regeneration in the CDE diet.

4.5 Discussion

As previously highlighted, the reproducible expansion of a stereotypical HPC niche is observed in a variety of rodent models in addition to human disease. This niche, consisting of macrophages and myofibroblasts, is not apparent in the healthy liver tissue, but instead appears to form synchronously along with HPC expansion. While each of these cell populations is present within the healthy liver and therefore may migrate into juxtaposition with expanding HPCs during regeneration it is apparent that a large proportion of HPC niche cells are actively proliferating in-situ (Figure 3.5). Certainly both cell populations in question are capable of intrahepatic proliferation and moreover appear to do so within the HPC niche (Figure 4.1). These observations are in accordance with published studies in other disease models demonstrating active proliferation of macrophages and myofibroblasts within the liver (Aktas *et al.*, 2003; Friedman, 2008).

Figure 4.4 Hepatic myofibroblasts and macrophages may be bone marrow derived

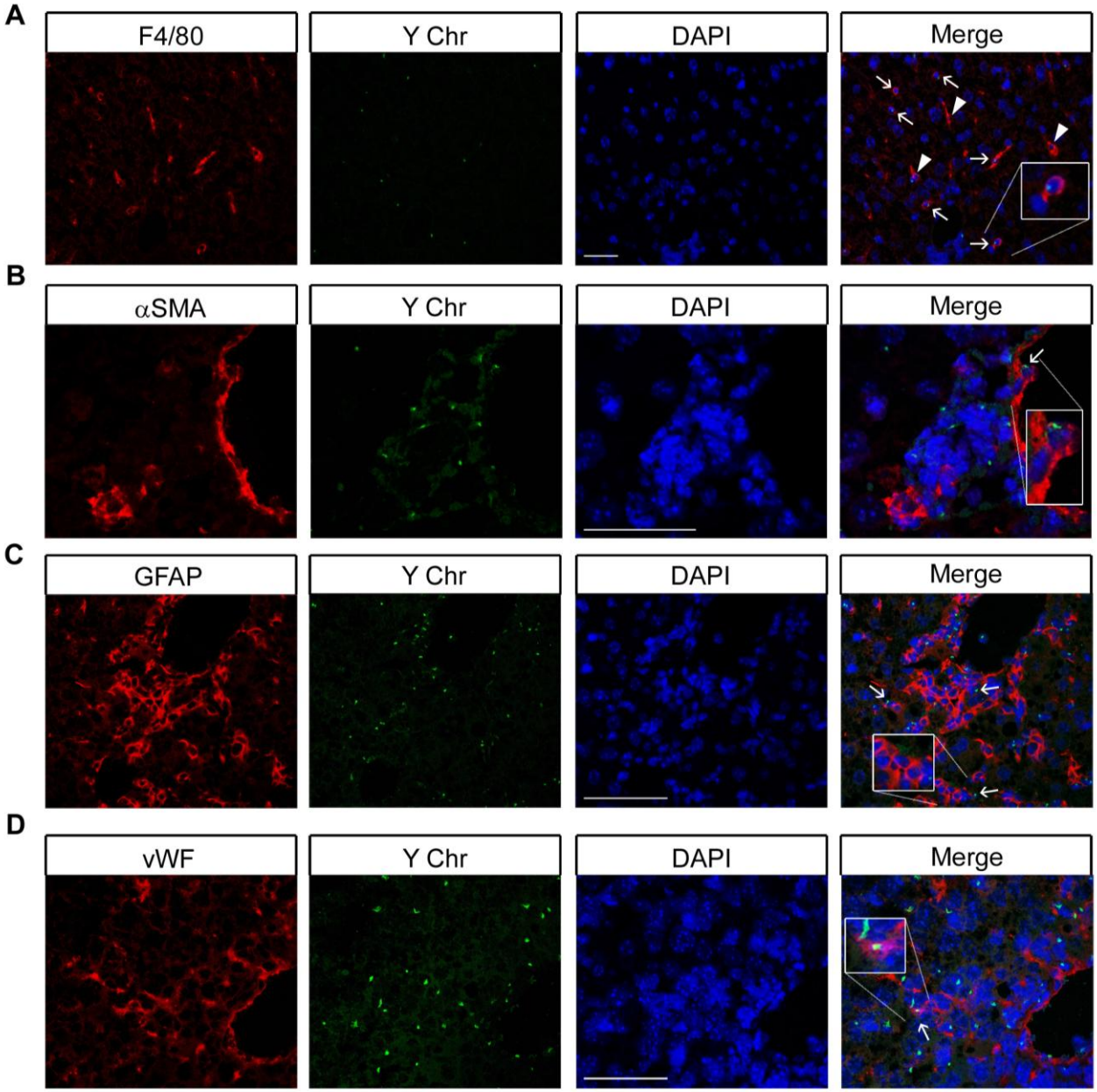

Following BM transplantation and CDE diet induction, (see Figure 4.2), non-parenchymal cell populations were investigated for potential BM origin by immunofluorescence and FISH. (A) The majority of F4/80^{+} macrophages are BM derived (arrows) whilst a significant minority apparently do not possess a Y chromosome. (B) Most myofibroblasts (αSMA) do not possess a Y-chromosome; however a small number, particularly perivascularly, are BM derived (arrow). (C) Hepatic stellate cells (GFAP) are not BM derived, nevertheless a significant proportion are found to be in direct contact with BM derived cells (arrow). (D) A minority of endothelial cells (vWF) are BM derived (arrow). All scale bars denote 50μm

Given also that both macrophages and hepatic myofibroblasts may be BM derived it is possible that elements of the HPC niche may be recruited from out with the liver in response to injury to form the HPC niche. In addition to intrahepatic proliferation I also find evidence that both populations may be derived from circulating cells which are most likely to be BM stem cell derived. Once again these observations are in line with previous BM transplantation studies (Klein *et al.*, 2007; Russo *et al.*, 2006). This study however is performed in a characterised model of HPC activation and therefore is a significant addition to our understanding of cellular recruitment in the context of intrahepatic stem/progenitor cell activation.

Figure 4.5 Niche macrophages are the recruited element in the CDE diet

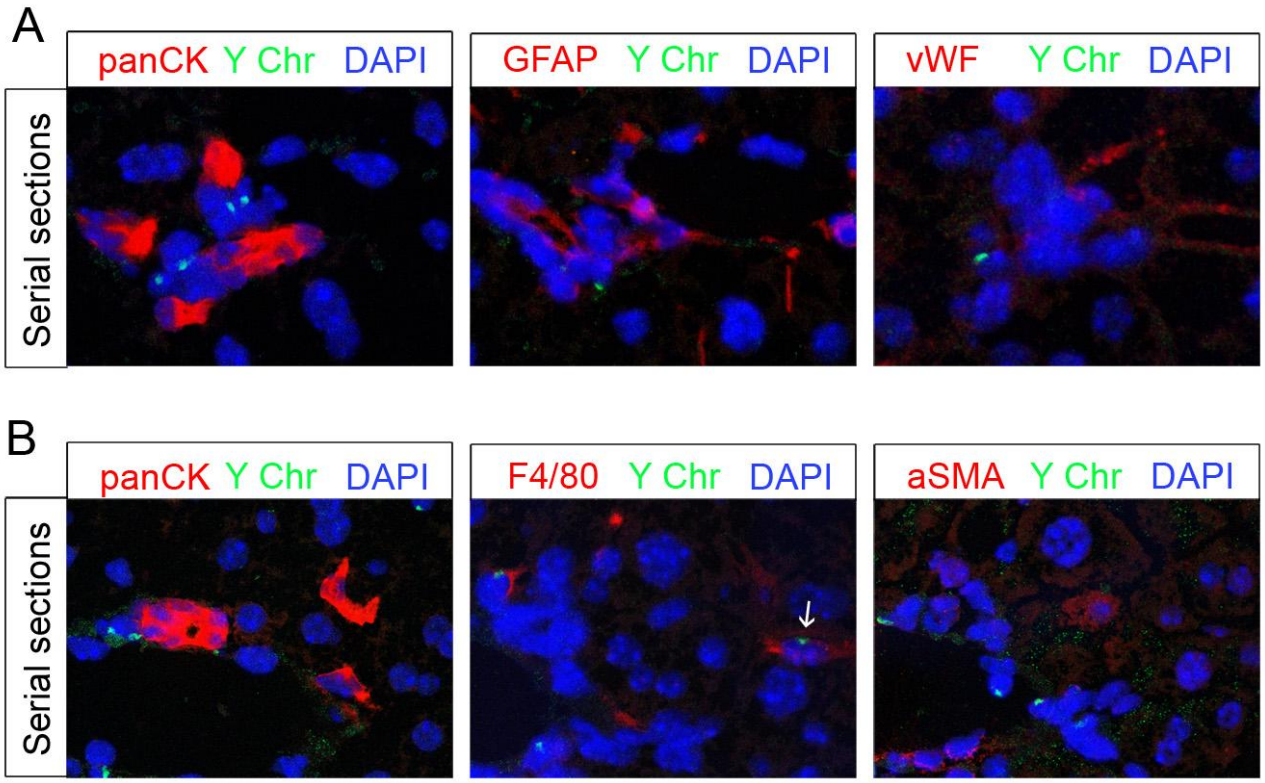

(A) and (B) Confocal analysis of serial sections of sex-mismatched mice treated with the CDE diet. Staining with panCK demonstrated closely localised cells positive for GFAP, vWF, F4/80 and aSMA positive cells. (B) F4/80 but not GFAP, aSMA, or panCK cells are Y chromosome positive.

For all assessment of the Y chromosome by FISH confocal microscopy was used in order to prevent the false association of chromosomes from one cell with that of an overlying nucleus of another. Using confocal microscopy and thin tissue sections (3μm) even in untransplanted male mice controls not all nuclei appear to contain a Y chromosome due to the three dimensional structure of the nucleus and its two dimensional analysis. For accurate quantification of the numbers of BM derived cells previous studies have used a correction factor based on the probability of finding a Y-chromosome positive cell but failing to identify the Y chromosome in that two dimensional plane (Russo et al.., 2006). Accurate quantification therefore is dependent also on the size of the nucleus in question. In order to track cells to the HPC niche I have been interested to observe whether this phenomenon occurs and not necessarily to what extent it occurs. While the identification of a Y-chromosome in any given male nucleus is relatively high I would predict that I have failed to identify every single BM derived cell in each individual image. Crucially I have not made attempts to quantify the extent to which this occurs, but merely have aimed to use this tool to identify both the presence of recruited cells as well as their nature in this study.

Using BM transplantation in this study it was possible to demonstrate that BM derived cells are recruited into juxtaposition with HPCs. It seems logical that this recruitment occurs during the period of HPC induction. Although this study does not directly address that question, it is possible although unlikely that the recruitment of niche cells and in particular macrophages occurred during the period of recovery when haematological repopulation had occurred but in the absence of injury. It seems likely however, that macrophages are directly recruited from the circulating pool during injury. The disproportionately high proportion of Y-chromosome negative macrophages seen in the liver during injury is testament to the longevity of these cells, as has been observed by other studies (Klein *et al.*, 2007). If the recruitment of intrahepatic macrophages to the HPC niche were occuring by stochastic process, a low proportion of niche macrophages would be expected to be observed throughout the liver, and yet examples of Y-

chromosome$^+$ niche macrophages are easily identifiable implying that this is not the case.

The observation that panCK$^+$ HPCs are not BM derived is consistent with previous reports both in the CDE diet (Tonkin *et al.*, 2008) and other models (Wang *et al.*, 2003a). As discussed previously HPCs are not believed, in most models, to be derived from the BM (Chapter 1). While some convincing reports using alternative methodologies of transplantation have demonstrated BM derived HPCs (Sun *et al.*, 2009), it is probable that strong immunological pressure towards selection of BM derived vs. transplanted HPCs in such models may be responsible for this phenomenon in this model system. The work presented in this thesis adds to the field, not only as a further report that HPCs in the models used in this work are not BM derived, but additionally also addresses the question of whether retrorsine or other toxins used in previous HPC induction regimes in some way inhibits the generation of HPCs from the BM (Vig *et al.*, 2006). These concerns regarding toxin effects on HPCs were raised regarding the discrepancy between the two sets of previous reports. In this work we have disproved that the use of such toxins is responsible for the failure to observe BM derived HPCs in the murine models such as those by Vig *et al.*

The demonstration in this thesis that HPCs are intimately surrounded by macrophages of BM origin provides a potential link between the BM and the intrahepatic stem/progenitor cells during injury, whereby the BM does not directly contribute to these cells but may influence their behaviour. Intriguingly whilst there is localisation and recruitment of macrophages to the HPC niche during injury, there is not a corresponding increase in hepatic macrophages. Indeed while macrophages appear to localise with HPCs there is a reduction in total hepatic macrophages during CDE diet HPC induction (Figure 3.11). This may be due to emigration or death of other parenchymal macrophages in the context of liver injury. This overall reduction in the hepatic macrophage population makes the presence and association of macrophages with the HPC niche even more striking.

In contrast to previous work in using BM tracking strategies with models of fibrosis in which significant numbers of myofibroblasts are noted to be of BM origin (Russo *et al.*, 2006) only a handful of BM derived myofibroblasts were observed in this study in the CDE diet. While this was the case no instance of BM derived myofibroblasts in direct contact with HPCs were observed. This work is therefore not at odds with the previous observations that scar associated myofibroblasts may be BM derived. Instead it provides a potential argument for differential populations of hepatic myofibroblasts within the liver with scar associated myofibroblasts being a more mobile population than those associated with HPCs. It is however possible that over the longer term HPC induction may be associated with significant recruitment of BM derived niche myofibroblasts.

4.6 Conclusions

- HPC niche elements are capable of intrahepatic proliferation during HPC activation
- HPCs are not bone marrow derived
- Bone marrow derived macrophages are recruited to the HPC niche during regeneration

Chapter 5: Macrophages as functional cells within the HPC niche

5.1 Hypothesis

- As a constituent of the HPC niche, macrophages play a functional role in controlling HPC activation

5.2 Aims

Based on the results of the previous chapter where active recruitment of macrophages to positions directly juxtaposed to HPCs during injury was observed, I wished to examine the functional effects of macrophages in the niche on HPC activation. To do so, methods of manipulating macrophage function in the liver were used including:

- Depletion of macrophage *in vivo* during HPC activation

- Adoptive transfer of bone marrow and macrophages to healthy liver

5.3 Introduction to models of macrophage manipulation

Depletion of macrophages provides an experimental approach to examine their functional roles in modulating HPC behaviour. Currently a number of depletion methods are described for macrophages including Liposomal Clodronate, Gadolinium Chloride and the DTR transgenic mouse system (Duffield *et al.*, 2005; Lee *et al.*, 2004;

Van Rooijen and Sanders, 1996). These varying depletion techniques have individual advantages and disadvantages. Liposomal clodronate, for example, is a substance that is selectively taken up by phagocytes which then die by apoptosis (van Rooijen *et al.*, 1996). It acts rapids and specifically and has been used successfully in the past to ablate hepatic macrophages/Kupffer cells in both rats (Sturm *et al.*, 2005; Van Rooijen and Sanders, 1996) and mice (Rivera *et al.*, 2007; Yamamoto *et al.*, 1996).

The effect of liposomal clodronate is related to the ingestion of clodronate by phagocytes by means of a liposomal vehicle. Neither clodronate, nor liposomes, are themselves toxic. Free clodronate, as a large molecule will not readily cross cell membranes. As liposomes are actively phagocytosed by macrophages, ingestion of liposomes results in uptake of clodronate which, once delivered into phagocytes will not escape from the cell. Therefore clodronate is accumulated intracellularly resulting in eventual toxicity and death by apoptosis (van Rooijen *et al.*, 1996).

The CD11b-DTR transgenic mouse system has been used successfully to deplete hepatic macrophages also (Duffield *et al.*, 2005). This system employs the use of a human EGF receptor (a relative of F4/80) which is the target for the highly toxic diphtheria toxin (DT). Whilst humans are highly susceptible to DT, normal mice are not. By expressing hEGF receptor under the control of the CD11b promoter, murine macrophages express hEGF thus rendering them susceptible to the toxic effects of DT. This therefore allows the depletion of $CD11b^{+}$ macrophages resulting in the incomplete deletion of hepatic macrophages depletion in a chronic liver injury model (Duffield *et al.*, 2005).

Given the variety of options for experimental hepatic macrophage depletion I initially set out to test the efficacy of macrophage depletion in the liver by the various methods available.

To test the CD11b-DTR system transgenic mice and WT controls were exposed to a range of DT doses. Liver analysis by immunohistochemistry for the F4/80 antigen revealed only partial depletion 24 hours after toxin administration (Figure 5.1C). Furthermore additional analysis revealed significant off-target effects of the transgenic models on other leukocyte populations including both B lymphocytes and $CD4^+$ and $CD8^+$ T lymphocytes (Figure 5.1F).

Given the only partial depletion and particularly the non-specific nature of the CD11b-DTR system I elected to trial liposomal clodronate delivered by i.v. injection. Analysis was performed at 24 to 72 hours post injection in otherwise healthy mice and revealed complete hepatic macrophage depletion over this time period (Figure 5.2A and B). Depletion of splenic macrophages was also observed over this time period although partial recovery was seen within the spleen only at 72 hours (Figure 5.2B). Having demonstrated effective and complete depletion of hepatic macrophages for over 72 hours following injection of liposomal clodronate, a trial of repeated dosing was used to assess whether ongoing complete hepatic macrophage depletion could be achieved following repeated liposomal clodronate administration. To exclude an improved reconstitution of hepatic macrophages following such repeated dosing, liposomal clodronate was given by injection every 72 hours. Tissue analysis was once again performed 72 hours following the last dose in this repeated dose strategy. Using the repeated dosing, ongoing and complete depletion of hepatic macrophages was achieved and occurred in the absence of clinical side effects (Figure 5.2C).

Figure 5.1 Transgenic DTR mouse mediated deletion of hepatic macrophages

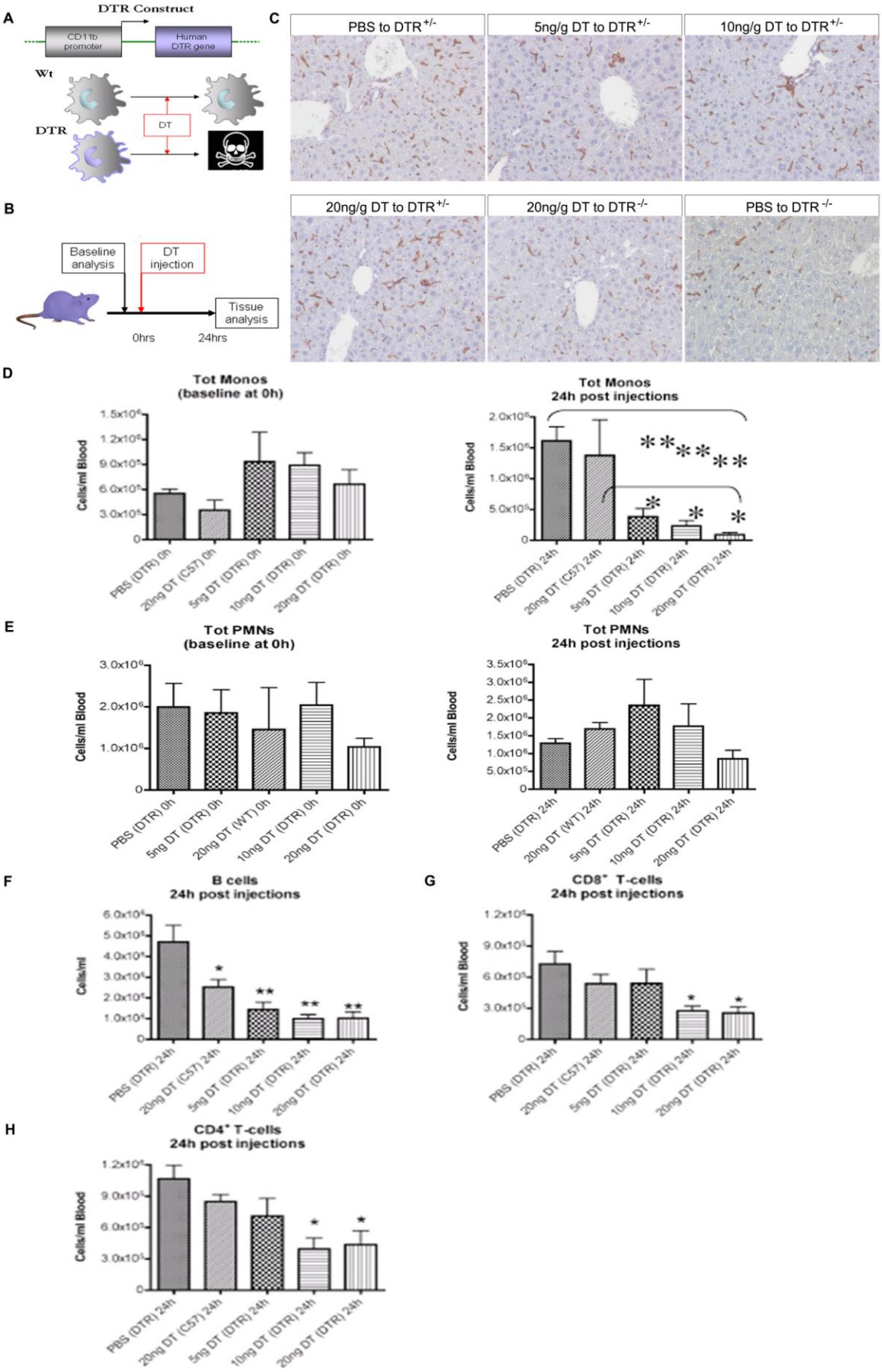

The Diphtheria Toxin Receptor (DTR) transgenic mouse construct places the human DTR under the CD11b promoter. (A). (B) DTR heterozygote mice and wild type controls were assessed 24 hours following a variety of doses of i.p. DT. (C) No significant depletion of hepatic F4/80$^+$ macrophages were observed following 24 hours in DTR mice treated with up to 20ng/g DT. (D) No significant variation is seen in peripheral monocyte numbers at baseline between animals, but a significant and dose dependent reduction in circulating monocytes is observed 24 hours following DT administration. (E) No significant changes in circulating neutrophil number is observed following DT treatment, while reductions of circulating B220$^+$ B lymphocytes along with CD8$^+$ and CD4$^+$ lymphocytes are noted in DT treated animals vs. control (F). FACS analysis performed with the help of Dr Tiina Kipari (p values denote Mann Whitney tests *$p<0.05$, **$p<0.01$). All scale bars denote 50μm.

To examine the functional role of macrophages in modulating HPCs behaviour an experimental protocol combining complete hepatic macrophage depletion with CDE diet mediated HPC activation was used over a 12 day period (Figure 5.3A). Firstly the efficacy of macrophage depletion by liposomal clodronate was assessed in this scenario. Complete depletion of hepatic macrophages was once again observed when repeated tail vein injections of liposomal clodronate were delivered every 72 hours during the CDE diet model. This depletion was seen both at early (Day 6) and late (Day 12) time points, each of which were 72 hours after the last liposomal clodronate injection (Figure 5.3B and C). Quantification of macrophages at sacrifice at day 12 reveal exceptionally efficient long lasting depletion of macrophages with a mean of 225 F4/80$^+$ macrophages per field in vehicle control mouse liver reduced to 0.72 per field in liposomal clodronate treated animals. There was no difference in the administration of PBS to untreated controls with 225 versus 234 F4/80$^+$ macrophages per field respectively.

Figure 5.2 Liposomal clodronate mediated deletion of hepatic macrophages

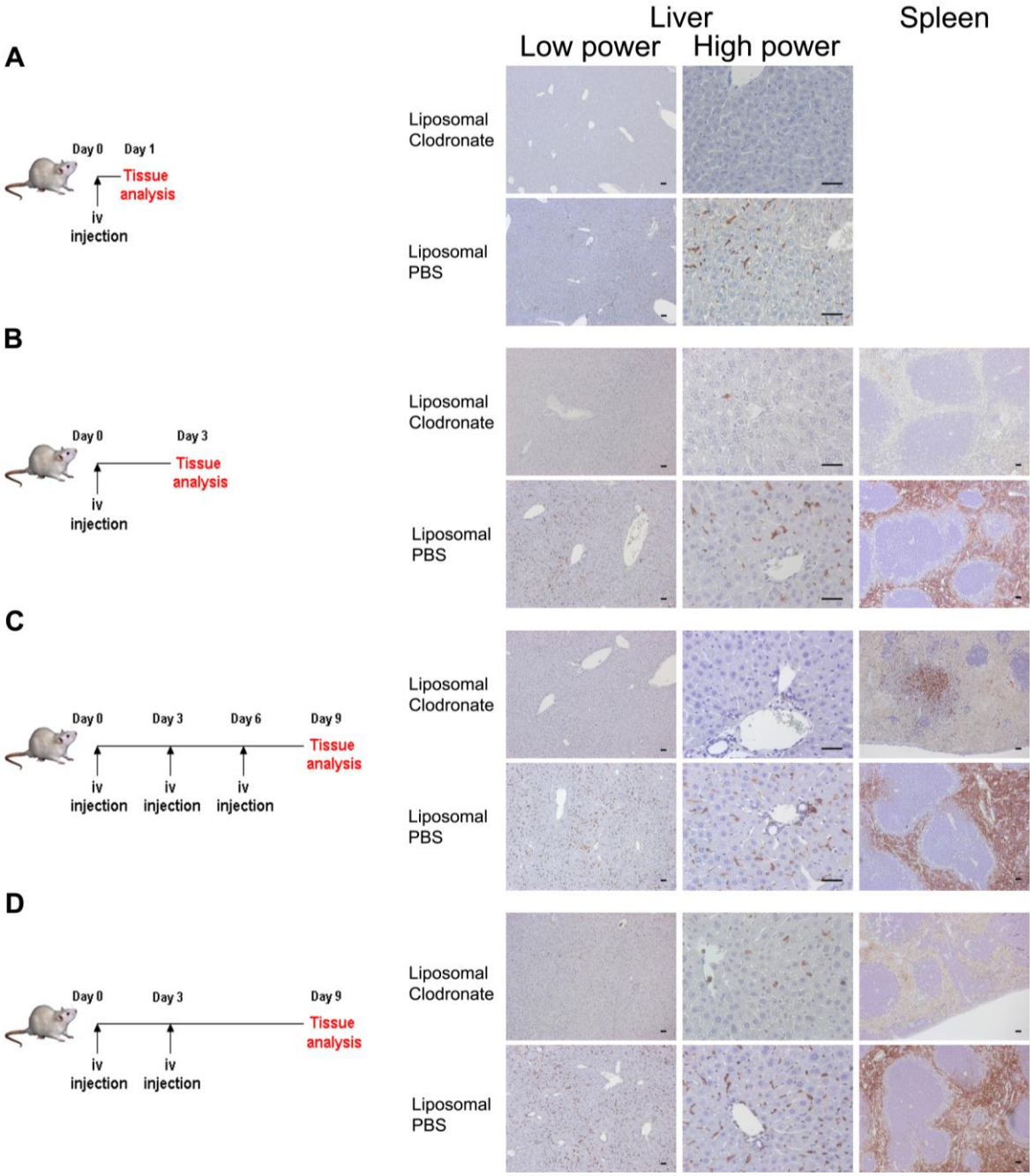

Liposomal clodronate was delivered via tail vein injection to healthy C57Bl6 mice to assess the efficacy and duration of deletion of F4/80^{+} macrophages by immunohistochemical analysis as outlined in each panel. (A) One day following injection complete depletion of hepatic macrophages was observed compared to control. (B) Similarly 3 days following a single injection of liposomal clodronate complete depletion of both hepatic macrophages and splenic macrophages is observed vs. control. (C) Using repeated injections to assess the efficacy of a prolonged macrophage depletion regime, complete depletion was once again observed 3 days but not 6 days (D) following final dose of liposomal clodronate. All scale bars denote 50μm.

5.4 Macrophages are not required for HPC expansion but influence HPC cell fate

The effect on HPC behaviour of continuous macrophage depletion during CDE diet induced HPC activation was then assessed. Examining HPC number in 3 repeated experiments (each n≥10) there was consistently no effect of the macrophage depletion on HPC expansion as assessed by the number of panCK$^+$ HPCs (Figure 5.3D and E). Quantification of panCK$^+$ HPCs confirms no effect of liposomal clodronate on HPC number following 12 days of CDE diet (mean per field 14.7 versus 10.57; n=10 each group; p=0.182 T test).

Other features were also examined in the context of macrophage depletion during the CDE diet. Dramatic increases were noted in serum transaminases with ALT increased from a mean of 228 to 735IU/L when CDE treated mice were treated with liposomal clodronate (Figure 5.3F). Significant increases were also observed in AST, Alkaline Phosphatase and Albumin following liposomal clodronate treatment (Figure 5.3G-I). Liver weights showed a consistent but non-significant trend towards enlargement following macrophage depletion. Mean relative liver weights at 6 and 12 days were 0.052 versus 0.046 (p=0.1; Mann Whitney) and 0.066 versus 0.58 (p=0.19) for Liposomal Clodronate and vehicle control animals receiving the CDE diet respectively (Figure 5.3J). No off target effects of liposomal clodronate were observed on morphology or cell number using *in vitro* HPCs culture versus PBS control (Personal Communication: Luke Boulter).

Figure 5.3 Macrophage depletion using CDE diet plus Liposomal clodronate

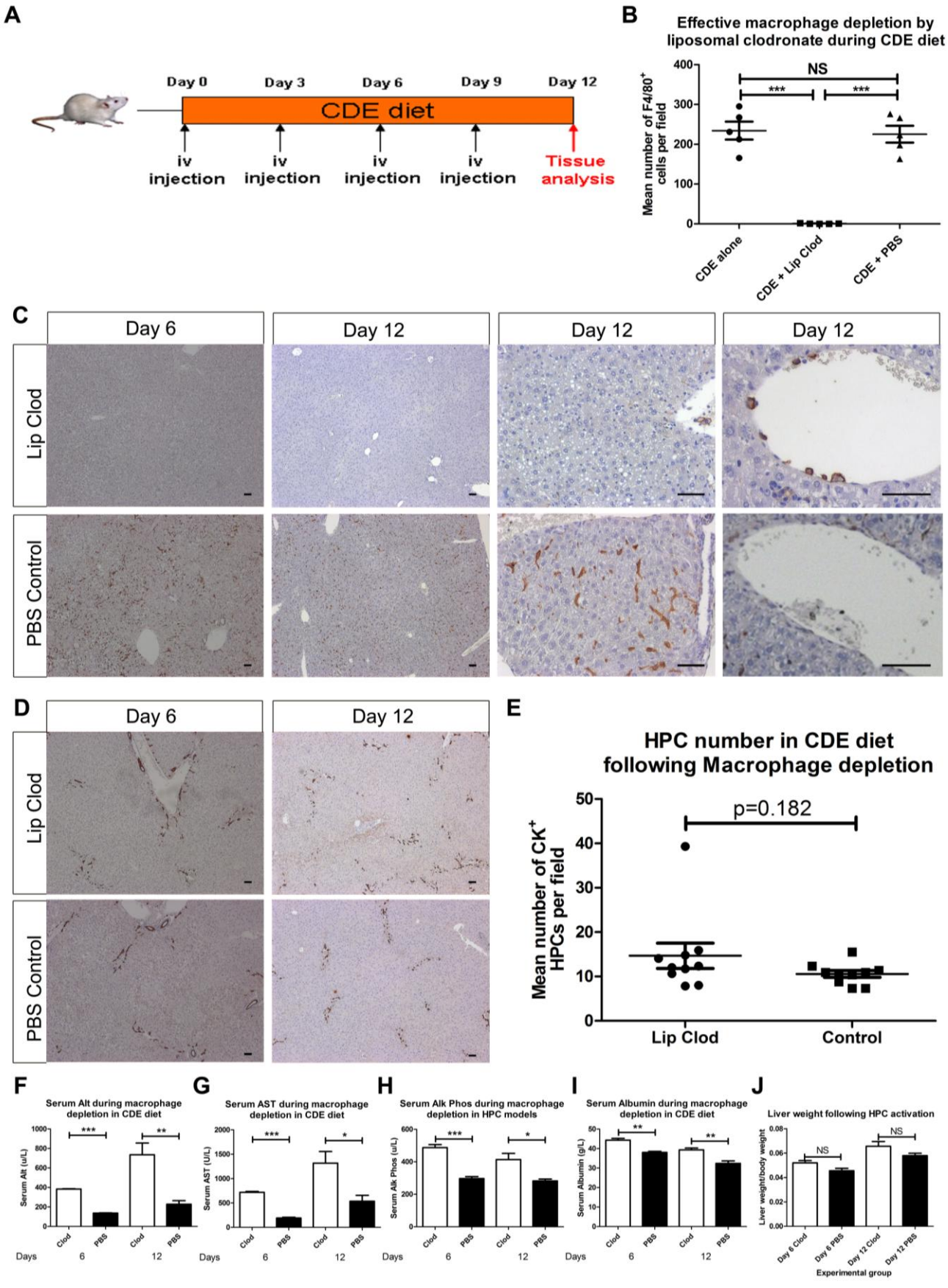

Following an experimental protocol (A) combining repeated liposomal clodronate injections during the CDE diet, highly efficient macrophage depletion (B) is noted by F4/80 immunohistochemistry at 6 and 12 days (C). Each group n= 5, p values denote one way Anova with Bonferroni multiple comparison, ***=P<0.001. No change in panCK$^+$ HPC number during the CDE diet in the presence of complete macrophage depletion (D and E). Each group n=15, p value denote T test result. Changes are noted in serum biochemistry at both 6 and 12 days. (F) Alt mean 384 vs. 137 (n=3; p<0.0001) at day 6 and 736 vs. 228 (n=5; p=0.0037) at day 12. (G) AST mean 719 vs. 191 (n=3; p<0.0001) at day 6 and 1317 vs. 536 (n=5; p=0.0195) at day 12. (H) Alk Phos mean 487 vs. 191 (n=3; p=0.0009) at day 6 and 414 vs. 132 (n=5; p=0.0107) at day 12. (I) Albumin mean 44.3 vs. 38.0 (n=3; p=0.004) at day 6 and 39.32 vs. 32.41 (n=5; p=0.0024) at day 12. Values are given for liposomal clodronate vs. vehicle control. (J) Liver size as assessed by liver weight/body weight demonstrates a consistent trends towards liver enlargement following liposomal clodronate treated livers vs. vehicle control p=0.10 and 0.19 for days 6 and 12 respectively.

A striking feature of macrophage depletion on HPC activation was noted when EpCAM$^+$ HPCs were analysed. While CDE diet consistently produces infiltrating cords of HPCs in the presence of macrophages, when macrophages were depleted areas were present with a markedly altered phenotype (Figure 5.4A). Here a ductular proliferation of EpCAM$^+$ cells surrounding a small and tortuous central lumen was observed. These changes were noted sporadically and were scattered throughout the liver parenchyma, but did not occur entirely at the exclusion of the infiltrating EpCAM$^+$ cells.

As the ductular morphology was particularly prominent on EpCAM identification but less so when assessment used panCK or Dlk1 as an HPC marker, the colocalisaiton of these markers was assessed. Due to the antibodies being raised in the same species a serial section approach was used to address this question. When serial sections stained with Dlk1, panCK, and EpCAM were examined in the macrophage replete and macrophage deplete CDE diet models striking overlap between the three HPC markers is observed (Figure 5.4B).

The ductular morphology of HPC expansion in the CDE diet is reminiscent of that observed previously in the DDC diet where $EpCAM^+$ cells also expand in a ductular morphology. Therefore I hypothesised that the absence of macrophage led to this altered morphology via a signalling mechanism which directs the fate choice of HPC down a biliary rather than hepatocellular differentiation pathway. While effects of certain signalling pathways discussed previously (Chapter 1) are known to influence HPC differentiation, a central candidate in this pathway is Notch signalling.

In collaboration with Luke Boulter, I therefore asked whether any consistent differences could be identified distinguishing HPCs in the DDC and CDE dietary models. The Notch inhibitor Numb was chosen as a potential candidate as it may link paracrine signalling from macrophages to alterations in the Notch signalling pathway which is known to be a crucial regulator of biliary differentiation (Chapter 1).

Using immunohistochemical examination Numb is identified in HPCs in the resting liver and is also present in HPCs in the CDE diet. Notably upon activation of HPCs in the DDC diet these cells markedly reduce Numb expression (Figure 5.4C), corresponding with a reduction in whole liver Numb gene expression (Figure 5.4D). To examine the effects of macrophage depletion upon Numb expression by HPCs from the CDE dietary model, HPCs were isolated using a liver perfusion technique followed by density centrifugation, and purification by FACS isolation of the $CD45^-$ HPC fraction. When this fraction from liposomal clodronate treated mice and PBS treated controls were compared a marked reduction in Numb expression was observed in HPCs from the macrophage depleted livers (Figure 5.4E).

Figure 5.4 Altered phenotype following macrophage depletion and Numb

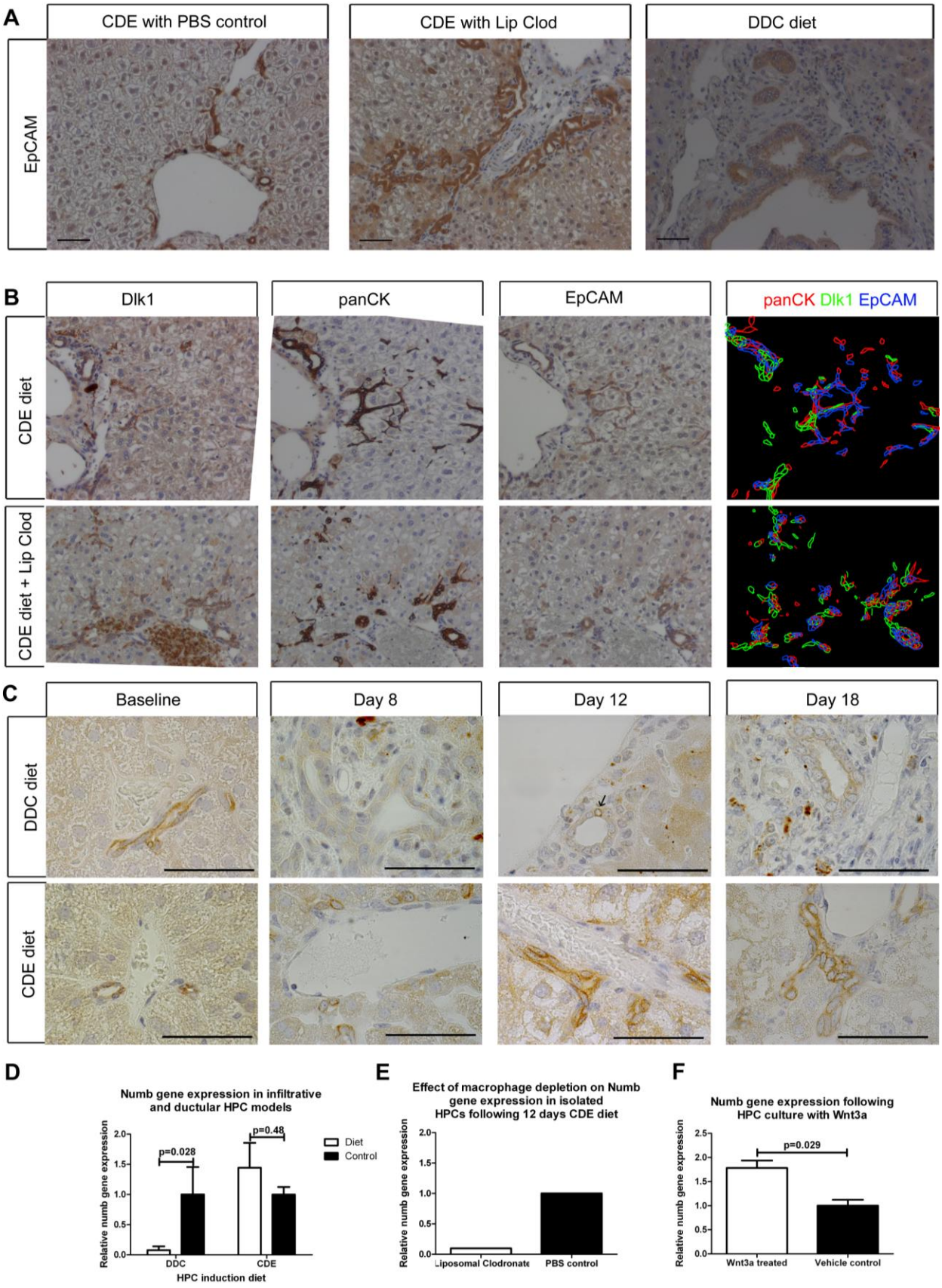

Following 12 days of the CDE diet with concurrent macrophage depletion as outlined in Figure 5.3A immunohistochemical analysis of $EpCAM^+$ HPCs was performed (A) and compared to DDC treated mice. A ductular morphology is seen in both macrophage depleted CDE diet and control DDC diet but not in control CDE diet. (B) HPC markers Dlk1, panCK, and EpCAM were assessed in serial sections revealing co-localisation of the HPC markers. (C) Immunohistochemical identification of Numb in HPCs. After 8 days of DDC diet there is widespread reduction of Numb expression by HPCs. A small number of DDC induced HPCs continue to express Numb (Arrow). Infiltrating HPCs in the CDE diet continue to express Numb. (D) Corresponding changes in Numb expression is seen by whole liver RT-PCR (n=4 each group; mean 0.078 vs. 1 and 1.44 vs. 1 for DDC and CDE vs. control respectively; p values denote Mann Whitney tests). (E) Reduced Numb gene expression in HPC isolated from macrophage depleted vs. macrophage replete livers following 12 days of CDE diet (pooled samples from n=5; mean relative Numb gene 0.097 vs. 1). (F) Elevated Numb expression in *in vitro* HPC cultures following addition of recombinant Wnt3a vs. DMSO vehicle control (n=4 each group, relative gene expression 1.78 vs. control, p value denotes Mann Whitney test). Work performed in collaboration with Luke Boulter. All scale bars denote 50μm.

5.5 Macrophage derived Wnt as the potential mechanism for influencing cell fate

The previous observations that (1) a central difference between the CDE and DDC diets is the loss of Numb expression during the DDC's ductular HPC activation, and (2) that a conversion of the HPC phenotype from infiltrative to ductular when macrophages are depleted in the CDE diet together with a loss of HPC Numb expression links the presence of macrophages and Numb expression. This therefore led to the hypothesis that paracrine signalling by macrophages directly influences HPC Numb expression and subsequently HPC cell fate choice.

As discussed previously the Wnt family of secreted signalling molecules have been reported to exert control over Numb expression (Chapter 1). Therefore, to examine a mechanism whereby macrophages directly influence Numb expression by HPCs, the role of paracrine Wnt signalling was investigated in this system. Firstly, when HPCs were cultured in the presence of Wnt3a their expression of Numb increases (Figure

5.4F). This data supports the hypothesis that macrophages promote Numb gene expression in HPCs in the CDE dietary model. This therefore implicated Numb as a part of a functional pathway by which macrophages promote an infiltrative morphology in the CDE diet.

Having demonstrated that HPC Numb expression may be increased by soluble Wnt we then asked whether macrophages make Wnts in the context of HPC activation. To examine this directly in an *in vivo* context, livers from CDE and DDC treated animals were digested and the hepatic macrophages isolated by FACS based on F4/80 expression. These isolated and purified ex vivo macrophages were subsequently analysed by RT-PCR for Wnt3a gene expression (Figure 5.5A). No significant changes were observed in hepatic macrophage Wnt3a gene expression. However a non-significant trend towards increased Wnt3a expression was observed in the CDE diet versus control.

Axin2 is an established marker of Wnt reception. Using an alternative approach to assess Wnt signal reception by HPCs *in vivo*, Axin2 gene expression by HPCs *in vivo* was examined in the CDE dietary model following macrophage depletion. Markedly reduced Axin2 gene expression is observed in purified HPCs isolated from the livers of liposomal clodronate treated mice undergoing the CDE diet versus CDE diet alone control (Figure 5.5B). In the same samples the effects of macrophage depletion upon HPC fate choice was assessed by examining the gene expression of hepatocytic (HNF4α) and biliary (HNF1β and HNF6) lineage markers (Figure 5.5C). A shift in expression of hepatocytic lineage markers to biliary lineage markers is observed in response to macrophage depletion (Figure 5.5C) in keeping with the changes from an infiltrative to a ductular HPC phenotype (Figure 5.4A). Similarly when the effects of Wnt are examined on HPC culture an increase in hepatocyte lineage HNF4α is observed (Figure 5.5D) together with no change in the biliary lineage marker HNF1β (Figure 5.5E).

Given the evidence for Wnt modulation of Numb as a mechanism by which HPC behaviour may be influenced by macrophages, I went onto investigate the role of Wnt in the CDE and DDC dietary models and whether correlating changes to HPCs occur during macrophage depletion in the CDE diet and macrophage replete DDC and CDE diets. Firstly whole liver changes in Wnt signal pathway were analysed at the transcription level and revealed upregulation of Wnt targets including cyclin D1, Jun, and c-myc consistent with a state of Wnt pathway activation in both the CDE and DDC models (Figure 5.6). Furthermore significant differences were observed in Wnt gene expression in each diet versus respective control, implying different hepatic Wnt expression signatures exist in the CDE and the DDC diets (Figure 5.6A). It is noted that whole liver gene expression of Wnt3a shows different trends to those observed for isolated hepatic macrophages (Figure 5.5A).

Many other alterations in Wnt related gene expression were observed in this study (see Appendix). Notable changes were observed in the expression of soluble Wnt inhibitors WIF and sFz (Figure 5.6C and D). To investigate the specific reception of Wnt by HPCs in the CDE diet I employed the use of the BATgal reporter mouse (Maretto *et al.*, 2003), which were a kind gift from Peter Hohenstein (MRC HGU Unit, Edinburgh). BATgal^{+} mice (Figure 5.7A) were fed either the CDE or control diet for up to 2 weeks to induce HPCs (Figure 5.7B). Their livers were then examined for the presence of β-galactosidase reporter expression by X-gal staining. No cells in the livers of either CDE diet treated or control BATgal^{+} mice were demonstrated (Figure 5.7C). Positive control liver used the constitutive expression of β-galactosidase in ROSA-26 mice and confirmed the staining assay performed correctly (Figure 5.7C). Failure of β-galactosidase expression in the adult BATgal mice was confirmed with an absence of expression of reporter β-galactosidase observed in the intestinal crypts of any of the BATgal^{+} mice (Figure 5.7C).

Figure 5.5 Macrophage depletion leads to loss of Numb and altered HPC fate

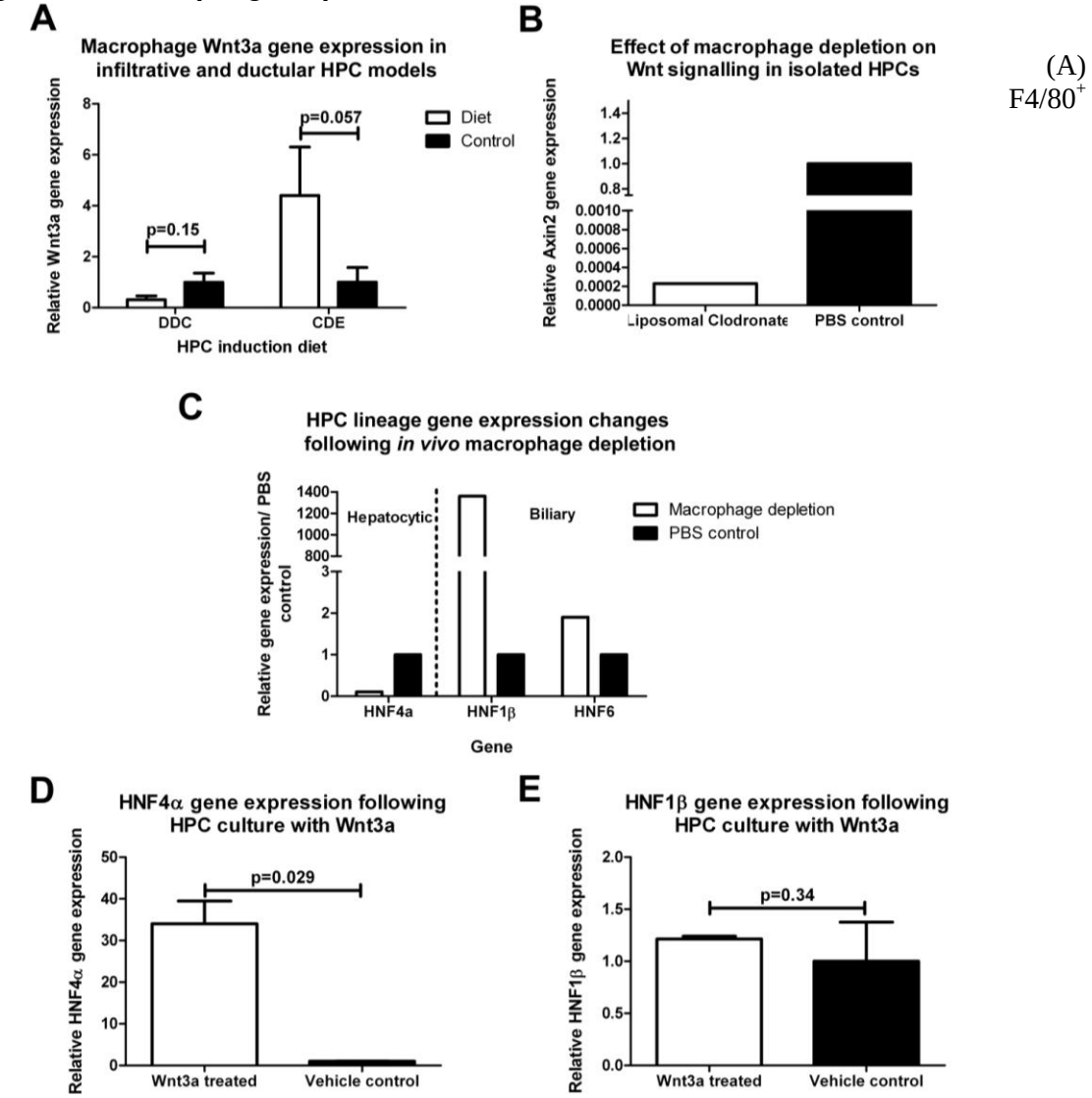

(A) F4/80^{+}

Macrophages purified by FACS after 12 days from livers of mice treated with CDE and DDC or respective control diets were analysed by RT-PCR for Wnt3a gene expression. A trend to reduction is observed in the DDC diet with a significant increase in macrophage Wnt3a gene expression is observed in the CDE diet (n=4 each group vs. control; 0.32 vs. 1 and 4.4 vs. 1 respectively; p values denote Mann Whitney test). (B) Analysis of purified HPCs from livers of liposomal clodronate vs. PBS control animals following 12 days of CDE diet (see Figure 5.3A) reveals markedly reduced Axin2 gene expression (pooled HPCs from n=5 each group; relative Axin2 expression in purified HPCs from livers <0.001 vs. PBS control). (C) Isolated HPCs from macrophage deplete CDE treated liver additionally show lower expression of HNF4α (0.11), but higher expression of HNF1β (1359) and HNF6 (1.90) relative to control CDE treated livers. (D) Elevated HNF4α but not HNF1β (E) gene expression is observed in *in vitro* HPC cultures following addition of recombinant Wnt3a vs. DMSO vehicle control (n=4 each group, relative gene expression 33.4 and 1.21 vs. control respectively, p values denote Mann Whitney test). Work performed in collaboration with Luke Boulter.

Given the failure of the transgenic reporter system in my hands, alternative strategies were employed to examine Wnt signal reception in HPCs. Firstly β-catenin, particularly its nuclear localisation, was examined by immunohistochemistry as a marker of active Wnt signal reception. This study revealed that high levels of β-catenin as observed in cells with HPC morphology in the CDE diet (Figure 5.7D). Lower levels were observed in the DDC diet and when the CDE diet was treated with liposomal clodronate. Sox-9 is an additional marker of active Wnt signal reception (Blache *et al.*, 2004). Changes in Sox-9 were also observed and again were consistent with increased Wnt signal reception by HPCs in the macrophage replete CDE diet than both the macrophage deplete CDE diet and macrophage replete DDC diet models (Figure 5.7).

The possibility of differentiated HPCs or hepatocytes being influenced by increased Wnt signal transduction was tested by a hepatocytes specific induction of APC deletion ($AhCre^{+}$ $APC^{flox/flox}$; see Chapter 6). Previously, highly efficient knockout of APC has been shown in this model (Reed *et al.*, 2008). When HPC activation is examined in the same mice, no evidence of HPC activation or altered HPC phenotype was observed in the context of active β-catenin signalling targeted to hepatocytes (Figure 5.7 E and F).

Figure 5.6 Wnt pathway activity in models of different HPC activation

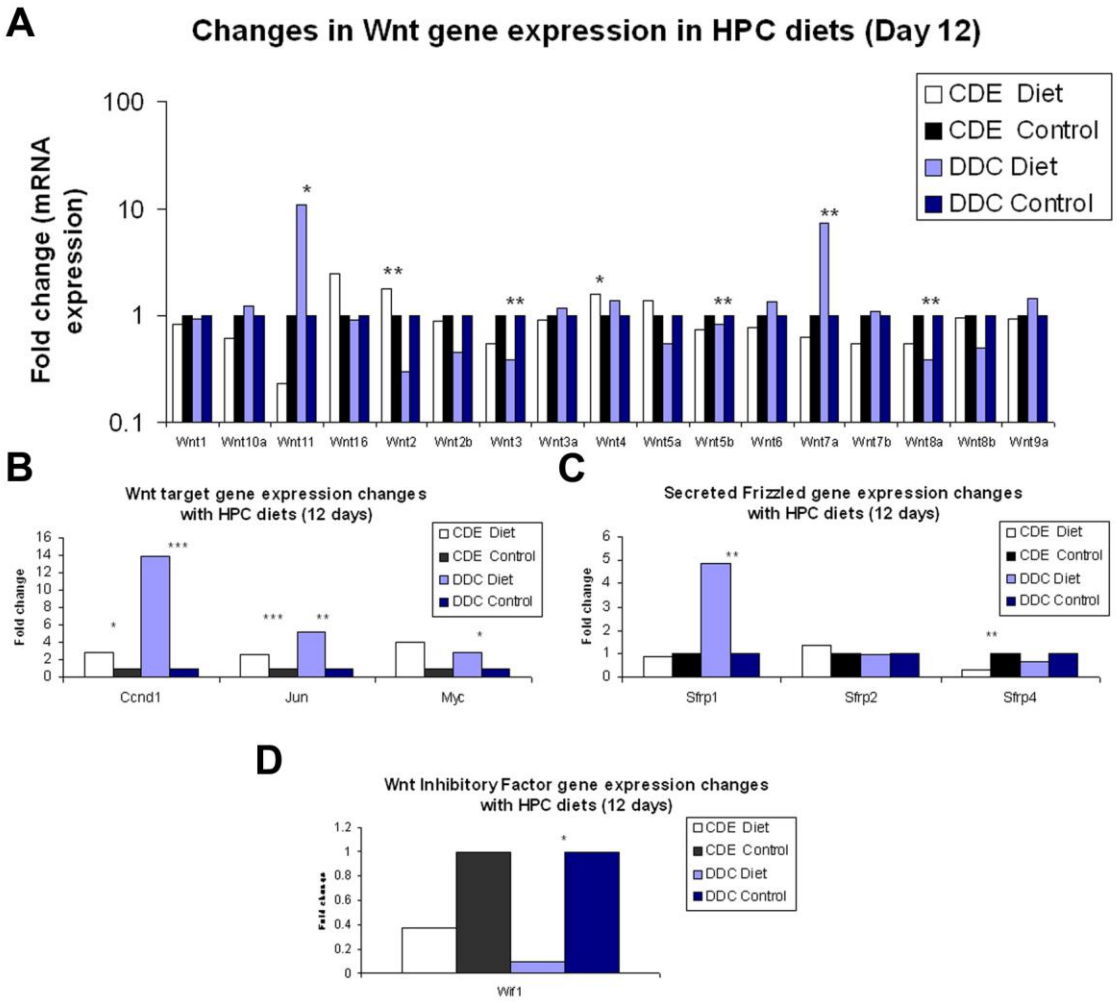

Whole liver was examined for Wnt related gene expression from C57Bl6 or S129 mice treated with 12 days of CDE or DDC diet respectively were compared to strain matched controls (n=3 each group). (A) Wnt gene expression varies between CDE and DDC diet and respectively control and Wnt target genes (B) Cyclin D1 (ccdn1), c-Jun (Jun) and c-Myc (Myc) are significantly increased in both the CDE and DDC diets vs. respective controls. Variations are also seen in expression of secreted Frizzled (sFz) and Wnt inhibitory factor (WIF) gene expression (C and D respectively) in the CDE and DDC diets vs. respective controls. Additional data in Appendix. (*p<0.05, **p<0.01, ***p<0.001). Performed with n=3 each group.

Figure 5.7 Wnt activity in CDE diet and failure of BATgal reporter system

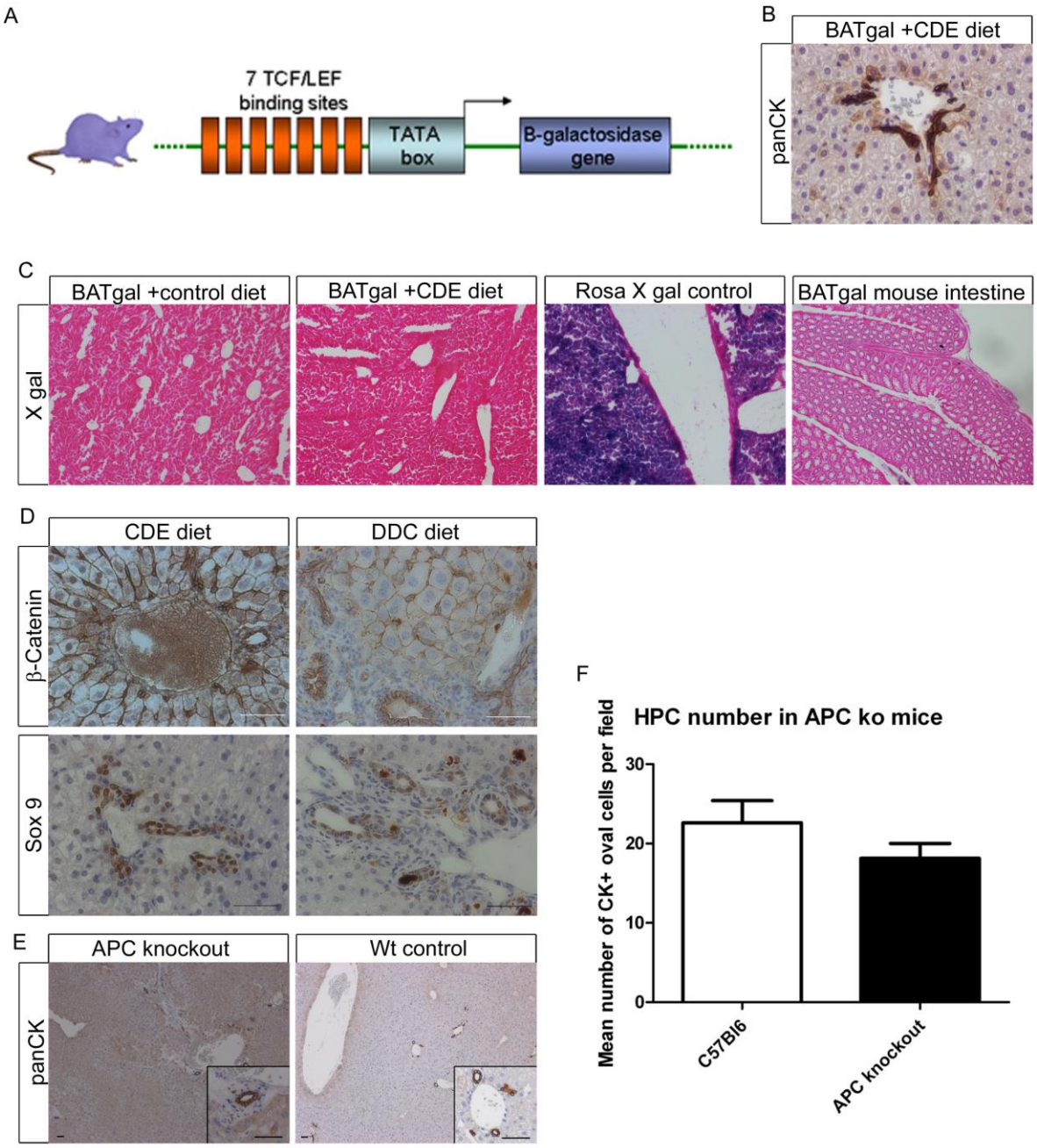

(A) The BATgal reporter construct used to test Wnt signal reception *in vivo* by activated HPCs during the CDE diet (B). (C) Xgal staining of liver and intestine in the BATgal reporter mice reveal no expression of β-galactosidase as compared to ROSA26 control. (D) Immunohistochemical staining for β-catenin and Sox-9 in HPC model identifies cells Wnt signalling in cells with HPC morphology; staining performed by Dr Alicia Cole. (E) 4 days following 80mg/kg βNF induction in $AhCre^{+}$ $APC^{flox/flox}$ mice HPC activation was assessed versus $AhCre^{-}$ $APC^{flox/flox}$ control with no alteration in morphology or expansion (F) in HPCs identified (n=≥3 each group). All scale bars denote 50μm.

5.6 Niche engraftment by macrophages is sufficient for HPC activation in the absence of injury

5.61 Background to experimental methods

Macrophages have been described to play a role in stem cell niches in other organs in the context of injury. In published models, macrophages are described to increase the numbers of stem cells and promote wound healing. My results suggest that in the liver, macrophages play a role in specifying progenitor cell fate in the context of injury. While no effect on HPC expansion as measured by cell number was observed, it is possible that macrophages may also play a role in HPC expansion. We therefore sought to ask the question of whether macrophages are capable of stimulating HPCs in the liver. To address this question using the numbers and proliferation of HPCs as a readout we utilised the known propensity of BM derived cells to engraft in multiple tissues even in the absence of injury. We elected to utilise an approach of delivering macrophages and whole BM via peripheral vein. This offers the advantage of being minimally invasive which is of benefit with regards to simplification of the model, in addition to mimicking what is frequently used in BM transplantation studies and human therapy.

Multiple studies in the field of BM transplantation have tracked the efficiency of BM engraftment in organs following infusion via a peripheral vein. The liver, BM and lung are the principle sites of engraftment in an un-irradiated mouse recipient of whole BM with each organ experiencing approximately the same proportion of donor cell engraftment (Cui *et al.*, 1999). Importantly each tissue appears to show different dynamics of cellular engraftment with variability in engraftment seen both over time in organs and between different organs.

Recently, several studies have suggested beneficial effects in human patients with liver injury following the intravenous delivery of BMCs. These effects have included endpoints such as liver function and regeneration (Houlihan and Newsome, 2008).

Therapy using BMC is clinically attractive from a variety of perspectives. The BM is readily available under minimal invasive techniques, and provides an autologous source with consequent immunological advantages. Furthermore donor BMCs may be purified, expanded and manipulated to enrich for beneficial effects or populations. Previously reports that BMCs themselves may adopt an epithelial phenotype in the liver are now thought to be unfounded or to occur at an insignificant magnitude (Chapter 1). None-the-less the effects of BMCs in humans and murine studies along with their known trafficking into the liver, may suggest that following engraftment their effects upon resident liver cell populations may be elicited by paracrine signalling. Such a paracrine signalling mechanism is yet to be described in the literature. Furthermore the effects I have observed previously of trafficking of macrophages into the HPC niche where they can influence HPC behaviour may provide a mechanism by which BMC therapy results in the beneficial effects described to date.

5.62 Transfer of syngeneic BMCs to healthy mice results in HPC activation in healthy recipient mice

I therefore sought to utilise the propensity of BMCs to engraft within the liver to investigate whether macrophages may play a role in HPC activation. My experimental model used healthy un-irradiated mice which received unfractionated BMC from in-bred littermates. Using male to female BMC transfer tracking of donor derived BMC is possible using the presence of the Y-Chromosome as a marker as previously described (Chapter 4).

Initial observations were made in female mice which received a single transfer of 10^7 unfractionated BMCs from male donors (to allow cell tracking via the Y chromosome). These animals showed a consistent, periportal expansion of panCK, Dlk1 and EpCAM positive HPCs, from day 7 post transfer onward which lasted for up to 6 weeks (Figure 5.8). This effect was observed in both recipient of sex-mismatched and sex-matched BMC. Irradiation of BMCs prior to infusion rendered them incapable of inducing HPC

activation (Figure 5.8), In both instances HPC activation is observed to occur in earnest between 1 and 6 weeks following BMC transfer. Examination of proliferation using BrdU at early time points demonstrates that as early as 1 day following BMC transfer proliferation is seen within the HPC compartment (Figure 5.8). The HPC expansion seen histologically is mirrored by an increase in HPC RNA expression with significant increase in CK19 gene expression along with consistent trends to increased expression in EpCAM, and Fn14 gene observed also (Figure 5.8).

Further examination of mice receiving BMC transfer revealed a number of other striking effects. Firstly following a period of initial reduction in liver size, a consistent and significant increase in size of livers is observed in mice following BMC transfer returning to normal size over a period of 2-6 months (Figure 5.9). This increased liver size occurred between 3 and 6 weeks following BMC transfer, and therefore is associated with the expansion of HPCs. In the longer term this relative hepatomegaly normalises with no difference in liver size 100 days post BMC transfer.

Serum analysis performed following BMC transfer reveals a relative reduction in serum albumin immediately following HPC transfer. This occurs along with an increase in whole liver albumin gene expression (Figure 5.9).

In all previous models of HPC induction described to date, a significant hepatocellular injury is observed and is believed to drive resultant HPC activation. Histological analysis of specimens following BMC transfer however revealed no evidence of significant hepatocellular injury at any time point (Figure 5.8). Therefore I sought to investigate whether any detectable evidence of liver inflammation or hepatocyte injury occurred using a number of different methods. Despite the administration of BMC containing a large leukocyte population no prominent $CD45^+$ infiltrate was observed in the liver by immunohistochemistry (Figure 5.10A). Furthermore there was no elevation of serum transaminases in mice treated with BMC transfer (Figure 5.10B and C).

Figure 5.8 Whole BM transfer results in HPC activation in healthy liver

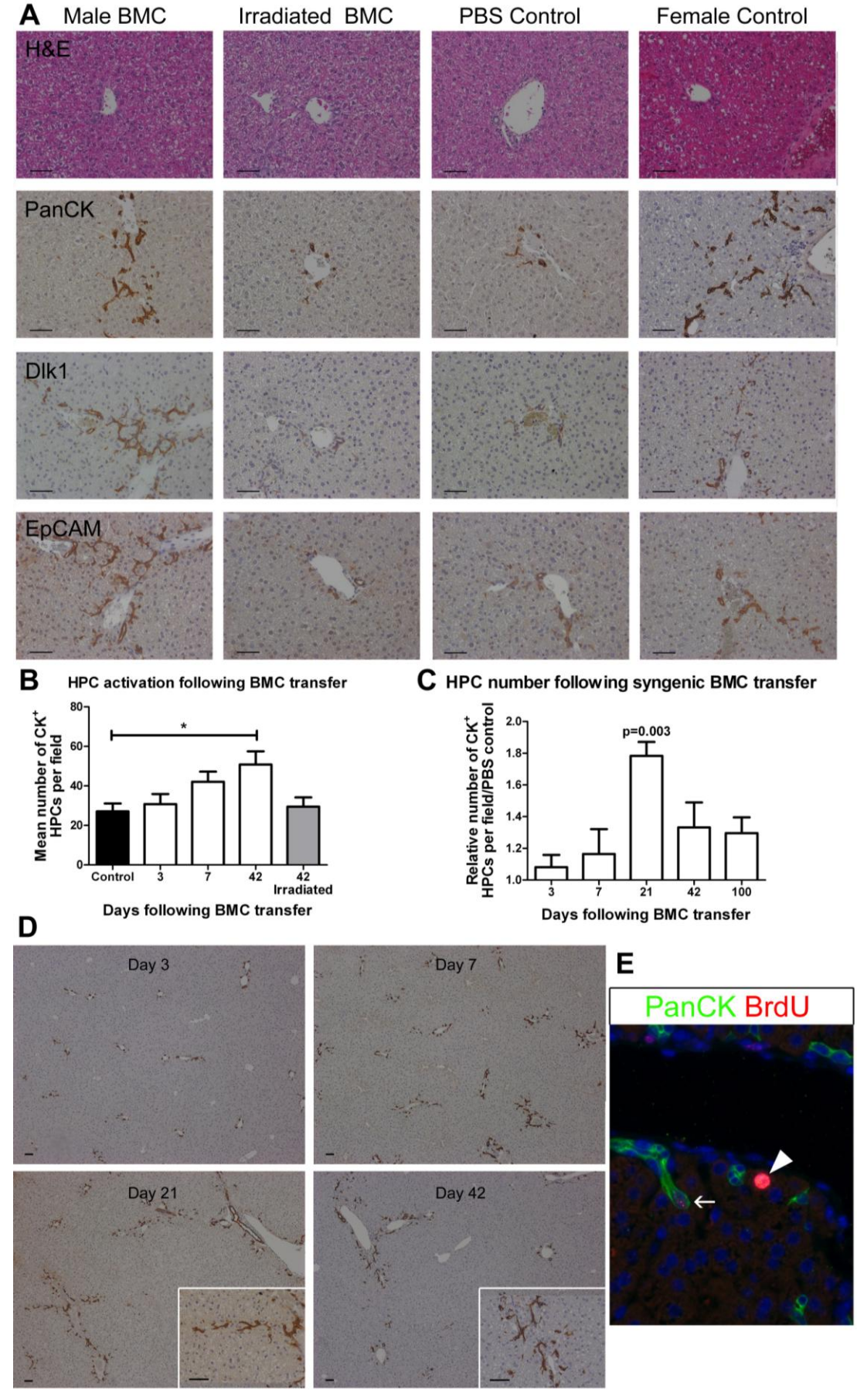

(A) Absence of injury with simultaneous expansion of HPCs in female mouse liver 42 days following tail vein injection of 10^7 BMCs from inbred male donors. Male BMC transfer experiments were repeated 4 times, each with n=5 animals per group. (B) Quantification of HPCs over time following after transfer of 10^7 male BMCs (n=5 each group, except n=2 at day 3,7 and 21). Data is presented as mean number of cells per field±SEM. (C) Quantification of HPCs over time following after transfer of 10^7 syngeneic BMCs from inbred female donors (n=5 each group). Data is presented as relative change in cells per x200 magnification field (experimental mean/time matched control mean)±SEM. (D) PanCK$^+$ HPCs in inbred female recipients of syngeneic BMC transfer with corresponding HPC quantification. (E) Proliferation of HPCs is seen as early as 1 Day following cell transfer (BrdU 2 hours prior to tissue harvest), with progressive expansion over subsequent 3 weeks. All scale bars denote 50μm.

Figure 5.9 Functional consequences of whole bone marrow transfer

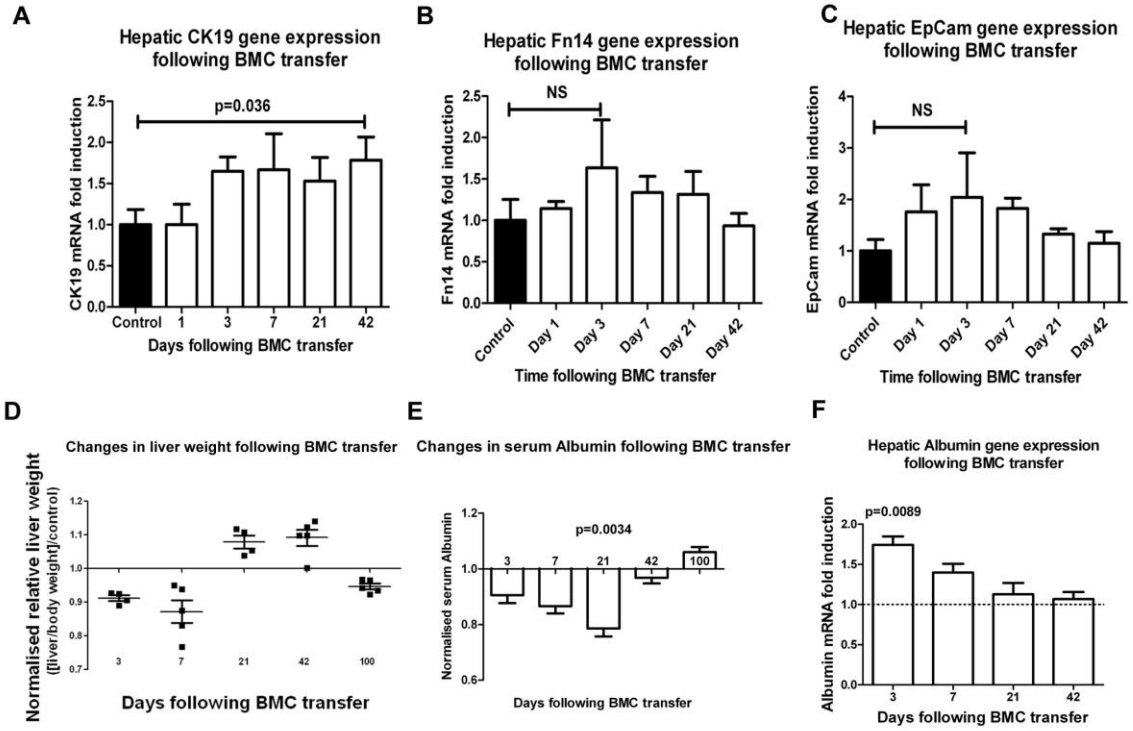

(A-C) HPC marker gene expression is raised in whole liver following syngeneic BMC transfer (CK19, Fn14 and EpCAM respectively). Values represent fold change versus 24 hours post PBS transfer, mean±SEM. (D) Liver size assessed by relative liver weight (liver weight/body weight)/(control liver weight/control body weight) following syngeneic BMC transfer (n≥4 each group). p values denote t-test result vs. control. (E) Initial reduction in serum albumin is followed by increases in serum albumin and occurs following increases in whole liver Albumin gene expression (F).

HPC activation is strongly associated with carcinogenesis in both human disease and rodent HPC models. I therefore wished to examine whether the transient induction of HPCs in the BMC transfer model resulted in long term side effects. Examining mice (n=5) for 400 days following BMC transfer no adverse effects were seen. Specifically careful examination of livers at harvesting revealed no macroscopic or microscopic evidence of liver tumours. Histologically the livers appeared normal and while relative increases in HPCs were seen compared to young mice, no changes were seen against aged matched controls (Figure 5.11). Additionally no biochemical abnormality was observed in mice 400 days following BMC transfer (Bilirubin 8±3.12, ALT 27±7.19, AST 299±211, Albumin 35±0.63; Mean±SEM; n=5).

5.63 Bone marrow transfer results in transient liver engraftment by donor-derived macrophages

To examine the biology of donor cells within the recipient liver, two independent cell-tracking strategies were employed. Firstly Y chromosome detection from the sex-mismatched BMC transfer group was performed. In addition, a separate series of GFP mismatched BMC transfer experiments were performed whereby GFP^+ donor BMCs were delivered to WT littermates. Examination of both series of experiments demonstrated rapid, albeit transient, engraftment of the recipient liver with donor–derived cells, with no evidence of detectable transdifferentiation of donor BMCs into HPCs or hepatocytes (Figure 5.12). Whilst after one day following transfer, donor cells were seen throughout all three zones of the hepatic lobule with no specific localisation (Figure 5.12A), from 3 days following transfer, donor-derived cells were found directly adjacent to bile ductules and HPCs, and frequently made direct physical contact with the $panCK^+$ progenitors (Figure 5.12B and C). By seven days following BMC transfer the numbers of engrafted cells was considerably lower than at either of the previous time points examined. Again cells were seen in direct contact with $panCK^+$ HPCs. After 21 days following BMC transfer no convincing donor derived cells were seen in the recipient livers.

Figure 5.10 Absence of injury or inflammation following BMC transfer

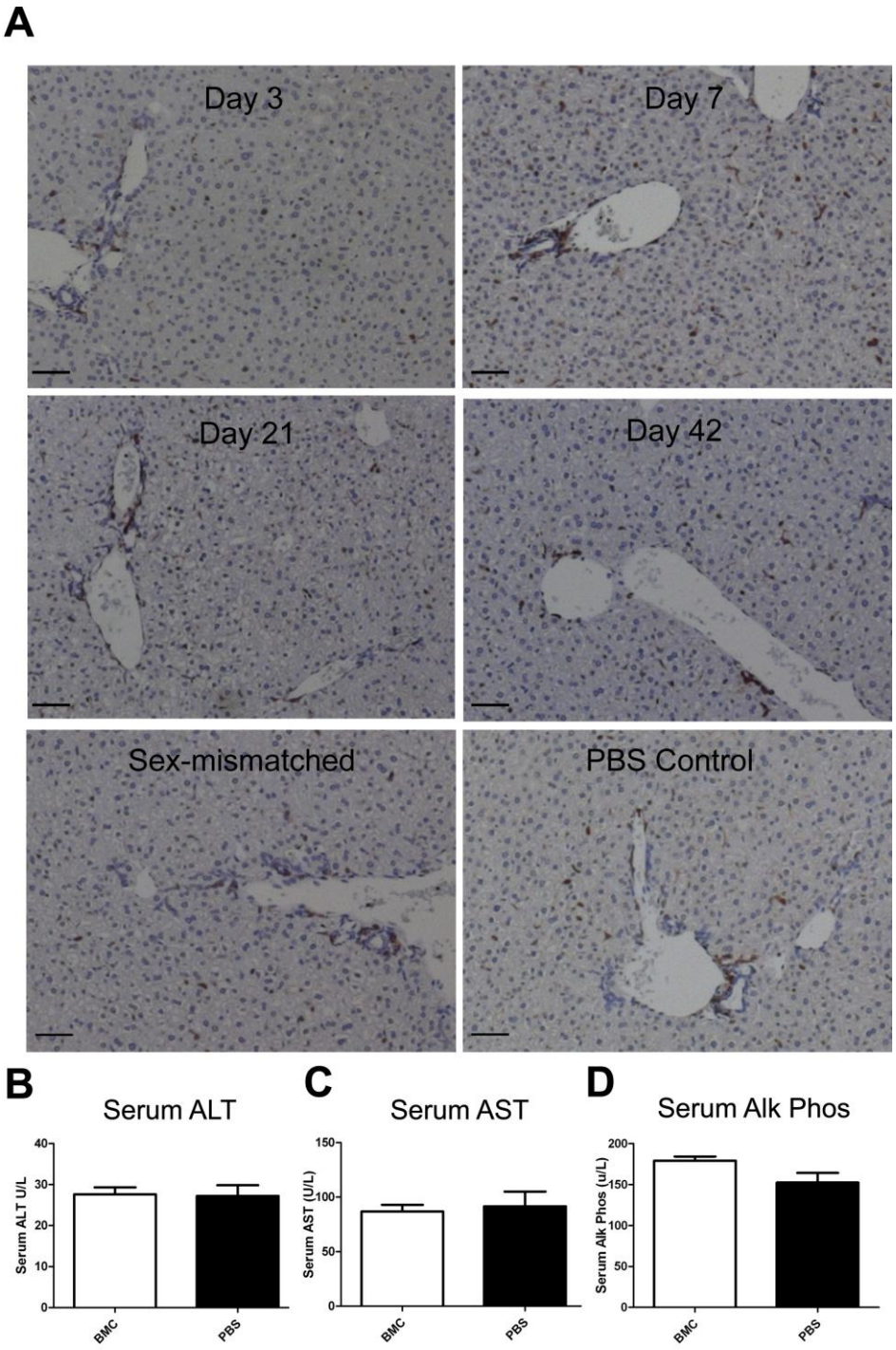

(A) Immunohistochemical analysis of liver for CD45 expression shows no evidence of leukocyte infiltration following BMC transfer compared to PBS control at any time following syngeneic or sex-mismatched BMC injection. All scale bars denote 50μm. No changes in serum Alt (B) AST (C) or Alk Phos (D) are observed 21 days following BMC transfer (all $p>0.05$ by T test, n=5 each group).

Figure 5.11 Absence of long term side effects following BMC transfer

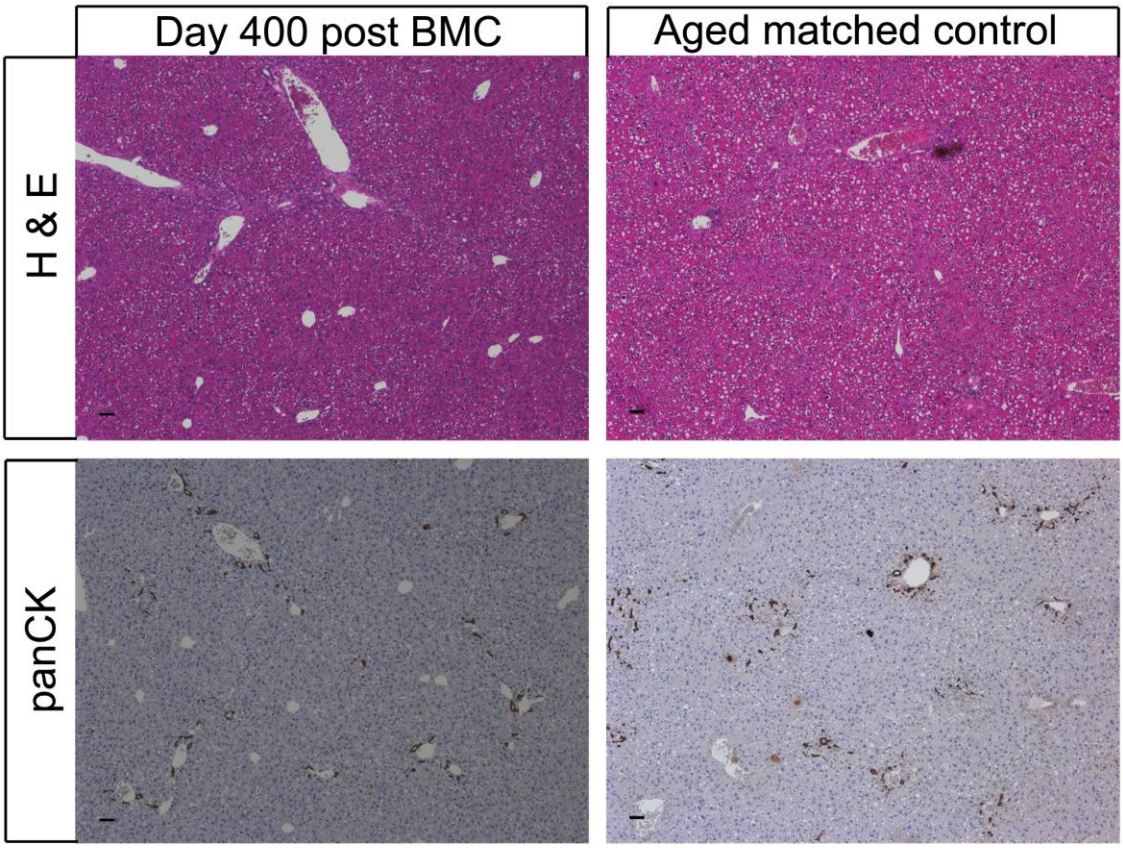

Microscopic examination of livers 400 days following peripheral vein infusion with 10^7 BMCs from an inbred male donor reveals no evidence of injury or carcinogenesis. Additionally no expansion of panCK$^+$ HPCs was observed (B). All scale bars denote 50μm.

In order to quantify the numbers of donor cells within the liver two independent strategies were performed. Firstly whole liver gDNA was assessed by qPCR for the presence of the Y chromosome in the sex-mismatched model. Additionally, as no evidence of transdifferentiation to hepatocytes was observed from donor BMCs, the non-parenchymal cell fraction was assessed for GFP$^+$ expression in the GFP mismatched model. Interestingly both methods revealed similar dynamics of loss of engrafted cells within the liver over time. Donor derived cells were consistently undetectable in recipient livers by 42 days post injection (Figure 5.13).

Figure 5.12 Localised engraftment to the HPC niche following BMC transfer

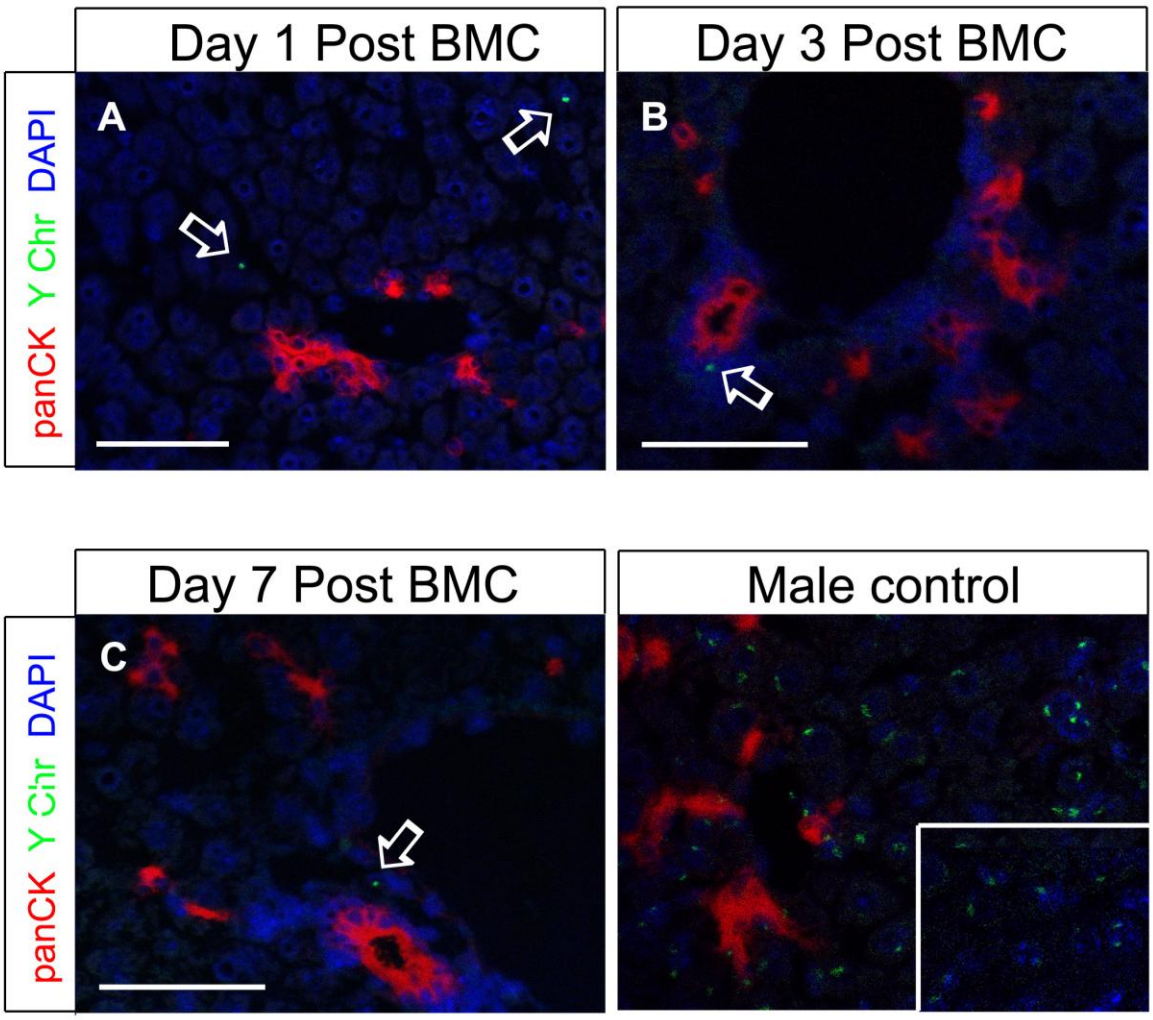

In the sex-mismatched BMC transfer model engrafted cells within perfused liver were assessed following immunohistochemical and FISH analysis by confocal microscopy. No hepatocytes or panCK$^+$ HPCs were identified as donor derived. One day following BMC transfer small donor derived cells were scattered throughout the parenchyma, however by 3 and 7 days a significant proportion of donor derived cells were in direct contact with panCK$^+$ HPCs. Male control demonstrates all cell populations contain Y chromosome$^+$ cells; insert antibody isotype control. All scale bars denote 50μm.

Figure 5.13 Transient cellular engraftment following BMC transfer

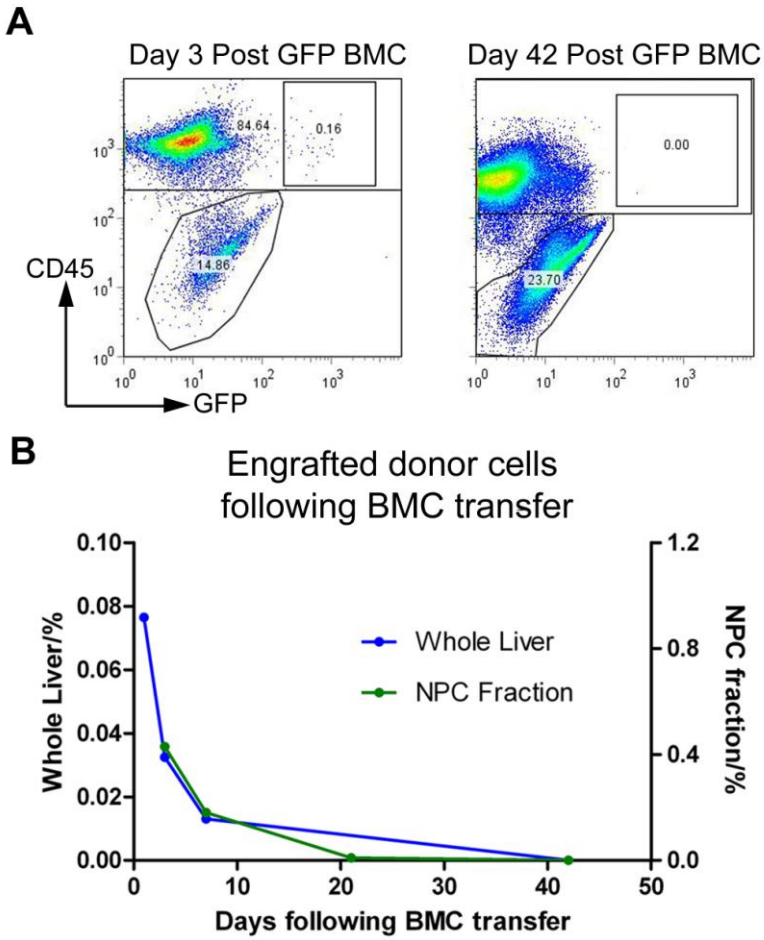

Following BMC infusion, cellular engraftment was assessed in perfused liver by two independent methods. Firstly NPCs were isolated by density centrifugation at multiple time points following GFP-mismatched BMC transfer. NPC were then assessed by FACS for GFP expression along-side CD45. (A) Representative FACS plots shown for examination at days 3 and 42 following BMC transfer. In addition qPCR for Y chromosome gDNA was performed on whole liver following sex-mismatched BMC transfer. (B) Data for each method of quantification is presented (green-GFP mismatched FACS, blue-sex-mismatch qPCR).

To characterise the phenotype of engrafted, donor-derived cells FACS selection of GFP^+ cells in wild type liver was performed 3 days post BMC delivery. The resultant cell isolate was exclusively $CD45^+$ (Figure 5.13A), and the majority (81%) were $F4/80^+$ macrophages (Figure 5.14A). The identity of engrafted BMCs as macrophages was then confirmed by *in situ* co-staining of Y chromosome and F4/80 in liver sections (Figure 5.14B).

Figure 5.14 Macrophages from whole BMC engraft following transfer

(A) Examination of extracted GFP^+ cells from recipient livers 3 days following infusion of 10^7 GFP^+ BMC by F4/80 immunocytochemistry reveals 81% of cells engrafted donor derived cells are macrophages. Contemporaneous staining control for F4/80 using BM. (B) Immunohistochemistry for F4/80 reveals engraftment of macrophages within the liver 3 days following infusion in the sex-mismatched tracking model also. All scale bars denote 50μm.

5.64 Macrophages are themselves capable of activating an HPC response

The experiments described above suggest a central role for macrophages in the activation of HPCs following BMC transfer. Thus, I hypothesised that *in vitro* matured macrophages would stimulate an HPC response to a similar or greater magnitude than that seen with whole BMC. Twenty one days following transfer of 10^7 $F4/80^+$ macrophages to healthy mice, livers and serum were analysed. Macrophage specific cell transfer once again resulted in absence of hepatic inflammation (Figure 5.15A and B). Nonetheless increased serum albumin was observed (Figure 5.15D), together with a robust activation of HPC proliferation (Figure 5.15F and G). These effects are analogous to the response seen with BMCs as hypothesised. In keeping with the activation of HPCs serum Alkaline Phosphatase was significantly elevated in macrophage treated mice (Figure 5.15C).

Figure 5.15 Macrophage transfer recapitulates whole BMC transfer

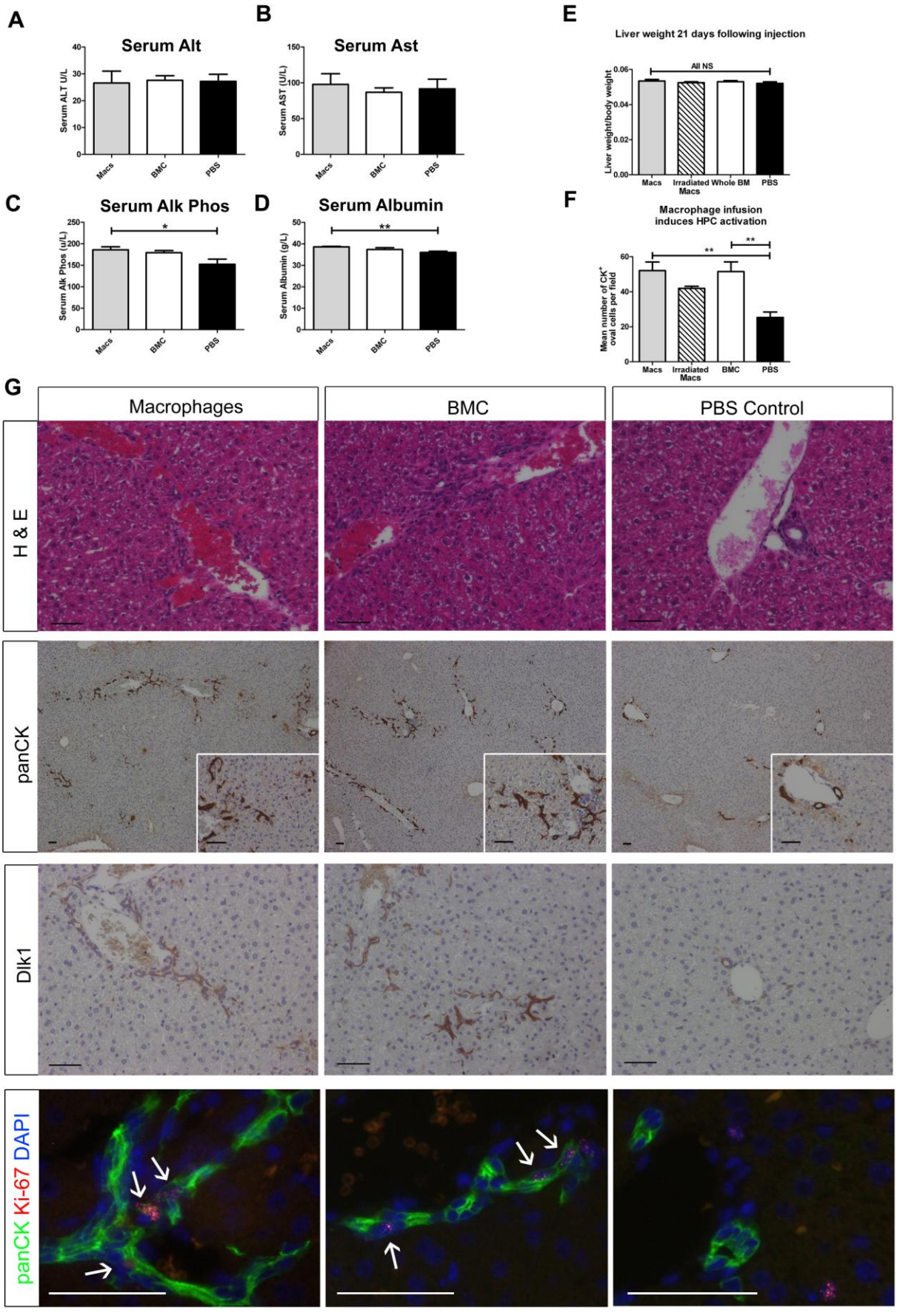

Mouse serum taken twenty one days following infusion of 10^7 F4/80$^+$ macrophages given via tail vein injection shows no change in ALT (A), or AST (B) compared to control. (C) Alkaline Phosphatase show significant rise in macrophage treated animals (186 vs. 182 vs. 152U/l in Mac vs. BMC vs. PBS treated mice, n=5 each). (D) Serum Albumin shows significant rise vs. PBS control (38.6 vs. 38.2 vs. 36.0g/l in Mac vs. BMC vs. PBS treated mice, n=5 each). (E) No significant change in liver weight : body weight following cell therapy at 21 days 0.054, 0.052, 0.053, 0.052 in mice given Macs alone, irradiated Macs, BMC, and PBS control respectively (n=5 each group). (F) Quantification of panCK$^+$ HPCs 21 days following cell therapy, with corresponding immunohistochemical analysis (G). All scale bars denote 50μm, *p<0.05, **p<0.01.

5.7 HPC activation following BMC transfer is dependent on TWEAK-Fn14 signalling

To determine the mechanism by which engrafted BM-derived macrophages stimulate the HPC response, I screened whole liver RNA for the presence of growth factors known to be associated with HPC proliferation, including: HGF, IFNγ, TNF, IL6, LTα, LTβ, OSM, and TWEAK. Expression of LTα, LTβ and OSM were not reliably detected in liver unlike in positive control (E15 liver/spleen/thymus). No significant changes in hepatic expression of IL6, TNF or IFNγ were observed following BMC transfer (Figure 5.17A-C). In contrast TWEAK mRNA levels were strongly induced during the first week following BMC transfer and returned to normal (Figure 5.17D) as engrafted cells were lost from the liver (Figure 5.13). Hepatic HGF showed a non-significant trend towards increased gene expression also (Figure 5.17E).

Figure 5.16 Fate of HPCs following macrophage transfer

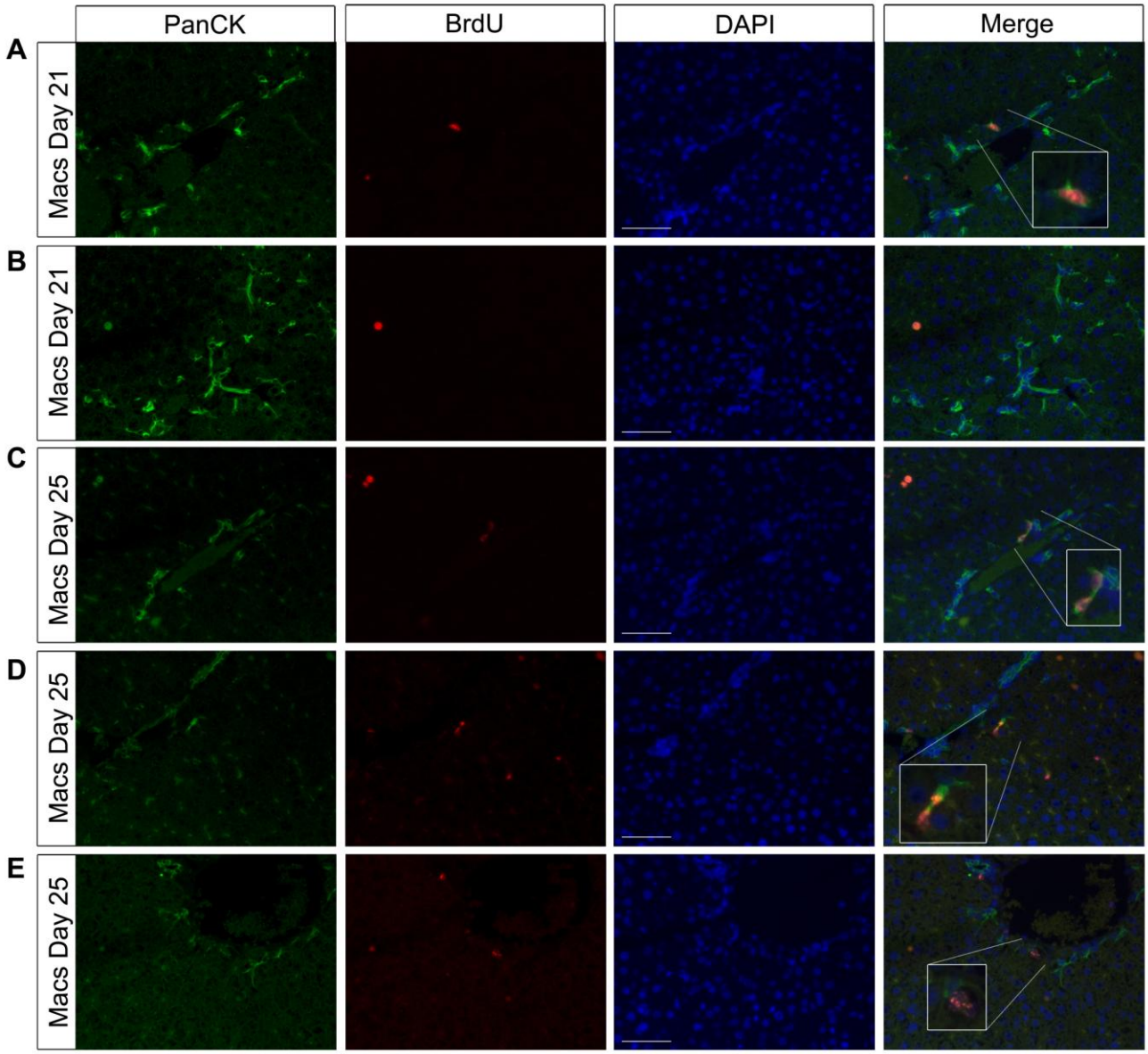

Immunohistochemical analysis of liver using PanCK (green), BrdU (red) and DAPI (blue) following transfer of 10^7 macrophages. BrdU (50mg/kg) is administered 21 following cell transfer and tissue analysed either 2 hours later (day 21) or 4 days later (day 25). (A) Early analysis following BrdU pulse reveals panCK$^+$ cells with uptake of BrdU label. Non-parenchymal cells also infrequently take up BrdU (A) as do hepatocytes (B). Later analysis 4 days following BrdU reveals clusters of BrdU$^+$ cells particularly in periportal areas (C-E). Clusters of panCK$^+$ BrdU$^+$ cells are observed (C) in addition to clusters of BrdU$^+$ cells containing both hepatocytes and panCK$^+$ HPCs (D). Clusters of BrdU$^+$ hepatocytes are also observed in the periportal areas in direct juxtaposition to panCK$^+$ HPCs (E). All scale bars denote 50μm.

Figure 5.17 Screening cytokines reveals TWEAK as a potential signal for HPC activation

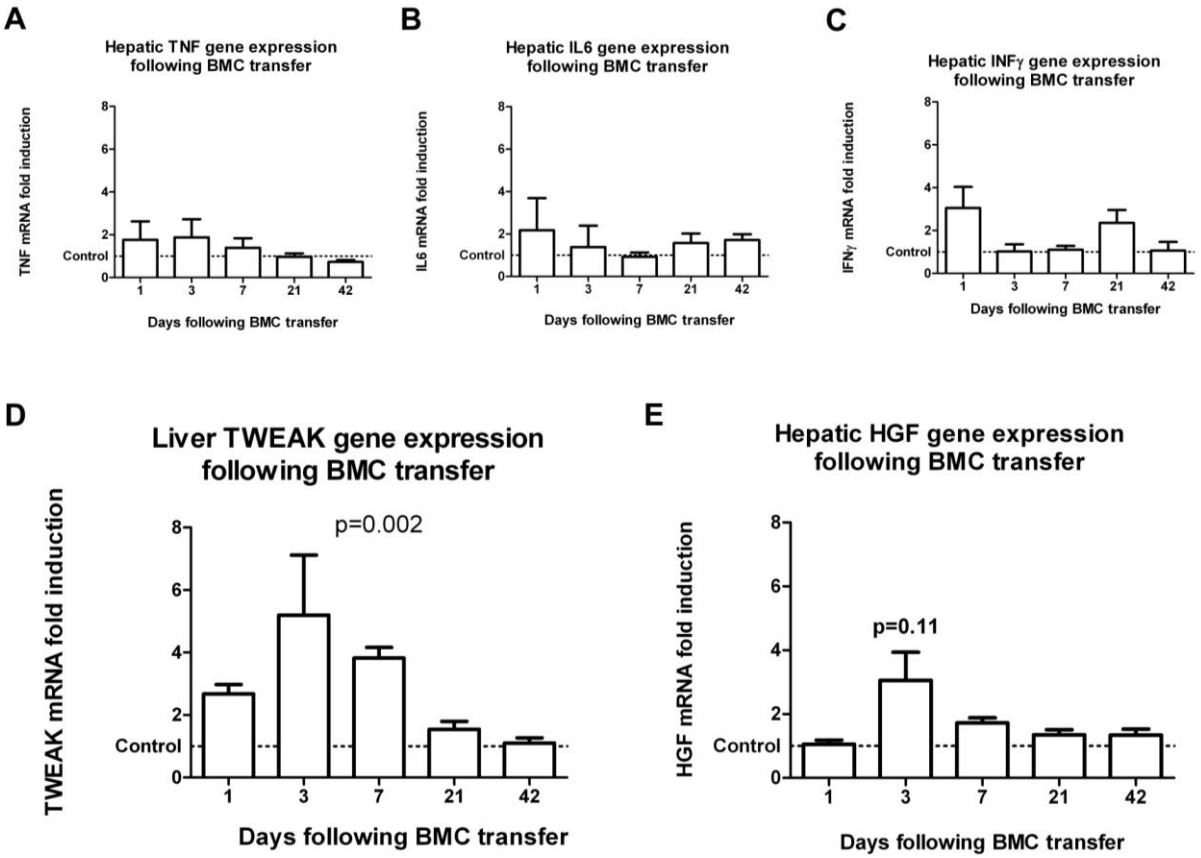

Analysis of whole liver mRNA expression by qRT-PCR was performed 1-42 days following infusion of 10^7 syngeneic BMC into healthy female C57/Bl6 mice (n=5 each group) and compared to PBS treated control. P values denote T test value vs. PBS treated control.

Having observed that TWEAK expression in whole liver follows a pattern similar to the engraftment of macrophages within the liver, I therefore sought to investigate if the increased expression of TWEAK following syngeneic BMC therapy originated from the donor derived macrophages. Initially I assessed whether TWEAK expression was a characteristic of mature macrophages in the absence of infusion. *In vitro* differentiated pure populations of F4/80$^+$ macrophages express high levels of TWEAK mRNA compared to undifferentiated and purified BMCs (Figure 5.18B). Then, aiming to assess if engrafted donor-derived cells were the source of TWEAK signalling post BMC

therapy, GFP^+ donor-derived cells were sorted from perfused wild-type recipient livers and examined for TWEAK expression 3 days following GFP-mismatched BMC transfer. Relative to whole BM, TWEAK mRNA levels were 2.8-fold elevated in the GFP^+ pullout fraction (Figure 5.18B) consistent with TWEAK production in-situ by donor derived macrophages following BMC transfer.

To test the hypothesis that TWEAK signalling mediates HPC expansion following BMC transfer, I used recipient mice lacking the Fn14 TWEAK receptor ($Fn14^{-/-}$) and compared the extent of HPC response invoked by transfer of wild-type BMCs between these and WT recipient controls. In the absence of Fn14, HPC expansion was entirely abrogated (Figure 5.19). In $Fn14^-$ recipients no evidence of expansion of HPCs expressing panCK, Dlk1 or EpCAM is observed 42 days following intravenous BMC transfer in contrast to when BMC is given to healthy wild type recipients.

Figure 5.18 Engrafted macrophages produce TWEAK within the liver

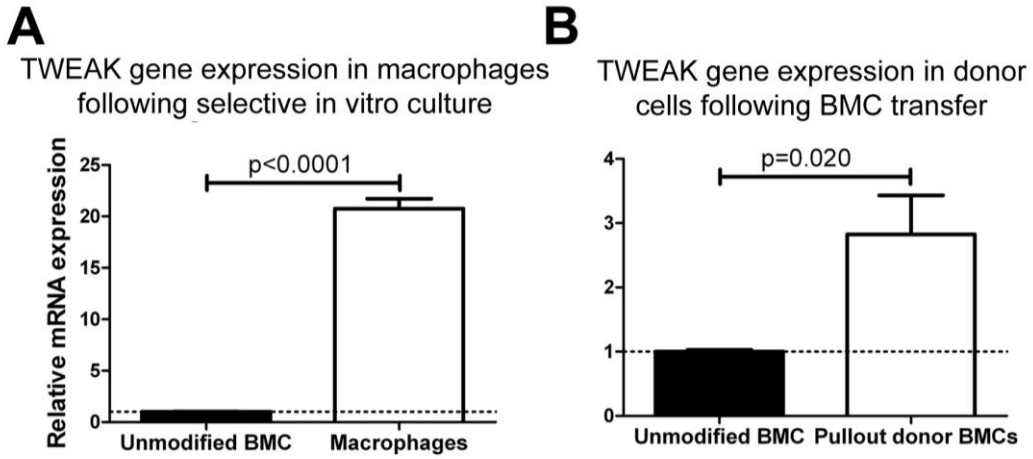

Analysis of TWEAK gene expression by qRT-PCR performed on *in vitro* differentiated macrophages revealed 20.8±0.96 (mean±SEM) times increased expression of TWEAK in enriched macrophages vs. whole BMC control (A). 3 days following GFP-mismatched BMC transfer donor derived GFP+ cells were sorted by FACS from the pooled NPC fraction from the whole livers of 3 mice. TWEAK gene expression in this cell population was 2.83±0.60 (mean±SEM) times higher assessed vs. whole BMC control. P values denote T test result vs. control, n=3-5 each group.

Figure 5.19 BMC mediated HPC activation is dependent on TWEAK signalling

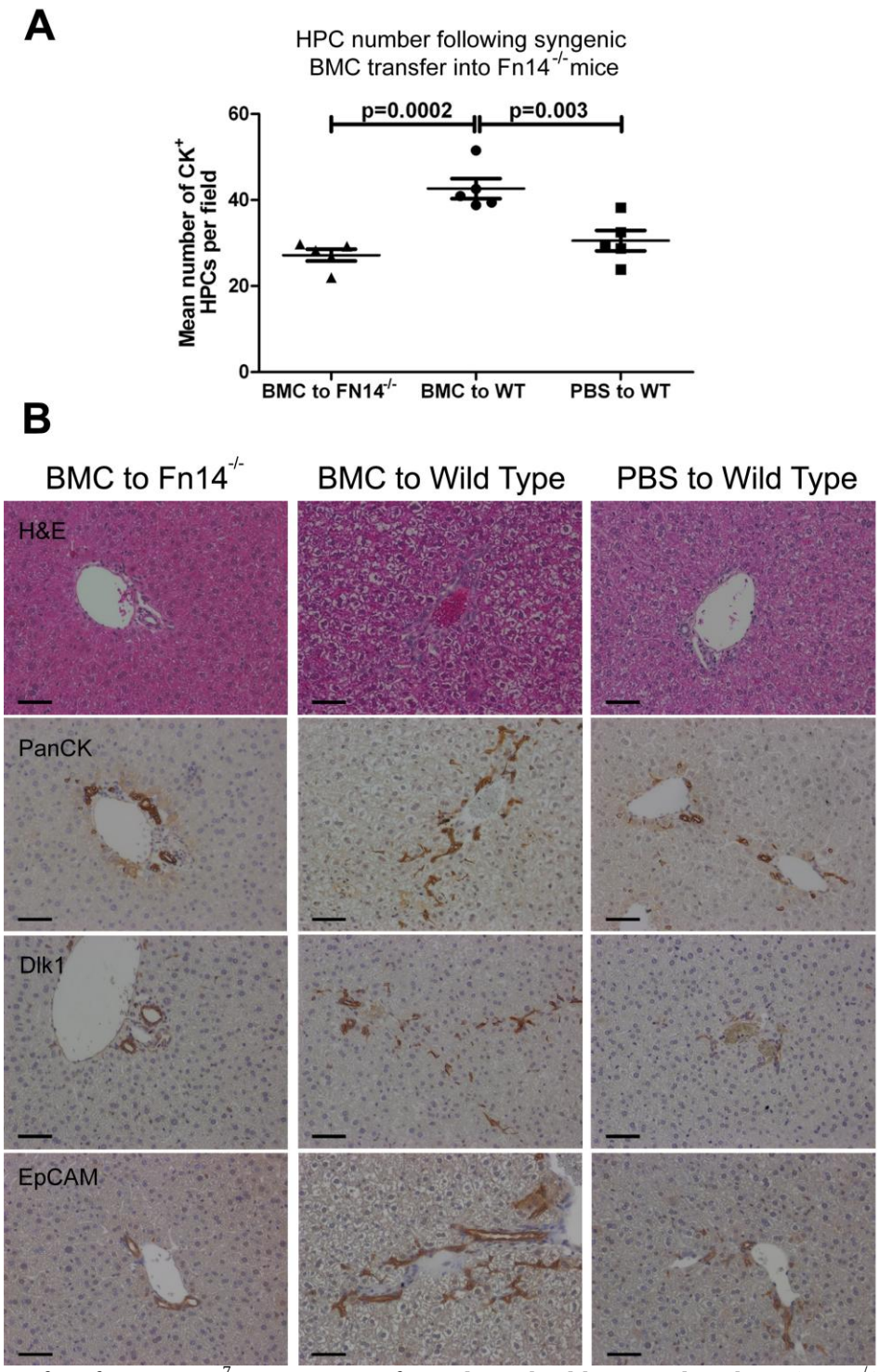

(A) Transfer of murine 10^7 BMC was performed into healthy Fn14 knockout ($Fn14^{-/-}$) and Wild type female mice recipients. The HPC response was assessed by panCK+ HPC expansion (A) together with immunohistochemical analysis for panCK, Dlk1 and EpCAM (B). All groups n=5. p values given for T test. All scale bars denote 50μm.

A series of changes are described to occur with age in the behaviour of stem and progenitor cells in the BM (Mayack *et al.*, 2010; Warren and Rossi, 2009). Described changes include an increased propensity of haematopoietic stem cells to differentiate towards myeloid rather than lymphoid lineages (Gazit *et al.*, 2008). I therefore asked whether aged BMC were capable of induction of HPC activation in a similar fashion to BMC isolated from young mice examined previously. Identical changes in HPC activation were observed when BMCs from old donors (18 months old) were given to young female mice compared to when BMCs from young donors (6 weeks) are used (Figure 5.20).

Changes in the haematopoietic potential of the old and young donor BM used in the experiment described previously was performed along with that from age matched mice injured with the CDE diet. Haematopoietic potential was assessed *in vitro* from freshly isolated BM using colony forming assays. A variety of colony phenotypes can be distinguished from this assay. Each phenotype represents the different potential of colony forming cells from varying stages of the leukocyte/erythrocyte lineage. The relative frequency of each colony forming unit from each group of mice was as predicted. No changes were observed with aging upon the frequency of committed haematopoietic progenitors (Figure 5.20C). However, a significant loss of multipotent colony forming stem cells was observed in the aged mouse upon exposure to the CDE diet (Figure 5.20D).

Figure 5.20 Effect of aged BMC on HPC expansion

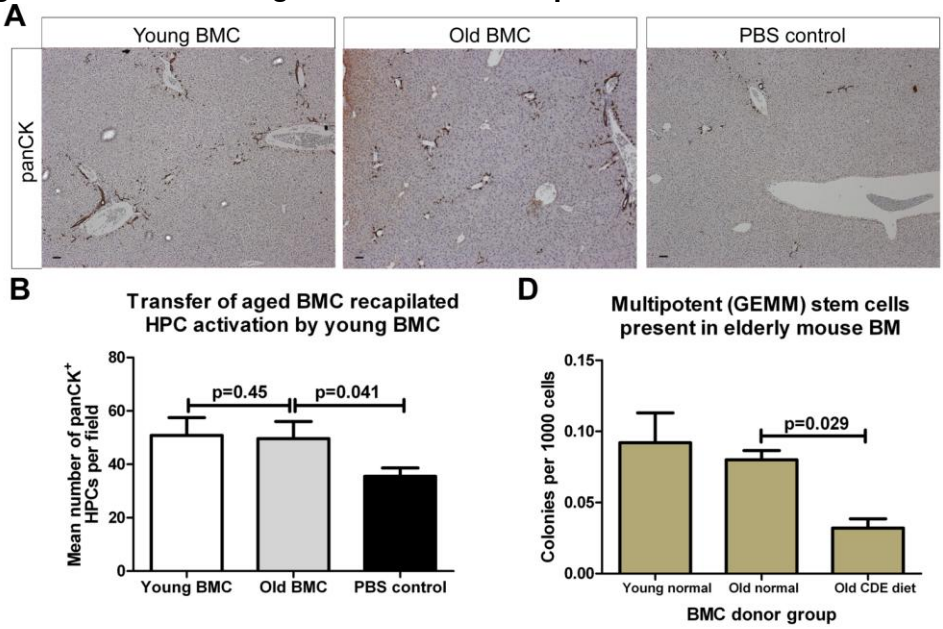

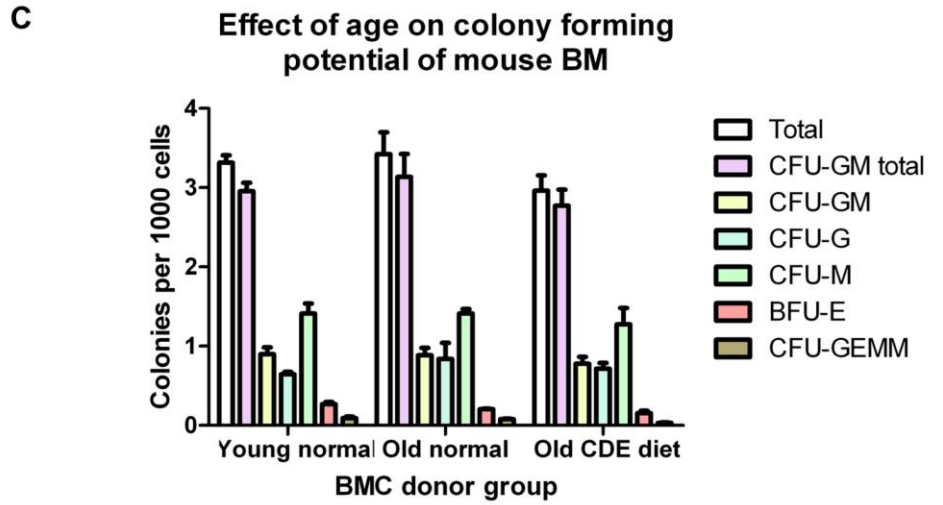

	Total	CFU-GM total	CFU-GM	CFU-G	CFU-M	BFU-E	CFU-GEMM
Young uninjured	3.316	2.956	0.9	0.644	1.412	0.268	0.092
Old uninjured	3.42	3.136	0.884	0.84	1.412	0.204	0.08
Old CDE diet	2.96	2.772	0.78	0.716	1.276	0.156	0.032

(A) 42 days following i.v. injection of 10^7 male BMC from either 6 week (young) or 18 month (old) mice, recipient mouse liver was assessed for HPC expansion by panCK immunohistochemistry and panCK$^+$ HPCs quantified (B). Scale bars denote 50μm. BMCs were extracted from healthy young and old mice in addition to old mice exposed to 12 days of CDE diet, and colony forming assay performed in methocult media. Data is presented as number of colonies per 1000 BMCs. Data is presented for total colonies, total granulocyte/monocyte/mixed granulocyte and monocyte (GM total), mixed granulocyte/monocyte (GM), granulocyte (G), monocyte (M), erythriod (E) and granulocyte/monocyte/erythroid/monocyte/megakaryocyte (GEMM) colonies (C). Numerical data represents mean for each group (n=4 each). GEMM colonies data is presented separately (D). p values denote Mann Whitney test.

5.8 Discussion

The question of what role macrophages play in the regenerative process in the liver from HPCs has been raised by earlier work in this thesis and many other studies (Yin *et al.*, 1999; Paku *et al.*, 2001; Pull *et al.*, 2005; Gyorki *et al.*, 2009; Lorenzini *et al.*, 2010). The work presented here demonstrates macrophages play a central functional role in controlling HPC activation and modulating the HPC regenerative response to injury. Following successful depletion of hepatic macrophages I demonstrate a role for macrophages in shaping the phenotype of bipotential HPCs, driving a hepatocytic differentiation and thereby promoting hepatocellular regeneration in response to the CDE diet. This mechanism for this influence appears to be via paracrine Wnt signalling, which inturn modulates HPC Numb expression leading to inhibition of Notch mediated cholangiocyte differentiation. Furthermore, work performed by the adoptive transfer of macrophage demonstrates that, even in the absence of local hepatocellular injury, macrophages promote the expansion of otherwise unstimulated HPCs. This phenomenon appears to be via an alternative paracrine signalling pathway utilising the TNF related TWEAK signal which acts on Fn14 receptors of the HPCs themselves.

5.81 Macrophage depletion during the CDE diet

As demonstrated in this work the Liposomal Clodronate is an exceptionally efficient method for depleting hepatic macrophages. Cellular depletion of $F4/80^{+}$ macrophages using liposomal clodronate in my hands is consistent with previous reports of F4/80 depletion both in the liver and spleen of mice 3 days following a repeated dosing strategy (Nishioka *et al.*, 2007) with return seen 5 days following injection (Yamamoto *et al.*, 1996). Here liposomal clodronate treatment a rebound in peripheral blood monocytes has been reported from 1-5 days post treatment. This increase in circulating monocytes is postulated to result from compensatory increased production of fresh BM derived monocytes during the tissue macrophage repopulation phase, following

macrophage depletion (Yamamoto *et al.*, 1996). Interestingly, in the model system used in this work, I have observed large numbers of F4/80^{+} macrophages adherent to the hepatic vasculature following hepatic injury and repeated intrahepatic macrophage depletion (Figure 5.3C). I propose that this observation is a result of active macrophage repopulation following depletion and subsequent intravascular repletion. This itself offers as an elegant model for the studying the kinetics and biology of macrophage recruitment to the liver.

Effective macrophage depletion in the healthy liver using the DTR deletion system in transgenic mice was not achieved in my hands. This is clearly in contrast to other studies (Cailhier *et al.*, 2005; Duffield *et al.*, 2005). In previous studies, efficient and significant depletion of peritoneal macrophages was seen between 8hr and 4 days following i.p. DT injection at up to 25ng/g (Cailhier *et al.*, 2005). Alternatively depletion of hepatic macrophages has been dsecribed 24 hours after repeated doses of 10-25ng/g DT via either i.p. or i.v. injection (Duffield *et al.*, 2005). The discrepancy between the published findings and my results in this work probably lies in the differing time between DT delivery and tissue analysis in these different studies. None-the-less my findings support what is apparent from the previous studies that intrahepatic macrophage depletion by liposomal clodronate is significantly more effective than in the CD11b-DTR transgenic system. In the work presented here liposomal clodronate was chosen not only for its improved rapidity of hepatic macrophage depletion and the improved specificity of action regarding other leukocyte subsets.

In contrast to the CD11b-DTR system, Liposomal clodronate is described to play a specific macrophage depletion role without off target effects, including neutrophils (Kitamoto *et al.*, 2009; Monkkonen *et al.*, 1994; Van Rooijen, 1989). An elevation in numbers of peripheral neutrophil numbers have however been described following liposomal clodronate but are believed to be secondary to reduced monocyte mediated neutrophil clearance (Yamamoto *et al.*, 1996).

Consistent changes in serum biochemistry are seen following liposomal clodronate administration during the CDE diet in this study. Transaminases in particular are strikingly increased following liposomal clodronate treatment. This may reflect increased cellular injury but is more likely to be explained by a failure of phagocytosis of apoptotic hepatocytes which are then able to liberate transaminases directly. This would be consistent with the relatively mild rise in transaminases seen following apoptosis, however if large scale hepatocyte apoptosis is induced, e.g. by ectopic FAS expression, then dramatic changes in serum transaminases are observed consistent with a saturation of hepatocyte phagocytosis by macrophages (Feldmann *et al.*, 1998).

Considering the above and the demonstration from Chapters 3 and 4 that macrophages are actively recruited into the HPC niche during HPC activation it was surprising that HPC number did not change following the complete depletion of hepatic macrophages. This result may imply that macrophages play little or no role in modulating the expansion of HPCs. Alternatively it is possible that the effects of macrophages upon HPCs are more subtle than merely influencing overall numbers of HPCs and may instead affect HPC generation, death and/or differentiation rate. HPCs are understood to be bipotential cells capable of either hepatocyte or biliary specification. It appears that in different injury models different phenotypes of HPCs are observed. It is assumed that these differences in observed HPC morphology are a feature of the models and related to the principle site of injury and therefore regenerative requirement. In other words models in which biliary injury predominates stimulate a biliary phenotype of HPCs due to a preponderance of HPC differentiation into freshly formed cholangiocytes. Whether HPC phenotype within a single injury model can be influenced by factors excluding the method of injury is a question which to my knowledge has not been answered previously. However in this work I clearly demonstrate that macrophages play a central role in the determination of HPC behaviour.

5.81A HPC quantification as a method for assessing HPC activation

Measuring HPC number, as a marker of HPC activation, is a widely used and appropriate method for the assessment of HPC activation. It is, however, naturally a function both of HPC production and loss. HPC production is dependent on their formation, almost certainly in the main from HPCs themselves. Certainly all models studied in this work and other related published work provides compelling evidence that HPCs are capable of proliferation both *in vivo* and *in vitro*. Any reduction in HPC number is most simply a function of a combination of their death, or loss by differentiation into other cell populations, outweighing any production from precursor sources. It is probable that HPC death, most likely via apoptosis is also a means by which the number of observed HPCs may be influenced. None-the-less, although these features were not specifically quantified in this study, as HPC number remains entirely stable it is likely that both the generation and loss of panCK$^+$ HPCs are not dramatically altered during macrophage deficiency.

To study HPC biology the choice of marker used to identify this population is crucial. For historical reasons the majority of this work has used panCK as a marker for HPCs. As discussed previously in Chapter 1, panCK is a validated HPC marker. It is clear, however, that there is heterogeneity within HPCs. EpCAM is now a well validated HPC marker with, in my opinion, more supporting evidence for it use as a marker currently, than panCK. EpCAM therefore, may be of more relevance to study HPC biology. None-the-less my work demonstrates that the two markers appear to colocalise very closely frequently and whilst not always doing so, both panCK and EpCAM appear to mark the same population in most instances (Figure 5.4B). This demonstration of Dlk1, EpCAM and panCK made in this work is the first such description within HPCs.

5.81B Mechanism of action of macrophage influence upon HPC cell fate

The observation that HPC morphology can be altered by the presence/absence of macrophages in the CDE dietary model is a core observation of this work. The switch from an infiltrative, single file HPC response in the CDE diet to a non-infiltrative ductular HPC response with macrophage depletion suggests that macrophages are responsible for the former phenotype. In this work I have utilised a variety of markers of lineage commitment, including HNF4α, HNF1β, and HNF6, which are well established in this field as markers of lineage commitment for hepatic progenitor cells (Rountree *et al.*, 2007; Zaret, 2002). HNF1β, and HNF6 are described as inhibited by the action of the pro-hepatocytic CEBPα during development (Yamasaki *et al.*, 2006; Hunter *et al.*, 2007; Tanimizu *et al.*, 2004). These factors are viewed as specific for cholangiocyte (biliary) differentiation, while HNF4α is widely regarded as a marker of hepatocellular lineage commitment. An important extension of this thesis in the future will be to further characterise cell fate choice using differentiation into functional hepatocytes and cholangiocytes.

With respect to the factors controlling cell fate choice the most striking feature in this work is the marked alteration in the morphology of HPCs in the CDE diet upon the depletion of macrophages using liposomal clodronate (Figure 5.4A). The identification of Numb as a central difference between the phenotypes of infiltrating and ductular HPCs was originally made by Luke Boulter. This observation correlates with downstream changes in Notch pathway activation in the different models as assessed by Hes gene expression (personal communication by Luke Boulter). Given the role of Notch pathway signalling in the formation of the intrahepatic biliary tree (see Chapter 1) the novel identification of Numb, a known inhibitor of Notch signalling, provides a mechanism by which fate choice in HPCs may be regulated. Therefore these two central observations associate macrophage function and Notch signalling control over HPC fate choice.

The question then arising is how Numb itself is controlled during HPC activation? It is clear from this work that Numb is expressed by the biliary tree in the uninjured liver but

upon activation in a ductular proliferation model, Numb is lost in DDC whilst its is maintained during the infiltrative HPC response in CDE diet (Figure 5.4C and D). It is also apparent that the addition of Wnt to HPC culture results in upregulation of Numb (Figure 5.4E), and that depletion of macrophages results in a reduction in Numb expression by HPCs *in vivo*. Numb has been described as a direct target of Wnt. In contrast to work in embryology where Wnt3a has been described to modulate Numb at the post transcriptional level (Katoh, 2006a), in this work we demonstrate that Wnt3a is able to effect Numb at the gene transcriptional level. This observation is in keeping with other previous reports of control at the level of gene transcription (Holowacz *et al.*, 2006), and furthermore, is in keeping with the observation that mammalian Numb gene lies in close proximity to TCF/LEF binding sites which in primates and humans even lie within the Numb promoter (Katoh, 2006b). These observations all support a role for the modulation of Numb gene expression by the Wnt signalling pathway.

The results presented in this work demonstrate a trend towards increased Wnt3a production by macrophages following CDE diet treatment. Clearly other Wnts may additionally be produced by macrophages in the context of the two dietary models. Macrophages have been described to produce Wnts in a variety of settings, typically in response to a hostile or injured environment (Staal *et al.*, 2008; Blumenthal *et al.*, 2006; Pereira *et al.*, 2009). Given the description of Wnt3a's role in modulating Numb behaviour (Katoh, 2006a) and the role for recombinant Wnt3a in stimulating hepatocyte differentiation both in the adult and development (Figure 5.5D and Hay *et al.*, 2008; Ober *et al.*, 2006) it is a clear candidate for the signalling mechanism from macrophages to HPCs. Additionally Wnt3a is the paradigm of canonical Wnt signalling, a feature suggested to occur in HPCs by their elevation in nuclear β-catenin (Figure 5.6H). Here I show detectable and active Wnt3a gene transcription in isolated and purified hepatic macrophages, an observation not previously reported.

A recent study using Wnt1 knockdown in the rat PH/AAF model supports a role for Wnt1 in the differentiation of HPCs into hepatocytes (Williams *et al.*, 2010). Although

no changes in whole liver Wnt1 expression were observed in my work it is possible that local periportal expression of Wnt1, particularly as this is observed by Williams *et al.*, may exist. Further elucidation of the regional and cellular expression of the Wnts in the regenerating liver will undoubtedly broaden our understanding of this family of proteins in regulating stem/progenitor cell behaviour in the future. Macrophage expression of other Wnts, including Wnt2, has been described previously in the mouse. In the liver expression of a number of Wnts by macrophages has been suggested also (Zeng *et al.*, 2007). Wnt2 signal predominantly via the canonical (β-catenin) dependent pathway (Lobov *et al.*, 2005). It is interesting to note that whole liver Wnt2a is increased in the CDE diet but reduced in the DDC diet (Figure 5.6A) and that based on Ct values is the second most highly expressed Wnt mRNA in the liver during CDE or DDC diet behind Wnt 5a (see Appendix). In the first instance however, I elected to examine the effect of Wnt3a on HPCs in culture as this is a commercially available recombinant protein and is the archetypical example of a canonical Wnt signal. Further investigations of the effects of other Wnts including Wnt 5a upon HPCs are warranted in addition to those of Wnt 3 reported here in the future.

In contrast to the previous report of Wnt4 expression in a mixed population of stellate and Kupffer cells in mouse liver (Zeng *et al.*, 2007) I did not detect Wnt4 transcript in isolated hepatic macrophages. These results therefore imply that Wnt4 is expressed by hepatic stellate cells, a result not specifically confirmed in this work. This further highlights the likelihood that Wnt expression is almost certainly highly complex, delivered from multiple cellular sources, and comes under additional control by a variety of other regulatory proteins such as WIF, sFz which are also modulated during HPC activation (Appendix 1) and are well described to play central regulatory role in the Wnt signalling pathway (Bi *et al.*, 2009).

A previous study performed using FVB mice has reported changes following 3 weeks of the DDC diet on the gene expression of a number of selected Wnts (Hu *et al.*, 2007). In comparison to my work many similarities and differences are observed. I did not

observe the large increases in Wnts 1, 5b, 7b and 11 previously reported. My observations regarding the changes observed between Wnt 6 and particularly the large increase in Wnt 7a were however consistent with that of Hu *et al.* (Hu *et al.*, 2007). In the normal whole liver my observations were broadly in keeping with the previous descriptions of comparatively high expression of Wnts 1, 2, 2b, 4, 5a, 5b and 11 (Zeng *et al.*, 2007) . In contrast to the published report which was performed in older C57Bl6 mice I additionally observed consistent expression of Wnts 3a, 6, 7a and 16 in the healthy liver. Whether these inconsistencies between these data reported in this study and previous publications are due to the changes in length of diet exposure, mouse age or strain are not clear, however a combination of these factors seem likely to explain these discrepancies.

From the observations that macrophages produce Wnts *in situ* (Figure 5.5A) and that HPCs show reduced response to Wnt when macrophages are depleted (Figure 5.5B), I propose that the functional effects of macrophage depletion during HPC activation are mediated through a loss of Wnt expression. This loss of Wnt reception by HPCs leads to a subsequent reduction in their Numb expression, with downstream effects on the Notch signalling pathway resulting in alteration in progenitor cell fate choice. While this has not been formally tested in this work, we are planning to do this as part of ongoing study into HPC biology. The role of Numb may also be directly assessed by knockdown using siRNA in the BMOL HPC line. Additionally using HPC/macrophage co-culture the effects of paracrine signalling by macrophages to HPCs may be dissected. When used in conjunction with interference with Wnt signalling by the use of recombinant Wnt inhibitors such as WIF and sFz we will be able to address the role of macrophage derived Wnt on cell fate choices by HPCs.

As briefly introduced previously, it is interesting to note that there is no apparent alteration in the localisation of macrophages and HPC in either the DDC or CDE dietary models. It appears that alterations in macrophage function between the two models account for the changes in Numb and secondarily HPC morphology. To address this

question directly the HPC phenotype could be monitored following adoptive transfer of macrophages from the CDE diet treated liver to a DDC treated mouse and vice versa. I would predict that in this instance Wnt-producing macrophages form the CDE treated liver would have a dominant effect, promoting a switch to an infiltrative HPC phenotype in this model. Similarly, it would also be fascinating to examine the effects of switching the CDE diet to DDC diet and vice versa to examine whether one HPC phenotype (infiltrative or ductular) is dominant. Should such experiments further support a role for macrophages in the establishment of HPC phenotype during regeneration then a central question remains why they should behave differently in the CDE and DDC models? I would propose that this is a function imposed upon them by their local environment and most likely in response to the local requirements for regeneration in the two model systems.

A further implication of the work presented here is that the recruitment of macrophages to influence cell fate may explain other observations in liver regeneration made previously by other groups. For example T3 is reported to influence macrophage migration and/or phenotype and separately described to improve the hepatocellular differentiation of HPCs. Raised T3 promotes the accumulation of younger recently immigrated macrophages (Gomes *et al.*, 2004). It is therefore possible that the effects of T3 seen on improving hepatocyte differentiation of HPCs in the rat model (Laszlo *et al.*, 2008) may be explained by secondary effects upon HPC differentiation mediated by an accumulated macrophage population.

5.81C Failure of the BATgal transgenic reporter system in the adult liver

The use of Wnt reporter mice is a widely used and accepted practice for studying Wnt signalling. A variety of such reporter strains are in wide use. In general TCF/LEF elements or Axin2 promoters are used to drive a detectable protein such as GFP or β-galactosidase (Barolo, 2006). BATgal mice were one of the first such reporter mice to

be developed by Stephano Piccolo *et al.*. I opted to use these mice to study Wnt signal reception by HPCs at an early stage in this work prior to the publications by other groups using alternative transgenic reporter systems (Hu *et al.*, 2007). Unfortunately in none of the adult BATgal^{+} animals in my work was β-galactosidase detected. Interestingly this failure of β-galactosidase expression was also observed in the intestine, where Wnt reception has been repeated shown by other groups (Clarke, 2006). Failure of β-galactosidase expression in the BATgal mice was not due to its technical failure of detection as it was reliably and consistently detected in contemporaneous ROSA26 positive controls (Figure 5.6). BATgal mice have been used repeatedly and successfully only in neonatal studies (Liebner *et al.*, 2004; Maretto *et al.*, 2003). No reports exist to date of successful BATgal reporting in the adult. It therefore appears that for epigenetic reasons, silencing of the BATgal reporter construct appears to occur in the adult mice.

5.82 The role of macrophages in stimulating HPC expansion in the absence of injury

An urgent need exists to develop therapies for liver disease. The potential for manipulating the endogenous HPC population is both a feasible and attractive option. Genetic modification has shown the potential to influence HPC activity (Jakubowski *et al.*, 2005; Knight *et al.*, 2000) as has indirect (Spahr *et al.*, 2008) and direct pharmaceutical targeting of HPC function (Knight *et al.*, 2008). The findings reported in this work highlight another therapeutic avenue by which host HPCs can be modulated exogenously. I propose that the pathway of macrophage recruitment and TWEAK mediated HPC stimulation as a mechanism by which autologous BMC therapy may be beneficial in human liver disease. Animal models of BMC therapy for liver disease and clinical autologous BMC therapy studies are already underway with encouraging preliminary results (Gaia *et al.*, 2006; Houlihan and Newsome, 2008; Terai *et al.*, 2005; Yannaki *et al.*, 2006). However until now there has been little or no mechanistic insight into how such "Bone Marrow Therapy" may be having its beneficial effect.

The novel observation reported here that a single infusion of either unfractionated BMCs or purified macrophages results in activation of an HPC response provides an explanation for how BM based therapy may be beneficial in chronic liver disease. Following whole BMC transfer, donor-derived macrophages engraft in recipient liver and stimulate HPC activation through a proposed paracrine mechanism involving the known HPC mitogen, TWEAK. The beneficial effects of BMC transfer on recipient liver is exemplified by the observed changes in liver growth and enhanced hepatic function which, I propose is due to increased parenchymal mass resulting from differentiation of HPCs.

In other organs and in the context of injury, previously published reports imply that macrophages can modulate stem cell behaviour. These observations suggest a role for macrophages in linking the response to injury to the commencement of regeneration (Pull *et al.*, 2005; Seno *et al.*, 2009). My observations both support, and extend these observations. I demonstrate that macrophages are able to modulate stem/progenitor cell behaviour, even in the absence of injury. Furthermore, my data supports the importance of the stem cell niche in this function, as donor-derived macrophages localise specifically to periportal liver regions where HPC expansion is known to originate from.

Using BMC transfer I have observed a consistent and reproducible HPC expansion in the livers of healthy uninjured and un-irradiated mice. Mice are described to show immunogenicity to sex-mismatched grafts in transplantation studies. None-the-less the observation that this effect occurs either when sex-matched or sex-mismatched BMC are used argues strongly against the response being due to a minor histocompatability reaction in the sex-mismatched BMC groups. The loss of HPC activation upon irradiation of the donor BMC further supports the requirement for functionality of BMCs and strongly argues against the involvement of either a bystander reaction to debris, or immunogenic antigens via a minor histocompatability reaction.

Interestingly when differentiated macrophages are delivered instead of whole BMC, the HPC response is only partially reversible by irradiation of the donor cells. Irradiation is believed to principally damage proliferating cells, with other quiescent cell populations such as fibroblasts being relatively resistant to even lethal irradiation (von Holzen *et al.*, 2007). Therefore, this implies that precursors in the BMC are responsible for the HPC activation while more mature cells in the differentiated macrophage population are capable of HPC activation in the absence of further proliferation. Certainly, the data examining the effects of differentiation on TWEAK expression in macrophages shows highly increased TWEAK production following macrophage differentiation (Figure 5.18A). This then suggests that upon differentiation macrophages are already in a state where they may induce HPC activation without further differentiation. The previous report showing that TWEAK production in the healthy liver in a transgenic mouse model is sufficient to induce HPC activation is therefore in keeping with these observations (Jakubowski *et al.*, 2005). Additionally the increase in TWEAK expression upon macrophage maturity suggests that TWEAK production is a function of macrophage maturity, although this remains to be conclusively tested. Additionally whether alterations in macrophage homing and engraftment in a healthy liver occur in immature versus mature macrophages is worthy of further investigation.

The demonstration that HPC activation, in response to BMC transfer, is lost in constitutive $Fn14^{-/-}$ mice is strong evidence for the TWEAK/Fn14 signalling pathway in HPC activation. TWEAK ligand and the Fn14 receptor are believed to be monogamous with regard to signal transduction (Winkles, 2008). None-the-less, TWEAK is also described to bind the scavenger receptor CD163 which is likely to add a further layer of control to TWEAK paracrine signalling (Bover *et al.*, 2007). As previously discussed, CD163 (also known as ED2) is a marker for mature tissue resident macrophages (Bilzer *et al.*, 2006). The data presented in this thesis suggests that even following engraftment, macrophages continue to produce TWEAK. Whether they continue to do so following longer term engraftment, is not directly addressed and is an interesting question which in the future may be addressed by adaptation of the methodologies used here. It is however

possible that in their immature and recently recruited state, macrophages are rich producers of TWEAK, but that with increasing CD163 expression mature tissue resident macrophages inhibit TWEAK/Fn14 signalling. Furthermore, CD163 expression by resident macrophages is not static, being induced by IL-10 and IL-6 while pro-inflammatory mediators like lipopolysaccharide, IFN-γ and TNF-α, suppress CD163 expression (Buechler *et al.*, 2000). This may then imply that freshly recruited macrophages provide more of a regenerative stimulus while more mature macrophages persistent in injured tissue are less pro-regenerative and perhaps more profibrotic. Additionally this process may be a further mechanism by which TWEAK mediated regeneration may be targeted therapeutically. It will be important to observe the changes in TWEAK signalling which result from manipulation of these cytokines.

The changes in liver structure and function which occur following either BMC or macrophage transfer appear to be temporality associated with the expansion of HPCs. The relative increase in liver size occurs between 3 and 6 weeks following BMC transfer and therefore is associated with, but lags slightly behind, the expansion of HPCs. This relative hepatomegaly occurs following a period of relative reduction in liver size immediately following BMC transfer and therefore may represent a compensatory hypertrophy. Interestingly in the longer term when HPC expansion normalises so does liver size; once again linking, by association, HPC expansion and liver growth.

The data presented in this work provides strong evidence that macrophages are the cells within (or a product of cells within) whole BMC which are responsible for the activation of HPCs. Macrophages recapitulate the HPC activation observed following whole BMC transfer. Donor derived macrophages are identified in the right place at the right time, specifically in juxtaposition to HPCs as the HPC expansion begins. Additionally macrophages are the overwhelmingly dominant donor derived population within the recipient liver at this time. Finally, engrafted macrophages are producing TWEAK signal in situ. TWEAK is not only known to be mitogenic to HPCs

(Jakubowski *et al.*, 2005; Tirnitz-Parker *et al.*, 2010) but additionally I demonstrate that HPC activation is reliant upon TWEAK signalling in this model.

The failure of macrophage infusion to produce a more marked activation of HPC than BMC is striking. Given that only a minor proportion of BMCs are (or may become) of monocyte lineage, a significantly larger number of macrophages are infused when a pure population of 10^7 macrophages are infused compared to 10^7 unfractioned BMCs. The apparently high levels of TWEAK expression by *in vitro* differentiated macrophages were predicted at the time to lead to heightened HPC activation. The reason for the failure of macrophages to produce a greater HPC activation compared to BMC is not currently clear. It is conceivable that the pathway of HPC activation in this scenario is saturated upon delivery of 10^7 cells in both instances. Further planned dose response studies are likely to directly address this question.

The work presented here does not exclude the possibility that other populations within whole BMC are capable of HPC activation. I plan to address this question with future work using purified leukocyte and mesenchymal cell populations in transfer experiments. Additionally experiments with the CD11b-DTR mouse system will permit the conditional ablation of $CD11b^+$ macrophages from whole BMC derived from a DTR donor, within a wild type recipient. It is not inconceivable that other cell populations may be able to active HPCs. Lymphocytes, themselves described to activate HPCs (Strick-Marchand *et al.*, 2008), are known to be recruited to the liver by activated myofibroblasts (Holt *et al.*, 2009). Lymphocytes, in similarity to macrophages, express a host of cytokines which are known to be mitogenic for HPCs when delivered by paracrine signalling (see Chapter 1). Be this the case or not, the implications of the work presented here highlight the potential for the use of macrophages from a readily available autologous source as a means to therapeutically manipulate liver regeneration. Whether other leukocyte populations may show the same potential remains to be examined.

Previous reports support the proposal that macrophages may influence progenitor cell behaviour *in vivo* (see Chapter 1). Recruitment of haematopoietic stem cells via CCR2 to the sites of injury has been observed to promote tissue repair and regeneration (Si *et al.*, 2010). M-CSF deficient op/op mice are well described to have regenerative deficiencies in the liver in addition to other adult organs (Amemiya *et al.*, 2009). It is possible that the influx of leukocytes which typically occurs following liver injury is an integral mechanism by which regeneration is stimulated. Therefore the artificial influx of macrophages following adoptive transfer into a healthy organ which I describe in this study may stimulate this regenerative response even in the absence of injury.

My work to date has not addressed the mechanism by which macrophages given by peripheral vein infusion migrate to the liver. As introduced in Chapter 1, this observation is well established although the specific engraftment in a selected few organs would suggest a targeting recruitment of leukocytes. Macrophages are known to express CXCR4. I would propose that our findings mirror the SDF1/CXCR4 axis previously described by Kollet *et al.* where expression of SDF by bile ducts results in the recruitment of $CD34^{+}/CXCR4^{+}$ progenitor cells following tail vein injection (Kollet *et al.*, 2003). Recruitment of lymphocytes has also been described to the liver via a host of chemokines, and in analogous fashion it is likely that macrophage recruitment to the HPC niche is promoted by a similarly complex cocktail of chemokines (Holt *et al.*, 2009). Additional studies are being performed in the $Fn14^{-/-}$ mice to investigate the possibility that the failure of HPC activation in this model is not due to a failure of engraftment of donor derived BMC/macrophages. Additionally, this axis is being investigated using TWEAK knockout mice as donors in BMC and macrophage transfer studies and furthermore by using TWEAK neutralising antibody in wild type to wild type cell transfers.

5.83 The use of macrophages as therapy for liver disease

The CCl_4 model used to assess the effect of macrophage therapy on HPC expansion is a widely used and well validated method of induction of injury and fibrosis (Friedman, 2008; Henderson and Iredale, 2007; Russo *et al.*, 2006; Duffield *et al.*, 2005). Using 12 weeks treatment reproducably induces significant fibrosis which falls short of cirrhosis histologically. Mice in this CCl_4 model were originally established to investigate the effect of macrophage therapy upon fibrosis remodeling and resolution. Ongoing work using such fibrosis models will be a crucial next step in the validation of macrophage mediated HPC expansion as a therapeutically useful strategy for human chronic liver disease. Preliminary work in this area by myself and others in the Forbes laboratory has shown consistent but often non-significant trends to increased HPC activation following macrophage infusion during CCl_4 mediated hepatic fibrosis. Further work to address this issue both in rodents and potentially also in human studies will be vital if such a therapy is developed in the future and may be performed in additional injury models.

Changes in BM and macrophage function are well recognised with age (Gazit *et al.*, 2008; Kohut *et al.*, 2004; Lloberas and Celada, 2002). The burden of liver disease particularly in the UK is predominantly in an aged population (Leon and McCambridge, 2006). The predominant focus of my work investigating the role of macrophage and BMC stimulation on HPC has been performed in young mice (6-8 weeks) receiving cells from similarly young mice. I have also investigated the effects of using aged BMC in stimulation of HPCs and found that the effect is reproduced when aged BMC are delivered and that there is no attenuation of HPC activation in this instance (Figure 5.20). Further studies to confirm whether aged mice will respond in a similar manner to cell infusion as young mice are needed. However the preliminary study presented here demonstrates the potential efficacy of such a cell therapy in elderly patients.

The description of a paracrine signalling mechanism between donor macrophages and host cells following BMC therapy is, to my knowledge, the first in liver. Furthermore, the strategy of using peripherally applied autologous cells to modulate the regenerative response of the HPC compartment is entirely novel. In contrast to traditional

stem/progenitor cell transplantation, this approach relies on the transient survival of infused cells, used not as direct precursors for tissue regeneration, but instead to target endogenous stem cells and utilise the liver's own regenerative capabilities. This approach to regenerative medicine from a therapeutic standpoint offers several key advantages over others currently under investigation, including the ready availability of donor cells from an autologous source; the feasibility of the approach; and finally, our demonstration that the mechanism of action involves simple paracrine signalling between donor and host liver cells. Rigorous characterisation of the stem/progenitor cell response invoked in host liver by cell therapy will be crucial to directing this work in a safe and efficacious manner. Regardless, I believe this type of work exemplifies basic stem/progenitor cell science that has genuine translational human impact.

5.9 Conclusions

- Macrophages influence HPC cell phenotype during *in vivo* expansion while not influencing the magnitude of expansion in response to injury

- Macrophages stimulate HPC activation and alteration in liver structure and function in the absence of injury

- Macrophage derived TWEAK and Wnt are key signals influencing HPC behaviour

- Macrophage based cell therapy has the potential to be effective in human liver disease

Chapter 6: Hepatocyte MDM2 deletion reveals the potential of HPC mediated regeneration

6.1 Hypothesis

- A transgenic model using inducible hepatocyte specific deletion of MDM2 will provide a novel model of HPC activation

6.2 Aims

- To study a conditional model with complete functional repopulation of the liver by HPCs.

6.3 Background to p53 function and the AhCre MDM2^{flox} model

The use of genetic manipulation is a powerful tool for the examination of genes and proteins in biology. Genetic engineering may be used in an *in vivo* context where DNA that originated from the same (cisgenic) or different (transgenic) species is added or altered. Genes may be manipulated by insertion or by their replacement, resulting in permanent expression or loss. Alternatively regulatory elements may be added in the form of promoters which allow gene expression under certain conditions; for example a tissue specific or cell population specific context. Furthermore, some genetic constructs allow exogenous control or inducibility. Such systems include tetracycline or tamoxifen inducibility where gene transcription and protein localisation may be controlled by the addition of the exogenous substances. Genetic recombination using either the Cre/Lox or Flp/FRT systems allows the site directed recombination of DNA under controlled

conditions both *in vitro* and *in vivo*. By combining specific genetic promoters with this technology recombination may be once again targeted to specific tissues or cell populations. Furthermore by adding an inducible element of control the recombination event may be induced in particular tissues or cells, as and when required. Using such technology the loss or alteration of a gene can be studied in one target organ of interest. This is possible even if experimental animals cannot survive the loss of this gene in other organs or during development. Furthermore genetic recombination allows examination of manipulation of specific cell populations in an otherwise wild-type environment *in vivo*.

Expression of the site specific DNA recombinase enzyme (Cre recombinase or Flippase recombinase) can be used to alter the genetic sequence by recombination at predetermined sites containing specific DNA sequences (lox P or Flippase Recognition Target [FRT] respectively). Two of each of these short palindromic sequences containing an asymmetric sequence are used to enable such recombination, which occurs a result of each double stranded DNA being cut by the recombinase protein. The broken strands are then rejoined with DNA ligase; both quickly and efficiently. The results of recombination depend on the position and orientation of the loxP sites. For two loxP sites on the same chromosome arm, inverted loxP site will cause an inversion, while a direct repeat will result in a deletion event together with the production of a short circular DNA excision fragment (Mallo, 2006).

The AhCre inducible activation system was originally described as a mechanism of targeting Cre recombinase expression in an inducible manner to the gastrointestinal tract (Ireland *et al.*, 2004). This report also described the induction of Cre recombinase within the liver in addition to the intestine together with lower expression in gallbladder and pancreas. Here Cre recombinase expression in the liver was shown to occur throughout the lobule, with no hepatic zone failing to undergo recombination. The AhCre system utilises the promoter element of the rat cytochrome P4501A1 (CYP1A1, also known as aryl hydrocarbon hydroxylase) gene to regulate Cre recombinase

expression (Campbell *et al.*, 1996). This promoter element is normally silent as demonstrated by the very low spontaneous recombination of floxed reporter elements. The promoter element is however strongly activated upon the cells exposure to defined lipophilic xenobiotics such as β-naphthoflavone (βNF). Such xenobiotics act by binding to a cytoplasmic basic helix-loop-helix DNA-binding aryl hydrocarbon receptor (AhR), resulting in the dissociation of a Hsp90 dimer bound to the AhR (Matsushita *et al.*, 1993). The AhR is then able to bind to an AhR nuclear translocator (Arnt). This AhR/Arnt complex then binds, probably as part of a larger protein complex containing other DNA binding factors, to the xenobiotic responsive element of DNA which drives the inducible expression of the CYP1A1 gene (Figure 6.1B). It is thought that this induction mechanism has evolved as system by which cells are able to degrade lipophilic xenobiotics only when required to do, thereby conserving unnecessary energy through the needless constitutive expression of CYP1A1 in the absence of lipophilic xenobiotics (Beresford, 1993; Guengerich *et al.*, 1982). This system is in many ways analogous to that of the lac operon used by bacteria to control the expression of β-galactosidase (Jacob and Monod, 1961).

The AhCre system may be used to facilitate population specific recombination as described by Ireland *et al.*. Cytochromes are enzymes classically associated with hepatocytes, however as described above extrahepatic recombination has additionally been observed in other epithelial tissues (Ireland *et al.*, 2004). Within the liver, immunohistochemical analysis of CYP1A1 expression demonstrates a pan-lobular expression, and although basal expression is higher in zone 3, this gradient is lost upon induction with lipophilic xenobiotics such as βNF (Baron *et al.*, 1982). In a study investigating the spontaneous activation in the R26R reporter (Cre inducible β-galactosidase) very little spontaneous activation of the reporter was seen in the livers of mice in the absence of induction with xenobiotics (Kemp *et al.*, 2004).

Using loxP mediated targeting the AhCre promoter therefore offers a mechanism of hepatocyte specific genetic recombination within the liver and consequently is a

powerful tool for researchers in the field of hepatic regeneration. The choice of genetic target offers the potential to examine a variety of biological effects of hepatocyte manipulation.

From a HPC regenerative standpoint there is a need to develop effective models for HPC induction as the mouse models previously described produce a rather limited induction of HPCs, particularly in comparison to what may occur in human disease (Chapter 1). Furthermore the models in mice do so via an uncharacterised mechanism, hence dissecting the mechanism controlling HPC activation in such models becomes particularly challenging.

As previously discussed, the activation of HPCs occurs when the regenerative capacity of hepatocytes is overwhelmed leading to activation of the facultative HPCs. Therefore either massive injury is required, which itself brings with it the problem of morbidity and mortality, or inhibition of hepatocyte mediated hepatocyte regeneration is required. Hepatocyte senescence may be induced to varying degrees by a variety of toxic stimuli and does so by a complex process which includes the induction of p21 and p16 (Chapter 1.31). The growth arrest proteins, p21 and p16, are downstream of p53 which is seen as the master controller of cell fate choice. p53 itself, stands at the junction of an extremely complex network of cellular signalling and assimilates and integrates different input signals such as oncogene activation, DNA damage, oxidative stress and mitotic impairment (Vousden and Lu, 2002). As a result of these inputs p53 controls a variety of processes. For example, p53 is known to modulate DNA repair, cell cycle arrest, senescence or even apoptosis. Fine control over these processes is achieved through integration of signalling pathways. For example in the case of p53's control over apoptosis, regulation is achieved not only dependent upon the degree of p53 phosphorylation but also the length of time phosphorylated p53 exists within the cell. Recent evidence suggests that low level and transient p53 activation results in the transcription of a programme acting predominantly to block the cell cycle while attenuating transcription of pro-apoptotic genes (Das *et al.*, 2007). When more

prolonged or more pronounced p53 activation occurs another set of pro-apoptotic genes, such as Bax, Perp, Puma and Noxa, are transcribed (Aylon and Oren, 2007; Wang *et al.*, 2007). In summary therefore, prolonged activation of p53 has the potential not only to induce growth arrest and senescence within a cell, but also its eventual death by apoptosis (Aylon and Oren, 2007).

Figure 6.1 Introduction to the AhCre MDM2^{flox} model

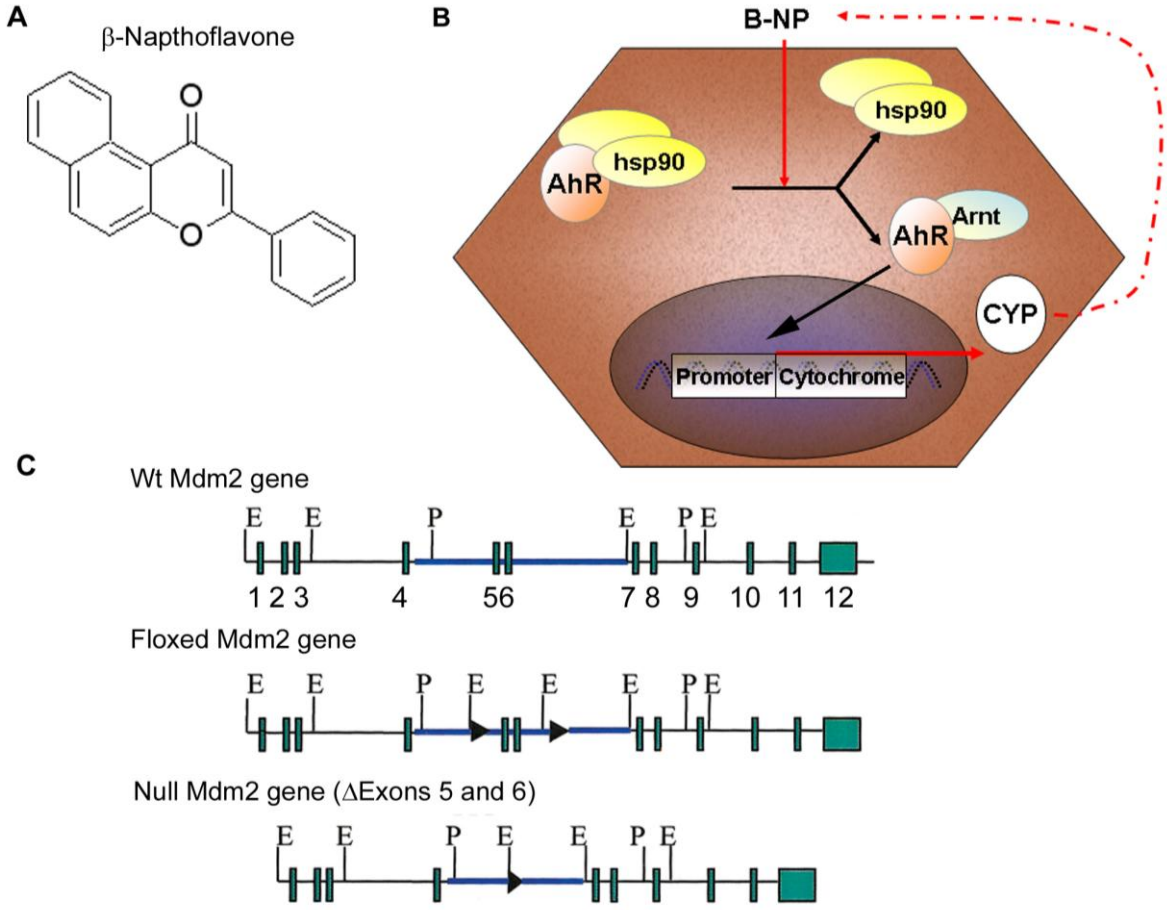

The arylhydrocarbon β-Napthoflavone (βNF) is used to induce the expression of Cre Recombinase in the AhCre promoter system (A). The physiological role of CYP1A1 is to metabolise arylhydrocarbons. (B) Following the exogenous addition of βNF, the arylhydrocarbon receptor (AhR) translocates to the hepatocyte nucleus, and upon binding to the CYP1A1 promoter induces CYP1A1 gene expression. (C) The transgenic MDM2 construct utilises the insertion of Lox P sites (arrows) between exons 4 and 5, and 6 and 8. Upon exposure to Cre Recombinase the floxed segment containing exons 5 and 6 is removed from gDNA resulting in a null MDM2 allele. Exons are represented by green boxes, adapted from Grier *et al.* 2002.

Murine Double Minute 2 (MDM2), a gene found on mouse chromosome 9, is a key negative regulator of the p53 tumour suppressor. Unsurprisingly MDM2 is frequently a site of oncogenesis (Momand *et al.*, 1992), being amplified in many tumour types (Cahilly-Snyder *et al.*, 1987; Evans *et al.*, 2001). MDM2 functions both as an E3 ubiquitin ligase, that recognises p53, and an inhibitor of p53 transcriptional activation. MDM2's transcription is itself promoted by p53, and therefore MDM2 acts as an important negative feedback loop controlling p53 function. Many oncogenic mutations have been described acting to increase levels of MDM2 expression thereby dampening p53 function. Indeed the demonstration that the generation of cancer in p53 knockout mice is not affected by MDM2 or MDM4 knockout suggests that the major anticancer role of these proteins is via p53.

Constitutive deletion of MDM2 is embryonic lethal, however rescue of such mice occurs in the context of p53 deletion, confirming p53's importance in MDM2 function (Jones *et al.*, 1995; Montes de Oca Luna *et al.*, 1995). More recently a floxed construct of the murine MDM2 gene has been produced by placing loxP sequences within introns of the MDM2 gene, to conditionally deletion exons 5 and 6 (Grier *et al.*, 2002). Exons 5 and 6 of MDM2 constitute the majority of its p53 binding domain (de Oca Luna *et al.*, 1996). Homozygous floxed MDM2 mice ($MDM2^{flox/flox}$) display no abnormal phenotype in the absence of recombination and yet recapitulate embryonic lethality when the floxed exons 5 and 6 are deleted (Grier *et al.*, 2002).

Therefore, I hypothesised that the hepatocyte specific deletion of MDM2 in the liver may provide an appropriate environment for HPC induction by the hepatocyte specific upregulation of p53. I hypothesised that this accumulation of p53 would lead to impaired entry into cell cycle of hepatocytes; and furthermore may induce hepatocellular loss by the induction of apoptosis in recombined hepatocytes. Therefore, in this environment, in which a variable degree of hepatocellular injury may be induced together with a widespread failure of hepatocyte mediated hepatocellular replication, one would predict that regeneration would occur from an HPC source.

To test this hypothesis, mice containing the AhCre construct were crossed with $MDM2^{flox}$ mice to produce $AhCre^{+}$ $MDM2^{flox/flox}$ offspring. Resultant off-spring were born at Mendelian ratios suggesting no embryonic phenotype. These mice were healthy and appeared entirely normal as adults.

6.4 Highly efficient inducible hepatocyte specific recombination in the AhCre $MDM2^{flox}$ model

Following induction with 80mg/kg βNF, male mice $AhCre^{+}$ $MDM2^{flox/flox}$ were assessed for efficiency and specificity of recombination along with uninduced $AhCre^{+}$ $MDM2^{flox/flox}$, and induced $AhCre^{+}$ $MDM2^{flox/wt}$ controls. In induced $AhCre^{+}$ $MDM2^{flox/flox}$ mice, high levels of nuclear p53 protein are seen in hepatocytes throughout the hepatic lobule, including those abutting the limiting plate in zone 1 and central vein in zone 3 (Figure 6.2). To assess the recombination efficiency following a single 80mg/kg βNF induction, assessment of hepatocytes with raised p53 expression was performed in mice 2 days following induction which confirmed highly efficient hepatocyte specific genetic recombination of the MDM2 gene (Figure 6.2).

The efficiency of recombination in this model was examined in more detail using a gDNA qPCR based approach. Using two primer sets in parallel to amplify a segment within the floxed region of the MDM2 gene construct, along with a reference segment out with the floxed segment, the efficiency of deletion of the floxed segment was assessed. Firstly a methodology for highly pure hepatocyte enrichment was developed using 3 sequential density gradient centrifugation steps. All cells, isolated using this protocol were large with hepatocyte-like morphology at cytological assessment (Figure 6.6A). Cells were assessed for purity by CYP2D6 immunocytochemistry (Figure 6.6B). 415/415 cells expressing CYP2D6 corresponding to >99% purity ($p<0.05$).

When hepatocytes and non-parenchymal cells were isolated and purified following induction in male AhCre^{+} MDM2$^{flox/flox}$ mice and the efficiency of recombination assessed quantitatively by gDNA qPCR only 3.2% of MDM2 genes in hepatocytes failed to undergo MDM2 inactivation. Hepatocytes, but not other non-parenchymal cells, underwent recombination in keeping with the known expression of CYP1A1 by hepatocytes (Oinonen and Lindros, 1998). Of the non-parenchymal cell fraction only 0.8% of MDM2 genes underwent MDM2 gene inactivation.

6.5 Hepatic phenotype following hepatocyte specific MDM2 gene deletion

6.51 Induced hepatocyte senescence in the AhCre MDM2^{flox} model

Following induction with βNF, AhCre^{+} MDM2$^{flox/flox}$ mice clinically lose weight and develop bilirubinuria (as confirmed by urine dipstick), approximately 4 days following induction. Given the increases observed in p53 protein, I then asked whether this over expression had functional consequences which may be responsible for these clinical signs. Firstly levels of p21 were seen to rise at both the protein and RNA level (Figure 6.3A and B). Other downstream targets of p53 such as p16 also increased following induction but over a slower time course (Figure 6.3C).

Increases in p53, p21 and p16 were hypothesised to give rise to senescence in the recombined hepatocytes. This was tested by examining the presence of the senescent marker β-galactosidase. Following recombination in the AhCre^{+} MDM2$^{flox/flox}$ mice, β-galactosidase was seen to be widely expressed by hepatocytes following the induction with βNF (Figure 6.3B).

Figure 6.2 Highly efficient recombination following βNF induction

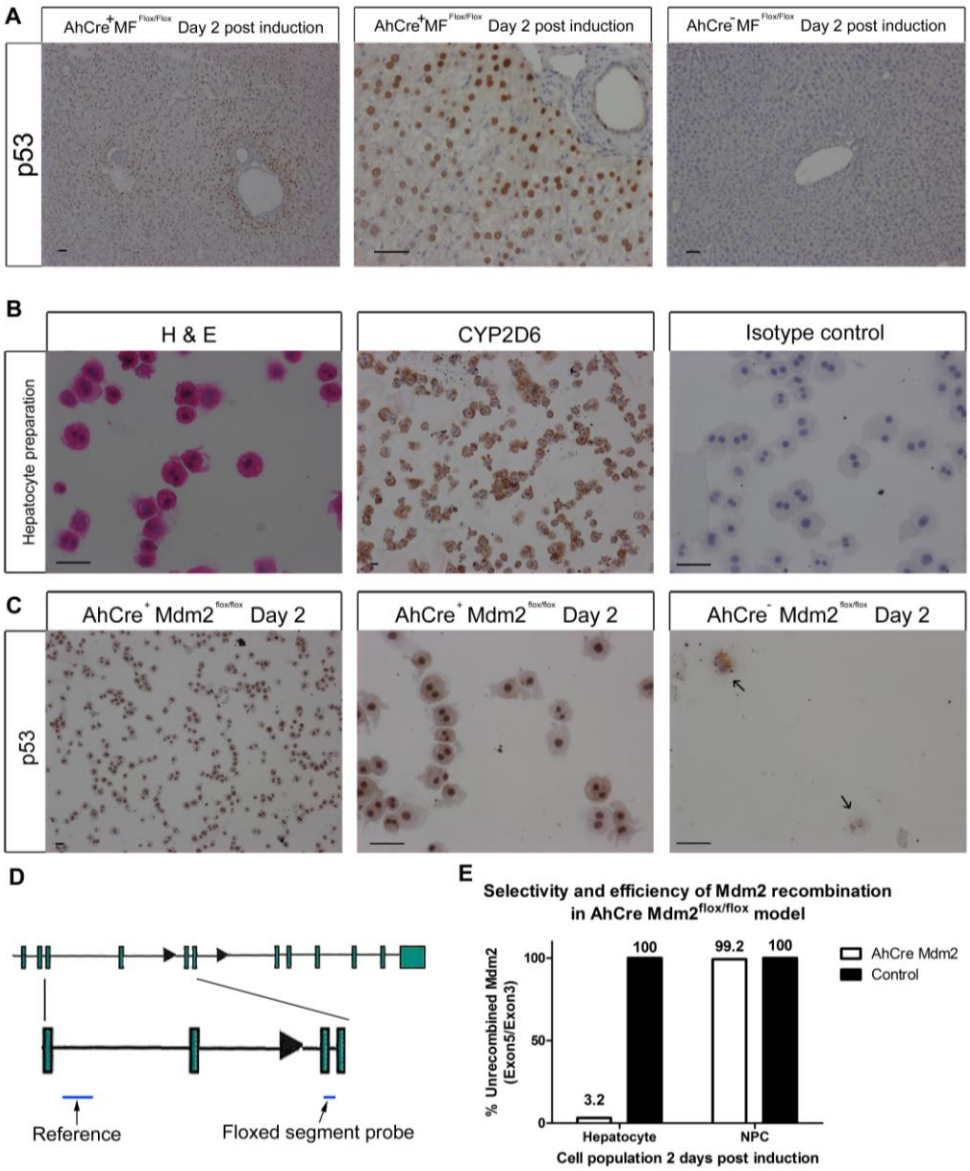

(A) 2 days following induction with 80mg/kg i.p. βNF mouse liver analysed with p53 immunohistochemistry demonstrated widespread upregulation of nuclear p53 in male AhCre^{+} MDM2$^{flox/flox}$ mice vs. male AhCre^{-}MDM2$^{flox/flox}$ controls. An absence of p53 upregulation in identically treated AhCre^{+} MDM2$^{flox/wt}$ mice. (B) Using an optimised method of isolating pure populations of primary hepatocyte, a >99% pure population of hepatocytes was obtained as assessed by CYP2D6 expression. (C) Hepatocytes isolated 2 days following induction using 80mg/kg i.p. βNF in female AhCre^{+} MDM2$^{flox/flox}$ mice and AhCre^{-} MDM2$^{flox/flox}$ were assessed for p53 expression the overwhelming majority of these hepatocytes are p53^{hi}. (D) Combination of qPCR primers sets directed at regions outside (reference sequence) and inside the floxed segment of the MDM2 gene were used for detection of gDNA from purified isolated hepatocytes and isolated non-parenchymal cells (NPC) 2 days following induction in male AhCre^{+} MDM2$^{flox/flox}$ vs. AhCre^{-} MDM2$^{flox/flox}$ control mice 2 days following βNF (; n=3 each group).

Figure 6.3 Hepatocyte specific MDM2 deletion results in hepatocyte senescence

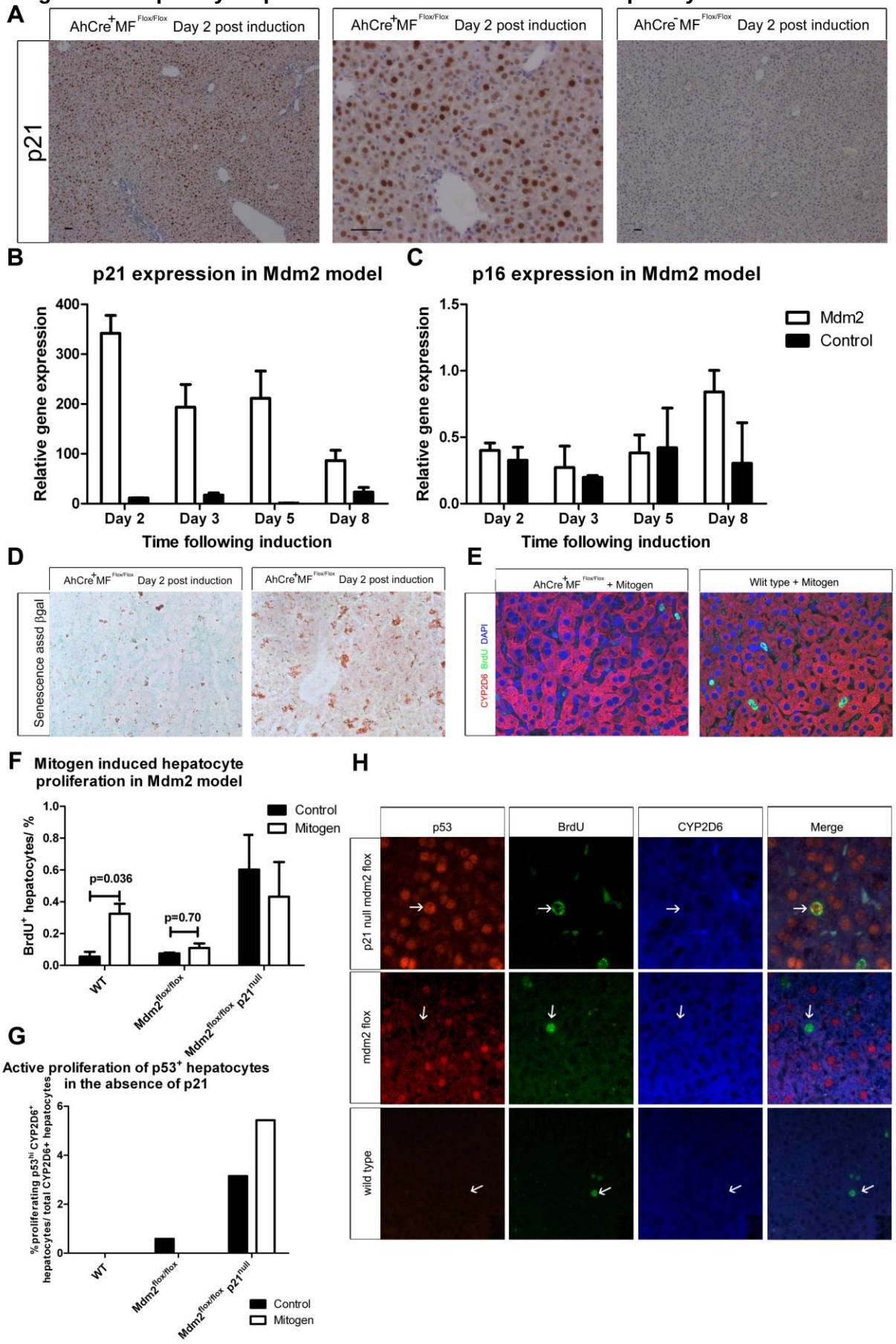

(A) 2 days following induction with 80mg/kg i.p. βNF mouse liver analysed with p21 immunohistochemistry demonstrated widespread upregulation of nuclear p21 in male $AhCre^{+}$ $MDM2^{flox/flox}$ mice vs. male $AhCre^{-}$ $MDM2^{flox/flox}$ controls consistent with elevation at the RNA transcript level over time (B). p16, a downstream prosenescent target of p53, is also elevated over time following MDM2 inactivation (C). (D) Senescence associated β-galactosidase expression 4 days following βNF induction. Using a mitogen cocktail of HGF and T3 (250μg/kg and 4mg/kg respectively) was administered to normal controls, $AhCre^{+}$ $MDM2^{flox/flox}$ mice and $AhCre^{+}$ $MDM2^{flox/flox}$ $p21^{nul}$ mice 3 days following 80mg/kg βNF. (E) Representative images in Wt and $AhCre^{+}$ $MDM2^{flox/flox}$ proliferation are shown for dual immunohistochemistry for CYP2D6 (red) and BrdU (green). (F) Proliferation, 24 hours later, was assessed by immunohistochemistry for BrdU in $CYP2D6^{+}$ hepatocytes (n≥3 each group). (G) Analysis of p53 status of $BrdU^{+}$ $CYP2D6^{+}$ hepatocytes following mitogen and control treatment with representative immunohistochemical analysis (H) performed using p53 (red), BrdU (green) and CYP2D6 (blue). No proliferation of $p53^{hi}$ hepatocytes is seen in WT controls while only a single cell was $p53^{hi}$ proliferating hepatocytes was observed in $AhCre^{+}$ $MDM2^{flox/flox}$ $p21^{WT}$ mice. In contrast, frequent $p53^{hi}$ proliferating hepatocytes are observed in $AhCre^{+}$ $MDM2^{flox/flox}$ $p21^{null}$ mice. All scale bars denote 50μm.

Hepatocyte senescence was also tested functionally by assessing whether recombined hepatocytes are able to respond to a combination of known mitogens (T3 and HGF), by entering cell cycle. When this mitogen cocktail is administered *in vivo*, significant entry into S-phase is observed within the hepatocyte population in control mice. This effect however, is lost when the mitogen cocktail is given to $AhCre^{+}$ $MDM2^{flox/flox}$ mice after hepatocyte specific MDM2 deletion (Figure 6.3E and F). Therefore, a combination of senescence associated markers and failure to respond to normally mitogenic stimuli indicates a state of senescence is achieved in hepatocytes following induction in the AhCre $MDM2^{flox}$ model.

Induced hepatocyte senescence is p21 dependent

To test whether the senescence phenotype induced in hepatocytes following MDM2 deletion was dependent on p21 function, $AhCre^{+}$ $MDM2^{flox/flox}$ mice were bred onto a $p21^{null}$ background. When the same *in vivo* mitogen stimuli used previously were applied to these mice hepatocytes did respond to the mitogen cocktail and enter cell cycle even after induction using βNF. This was in contrast to their $p21^{wt}$ controls which did not respond to the mitogen cocktail (Figure 6.3F). This therefore demonstrates that p21 plays a central role in the induction of senescence following MDM2 loss. Further detailed examination of the characteristics of the proliferating cells in this model revealed that the increased proliferation in the $p21^{null}$ mice, versus $p21^{wt}$ mice, occurred in $p53^{hi}$ hepatocytes (Figure 6.3G and H).

6.52 Induced hepatocellular injury in the AhCre MDM^{flox} model

Following induction, in $AhCre^{+}$ $MDM2^{flox/flox}$ mice, dramatic rises in ALT, AST, bilirubin and alkaline phosphatase are observed (Figure 6.4A-D). Derangement of liver function is observed with increase in Alt from a baseline of 42U/L to a peak of 471U/L 2 days following induction (Figure 6.4C). Similarly AST increases from a baseline of 246

to 1170U/L (Figure 6.4B). Associated increases in bilirubin and alkaline Phosphatase and a reduction in serum albumin are also witnessed, in keeping with hepatic injury (Figures 6.4C-E respectively). The onset of bilirubinuria, along with associated derangement of the liver function tests provides a rudimentary assessment of liver injury in these mice. Liver injury was also assessed histologically, revealing evidence of profound hepatocellular death (Figure 6.4F).

Hepatocyte apoptosis was assessed using TUNEL staining demonstrating the occurrence of significant and widespread hepatocyte apoptosis (Figure 6.4G). Furthermore, a p53 dependent pro-apoptotic program consisting of Bax 1 and PUMA is activated following βNF induction (Figure 6.4H and I). Highest expression of both Bax 1 and PUMA occurs 2 days following induction with 11.7 and 2.72 times expression of induced control mice observed respectively. Together, these results show that the loss of MDM2 function and consequent elevation of p53 results in injury, together with the previously observed senescence.

6.53 Induced massive HPC activation in the AhCre MDM2^{flox} model

Given the induction of both hepatocyte senescence and hepatocellular injury following βNF induction in the AhCre^{+} MDM2$^{flox/flox}$ model, I hypothesised that HPC activation would also occur in response to this regenerative stimulus. Using a variety of HPC markers, including panCK, Dlk1 and EpCAM, a progressive and massive HPC activation is observed in the AhCre^{+} MDM2^{flox} model (Figure 6.5). In similarity to the phenotype of HPC activation in the murine CDE diet or rat PH/AAF model, HPC activation in this instance occurs in an infiltrating phenotype. Here HPCs extend as cords rather than ducts and infiltrate into the hepatic parenchyma (Figure 6.5A). Consistent with the histological evidence of significant HPC activation an elevation of HPC markers at the RNA level is observed in whole liver following βNF induction (Figure 6.5E-G).

Figure 6.4 Hepatocyte specific MDM2 deletion results in hepatocellular injury

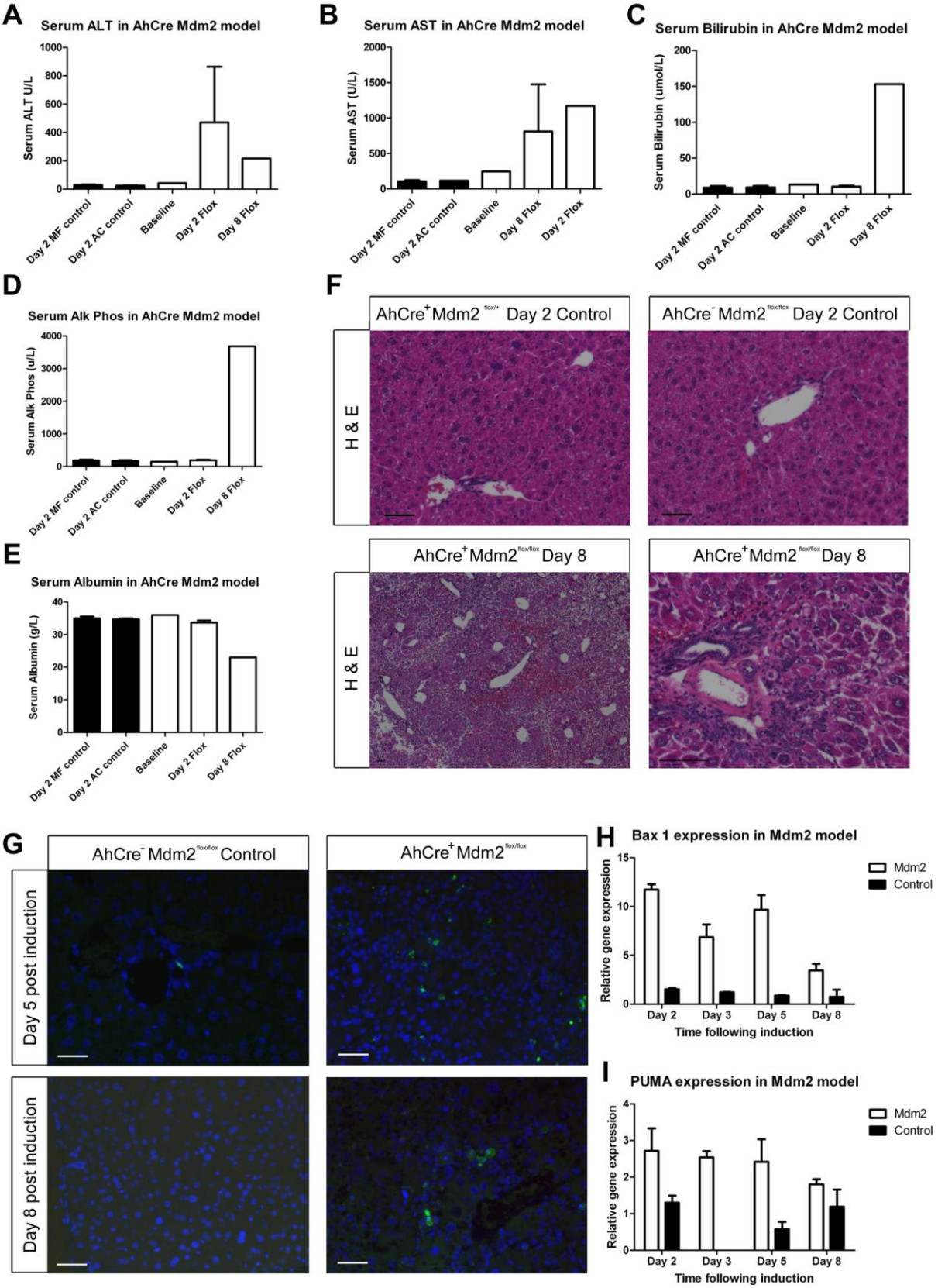

Serum liver function derangement occurs following induction with 80mg/kg i.p. βNF in male AhCre^{+} MDM2$^{flox/flox}$ but not in uninduced AhCre^{+} MDM2$^{flox/flox}$ or induced AhCre^{-} MDM2$^{flox/flox}$ controls: (A) ALT (B) AST (C) Bilirubin (D) Alkaline Phosphatase and (E) Albumin. (F) Normal hepatic parenchyma in induced controls (AhCre^{+} MDM2$^{flox/+}$ and AhCre^{-} MDM2$^{flox/flox}$ respectively), but widespread parenchymal injury is observed on H&E staining 8 days following induction with 80mg/kg i.p. βNF in male AhCre^{+} MDM2$^{flox/flox}$ mice. (G) TUNEL staining (Alexa 488 detection; green and DAPI; blue) reveals widespread parenchymal apoptosis 5 and 8 days following induction compared to AhCre^{-} MDM2$^{flox/flox}$ controls given 80mg/kg i.p. βNF (a rare apoptotic cells in day 5 control mice is shown while representative field shown for day 8 control). Whole liver analysis by qRT-PCR for apoptosis associated gene Bax 1(H) and PUMA (I). (n=3 for all AhCre^{+} MDM2$^{flox/flox}$ data points, control data for days 2 and 5 n=3, and n=2 for days 3 and 8). All scale bars denote 50μm.

The HPC activation which occurs following induction in the AhCre MDM2^{flox} model is striking, with large numbers of HPCs observed as early as 8 days following induction of genetic recombination. This response is much more rapid than the HPC expansion observed with the CDE diet (Chapter 3). Furthermore, the magnitude of the HPC response in the AhCre^{+} MDM2^{flox} model is significantly greater than the CDE diet (243 vs. 61 HPCs per field respectively; Figure 6.5).

Following highly efficient and specific hepatocyte recombination in male AhCre^{+} MDM2$^{flox/flox}$, morbidity with hunching piloerection and social withdrawal and even occasional mortality occurred. Together with the changes described above, this implied that these clinical consequences were related to liver injury. I therefore asked whether these side effects were associated with the degree of induction in hepatocytes? Using identical induction doses of βNF in aged matched female mice, induction of widespread p53 over-expression is noted in the liver 2 days following induction (Figure 6.6A). However while widespread, the p53 upregulation in female mice, it was induced at obviously reduced efficiency in comparison to male mice receiving the same induction regime.

Using qPCR (as previously described in Figure 6.2) to assess recombination in this population 19% of MDM2 genes retained the floxed segment of the gene corresponding

to 81% recombination at the chromosome level (Figure 6.6C). While not as efficient as the recombination in the similar male AhCre^{+} MDM2$^{flox/-}$ model (see Section 6.41), this remains a highly efficient induction system. When induced, with this resultant lower efficiency, female mice did not display the severity or frequency of clinical side effects observed in their, more efficiently induced, male counterparts.

6.6 Characterisation of hepatic phenotype in alternative models of transgenic MDM2 deletion in AhCre MDM2^{flox} models

The effect of the lower proportion of hepatocyte recombination on the resultant HPC activation was then assessed in the female AhCre^{+} MDM2$^{flox/flox}$ mice. In this model, an attenuated expansion of panCK^{+} HPCs is observed peaking again at approximately 6-8 days following induction (Figure 6.6B). Here no animal mortality was observed, with all mice surviving to at least 45 days without significant morbidity. This is in significant contrast to universal requirement for humane euthanasia by day 9 following induction in male mice given the identical induction regime.

An alternative induction protocol in male AhCre^{+} MDM2$^{flox/flox}$ mice, using lower induction doses (40mg/kg βNF), results again in lower efficiency of p53 induction and minimal expansion of HPCs (Figure 6.6D). Once again this induction is associated with no significant mouse morbidity or mortality that observed with the previous higher dose (80mg/kg βNF) in male mice. These results are, once again, in keeping with a dose dependent induction of recombination. Similarly higher induction doses (3x80mg/kg βNF) in female AhCre^{+} MDM2$^{flox/flox}$ mice results once again in mortality.

Figure 6.5 Progressive activation of HPC following induction in the AhCre MDM2 model

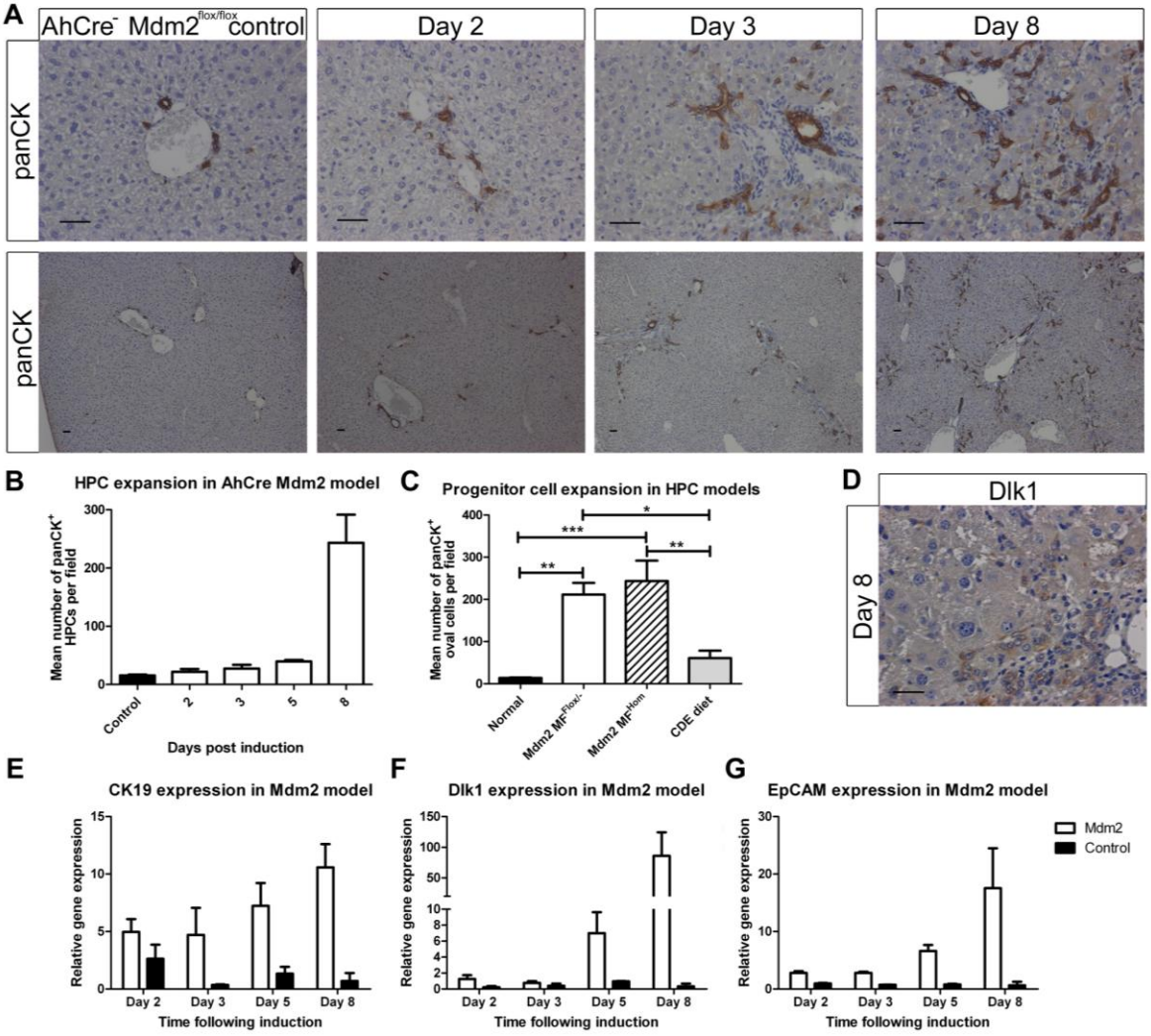

(A) Following induction with 80mg/kg i.p. βNF a progressive and dramatic expansion of panCK^{+} HPCs is observed within the liver. (B) Quantification of HPCs over time (n≥3 each group) reveals an increased HPC expansion compared to the CDE diet (C), data is presented for AhCre^{+} MDM2$^{flox/-}$ and MDM2$^{flox/flox}$ (hom) mice at time of maximum HPC expansion (day 19 and 8 respectively) vs. maximal HPC expansion in CDE diet (Day 12). (D) HPCs express Dlk1. Corresponding changes in mRNA expression of HPC markers CK19, Dlk1 and EpCAM (E-G respectively)are observed vs. control in the AhCre MDM2^{flox} model (all MDM2 time points n=3, all controls n≥3). *p<0.05, **p<0.01, ***p<0.001 by Mann Whitney test, all scale bars denote 50μm.

Figure 6.6 Reduced recombination and HPC activation in female mice

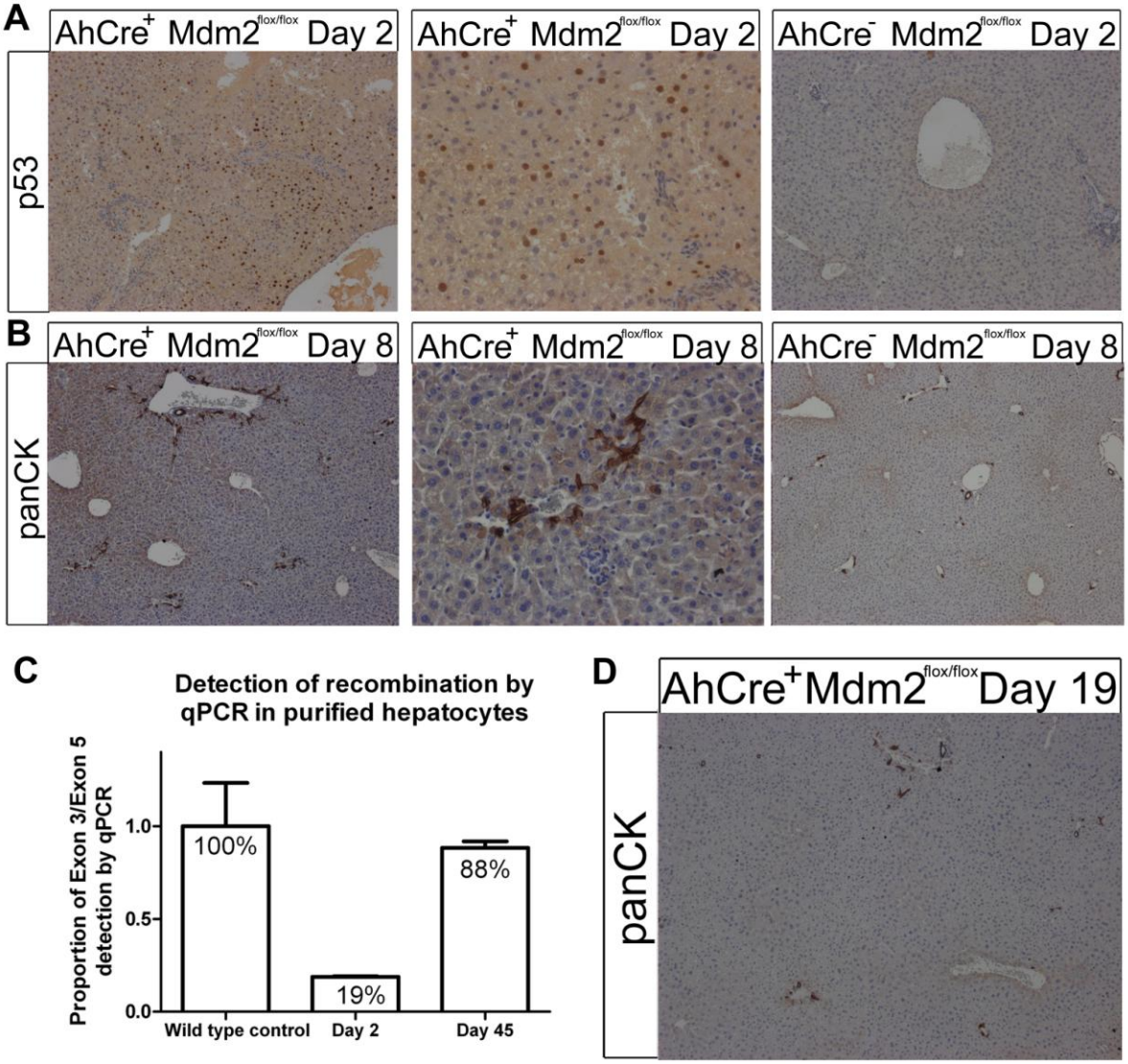

Induction with 80mg/kg i.p. βNF in female AhCre^{+} MDM2$^{flox/flox}$ mice leads to widespread but incomplete p53 upregulation in hepatocytes 2 days following induction, while no p53 over expression is observed in AhCre^{-} MDM2$^{flox/flox}$ controls following βNF (A). Expansion of panCK^{+} HPCs at day 8 in AhCre^{+} MDM2$^{flox/flox}$ compared to AhCre^{-} controls (B). qPCR analysis of purified hepatocytes gDNA from female AhCre^{+} MDM2$^{flox/flox}$ over time reveals reduced efficiency of recombination with only 81% of MDM2 genes being inactivated 2 days following induction. This levels falls with time to only 12% 45 days post induction (C). Male AhCre^{+} MDM2$^{flox/flox}$ mice survive beyond 19 days without HPC expansion when induced with the lower 40mg/kg i.p. βNF induction regime (D).

Figure 6.7 Efficient recombination but delayed hepatic injury in AhCre MDM2$^{-/flox}$ mice

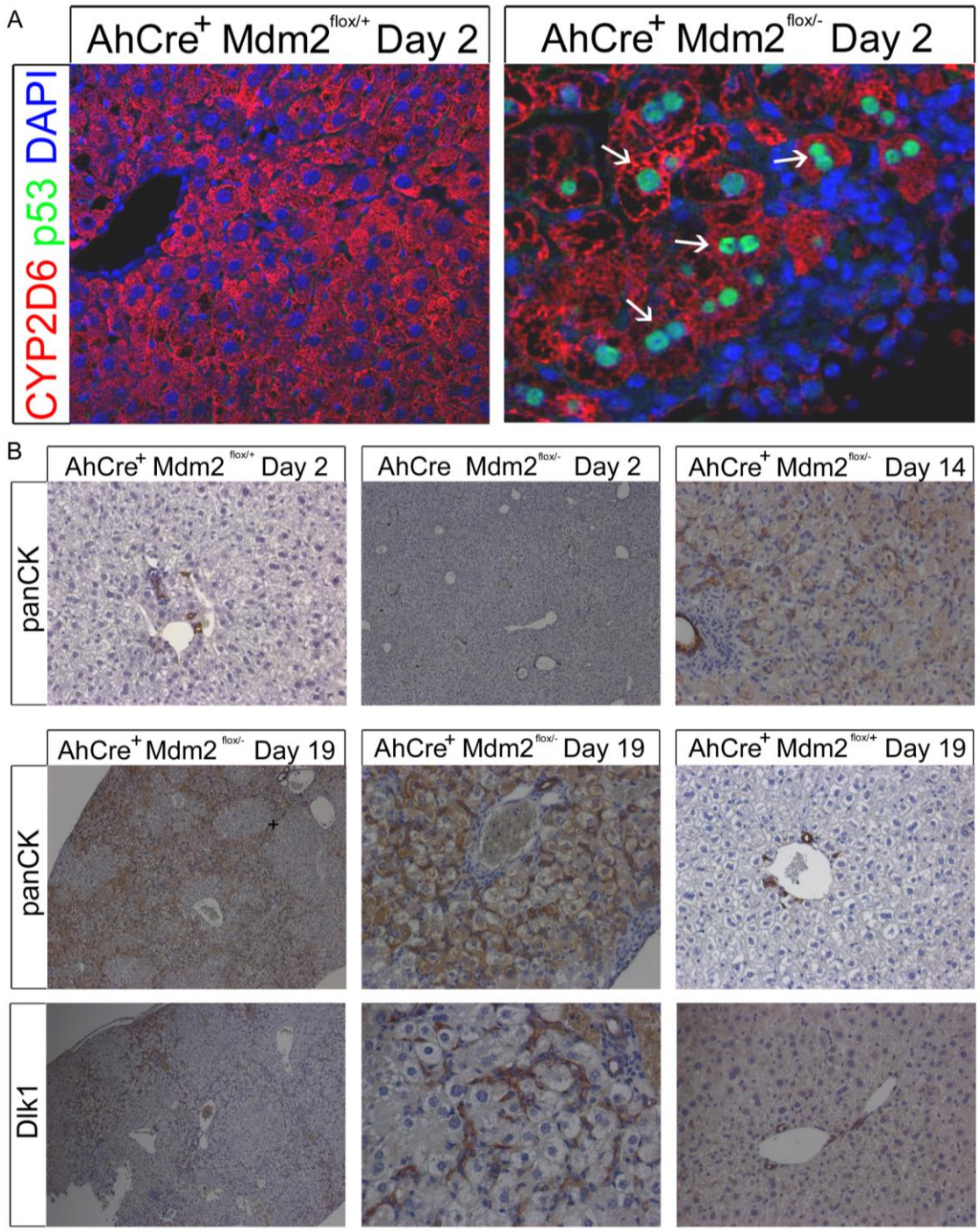

When a high dose induction (80mg/kg βNF) is performed in male AhCre^{+} MDM2$^{flox/-}$ mice, exceptionally efficient hepatocyte specific p53 upregulation is observed by immunohistochemistry (A) for CYP2D6 (red) p53 (green) and DAPI (blue) together with a progressive panCK^{+} and Dlk1^{+} HPC expansion over 3 weeks (B).

6.61 Hepatic parenchymal repopulation in the AhCre^{+} MDM2$^{flox/-}$ model

In an alternative model of MDM2 inactivation, congenitally heterozygous MDM2 deficient mice (which show no overt phenotype mice), were crossed onto an MDM2^{flox} background to generate AhCre^{+} MDM2$^{flox/-}$ mice. Following MDM2^{flox} inactivation by administration of 80mg/kg βNF highly efficient recombination was once again observed by hepatocyte specific p53 upregulation (Figure 6.7A). This effect is comparable to that previously described in AhCre^{+} MDM2$^{flox/flox}$ male mice (section 6.2). Once again in this context, a dramatic expansion of panCK^{+} and Dlk1^{+} HPCs is observed (Figure 6.7B, see also Figure 6.5C), as with male AhCre^{+} MDM2$^{flox/flox}$ mice. However, in contrast to the homozygote AhCre^{+} MDM2$^{flox/flox}$ mice, these heterozygote deficient AhCre^{+} MDM2$^{flox/-}$ mice remain healthy over the period of the first two weeks, with a minority of mice developing clinical signs of liver injury between 14 and 21 days. These signs were indistinguishable to those observed in AhCre^{+} MDM2$^{flox/flox}$ mice at approximately 1 week post-induction. Most heterozygote mice however survived without the need for humane euthanasia. The development of clinical signs is once again consistent with the contemporaneous development of dramatic HPC activation. Analysis of liver injury both histologically and by TUNEL assay reveals marked hepatocellular injury and apoptosis over this period (Figure 6.8A and B). Serum analysis also confirms the presence of liver injury with raised transaminases and bilirubin (Figure 6.8C and D).

In summary therefore, differing levels of hepatocyte recombination may be achieved together with different levels of resultant liver injury occurring over defined but variable time courses by using different induction regimes. Differing induction regimes used here took the form of dose adjustments of βNF, altering the mouse sex, and/or genotype.

Figure 6.8 Hepatocellular injury and apoptosis in the AhCre^{+} MDM2$^{flox/-}$ model

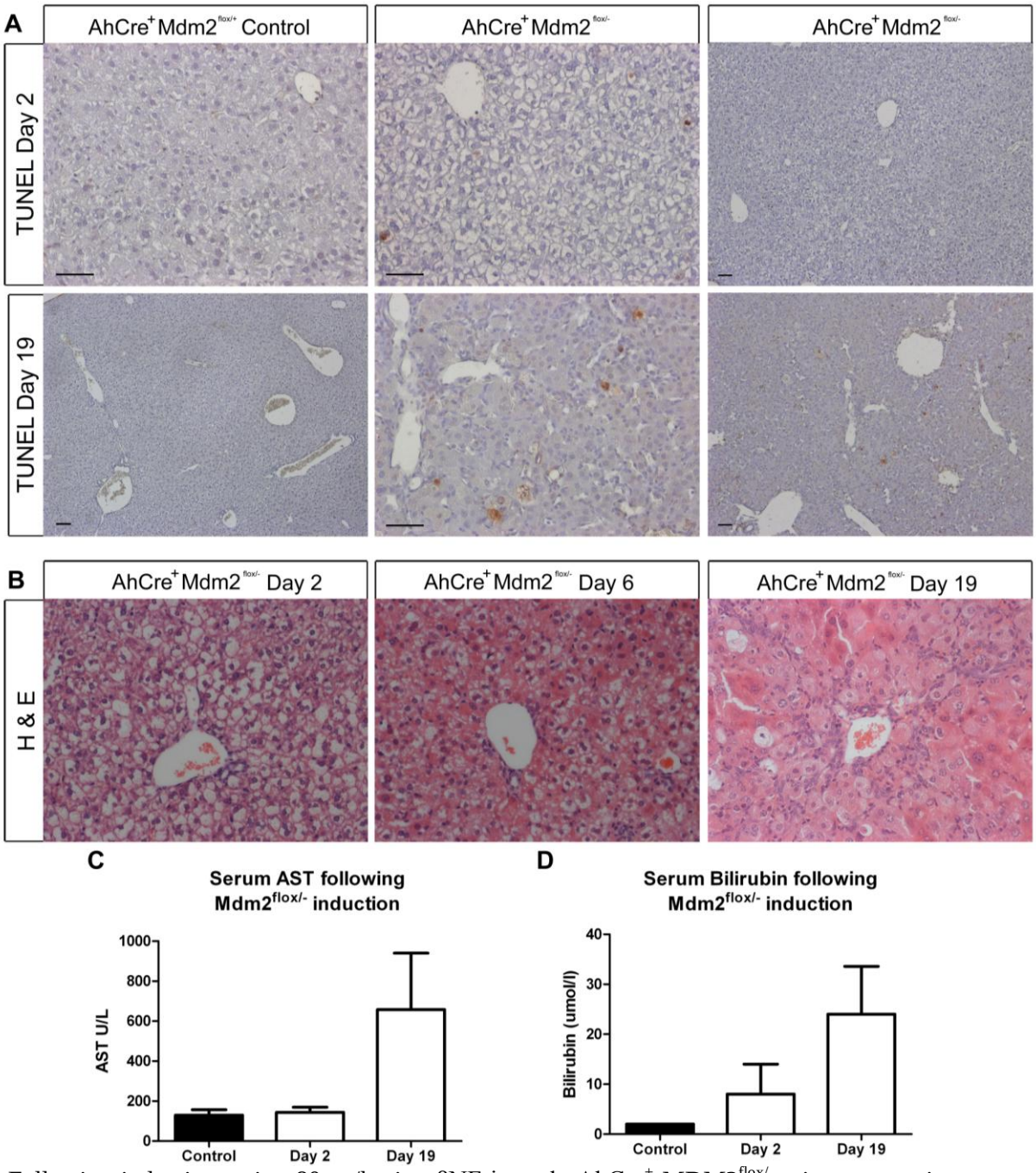

Following induction, using 80mg/kg i.p. βNF in male AhCre^{+} MDM2$^{flox/-}$ mice, apoptosis was assessed by TUNEL assay (A) together with liver injury by H&E (B). Apoptotic cells (brown) can be seen as early as 2 days following induction with increased numbers 19 days post induction. Corresponding serum analysis for AST (C) and Bilirubin (D); n≥5 each group (AST $P<0.0001$; T test).

In each of the models described above both the number and proportion of $p53^{hi}$ hepatocytes in livers reduced over time after induction. This implies a gradual loss of $p53^{hi}$ recombined hepatocytes. As widespread hepatocyte apoptosis occurs following recombination, the reduction in overall $p53^{hi}$ hepatocyte number might be expected. Therefore the change in proportion of $p53^{hi}$ hepatocytes was not necessarily unexpected, however it was also clear that liver function and architecture returned to normal over a period of time (Figure 6.9A). This was also accompanied resolution of HPC activation.

With the hypothesis that HPCs were the precursor source for hepatocyte regeneration in this model, I asked whether there was evidence of HPC mediated regeneration in the AhCre $MDM2^{flox}$ model. To do so, I utilised the observation that all hepatocytes could be induced to undergo recombination to lineage trace hepatocyte versus non-hepatocyte mediated regeneration of freshly derived hepatocytes in this model.

As previously described, hepatocyte proliferation (assessed by BrdU incorporation) following recombination was extremely rare (Figure 6.3), implying a limited role of hepatocyte mediated hepatocyte regeneration. Furthermore the rare hepatocytes identified in cell cycle 4 days following recombination were overwhelmingly $p53^{low}$, and therefore likely themselves to be from a non-recombined precursor source. The permanent genetic recombination in the hepatocyte population following induction affords an ability to separate regeneration from a recombined (e.g. hepatocyte source) from a non-recombined (e.g. progenitor cell source). In support of an HPC mediated regenerative response in this model I observed a reducing proportion of $p53^{hi}$ hepatocytes over time, even in the highly efficient recombination models (Figure 6.9C).

Therefore, in this novel model, an unrecombined and undifferentiated source of hepatocytes is responsible for the replenishment of freshly derived hepatocytes. I therefore assessed whether HPCs may be the source of these freshly regenerated hepatocytes in this model. As previously described a large expansion of HPCs is observed following induction (Figures 6.5 and 6.7).

Figure 6.9 Regeneration of hepatocytes from a precursor source

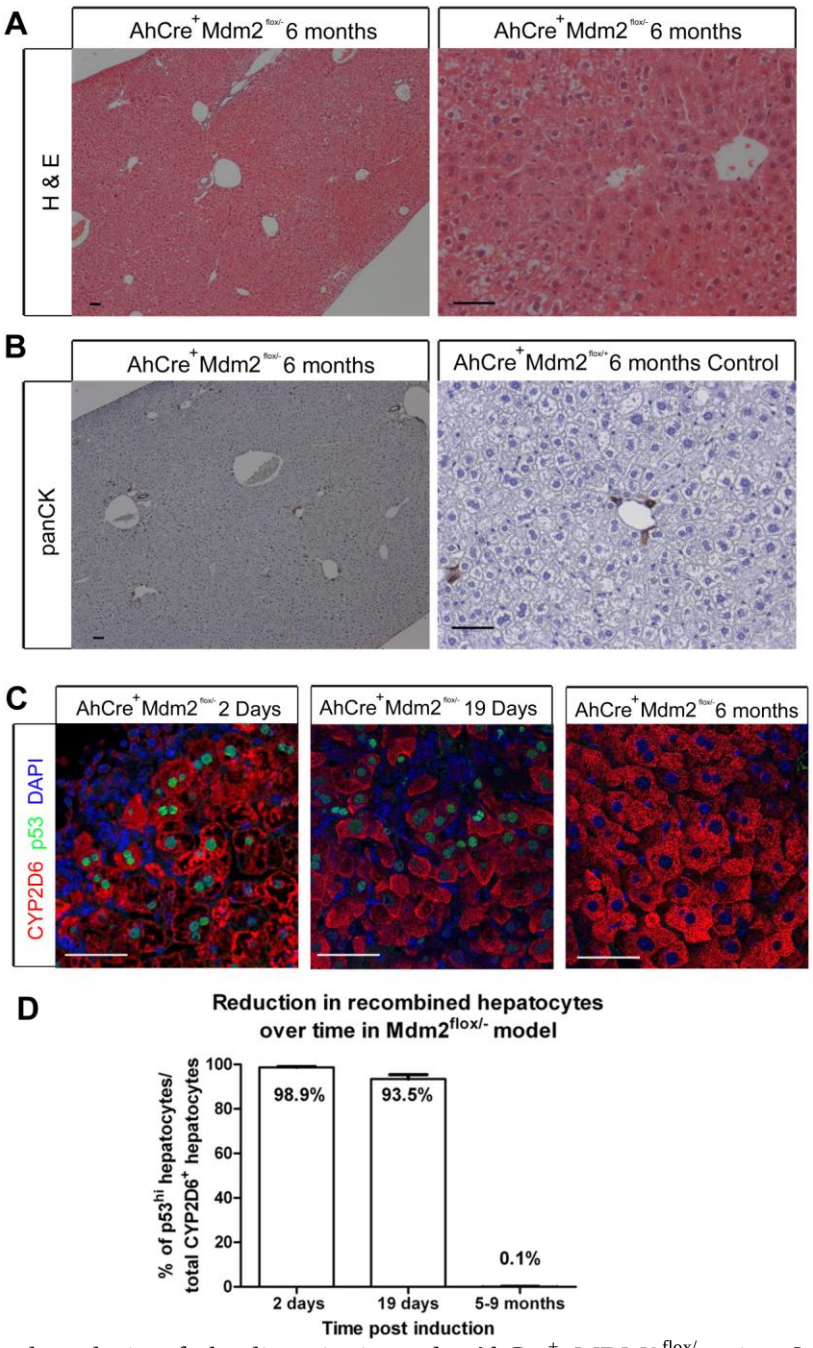

Histological analysis of the liver in in male AhCre^{+} MDM2$^{flox/-}$ mice 6 months following induction with 80mg/kg i.p. βNF by H&E (A) and panCK immunohistochemistry (B) reveals resolution of injury an associated loss of HPC activation over time. Assessment of proportion of recombined hepatocytes over time using detection of CYP2D6 (red) and p53 (green) in the same groups of mice (C) with quantification of recombined hepatocytes expressed % total hepatocytes with p53 upregulation (n≥3 each groups; 0% in AhCre^{+} MDM2$^{flox/+}$ control mice at each time point). All scale bars denote 50μm.

In order for panCK$^+$ HPCs to be a potential source of regeneration of hepatocytes in this model they must themselves not undergo genetic recombination of the MDM2 locus in response to βNF induction. Once again using p53 upregulation as a marker of MDM2 gene deletion, there was no evidence of recombination in the panCK$^+$ HPC compartment (Figure 6.10). Additionally in the portal areas p53^{low} hepatocytes were observed and were often in direct contact with panCK$^+$ HPCs.

6.7 In vitro hepatocyte differentiation of HPCs isolated from actively regenerating AhCre MDM2^{flox} livers

To investigate the potential for HPCs derived from the MDM2 model to differentiate into hepatocytes *in vitro*, HPCs were extracted and subsequently cultured under differentiation conditions. HPCs were isolated at the time of peak HPC activation (eight days following induction), and purified and then cultured *in vitro*. These cells retained small, HPC like morphology until cultured under differentiation conditions, following which they developed a hepatocyte like morphology. Analysis of expression patterns of the hepatocyte marker HNF4α demonstrated that HPCs *in vitro* may differentiate into hepatocyte-like cells under differentiation conditions (Figure 6.11A and B).

RNA expression analysis of these populations revealed a reduction in HPC markers without the consistent development of a differentiated hepatocellular-like phenotype (Figure 6.11C). While Dlk expression fell under differentiation conditions, Fn14 gene expression was increased and no significant changes were identified in CK19, EpCAM, HNF3β, HNF4α, and HNF1β (Figure 6.12). Albumin gene expression fell significantly during differentiation conditions but was strikingly lower than hepatocyte control in both undifferentiated and differentiated HPCs. Asialoglycoprotein gene expression was not detected consistently in either HPC population (sensitivity 4000x less than hepatocyte control).

Figure 6.10 HPCs are not phenotypically affected by induction in the AhCre MDM2^{flox} model

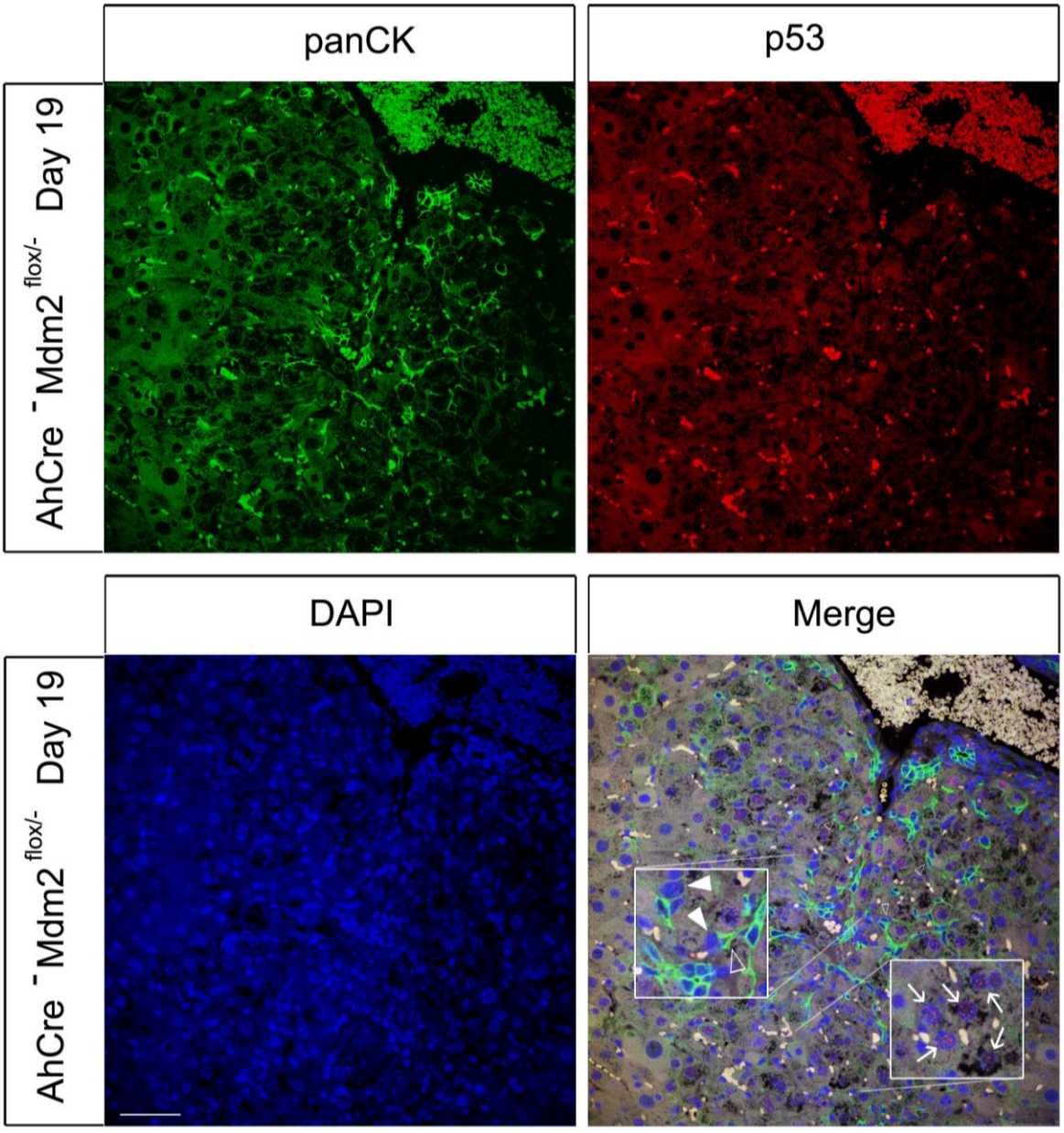

Confocal analysis following immunohistochemical identification of p53 status of panCK^{+} HPCs 19 days following induction with 80mg/kg i.p. βNF in AhCre^{+} MDM2$^{flox/-}$ mice. p53^{hi} hepatocytes are observed within the parenchyma (arrows). panCK^{+} HPCs are not p53^{hi} (hollow arrowheads). Additionally p53^{lo} hepatocytes are observed in the portal tract often in direct contact with panCK^{+} HPCs (solid arrowheads). Scale bar denotes 50μm.

Figure 6.11 *In vitro* evidence for HPC mediated regeneration

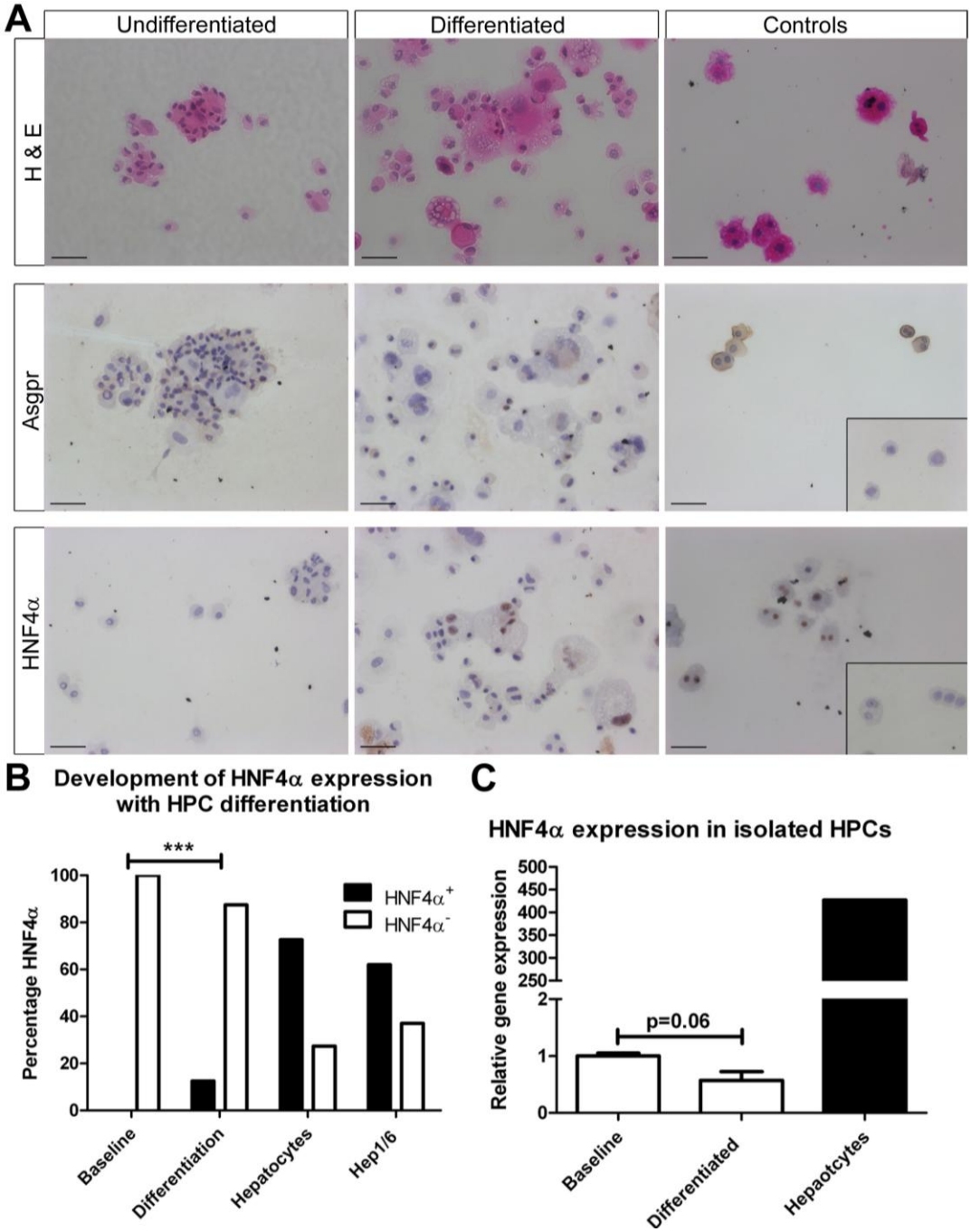

(A)

NPCs were isolated from male AhCre^{+} MDM2$^{flox/flox}$ mice 8 days after βNF induction (1x80mg/kg; n=3). NPCs were cultured for 14 days in low serum HPC media to remove contaminating endothelia at which point no cells (n=308 from 4 independent experiments) expressed HNF4α (E). Following HPC differentiation HNF4α expression was noted on 12.6% of cells (n=1145 from 4 independent experiments). No significant changes in HNF4α (C), HNF3β were seen on a population basis following 5 days in differentiation media. RNA analysis performed in triplicates from n=4 samples in each group.

Figure 6.12 Gene analysis following *in vitro* differentiation of HPCs

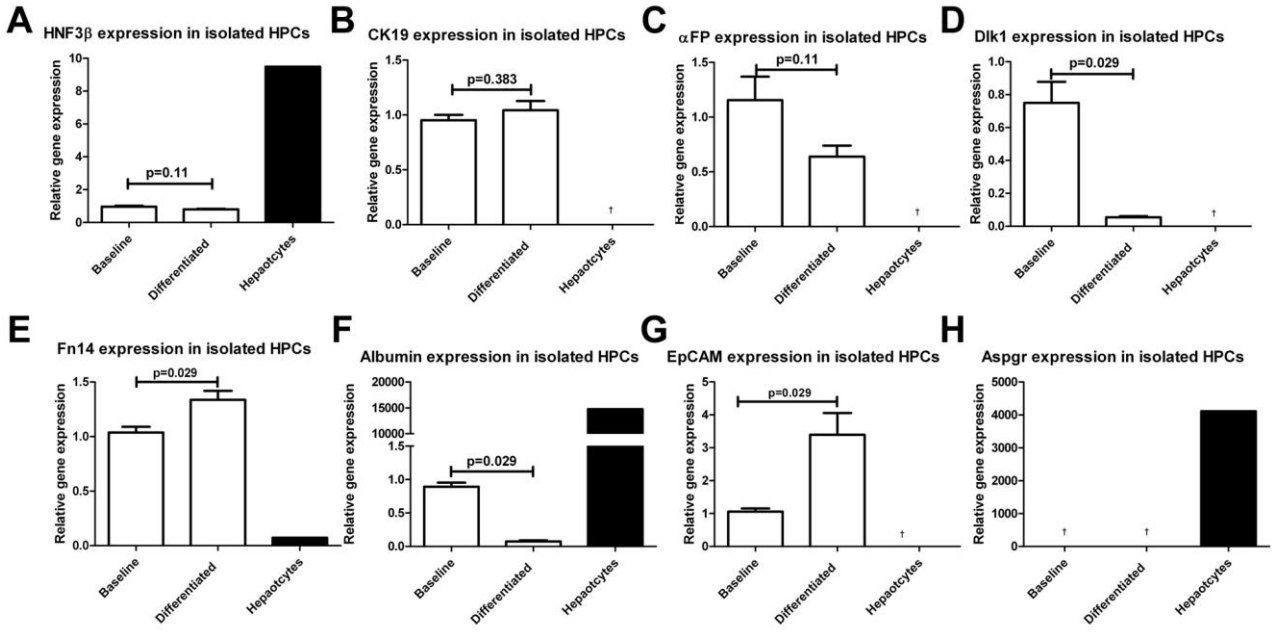

RNA analysis of HPC and hepatocytic gene expression on a population basis from *in vitro* cultures HPCs as shown previously in Figure 6.11. Gene expression of HNF3β (A), CK19 (B) and αFP (C) did not change upon differentiation of HPCs *in vitro* while Dlk gene expression fell (D) during this time while Fn14 (E) EpCAM (F) and Albumin (G) gene expression increased. Asialoglycoprotein expression was not detected in either HPC population (H) RNA analysis performed in triplicates from n=4 samples in each group.

6.8 Relationship of HPCs to hepatocyte regeneration in vivo in the AhCre MDM2^{flox} model

In order to examine the differentiation capacity of panCK^{+} HPCs *in vivo* a BrdU pulse-chase strategy was used. Following initial trials of BrdU delivered at either 2,4,5, or 8 days following induction it was noted that if BrdU was delivered 2 days following induction a high proportion of BrdU labelled cells were panCK^{+} (Figure 6.13A). This time point represented the period with the largest proportional BrdU labeling of panCK^{+} HPCs, none-the-less BrdU label expression was not isolated to the panCK^{+} population even at this optimal time point. When BrdU was administered at day 2 and liver

analysis performed 2 days later, limited BrdU expression was observed in control animals, whilst in experimental animals a dramatic periportal BrdU labelling was observed in the AhCre^{+} MDM2$^{flox/flox}$ model (Figure 6.13A). BrdU labelled cells in the periportal area included cells with hepatocyte like phenotypes (Figure 6.13B) and cells with enlarged nuclei but with intermediate expression of panCK, analogous to small hepatocyte like cells (Figure 6.13C). Additionally when female mice were given BrdU 4 days following induction were assessed at day 8 clustered of periportal BrdU^{+} cells were observed containing both BrdU^{+} panCK^{+} cells and BrdU^{+} hepatocytes (Figure 6.13D).

Examination between the relationship of HPCs and liver regeneration in the repopulating AhCre MDM2$^{flox/-}$ model was performed by assessing the identity of proliferating cells during the period of hepatocyte repopulation. At this time large numbers of proliferating (Ki-67^{+}) hepatocytes are observed (Figure 6.14).

6.9 Absence of long term sequelae following complete hepatic parenchymal regeneration in the AhCre MDM2$^{flox/-}$ model

When large scale hepatocyte labeling is applied to AhCre^{+} MDM2$^{flox/flox}$ mice, significant morbidity and mortality ensues. Therefore, in this model it is not possible to ask the question: what are the functional consequences of regeneration of hepatocytes from HPCs? I therefore sought to examine whether this question could be addressed using an alternative model in which large scale hepatocyte repopulation was once again observed but in which the clinical consequences were not as severe. Working under the hypothesis that the improved outcome previously noted in fully induced AhCre^{+} MDM2$^{flox/-}$ mice was due to the partial compensation of chronically reduced MDM2 expression in p53 regulation, I examined hepatic repopulation in these mice. Once again using p53 as a marker for MDM2 recombination, following full induction long term restoration of hepatocytes was observed in these mice (Figure 6.19). I then sought to address whether any long term sequelae were observed following complete hepatocyte

repopulation alongside dramatic HPC induction. No hepatocellular carcinomas were observed in this cohort (n=6) and detailed analysis by H&E (Figure 6.9A) and by Pico Sirius Red staining revealed a normalisation of liver architecture in the absence of fibrosis (Figure 6.15).

Figure 6.13 Product precursor relationship from HPCs to hepatocytes *in vivo*

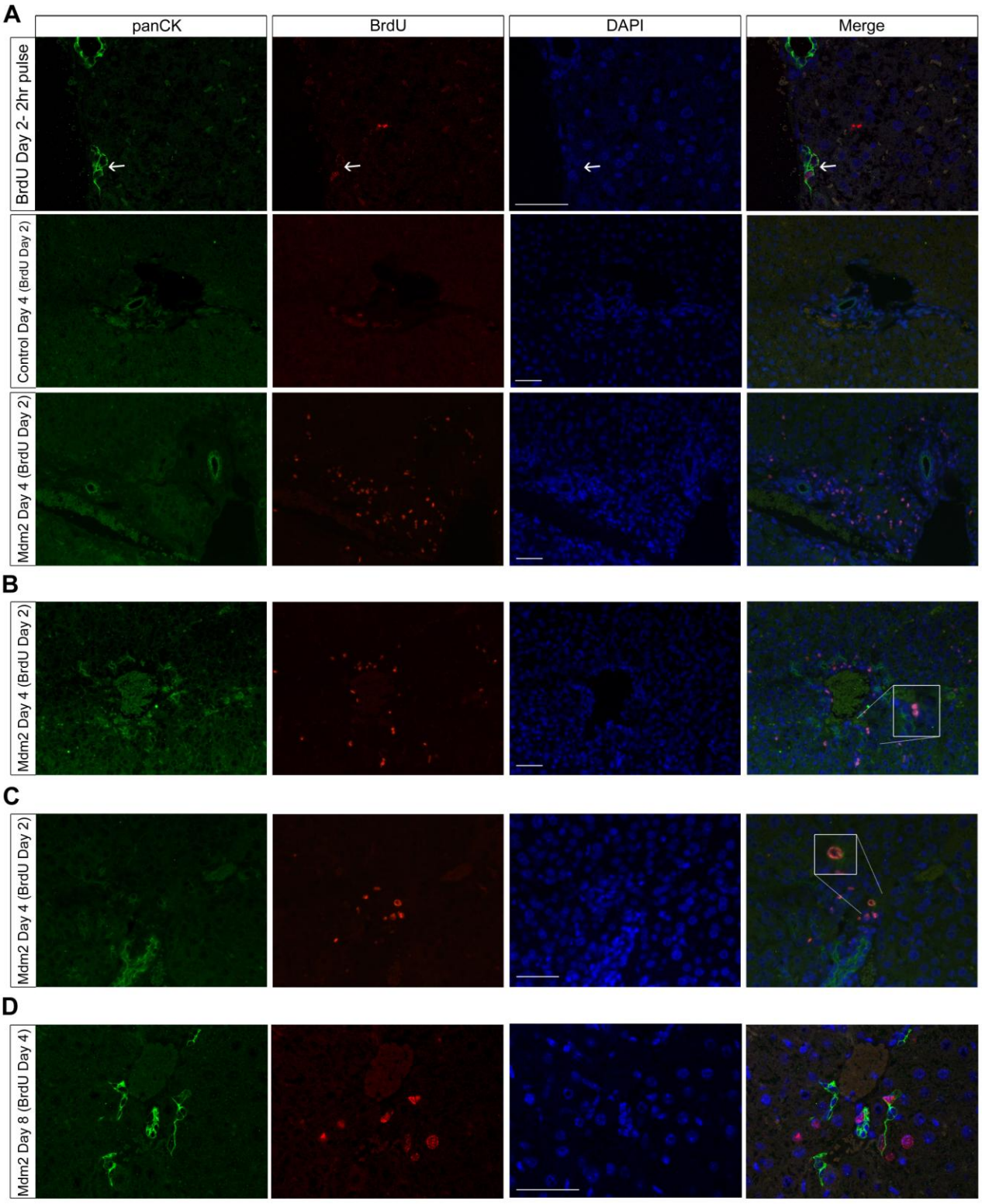

Immunohistochemical analysis for panCK (green) and BrdU (red) in $AhCre^{+}$ $Mm2^{flox/flox}$ mice treated with BrdU. (A) When BrdU is administered 2 days following induction with 1x80mg/kg βNF in male $AhCre^{+}$ $MDM2^{flox/flox}$ mice, analysis 2 hours following BrdU reveals frequent BrdU labelling in $panCK^{+}$ HPCs. When mice are then analysed a further 2 days after BrdU, BrdU is observed in large numbers of $panCK^{-}$ periportal cells. Control ($AhCre^{-}$ $Mm2^{flox/flox}$) animals given the same regime of βNF and BrdU show only very limited BrdU label in the portal areas 2 days following BrdU administration. Further analysis of $AhCre^{+}$ $Mm2^{flox/flox}$ 2 days following BrdU reveals $BrdU^{+}$ hepatocyte-like cells in the portal areas some which do not (B) and some which do possess weak $panCK^{+}$ expression (B) and (C) respectively. (D) When female $AhCre^{+}$ $Mm2^{flox/flox}$ are induced with 1x80mg/kg βNF, given BrdU 4 days later, and liver analysis performed after a further 4 days, periportal clusters of $BrdU^{+}$ cells are observed containing both $panCK^{+}$ HPCs and hepatocytes. Scale bar denotes 50μm.

Figure 6.14 Generation of proliferating hepatocytes from HPCs

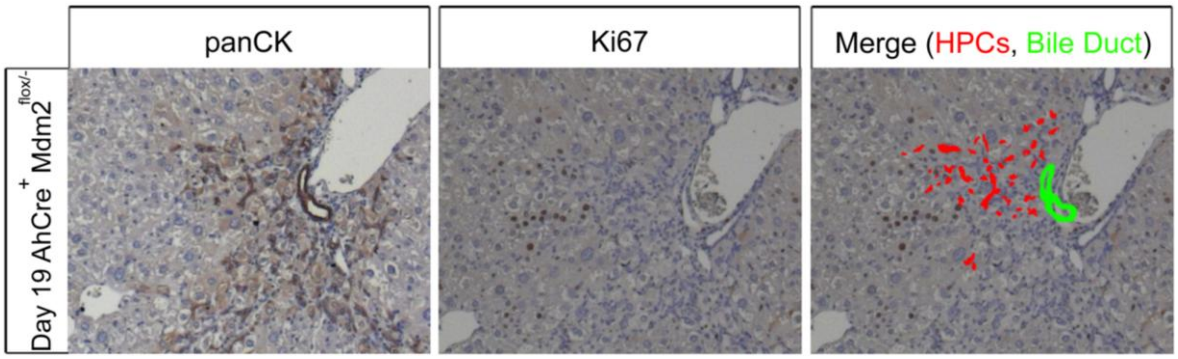

Serial section immunohistochemical analysis of livers 19 days following 1x80mg/kg βNF induction AhCre^{+} MDM2$^{flox/-}$ mice. HPCs are assessed by panCK and proliferation by Ki-67. When the relationship between cords of Ki-67 positive hepatocytes to HPCs is assessed each stream of proliferating hepatocytes can be observed to lie in direct opposition to the distal tip of an HPC cord.

6.10 Manipulation of HPC results in altered regeneration in the AhCre MDM2^{flox} model

Having previously demonstrated a role for TWEAK in the activation of HPCs following macrophage infusion I hypothesised that TWEAK would also be mitogenic stimulus in HPC mediated regeneration in the AhCre MDM2^{flox} model. To test this and observe the functional consequences of impaired TWEAK signalling in HPC mediated regeneration this pathway was manipulated both by impaired and augmented TWEAK signalling in the *in vivo* model. To examine impaired TWEAK signalling, AhCre^{+} MDM2$^{flox/flox}$ mice were bred with Fn14$^{-/-}$ mice and the offspring crossed to produce AhCre^{+} MDM2$^{flox/flox}$ Fn14$^{-/-}$ mice. Augmentation of TWEAK signaled was achieved by delivery of an Fn14 receptor agonist antibody (Fn14Ab).

Figure 6.15 Absence of fibrosis following complete hepatic repopulation by HPCs

Analysis of fibrosis over time in the AhCre MDM2$^{flox/-}$ model using picosirius red histochemistry

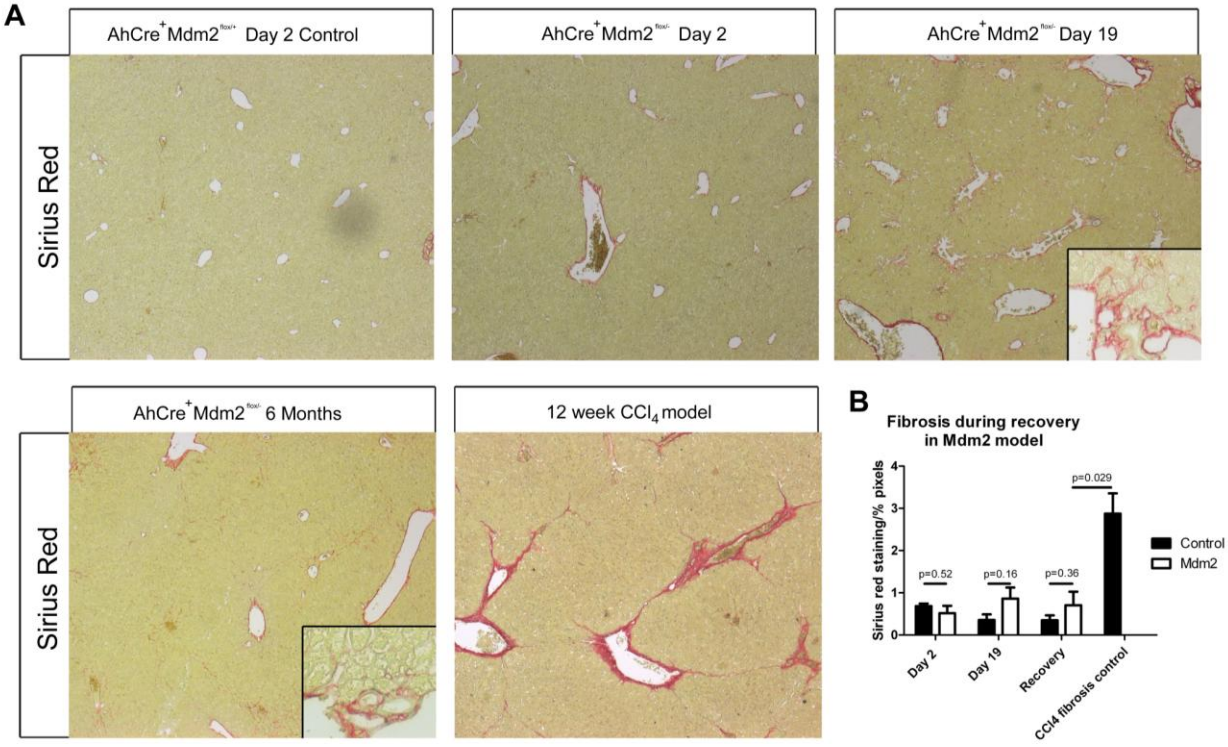

reveals normal baseline appearances of the liver and no fibrosis 2 days following induction with 1x80mg/kg βNF (A). Localised minor increases in picosirius red staining are seen in periportal regions 19 days following induction (inset). Near complete resolution of periportal fibrosis is observed 6 months following induction at the time of complete hepatic reconstitution. Comparison is made to the fibrosis observed in a 12 week CCl_4 model (courtesy of Jules Thorn Group). (B) Quantification of fibrosis using image analysis reveals no significant change in fibrosis at any time point following induction in the AhCre^{+} MDM2$^{flox/-}$ model vs. induced AhCre^{+} MDM2$^{+/flox}$ controls. P values denote T test results.

When examined 4 days following induction under these conditions effect on the number of HPCs were clearly visible with TWEAK signalling manipulation. A reduced HPC response was observed in the context of Fn14 deficiency, whilst an augmented HPC activation was seen in mice given the stimulatory TWEAK antibody (Figure 6.16A and B). As previously described, this model would be expected to lead to moderate clinical sequelae not before day 6. The AhCre^{+} MDM2$^{flox/flox}$ Fn14$^{-/-}$ however, exhibited severe clinical side effects as early as day 3 which lead to the requirement for humane

euthanasia 4 days following induction in all mice tested. These clinical signs were indistinguishable from those described in their Fn14 competent counterpart but occurred with greater severity and at an earlier time point.

Figure 6.16 TWEAK dependent regeneration in the AhCre MDM2^{flox} model

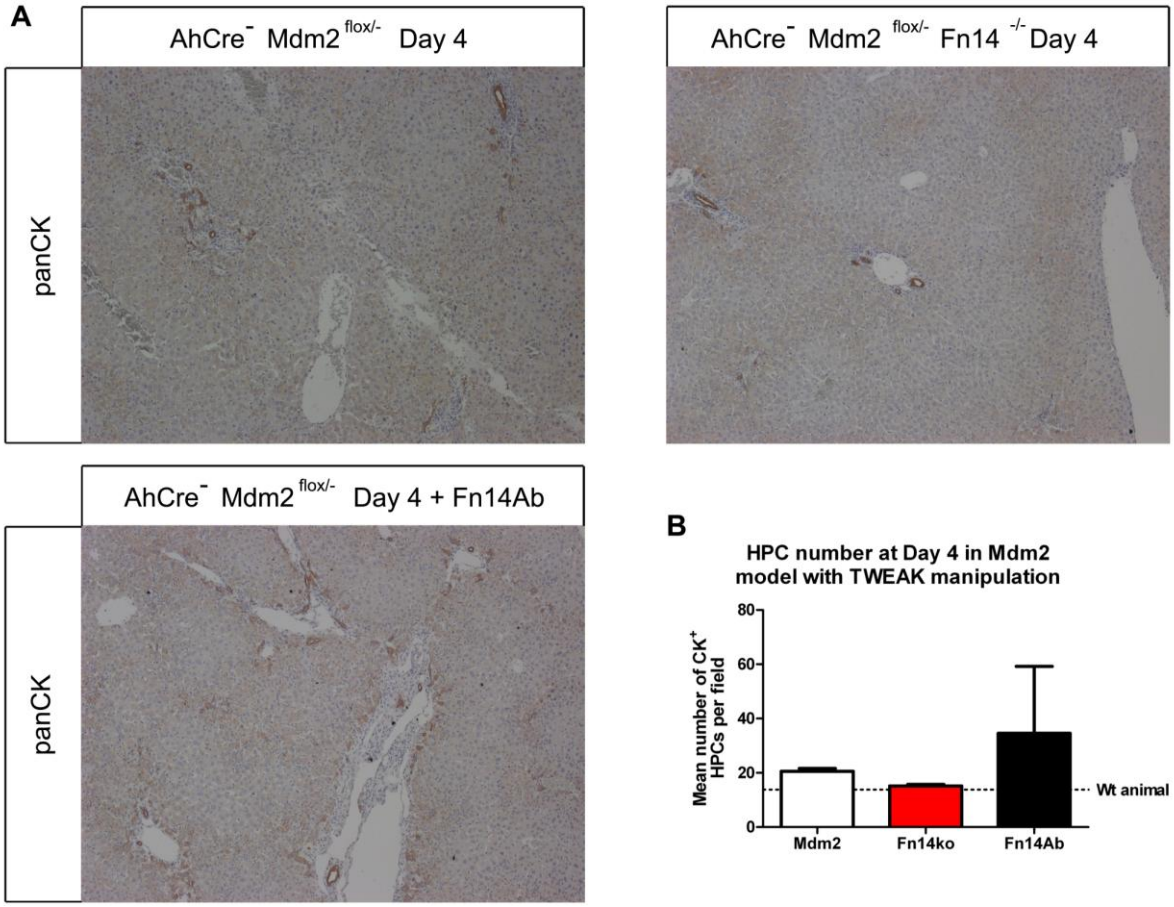

To assess the functional role of TWEAK signalling in HPC expansion in the MDM2 model male induction AhCre^{+} MDM2$^{flox/flox}$ mice were induced with 1x80mg/kg βNF and the HPC response assessed after 4 days and compared to AhCre^{+} MDM2$^{flox/flox}$ bred onto a Fn14 knockout background and AhCre^{+} MDM2$^{flox/flox}$ receiving Fn14 stimulating antibody given 1 day prior to and 1,2, and 3 days following induction. When HPC activation was assessed by quantification of panCK^{+} HPCs and compared to normal controls relative activation was observed in AhCre^{+} MDM2$^{flox/flox}$ (MDM2) but this activation is lost on an Fn14$^{-/-}$ (Fn14^{ko}) background. HPC activation is hyper-stimulated when AhCre^{+} MDM2$^{flox/flox}$ are treated with Fn14 stimulating antibody (Fn14Ab) at day 2 and 4 following induction with 80mg/kg βNF. Control mice received IgG2a control antibody. Values are presented as mean±SEM for MDM2, Fn14^{ko} and Fn14Ab (20.53±1.1, 5.18±0.6, 34.55±24.6 respectively).

6.11 Discussion

6.11A Efficiency of transgenic induction in AhCre MDM2^{flox} model

The use of transgenic technology has provided an exceptionally powerful tool in the study of cellular biology and has offered great insights into stem cells. The use of inducible transgene activation/deactivation permits the detailed examination of the effects of a specific abnormality generated in an otherwise normal *in vivo* system. It is however, highly dependent upon the efficient and specific targeting of transgene alteration. In addition to facilitating examination the effects of genetic manipulation within this population, the AhCre inducible promoter system offers other utilities. Whilst the identity of the hepatic stem cell remains elusive the opportunity to utilise an inducible hepatocyte specific promoter is particularly appealing, as it permits the separation of a differentiated hepatocyte population from that of hepatocyte precursors. By observing the fate of genetically altered populations, the fate of hepatocytes may be observed, and additionally all hepatocytes which arise from progenitors may be differentiated from this originally labeled population.

The elegance of the AhCre MDM2^{flox} model in the liver is that it induces changes in the hepatocyte population specifically and extremely efficiently. This specificity has previously been implied but not examined specifically (Ireland *et al.*, 2004). The inducibility of cytochromes is a key feature of differentiated hepatocytes (Hay *et al.*, 2008) and therefore the demonstration in this work that within the liver only hepatocytes undergo genetic recombination in response to βNF induction is not surprising. What is particularly impressive in this system is the efficiency with which recombination can be achieved (Figure 6.2). Assessing this efficiency either by examining downstream changes in cell gene expression, for examples p53 or p21 (Figures 6.2 and 6.3), or examination directly the efficiency of deletion of the MDM2 gene of the gene (Figure 6.6) reveals recombination up to the limits of detection in the most efficient

recombination models. The limits of detection, in this setting using quantification of p53/CYP2D6 dual immunohistochemistry, relies on the accurate assignment of hepatocyte identity and assessment of p53 status, each of which is made independently by the methodology employed. Therefore potential false negatives may arise by the inappropriate allocation of hepatocyte morphology to any nucleus or by assigning a either $p53^{hi}$ or $p53^{low}$ phenotype to a $p53^{intermediate}$ cell.

Analysis prior to induction in $AhCre^{+}$ $MDM2^{flox/-}$ control mice reveals that a single functional MDM2 gene is sufficient for cellular function. Likewise, induction in $AhCre^{+}$ $MDM2^{flox/wt}$ confirmed that p53 up-regulation does not result from the loss of a single functional MDM2 allele in a mouse with two previously functioning MDM2 alleles. This observation is a crucial control as it implies that the p53 upregulation observed in $AhCre^{+}$ $MDM2^{flox/flox}$ mice results from the deletion of the floxed segment from both floxed MDM2 genes. Furthermore, the p53 upregulation observed following induction in $AhCre^{+}$ $MDM2^{flox/-}$ mice is a reflection of the recombination of the floxed MDM2 allele and not an indirect effect of βNF upon the liver itself. Therefore it follows that recovery of hepatocytes with a floxed segment must therefore occur from cells which contain at least one floxed allele which at no point underwent recombination.

The efficiency of the AhCre construct for induction of hepatocyte specific recombination also lends itself to labelling the hepatocyte population for lineage tracing studies. Whilst the AhCre $MDM2^{flox}$ model allows lineage tracing of the hepatocyte population, a key feature of this model is that an altered phenotype is synchronously imposed upon the labelled hepatocytes by the dis-inhibition of p53. Using the AhCre inducer with a purely labelling construct such as Lox-Stop-Lox EYFP (Srinivas *et al.*, 2001; Wang *et al.*, 2009) would in theory permit the analysis of the hepatocyte population in an otherwise healthy liver. Furthermore, in addition to lineage tracing or the induction of deleterious effects upon hepatocytes, positive or pro-survival genes could be induced using a similar methodology.

6.11B Induced hepatocyte senescence in the AhCre MDM2^{flox} model

Over expression of p53 in other environments is strongly associated with the development of a senescent phenotype (Xue *et al.*, 2007; Brooks and Gu, 2006). I therefore hypothesised that increased hepatocyte p53 following disabling MDM2 function may result in cell cycle arrest. To test this hypothesis senescence associated β-galactosidase was examined revealing widespread expression in contrast to control mice.

β-galactosidase expression is associated with a senescent phenotype in the liver amongst other organs (Paradis *et al.*, 2001). None-the-less, I wished to test directly whether these cells were senescent by delivering a stimulus which is capable of inducing proliferation in wild type hepatocytes. The combination of HGF and T3 used here induced significant elevation in BrdU incorporation by hepatocytes in keeping with their effects in the rat (Forbes *et al.*, 2000). When applied to AhCre MDM2^{flox} mice following induction this mitogen cocktail failed to induce hepatocyte proliferation (Figure 6.3). Increased non-parenchymal cell proliferation was however observed (Figure 6.3E). Analysis was performed to exclude the detection of such non-parenchymal assessment using colocalisation of nuclear BrdU in CYP2D6^{+} hepatocytes. As such any effects of the mitogen cocktail on the proliferation of other non-parenchymal cell populations including HPCs which are described to be sensitive to the effects of this cocktail are minimised (Bird *et al.*, 2008; Laszlo *et al.*, 2008).

In AhCre MDM2$^{flox/fllox}$ mice, a relative failure to proliferate upon exposure to exogenous mitogenic stimulus is observed, however hepatocyte proliferation is not entirely impaired when examined 4 days following βNF induction. Interestingly while exceptionally efficient p53 induction is seen at day 2 following induction, when analysis was performed for the p53 status of proliferating hepatocytes in the AhCre MDM2^{flox} model virtually all proliferating hepatocytes were p53^{normal} (only a single p53^{hi} hepatocyte contained nuclear BrdU in the examination of entire sections from 6 recombined animals). The observation that p53^{normal} status at day 4 only occurs in a

small minority of hepatocytes implies these cells represent freshly derived hepatocytes from a non-recombined source, which in the presence of exceptionally efficient hepatocyte recombination two days previously may point to a hepatocyte precursor cell as the source of these freshly derived hepatocytes.

As a downstream target of p53, p21 is thought to be key in the induction of senescence by p53 (Aylon and Oren, 2007; Wiebusch and Hagemeier, 2010). Indeed elevation of p21 is observed both at the transcript and protein level following upregulation of p53 in hepatocytes following MDM2 loss of function. Further evidence of the function of the high levels of p53 observed is that elevation of p16 transcripts also (Figure 6.3). Given the suspected involvement of p21 in p53 induced senescence, I therefore sought to examine the effects of p21 deficiency on hepatocyte senescence in the AhCre MDM2^{flox} model. Using hepatocyte specific p53 upregulation in constitutively deficient p21 mice the ability of hepatocytes to proliferate was once again tested. This revealed that both in the presence and absence of exogenous mitogenic stimulation increased hepatocyte proliferation was observed in p21^{null} mice, demonstrating that p21 deficiency at least partially resolves the failure to proliferate in p53^{hi} hepatocytes. Further investigation of the p53 status of proliferating hepatocytes in this model revealed that large numbers, approximately 4% (vs. <0.05% in p21^{wt}), of all proliferating hepatocytes were p53^{hi} confirming that p21 deficiency allows hepatocytes to escape p53 induced senescence. It is likely that the failure of mitogen to significantly affect the rate of hepatocyte proliferation in the p21^{null} model is reflective of the endogenous regenerative stimulus in the model supplied as a result of the significant hepatocellular injury observed.

6.11C Liver injury and associated HPC activation in the AhCre MDM2^{flox} model

The work described here has shown that the AhCre^{+} MDM2^{flox} model induces hepatocyte senescence and hepatocellular injury with a resultant HPC activation. As hypothesised, there is dramatic induction of apoptosis as assessed by TUNEL staining throughout the liver lobule (Figure 6.4G) together with hepatocyte death observed

histologically (Figure 6.4F). In keeping with these observations elevations of serum transaminase are observed in AhCre^{+} MDM2$^{flox/flox}$ and AhCre^{+} MDM2$^{flox/-}$ following induction with βNF, which is not observed in induced AhCre^{-} MDM2$^{flox/flox}$ controls (Figures 6.4A and B).

The demonstration of large scale HPC activation in the AhCre MDM2^{flox} model associated with widespread liver injury, is once again in keeping with the apparent requirement for liver injury in order to observe HPC activation (Bird *et al.*, 2008; Santoni-Rugiu *et al.*, 2005). Interestingly the only previous report of HPC activation without documented liver injury is in the hepatic specific expression of TWEAK (Jakubowski *et al.*, 2005). In this study while no increased hepatocyte apoptosis was observed at the time of HPC activation other markers of liver injury, crucially serum transaminases, were not examined in this study. The previous observations reported in this work that BMC or macrophage infusion results in HPC activation via a TWEAK dependent mechanism in the absence of liver injury (Chapter 5), are nonetheless consistent with the report by Jakubowski *et al.*

A key limitation in the study of the mechanism of HPC activation to date, is the lack of an understanding of the mechanism by which the established mouse dietary models (namely the CDE and DDC diets) lead to injury and hence HPC activation. Liver injury in these model is now well described in these models, both in this work Chapter 3) and that previously (Akhurst *et al.*, 2001; Preisegger *et al.*, 1999). It has been assumed that this liver injury is responsible for the stimulation of HPC mediated expansion. None-the-less, study of whether HPC activation is directly linked to concurrent injury has been impossible, as the mechanism by which dietary manipulation results in hepatocellular injury is unknown, in either diet. This development of a characterised mechanism of hepatocellular injury induction together with synchronous HPC activation may permit the relationship and mechanistic pathway between liver injury and HPC activation to be examined.

In the AhCre MDM2^{flox} model, examination using specific HPC markers, either at the protein or mRNA level, shows a progressive and marked expansion of HPCs following induction with βNF. This expansion is significantly more dramatic than existing models of HPC activation such as the CDE diet (>3 times HPC numbers). The AhCre MDM2^{flox} model, therefore, offers a valuable tool with which to study both HPC biology and hepatocellular senescence in the future. The features of the exceptionally dramatic HPC expansion, coupled with a defined molecular signal initiating the response may permit a powerful and detailed interrogation of the molecular pathway by which injury stimulates HPCs in the future.

The varying phenotypes in the different AhCre MDM2^{flox} models examined in this work, provide a useful method for examining HPC activation under varying conditions. It appears that hepatocyte senescence is induced following p53 upregulation in either the setting of MDM2$^{flox/flox}$ or MDM2$^{flox/-}$ recombination and in mice of either sex (Figure 6.3). The reduced efficiency of recombination in female mice appears intimately linked to the less severe clinical phenotype observed compared to male mice. I propose that the mechanism by which this occurs results both as a from the eventual death of a smaller hepatocyte population and also the presence of a larger unrecombined and therefore non-senescent hepatocyte population. This non-senescent hepatocyte population may then able to proliferate actively during liver injury and result in maintained liver function and heightened hepatocellular regeneration. Accordingly HPC activation would be expected to be reduced in this context. Indeed this is what is observed experimentally in these animals (Figure 6.7).

Examination of mice in which a dramatic HPC expansion was noted often revealed differing clinical outcomes. When AhCre^{+} MDM2$^{flox/-}$ mice are used instead of MDM2$^{flox/flox}$ mice, recombination was equally efficient, and yet mortality was higher in the MDM2$^{flox/flox}$ than their MDM2$^{flox/-}$ counterparts. The necessity for the deletion of both MDM2 alleles for observed p53 elevation and consequent functional downstream effects has been previously discussed. The complete loss of MDM2 function in

$MDM2^{flox/flox}$ and $MDM2^{flox/-}$ mice might be expected to lead to an identical phenotype but is not in practice. In the $MDM2^{flox/flox}$ liver injury and associated severe clinical effects occur over 1 week, while in the $MDM2^{flox/-}$ model the injury is delayed for approximately 3 weeks and is less clinically severe (Figures 6.5 and 6.7). It therefore appears that the complete loss of MDM2 gene function from a homozygous state results in more rapid entry into a pro-apoptotic programme than the complete loss from a heterozygote deficient state. This may perhaps be explained by a degree of compensation in heterozygote MDM2 deficient cells, which could delay the onset of apoptosis. Further investigation of the degree p53 accumulation in these cells and alterations in other p53 interacting proteins between the cells of $MDM2^{wt/-}$ and $MDM2^{wt/wt}$ mice would be worthwhile future work in this area. The clinical implications of altered susceptibility of cells to enter apoptosis in the context of similar p53 upregulation would potentially provide therapies to prevent apoptotic mediated organ failure or induce/promote apoptotic mediated clearance of neoplasia.

The use of the $AhCre^{+}$ $MDM2^{flox/-}$ model is particularly intriguing as it permits the examination of a full recovery from a state of complete hepatocyte recombination following induction. This therefore affords the examination of reconstitution of the hepatic parenchyma from a non-recombined source. As differentiated parenchymal hepatocytes are all labelled by the deletion of the MDM2 gene segment, the non-recombined source is by definition a hepatocyte precursor population. At the time of induction this precursor cell is in an undifferentiated state and therefore unaffected by the addition of βNF. This precursor is, therefore, an hepatic progenitor cell as it demonstrates its potential to form differentiated hepatocytes. This system does not however necessarily ascribe a particular phenotype, such as expression of the classically accepted HPC markers such as panCK, Dlk1 or EpCAM, to this progenitor cell population.

Following the demonstration of repopulation of the hepatic parenchyma from a precursor source I sought to investigate the potential of HPCs (defined by the expression

of panCK) to play a role in this regenerative process. Multiple lines of evidence suggest a product precursor relationship between the panCK$^+$ HPC population and differentiated hepatocytes. Firstly HPCs expansion is observed over the time course of hepatocyte repopulation (Figures 6.5 and 6.7), in keeping other models of liver regeneration. Secondly, isolated and enriched HPCs from during this regenerative phase are capable of differentiating into hepatocyte like cells *in vitro* (Figure 6.12). The clustering of BrdU labelled hepatocytes adjacent to HPCs following BrdU pulse-chase labelling provides further strong evidence of this product precursor relationship *in vivo* (Figure 6.13). This is additionally supported by the presence of freshly generated hepatocytes in the areas of HPC activity *in vivo* (Figures 6.10 and 6.13) and furthermore by the observation that the HPC population remains unrecombined following βNF recombination (Figure 6.11). Additionally, replicating hepatocytes are observed as cords during the regenerative phase (Figure 6.14). The nature of these hepatocytes as cords strongly implies a relationship of each of these regenerating hepatocytes to one another. Crucially each of these cords of replicating hepatocytes additionally relates back to the distal tip of an HPC cord (Figure 6.14). Finally direct intervention to manipulated HPC mediated activation via both stimulation and blockade of TWEAK-Fn14 mediated signalling affects the clinical outcome, mechanistically linking HPC mediated regeneration to liver function itself (Figure 6.16). This observation of reduced HPC expansion coupled with a syndrome consistent with failed liver regeneration implies that Fn14 signalling is functionally necessary for adequate HPC activation in this model.

This description that liver regeneration is exceptionally effective and efficient is not the first. Interrogation of regeneration in partial hepatectomy models have shown for many years that large scale hepatocyte replacement may occur rapidly and efficiently (Fausto *et al.*, 2006), and the addition of AAF to this model strongly supports the proposal that such regeneration may occur from a precursor source if so required (Alison, 1998). In these models, in which an impressive form of compensatory hyperplasia occurs, what is not clear is to what extent the liver parenchyma may be regenerated from such cells.

Additional elegant transplantation studies using HPCs have demonstrated the rescue of metabolic deficiency in transgenic animals using wild type donor derived cells (Wang *et al.*, 2003a). Furthermore these studies have done much to clarify the identity of the repopulating cell. Whilst they have provided evidence that small clusters of donor derived cells may form within the liver, they have not yet shown large scale repopulation. This may be a feature of the requirement of only a small mass of metabolically competent cells to rescue this disease model. However, to date the potential of HPCs to repopulate the hepatic parenchyma on a larger scale has not been examined.

The AhCre MDM2^{flox} model, therefore, adds significantly to the field of liver regeneration. This novel model has allowed the extensive repopulation potential of the HPC precursor compartment to be examined. This model, described here, has shown the entire repopulation of the hepatic parenchyma in the short term from a repopulating progenitor population.

6.11D Examination of the product precursor relationship between HPCs and hepatocytes in the AhCre MDM2^{flox} model

Utilising the lineage tracing function of this model I show the regeneration of the entire hepatocyte population from a non-hepatocyte precursors. Direct lineage tracing of the precursor population (as defined by a specific marker) is not performed, however by a number of methods I demonstrate that HPCs can and do form hepatocytes in this model. Firstly, following extraction and purification, HPCs are capable of hepatocellular differentiation (Figure 6.11). This observation, while relevant for this novel model, is not in itself surprising. HPCs defined by a number of markers have been described as capable of hepatocyte differentiation (Rountree *et al.*, 2007; Okabe *et al.*, 2009; Lorenzini *et al.*, 2010; Conigliaro *et al.*, 2008; Lazaro *et al.*, 1998). Furthermore, spatial association of CK19^{+} HPCs and regenerative nodules has been observed in

human liver disease (Lin *et al.*, 2010) by utilising a system of clonal analysis discussed previously (Fellous *et al.*, 2009)

It is also unsurprising that results of RNA analysis do not at least superficially correlate with data from immunohistochemical analysis of HNF4α. HNF4α acts as a transcription factor promoting transcription any genes including HNF1α, itself a transcription factor which regulates α-1-antitrypsin, and transthyretin genes. Active HNF4α is therefore located in the nucleus and this is regarded as a marker of committed hepatocytes (Hay *et al.*, 2008). HNF4α is understood to be strongly regulated at both the post transcriptional levels, and therefore whilst no change is noted in HNF4α RNA upon HPC differentiation in culture this is not incompatible with the observation that a minority of these cells expression high levels of nuclear HNF4α protein.

What is clear from the RNA analysis between undifferentiated and differentiated hepatocytes is that whilst there is evidence of loss of primitive HPC markers e.g. Dlk1, there is little change in differentiated hepatocyte gene marker expression, particularly with reference to hepatocyte controls. Most of the genes remain exceptionally low (10-100 000 times lower) than in purified hepatocyte populations. Whilst cells in the *in vitro* culture system at this time develop hepatocyte-like morphology at the time of analysis it is probable that a full genetic hepatocyte programme is not activated at this relatively early stage of development. Clearly further analysis of this *in vitro* differentiating population is desirable, together with optimising the differentiation conditions.

None-the-less, importantly I go onto show using pulse-chase labeling periportal clusters of hepatocytes often containing HPCs (Figure 6.13). The absence of hepatocyte labeling during the pulse period implies that these periportal hepatocytes have indeed been regenerated from a precursor source. Furthermore, their spatial localisation together with their association within clusters containing HPCs, implies a clonal origin from a periportal cell. This is in keeping with the uptake of BrdU by periportal panCK$^+$

HPCs during the pulse phase 2 days previously. So these HPCs, which are capable of forming hepatocytes, actually do so in this *in vivo* model. This interpretation is in keeping with the *in vitro* data where differentiation of an enriched and hepatocyte free (as defined by absence of HNF4α) HPC culture occurs producing hepatocytes (as defined by presence of nuclear HNF4α).

Crucially, given that HPCs do form hepatocytes *in vivo*, this model goes onto address the question of to what extent they do so. Using wash out of label retention (loss of recombined MDM2) in the hepatocyte population, it is demonstrated that hepatocytes may, to all intents and purposes (>95%), be completely restored from a precursor pool. With this work, I do not exclude the potential contribution of other precursor populations. I can however see no evidence, either spatially or by pulse-chase labeling, of a significant contribution by any other precursor population to hepatocyte regeneration.

Together with the observation of significant HPC differentiation into hepatocytes, this is strong evidence for repopulation of the liver by this precursor source. By extension it seems likely that this repopulation occurs from an even more primitive stem cell derived, population.

The application of lineage tracing

The gold standard for demonstration of in-situ product-precursor relationships currently *in vivo* is the use of transgenic controlled activation of markers genes which display no active phenotype aside from permitted identification of labelled cells. The AhCre MDM2^{flox} system described in this work clearly differs significantly from this strategy. Instead of aiming to label the stem/progenitor cell population and watch over time, for the passage of label into the differentiated parenchyma, I have adopted a strategy to completely label the parenchyma and observe washout of this label from an

un-modified precursor population. While providing information regarding the quantity of generation of the parenchyma, this strategy provides no information regarding the phenotype of the precursor population aside from these cells did not undergo recombination at the time of βNF induction. Further specific analysis investigating the product precursor relationship of panCK$^+$ HPC to hepatocytes is described above but falls short of the definitive clarification of this relationship using transgenic labelling of the precursor population.

Published reports in the liver of lineage tracing experiments in the mouse have provided some information regarding the potential nature of hepatocyte precursors during liver regeneration. Using a constitutively active Foxl1-Cre mouse a small number of hepatocytes (0.5% max) were seen following biliary injury. Interestingly whilst this occurred in an injury model, the proportion of hepatocytes derived from Foxl1$^+$ precursors during development and physiological liver homeostasis was extremely low suggesting that while Foxl1$^+$ cells may have the potential to become hepatocytes, in reality (and even during injury) their propensity to support liver function is very low indeed (Sackett *et al.*, 2009). Another constitutively active lineage tracing system, this time under the control of a GFAP promoter has also been used to track precursors of hepatocytes (Yang *et al.*, 2008). In this model larger numbers of labelled hepatocytes are seen following exposure to a dietary injury model. None-the-less, again the low level of labelled hepatocytes prior to dietary initiation calls into question how relevant GFAP$^+$ precursors are during development and adult homeostasis. Additionally it is apparent that while GFAP is classically a marker of hepatic stellate cells, it is also a marker of HPCs and cholangiocytes (Yang *et al.*, 2008). Therefore the question of the role of hepatic stellate cells in the formation of hepatocytes remains in doubt. It seems more plausible that these finding represent the differentiation of HPCs which transiently at least express GFAP, into hepatocytes. Whether all HPCs express GFAP and at what point in their differentiation is a question that requires further investigation. The relationship between both the Foxl1$^+$ and/or GFAP$^+$ cells and the panCK$^+$ HPCs studied in detail in this thesis are not known.

The use of an additional Cre-Lox mediated labelling of the stem/progenitor cell population is limited in the AhCre MDM2^{flox} model as induction of Cre-recombinase will result in non selective deletion of MDM2 and activation of a lineage marker in hepatocytes and progenitor cells respectively. Alternative combinations of transgenic labeling are required. For example a progenitor cell driven Flp may be used with AhCre together with marker^{FRT} and MDM2^{flox} may permit this question to be directly addressed. The choice of progenitor cell marker promoter used to drive Flp in such a system will be central to its success or failure. While panCK has proved to be a useful antibody for identifying the HPC population in this study, this antibody is believed to recognise a number of cytokeratins over and above CK19, as discussed previously. A CK19 promoter would appear a rational choice but will not limit expression to the HPC population as it is also actively expressed in the cholangiocyte population along with other HPC markers including EpCAM and Dlk1. Members of the LGR family and CD133 show promise as potential targets for stem cell lineage markers in the future.

6.11E Implications and future directions

The implications of this work are profound and wide-ranging. From the hepatic perspective these findings place HPCs at the heart of the process of liver regeneration. This therefore exposes them as a highly attractive target for regenerative therapy. Therapeutic manipulation of HPCs has been achieved to date on many levels. Genetic manipulation has shown the potential to influence HPC activity is a variety of systems (Jakubowski *et al.*, 2005; Knight *et al.*, 2000). Small molecule manipulation of HPC mediated activation has also been observed in humans (Spahr *et al.*, 2008) via indirect methods. Additionally direct pharmaceutical manipulation of HPCs has been observed in mice, as a proof of concept (Knight *et al.*, 2008). Given the repopulation potential of HPCs, the ability to influence HPC behaviour *in vivo* may prove to have profound potential in the development of regenerative therapies for liver disease.

The fundamental potential of HPCs in liver regeneration also draws attention to the role of hepatocyte mediated liver regeneration and whether there is any particular relationship between the freshly generated hepatocytes from precursors and ongoing liver regeneration. As previously discussed in Chapter 1, whilst evidence exist for the potential of nearly the entire population of hepatocytes to display the potential for regeneration, intriguing work recently published examining clonality of liver patches in the human liver has demonstrated the relationship of proliferating hepatocytes to the portal tract (Fellous *et al.*, 2009). It is conceivable therefore that all hepatocytes are not equal from a regenerative standpoint, and that regeneration from hepatocytes may preferentially occur from those hepatocytes arising more recently from precursors.

From the stem cell perspective the observation of entire hepatic parenchymal repopulation from a precursor source is the first demonstration of solid organ regeneration from a stem cell *in vivo*. Whilst it is widely accepted that other organ systems with typically high cellular turnover (for example skin, intestine and blood) may be repopulated from stem cells, to date only complete repopulation of the BM from stem cell populations have been experimentally demonstrated. Regeneration of single organ units in the skin and intestine has been shown from individual stem cell populations (Barker *et al.*, 2010; Fuchs and Nowak, 2008). The observation that the liver, an organ with a vastly reduced cell turnover, may be similarly repopulated by precursors highlights the possibility that other solid organs for example kidney, pancreas, heart, lung or even brain may be similarly capable of large scale regeneration from progenitors. Similar systems of selective targeting of MDM2 deletion in the differentiated parenchyma of these other organs could conceivably be employed to address this question.

A number of further questions therefore arise from the observations reported in this work. Can I more definitively identify the characteristics and phenotype of the hepatic stem cell population? If HPCs can regenerate a liver once, can they do it repeatedly? What are the implications for the liver when regeneration occurs from HPCs versus that

which occurs from differentiated hepatocytes? Do liver cancers come from differentiated hepatocytes and/or from HPCs? Many of these questions are directly addressable using the AhCre model described in this work. For example provisional work examining the functional effects of regeneration from HPCs has shown that the liver is functionally normal and that no significant associated fibrosis is observed following complete hepatocytic parenchymal regeneration from HPCs (Figures 6.9 and 6.14). Additional study examining the effect of re-induction of the regenerated liver with further doses of βNF following complete regeneration can be used to examine the repeated repopulation potential of HPCs.

The $AhCre^{+}$ $MDM2^{flox}$ model described here is a novel model of HPC activation and is the first in the mouse to utilise transgenic technology to activate HPCs via a characterised mechanism. Moreover the activation of HPCs in this model may be dramatic and occurs to a much larger extent than other murine models (Jelnes *et al.*, 2007; Santoni-Rugiu *et al.*, 2005), and may be induced to varying degrees depending on mouse sex and induction regime. I therefore believe that it represents a highly useful tool for the study of HPC biology in the future.

It is of significant interest to note that in the context of large scale organ regeneration from HPCs, there are no long term side effects, albeit in a small cohort of mice. Specifically no mice developed cancers and upon further detailed examination there was no evidence of significant residual fibrosis in spite of the dramatic injury and HPC activation which has occurred. There have been significant concerned raised about the potential side effects of HPC activity both in terms of fibrosis and HCC (Knight *et al.*, 2005b).

A number of significant questions remain. Firstly and crucially what is/are the identity of the stem cells within the liver from which HPCs arise? A number of key technologies are required to answer this question. Development of a suitable lineage tracing system using a marker analogous to that of LGR5 in the intestine is undoubtedly a keystone in

our understanding. In addition, the development of a suitable transplantation model for HPCs and precursors will provide crucial validation of any putative hepatic stem cells. The $FAH^{-/-}$ murine system described by Grompe *et al.* may be used in such a fashion (Wang *et al.*, 2003a). I believe also that the lethality of MDM2 deletion when performed on an $Fn14^{-/-}$ background may provide the opportunity for a model of stem cell/HPC transplantation due to the combination of regenerative stimulus and the relative selective advantage an $Fn14^{wt}$ HPC would be expected to enjoy in such a context.

6.12 Conclusion

In conclusion, the AhCre^{+} MDM2^{flox} model provides a new and novel approach to study HPC biology, as well as the biology of hepatocyte senescence *in vivo*. Interrogation of this model to date has demonstrated massive HPC expansion and the likely mechanistic drive for such an expansion. Utilising the hepatocyte lineage tracing capability of the model I have been able to demonstrate large scale parenchymal repopulation within an adult solid organ *in vivo* from a progenitor cell source.

Furthermore, I go onto to characterise this activation of HPCs and demonstrated not only that these cells may form hepatocytes but that they do so to a large extent

Thesis Conclusions

In summary the work presented in this thesis provides a description of the environment surrounding HPCs, the functional effects of the macrophage component of the niche and the potential of HPCs to regenerate the liver parenchyma. This HPC niche is stereotypical in nature and is comprised of macrophages and myofibroblasts together with a laminin rich basement membrane and these associations are conserved across a wide variety of models and species (Chapter 3).

Upon injury to the liver, the niche expands by the proliferation of cells. Macrophages are actively recruited into the expanding niche from the bone marrow while other niche populations proliferate *in situ* (Chapter 4). Macrophages within the niche provide a functional role in stimulating the shaping the phenotype of expanding HPCs. They do this by the secretion of a variety of signals including Wnt and TWEAK (Chapter 5).

Macrophages delivered intravenously engraft transiently within the liver and home to the HPC niche. Upon doing so, and even in the absence of injury, macrophages may stimulate HPC activation resulting in changes in both liver structure and function. This process is dependent upon the paracrine delivery of TWEAK from macrophages to endogenous HPCs (Chapter 5). Such a mechanism provides the potential for targeting therapy to stimulate HPC mediated regeneration during liver disease.

Finally I go onto to describe the potential for HPC mediated regeneration of hepatocytes. I show that the hepatic parenchyma may be completely and rapidly reconstituted precursor HPCs, and that this regeneration may occur without the development of side effects such as fibrosis and carcinogenesis. Regeneration from HPCs may be inhibited by interference with TWEAK signalling and doing so prevents HPC activation and may result in liver failure in this model of liver injury (Chapter 6). The demonstration of hepatic regeneration by HPC is the first demonstration of regeneration of an adult mammalian solid organ from stem cells *in vivo*.

References

Abe, S., Lauby, G., Boyer, C., Rennard, S.I., and Sharp, J.G. (2003). Transplanted BM and BM side population cells contribute progeny to the lung and liver in irradiated mice. Cytotherapy *5*, 523-533.

Akhurst, B., Croager, E.J., Farley-Roche, C.A., Ong, J.K., Dumble, M.L., Knight, B., and Yeoh, G.C. (2001). A modified choline-deficient, ethionine-supplemented diet protocol effectively induces oval cells in mouse liver. Hepatology *34*, 519-522.

Akhurst, B., Matthews, V., Husk, K., Smyth, M.J., Abraham, L.J., and Yeoh, G.C. (2005). Differential lymphotoxin-beta and interferon gamma signaling during mouse liver regeneration induced by chronic and acute injury. Hepatology *41*, 327-335.

Aktas, S., Diniz, G., and Ortac, R. (2003). Quantitative analysis of ductus proliferation, proliferative activity, Kupffer cell proliferation and angiogenesis in differential diagnosis of biliary atresia and neonatal hepatitis. Hepatogastroenterology *50*, 1811-1813.

Alison, M. (1998). Liver stem cells: a two compartment system. Curr Opin Cell Biol *10*, 710-715.

Alison, M.R. (2005). Liver stem cells: implications for hepatocarcinogenesis. Stem Cell Rev *1*, 253-260.

Alison, M.R., Golding, M., Sarraf, C.E., Edwards, R.J., and Lalani, E.N. (1996). Liver damage in the rat induces hepatocyte stem cells from biliary epithelial cells. Gastroenterology *110*, 1182-1190.

Alison, M.R., Islam, S., and Lim, S.M. (2009). Cell therapy for liver disease. Curr Opin Mol Ther *11*, 364-374.

Alison, M.R., Murphy, G., and Leedham, S. (2008). Stem cells and cancer: a deadly mix. Cell Tissue Res *331*, 109-124.

Alison, M.R., Poulsom, R., Jeffery, R., Dhillon, A.P., Quaglia, A., Jacob, J., Novelli, M., Prentice, G., Williamson, J., and Wright, N.A. (2000). Hepatocytes from non-hepatic adult stem cells. Nature *406*, 257.

Alix, J.H. (1982). Molecular aspects of the *in vivo* and *in vitro* effects of ethionine, an analog of methionine. Microbiol Rev *46*, 281-295.

Alvarez-Dolado, M., Pardal, R., Garcia-Verdugo, J.M., Fike, J.R., Lee, H.O., Pfeffer, K., Lois, C., Morrison, S.J., and Alvarez-Buylla, A. (2003). Fusion of bone-marrow-derived cells with Purkinje neurons, cardiomyocytes and hepatocytes. Nature *425*, 968-973.

Amemiya, H., Kono, H., and Fujii, H. (2009). Liver Regeneration is Impaired in Macrophage Colony Stimulating Factor Deficient Mice After Partial Hepatectomy: The Role of M-CSF-Induced Macrophages. J Surg Res.

Apte, U., Gkretsi, V., Bowen, W.C., Mars, W.M., Luo, J.H., Donthamsetty, S., Orr, A., Monga, S.P., Wu, C., and Michalopoulos, G.K. (2009). Enhanced liver regeneration following changes induced by hepatocyte-specific genetic ablation of integrin-linked kinase. Hepatology *50*, 844-851.

Apte, U., Thompson, M.D., Cui, S., Liu, B., Cieply, B., and Monga, S.P. (2007). Wnt/beta-catenin signaling mediates oval cell response in rodents. Hepatology.

Apte, U., Zeng, G., Muller, P., Tan, X., Micsenyi, A., Cieply, B., Dai, C., Liu, Y., Kaestner, K.H., and Monga, S.P. (2006). Activation of Wnt/beta-catenin pathway during hepatocyte growth factor-induced hepatomegaly in mice. Hepatology *44*, 992-1002.

Arends, B., Vankelecom, H., Vander Borght, S., Roskams, T., Penning, L.C., Rothuizen, J., and Spee, B. (2009). The dog liver contains a "side population" of cells with hepatic progenitor-like characteristics. Stem Cells Dev *18*, 343-350.

Artavanis-Tsakonas, S., Rand, M.D., and Lake, R.J. (1999). Notch signaling: cell fate control and signal integration in development. Science *284*, 770-776.

Aumailley, M., Bruckner-Tuderman, L., Carter, W.G., Deutzmann, R., Edgar, D., Ekblom, P., Engel, J., Engvall, E., Hohenester, E., Jones, J.C., *et al.* (2005). A simplified laminin nomenclature. Matrix Biol *24*, 326-332.

Aylon, Y., and Oren, M. (2007). Living with p53, dying of p53. Cell *130*, 597-600.

Baba, S., Fujii, H., Hirose, T., Yasuchika, K., Azuma, H., Hoppo, T., Naito, M., Machimoto, T., and Ikai, I. (2004). Commitment of bone marrow cells to hepatic stellate cells in mouse. J Hepatol *40*, 255-260.

Baker, A., Ralphs, M., and Griffiths, C. (2008). Health Service Quarterly, O.o.N. Statistics, ed. (Palgrave MacMillan), pp. 59-60.

Barker, N., Huch, M., Kujala, P., van de Wetering, M., Snippert, H.J., van Es, J.H., Sato, T., Stange, D.E., Begthel, H., van den Born, M., *et al.* (2010). Lgr5(+ve) stem cells drive self-renewal in the stomach and build long-lived gastric units *in vitro*. Cell Stem Cell *6*, 25-36.

Barker, N., van Es, J.H., Kuipers, J., Kujala, P., van den Born, M., Cozijnsen, M., Haegebarth, A., Korving, J., Begthel, H., Peters, P.J., *et al.* (2007). Identification of stem cells in small intestine and colon by marker gene Lgr5. Nature *449*, 1003-1007.

Barolo, S. (2006). Transgenic Wnt/TCF pathway reporters: all you need is Lef? Oncogene *25*, 7505-7511.

Baron, J., Redick, J.A., and Guengerich, F.P. (1982). Effects of 3-methylcholanthrene, beta-naphthoflavone, and phenobarbital on the 3-methylcholanthrene-inducible isozyme of cytochrome P-450 within centrilobular, midzonal, and periportal hepatocytes. J Biol Chem *257*, 953-957.

Benhamouche, S., Decaens, T., Godard, C., Chambrey, R., Rickman, D.S., Moinard, C., Vasseur-Cognet, M., Kuo, C.J., Kahn, A., Perret, C., *et al.* (2006). Apc tumor suppressor gene is the "zonation-keeper" of mouse liver. Dev Cell *10*, 759-770.

Beresford, A.P. (1993). CYP1A1: friend or foe? Drug Metab Rev 25, 503-517.

Bergmeyer, H. U., Scheibe, P., and Wahlefeld, A. W. (1978). Optimisation of Methods for Aspartate Aminotransferase and Alanine Aminotransferase. Clin Chem 24, 58-73

Bi, Y., Huang, J., He, Y., Zhu, G.H., Su, Y., He, B.C., Luo, J., Wang, Y., Kang, Q., Luo, Q., *et al.* (2009). Wnt antagonist SFRP3 inhibits the differentiation of mouse hepatic progenitor cells. J Cell Biochem *108*, 295-303.

Bilzer, M., Roggel, F., and Gerbes, A.L. (2006). Role of Kupffer cells in host defense and liver disease. Liver Int *26*, 1175-1186.

Bioulac-Sage, P., Rebouissou, S., Thomas, C., Blanc, J.F., Saric, J., Sa Cunha, A., Rullier, A., Cubel, G., Couchy, G., Imbeaud, S., *et al.* (2007). Hepatocellular adenoma subtype classification using molecular markers and immunohistochemistry. Hepatology *46*, 740-748.

Birchmeier, C., and Birchmeier, W. (1993). Molecular aspects of mesenchymal-epithelial interactions. Annu Rev Cell Biol *9*, 511-540.

Bird, T.G., Lorenzini, S., and Forbes, S.J. (2008). Activation of stem cells in hepatic diseases. Cell Tissue Res *331*, 283-300.

Bisgaard, H.C., Holmskov, U., Santoni-Rugiu, E., Nagy, P., Nielsen, O., Ott, P., Hage, E., Dalhoff, K., Rasmussen, L.J., and Tygstrup, N. (2002). Heterogeneity of ductular reactions in adult rat and human liver revealed by novel expression of deleted in malignant brain tumor 1. Am J Pathol *161*, 1187-1198.

Bisgaard, H.C., Muller, S., Nagy, P., Rasmussen, L.J., and Thorgeirsson, S.S. (1999). Modulation of the gene network connected to interferon-gamma in liver regeneration from oval cells. Am J Pathol *155*, 1075-1085.

Blache, P., van de Wetering, M., Duluc, I., Domon, C., Berta, P., Freund, J.N., Clevers, H., and Jay, P. (2004). SOX9 is an intestine crypt transcription factor, is regulated by the Wnt pathway, and represses the CDX2 and MUC2 genes. J Cell Biol *166*, 37-47.

Blumenthal, A., Ehlers, S., Lauber, J., Buer, J., Lange, C., Goldmann, T., Heine, H., Brandt, E., and Reiling, N. (2006). The Wingless homolog WNT5A and its receptor Frizzled-5 regulate inflammatory responses of human mononuclear cells induced by microbial stimulation. Blood *108*, 965-973.

Boltz-Nitulescu, G., Wiltschke, C., Holzinger, C., Fellinger, A., Scheiner, O., Gessl, A., and Forster, O. (1987). Differentiation of rat bone marrow cells into macrophages under the influence of mouse L929 cell supernatant. J Leukoc Biol *41*, 83-91.

Boulton, R.A., Alison, M.R., Golding, M., Selden, C., and Hodgson, H.J. (1998). Augmentation of the early phase of liver regeneration after 70% partial hepatectomy in rats following selective Kupffer cell depletion. J Hepatol *29*, 271-280.

Bouwens, L., Baekeland, M., De Zanger, R., and Wisse, E. (1986). Quantitation, tissue distribution and proliferation kinetics of Kupffer cells in normal rat liver. Hepatology *6*, 718-722.

Bover, L.C., Cardo-Vila, M., Kuniyasu, A., Sun, J., Rangel, R., Takeya, M., Aggarwal, B.B., Arap, W., and Pasqualini, R. (2007). A previously unrecognized protein-protein interaction between TWEAK and CD163: potential biological implications. J Immunol *178*, 8183-8194.

Brack, A.S., Conboy, M.J., Roy, S., Lee, M., Kuo, C.J., Keller, C., and Rando, T.A. (2007). Increased Wnt signaling during aging alters muscle stem cell fate and increases fibrosis. Science *317*, 807-810.

Bralet, M.P., Branchereau, S., Brechot, C., and Ferry, N. (1994). Cell lineage study in the liver using retroviral mediated gene transfer. Evidence against the streaming of hepatocytes in normal liver. Am J Pathol *144*, 896-905.

Bray, S.J. (2006). Notch signalling: a simple pathway becomes complex. Nat Rev Mol Cell Biol *7*, 678-689.

Bray, S.J., Takada, S., Harrison, E., Shen, S.C., and Ferguson-Smith, A.C. (2008). The atypical mammalian ligand Delta-like homologue 1 (Dlk1) can regulate Notch signalling in Drosophila. BMC Dev Biol *8*, 11.

Brooks, C.L., and Gu, W. (2006). p53 ubiquitination: MDM2 and beyond. Mol Cell *21*, 307-315.

Brooling, J.T., Campbell, J.S., Mitchell, C., Yeoh, G.C., and Fausto, N. (2005). Differential regulation of rodent hepatocyte and oval cell proliferation by interferon gamma. Hepatology *41*, 906-915.

Buchman, A.L., Ament, M.E., Sohel, M., Dubin, M., Jenden, D.J., Roch, M., Pownall, H., Farley, W., Awal, M., and Ahn, C. (2001). Choline deficiency causes reversible hepatic abnormalities in patients receiving parenteral nutrition: proof of a human choline requirement: a placebo-controlled trial. JPEN J Parenter Enteral Nutr *25*, 260-268.

Buechler, C., Ritter, M., Orso, E., Langmann, T., Klucken, J., and Schmitz, G. (2000). Regulation of scavenger receptor CD163 expression in human monocytes and macrophages by pro- and antiinflammatory stimuli. J Leukoc Biol *67*, 97-103.

Burke, Z.D., and Tosh, D. (2006). The Wnt/beta-catenin pathway: master regulator of liver zonation? Bioessays *28*, 1072-1077.

Burkly, L.C., Michaelson, J.S., Hahm, K., Jakubowski, A., and Zheng, T.S. (2007). TWEAKing tissue remodeling by a multifunctional cytokine: role of TWEAK/Fn14 pathway in health and disease. Cytokine *40*, 1-16.

Cadoret, A., Ovejero, C., Saadi-Kheddouci, S., Souil, E., Fabre, M., Romagnolo, B., Kahn, A., and Perret, C. (2001). Hepatomegaly in transgenic mice expressing an oncogenic form of beta-catenin. Cancer Res *61*, 3245-3249.

Cahilly-Snyder, L., Yang-Feng, T., Francke, U., and George, D.L. (1987). Molecular analysis and chromosomal mapping of amplified genes isolated from a transformed mouse 3T3 cell line. Somat Cell Mol Genet *13*, 235-244.

Cailhier, J.F., Partolina, M., Vuthoori, S., Wu, S., Ko, K., Watson, S., Savill, J., Hughes, J., and Lang, R.A. (2005). Conditional macrophage ablation demonstrates that resident macrophages initiate acute peritoneal inflammation. J Immunol *174*, 2336-2342.

Camargo, F.D., Finegold, M., and Goodell, M.A. (2004). Hematopoietic myelomonocytic cells are the major source of hepatocyte fusion partners. J Clin Invest *113*, 1266-1270.

Campbell, S.J., Carlotti, F., Hall, P.A., Clark, A.J., and Wolf, C.R. (1996). Regulation of the CYP1A1 promoter in transgenic mice: an exquisitely sensitive on-off system for cell specific gene regulation. J Cell Sci *109 (Pt 11)*, 2619-2625.

Carpentier, B., Gautier, A., and Legallais, C. (2009). Artificial and bioartificial liver devices: present and future. Gut *58*, 1690-1702.

Cassiman, D., Libbrecht, L., Sinelli, N., Desmet, V., Denef, C., and Roskams, T. (2002). The vagal nerve stimulates activation of the hepatic progenitor cell compartment via muscarinic acetylcholine receptor type 3. Am J Pathol *161*, 521-530.

Cheng, J.H., She, H., Han, Y.P., Wang, J., Xiong, S., Asahina, K., and Tsukamoto, H. (2008). Wnt antagonism inhibits hepatic stellate cell activation and liver fibrosis. Am J Physiol Gastrointest Liver Physiol *294*, G39-49.

Chiba, T., Kita, K., Zheng, Y.W., Yokosuka, O., Saisho, H., Iwama, A., Nakauchi, H., and Taniguchi, H. (2006). Side population purified from hepatocellular carcinoma cells harbors cancer stem cell-like properties. Hepatology *44*, 240-251.

Chinzei, R., Tanaka, Y., Shimizu-Saito, K., Hara, Y., Kakinuma, S., Watanabe, M., Teramoto, K., Arii, S., Takase, K., Sato, C., *et al.* (2002). Embryoid-body cells derived from a mouse embryonic stem cell line show differentiation into functional hepatocytes. Hepatology *36*, 22-29.

Chitnis, A.B. (1995). The role of Notch in lateral inhibition and cell fate specification. Mol Cell Neurosci *6*, 311-321.

Clarke, A.R. (2006). Wnt signalling in the mouse intestine. Oncogene *25*, 7512-7521.

Coady, J.M., Santangelo, M.V., and Toto, P.D. (1967). Gamma-irradiated mouse incisor. J Dent Res *46*, 681-685.

Colletti, M., Cicchini, C., Conigliaro, A., Santangelo, L., Alonzi, T., Pasquini, E., Tripodi, M., and Amicone, L. (2009). Convergence of Wnt signaling on the HNF4alpha-driven transcription in controlling liver zonation. Gastroenterology *137*, 660-672.

Conigliaro, A., Colletti, M., Cicchini, C., Guerra, M.T., Manfredini, R., Zini, R., Bordoni, V., Siepi, F., Leopizzi, M., Tripodi, M., *et al.* (2008). Isolation and characterization of a murine resident liver stem cell. Cell Death Differ *15*, 123-133.

Croker, B.A., Krebs, D.L., Zhang, J.G., Wormald, S., Willson, T.A., Stanley, E.G., Robb, L., Greenhalgh, C.J., Forster, I., Clausen, B.E., *et al.* (2003). SOCS3 negatively regulates IL-6 signaling *in vivo*. Nat Immunol *4*, 540-545.

Cui, J., Wahl, R.L., Shen, T., Fisher, S.J., Recker, E., Ginsburg, D., and Long, M.W. (1999). Bone marrow cell trafficking following intravenous administration. Br J Haematol *107*, 895-902.

Das, S., Raj, L., Zhao, B., Kimura, Y., Bernstein, A., Aaronson, S.A., and Lee, S.W. (2007). Hzf Determines cell survival upon genotoxic stress by modulating p53 transactivation. Cell *130*, 624-637.

De Alwis, N., Hudson, G., Burt, A.D., Day, C.P., and Chinnery, P.F. (2009). Human liver stem cells originate from the canals of Hering. Hepatology *50*, 992-993.

de Boer, C.J., van Krieken, J.H., Janssen-van Rhijn, C.M., and Litvinov, S.V. (1999). Expression of Ep-CAM in normal, regenerating, metaplastic, and neoplastic liver. J Pathol *188*, 201-206.

de La Coste, A., Romagnolo, B., Billuart, P., Renard, C.A., Buendia, M.A., Soubrane, O., Fabre, M., Chelly, J., Beldjord, C., Kahn, A., *et al.* (1998). Somatic mutations of the beta-catenin gene are frequent in mouse and human hepatocellular carcinomas. Proc Natl Acad Sci U S A *95*, 8847-8851.

de Oca Luna, R.M., Tabor, A.D., Eberspaecher, H., Hulboy, D.L., Worth, L.L., Colman, M.S., Finlay, C.A., and Lozano, G. (1996). The organization and expression of the mdm2 gene. Genomics *33*, 352-357.

De Silvestro, G., Vicarioto, M., Donadel, C., Menegazzo, M., Marson, P., and Corsini, A. (2004). Mobilization of peripheral blood hematopoietic stem cells following liver resection surgery. Hepatogastroenterology *51*, 805-810.

De Vos, R., and Desmet, V. (1992). Ultrastructural characteristics of novel epithelial cell types identified in human pathologic liver specimens with chronic ductular reaction. Am J Pathol *140*, 1441-1450.

Demetris, A.J., Seaberg, E.C., Wennerberg, A., Ionellie, J., and Michalopoulos, G. (1996). Ductular reaction after submassive necrosis in humans. Special emphasis on analysis of ductular hepatocytes. Am J Pathol *149*, 439-448.

Dixon, L.R., and Crawford, J.M. (2007). Early histologic changes in fibrosing cholestatic hepatitis C. Liver Transpl *13*, 219-226.

Domogatskaya, A., Rodin, S., Boutaud, A., and Tryggvason, K. (2008). Laminin-511 but not -332, -111, or -411 enables mouse embryonic stem cell self-renewal *in vitro*. Stem Cells *26*, 2800-2809.

Dorrell, C., Erker, L., Lanxon-Cookson, K.M., Abraham, S.L., Victoroff, T., Ro, S., Canaday, P.S., Streeter, P.R., and Grompe, M. (2008). Surface markers for the murine oval cell response. Hepatology *48*, 1282-1291.

Douglass, A., Wallace, K., Koruth, M., Barelle, C., Porter, A.J., and Wright, M.C. (2008a). Targeting liver myofibroblasts: a novel approach in anti-fibrogenic therapy. Hepatol Int *2*, 405-415.

Douglass, A., Wallace, K., Parr, R., Park, J., Durward, E., Broadbent, I., Barelle, C., Porter, A.J., and Wright, M.C. (2008b). Antibody-targeted myofibroblast apoptosis reduces fibrosis during sustained liver injury. J Hepatol *49*, 88-98.

Dudas, J., Elmaouhoub, A., Mansuroglu, T., Batusic, D., Tron, K., Saile, B., Papoutsi, M., Pieler, T., Wilting, J., and Ramadori, G. (2006). Prospero-related homeobox 1 (Prox1) is a stable hepatocyte marker during liver development, injury and regeneration, and is absent from "oval cells". Histochem Cell Biol *126*, 549-562.

Duffield, J.S., Forbes, S.J., Constandinou, C.M., Clay, S., Partolina, M., Vuthoori, S., Wu, S., Lang, R., and Iredale, J.P. (2005). Selective depletion of macrophages reveals distinct, opposing roles during liver injury and repair. J Clin Invest *115*, 56-65.

Duncan, A.W., Dorrell, C., and Grompe, M. (2009). Stem cells and liver regeneration. Gastroenterology *137*, 466-481.

Evans, S.C., Viswanathan, M., Grier, J.D., Narayana, M., El-Naggar, A.K., and Lozano, G. (2001). An alternatively spliced HDM2 product increases p53 activity by inhibiting HDM2. Oncogene *20*, 4041-4049.

Evarts, R.P., Hu, Z., Fujio, K., Marsden, E.R., and Thorgeirsson, S.S. (1993). Activation of hepatic stem cell compartment in the rat: role of transforming growth factor alpha, hepatocyte

growth factor, and acidic fibroblast growth factor in early proliferation. Cell Growth Differ *4*, 555-561.

Evarts, R.P., Nagy, P., Marsden, E., and Thorgeirsson, S.S. (1987). A precursor-product relationship exists between oval cells and hepatocytes in rat liver. Carcinogenesis *8*, 1737-1740.

Evarts, R.P., Nagy, P., Nakatsukasa, H., Marsden, E., and Thorgeirsson, S.S. (1989). *In vivo* differentiation of rat liver oval cells into hepatocytes. Cancer Res *49*, 1541-1547.

Evarts, R.P., Nakatsukasa, H., Marsden, E.R., Hu, Z., and Thorgeirsson, S.S. (1992). Expression of transforming growth factor-alpha in regenerating liver and during hepatic differentiation. Mol Carcinog *5*, 25-31.

Falkowski, O., An, H.J., Ianus, I.A., Chiriboga, L., Yee, H., West, A.B., and Theise, N.D. (2003). Regeneration of hepatocyte 'buds' in cirrhosis from intrabiliary stem cells. J Hepatol *39*, 357-364.

Fallowfield, J.A., Mizuno, M., Kendall, T.J., Constandinou, C.M., Benyon, R.C., Duffield, J.S., and Iredale, J.P. (2007). Scar-associated macrophages are a major source of hepatic matrix metalloproteinase-13 and facilitate the resolution of murine hepatic fibrosis. J Immunol *178*, 5288-5295.

Farber, E. (1956). Similarities in the sequence of early histological changes induced in the liver of the rat by ethionine, 2-acetylamino-fluorene, and 3'-methyl-4-dimethylaminoazobenzene. Cancer Res *16*, 142-148.

Faris, R.A., and Hixson, D.C. (1989). Selective proliferation of chemically altered rat liver epithelial cells following hepatic transplantation. Transplantation *48*, 87-92.

Fausto, N., Campbell, J.S., and Riehle, K.J. (2006). Liver regeneration. Hepatology *43*, S45-53.

Feldmann, G., Lamboley, C., Moreau, A., and Bringuier, A. (1998). Fas-mediated apoptosis of hepatic cells. Biomed Pharmacother *52*, 378-385.

Fellous, T.G., Islam, S., Tadrous, P.J., Elia, G., Kocher, H.M., Bhattacharya, S., Mears, L., Turnbull, D.M., Taylor, R.W., Greaves, L.C., *et al.* (2009). Locating the stem cell niche and tracing hepatocyte lineages in human liver. Hepatology *49*, 1655-1663.

Fischer, M., Goldschmitt, J., Peschel, C., Brakenhoff, J.P., Kallen, K.J., Wollmer, A., Grotzinger, J., and Rose-John, S. (1997). I. A bioactive designer cytokine for human hematopoietic progenitor cell expansion. Nat Biotechnol *15*, 142-145.

Fleming, H.E., Janzen, V., Lo Celso, C., Guo, J., Leahy, K.M., Kronenberg, H.M., and Scadden, D.T. (2008). Wnt signaling in the niche enforces hematopoietic stem cell quiescence and is necessary to preserve self-renewal *in vivo*. Cell Stem Cell *2*, 274-283.

Forbes, S.J., Russo, F.P., Rey, V., Burra, P., Rugge, M., Wright, N.A., and Alison, M.R. (2004). A significant proportion of myofibroblasts are of bone marrow origin in human liver fibrosis. Gastroenterology *126*, 955-963.

Forbes, S.J., Themis, M., Alison, M.R., Selden, C., Coutelle, C., and Hodgson, H.J. (1998). Retroviral gene transfer to the liver *in vivo* during tri-iodothyronine induced hyperplasia. Gene Ther *5*, 552-555.

Forbes, S.J., Themis, M., Alison, M.R., Shiota, A., Kobayashi, T., Coutelle, C., and Hodgson, H.J. (2000). Tri-iodothyronine and a deleted form of hepatocyte growth factor act synergistically to enhance liver proliferation and enable *in vivo* retroviral gene transfer via the peripheral venous system. Gene Ther *7*, 784-789.

Friedman, S.L. (2008). Hepatic stellate cells: protean, multifunctional, and enigmatic cells of the liver. Physiol Rev *88*, 125-172.

Fuchs, E., and Nowak, J.A. (2008). Building epithelial tissues from skin stem cells. Cold Spring Harb Symp Quant Biol *73*, 333-350.

Fuchs, E., Tumbar, T., and Guasch, G. (2004). Socializing with the neighbors: stem cells and their niche. Cell *116*, 769-778.

Fujii, H., Hirose, T., Oe, S., Yasuchika, K., Azuma, H., Fujikawa, T., Nagao, M., and Yamaoka, Y. (2002). Contribution of bone marrow cells to liver regeneration after partial hepatectomy in mice. J Hepatol *36*, 653-659.

Furst, G., Schulte am Esch, J., Poll, L.W., Hosch, S.B., Fritz, L.B., Klein, M., Godehardt, E., Krieg, A., Wecker, B., Stoldt, V., *et al.* (2007). Portal vein embolization and autologous CD133+ bone marrow stem cells for liver regeneration: initial experience. Radiology *243*, 171-179.

Gaia, S., Smedile, A., Omede, P., Olivero, A., Sanavio, F., Balzola, F., Ottobrelli, A., Abate, M.L., Marzano, A., Rizzetto, M., *et al.* (2006). Feasibility and safety of G-CSF administration to induce bone marrow-derived cells mobilization in patients with end stage liver disease. J Hepatol *45*, 13-19.

Gao, Z., McAlister, V.C., and Williams, G.M. (2001). Repopulation of liver endothelium by bone-marrow-derived cells. Lancet *357*, 932-933.

Gasbarrini, A., Rapaccini, G.L., Rutella, S., Zocco, M.A., Tittoto, P., Leone, G., Pola, P., Gasbarrini, G., and Di Campli, C. (2006). Rescue therapy by portal infusion of autologous stem cells in a case of drug-induced hepatitis. Dig Liver Dis.

Gazit, R., Weissman, I.L., and Rossi, D.J. (2008). Hematopoietic stem cells and the aging hematopoietic system. Semin Hematol *45*, 218-224.

Gebhardt, R. (1992). Metabolic zonation of the liver: regulation and implications for liver function. Pharmacol Ther *53*, 275-354.

Gebhardt, R., and Hovhannisyan, A. (2010). Organ patterning in the adult stage: the role of Wnt/beta-catenin signaling in liver zonation and beyond. Dev Dyn *239*, 45-55.

Gehling, U.M., Willems, M., Dandri, M., Petersen, J., Berna, M., Thill, M., Wulf, T., Muller, L., Pollok, J.M., Schlagner, K., *et al.* (2005). Partial hepatectomy induces mobilization of a unique population of haematopoietic progenitor cells in human healthy liver donors. J Hepatol *43*, 845-853.

Geisler, F., Nagl, F., Mazur, P.K., Lee, M., Zimber-Strobl, U., Strobl, L.J., Radtke, F., Schmid, R.M., and Siveke, J.T. (2008). Liver-specific inactivation of Notch2, but not Notch1, compromises intrahepatic bile duct development in mice. Hepatology *48*, 607-616.

Girgenrath, M., Weng, S., Kostek, C.A., Browning, B., Wang, M., Brown, S.A., Winkles, J.A., Michaelson, J.S., Allaire, N., Schneider, P., *et al.* (2006). TWEAK, via its receptor

Fn14, is a novel regulator of mesenchymal progenitor cells and skeletal muscle regeneration. Embo J *25*, 5826-5839.

Gomes, L.F., Lorente, S., Simon-Giavarotti, K.A., Areco, K.N., Araujo-Peres, C., and Videla, L.A. (2004). Tri-iodothyronine differentially induces Kupffer cell ED1/ED2 subpopulations. Mol Aspects Med *25*, 183-190.

Goncalves, L.A., Vigario, A.M., and Penha-Goncalves, C. (2007). Improved isolation of murine hepatocytes for *in vitro* malaria liver stage studies. Malar J *6*, 169.

Gordon, G.J., Coleman, W.B., and Grisham, J.W. (2000). Temporal analysis of hepatocyte differentiation by small hepatocyte-like progenitor cells during liver regeneration in retrorsine-exposed rats. Am J Pathol *157*, 771-786.

Gordon, M.Y., Levicar, N., Pai, M., Bachellier, P., Dimarakis, I., Al-Allaf, F., M'Hamdi, H., Thalji, T., Welsh, J.P., Marley, S.B., *et al.* (2006). Characterization and clinical application of human CD34+ stem/progenitor cell populations mobilized into the blood by granulocyte colony-stimulating factor. Stem Cells *24*, 1822-1830.

Grier, J.D., Yan, W., and Lozano, G. (2002). Conditional allele of mdm2 which encodes a p53 inhibitor. Genesis *32*, 145-147.

Guengerich, F.P., Dannan, G.A., Wright, S.T., Martin, M.V., and Kaminsky, L.S. (1982). Purification and characterization of liver microsomal cytochromes p-450: electrophoretic, spectral, catalytic, and immunochemical properties and inducibility of eight isozymes isolated from rats treated with phenobarbital or beta-naphthoflavone. Biochemistry *21*, 6019-6030.

Gyorki, D.E., Asselin-Labat, M.L., van Rooijen, N., Lindeman, G.J., and Visvader, J.E. (2009). Resident macrophages influence stem cell activity in the mammary gland. Breast Cancer Res *11*, R62.

Hansson, G.K. (2007). Medicine. LIGHT hits the liver. Science *316*, 206-207.

Hashimoto, S., Yamada, M., Yanai, N., Kawashima, T., and Motoyoshi, K. (1996). Phenotypic change and proliferation of murine Kupffer cells by colony-stimulating factors. J Interferon Cytokine Res *16*, 237-243.

Hasuike, S., Ido, A., Uto, H., Moriuchi, A., Tahara, Y., Numata, M., Nagata, K., Hori, T., Hayashi, K., and Tsubouchi, H. (2005). Hepatocyte growth factor accelerates the proliferation of hepatic oval cells and possibly promotes the differentiation in a 2-acetylaminofluorene/partial hepatectomy model in rats. J Gastroenterol Hepatol *20*, 1753-1761.

Hatch, H.M., Zheng, D., Jorgensen, M.L., and Petersen, B.E. (2002). SDF-1alpha/CXCR4: a mechanism for hepatic oval cell activation and bone marrow stem cell recruitment to the injured liver of rats. Cloning Stem Cells *4*, 339-351.

Hay, D.C., Fletcher, J., Payne, C., Terrace, J.D., Gallagher, R.C., Snoeys, J., Black, J.R., Wojtacha, D., Samuel, K., Hannoun, Z., *et al.* (2008). Highly efficient differentiation of hESCs to functional hepatic endoderm requires ActivinA and Wnt3a signaling. Proc Natl Acad Sci U S A *105*, 12301-12306.

Hayward, P., Kalmar, T., and Arias, A.M. (2008). Wnt/Notch signalling and information processing during development. Development *135*, 411-424.

He, X. (2006). Unwinding a path to nuclear beta-catenin. Cell *127*, 40-42.

Heinrich, P.C., Behrmann, I., Haan, S., Hermanns, H.M., Muller-Newen, G., and Schaper, F. (2003). Principles of interleukin (IL)-6-type cytokine signalling and its regulation. Biochem J *374*, 1-20.

Henderson, N.C., and Iredale, J.P. (2007). Liver fibrosis: cellular mechanisms of progression and resolution. Clin Sci (Lond) *112*, 265-280.

Herrera, M.B., Bruno, S., Buttiglieri, S., Tetta, C., Gatti, S., Deregibus, M.C., Bussolati, B., and Camussi, G. (2006). Isolation and characterization of a stem cell population from adult human liver. Stem Cells *24*, 2840-2850.

Higashiyama, R., Inagaki, Y., Hong, Y.Y., Kushida, M., Nakao, S., Niioka, M., Watanabe, T., Okano, H., Matsuzaki, Y., Shiota, G., *et al.* (2007). Bone marrow-derived cells express matrix metalloproteinases and contribute to regression of liver fibrosis in mice. Hepatology *45*, 213-222.

Hirose, Y., Itoh, T., and Miyajima, A. (2009). Hedgehog signal activation coordinates proliferation and differentiation of fetal liver progenitor cells. Exp Cell Res *315*, 2648-2657.

Holic, N., Suzuki, T., Corlu, A., Couchie, D., Chobert, M.N., Guguen-Guillouzo, C., and Laperche, Y. (2000). Differential expression of the rat gamma-glutamyl transpeptidase gene promoters along with differentiation of hepatoblasts into biliary or hepatocytic lineage. Am J Pathol *157*, 537-548.

Holowacz, T., Zeng, L., and Lassar, A.B. (2006). Asymmetric localization of numb in the chick somite and the influence of myogenic signals. Dev Dyn *235*, 633-645.

Holt, A.P., Haughton, E.L., Lalor, P.F., Filer, A., Buckley, C.D., and Adams, D.H. (2009). Liver myofibroblasts regulate infiltration and positioning of lymphocytes in human liver. Gastroenterology *136*, 705-714.

Houlihan, D.D., and Newsome, P.N. (2008). Critical review of clinical trials of bone marrow stem cells in liver disease. Gastroenterology *135*, 438-450.

Hsia, C.C., Thorgeirsson, S.S., and Tabor, E. (1994). Expression of hepatitis B surface and core antigens and transforming growth factor-alpha in "oval cells" of the liver in patients with hepatocellular carcinoma. J Med Virol *43*, 216-221.

Hu, M., Kurobe, M., Jeong, Y.J., Fuerer, C., Ghole, S., Nusse, R., and Sylvester, K.G. (2007). Wnt/beta-catenin signaling in murine hepatic transit amplifying progenitor cells. Gastroenterology *133*, 1579-1591.

Hu, Z., Evarts, R.P., Fujio, K., Marsden, E.R., and Thorgeirsson, S.S. (1993). Expression of hepatocyte growth factor and c-met genes during hepatic differentiation and liver development in the rat. Am J Pathol *142*, 1823-1830.

Hu, Z., Evarts, R.P., Fujio, K., Marsden, E.R., and Thorgeirsson, S.S. (1995). Expression of fibroblast growth factor receptors flg and bek during hepatic ontogenesis and regeneration in the rat. Cell Growth Differ *6*, 1019-1025.

Hume, D.A., Loutit, J.F., and Gordon, S. (1984). The mononuclear phagocyte system of the mouse defined by immunohistochemical localization of antigen F4/80: macrophages of bone and associated connective tissue. J Cell Sci *66*, 189-194.

Hunter, M.P., Wilson, C.M., Jiang, X., Cong, R., Vasavada, H., Kaestner, K.H., and Bogue, C.W. (2007). The homeobox gene Hhex is essential for proper hepatoblast differentiation and bile duct morphogenesis. Dev Biol *308*, 355-367.

Iakova, P., Awad, S.S., and Timchenko, N.A. (2003). Aging reduces proliferative capacities of liver by switching pathways of C/EBPalpha growth arrest. Cell *113*, 495-506.

Ide, M., Kuwamura, M., Kotani, T., Sawamoto, O., and Yamate, J. (2005). Effects of gadolinium chloride (GdCl(3)) on the appearance of macrophage populations and fibrogenesis in thioacetamide-induced rat hepatic lesions. J Comp Pathol *133*, 92-102.

Ireland, H., Kemp, R., Houghton, C., Howard, L., Clarke, A.R., Sansom, O.J., and Winton, D.J. (2004). Inducible Cre-mediated control of gene expression in the murine gastrointestinal tract: effect of loss of beta-catenin. Gastroenterology *126*, 1236-1246.

Jacob, F., and Monod, J. (1961). Genetic regulatory mechanisms in the synthesis of proteins. J Mol Biol *3*, 318-356.

Jakubowski, A., Ambrose, C., Parr, M., Lincecum, J.M., Wang, M.Z., Zheng, T.S., Browning, B., Michaelson, J.S., Baetscher, M., Wang, B., *et al.* (2005). TWEAK induces liver progenitor cell proliferation. J Clin Invest *115*, 2330-2340.

Jakubowski, A., Browning, B., Lukashev, M., Sizing, I., Thompson, J.S., Benjamin, C.D., Hsu, Y.M., Ambrose, C., Zheng, T.S., and Burkly, L.C. (2002). Dual role for TWEAK in angiogenic regulation. J Cell Sci *115*, 267-274.

Jelnes, P., Santoni-Rugiu, E., Rasmussen, M., Friis, S.L., Nielsen, J.H., Tygstrup, N., and Bisgaard, H.C. (2007). Remarkable heterogeneity displayed by oval cells in rat and mouse models of stem cell-mediated liver regeneration. Hepatology *45*, 1462-1470.

Jensen, C.H., Jauho, E.I., Santoni-Rugiu, E., Holmskov, U., Teisner, B., Tygstrup, N., and Bisgaard, H.C. (2004). Transit-amplifying ductular (oval) cells and their hepatocytic progeny are characterized by a novel and distinctive expression of delta-like protein/preadipocyte factor 1/fetal antigen 1. Am J Pathol *164*, 1347-1359.

Jian, H., Shen, X., Liu, I., Semenov, M., He, X., and Wang, X.F. (2006). Smad3-dependent nuclear translocation of beta-catenin is required for TGF-beta1-induced proliferation of bone marrow-derived adult human mesenchymal stem cells. Genes Dev *20*, 666-674.

Jin-no, K., Tanimizu, M., Hyodo, I., Kurimoto, F., and Yamashita, T. (1997). Plasma level of basic fibroblast growth factor increases with progression of chronic liver disease. J Gastroenterol *32*, 119-121.

Jones, S.N., Roe, A.E., Donehower, L.A., and Bradley, A. (1995). Rescue of embryonic lethality in MDM2-deficient mice by absence of p53. Nature *378*, 206-208.

Jung, J., Zheng, M., Goldfarb, M., and Zaret, K.S. (1999). Initiation of mammalian liver development from endoderm by fibroblast growth factors. Science *284*, 1998-2003.

Jung, Y., Brown, K.D., Witek, R.P., Omenetti, A., Yang, L., Vandongen, M., Milton, R.J., Hines, I.N., Rippe, R.A., Spahr, L., *et al.* (2008). Accumulation of hedgehog-responsive progenitors parallels alcoholic liver disease severity in mice and humans. Gastroenterology *134*, 1532-1543.

Kakinuma, S., Ohta, H., Kamiya, A., Yamazaki, Y., Oikawa, T., Okada, K., and Nakauchi, H. (2009). Analyses of cell surface molecules on hepatic stem/progenitor cells in mouse fetal liver. J Hepatol *51*, 127-138.

Kasahara, M., Kiuchi, T., Inomata, Y., Uryuhara, K., Sakamoto, S., Ito, T., Fujimoto, Y., Ogura, Y., Oike, F., and Tanaka, K. (2003). Living-related liver transplantation for Alagille syndrome. Transplantation *75*, 2147-2150.

Katoh, M. (2006a). Notch ligand, JAG1, is evolutionarily conserved target of canonical WNT signaling pathway in progenitor cells. Int J Mol Med *17*, 681-685.

Katoh, M. (2006b). NUMB is a break of WNT-Notch signaling cycle. Int J Mol Med *18*, 517-521.

Kawakita, T., Shiraki, K., Yamanaka, Y., Yamaguchi, Y., Saitou, Y., Enokimura, N., Yamamoto, N., Okano, H., Sugimoto, K., Murata, K., *et al.* (2005). Functional expression of TWEAK in human colonic adenocarcinoma cells. Int J Oncol *26*, 87-93.

Kemp, R., Ireland, H., Clayton, E., Houghton, C., Howard, L., and Winton, D.J. (2004). Elimination of background recombination: somatic induction of Cre by combined transcriptional regulation and hormone binding affinity. Nucleic Acids Res *32*, e92.

Kiel, M.J., and Morrison, S.J. (2008). Uncertainty in the niches that maintain haematopoietic stem cells. Nat Rev Immunol *8*, 290-301.

Kinoshita, T., Sekiguchi, T., Xu, M.J., Ito, Y., Kamiya, A., Tsuji, K., Nakahata, T., and Miyajima, A. (1999). Hepatic differentiation induced by oncostatin M attenuates fetal liver hematopoiesis. Proc Natl Acad Sci U S A *96*, 7265-7270.

Kinosita, R. (1937). Studies on the cancerogenic chemical substances. Trans Soc Pathol Jpn *27*, 329-334.

Kinugasa, A., and Thurman, R.G. (1986). Differential effect of glucagon on gluconeogenesis in periportal and pericentral regions of the liver lobule. Biochem J *236*, 425-430.

Kirillova, I., Chaisson, M., and Fausto, N. (1999). Tumor necrosis factor induces DNA replication in hepatic cells through nuclear factor kappaB activation. Cell Growth Differ *10*, 819-828.

Kirkwood, T.B. (2005). Understanding the odd science of aging. Cell *120*, 437-447.

Kirstetter, P., Anderson, K., Porse, B.T., Jacobsen, S.E., and Nerlov, C. (2006). Activation of the canonical Wnt pathway leads to loss of hematopoietic stem cell repopulation and multilineage differentiation block. Nat Immunol *7*, 1048-1056.

Kisseleva, T., Uchinami, H., Feirt, N., Quintana-Bustamante, O., Segovia, J.C., Schwabe, R.F., and Brenner, D.A. (2006). Bone marrow-derived fibrocytes participate in pathogenesis of liver fibrosis. J Hepatol *45*, 429-438.

Kitamoto, K., Machida, Y., Uchida, J., Izumi, Y., Shiota, M., Nakao, T., Iwao, H., Yukimura, T., Nakatani, T., and Miura, K. (2009). Effects of liposome clodronate on renal leukocyte populations and renal fibrosis in murine obstructive nephropathy. J Pharmacol Sci *111*, 285-292.

Klein, I., Cornejo, J.C., Polakos, N.K., John, B., Wuensch, S.A., Topham, D.J., Pierce, R.H., and Crispe, I.N. (2007). Kupffer cell heterogeneity: functional properties of bone marrow-derived and sessile hepatic macrophages. Blood.

Knight, B., Akhurst, B., Matthews, V.B., Ruddell, R.G., Ramm, G.A., Abraham, L.J., Olynyk, J.K., and Yeoh, G.C. (2007). Attenuated liver progenitor (oval) cell and fibrogenic responses to the choline deficient, ethionine supplemented diet in the BALB/c inbred strain of mice. J Hepatol *46*, 134-141.

Knight, B., Matthews, V.B., Akhurst, B., Croager, E.J., Klinken, E., Abraham, L.J., Olynyk, J.K., and Yeoh, G. (2005a). Liver inflammation and cytokine production, but not acute phase protein synthesis, accompany the adult liver progenitor (oval) cell response to chronic liver injury. Immunol Cell Biol *83*, 364-374.

Knight, B., Matthews, V.B., Olynyk, J.K., and Yeoh, G.C. (2005b). Jekyll and Hyde: evolving perspectives on the function and potential of the adult liver progenitor (oval) cell. Bioessays *27*, 1192-1202.

Knight, B., Tirnitz-Parker, J.E., and Olynyk, J.K. (2008). C-kit inhibition by imatinib mesylate attenuates progenitor cell expansion and inhibits liver tumor formation in mice. Gastroenterology *135*, 969-979, 979 e961.

Knight, B., and Yeoh, G.C. (2005). TNF/LTalpha double knockout mice display abnormal inflammatory and regenerative responses to acute and chronic liver injury. Cell Tissue Res *319*, 61-70.

Knight, B., Yeoh, G.C., Husk, K.L., Ly, T., Abraham, L.J., Yu, C., Rhim, J.A., and Fausto, N. (2000). Impaired preneoplastic changes and liver tumor formation in tumor necrosis factor receptor type 1 knockout mice. J Exp Med *192*, 1809-1818.

Kodama, Y., Hijikata, M., Kageyama, R., Shimotohno, K., and Chiba, T. (2004). The role of notch signaling in the development of intrahepatic bile ducts. Gastroenterology *127*, 1775-1786.

Kofman, A.V., Morgan, G., Kirschenbaum, A., Osbeck, J., Hussain, M., Swenson, S., and Theise, N.D. (2005). Dose- and time-dependent oval cell reaction in acetaminophen-induced murine liver injury. Hepatology *41*, 1252-1261.

Kohler, C., Bell, A.W., Bowen, W.C., Monga, S.P., Fleig, W., and Michalopoulos, G.K. (2004). Expression of Notch-1 and its ligand Jagged-1 in rat liver during liver regeneration. Hepatology *39*, 1056-1065.

Kohut, M.L., Senchina, D.S., Madden, K.S., Martin, A.E., Felten, D.L., and Moynihan, J.A. (2004). Age effects on macrophage function vary by tissue site, nature of stimulant, and exercise behavior. Exp Gerontol *39*, 1347-1360.

Koivisto, U.M., Hubbard, A.L., and Mellman, I. (2001). A novel cellular phenotype for familial hypercholesterolemia due to a defect in polarized targeting of LDL receptor. Cell *105*, 575-585.

Kollet, O., Shivtiel, S., Chen, Y.Q., Suriawinata, J., Thung, S.N., Dabeva, M.D., Kahn, J., Spiegel, A., Dar, A., Samira, S., *et al.* (2003). HGF, SDF-1, and MMP-9 are involved in stress-induced human CD34+ stem cell recruitment to the liver. J Clin Invest *112*, 160-169.

Komuves, L.G., Feren, A., Jones, A.L., and Fodor, E. (2000). Expression of epidermal growth factor and its receptor in cirrhotic liver disease. J Histochem Cytochem *48*, 821-830.

Kordes, C., Sawitza, I., and Haussinger, D. (2008). Canonical Wnt signaling maintains the quiescent stage of hepatic stellate cells. Biochem Biophys Res Commun *367*, 116-123.

Kordes, C., Sawitza, I., and Haussinger, D. (2009). Hepatic and pancreatic stellate cells in focus. Biol Chem *390*, 1003-1012.

Kubota, K., Soeda, J., Misawa, R., Mihara, M., Miwa, S., Ise, H., Takahashi, M., and Miyagawa, S. (2008). Bone marrow-derived cells fuse with hepatic oval cells but are not involved in hepatic tumorigenesis in the choline-deficient ethionine-supplemented diet rat model. Carcinogenesis *29*, 448-454.

Lagasse, E., Connors, H., Al-Dhalimy, M., Reitsma, M., Dohse, M., Osborne, L., Wang, X., Finegold, M., Weissman, I.L., and Grompe, M. (2000). Purified hematopoietic stem cells can differentiate into hepatocytes *in vivo*. Nat Med *6*, 1229-1234.

Larsen, S.R., Kingham, J.A., Hayward, M.D., and Rasko, J.E. (2006). Damage to incisors after nonmyeloablative total body irradiation may complicate NOD/SCID models of hemopoietic stem cell transplantation. Comp Med *56*, 209-214.

Laszlo, V., Dezso, K., Baghy, K., Papp, V., Kovalszky, I., Safrany, G., Thorgeirsson, S.S., Nagy, P., and Paku, S. (2008). Triiodothyronine accelerates differentiation of rat liver progenitor cells into hepatocytes. Histochem Cell Biol.

Lathia, J.D., Patton, B., Eckley, D.M., Magnus, T., Mughal, M.R., Sasaki, T., Caldwell, M.A., Rao, M.S., Mattson, M.P., and ffrench-Constant, C. (2007). Patterns of laminins and integrins in the embryonic ventricular zone of the CNS. J Comp Neurol *505*, 630-643.

Lazaro, C.A., Rhim, J.A., Yamada, Y., and Fausto, N. (1998). Generation of hepatocytes from oval cell precursors in culture. Cancer Res *58*, 5514-5522.

Leahy, D.J. (2004). Structure and function of the epidermal growth factor (EGF/ErbB) family of receptors. Adv Protein Chem *68*, 1-27.

Lee, C.M., Yeoh, G.C., and Olynyk, J.K. (2004). Differential effects of gadolinium chloride on Kupffer cells *in vivo* and *in vitro*. Int J Biochem Cell Biol *36*, 481-488.

Lemoli, R.M., Catani, L., Talarico, S., Loggi, E., Gramenzi, A., Baccarani, U., Fogli, M., Grazi, G.L., Aluigi, M., Marzocchi, G., *et al.* (2006). Mobilization of bone marrow-derived hematopoietic and endothelial stem cells after orthotopic liver transplantation and liver resection. Stem Cells *24*, 2817-2825.

Leon, D.A., and McCambridge, J. (2006). Liver cirrhosis mortality rates in Britain from 1950 to 2002: an analysis of routine data. Lancet *367*, 52-56.

Libbrecht, L., Desmet, V., Van Damme, B., and Roskams, T. (2000). Deep intralobular extension of human hepatic 'progenitor cells' correlates with parenchymal inflammation in chronic viral hepatitis: can 'progenitor cells' migrate? J Pathol *192*, 373-378.

Liebner, S., Cattelino, A., Gallini, R., Rudini, N., Iurlaro, M., Piccolo, S., and Dejana, E. (2004). Beta-catenin is required for endothelial-mesenchymal transformation during heart cushion development in the mouse. J Cell Biol *166*, 359-367.

Lim, R., Knight, B., Patel, K., McHutchison, J.G., Yeoh, G.C., and Olynyk, J.K. (2006). Antiproliferative effects of interferon alpha on hepatic progenitor cells *in vitro* and *in vivo*. Hepatology *43*, 1074-1083.

Lin, W.R., Lim, S.N., McDonald, S.A., Graham, T., Wright, V.L., Peplow, C.L., Humphries, A., Kocher, H.M., Wright, N.A., Dhillon, A.P., *et al.* (2010). The histogenesis of regenerative nodules in human liver cirrhosis. Hepatology *51*, 1017-1026.

Lloberas, J., and Celada, A. (2002). Effect of aging on macrophage function. Exp Gerontol *37*, 1325-1331.

Lo, J.C., Wang, Y., Tumanov, A.V., Bamji, M., Yao, Z., Reardon, C.A., Getz, G.S., and Fu, Y.X. (2007). Lymphotoxin beta receptor-dependent control of lipid homeostasis. Science *316*, 285-288.

Lobov, I.B., Rao, S., Carroll, T.J., Vallance, J.E., Ito, M., Ondr, J.K., Kurup, S., Glass, D.A., Patel, M.S., Shu, W., *et al.* (2005). WNT7b mediates macrophage-induced programmed cell death in patterning of the vasculature. Nature *437*, 417-421.

Locksley, R.M., Killeen, N., and Lenardo, M.J. (2001). The TNF and TNF receptor superfamilies: integrating mammalian biology. Cell *104*, 487-501.

Logeat, F., Bessia, C., Brou, C., LeBail, O., Jarriault, S., Seidah, N.G., and Israel, A. (1998). The Notch1 receptor is cleaved constitutively by a furin-like convertase. Proc Natl Acad Sci U S A *95*, 8108-8112.

Loomes, K.M., Russo, P., Ryan, M., Nelson, A., Underkoffler, L., Glover, C., Fu, H., Gridley, T., Kaestner, K.H., and Oakey, R.J. (2007). Bile duct proliferation in liver-specific Jag1 conditional knockout mice: effects of gene dosage. Hepatology *45*, 323-330.

Lorenzini, S., Bird, T.G., Boulter, L., Bellamy, C., Samuel, K., Aucott, R., Clayton, E., Andreone, P., Bernardi, M., Golding, M., *et al.* (2010). Characterization of a stereotypical cellular and extracellular adult liver progenitor cell niche in rodents and diseased human liver. Gut *59*, 645-54.

Lowes, K.N., Brennan, B.A., Yeoh, G.C., and Olynyk, J.K. (1999). Oval cell numbers in human chronic liver diseases are directly related to disease severity. Am J Pathol *154*, 537-541.

Loyer, P., Ilyin, G., Cariou, S., Glaise, D., Corlu, A., and Guguen-Guillouzo, C. (1996). Progression through G1 and S phases of adult rat hepatocytes. Prog Cell Cycle Res *2*, 37-47.

Lozier, J., McCright, B., and Gridley, T. (2008). Notch signaling regulates bile duct morphogenesis in mice. PLoS One *3*, e1851.

Lu, L., Li, Y., Kim, S.M., Bossuyt, W., Liu, P., Qiu, Q., Wang, Y., Halder, G., Finegold, M.J., Lee, J.S., *et al.* (2009). Hippo signaling is a potent *in vivo* growth and tumor suppressor pathway in the mammalian liver. Proc Natl Acad Sci U S A *107*, 1437-1442.

Ma, G., Xiao, Y., and He, L. (2008). Recent progress in the study of Hedgehog signaling. J Genet Genomics *35*, 129-137.

MacKay, G.E., Keighren, M.A., Wilson, L., Pratt, T., Flockhart, J.H., Mason, J.O., Price, D.J., and West, J.D. (2005). Evaluation of the mouse TgTP6.3 tauGFP transgene as a lineage marker in chimeras. J Anat *206*, 79-92.

Mallo, M. (2006). Controlled gene activation and inactivation in the mouse. Front Biosci *11*, 313-327.

Mandache, E., Vidulescu, C., Gherghiceanu, M., Dragomir, P., and Popescu, L.M. (2002). Neoductular progenitor cells regenerate hepatocytes in severely damaged liver: a comparative ultrastructural study. J Cell Mol Med *6*, 59-73.

Maretto, S., Cordenonsi, M., Dupont, S., Braghetta, P., Broccoli, V., Hassan, A.B., Volpin, D., Bressan, G.M., and Piccolo, S. (2003). Mapping Wnt/beta-catenin signaling during mouse development and in colorectal tumors. Proc Natl Acad Sci U S A *100*, 3299-3304.

Marsden, E.R., Hu, Z., Fujio, K., Nakatsukasa, H., Thorgeirsson, S.S., and Evarts, R.P. (1992). Expression of acidic fibroblast growth factor in regenerating liver and during hepatic differentiation. Lab Invest *67*, 427-433.

Marshall, A., Rushbrook, S., Davies, S.E., Morris, L.S., Scott, I.S., Vowler, S.L., Coleman, N., and Alexander, G. (2005). Relation between hepatocyte G1 arrest, impaired hepatic regeneration, and fibrosis in chronic hepatitis C virus infection. Gastroenterology *128*, 33-42.

Martin, P., D'Souza, D., Martin, J., Grose, R., Cooper, L., Maki, R., and McKercher, S.R. (2003). Wound healing in the PU.1 null mouse--tissue repair is not dependent on inflammatory cells. Curr Biol *13*, 1122-1128.

Martinez, F.O., Helming, L., and Gordon, S. (2009). Alternative activation of macrophages: an immunologic functional perspective. Annu Rev Immunol *27*, 451-483.

Matsumoto, K., Yoshitomi, H., Rossant, J., and Zaret, K.S. (2001). Liver organogenesis promoted by endothelial cells prior to vascular function. Science *294*, 559-563.

Matsushita, N., Sogawa, K., Ema, M., Yoshida, A., and Fujii-Kuriyama, Y. (1993). A factor binding to the xenobiotic responsive element (XRE) of P-4501A1 gene consists of at least two helix-loop-helix proteins, Ah receptor and Arnt. J Biol Chem *268*, 21002-21006.

Matthews, V.B., Klinken, E., and Yeoh, G.C. (2004). Direct effects of interleukin-6 on liver progenitor oval cells in culture. Wound Repair Regen *12*, 650-656.

Matthews, V.B., Knight, B., Tirnitz-Parker, J.E., Boon, J., Olynyk, J.K., and Yeoh, G.C. (2005). Oncostatin M induces an acute phase response but does not modulate the growth or maturation-status of liver progenitor (oval) cells in culture. Exp Cell Res *306*, 252-263.

Mavier, P., Martin, N., Couchie, D., Preaux, A.M., Laperche, Y., and Zafrani, E.S. (2004). Expression of stromal cell-derived factor-1 and of its receptor CXCR4 in liver regeneration from oval cells in rat. Am J Pathol *165*, 1969-1977.

Mayack, S.R., Shadrach, J.L., Kim, F.S., and Wagers, A.J. (2010). Systemic signals regulate ageing and rejuvenation of blood stem cell niches. Nature *463*, 495-500.

McCright, B., Lozier, J., and Gridley, T. (2002). A mouse model of Alagille syndrome: Notch2 as a genetic modifier of Jag1 haploinsufficiency. Development *129*, 1075-1082.

McDaniell, R., Warthen, D.M., Sanchez-Lara, P.A., Pai, A., Krantz, I.D., Piccoli, D.A., and Spinner, N.B. (2006). NOTCH2 mutations cause Alagille syndrome, a heterogeneous disorder of the notch signaling pathway. Am J Hum Genet *79*, 169-173.

Menthena, A., Deb, N., Oertel, M., Grozdanov, P.N., Sandhu, J., Shah, S., Guha, C., Shafritz, D.A., and Dabeva, M.D. (2004). Bone marrow progenitors are not the source of expanding oval cells in injured liver. Stem Cells *22*, 1049-1061.

Metcalf, D., and Gearing, D.P. (1989). A myelosclerotic syndrome in mice engrafted with cells producing high levels of leukemia inhibitory factor (LIF). Leukemia *3*, 847-852.

Michalopoulos, G.K., Barua, L., and Bowen, W.C. (2005). Transdifferentiation of rat hepatocytes into biliary cells after bile duct ligation and toxic biliary injury. Hepatology *41*, 535-544.

Michalopoulos, G.K., Bowen, W.C., Mule, K., and Stolz, D.B. (2001). Histological organization in hepatocyte organoid cultures. Am J Pathol *159*, 1877-1887.

Michalopoulos, G.K., and DeFrances, M.C. (1997). Liver regeneration. Science *276*, 60-66.

Micsenyi, A., Tan, X., Sneddon, T., Luo, J.H., Michalopoulos, G.K., and Monga, S.P. (2004). Beta-catenin is temporally regulated during normal liver development. Gastroenterology *126*, 1134-1146.

Miner, J.H., and Yurchenco, P.D. (2004). Laminin functions in tissue morphogenesis. Annu Rev Cell Dev Biol *20*, 255-284.

Miyata, E., Masuya, M., Yoshida, S., Nakamura, S., Kato, K., Sugimoto, Y., Shibasaki, T., Yamamura, K., Ohishi, K., Nishii, K., *et al*. (2007). Hematopoietic origin of hepatic stellate cells in the adult liver. Blood.

Momand, J., Zambetti, G.P., Olson, D.C., George, D., and Levine, A.J. (1992). The mdm-2 oncogene product forms a complex with the p53 protein and inhibits p53-mediated transactivation. Cell *69*, 1237-1245.

Monga, S.P., Mars, W.M., Pediaditakis, P., Bell, A., Mule, K., Bowen, W.C., Wang, X., Zarnegar, R., and Michalopoulos, G.K. (2002). Hepatocyte growth factor induces Wnt-independent nuclear translocation of beta-catenin after Met-beta-catenin dissociation in hepatocytes. Cancer Res *62*, 2064-2071.

Monga, S.P., Monga, H.K., Tan, X., Mule, K., Pediaditakis, P., and Michalopoulos, G.K. (2003). Beta-catenin antisense studies in embryonic liver cultures: role in proliferation, apoptosis, and lineage specification. Gastroenterology *124*, 202-216.

Monkkonen, J., Taskinen, M., Auriola, S.O., and Urtti, A. (1994). Growth inhibition of macrophage-like and other cell types by liposome-encapsulated, calcium-bound, and free bisphosphonates *in vitro*. J Drug Target *2*, 299-308.

Montes de Oca Luna, R., Wagner, D.S., and Lozano, G. (1995). Rescue of early embryonic lethality in mdm2-deficient mice by deletion of p53. Nature *378*, 203-206.

Muller, M., Morotti, A., and Ponzetto, C. (2002). Activation of NF-kappaB is essential for hepatocyte growth factor-mediated proliferation and tubulogenesis. Mol Cell Biol *22*, 1060-1072.

Myung, S.J., Yoon, J.H., Gwak, G.Y., Kim, W., Lee, J.H., Kim, K.M., Shin, C.S., Jang, J.J., Lee, S.H., Lee, S.M., *et al.* (2007). Wnt signaling enhances the activation and survival of human hepatic stellate cells. FEBS Lett *581*, 2954-2958.

Nagato, M., Heike, T., Kato, T., Yamanaka, Y., Yoshimoto, M., Shimazaki, T., Okano, H., and Nakahata, T. (2005). Prospective characterization of neural stem cells by flow cytometry analysis using a combination of surface markers. J Neurosci Res *80*, 456-466.

Nagy, P., Bisgaard, H.C., Santoni-Rugiu, E., and Thorgeirsson, S.S. (1996). *In vivo* infusion of growth factors enhances the mitogenic response of rat hepatic ductal (oval) cells after administration of 2-acetylaminofluorene. Hepatology *23*, 71-79.

Nagy, P., Kiss, A., Schnur, J., and Thorgeirsson, S.S. (1998). Dexamethasone inhibits the proliferation of hepatocytes and oval cells but not bile duct cells in rat liver. Hepatology *28*, 423-429.

Naito, M., Hasegawa, G., Ebe, Y., and Yamamoto, T. (2004). Differentiation and function of Kupffer cells. Med Electron Microsc *37*, 16-28.

Nakayama, M., Kayagaki, N., Yamaguchi, N., Okumura, K., and Yagita, H. (2000). Involvement of TWEAK in interferon gamma-stimulated monocyte cytotoxicity. J Exp Med *192*, 1373-1380.

Naugler, W.E., Sakurai, T., Kim, S., Maeda, S., Kim, K., Elsharkawy, A.M., and Karin, M. (2007). Gender disparity in liver cancer due to sex differences in MyD88-dependent IL-6 production. Science *317*, 121-124.

Nejak-Bowen, K., and Monga, S.P. (2008). Wnt/beta-catenin signaling in hepatic organogenesis. Organogenesis *4*, 92-99.

Nguyen, L.N., Furuya, M.H., Wolfraim, L.A., Nguyen, A.P., Holdren, M.S., Campbell, J.S., Knight, B., Yeoh, G.C., Fausto, N., and Parks, W.T. (2007). Transforming growth factor-beta differentially regulates oval cell and hepatocyte proliferation. Hepatology *45*, 31-41.

Nishioka, T., Kuroishi, T., Sugawara, Y., Yu, Z., Sasano, T., Endo, Y., and Sugawara, S. (2007). Induction of serum IL-18 with Propionibacterium acnes and lipopolysaccharide in phagocytic macrophage-inactivated mice. J Leukoc Biol *82*, 327-334.

Nusse, R. (2005). Wnt signaling in disease and in development. Cell Res *15*, 28-32.

Oakley, F., Mann, J., Ruddell, R.G., Pickford, J., Weinmaster, G., and Mann, D.A. (2003). Basal expression of IkappaBalpha is controlled by the mammalian transcriptional repressor RBP-J (CBF1) and its activator Notch1. J Biol Chem *278*, 24359-24370.

Oben, J.A., Roskams, T., Yang, S., Lin, H., Sinelli, N., Li, Z., Torbenson, M., Huang, J., Guarino, P., Kafrouni, M., *et al.* (2003). Sympathetic nervous system inhibition increases hepatic progenitors and reduces liver injury. Hepatology *38*, 664-673.

Ober, E.A., Verkade, H., Field, H.A., and Stainier, D.Y. (2006). Mesodermal Wnt2b signalling positively regulates liver specification. Nature *442*, 688-691.

Ochsner, S.A., Strick-Marchand, H., Qiu, Q., Venable, S., Dean, A., Wilde, M., Weiss, M.C., and Darlington, G.J. (2007). Transcriptional profiling of bipotential embryonic liver cells to identify liver progenitor cell surface markers. Stem Cells *25*, 2476-2487.

Oertel, M., Menthena, A., Chen, Y.Q., Teisner, B., Jensen, C.H., and Shafritz, D.A. (2008). Purification of fetal liver stem/progenitor cells containing all the repopulation potential for normal adult rat liver. Gastroenterology *134*, 823-832.

Oh, S.H., Witek, R.P., Bae, S.H., Zheng, D., Jung, Y., Piscaglia, A.C., and Petersen, B.E. (2007). Bone marrow-derived hepatic oval cells differentiate into hepatocytes in 2-acetylaminofluorene/partial hepatectomy-induced liver regeneration. Gastroenterology *132*, 1077-1087.

Ohlstein, B., Kai, T., Decotto, E., and Spradling, A. (2004). The stem cell niche: theme and variations. Curr Opin Cell Biol *16*, 693-699.

Oikawa, T., Kamiya, A., Kakinuma, S., Zeniya, M., Nishinakamura, R., Tajiri, H., and Nakauchi, H. (2009). Sall4 regulates cell fate decision in fetal hepatic stem/progenitor cells. Gastroenterology *136*, 1000-1011.

Oinonen, T., and Lindros, K.O. (1998). Zonation of hepatic cytochrome P-450 expression and regulation. Biochem J *329 (Pt 1)*, 17-35.

Okabe, M., Tsukahara, Y., Tanaka, M., Suzuki, K., Saito, S., Kamiya, Y., Tsujimura, T., Nakamura, K., and Miyajima, A. (2009). Potential hepatic stem cells reside in EpCAM+ cells of normal and injured mouse liver. Development *136*, 1951-1960.

Olynyk, J.K., Yeoh, G.C., Ramm, G.A., Clarke, S.L., Hall, P.M., Britton, R.S., Bacon, B.R., and Tracy, T.F. (1998). Gadolinium chloride suppresses hepatic oval cell proliferation in rats with biliary obstruction. Am J Pathol *152*, 347-352.

Omori, N., Evarts, R.P., Omori, M., Hu, Z., Marsden, E.R., and Thorgeirsson, S.S. (1996). Expression of leukemia inhibitory factor and its receptor during liver regeneration in the adult rat. Lab Invest *75*, 15-24.

Overturf, K., Al-Dhalimy, M., Finegold, M., and Grompe, M. (1999). The repopulation potential of hepatocyte populations differing in size and prior mitotic expansion. Am J Pathol *155*, 2135-2143.

Overturf, K., al-Dhalimy, M., Ou, C.N., Finegold, M., and Grompe, M. (1997). Serial transplantation reveals the stem-cell-like regenerative potential of adult mouse hepatocytes. Am J Pathol *151*, 1273-1280.

Ozturk, M., Arslan-Ergul, A., Bagislar, S., Senturk, S., and Yuzugullu, H. (2009). Senescence and immortality in hepatocellular carcinoma. Cancer Lett *286*, 103-113.

Paku, S., Dezso, K., Kopper, L., and Nagy, P. (2005). Immunohistochemical analysis of cytokeratin 7 expression in resting and proliferating biliary structures of rat liver. Hepatology *42*, 863-870.

Paku, S., Schnur, J., Nagy, P., and Thorgeirsson, S.S. (2001). Origin and structural evolution of the early proliferating oval cells in rat liver. Am J Pathol *158*, 1313-1323.

Paradis, K., Blazar, B., and Sharp, H.L. (1989). Rapid repopulation and maturation of Kupffer cells from the bone marrow in a murine bone marrow transplant model. . In Cells of the Hepatic Sinusoid, E. Wisse, ed., pp. 410–412.

Paradis, V., Youssef, N., Dargere, D., Ba, N., Bonvoust, F., Deschatrette, J., and Bedossa, P. (2001). Replicative senescence in normal liver, chronic hepatitis C, and hepatocellular carcinomas. Hum Pathol *32*, 327-332.

Park, D.Y., and Suh, K.S. (1999). Transforming growth factor-beta1 protein, proliferation and apoptosis of oval cells in acetylaminofluorene-induced rat liver regeneration. J Korean Med Sci *14*, 531-538.

Pearson, A.E., and Phelps, T.A. (1981). Radiation effects on mouse incisor teeth following whole-body doses of up to 16 gray. Int J Radiat Biol Relat Stud Phys Chem Med *39*, 409-417.

Pellegrini, L. (2001). Role of heparan sulfate in fibroblast growth factor signalling: a structural view. Curr Opin Struct Biol *11*, 629-634.

Pereira, C.P., Bachli, E.B., and Schoedon, G. (2009). The wnt pathway: a macrophage effector molecule that triggers inflammation. Curr Atheroscler Rep *11*, 236-242.

Petersen, B.E., Bowen, W.C., Patrene, K.D., Mars, W.M., Sullivan, A.K., Murase, N., Boggs, S.S., Greenberger, J.S., and Goff, J.P. (1999). Bone marrow as a potential source of hepatic oval cells. Science *284*, 1168-1170.

Petersen, B.E., Grossbard, B., Hatch, H., Pi, L., Deng, J., and Scott, E.W. (2003). Mouse A6-positive hepatic oval cells also express several hematopoietic stem cell markers. Hepatology *37*, 632-640.

Pi, L., Oh, S.H., Shupe, T., and Petersen, B.E. (2005). Role of connective tissue growth factor in oval cell response during liver regeneration after 2-AAF/PHx in rats. Gastroenterology *128*, 2077-2088.

Pintilie, D.G., Shupe, T.D., Oh, S.H., Salganik, S.V., Darwiche, H., and Petersen, B.E. (2010). Hepatic stellate cells' involvement in progenitor-mediated liver regeneration. Lab Invest *90*, 1199-1208.

Plum, W., Tschaharganeh, D.F., Kroy, D.C., Corsten, E., Erschfeld, S., Dierssen, U., Wasmuth, H., Trautwein, C., and Streetz, K.L. (2010). Lack of glycoprotein 130/signal transducer and activator of transcription 3-mediated signaling in hepatocytes enhances chronic liver injury and fibrosis progression in a model of sclerosing cholangitis. Am J Pathol *176*, 2236-2246.

Plumpe, J., Malek, N.P., Bock, C.T., Rakemann, T., Manns, M.P., and Trautwein, C. (2000). NF-kappaB determines between apoptosis and proliferation in hepatocytes during liver regeneration. Am J Physiol Gastrointest Liver Physiol *278*, G173-183.

Porretti, L., Cattaneo, A., Colombo, F., Lopa, R., Rossi, G., Mazzaferro, V., Battiston, C., Svegliati-Baroni, G., Bertolini, F., Rebulla, P., *et al.* (2010). Simultaneous characterization of progenitor cell compartments in adult human liver. Cytometry A *77*, 31-40.

Pownall, M.E., Tucker, A.S., Slack, J.M., and Isaacs, H.V. (1996). eFGF, Xcad3 and Hox genes form a molecular pathway that establishes the anteroposterior axis in Xenopus. Development *122*, 3881-3892.

Preisegger, K.H., Factor, V.M., Fuchsbichler, A., Stumptner, C., Denk, H., and Thorgeirsson, S.S. (1999). Atypical ductular proliferation and its inhibition by transforming growth factor beta1 in the 3,5-diethoxycarbonyl-1,4-dihydrocollidine mouse model for chronic alcoholic liver disease. Lab Invest *79*, 103-109.

Pritchard, M.T., and Nagy, L.E. (2010). Hepatic fibrosis is enhanced and accompanied by robust oval cell activation after chronic carbon tetrachloride administration to Egr-1-deficient mice. Am J Pathol *176*, 2743-2752.

Pull, S.L., Doherty, J.M., Mills, J.C., Gordon, J.I., and Stappenbeck, T.S. (2005). Activated macrophages are an adaptive element of the colonic epithelial progenitor niche necessary for regenerative responses to injury. Proc Natl Acad Sci U S A *102*, 99-104.

Qin, X., Zhang, H., Zhou, X., Wang, C., Zhang, H., Zhang, X., and Ye, L. (2007). Proliferation and migration mediated by Dkk-1/Wnt/beta-catenin cascade in a model of hepatocellular carcinoma cells. Transl Res *150*, 281-294.

Reed, K.R., Athineos, D., Meniel, V.S., Wilkins, J.A., Ridgway, R.A., Burke, Z.D., Muncan, V., Clarke, A.R., and Sansom, O.J. (2008). B-catenin deficiency, but not Myc deletion, suppresses the immediate phenotypes of APC loss in the liver. Proc Natl Acad Sci U S A *105*, 18919-18923.

Rhim, J.A., Sandgren, E.P., Degen, J.L., Palmiter, R.D., and Brinster, R.L. (1994). Replacement of diseased mouse liver by hepatic cell transplantation. Science *263*, 1149-1152.

Rijsewijk, F., Schuermann, M., Wagenaar, E., Parren, P., Weigel, D., and Nusse, R. (1987). The Drosophila homolog of the mouse mammary oncogene int-1 is identical to the segment polarity gene wingless. Cell *50*, 649-657.

Rivera, C.A., Adegboyega, P., van Rooijen, N., Tagalicud, A., Allman, M., and Wallace, M. (2007). Toll-like receptor-4 signaling and Kupffer cells play pivotal roles in the pathogenesis of non-alcoholic steatohepatitis. J Hepatol *47*, 571-579.

Rock, J.R., Onaitis, M.W., Rawlins, E.L., Lu, Y., Clark, C.P., Xue, Y., Randell, S.H., and Hogan, B.L. (2009). Basal cells as stem cells of the mouse trachea and human airway epithelium. Proc Natl Acad Sci U S A *106*, 12771-12775.

Rosenberg, D., Ilic, Z., Yin, L., and Sell, S. (2000). Proliferation of hepatic lineage cells of normal C57BL and interleukin-6 knockout mice after cocaine-induced periportal injury. Hepatology *31*, 948-955.

Roskams, T. (2003). Progenitor cell involvement in cirrhotic human liver diseases: from controversy to consensus. J Hepatol *39*, 431-434.

Roskams, T. (2006). Liver stem cells and their implication in hepatocellular and cholangiocarcinoma. Oncogene *25*, 3818-3822.

Roskams, T., De Vos, R., van den Oord, J.J., and Desmet, V. (1991). Cells with neuroendocrine features in regenerating human liver. APMIS Suppl *23*, 32-39.

Roskams, T., Yang, S.Q., Koteish, A., Durnez, A., DeVos, R., Huang, X., Achten, R., Verslype, C., and Diehl, A.M. (2003a). Oxidative stress and oval cell accumulation in mice and humans with alcoholic and nonalcoholic fatty liver disease. Am J Pathol *163*, 1301-1311.

Roskams, T.A., Libbrecht, L., and Desmet, V.J. (2003b). Progenitor cells in diseased human liver. Semin Liver Dis *23*, 385-396.

Rountree, C.B., Barsky, L., Ge, S., Zhu, J., Senadheera, S., and Crooks, G.M. (2007). A CD133-expressing murine liver oval cell population with bilineage potential. Stem Cells *25*, 2419-2429.

Ruffell, D., Mourkioti, F., Gambardella, R., Kirstetter, F., Lopez, R. G., Rosenthal, N., and Nerlov, C. (2009). A CREB-C/EBP cascade induces M2 macrophagespecific gene expression and promotes muscle injury repair. Am J Path 106, 17475–17480

Russo, F.P., Alison, M.R., Bigger, B.W., Amofah, E., Florou, A., Amin, F., Bou-Gharios, G., Jeffery, R., Iredale, J.P., and Forbes, S.J. (2006). The bone marrow functionally contributes to liver fibrosis. Gastroenterology *130*, 1807-1821.

Sackett, S.D., Li, Z., Hurtt, R., Gao, Y., Wells, R.G., Brondell, K., Kaestner, K.H., and Greenbaum, L.E. (2009). Foxl1 is a marker of bipotential hepatic progenitor cells in mice. Hepatology *49*, 920-929.

Sanchez, A., Alvarez, A.M., Pagan, R., Roncero, C., Vilaro, S., Benito, M., and Fabregat, I. (2000). Fibronectin regulates morphology, cell organization and gene expression of rat fetal hepatocytes in primary culture. J Hepatol *32*, 242-250.

Sanchez, A., Factor, V.M., Schroeder, I.S., Nagy, P., and Thorgeirsson, S.S. (2004). Activation of NF-kappaB and STAT3 in rat oval cells during 2-acetylaminofluorene/partial hepatectomy-induced liver regeneration. Hepatology *39*, 376-385.

Santoni-Rugiu, E., Jelnes, P., Thorgeirsson, S.S., and Bisgaard, H.C. (2005). Progenitor cells in liver regeneration: molecular responses controlling their activation and expansion. Apmis *113*, 876-902.

Sato, T., Vries, R.G., Snippert, H.J., van de Wetering, M., Barker, N., Stange, D.E., van Es, J.H., Abo, A., Kujala, P., Peters, P.J., *et al.* (2009). Single Lgr5 stem cells build crypt-villus structures *in vitro* without a mesenchymal niche. Nature *459*, 262-265.

Sawitza, I., Kordes, C., Reister, S., and Haussinger, D. (2009). The niche of stellate cells within rat liver. Hepatology *50*, 1617-1624.

Saxena, R., Theise, N.D., and Crawford, J.M. (1999). Microanatomy of the human liver-exploring the hidden interfaces. Hepatology *30*, 1339-1346.

Schaller, E., Macfarlane, A.J., Rupec, R.A., Gordon, S., McKnight, A.J., and Pfeffer, K. (2002). Inactivation of the F4/80 glycoprotein in the mouse germ line. Mol Cell Biol *22*, 8035-8043.

Schlotzer-Schrehardt, U., Dietrich, T., Saito, K., Sorokin, L., Sasaki, T., Paulsson, M., and Kruse, F.E. (2007). Characterization of extracellular matrix components in the limbal epithelial stem cell compartment. Exp Eye Res *85*, 845-860.

Schmelzer, E., Zhang, L., Bruce, A., Wauthier, E., Ludlow, J., Yao, H.L., Moss, N., Melhem, A., McClelland, R., Turner, W., *et al.* (2007). Human hepatic stem cells from fetal and postnatal donors. J Exp Med *204*, 1973-1987.

Schwartz, R.E., Reyes, M., Koodie, L., Jiang, Y., Blackstad, M., Lund, T., Lenvik, T., Johnson, S., Hu, W.S., and Verfaillie, C.M. (2002). Multipotent adult progenitor cells from bone marrow differentiate into functional hepatocyte-like cells. J Clin Invest *109*, 1291-1302.

Sekine, S., Gutierrez, P.J., Lan, B.Y., Feng, S., and Hebrok, M. (2007). Liver-specific loss of beta-catenin results in delayed hepatocyte proliferation after partial hepatectomy. Hepatology *45*, 361-368.

Sekine, S., Lan, B.Y., Bedolli, M., Feng, S., and Hebrok, M. (2006). Liver-specific loss of beta-catenin blocks glutamine synthesis pathway activity and cytochrome p450 expression in mice. Hepatology *43*, 817-825.

Seno, H., Miyoshi, H., Brown, S.L., Geske, M.J., Colonna, M., and Stappenbeck, T.S. (2009). Efficient colonic mucosal wound repair requires Trem2 signaling. Proc Natl Acad Sci U S A *106*, 256-261.

Shay, J.W., Pereira-Smith, O.M., and Wright, W.E. (1991). A role for both RB and p53 in the regulation of human cellular senescence. Exp Cell Res *196*, 33-39.

Shen, Q., Wang, Y., Kokovay, E., Lin, G., Chuang, S.M., Goderie, S.K., Roysam, B., and Temple, S. (2008). Adult SVZ stem cells lie in a vascular niche: a quantitative analysis of niche cell-cell interactions. Cell Stem Cell *3*, 289-300.

Shinozuka, H., Lombardi, B., Sell, S., and Iammarino, R.M. (1978). Early histological and functional alterations of ethionine liver carcinogenesis in rats fed a choline-deficient diet. Cancer Res *38*, 1092-1098.

Shiota, G., Okano, J., Kawasaki, H., Kawamoto, T., and Nakamura, T. (1995). Serum hepatocyte growth factor levels in liver diseases: clinical implications. Hepatology *21*, 106-112.

Shmelkov, S.V., Butler, J.M., Hooper, A.T., Hormigo, A., Kushner, J., Milde, T., St Clair, R., Baljevic, M., White, I., Jin, D.K., *et al.* (2008). CD133 expression is not restricted to stem cells, and both CD133+ and CD133- metastatic colon cancer cells initiate tumors. J Clin Invest *118*, 2111-2120.

Shmelkov, S.V., St Clair, R., Lyden, D., and Rafii, S. (2005). AC133/CD133/Prominin-1. Int J Biochem Cell Biol *37*, 715-719.

Si-Tayeb, K., Noto, F.K., Nagaoka, M., Li, J., Battle, M.A., Duris, C., North, P.E., Dalton, S., and Duncan, S.A. (2010). Highly efficient generation of human hepatocyte-like cells from induced pluripotent stem cells. Hepatology *51*, 297-305.

Si, Y., Tsou, C.L., Croft, K., and Charo, I.F. (2010). CCR2 mediates hematopoietic stem and progenitor cell trafficking to sites of inflammation in mice. J Clin Invest *120*, 1192-1203.

Sicklick, J.K., Li, Y.X., Melhem, A., Schmelzer, E., Zdanowicz, M., Huang, J., Caballero, M., Fair, J.H., Ludlow, J.W., McClelland, R.E., *et al.* (2006). Hedgehog signaling maintains resident hepatic progenitors throughout life. Am J Physiol Gastrointest Liver Physiol *290*, G859-870.

Sodhi, D., Micsenyi, A., Bowen, W.C., Monga, D.K., Talavera, J.C., and Monga, S.P. (2005). Morpholino oligonucleotide-triggered beta-catenin knockdown compromises normal liver regeneration. J Hepatol *43*, 132-141.

Song, H., Mak, K.K., Topol, L., Yun, K., Hu, J., Garrett, L., Chen, Y., Park, O., Chang, J., Simpson, R.M., *et al.* (2010). Mammalian Mst1 and Mst2 kinases play essential roles in organ size control and tumor suppression. Proc Natl Acad Sci U S A *107*, 1431-1436.

Spahr, L., Lambert, J.F., Rubbia-Brandt, L., Chalandon, Y., Frossard, J.L., Giostra, E., and Hadengue, A. (2008). Granulocyte-colony stimulating factor induces proliferation of hepatic progenitors in alcoholic steatohepatitis: a randomized trial. Hepatology *48*, 221-229.

Spradling, A., Drummond-Barbosa, D., and Kai, T. (2001). Stem cells find their niche. Nature *414*, 98-104.

Srinivas, S., Watanabe, T., Lin, C.S., William, C.M., Tanabe, Y., Jessell, T.M., and Costantini, F. (2001). Cre reporter strains produced by targeted insertion of EYFP and ECFP into the ROSA26 locus. BMC Dev Biol *1*, 4.

Staal, F.J., Luis, T.C., and Tiemessen, M.M. (2008). WNT signalling in the immune system: WNT is spreading its wings. Nat Rev Immunol *8*, 581-593.

Stanulovic, V.S., Kyrmizi, I., Kruithof-de Julio, M., Hoogenkamp, M., Vermeulen, J.L., Ruijter, J.M., Talianidis, I., Hakvoort, T.B., and Lamers, W.H. (2007). Hepatic HNF4alpha deficiency induces periportal expression of glutamine synthetase and other pericentral enzymes. Hepatology *45*, 433-444.

Stappenbeck, T.S., and Miyoshi, H. (2009). The role of stromal stem cells in tissue regeneration and wound repair. Science *324*, 1666-1669.

Streetz, K.L., Tacke, F., Leifeld, L., Wustefeld, T., Graw, A., Klein, C., Kamino, K., Spengler, U., Kreipe, H., Kubicka, S., *et al*. (2003). Interleukin 6/gp130-dependent pathways are protective during chronic liver diseases. Hepatology *38*, 218-229.

Strick-Marchand, H., Masse, G.X., Weiss, M.C., and Di Santo, J.P. (2008). Lymphocytes support oval cell-dependent liver regeneration. J Immunol *181*, 2764-2771.

Sturm, E., Havinga, R., Baller, J.F., Wolters, H., van Rooijen, N., Kamps, J.A., Verkade, H.J., Karpen, S.J., and Kuipers, F. (2005). Kupffer cell depletion with liposomal clodronate prevents suppression of Ntcp expression in endotoxin-treated rats. J Hepatol *42*, 102-109.

Subrata, L.S., Lowes, K.N., Olynyk, J.K., Yeoh, G.C., Quail, E.A., and Abraham, L.J. (2005). Hepatic expression of the tumor necrosis factor family member lymphotoxin-beta is regulated by interleukin (IL)-6 and IL-1beta: transcriptional control mechanisms in oval cells and hepatoma cell lines. Liver Int *25*, 633-646.

Sullivan, G.J., Hay, D.C., Park, I.H., Fletcher, J., Hannoun, Z., Payne, C.M., Dalgetty, D., Black, J.R., Ross, J.A., Samuel, K., *et al.* (2010). Generation of functional human hepatic endoderm from human induced pluripotent stem cells. Hepatology *51*, 329-335.

Sun, Z., Zhang, X., Locke, J.E., Zheng, Q., Tachibana, S., Diehl, A.M., and Williams, G.M. (2009). Recruitment of host progenitor cells in rat liver transplants. Hepatology *49*, 587-597.

Suzuki, A., Iwama, A., Miyashita, H., Nakauchi, H., and Taniguchi, H. (2003). Role for growth factors and extracellular matrix in controlling differentiation of prospectively isolated hepatic stem cells. Development *130*, 2513-2524.

Suzuki, A., Sekiya, S., Onishi, M., Oshima, N., Kiyonari, H., Nakauchi, H., and Taniguchi, H. (2008). Flow cytometric isolation and clonal identification of self-renewing bipotent hepatic progenitor cells in adult mouse liver. Hepatology *48*, 1964-1978.

Takayama, H., La Rochelle, W.J., Anver, M., Bockman, D.E., and Merlino, G. (1996). Scatter factor/hepatocyte growth factor as a regulator of skeletal muscle and neural crest development. Proc Natl Acad Sci U S A *93*, 5866-5871.

Takeishi, T., Hirano, K., Kobayashi, T., Hasegawa, G., Hatakeyama, K., and Naito, M. (1999). The role of Kupffer cells in liver regeneration. Arch Histol Cytol *62*, 413-422.

Tan, X., Apte, U., Micsenyi, A., Kotsagrelos, E., Luo, J.H., Ranganathan, S., Monga, D.K., Bell, A., Michalopoulos, G.K., and Monga, S.P. (2005). Epidermal growth factor receptor: a novel target of the Wnt/beta-catenin pathway in liver. Gastroenterology *129*, 285-302.

Tanimizu, N., Nishikawa, M., Saito, H., Tsujimura, T., and Miyajima, A. (2003). Isolation of hepatoblasts based on the expression of Dlk/Pref-1. J Cell Sci *116*, 1775-1786.

Tanimizu, N., Tsujimura, T., Takahide, K., Kodama, T., Nakamura, K., and Miyajima, A. (2004). Expression of Dlk/Pref-1 defines a subpopulation in the oval cell compartment of rat liver. Gene Expr Patterns *5*, 209-218.

Taoudi, S., Gonneau, C., Moore, K., Sheridan, J.M., Blackburn, C.C., Taylor, E., and Medvinsky, A. (2008). Extensive hematopoietic stem cell generation in the AGM region via maturation of VE-cadherin+CD45+ pre-definitive HSCs. Cell Stem Cell *3*, 99-108.

Tate, M.C., Garcia, A.J., Keselowsky, B.G., Schumm, M.A., Archer, D.R., and LaPlaca, M.C. (2004). Specific beta1 integrins mediate adhesion, migration, and differentiation of neural progenitors derived from the embryonic striatum. Mol Cell Neurosci *27*, 22-31.

Tee, L.B., Kirilak, Y., Huang, W.H., Smith, P.G., Morgan, R.H., and Yeoh, G.C. (1996). Dual phenotypic expression of hepatocytes and bile ductular markers in developing and preneoplastic rat liver. Carcinogenesis *17*, 251-259.

Teoh, N., Pyakurel, P., Dan, Y.Y., Swisshelm, K., Hou, J., Mitchell, C., Fausto, N., Gu, Y., and Farrell, G. (2010). Induction of p53 Renders ATM-Deficient Mice Refractory to Hepatocarcinogenesis. Gastroenterology *138*, 1155-1165 e1152.

Terada, R., Yamamoto, K., Hakoda, T., Shimada, N., Okano, N., Baba, N., Ninomiya, Y., Gershwin, M.E., and Shiratori, Y. (2003). Stromal cell-derived factor-1 from biliary epithelial cells recruits CXCR4-positive cells: implications for inflammatory liver diseases. Lab Invest *83*, 665-672.

Terai, S., Ishikawa, T., Omori, K., Aoyama, K., Marumoto, Y., Urata, Y., Yokoyama, Y., Uchida, K., Yamasaki, T., Fujii, Y., *et al.* (2006). Improved liver function in patients with liver cirrhosis after autologous bone marrow cell infusion therapy. Stem Cells *24*, 2292-2298.

Terai, S., Sakaida, I., Nishina, H., and Okita, K. (2005). Lesson from the GFP/CCl4 model--translational research project: the development of cell therapy using autologous bone marrow cells in patients with liver cirrhosis. J Hepatobiliary Pancreat Surg *12*, 203-207.

Theise, N.D., Nimmakayalu, M., Gardner, R., Illei, P.B., Morgan, G., Teperman, L., Henegariu, O., and Krause, D.S. (2000). Liver from bone marrow in humans. Hepatology *32*, 11-16.

Theise, N.D., Saxena, R., Portmann, B.C., Thung, S.N., Yee, H., Chiriboga, L., Kumar, A., and Crawford, J.M. (1999). The canals of Hering and hepatic stem cells in humans. Hepatology *30*, 1425-1433.

Theocharis, S.E., Margeli, A.P., Skaltsas, S.D., Skopelitou, A.S., Mykoniatis, M.G., and Kittas, C.N. (1997). Effect of interferon-alpha2b administration on rat liver regeneration after partial hepatectomy. Dig Dis Sci *42*, 1981-1986.

Thorgeirsson, S.S., and Grisham, J.W. (2006). Hematopoietic cells as hepatocyte stem cells: a critical review of the evidence. Hepatology *43*, 2-8.

Tilg, H., Wilmer, A., Vogel, W., Herold, M., Nolchen, B., Judmaier, G., and Huber, C. (1992). Serum levels of cytokines in chronic liver diseases. Gastroenterology *103*, 264-274.

Timchenko, N.A., Wilde, M., Kosai, K.I., Heydari, A., Bilyeu, T.A., Finegold, M.J., Mohamedali, K., Richardson, A., and Darlington, G.J. (1998). Regenerating livers of old rats contain high levels of C/EBPalpha that correlate with altered expression of cell cycle associated proteins. Nucleic Acids Res *26*, 3293-3299.

Tirnitz-Parker, J.E., Tonkin, J.N., Knight, B., Olynyk, J.K., and Yeoh, G.C. (2007). Isolation, culture and immortalisation of hepatic oval cells from adult mice fed a choline-deficient, ethionine-supplemented diet. Int J Biochem Cell Biol *39*, 2226-2239.

Tirnitz-Parker, J.E., Viebahn, C.S., Jakubowski, A., Klopcic, B.R., Olynyk, J.K., Yeoh, G.C., and Knight, B. (2010). Tumor necrosis factor-like weak inducer of apoptosis is a mitogen for liver progenitor cells. Hepatology *52*, 291-302.

Tonkin, J.N., Knight, B., Curtis, D., Abraham, L.J., and Yeoh, G.C. (2008). Bone marrow cells play only a very minor role in chronic liver regeneration induced by a choline-deficient, ethionine-supplemented diet. Stem Cell Res *1*, 195-204.

Toyonaga, T., Hino, O., Sugai, S., Wakasugi, S., Abe, K., Shichiri, M., and Yamamura, K. (1994). Chronic active hepatitis in transgenic mice expressing interferon-gamma in the liver. Proc Natl Acad Sci U S A *91*, 614-618.

Tsamandas, A.C., Syrokosta, I., Thomopoulos, K., Zolota, V., Dimitropoulou, D., Liava, A., Coupoulou, A.A., Siagris, D., Petsas, T., Karatza, C., *et al.* (2006). Potential role of hepatic progenitor cells expression in cases of chronic hepatitis C and their relation to response to therapy: a clinicopathologic study. Liver Int *26*, 817-826.

Tsuchiya, A., Heike, T., Fujino, H., Shiota, M., Umeda, K., Yoshimoto, M., Matsuda, Y., Ichida, T., Aoyagi, Y., and Nakahata, T. (2005). Long-term extensive expansion of mouse hepatic stem/progenitor cells in a novel serum-free culture system. Gastroenterology *128*, 2089-2104.

Tumanov, A.V., Christiansen, P.A., and Fu, Y.X. (2007). The role of lymphotoxin receptor signaling in diseases. Curr Mol Med *7*, 567-578.

Upton, A.C., Buffett, R.F., Forth, J., and Doherty, D.G. (1956). Radiation Induced "Dental Death" in Mice. Radiation Research *4*, 475-479.

van den Berg, T.K., and Kraal, G. (2005). A function for the macrophage F4/80 molecule in tolerance induction. Trends Immunol *26*, 506-509.

Van Hul, N.K., Abarca-Quinones, J., Sempoux, C., Horsmans, Y., and Leclercq, I.A. (2009). Relation between liver progenitor cell expansion and extracellular matrix deposition in a CDE-induced murine model of chronic liver injury. Hepatology *49*, 1625-1635.

Van Rooijen, N. (1989). The liposome-mediated macrophage 'suicide' technique. J Immunol Methods *124*, 1-6.

Van Rooijen, N., Kors, N., vd Ende, M., and Dijkstra, C.D. (1990). Depletion and repopulation of macrophages in spleen and liver of rat after intravenous treatment with liposome-encapsulated dichloromethylene diphosphonate. Cell Tissue Res *260*, 215-222.

Van Rooijen, N., and Sanders, A. (1996). Kupffer cell depletion by liposome-delivered drugs: comparative activity of intracellular clodronate, propamidine, and ethylenediaminetetraacetic acid. Hepatology *23*, 1239-1243.

van Rooijen, N., Sanders, A., and van den Berg, T.K. (1996). Apoptosis of macrophages induced by liposome-mediated intracellular delivery of clodronate and propamidine. J Immunol Methods *193*, 93-99.

Vassilopoulos, G., Wang, P.R., and Russell, D.W. (2003). Transplanted bone marrow regenerates liver by cell fusion. Nature *422*, 901-904.

Vig, P., Russo, F.P., Edwards, R.J., Tadrous, P.J., Wright, N.A., Thomas, H.C., Alison, M.R., and Forbes, S.J. (2006). The sources of parenchymal regeneration after chronic hepatocellular liver injury in mice. Hepatology *43*, 316-324.

Vivier, I., Marguet, D., Naquet, P., Bonicel, J., Black, D., Li, C.X., Bernard, A.M., Gorvel, J.P., and Pierres, M. (1991). Evidence that thymocyte-activating molecule is mouse CD26 (dipeptidyl peptidase IV). J Immunol *147*, 447-454.

Volpes, R., van den Oord, J.J., and Desmet, V.J. (1991). Distribution of the VLA family of integrins in normal and pathological human liver tissue. Gastroenterology *101*, 200-206.

Volpes, R., van den Oord, J.J., and Desmet, V.J. (1993). Integrins as differential cell lineage markers of primary liver tumors. Am J Pathol *142*, 1483-1492.

von Holzen, U., Pataer, A., Raju, U., Bocangel, D., Vorburger, S.A., Liu, Y., Lu, X., Roth, J.A., Aggarwal, B.B., Barber, G.N., *et al.* (2007). The double-stranded RNA-activated protein kinase mediates radiation resistance in mouse embryo fibroblasts through nuclear factor kappaB and Akt activation. Clin Cancer Res *13*, 6032-6039.

Voog, J., and Jones, D.L. (2010). Stem Cells and the Niche: A Dynamic Duo. Cell Stem Cell *6*, 103-115.

Vousden, K.H., and Lu, X. (2002). Live or let die: the cell's response to p53. Nat Rev Cancer *2*, 594-604.

Wagers, A.J. (2005). Stem cell grand SLAM. Cell *121*, 967-970.

Wands, J. (2007). Hepatocellular carcinoma and sex. N Engl J Med *357*, 1974-1976.

Wang, P., Yu, J., and Zhang, L. (2007). The nuclear function of p53 is required for PUMA-mediated apoptosis induced by DNA damage. Proc Natl Acad Sci U S A *104*, 4054-4059.

Wang, X., Foster, M., Al-Dhalimy, M., Lagasse, E., Finegold, M., and Grompe, M. (2003a). The origin and liver repopulating capacity of murine oval cells. Proc Natl Acad Sci U S A *100 Suppl 1*, 11881-11888.

Wang, X., Kruithof-de Julio, M., Economides, K.D., Walker, D., Yu, H., Halili, M.V., Hu, Y.P., Price, S.M., Abate-Shen, C., and Shen, M.M. (2009). A luminal epithelial stem cell that is a cell of origin for prostate cancer. Nature *461*, 495-500.

Wang, X., Montini, E., Al-Dhalimy, M., Lagasse, E., Finegold, M., and Grompe, M. (2002). Kinetics of liver repopulation after bone marrow transplantation. Am J Pathol *161*, 565-574.

Wang, X., Willenbring, H., Akkari, Y., Torimaru, Y., Foster, M., Al-Dhalimy, M., Lagasse, E., Finegold, M., Olson, S., and Grompe, M. (2003b). Cell fusion is the principal source of bone-marrow-derived hepatocytes. Nature *422*, 897-901.

Warren, L.A., and Rossi, D.J. (2009). Stem cells and aging in the hematopoietic system. Mech Ageing Dev *130*, 46-53.

Wege, H., Muller, A., Muller, L., Petri, S., Petersen, J., and Hillert, C. (2007). Regeneration in pig livers by compensatory hyperplasia induces high levels of telomerase activity. Comp Hepatol *6*, 6.

Wiebusch, L., and Hagemeier, C. (2010). p53- and p21-dependent premature APC/C-Cdh1 activation in G2 is part of the long-term response to genotoxic stress. Oncogene *29*, 3477-3489.

Wiemann, S.U., Satyanarayana, A., Tsahuridu, M., Tillmann, H.L., Zender, L., Klempnauer, J., Flemming, P., Franco, S., Blasco, M.A., Manns, M.P., *et al.* (2002). Hepatocyte telomere shortening and senescence are general markers of human liver cirrhosis. Faseb J *16*, 935-942.

Willenbring, H., Bailey, A.S., Foster, M., Akkari, Y., Dorrell, C., Olson, S., Finegold, M., Fleming, W.H., and Grompe, M. (2004). Myelomonocytic cells are sufficient for therapeutic cell fusion in liver. Nat Med *10*, 744-748.

Williams, J.M., Oh, S.H., Jorgensen, M., Steiger, N., Darwiche, H., Shupe, T., and Petersen, B.E. (2010). The role of the Wnt family of secreted proteins in rat oval "stem" cell-based liver regeneration: Wnt1 drives differentiation. Am J Pathol *176*, 2732-2742.

Winkles, J.A. (2008). The TWEAK-Fn14 cytokine-receptor axis: discovery, biology and therapeutic targeting. Nat Rev Drug Discov *7*, 411-425.

Wong, S., Gauthier, T., Kaita, K.D., and Minuk, G.Y. (1995). The differential effects of three forms of interferon alfa on hepatic regeneration after partial hepatectomy in the rat. Hepatology *22*, 883-886.

Wu, Y., Nan, L., Bardag-Gorce, F., Li, J., French, B.A., Wilson, L.T., Dedes, J., and French, S.W. (2005). The role of laminin-integrin signaling in triggering MB formation. An *in vivo* and *in vitro* study. Exp Mol Pathol *79*, 1-8.

Xue, W., Zender, L., Miething, C., Dickins, R.A., Hernando, E., Krizhanovsky, V., Cordon-Cardo, C., and Lowe, S.W. (2007). Senescence and tumour clearance is triggered by p53 restoration in murine liver carcinomas. Nature *445*, 656-660.

Yamada, Y., Nishimoto, E., Mitsuya, H., and Yonemura, Y. (2006). *In vitro* transdifferentiation of adult bone marrow Sca-1+ cKit- cells cocultured with fetal liver cells into hepatic-like cells without fusion. Exp Hematol *34*, 97-106.

Yamamoto, T., Naito, M., Moriyama, H., Umezu, H., Matsuo, H., Kiwada, H., and Arakawa, M. (1996). Repopulation of murine Kupffer cells after intravenous administration of liposome-encapsulated dichloromethylene diphosphonate. Am J Pathol *149*, 1271-1286.

Yamasaki, H., Sada, A., Iwata, T., Niwa, T., Tomizawa, M., Xanthopoulos, K.G., Koike, T., and Shiojiri, N. (2006). Suppression of C/EBPalpha expression in periportal hepatoblasts may stimulate biliary cell differentiation through increased Hnf6 and Hnf1b expression. Development *133*, 4233-4243.

Yamashita, T., Forgues, M., Wang, W., Kim, J.W., Ye, Q., Jia, H., Budhu, A., Zanetti, K.A., Chen, Y., Qin, L.X., *et al*. (2008). EpCAM and alpha-fetoprotein expression defines novel prognostic subtypes of hepatocellular carcinoma. Cancer Res *68*, 1451-1461.

Yamashita, T., Ji, J., Budhu, A., Forgues, M., Yang, W., Wang, H.Y., Jia, H., Ye, Q., Qin, L.X., Wauthier, E., *et al*. (2009). EpCAM-positive hepatocellular carcinoma cells are tumor-initiating cells with stem/progenitor cell features. Gastroenterology *136*, 1012-1024.

Yamazaki, S., Miki, K., Hasegawa, K., Sata, M., Takayama, T., and Makuuchi, M. (2003). Sera from liver failure patients and a demethylating agent stimulate transdifferentiation of murine bone marrow cells into hepatocytes in coculture with nonparenchymal liver cells. J Hepatol *39*, 17-23.

Yang, L., Jung, Y., Omenetti, A., Witek, R.P., Choi, S., Vandongen, H.M., Huang, J., Alpini, G.D., and Diehl, A.M. (2008). Fate-Mapping Evidence that Hepatic Stellate Cells are Epithelial Progenitors in Adult Mouse Livers. Stem Cells.

Yannaki, E., Anagnostopoulos, A., Kapetanos, D., Xagorari, A., Iordanidis, F., Batsis, I., Kaloyannidis, P., Athanasiou, E., Dourvas, G., Kitis, G., *et al.* (2006). Lasting amelioration in the clinical course of decompensated alcoholic cirrhosis with boost infusions of mobilized peripheral blood stem cells. Exp Hematol *34*, 1583-1587.

Yannaki, E., Athanasiou, E., Xagorari, A., Constantinou, V., Batsis, I., Kaloyannidis, P., Proya, E., Anagnostopoulos, A., and Fassas, A. (2005). G-CSF-primed hematopoietic stem cells or G-CSF per se accelerate recovery and improve survival after liver injury, predominantly by promoting endogenous repair programs. Exp Hematol *33*, 108-119.

Yasui, O., Miura, N., Terada, K., Kawarada, Y., Koyama, K., and Sugiyama, T. (1997). Isolation of oval cells from Long-Evans Cinnamon rats and their transformation into hepatocytes *in vivo* in the rat liver. Hepatology *25*, 329-334.

Yaswen, P., Hayner, N.T., and Fausto, N. (1984). Isolation of oval cells by centrifugal elutriation and comparison with other cell types purified from normal and preneoplastic livers. Cancer Res *44*, 324-331.

Yeoh, G.C., Ernst, M., Rose-John, S., Akhurst, B., Payne, C., Long, S., Alexander, W., Croker, B., Grail, D., and Matthews, V.B. (2007). Opposing roles of gp130-mediated STAT-3 and ERK-1/ 2 signaling in liver progenitor cell migration and proliferation. Hepatology *45*, 486-494.

Yin, L., Lynch, D., and Sell, S. (1999). Participation of different cell types in the restitutive response of the rat liver to periportal injury induced by allyl alcohol. J Hepatol *31*, 497-507.
Yin, L., Sun, M., Ilic, Z., Leffert, H.L., and Sell, S. (2002). Derivation, characterization, and phenotypic variation of hepatic progenitor cell lines isolated from adult rats. Hepatology *35*, 315-324.

Yovchev, M.I., Zhang, J., Neufeld, D.S., Grozdanov, P.N., and Dabeva, M.D. (2009). Thymus cell antigen-1-expressing cells in the oval cell compartment. Hepatology *50*, 601-611.
Yurchenco, P.D., Amenta, P.S., and Patton, B.L. (2004). Basement membrane assembly, stability and activities observed through a developmental lens. Matrix Biol *22*, 521-538.

Zaret, K.S. (2002). Regulatory phases of early liver development: paradigms of organogenesis. Nat Rev Genet *3*, 499-512.

Zeisel, S.H., and Blusztajn, J.K. (1994). Choline and human nutrition. Annu Rev Nutr *14*, 269-296.

Zeng, G., Awan, F., Otruba, W., Muller, P., Apte, U., Tan, X., Gandhi, C., Demetris, A.J., and Monga, S.P. (2007). Wnt'er in liver: expression of Wnt and frizzled genes in mouse. Hepatology *45*, 195-204.

Zhang, W., Chen, X.P., Zhang, W.G., Zhang, F., Xiang, S., Dong, H.H., and Zhang, L. (2009). Hepatic non-parenchymal cells and extracellular matrix participate in oval cell-mediated liver regeneration. World J Gastroenterol *15*, 552-560.

Zheng, D., Oh, S.H., Jung, Y., and Petersen, B.E. (2006). Oval cell response in 2-acetylaminofluorene/partial hepatectomy rat is attenuated by short interfering RNA targeted to stromal cell-derived factor-1. Am J Pathol *169*, 2066-2074.

Zhou, D., Conrad, C., Xia, F., Park, J.S., Payer, B., Yin, Y., Lauwers, G.Y., Thasler, W., Lee, J.T., Avruch, J., *et al*. (2009). Mst1 and Mst2 maintain hepatocyte quiescence and suppress hepatocellular carcinoma development through inactivation of the Yap1 oncogene. Cancer Cell *16*, 425-438.

Znoyko, I., Sohara, N., Spicer, S.S., Trojanowska, M., and Reuben, A. (2005). Expression of oncostatin M and its receptors in normal and cirrhotic human liver. J Hepatol *43*, 893-900.

Appendix 1 Publications arising from this thesis

Bird, T.G., Lorenzini, S., and Forbes, S.J. (2008). Activation of stem cells in hepatic diseases. Cell Tissue Res *331*, 283-300.

Lorenzini, S., Bird, T.G., Boulter, L., Bellamy, C., Samuel, K., Aucott, R., Clayton, E., Andreone, P., Bernardi, M., Golding, M., *et al*. (2010). Characterization of a stereotypical cellular and extracellular adult liver progenitor cell niche in rodents and diseased human liver. Gut *59*, 645-54.

Cell Tissue Res
DOI 10.1007/s00441-007-0542-z

REVIEW

Activation of stem cells in hepatic diseases

T. G. Bird · S. Lorenzini · S. J. Forbes

Received: 1 June 2007 / Accepted: 23 October 2007

Abstract The liver has enormous regenerative capacity. Following acute liver injury, hepatocyte division regenerates the parenchyma but, if this capacity is overwhelmed during massive or chronic liver injury, the intrinsic hepatic progenitor cells (HPCs) termed oval cells are activated. These HPCs are bipotential and can regenerate both biliary epithelia and hepatocytes. Multiple signalling pathways contribute to the complex mechanism controlling the behaviour of the HPCs. These signals are delivered primarily by the surrounding microenvironment. During liver disease, stem cells extrinsic to the liver are activated and bone-marrow-derived cells play a role in the generation of fibrosis during liver injury and its resolution. Here, we review our current understanding of the role of stem cells during liver disease and their mechanisms of activation.

Keywords Liver regeneration · Liver cirrhosis · Oval cells · Stem cells · Bone marrow

Abbreviations

αFP	Alpha-fetoprotein
AAF	2-N-acetylaminofluorene
BDL	Bile duct ligation
BM	Bone marrow
BMSC	Bone marrow stem cell
CCl_4	Carbon tetrachloride
CDE	Choline-deficient ethionine-supplemented
CK	Cytokeratin
CTGF	Connective tissue growth factor
DDC	3,5-Diethoxycarbonlyl-1,4-dihydrocollidine-supplemented
DPPIV	Dipeptidyl peptidase IV
ECM	Extracellular matrix
ERK	Extracellular signal-regulated kinase
EGF	Epidermal growth factor
FAH $^{-/-}$	Fumarylacetoacetate hydrolase knockout
FGF	Fibroblast growth factor
FGFR	FGF receptor
G-CSF	Granulocyte colony-stimulating factor
HGF	Hepatocyte growth factor
HCC	Hepatocellular carcinoma
HPC	Hepatic progenitor cell
IFN	Interferon
IL	Interleukin
JAK	Janus kinase
LIF	Leukaemia inhibitor factor
LIFR	LIF receptor
LT	Lymphotoxin
MMP	Metalloproteinase
OC	Oval cell
OSM	Oncostatin M
OSMR	OSM receptor
PH	Partial hepatectomy
PPAR	Peroxisome-proliferator-activated receptor
SCF	Stem cell factor
SDF-1	Stromal-cell-derived factor 1
SgIGSF	Spermatogenic immunoglobulin superfamily
STAT	Signal transductor and activator of transcription

This work was supported by a Wellcome Trust Clinical Training Fellowship to T.G.B.; S.L. is supported by an EASL Sheila Sherlock Fellowship Post-Doctoral Fellowship.

T. G. Bird (✉) · S. Lorenzini · S. J. Forbes
MRC/University of Edinburgh Centre for Inflammation Research,
The Queen's Medical Research Institute, University of Edinburgh,
47 Little France Crescent,
Edinburgh EH16 4TJ, UK
e-mail: tbird@staffmail.ed.ac.uk

TGF	Transforming growth factor
TNF	Tumour necrosis factor
TWEAK	TNF-like weak induction of apoptosis
uPA	Urokinase-type plasminogen activator

Introduction

Chronic liver disease is common and has severe clinical consequences that arise from the loss of functional hepatocytes and excessive scar formation. Currently, therapies are insufficient to treat these disorders effectively. Great interest has therefore been shown in characterising the regenerative capacity of the liver in order to manipulate this process therapeutically. The liver has an exceptional regenerative capacity that is now appreciated to occur both by replication of differentiated hepatocytes and through activation of the intrahepatic stem cell compartment. Hepatic stem cells are described as facultative as they only participate in hepatocyte replacement when regeneration by mature hepatocytes is overwhelmed or impaired. At present, the consensus is that a bipotential hepatic progenitor cell (HPC) population expands in human liver diseases and a variety of animal models (Roskams et al. 2003b; Santoni-Rugiu et al. 2005). Stem-cell-directed therapy thus offers the hope of improving outcomes during chronic liver disease. Unsurprisingly, interest has more recently turned to delineating the control mechanisms of the HPCs. Together with indigenous hepatic stem cells, stem cells within the bone marrow (BM) are also activated during liver disease and play central roles in inflammation and tissue remodelling. Here, we aim to review critically the evidence for the presence of stem cells within the liver and the mechanisms of their activation, together with the role of extrahepatic stem cells during liver disease.

Somatic stem cells are expected to display certain characteristics: (1) self-renewal, (2) multipotentiality, (3) transplantability and (4) functional long-term tissue reconstitution. Stem cells themselves are required to maintain their undifferentiated state while dividing. Progenitor cells in contrast show a limited ability to self-renew. They comprise distinct subpopulations with variable lineage potential. Moreover, unlike stem cells, progenitor cells divide rapidly but cannot be serially transplanted and hence have been named transit amplifying cells (Shafritz et al. 2006). Activation in the context of stem cells refers to an expansion of cell number by proliferation combined with differentiation towards different lineages. HPCs are thought to be bipotential progenitors capable of forming either hepatocytes or cholangiocytes. In rodents, HPCs have historically been called oval cells (OCs) because of their histological appearance.

HPC characterisation

HPCs are heterogeneous, consisting of a spectrum of cells ranging from an immature phenotype to mature cholangiocytes and intermediate hepatocytes. Although markers for the most immature progenitor cells have not been identified, there are currently a variety of established markers for constituents of the HPC compartment (Table 1). Many HPC markers are expressed by mature cholangiocytes and hepatocytes and by embryonic bipotential hepatoblasts. No universal HPC marker, specific to this compartment, has been identified to date. This is likely to be a feature of the progressive differentiation of HPCs during which they vary

Table 1 Adult HPC markers with representative references

Oval cell marker and abbreviations	References
Adult biliary marker	
Cytokeratin 19 (CK19)	Bisgaard et al. 1993
CK7	Paku et al. 2005
CK14	Bisgaard et al. 1993
γ-Glutamyl transpeptidase (γGT)	Cameron et al. 1978
Glutathione-S-transferase P (GST-P)	Tee et al. 1992
Muscle pyruvate kinase (MPK)	Akhurst et al. 2005
OV-6 (recognises CK14 and CK19)	Bisgaard et al. 1993
OV1	Sanchez et al. 2004
A6	Engelhardt et al. 1993
OC.2 and OC.3	Hixson and Allison 1985
Connexin 43	Zhang and Thorgeirsson 1994
CX3Cl1	Yovchev et al. 2007
CD24	Yovchev et al. 2007
MUC1	Yovchev et al. 2007
Deleted in malignant brain tumour 1 (DMBT1)	Bisgaard et al. 2002
Adult hepatocyte markers	
Albumin	Tian et al. 1997
CK8	Libbrecht et al. 2000b
CK18	Libbrecht et al. 2000b
α1-Antitrypsin	Gauldie et al. 1980
Hepatocyte nuclear factor 4 (HNF4)	Nagy et al. 1994
HBD.1	Faris et al. 1991
c-Met	Hu et al. 1993
Fetal hepatocyte markers	
α-Fetoprotein (αFP)	Evarts et al. 1987
Delta-like protein (dlk)	Yovchev et al. 2007
Aldolase A and C	Lamas et al. 1987
c-Met	Hu et al. 1993
Cadherin 22	Yovchev et al. 2007
CD24	Yovchev et al. 2007
CD44	Kon et al. 2006
Adult haematopoietic markers	
c-kit	Fujio et al. 1994
CXCR4	Zheng et al. 2006
CD34	Omori et al. 1997
Sca-1	Petersen et al. 2003

their marker expression. Currently, there is a genuine requirement for a thorough understanding of the step-wise marker expression in HPCs akin to that described for the development of haematopoietic stem cells.

The early HPC markers described to date include c-kit, sca-1, NCAM, spermatogenic immunoglobulin superfamily (SgIGSF) and multidrug resistance transporters, which denote a side-population (SP) phenotype. The SP phenotype was originally described in the haematopoietic system and relates to the ability to efflux the dye Hoechst 33342. It appears to identify cells with immature characteristics, particularly with regard to hepatic embryogenesis (Tsuchiya et al. 2005) and carcinogenesis (Chiba et al. 2006). Another feature of immature cells is the absence of cytokeratin 7 (CK7) expression; CK7 is expressed as HPCs acquire a mature phenotype (Paku et al. 2005), which is in keeping with the demonstration of CK7 in the later stages of hepatic organogenesis (Shiojiri et al. 1991). Alpha-fetoprotein (αFP) is an OC marker that is also expressed during human hepatic embryogenesis and carcinogenesis. It appears to be present in intermediate ducts (Alpini et al. 1992) with prolonged expression for over 3 weeks following partial hepatectomy (PH) with retrorsine treatment (Gordon et al. 2000) and is also expressed by more differentiated hepatocyte-like cells in rats (Evarts et al. 1989). αFP expression is however notable by its absence during the OC response in mice (Jelnes et al. 2007).

Mechanisms of hepatic regeneration

The anatomical position of the liver and its physiological role place it in a toxin-rich environment. As such, it is required to tolerate frequent exposure to toxins. In addition, persistent insults such as viral disease, immunological or genetic disorders may continually challenge the liver. Evolutionarily, the liver has adapted to cope well with such insults and the regenerative capacity of the adult mammalian liver is immense. An injured liver is able to call upon a two-tier regenerative strategy comprised initially of mature hepatocyte followed, if need be, by HPCs (Alison 1998; Fig. 1).

Hepatocyte-mediated regeneration

Normally, the turnover of hepatocytes in the liver is slow with hepatocytes having a life span of approximately 1 year. Acute liver injury, for example PH, results in rapid and effective regeneration with hepatocytes undergoing mitosis leading to subsequent restoration of liver function within two cycles of division (Fausto et al. 2006). This process in pigs has recently been shown to include telomerase activation (Wege et al. 2007). Naturally, the question has been raised as to whether

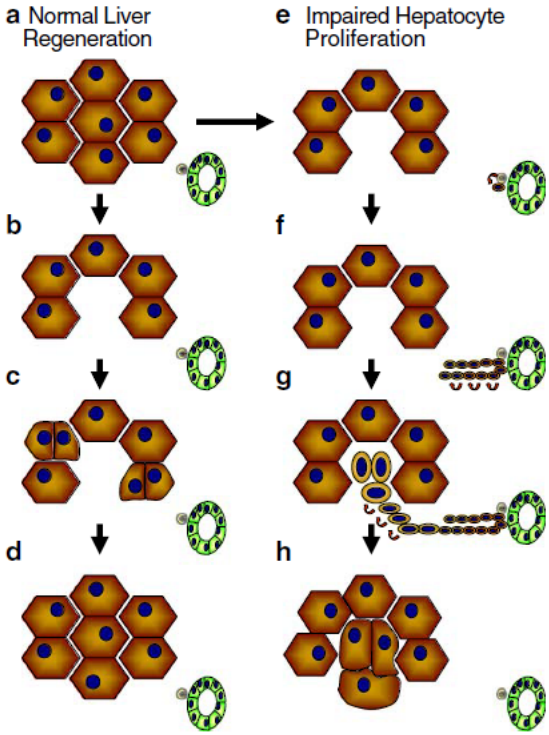

Fig. 1 Injury of the healthy liver (**a**) may be repaired in two ways. Either regeneration from the fully differentiated hepatocyte compartment (*brown*) is maintained (**b**) or it is impaired (**e**). In the case of maintained hepatocyte proliferation, replacement of damaged hepatocytes is quickly and efficiently achieved by division of pre-existing hepatocytes (**c**) resulting in the restoration of hepatocyte number (**d**) without expansion of HPCs. If hepatocyte injury occurs in the context of impaired hepatocyte proliferation (**e**), then stem cells (*grey*) located in the terminal biliary tree (*green*) are activated leading to the generation of a transit amplifying compartment (*black*, **f**), which spreads into the liver parenchyma (**g**). These cells are able to replace damaged hepatocytes, often forming regenerative nodules (**h**)

hepatocytes themselves function as stem cells. Landmark transplantation studies in fumarylacetoacetate hydrolase knockout (FAH $^{-/-}$) and urokinase-type plasminogen activator (uPA) transgenic mice have demonstrated that hepatocytes possess a virtually unlimited proliferative potential. They are capable of a least 69 cell divisions and can restore normal architecture and impaired function in the injured liver (Rhim et al. 1994; Overturf et al. 1997). Furthermore, Grompe and coworkers have shown, in the FAH$^{-/-}$ mouse, that adult hepatocytes expand clonally (Overturf et al. 1999) and may be serially transplanted (Overturf et al. 1997). These models however rely on a strong selection advantage against native hepatocytes. In addition, wild-type hepatocytes have been suggested to show multipotentiality when transplanted into the livers of dipeptidyl peptidase IV (DPPIV) knockout mice followed by PH and retrosine

treatment. DPPIV is an exopeptidase expressed on the bile canalicular surface of hepatocytes in addition to diffuse cytoplasmic expression by bile duct epithelia. Using this model, Michalopoulos et al. (2005) have shown that transplanted DPPIV$^+$ cells reconstitute bile ducts following bile duct ligation (BDL); the authors, in their previous work, note however that this hepatocyte infusion is not entirely pure (Michalopoulos et al. 2001). Notwithstanding, this study raises the possibility that hepatocytes may, in specific circumstances, display multipotentiality. Therefore, under certain conditions, hepatocytes may show many of the characteristics of stem cells. The models demonstrating self-renewal nevertheless share continual selection pressure for transplanted hepatocytes versus indigenous epithelia in the context of persistent liver injury. Whether human hepatocytes are capable of acting as true stem cells remains doubtful.

HPC-mediated regeneration

Rodent HPC models

The first description of candidate hepatic progenitor-like cells was made in 1937 (Kinosita 1937) with the subsequent naming of OCs in rodents following a report by Farber in 1956 (Farber 1956). These cells are characteristically 'small ovoid cells with scant lightly basophilic cytoplasm and pale blue-staining nuclei" and are not seen in the uninjured mammalian liver. In rodents, a variety of liver injury models have been used to induce an OC response (for a comprehensive list, see Santoni-Rugiu et al. 2005). PH alone in the otherwise uninjured rodent results in a regenerative response by the mature epithelial compartment but not by OCs. Analysis of carcinogenesis models such as 2-N-acetylaminofluorene (AAF) in combination with PH has demonstrated that the mitogenic stimulus of the PH may stimulate OCs when hepatocyte-mediated regeneration is inhibited (Solt and Farber 1976). AAF is converted to an active cytotoxic/mitoinhibitory N-hydroxy derivative by the cytochromes of mature hepatocytes (Alison 1998). OCs, by virtue of the low level expression of hepatocytic cytochromes, are resistant to this toxic effect and, as such, expand following AAF/PH. The carcinogenic alkaloid retrorsine specifically inhibits hepatocyte proliferation by a similar mechanism (Laconi et al. 1999) and, like AAF, has been used in combination with the mitogenic stimulus of PH or toxins, such as carbon tetrachloride (CCl_4) and allyl alcohol, to induce an OC response. Diets, such as the carcinogenic choline-deficient ethionine-supplemented (CDE) diet or the 3,5-diethoxycarbonlyl-1,4-dihydrocollidine -supplemented (DDC) diet, also stimulate an OC response and have more recently become increasingly popular models particularly in mice.

Investigation of OCs has made remarkable progress since the seminal work by Thorgeirsson and coworkers (Evarts et al. 1987, 1989) who demonstrated that rats treated with AAF followed by PH (AAF/PH) exhibited OC proliferation beginning in the periportal region. At later time points in these models, label-retaining basophilic hepatocytes were seen in the mid-parenchyma suggesting a precursor/product relationship. Further work has shown that OCs stream into regenerative nodules (Vig et al. 2006). The tracing of tritiated thymidine transfer from OCs to parenchymal cells in combination with differentiation markers has revealed the bipotentiality of HPCs, which are able to form either hepatocytes or cholangiocytes (Evarts et al. 1989; Holic et al. 2000). Indeed, HPCs themselves may express mature hepatocyte or biliary duct markers such as CK18 or CK19 (see Table 1. Observations by electron microscopy to study cell ultrastructure have shown a differentiation gradient of cells from more primitive progenitors to differentiated hepatocytes and cholangiocytes (De Vos and Desmet 1992; Mandache et al. 2002). This bipotentiality is furthermore demonstrated by the generation of stable OC lines that are capable of differentiating into cholangiocyte- or hepatocyte-like cells in vitro (Lazaro et al. 1998). In addition, these cells are also capable of engrafting following transplantation and expanding in the recipient liver (Faris and Hixson 1989; Yasui et al. 1997). Therefore, HPCs, in rodents at least, appear to possess the characteristics of progenitor cells, in addition to possessing a variety of markers implying stem cell function (e.g. c-kit, CD34 and flt3). Meticulous studies in rodents have demonstrated that OCs are predominantly derived from the terminal ducts, known as the canals of Hering, in the biliary tree (Saxena et al. 1999; Theise et al. 1999; Paku et al. 2001). Following activation, these OCs expand, forming ductular structures extending between the biliary tree and hepatocytes (Paku et al. 2001). This anatomical position at the interface between the parenchyma and the portal tract mesenchyme is also the site of bipotential hepatoblasts during hepatic organogenesis. Although differences have been noted (Dudas et al. 2006), many phenotypic and functional parallels exist between embryonic bipotential hepatoblasts and adult HPCs (Shafritz et al. 2006).

HPCs in human liver disease

In humans, HPC activation is believed to take the form of a ductular reaction. This is morphologically and immunohistochemically analogous to the rodent OC response. The clinical relevance of the HPC reactions is implied by its frequency in a wide variety of human liver diseases including fulminant hepatic failure, chronic viral hepatitis, alcoholic disease, non-alcoholic fatty liver disease, immune cholangio-

pathies and hereditary liver disorders (Roskams et al. 1991, 2003a, 2003b; Falkowski et al. 2003; Roskams 2003; Fig. 2). During acute liver injury, HPC regeneration may be seen occurring synchronously with a degree of hepatocyte replication. The presence of HPC activation during chronic liver disease however is probably a feature of eventual exhaustion of hepatocyte proliferation over many years or decades (Wiemann et al. 2002; Marshall et al. 2005). Characteristically, the magnitude of HPC activation corresponds to the severity of liver fibrosis and inflammation (Lowes et al. 1999; Libbrecht et al. 2000a; Roskams et al. 2003a). In addition, the more aggressive a hepatocellular injury, the higher the proportion of observed HPCs that resemble intermediate hepatocytes. This implies that an escalating hepatocyte deficiency promotes a greater degree of differentiation down the progenitor cell/hepatocyte axis (Roskams et al. 2003b).

Despite the apparently stereotyped HPC response seen across a wide range of human diseases, there is heterogeneity both between species and injury models (Jelnes et al. 2007). For example, the expression of αFP, which is characteristically seen in rodent OC reactions, is rare in the human ductular reaction. Differing characteristics are seen between models; for instance, the expression of DMBT1 (deleted in malignant brain tumour 1) is seen following hepatocelluar injury but not during human cholestatic liver disease or following BDL in rodents (Bisgaard et al. 2002). Consistent with an atypical HPC response in the BDL model, dexamethasone does not effect ductule formation following BDL in rats but inhibits OC activation following AAF/PH (Nagy et al. 1998).

In contrast to observations in rodents, the characteristics of stem cells have not been demonstrated in human ductular reactions to date. Sequential biopsies taken from patients have shown HPC proliferation and suggest their differentiation by observing a progressive increase in intermediate hepatocytes in association with their progressive extension into the liver lobule over time (Roskams et al. 1991; Demetris et al. 1996; Falkowski et al. 2003). Proliferating cells have been isolated from human liver capable of hepatocyte-like differentiation (Herrera et al. 2006). Further characterisation is required however to confirm these initial observations.

Mechanisms of HPC activation

The mechanisms controlling the HPC response are under intense investigation. In general, although many of the signals that control liver regeneration in the normal liver (i.e. via hepatocyte replication) are involved in HPC-mediated regeneration, acute liver injury does not significantly activate the HPC compartment. The most common context in which the HPC reaction is seen is when the cell cycle in hepatocyte regeneration is blocked either by toxins or replicative senescence in rodent models or human disease. Nevertheless, the two modes of liver regeneration are not entirely mutually exclusive, as HPC and hepatocyte replication can be observed simultaneously in some injury models (Rosenberg et al. 2000; Wang et al. 2003). This may simply be a function of the location, duration and/or magnitude of these specific signals. However, other factors such as cellular environment are likely to be highly relevant in generating the HPC response. Certainly, the wide range of candidate signals, with many showing only modest effects, suggests a significant signal redundancy in HPC control.

Observational studies show a correlation between liver disease severity and the magnitude of the HPC response (Lowes et al. 1999; Libbrecht et al. 2000a). A central role of inflammatory cytokines has also been suggested in rodents (Knight et al. 2005a). These observations are consistent with the dramatic inhibition of OC responses noted upon treatment with anti-inflammatory agents (Davies et al. 2006; Nagy et al. 1998). In terms of specific signals, many have been studied directly during HPC

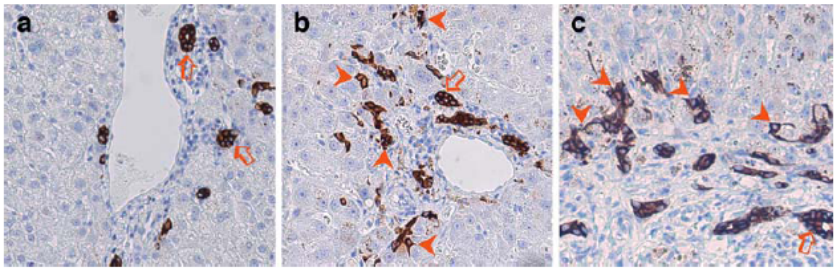

Fig. 2 Human ductular reaction in a patient with recurrent hepatitis C infection following cadaveric liver transplantation. **a** Pre-perfusion biopsy of donor liver prior to both implantation and hepatitis C infection; note the $CK7^+$ cells in the bile ducts (*arrows*). **b**, **c** Biopsies from the same liver 1 and 6 months, respectively, after transplantation and hepatitis C infection. These sections show $CK7^+$ HPCs (*arrowheads*) extending from the periportal regions into the parenchyma.

activation in vitro and in vivo (for an overview, see Table 2). Most of these signals are also seen during PH; however, they often exhibit differences in either the intensity or duration of the signal.

Tumour necrosis factor superfamily

Members of the pro-inflammatory tumour necrosis factor (TNF) superfamily include TNFα and TWEAK (TNF-like

Table 2 Key functional studies in animal models for investigating control mechanisms of OC activation. Manipulation of target signal is shown by *arrows*: ↑ indicates upregulation, whereas ↓ indicates inhibition of signalling. For OC models, *M* and *R* denote murine and rat studies, respectively (explanations of other abbreviations can be found in the Abbreviations list)

Signal	OC model	Effect on OCs	Reference
TNF			
↓ In vivo	50% CDE diet (M)	↓ Expansion	Knight et al. 2000
↑ In vitro	LE6 cells IV (R)	↑ Proliferation	Kirillova et al. 1999
↑ In vitro	LE6 cells IV (R)	↑ Mitogenesis	Brooling et al. 2005
TWEAK			
↑ In vivo	Uninjured (M)	↑ Expansion	Jakubowski et al. 2005
↑ In vivo	Uninjured adults (M)	↑ Expansion	
↓ In vivo	DDC diet (M)	↓ Expansion	
↑ In vitro	NRC line (R)	↑ Mitogenesis	
LTα			
↓ In vivo	CDE diet (M)	↓ Expansion	Knight and Yeoh 2005
LTβ			
↓ In vivo	CDE diet (M)	↓ Expansion	Akhurst et al. 2005
STAT3			
↑ In vivo	None (M)	↑ Expansion	Yeoh et al. 2007
↑ In vivo	CDE diet (M)	↑ Expansion, migration	Yeoh et al. 2007
IL6			
↓ In vivo	50% CDE diet (M)	↓ Proliferation	Knight et al. 2000
↑ In vitro	PIL2/PIL4 lines (M)	↑ Proliferation	Matthews et al. 2004
↑ In vivo	CDE diet (M)	↑ Expansion, proliferation	Yeoh et al. 2007
↓ In vivo	AAF/PH (R)	↓ Expansion	Nagy et al. 1998
OSM			
↑ In vitro	PIL2/PIL4 lines (M)	↓ Growth	Matthews et al. 2005
↑ In vitro	Primary OCs (M)	Equal growth	Matthews et al. 2005
IFNγ			
↑ In vivo	Uninjured (M)	OC-like expansion	Toyonaga et al. 1994
↓ In vivo	CDE diet (M)	↓ Expansion	Akhurst et al. 2005
↑ In vivo	2/3 PH (M)	↑ Expansion	Brooling et al. 2005
IFNα			
↑ In vitro	PIL2/PIL4 lines (M)	↓ Proliferation	Lim et al. 2006
↑ In vivo	CDE diet (M)	↓ Expansion, proliferation	
HGF			
↑ In vivo	AAF (R)	↑ Proliferation	Nagy et al. 1996
↑ In vivo	AAF/PH (R)	↑ Early expansion	Hasuike et al. 2005
↑ In vivo	AAF/PH (R)	↑ Expansion	Oe et al. 2005
EGF			
↑ In vivo	AAF (R)	↑ Proliferation	Nagy et al. 1996
↑ In vitro	MOC lines (M)	↑ Proliferation	Isfort et al. 1997
TGFβ			
↑ In vivo	DDC diet (M)	↓ Expansion	Preisegger et al. 1999
↑ In vitro	LE2/LE6 cells (R)	↓ Proliferation	Nguyen et al. 2007
SCF			
↓ In vivo	AAF/PH (R)	↓ Expansion	Matsusaka et al. 1999
Sympathetic nervous system			
↓ In vivo	50% CDE diet (M)	↓ Expansion	Oben et al. 2003
Parasympathetic nervous system			
↓ In vivo	Galactosamine (R)	↓ Expansion	Cassiman et al. 2002

weak induction of apoptosis), both of which appear to play pivotal roles in HPC activation. While many members of the TNF superfamily, including TNFα and lymphotoxin (LT), play important roles in both HPC and hepatocyte-mediated regeneration (Knight and Yeoh 2005; Fausto et al. 2006), TWEAK stands out by demonstrating differential effects on the mature hepatocyte and progenitor cell compartments (Jakubowski et al. 2005). TWEAK is upregulated during hepatic injury, both in rodents and in a variety of human diseases, and mediates pro-proliferative effects directly on OCs via the Fn14 receptor (Jakubowski et al. 2005). TWEAK is sufficient, although not necessary, to induce a modest OC response, whereas its inhibition results in an attenuated murine OC response. This therefore positions TWEAK as arguably the most important intercellular signal inducing the hepatic HPC response. It is produced predominantly by monocytes, particularly following interferon-γ (IFNγ) stimulation (Nakayama et al. 2000), and is initially expressed as a membrane -ound molecule that can also be released in a soluble form. TWEAK activates nuclear factor kappaB, which is pro-proliferative to OCs (Kirillova et al. 1999); it may also play a role in the proliferation of other mesenchymal progenitors (Girgenrath et al. 2006), including promoting angiogenesis (Jakubowski et al. 2002), and may contribute to hepatic embryogenesis and carcinogenesis (Kawakita et al. 2005).

TNFα production is increased during chronic human liver disease (Tilg et al. 1992). It is known to be predominantly produced by macrophages but also by other cells types, including lymphocytes and fibroblasts (Locksley et al. 2001), and is upregulated during the rodent OC response (Knight et al. 2000; Akhurst et al. 2005). Cellular activity is mediated via the TNF R1 and TNF R2 receptors. Administration of TNFα to OC lines in vitro results in proliferation (Kirillova et al. 1999). Furthermore, TNF R1 knockout mice show a markedly impaired OC response (Knight et al. 2000). No study to date, including that with TNFα/LTα knockout mice (Knight and Yeoh 2005), has shown an absolute requirement for TNFα but all suggest that TNFα is required for an optimal OC response.

LT-α, LT-β and LIGHT are also members of the TNF superfamily and are involved in a variety of processes including influencing cell survival and proliferation. LT-α, like TNF, binds TNF R1, which as described previously plays an important role in the control of the OC response. Its role in HPC activation is suggested but not confirmed by the demonstration that LT-α/TNFα double-knockout mice develop an attenuated OC response following the CDE diet (Knight and Yeoh 2005). LT-α may also act in combination with LT-β via the formation of a heterotrimer (LTα1β2), which is the ligand for a separate receptor; LT-β receptor (LT-βR). LT-β expression is upregulated during rodent OC activation and during chronic human liver disease. Both LT-β knockout and LT-βR knockout mice show a partially impaired OC response (Akhurst et al. 2005). Another ligand for LT-βR called LIGHT is potentially therefore also involved. LIGHT is predominantly expressed by lymphocytes (Hansson 2007) and, although its effects on HPCs have not been directly investigated, it is known to signal to hepatocytes via LT-βR (Lo et al. 2007).

GP130 activators

A variety of cytokines, including interleukin 6 (IL6), oncostatin M (OSM) and leukaemia inhibitor factor (LIF), act through the gp130 signalling pathway. Following homodimerisation, gp130 activates the JAK (Janus kinase)/STAT (signal transductor and activator of transcription) and ERK (extracellular signal-regulated kinase) pathways. STAT3 and its targets are upregulated during the rodent OC response and during human chronic liver disease (Sanchez et al. 2004; Subrata et al. 2005) and also play an established role in hepatocyte-mediated regeneration following PH (Fausto et al. 2006).

Aside from TWEAK, gp130 is the only signal demonstrated to date capable of initiating an OC response alone. This has been revealed in uninjured gp130^{Y757F} mice with constitutively active gp130 (Subrata et al. 2005). Another of the downstream targets of gp130, viz. the ERK-1/2 pathway, has been shown by the same investigators to be a negative regulator of OC expansion. Therefore, gp130 is potentially a key element in the activation and expansion of hepatic HPCs. IL-6 is the best characterised of the gp130 activators; it is produced by a variety of cell types including macrophages, fibroblasts and endothelia. Recent studies have demonstrated that IL-6 is pro-proliferative to the OC response and that IL-6 knockout mice demonstrate a reduced OC response (Fischer et al. 1997; Knight et al. 2000; Yeoh et al. 2007). Treatment of OC lines with IL-6 results in proliferation and migration (Matthews et al. 2004; Yeoh et al. 2007). IL-6 signals via the type I cytokine receptor CD126 (IL-6Rα) together with the signal transducing gp130 homodimer principally activating STAT3 (Yeoh et al. 2007). IL-6 expression increases in both acute and chronic human disease and rodent liver injury models (Streetz et al. 2003; Akhurst et al. 2005; Fausto et al. 2006). Thus, IL-6 is a key signal in hepatocyte proliferation but is not in itself capable of inducing an OC response (Yeoh et al. 2007). The source of IL-6 during liver injury is likely to be activated leucocytes, including Kupffer cells and lymphocytes (Streetz et al. 2003); however, IL6 production has also been described from HPCs themselves, raising the possibility of autocrine stimulation (Matthews et al. 2004).

LIF and OSM both participate in a variety of processes including the regulation of growth and differentiation. The action of LIF is mediated via the LIF receptor (LIFR), which is composed of LIFRβ and gp130. Its downstream

effect in OCs occurs predominantly via STAT1 (Kirillova et al. 1999). Both LIF and LIFR are upregulated during the OC reaction in the rat (Omori et al. 1996) and in human cirrhotic livers, with LIFRβ localising to proliferating $CK7^{+}$ intermediate hepatobiliary cells (Znoyko et al. 2005). Although the effects of LIF on HPC proliferation are not clear, it does have stimulatory effects on other progenitor cells, including murine haematopoietic progenitors (Metcalf and Gearing 1989). LIF has also been described to have effects of hepatocyte differentiation. Murine embryonic bodies when cultured with LIF are maintained in a undifferentiated state but differentiate into hepatocyte-like cells upon its removal (Chinzei et al. 2002). OSM also activates gp130, either via its own OSM receptor (OSMRβ) subunit or via LIFR (Heinrich et al. 2003). OSM influences extrahepatic progenitor cell activity and extracellular matrix (ECM) deposition, in addition to inducing an acute phase response. It is produced by hepatic macrophages in humans and is upregulated during both cirrhotic human liver disease (Znoyko et al. 2005) and the rodent OC reaction (Matthews et al. 2005). Both murine OCs and human intermediate hepatobiliary cells express OSMRβ, which induces activation of STAT3 (Znoyko et al. 2005; Matthews et al. 2005). OSM has been described to promote the proliferation and differentiation of fetal hepatoblasts (Kinoshita et al. 1999) and OCs lines (Yin et al. 1999, 2002), respectively. Conflicting data however have come from an immortalised p-53-deficient OC line (Matthews et al. 2005). Further investigation is required to clarify the role of OSM in HPC activation.

Interferon γ

There is strong evidence for a role of the inflammatory cytokine IFNγ in HPC activation. It is characteristically expressed by T lymphocytes and natural killer cells. Although it also activates the JAK-STAT pathway, in contrast to many gp130-mediated signals, INFγ signals predominantly through the STAT1 pathway (Croker et al. 2003). Its role in HPC activation was initially examined in a transgenic mouse with constitutive hepatic IFNγ expression by using a serum amyloid P component gene promoter. These mice demonstrated cords of small cells morphologically similar to OCs in the context of progressive liver inflammation (Toyonaga et al. 1994). Since then, OCs have been found to possess functional IFNγ receptors and IFNγ expression has been shown during the OC reaction (Bisgaard et al. 1999). Varying effects, including proliferation, are seen when IFNγ is administered to OC lines (Brooling et al. 2005). More consistent effects have been seen during in vivo manipulation, with reduced OC expansion being seen in IFNγ knockout mice (Akhurst et al. 2005) and IFNγ treatment stimulating an OC response following PH in mice (Brooling et al. 2005). These observations are consistent with the impaired OC response seen in BALB/c mice that lack Th1 signalling, of which IFNγ is a key component (Knight et al. 2007). Caution however should be exercised as reduced OC expansion has also been noted in vitro (Brooling et al. 2005) and IFNγ may have indirect effects upon the OC response via the inhibition of hepatocyte proliferation (Fausto et al. 2006). IFNγ has been proposed to be a factor in determining hepatocyte- versus HPC-mediated regeneration, although convincing data to support this hypothesis are lacking.

Type I interferons

The effects of the type 1 interferons (IFNα and IFNβ) on HPCs appear to differ significantly from that of IFNγ. IFNα signals predominantly through STAT3 in murine liver (Lim et al. 2006). Analysis of paired human liver biopsies reveals that both successful and unsuccessful IFNα treatment of hepatitis C virus is associated with a reduced number of HPCs (Lim et al. 2006; Tsamandas et al. 2006). This effect is not reliant on hepatitis C, as IFNα reduces OC proliferation both in vitro and in vivo in the absence of hepatitis C infection (Lim et al. 2006). Furthermore, IFNα appears to promote differentiation particularly into hepatocyte-like cells. The effects of IFNβ on HPCs are unknown, although, like IFNα, it impairs regeneration following PH alone (Wong et al. 1995; Theocharis et al. 1997). Its role in HPC activation therefore warrants further investigation.

Primary growth factors

The role of hepatocyte growth factor (HGF) in stimulating hepatocyte proliferation in the primed liver has been well described (Fausto et al. 2006). Like hepatocytes, OCs also express the HGF receptor c-Met (Hu et al. 1993; Muller et al. 2002). The expression of HGF is increased following PH/AAF in the rat (Evarts et al. 1993; Hu et al. 1993), as is uPA (Nagy et al. 1996), which can release HGF stored in its bound form on the ECM. HGF levels are also increased in the serum of patients with chronic liver disease and of those experiencing acute injury compared with healthy controls (Shiota et al. 1995). HGF is both mitogenic to, and promotes the differentiation of, OCs in vivo (Nagy et al. 1996; Hasuike et al. 2005). This is in concordance with similar effects on embryonic hepatic stem cells (Suzuki et al. 2003). There is therefore strong evidence for a role of HGF in influencing HPC behaviour; however, elevations of HGF in the context of PH alone are insufficient to stimulate HPC expansion.

Transforming growth factor-α (TGFα) and epidermal growth factor (EGF) are structurally related membrane-bound growth factors that bind the EGF receptor (EGFR) of adjacent cells, in turn initiating a variety of effects including

the upregulation of the EGFR and cell proliferation (Leahy 2004). Membrane-bound pro-TGFα may also be cleaved to release a soluble signal capable of autocrine and paracrine signalling. In rodents, TGFα and EGF are produced predominantly by stellate cells, which are known to line OC ductules (Paku et al. 2001), whereas the EGFR is expressed by OCs (Evarts et al. 1992). TGFα is upregulated following AAF/PH injury in rodents (Evarts et al. 1993) and both EGF and TGFα localise to ductular reactions in human chronic liver disease (Hsia et al. 1994; Komuves et al. 2000). EGF is mitogenic to OCs in vitro suggesting a role of both growth factors in HPC activation.

The fibroblast growth factors (FGFs) are a family of growth factors that bind their FGF receptors (FGFR) with the aid of heparin sulphate proteoglycans (Pellegrini 2001). FGFs are involved in hepatic embryogenesis (Jung et al. 1999) and are upregulated in both the rat AAF/PH model (Marsden et al. 1992) and during human chronic liver disease (Jin-no et al. 1997). Whereas FGFR2 is upregulated in a variety of liver injuries and is expressed by numerous cell types, FGFR1 in adult rats is upregulated specifically during HPC-inducing injury and is expressed by OCs (Hu et al. 1995). In keeping with their role in organogenesis, FGFs induce a hepatocyte-like phenotype in BM-derived "multipotent adult progenitor cells" in vitro (Schwartz et al. 2002).

Transforming growth factor-β

TGFβ is well known to limit hepatocyte-mediated regeneration by inhibiting hepatocyte proliferation and inducing apoptosis (Fausto et al. 2006) and is actively expressed by myofibroblasts following OC-inducing injury (Park and Suh 1999). Active expression of TGFβ in a transgenic mouse fed on the DDC diet results in a reduced OC response (Preisegger et al. 1999). Concordantly, TGFβ is inhibitory to OC lines in vitro (Nguyen et al. 2007), although TGFβ is less inhibitory of mitosis in OCs than in hepatocytes.

Stem cell factor

Stem cell factor (SCF) acts via the c-kit receptor and has well-described functions including the promotion of cell survival and the proliferation and differentiation of haematopoietic progenitor cells. Expression of SCF is increased in the AAF/PH model but not following PH alone. Its receptor, c-kit, is an established HPC marker. Functional investigation of c-kit by using a dysfunctional c-kit receptor suggests that SCF is pro-proliferative to OCs in the rat (Matsusaka et al. 1999). Interestingly, as discussed previously, gp130 and c-kit activation is regarded as the minimal requirement for the expansion of haematopoietic progenitors (Fischer et al. 1997) and, therefore, SCF is also potentially a key player in HPC activation.

Connective tissue growth factor

Connective tissue growth factor (CTGF) is a matrix-associated heparin-binding protein that mediates cell proliferation and differentiation and ECM remodelling in a variety of tissues. It is regulated by TGFβ and is known to be upregulated both in animal models of HPC activation (Pi et al. 2005) and human chronic liver disease (Paradis et al. 2001; Gressner et al. 2006). Inhibition of CTGF during rat OC proliferation results in reduced cellular proliferation and expression of αFP (Pi et al. 2005).

Stromal-cell-derived factor 1

The chemokine stromal-cell-derived factor 1 (SDF-1) uniquely binds to the CXCR4 receptor and plays a variety of roles including cell trafficking, proliferation and organogenesis. CXCR4 is expressed by a variety of progenitor cells and SDF-1 is upregulated during human chronic liver disease (Terada et al. 2003). There is however some disagreement over the source of SDF-1 during the hepatic OC response with reports suggesting either hepatocytic or periportal production (Hatch et al. 2002; Mavier et al. 2004; Zheng et al. 2006). None-the-less, SDF-1 is clearly upregulated following OC-inducing rodent injury. SDF-1 has been shown to be both pro-proliferative (Pi et al. 2005) and chemotactic (Hatch et al. 2002) to OCs.

Peroxisome-proliferator-activated receptor γ

Intracellular peroxisome-proliferator-activated receptors (PPAR) may also mediated a degree of OC control. Their principally described role is in the control of lipid metabolism in response to binding to fatty acid and eicosanoid ligands. Their pro-proliferative role during HPC activation is suggested by in vivo and in vitro studies showing that administration of a PPARγ inhibitor attenuates OC growth (Knight et al. 2005b). This effect may in part be mediated by prostaglandins, as PPARγ might be activated by prostaglandin J_2 (Forman et al. 1995). Prostaglandin production is inhibited by COX2 inhibitors, which themselves are known to inhibit the OC reaction (Davies et al. 2006).

Spermatogenic immunoglobulin superfamily

SgIGSF is an intercellular adhesion molecule that can bind either homophilically or heterophilically; it is expressed on HPCs both in humans and in rodents and appears to identify an immature phenotype (Ito et al. 2007). Signal inhibition by using a blocking antibody results in the inhibition of ductular formation in an in vitro model. The report of Ito et al. (2007) not only highlights this molecule

as a potential further addition to the already complex array of signals mediating OC control, but also emphasises the ongoing nature of the description of new pathways mediating such control.

Neural input

Fewer intermediate hepatobiliary cells are seen in transplanted graft livers that develop recurrent disease than in matched liver biopsies taken from untransplanted patients. This observation has led to the hypothesis that denervation as result of transplantation directly affects the HPC response. Expression of both adrenoreceptors and muscarinic receptors corresponding to the sympathetic and parasympathetic nervous system respectively has been described on OCs. The inhibition of the sympathetic or parasympathetic nervous systems either chemically or surgically in rodents results in the expansion or contraction of the HPC response, respectively (Cassiman et al. 2002; Oben et al. 2003). The mechanism of action of neurotransmitters on HPCs together with the demonstration that neurons make direct functional contract with these cells are topics that remain to be investigated.

As discussed above, a variety of signals have been implicated in the activation of HPCs (see Fig. 3). Many of these signals are known to be delivered by cells that are seen surrounding the HPC reaction. This raises the hypothesis of there being a specialised niche regulating HPC behaviour both physiologically and during disease. The ECM plays a key role in other stem cell niches and is seen surrounding HPCs (Paku et al. 2001); it is therefore also implicated in forming the hepatic stem cell niche.

Role of extrahepatic stem cell activation during liver disease

Over the last decade, the importance of BM stem cell (BMSC) activation during liver disease has become apparent. CD34-positive and CD133-positive cells appear to be upregulated following liver transplantation or PH in the diseased liver (De Silvestro et al. 2004; Gehling et al. 2005; Lemoli et al. 2006). Similarly, cells with haematopoietic stem cell markers are mobilised following liver injury in rodents (Fujii et al. 2002) and, in this context, are recruited to the liver (Kollet et al. 2003). There has been considerable interest in the possibility that the BM contributes to liver parenchymal and non-parenchymal cells. Furthermore, current data point towards a role in modulating hepatic fibrosis, in addition to the control of HPC behaviour outlined above.

Hepatic parenchymal regeneration by BM

Work carried out during the last 10 years has made apparent that OCs express a variety of markers, such as c-kit and sca-1, that had previously been thought of as haemato-

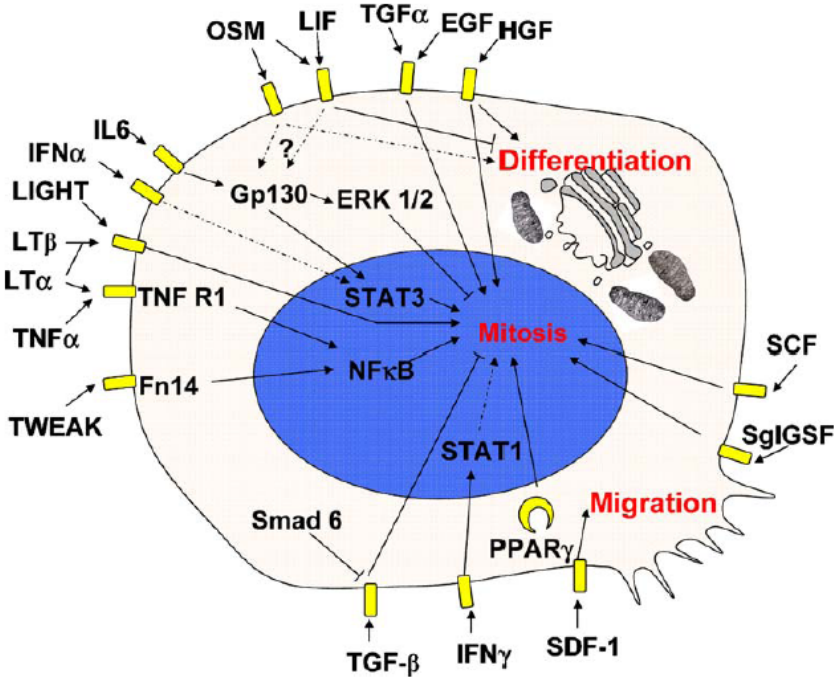

Fig. 3 A variety of signals influence HPC behaviour by modulating mitosis, differentiation and migration (abbreviations are explained in Table 1 and in the Abbreviations list)

poietic (see Table 1; Petersen et al. 2003). Furthermore, BM-derived stem cells have been shown to differentiate into hepatocyte-like cells in vitro (Yamazaki et al. 2003; Yamada et al. 2006). When hepatocytes were identified that expressed extrahepatic markers in both rodent (Petersen et al. 1999) and human liver (Alison et al. 2000; Theise et al. 2000), the exciting possibility that BM-derived cells were transdifferentiating into hepatocytes was raised. Examination by using Y chromosome tracking in human liver specimens from either female patients with a previous BM transplant from male donors, or male patients who had received a liver transplant from female donors demonstrated that a number (varying from 0%–40% depending upon the study) of hepatocytes possessed a Y chromosome (Thorgeirsson and Grisham 2006). The implication was, therefore, that BM-derived cells were crossing lineage boundaries via transdifferentiation to form hepatocytes. This was investigated in detail in rodents including the $FAH^{-/-}$ mouse, a model for human hereditary type I tyrosinaemia in which hepatic injury may be inhibited at will by the administration of a protective chemical ([2-(2-nitro-4-fluoromethylbenzoyl)-1,3-cyclohexanedione], NTBC). NTBC prevents hepatotoxicity by blocking the formation of fumarylacetoacetate. When $FAH^{-/-}$ mice are given BM and the protection of NTBC is gradually withdrawn, hepatocytes expressing markers of the transplanted BM are seen to reconstitute the mouse liver (Lagasse et al. 2000). Subsequent work however has convincingly shown that, instead of plasticity, monocyte-hepatocyte fusion is the mechanism by which BM cells rescue a genetically deficient phenotype in the $FAH^{-/-}$ mouse (Alvarez-Dolado et al. 2003; Vassilopoulos et al. 2003; Wang et al. 2003b; Camargo et al. 2004; Willenbring et al. 2004). These monocyte-hepatocyte fusion events are rare but rescue in the $FAH^{-/-}$ model is nevertheless attributable to the proliferation of these fusion cells (Wang et al. 2002). This occurs as selective pressure is applied against native hepatocytes lacking the correcting wild-type genes. In the absence of such selective pressure, however, significant hepatocytes replacement is rarely seen and, at most, occurs at a level far below that of native hepatocytes turnover (Yannaki et al. 2005; Thorgeirsson and Grisham 2006). Despite initial reports that HPCs may be in part BM-derived (Petersen et al. 1999), more recent studies suggest that this does not occur to any significant degree (Wang et al. 2003a; Menthena et al. 2004; Vig et al. 2006). OCs from BM transplanted mice neither express the BM-tracking marker to any significant degree nor show clustering suggestive of the expansion of BM-derived OCs. Importantly, transplantation of an OC fraction into the $FAH^{-/-}$ mouse in one study has shown that transplantable cells are not BM-derived (Wang et al. 2003a). Some ongoing uncertainty exists in this area, however, as a recent report suggests that the OCs may indeed be BM-derived (Oh et al. 2007). The study investigated $DPPIV^{+}$ cells after DPPIV-deficient rats were transplanted with wild-type BM. AAF/PH was used in these animals to induce an OC response and resulted in $DPPIV^{+}$ cells within the liver (Oh et al. 2007). DPPIV is however not a specific hepatocyte marker and is expressed by sinusoidal endothelia (Koivisto et al. 2001) and T lymphocytes (Vivier et al. 1991).

BM contribution to hepatic non-parenchymal cells

Kupffer cells/macrophages

Although approximately 80% of the liver mass is comprised of parenchymal epithelial cells, a number of other cell types play a variety of key physiological roles within the liver. Leucocyte-derived populations remain as resident monocytes (Kupffer cells), whereas other populations transiently traffic through the liver. At least a proportion of hepatic Kupffer cells are BM-derived (Abe et al. 2003; Higashiyama et al. 2007). Kupffer cells have been implicated in a variety of processes during hepatic disease including inflammation, regeneration, fibrosis and ECM remodelling. Administration of gadolinium chloride, which inhibits Kupffer cells, prevents the expansion of OCs positive for muscle pyruvate kinase, in response to BDL in rats (Olynyk et al. 1998). This is consistent with the intimate spatial relationship between Kupffer cells and OCs (Yin et al. 1999). Similarly, gadolinium chloride treatment is able to reduce fibrosis in thioacetamide-treated rats (Ide et al. 2005) consistent with the putative role of Kupffer cells and macrophages in the process of hepatic fibrosis and ECM remodelling. This role has been corroborated by using an inducible macrophage-specific depletion model in mice during or following CCl_4 injury; this work has demonstrated that both the generation and resolution of fibrosis are macrophage-dependent (Duffield et al. 2005). The mechanism of tissue remodelling may include the expression of the matrix-remodelling metalloproteinase MMP-9 by BM-derived $F4/80^{+}$ macrophages during the resolution of fibrosis following CCl_4 injury (Higashiyama et al. 2007).

Hepatic stellate cells

Sustained injury occurring in human chronic liver disease is usually accompanied by progressive fibrosis and potentially by cirrhosis resulting from excessive deposition of collagen and other components of the ECM. Central to this process is the population of matrix-secreting myofibroblasts, which, at least in part, are formed following the activation of hepatic stellate cells (Henderson and Iredale 2007). Myofibroblasts not only deposit ECM, but also alter its

degradation by the expression of tissue inhibitors of MMP. Investigations in rodent models by using labelled BM transplantation (Baba et al. 2004; Russo et al. 2006) or human studies following sex mis-matched liver or BM transplants (Forbes et al. 2004) have shown a significant BM contribution to populations of both hepatic stellate cells and myofibroblasts and this process does not appear to occur through cell fusion. Other studies of the BDL model have found only a small proportion (5%–10%) of collagen-producing cells are BM-derived (Kisseleva et al. 2006).

Endothelial progenitors

Capillaries extend alongside the smallest branches of the biliary tree during chronic rejection following liver transplantation, consistent with new vessel formation paralleling progenitor ductules (Gouw et al. 2006). A least a proportion of liver sinusoidal cells that expand following liver injury are BM-derived (Gao et al. 2001; Fujii et al. 2002; Taniguchi et al. 2006). These cells produce a variety of growth factors including HGF, EGF and TGFα, all of which have been implicated in modulating the HPC response (Taniguchi et al. 2006).

The BM is therefore able to produce a variety of cells in response to liver injury (Fig. 4). These various populations described to date orchestrate an assortment of functions during liver injury. BM-derived cells act as precursors to a variety of non-parenchymal cells. In doing so, the BM significantly contributes to the deposition, remodelling and resolution of hepatic fibrosis. The role of the BM in parenchymal cell regeneration appears to be minimal. Under carefully controlled experimental conditions, the BM can make dramatic contributions to hepatocyte regeneration, albeit via fusion with pre-existing hepatocytes rather than by transdifferentiation.

Functions of BM-derived stem cells during human liver disease

To date only a handful of clinical trials have investigated the role of stem cell mobilisation therapy or stem cell infusion in adults. G-CSF (granulocyte colony-stimulating factor) has been used to induce haematopoietic stem cell mobilisation to the peripheral blood of patients with cirrhosis (Gaia et al. 2006). In association with the mobilisation of CD34+ and CD133+ cells, only two out of eight patients showed moderate improvement in liver function. Trials of cell therapy have included a cohort of patients with liver cancer in whom portal vein embolisation was used to induce compensatory hypertrophy in the contralateral liver lobe prior to surgical resection. Thirteen patients underwent portal vein embolisation, six of whom received an infusion of autologous CD133+ BMSC. This non-randomised trial demonstrated a marginal but significant increase in liver volume and reduced time to surgery in patients receiving autologous BMSC infusions (Furst et al. 2007). Another uncontrolled study in five patients with cirrhosis investigated the effects of autologous $CD34^+$ BMSCs. Three of these patients showed transient improvements in biochemical markers such as bilirubin and albumin over the following 2 months (Gordon et al. 2006). A case report has described clinical improvement following infusion of autologous G-CSF mobilised $CD34^+$ BM cells in a single patient with hepatic failure (Gasbarrini et al. 2006). Autologous monocyte therapy has also been attempted by using a larger number of unsorted cells

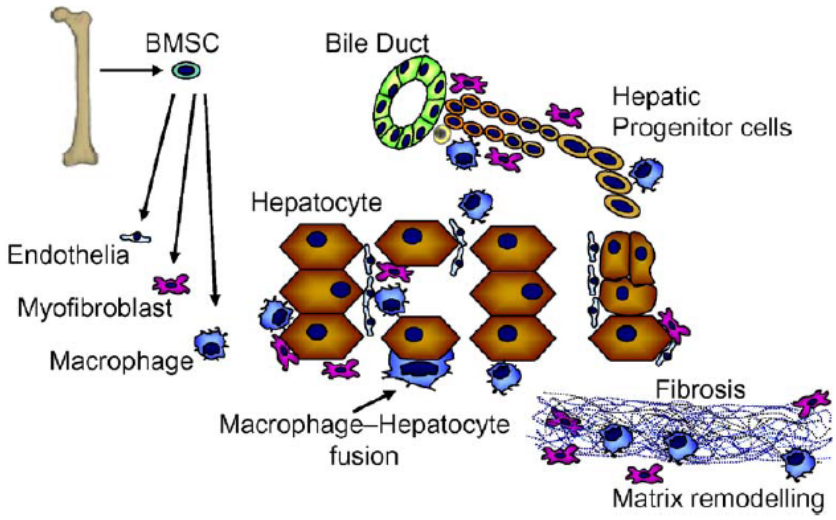

Fig. 4 Overview of HPC activation during liver injury. During hepatic injury, regeneration of hepatocytes may occur from hepatocytes or by expansion and differentiation of HPCs. Bone marrow stem cells (*BMSC*) are also activated forming macrophages, myofibroblasts and endothelial cells. Macrophages may fuse with hepatocytes. Macrophages and myofibroblasts also play key roles in both the production and resolution of fibrosis in the liver

extracted from the BM of cirrhotic patients. In the nine patients receiving BM, an improvement in the Child-Pugh score was noted with an increase in intrahepatic cell proliferation in the patients biopsied after treatment (Terai et al. 2006). Despite these encouraging reports, caution must be exercised. Only one of these trials used controls (non-randomised) and all were performed in a small number of patients. Engraftment or colonisation of infused cell was not investigated in any of the studies. Therefore, a considerable amount of further investigation is required in this area.

HPCs and cancer

A final consideration of the activation of stem cells during liver disease should include their potential role in carcinogenesis (see the review by Morrison and Alison in this issue). Chronic activation of HPCs occurs at a time when liver cancer develops. Inhibition of the rodent HPC response during the long-term CDE diet is associated with a reduction in the incidence of cancerous lesions (Knight et al. 2000). The occurrence of mixed forms of liver cancer with features of both hepatocellular carcinoma and cholangiocarcinoma is consistent with a bipotential HPC origin (Alison 2005; Roskams 2006), as are the similarities in gene expression between HCC subtypes and OCs (Lee et al. 2006). Clearly, these observations have implications for the use of HPC-directed therapies.

Concluding remarks

To date, a great deal has been learnt about stem cell activation, during liver disease, from experimental studies in well established rodent models. From a clinical perspective, an understanding of regenerative processes is essential in guiding patient management and for offering new therapies to harness or augment the impressive capacity of the liver for regeneration. Stem cells are at the hub of such regeneration in chronic liver disease but also appear to be involved in fibrogenesis and carcinogenesis within the liver.

References

Abe S, Lauby G, Boyer C, Rennard SI, Sharp JG (2003) Transplanted BM and BM side population cells contribute progeny to the lung and liver in irradiated mice. Cytotherapy 5:523–533

Akhurst B, Matthews V, Husk K, Smyth MJ, Abraham LJ, Yeoh GC (2005) Differential lymphotoxin-beta and interferon gamma signaling during mouse liver regeneration induced by chronic and acute injury. Hepatology 41:327–335

Alison M (1998) Liver stem cells: a two compartment system. Curr Opin Cell Biol 10:710–715

Alison MR (2005) Liver stem cells: implications for hepatocarcinogenesis. Stem Cell Rev 1:253–260

Alison MR, Poulsom R, Jeffery R, Dhillon AP, Quaglia A, Jacob J, Novelli M, Prentice G, Williamson J, Wright NA (2000) Hepatocytes from non-hepatic adult stem cells. Nature 406:257

Alpini G, Aragona E, Dabeva M, Salvi R, Shafritz DA, Tavoloni N (1992) Distribution of albumin and alpha-fetoprotein mRNAs in normal, hyperplastic, and preneoplastic rat liver. Am J Pathol 141:623–632

Alvarez-Dolado M, Pardal R, Garcia-Verdugo JM, Fike JR, Lee HO, Pfeffer K, Lois C, Morrison SJ, Alvarez-Buylla A (2003) Fusion of bone-marrow-derived cells with Purkinje neurons, cardiomyocytes and hepatocytes. Nature 425:968–973

Baba S, Fujii H, Hirose T, Yasuchika K, Azuma H, Hoppo T, Naito M, Machimoto T, Ikai I (2004) Commitment of bone marrow cells to hepatic stellate cells in mouse. J Hepatol 40:255–260

Bisgaard HC, Parmelee DC, Dunsford HA, Sechi S, Thorgeirsson SS (1993) Keratin 14 protein in cultured nonparenchymal rat hepatic epithelial cells: characterization of keratin 14 and keratin 19 as antigens for the commonly used mouse monoclonal antibody OV-6. Mol Carcinog 7:60–66

Bisgaard HC, Muller S, Nagy P, Rasmussen LJ, Thorgeirsson SS (1999) Modulation of the gene network connected to interferon-gamma in liver regeneration from oval cells. Am J Pathol 155:1075–1085

Bisgaard HC, Holmskov U, Santoni-Rugiu E, Nagy P, Nielsen O, Ott P, Hage E, Dalhoff K, Rasmussen LJ, Tygstrup N (2002) Heterogeneity of ductular reactions in adult rat and human liver revealed by novel expression of deleted in malignant brain tumor 1. Am J Pathol 161:1187–1198

Brooling JT, Campbell JS, Mitchell C, Yeoh GC, Fausto N (2005) Differential regulation of rodent hepatocyte and oval cell proliferation by interferon gamma. Hepatology 41:906–915

Camargo FD, Finegold M, Goodell MA (2004) Hematopoietic myelomonocytic cells are the major source of hepatocyte fusion partners. J Clin Invest 113:1266–1270

Cameron R, Kellen J, Kolin A, Malkin A, Farber E (1978) Gamma-glutamyltransferase in putative premalignant liver cell populations during hepatocarcinogenesis. Cancer Res 38:823–829

Cassiman D, Libbrecht L, Sinelli N, Desmet V, Denef C, Roskams T (2002) The vagal nerve stimulates activation of the hepatic progenitor cell compartment via muscarinic acetylcholine receptor type 3. Am J Pathol 161:521–530

Chiba T, Kita K, Zheng YW, Yokosuka O, Saisho H, Iwama A, Nakauchi H, Taniguchi H (2006) Side population purified from hepatocellular carcinoma cells harbors cancer stem cell-like properties. Hepatology 44:240–251

Chinzei R, Tanaka Y, Shimizu-Saito K, Hara Y, Kakinuma S, Watanabe M, Teramoto K, Arii S, Takase K, Sato C, Terada N, Teraoka H (2002) Embryoid-body cells derived from a mouse embryonic stem cell line show differentiation into functional hepatocytes. Hepatology 36:22–29

Croker BA, Krebs DL, Zhang JG, Wormald S, Willson TA, Stanley EG, Robb L, Greenhalgh CJ, Forster I, Clausen BE, Nicola NA, Metcalf D, Hilton DJ, Roberts AW, Alexander WS (2003) SOCS3 negatively regulates IL-6 signaling in vivo. Nat Immunol 4:540–545

Davies RA, Knight B, Tian YW, Yeoh GC, Olynyk JK (2006) Hepatic oval cell response to the choline-deficient, ethionine supplemented model of murine liver injury is attenuated by the administration of a cyclo-oxygenase 2 inhibitor. Carcinogenesis 27:1607–1616

De Silvestro G, Vicarioto M, Donadel C, Menegazzo M, Marson P, Corsini A (2004) Mobilization of peripheral blood hematopoietic stem cells following liver resection surgery. Hepatogastroenterology 51:805–810

De Vos R, Desmet V (1992) Ultrastructural characteristics of novel epithelial cell types identified in human pathologic liver specimens with chronic ductular reaction. Am J Pathol 140:1441–1450

Demetris AJ, Seaberg EC, Wennerberg A, Ionellie J, Michalopoulos G (1996) Ductular reaction after submassive necrosis in humans. Special emphasis on analysis of ductular hepatocytes. Am J Pathol 149:439–448

Dudas J, Elmaouhoub A, Mansuroglu T, Batusic D, Tron K, Saile B, Papoutsi M, Pieler T, Wilting J, Ramadori G (2006) Prospero-related homeobox 1 (Prox1) is a stable hepatocyte marker during liver development, injury and regeneration, and is absent from "oval cells". Histochem Cell Biol 126:549–562

Duffield JS, Forbes SJ, Constandinou CM, Clay S, Partolina M, Vuthoori S, Wu S, Lang R, Iredale JP (2005) Selective depletion of macrophages reveals distinct, opposing roles during liver injury and repair. J Clin Invest 115:56–65

Engelhardt NV, Factor VM, Medvinsky AL, Baranov VN, Lazareva MN, Poltoranina VS (1993) Common antigen of oval and biliary epithelial cells (A6) is a differentiation marker of epithelial and erythroid cell lineages in early development of the mouse. Differentiation 55:19–26

Evarts RP, Nagy P, Marsden E, Thorgeirsson SS (1987) A precursor-product relationship exists between oval cells and hepatocytes in rat liver. Carcinogenesis 8:1737–1740

Evarts RP, Nagy P, Nakatsukasa H, Marsden E, Thorgeirsson SS (1989) In vivo differentiation of rat liver oval cells into hepatocytes. Cancer Res 49:1541–1547

Evarts RP, Nakatsukasa H, Marsden ER, Hu Z, Thorgeirsson SS (1992) Expression of transforming growth factor-alpha in regenerating liver and during hepatic differentiation. Mol Carcinog 5:25–31

Evarts RP, Hu Z, Fujio K, Marsden ER, Thorgeirsson SS (1993) Activation of hepatic stem cell compartment in the rat: role of transforming growth factor alpha, hepatocyte growth factor, and acidic fibroblast growth factor in early proliferation. Cell Growth Differ 4:555–561

Falkowski O, An HJ, Ianus IA, Chiriboga L, Yee H, West AB, Theise ND (2003) Regeneration of hepatocyte "buds" in cirrhosis from intrabiliary stem cells. J Hepatol 39:357–364

Farber E (1956) Similarities in the sequence of early histological changes induced in the liver of the rat by ethionine, 2-acetylamino-fluorene, and 3′-methyl-4-dimethylaminoazobenzene. Cancer Res 16:142–148

Faris RA, Hixson DC (1989) Selective proliferation of chemically altered rat liver epithelial cells following hepatic transplantation. Transplantation 48:87–92

Faris RA, Monfils BA, Dunsford HA, Hixson DC (1991) Antigenic relationship between oval cells and a subpopulation of hepatic foci, nodules, and carcinomas induced by the "resistant hepatocyte" model system. Cancer Res 51:1308–1317

Fausto N, Campbell JS, Riehle KJ (2006) Liver regeneration. Hepatology 43:S45–53

Fischer M, Goldschmitt J, Peschel C, Brakenhoff JP, Kallen KJ, Wollmer A, Grotzinger J, Rose-John S (1997) A bioactive designer cytokine for human hematopoietic progenitor cell expansion. Nat Biotechnol 15:142–145

Forbes SJ, Russo FP, Rey V, Burra P, Rugge M, Wright NA, Alison MR (2004) A significant proportion of myofibroblasts are of bone marrow origin in human liver fibrosis. Gastroenterology 126:955–963

Forman BM, Tontonoz P, Chen J, Brun RP, Spiegelman BM, Evans RM (1995) 15-Deoxy-delta 12, 14-prostaglandin J2 is a ligand for the adipocyte determination factor PPAR gamma. Cell 83:803–812

Fujii H, Hirose T, Oe S, Yasuchika K, Azuma H, Fujikawa T, Nagao M, Yamaoka Y (2002) Contribution of bone marrow cells to liver regeneration after partial hepatectomy in mice. J Hepatol 36:653–659

Fujio K, Evarts RP, Hu Z, Marsden ER, Thorgeirsson SS (1994) Expression of stem cell factor and its receptor, c-kit, during liver regeneration from putative stem cells in adult rat. Lab Invest 70:511–516

Furst G, Schulte am Esch J, Poll LW, Hosch SB, Fritz LB, Klein M, Godehardt E, Krieg A, Wecker B, Stoldt V, Stockschlader M, Eisenberger CF, Modder U, Knoefel WT (2007) Portal vein embolization and autologous CD133+ bone marrow stem cells for liver regeneration: initial experience. Radiology 243:171–179

Gaia S, Smedile A, Omede P, Olivero A, Sanavio F, Balzola F, Ottobrelli A, Abate ML, Marzano A, Rizzetto M, Tarella C (2006) Feasibility and safety of G-CSF administration to induce bone marrow-derived cells mobilization in patients with end stage liver disease. J Hepatol 45:13–19

Gao Z, McAlister VC, Williams GM (2001) Repopulation of liver endothelium by bone-marrow-derived cells. Lancet 357:932–933

Gasbarrini A, Rapaccini GL, Rutella S, Zocco MA, Zocco P, Leone G, Pola P, Gasbarrini G, Di Campli C (2006) Rescue therapy by portal infusion of autologous stem cells in a case of drug-induced hepatitis. Dig Liver Dis 39:878–882

Gauldie J, Lamontagne L, Horsewood P, Jenkins E (1980) Immunohistochemical localization of alpha 1-antitrypsin in normal mouse liver and pancreas. Am J Pathol 101:723–735

Gehling UM, Willems M, Dandri M, Petersen J, Berna M, Thill M, Wulf T, Muller L, Pollok JM, Schlagner K, Faltz C, Hossfeld DK, Rogiers X (2005) Partial hepatectomy induces mobilization of a unique population of haematopoietic progenitor cells in human healthy liver donors. J Hepatol 43:845–853

Girgenrath M, Weng S, Kostek CA, Browning B, Wang M, Brown SA, Winkles JA, Michaelson JS, Allaire N, Schneider P, Scott ML, Hsu YM, Yagita H, Flavell RA, Miller JB, Burkly LC, Zheng TS (2006) TWEAK, via its receptor Fn14, is a novel regulator of mesenchymal progenitor cells and skeletal muscle regeneration. EMBO J 25:5826–5839

Gordon GJ, Coleman WB, Grisham JW (2000) Temporal analysis of hepatocyte differentiation by small hepatocyte-like progenitor cells during liver regeneration in retrorsine-exposed rats. Am J Pathol 157:771–786

Gordon MY, Levicar N, Pai M, Bachellier P, Dimarakis I, Al-Allaf F, M'Hamdi H, Thalji T, Welsh JP, Marley SB, Davies J, Dazzi F, Marelli-Berg F, Tait P, Playford R, Jiao L, Jensen S, Nicholls JP, Ayav A, Nohandani M, Farzaneh F, Gaken J, Dodge R, Alison M, Apperley JF, Lechler R, Habib NA (2006) Characterization and clinical application of human CD34+ stem/progenitor cell populations mobilized into the blood by granulocyte colony-stimulating factor. Stem Cells 24:1822–1830

Gouw AS, Heuvel MC van den, Boot M, Slooff MJ, Poppema S, Jong KP de (2006) Dynamics of the vascular profile of the finer branches of the biliary tree in normal and diseased human livers. J Hepatol 45:393–400

Gressner AM, Yagmur E, Lahme B, Gressner O, Stanzel S (2006) Connective tissue growth factor in serum as a new candidate test for assessment of hepatic fibrosis. Clin Chem 52:1815–1817

Hansson GK (2007) Medicine. LIGHT hits the liver. Science 316:206–207

Hasuike S, Ido A, Uto H, Moriuchi A, Tahara Y, Numata M, Nagata K, Hori T, Hayashi K, Tsubouchi H (2005) Hepatocyte growth factor accelerates the proliferation of hepatic oval cells and possibly promotes the differentiation in a 2-acetylaminofluorene/partial hepatectomy model in rats. J Gastroenterol Hepatol 20:1753–1761

Hatch HM, Zheng D, Jorgensen ML, Petersen BE (2002) SDF-1alpha/CXCR4: a mechanism for hepatic oval cell activation and bone

marrow stem cell recruitment to the injured liver of rats. Cloning Stem Cells 4:339–351

Heinrich PC, Behrmann I, Haan S, Hermanns HM, Muller-Newen G, Schaper F (2003) Principles of interleukin (IL)-6-type cytokine signalling and its regulation. Biochem J 374:1–20

Henderson NC, Iredale JP (2007) Liver fibrosis: cellular mechanisms of progression and resolution. Clin Sci (Lond) 112:265–280

Herrera MB, Bruno S, Buttiglieri S, Tetta C, Gatti S, Deregibus MC, Bussolati B, Camussi G (2006) Isolation and characterization of a stem cell population from adult human liver. Stem Cells 24:2840–2850

Higashiyama R, Inagaki Y, Hong YY, Kushida M, Nakao S, Niioka M, Watanabe T, Okano H, Matsuzaki Y, Shiota G, Okazaki I (2007) Bone marrow-derived cells express matrix metalloproteinases and contribute to regression of liver fibrosis in mice. Hepatology 45:213–222

Hixson DC, Allison JP (1985) Monoclonal antibodies recognizing oval cells induced in the liver of rats by N-2-fluorenylacetamide or ethionine in a choline-deficient diet. Cancer Res 45:3750–3760

Holic N, Suzuki T, Corlu A, Couchie D, Chobert MN, Guguen-Guillouzo C, Laperche Y (2000) Differential expression of the rat gamma-glutamyl transpeptidase gene promoters along with differentiation of hepatoblasts into biliary or hepatocytic lineage. Am J Pathol 157:537–548

Hsia CC, Thorgeirsson SS, Tabor E (1994) Expression of hepatitis B surface and core antigens and transforming growth factor-alpha in "oval cells" of the liver in patients with hepatocellular carcinoma. J Med Virol 43:216–221

Hu Z, Evarts RP, Fujio K, Marsden ER, Thorgeirsson SS (1993) Expression of hepatocyte growth factor and c-met genes during hepatic differentiation and liver development in the rat. Am J Pathol 142:1823–1830

Hu Z, Evarts RP, Fujio K, Marsden ER, Thorgeirsson SS (1995) Expression of fibroblast growth factor receptors flg and bek during hepatic ontogenesis and regeneration in the rat. Cell Growth Differ 6:1019–1025

Ide M, Kuwamura M, Kotani T, Sawamoto O, Yamate J (2005) Effects of gadolinium chloride ($GdCl_3$) on the appearance of macrophage populations and fibrogenesis in thioacetamide-induced rat hepatic lesions. J Comp Pathol 133:92–102

Isfort RJ, Cody DB, Stuard SB, Randall CJ, Miller C, Ridder GM, Doersen CJ, Richards WG, Yoder BK, Wilkinson JE, Woychik RPJ (1997)The combination of epidermal growth factor and transforming growth factor-beta induces novel phenotypic changes in mouse liver stem cell lines. J Cell Sci 110:3117–3129

Ito A, Nishikawa Y, Ohnuma K, Ohnuma I, Koma Y, Sato A, Enomoto K, Tsujimura T, Yokozaki H (2007) SgIGSF is a novel biliary-epithelial cell adhesion molecule mediating duct/ductule development. Hepatology 45:684–694

Jakubowski A, Browning B, Lukashev M, Sizing I, Thompson JS, Benjamin CD, Hsu YM, Ambrose C, Zheng TS, Burkly LC (2002) Dual role for TWEAK in angiogenic regulation. J Cell Sci 115:267–274

Jakubowski A, Ambrose C, Parr M, Lincecum JM, Wang MZ, Zheng S, Browning B, Michaelson JS, Baetscher M, Wang B, Bissell DM, Burkly LC (2005) TWEAK induces liver progenitor cell proliferation. J Clin Invest 115:2330–2340

Jelnes P, Santoni-Rugiu E, Rasmussen M, Friis SL, Nielsen JH, Tygstrup N, Bisgaard HC (2007) Remarkable heterogeneity displayed by oval cells in rat and mouse models of stem cell-mediated liver regeneration. Hepatology 45:1462–1470

Jensen CH, Jauho EI, Santoni-Rugiu E, Holmskov U, Teisner B, Tygstrup N, Bisgaard HC (2004) Transit-amplifying ductular (oval) cells and their hepatocytic progeny are characterized by a novel and distinctive expression of delta-like protein/preadipocyte factor 1/fetal antigen 1. Am J Pathol 164:1347–1359

Jin-no K, Tanimizu M, Hyodo I, Kurimoto F, Yamashita T (1997) Plasma level of basic fibroblast growth factor increases with progression of chronic liver disease. J Gastroenterol 32:119–121

Jung J, Zheng M, Goldfarb M, Zaret KS (1999) Initiation of mammalian liver development from endoderm by fibroblast growth factors. Science 284:1998–2003

Kawakita T, Shiraki K, Yamanaka Y, Yamaguchi Y, Saitou Y, Enokimura N, Yamamoto N, Okano H, Sugimoto K, Murata K, Nakano T (2005) Functional expression of TWEAK in human colonic adenocarcinoma cells. Int J Oncol 26:87–93

Kinoshita T, Sekiguchi T, Xu MJ, Ito Y, Kamiya A, Tsuji K, Nakahata T, Miyajima A (1999) Hepatic differentiation induced by oncostatin M attenuates fetal liver hematopoiesis. Proc Natl Acad Sci USA 96:7265–7270

Kinosita R (1937) Studies on the cancerogenic chemical substances. Trans Soc Pathol Jpn 27:329–334

Kirillova I, Chaisson M, Fausto N (1999) Tumor necrosis factor induces DNA replication in hepatic cells through nuclear factor kappaB activation. Cell Growth Differ 10:819–828

Kisseleva T, Uchinami H, Feirt N, Quintana-Bustamante O, Segovia JC, Schwabe RF, Brenner DA (2006) Bone marrow-derived fibrocytes participate in pathogenesis of liver fibrosis. J Hepatol 45:429–438

Knight B, Yeoh GC (2005) TNF/LTalpha double knockout mice display abnormal inflammatory and regenerative responses to acute and chronic liver injury. Cell Tissue Res 319:61–70

Knight B, Yeoh GC, Husk KL, Ly T, Abraham LJ, Yu C, Rhim JA, Fausto N (2000) Impaired preneoplastic changes and liver tumor formation in tumor necrosis factor receptor type 1 knockout mice. J Exp Med 192:1809–1818

Knight B, Matthews VB, Akhurst B, Croager EJ, Klinken E, Abraham LJ, Olynyk JK, Yeoh G (2005a) Liver inflammation and cytokine production, but not acute phase protein synthesis, accompany the adult liver progenitor (oval) cell response to chronic liver injury. Immunol Cell Biol 83:364–374

Knight B, Yeap BB, Yeoh GC, Olynyk JK (2005b) Inhibition of adult liver progenitor (oval) cell growth and viability by an agonist of the peroxisome proliferator activated receptor (PPAR) family member gamma, but not alpha or delta. Carcinogenesis 26:1782–1792

Knight B, Akhurst B, Matthews VB, Ruddell RG, Ramm GA, Abraham LJ, Olynyk JK, Yeoh GC (2007) Attenuated liver progenitor (oval) cell and fibrogenic responses to the choline deficient, ethionine supplemented diet in the BALB/c inbred strain of mice. J Hepatol 46:134–141

Koivisto UM, Hubbard AL, Mellman I (2001) A novel cellular phenotype for familial hypercholesterolemia due to a defect in polarized targeting of LDL receptor. Cell 105:575–585

Kollet O, Shivtiel S, Chen YQ, Suriawinata J, Thung SN, Dabeva MD, Kahn J, Spiegel A, Dar A, Samira S, Goichberg P, Kalinkovich A, Arenzana-Seisdedos F, Nagler A, Hardan I, Revel M, Shafritz DA, Lapidot T (2003) HGF, SDF-1, and MMP-9 are involved in stress-induced human CD34+ stem cell recruitment to the liver. J Clin Invest 112:160–169

Komuves LG, Feren A, Jones AL, Fodor E (2000) Expression of epidermal growth factor and its receptor in cirrhotic liver disease. J Histochem Cytochem 48:821–830

Kon J, Ooe H, Oshima H, Kikkawa Y, Mitaka T (2006) Expression of CD44 in rat hepatic progenitor cells. J Hepatol 45:90–98

Lagasse E, Connors H, Al-Dhalimy M, Reitsma M, Dohse M, Osborne L, Wang X, Finegold M, Weissman IL, Grompe M (2000) Purified hematopoietic stem cells can differentiate into hepatocytes in vivo. Nat Med 6:1229–1234

Lamas E, Kahn A, Guillouzo A (1987) Detection of mRNAs present at low concentrations in rat liver by in situ hybridization:

application to the study of metabolic regulation and azo dye hepatocarcinogenesis. J Histochem Cytochem 35:559–563

Laconi S, Curreli F, Diana S, Pasciu D, De Filippo G, Sarma DS, Pani P, Laconi E (1999) Liver regeneration in response to partial hepatectomy in rats treated with retrorsine: a kinetic study.J Hepatol 31:1069–1074

Lazaro CA, Rhim JA, Yamada Y, Fausto N (1998) Generation of hepatocytes from oval cell precursors in culture. Cancer Res 58:5514–5522

Leahy DJ (2004) Structure and function of the epidermal growth factor (EGF/ErbB) family of receptors. Adv Protein Chem 68:1–27

Lee JS, Heo J, Libbrecht L, Chu IS, Kaposi-Novak P, Calvisi DF, Mikaelyan A, Roberts LR, Demetris AJ, Sun Z, Nevens F, Roskams T, Thorgeirsson SS (2006) A novel prognostic subtype of human hepatocellular carcinoma derived from hepatic progenitor cells. Nat Med 12:410–416

Lemoli RM, Catani L, Talarico S, Loggi E, Gramenzi A, Baccarani U, Fogli M, Grazi GL, Aluigi M, Marzocchi G, Bernardi M, Pinna A, Bresadola F, Baccarani M, Andreone P (2006) Mobilization of bone marrow-derived hematopoietic and endothelial stem cells after orthotopic liver transplantation and liver resection. Stem Cells 24:2817–2825

Libbrecht L, Desmet V, Van Damme B, Roskams T (2000a) Deep intralobular extension of human hepatic "progenitor cells" correlates with parenchymal inflammation in chronic viral hepatitis: can "progenitor cells" migrate? J Pathol 192:373–378

Libbrecht L, Desmet V, Van Damme B, Roskams T (2000b) The immunohistochemical phenotype of dysplastic foci in human liver: correlation with putative progenitor cells. J Hepatol 33:76–84

Lim R, Knight B, Patel K, McHutchison JG, Yeoh GC, Olynyk JK (2006) Antiproliferative effects of interferon alpha on hepatic progenitor cells in vitro and in vivo. Hepatology 43:1074–1083

Lo JC, Wang Y, Tumanov AV, Bamji M, Yao Z, Reardon CA, Getz GS, Fu YX (2007) Lymphotoxin beta receptor-dependent control of lipid homeostasis. Science 316:285–288

Locksley RM, Killeen N, Lenardo MJ (2001) The TNF and TNF receptor superfamilies: integrating mammalian biology. Cell 104:487–501

Lowes KN, Brennan BA, Yeoh GC, Olynyk JK (1999) Oval cell numbers in human chronic liver diseases are directly related to disease severity. Am J Pathol 154:537–541

Mandache E, Vidulescu C, Gherghiceanu M, Dragomir P, Popescu LM (2002) Neoductular progenitor cells regenerate hepatocytes in severely damaged liver: a comparative ultrastructural study. J Cell Mol Med 6:59–73

Marsden ER, Hu Z, Fujio K, Nakatsukasa H, Thorgeirsson SS, Evarts RP (1992) Expression of acidic fibroblast growth factor in regenerating liver and during hepatic differentiation. Lab Invest 67:427–433

Marshall A, Rushbrook S, Davies SE, Morris LS, Scott IS, Vowler SL, Coleman N, Alexander G (2005) Relation between hepatocyte G1 arrest, impaired hepatic regeneration, and fibrosis in chronic hepatitis C virus infection. Gastroenterology 128:33–42

Matsusaka S, Tsujimura T, Toyosaka A, Nakasho K, Sugihara A, Okamoto E, Uematsu K, Terada N (1999) Role of c-kit receptor tyrosine kinase in development of oval cells in the rat 2-acetylaminofluorene/partial hepatectomy model. Hepatology 29:670–676

Matthews VB, Klinken E, Yeoh GC (2004) Direct effects of interleukin-6 on liver progenitor oval cells in culture. Wound Repair Regen 12:650–656

Matthews VB, Knight B, Timitz-Parker JE, Boon J, Olynyk JK, Yeoh GC (2005) Oncostatin M induces an acute phase response but does not modulate the growth or maturation-status of liver progenitor (oval) cells in culture. Exp Cell Res 306:252–263

Mavier P, Martin N, Couchie D, Preaux AM, Laperche Y, Zafrani ES (2004) Expression of stromal cell-derived factor-1 and of its receptor CXCR4 in liver regeneration from oval cells in rat. Am J Pathol 165:1969–1977

Menthena A, Deb N, Oertel M, Grozdanov PN, Sandhu J, Shah S, Guha C, Shafritz DA, Dabeva MD (2004) Bone marrow progenitors are not the source of expanding oval cells in injured liver. Stem Cells 22:1049–1061

Metcalf D, Gearing DP (1989) A myelosclerotic syndrome in mice engrafted with cells producing high levels of leukemia inhibitory factor (LIF). Leukemia 3:847–852

Michalopoulos GK, Bowen WC, Mule K, Stolz DB (2001) Histological organization in hepatocyte organoid cultures. Am J Pathol 159:1877–1887

Michalopoulos GK, Barua L, Bowen WC (2005) Transdifferentiation of rat hepatocytes into biliary cells after bile duct ligation and toxic biliary injury. Hepatology 41:535–544

Muller M, Morotti A, Ponzetto C (2002) Activation of NF-kappaB is essential for hepatocyte growth factor-mediated proliferation and tubulogenesis. Mol Cell Biol 22:1060–1072

Nagy P, Bisgaard HC, Thorgeirsson SS (1994) Expression of hepatic transcription factors during liver development and oval cell differentiation. J Cell Biol 126:223–233

Nagy P, Bisgaard HC, Santoni-Rugiu E, Thorgeirsson SS (1996) In vivo infusion of growth factors enhances the mitogenic response of rat hepatic ductal (oval) cells after administration of 2-acetylaminofluorene. Hepatology 23:71–79

Nagy P, Kiss A, Schnur J, Thorgeirsson SS (1998) Dexamethasone inhibits the proliferation of hepatocytes and oval cells but not bile duct cells in rat liver. Hepatology 28:423–429

Nakayama M, Kayagaki N, Yamaguchi N, Okumura K, Yagita H (2000) Involvement of TWEAK in interferon gamma-stimulated monocyte cytotoxicity. J Exp Med 192:1373–1380

Nguyen LN, Furuya MH, Wolfraim LA, Nguyen AP, Holdren MS, Campbell JS, Knight B, Yeoh GC, Fausto N, Parks WT (2007) Transforming growth factor-beta differentially regulates oval cell and hepatocyte proliferation. Hepatology 45:31–41

Neirhoff D, Ogawa A, Oertel M, Chen YQ, Shafritz DA (2005) Purification and characterization of mouse fetal liver epithelial cells with high in vivo repopulation capacity. Hepatology 42:130–139

Oben JA, Roskams T, Yang S, Lin H, Sinelli N, Li Z, Torbenson M, Huang J, Guarino P, Kafrouni M, Diehl AM (2003) Sympathetic nervous system inhibition increases hepatic progenitors and reduces liver injury. Hepatology 38:664–673

Oe H, Kaido T, Mori A, Onodera H, Imamura M (2005) Hepatocyte growth factor as well as vascular endothelial growth factor gene induction effectively promotes liver regeneration after hepatectomy in Solt-Farber rats.Hepatogastroenterology 52:1393–1397

Oh SH, Witek RP, Bae SH, Zheng D, Jung Y, Piscaglia AC, Petersen BE (2007) Bone marrow-derived hepatic oval cells differentiate into hepatocytes in 2-acetylaminofluorene/partial hepatectomy-induced liver regeneration. Gastroenterology 132:1077–1087

Olynyk JK, Yeoh GC, Ramm GA, Clarke SL, Hall PM, Britton RS, Bacon BR, Tracy TF (1998) Gadolinium chloride suppresses hepatic oval cell proliferation in rats with biliary obstruction. Am J Pathol 152:347–352

Omori N, Evarts RP, Omori M, Hu Z, Marsden ER, Thorgeirsson SS (1996) Expression of leukemia inhibitory factor and its recep tor during liver regeneration in the adult rat. Lab Invest 75: 15–24

Omori N, Omori M, Evarts RP, Teramoto T, Miller MJ, Hoang TN, Thorgeirsson SS (1997) Partial cloning of rat CD34 cDNA and expression during stem cell-dependent liver regeneration in the adult rat. Hepatology 26:720–727

Overturf K, Al-Dhalimy M, Ou CN, Finegold M, Grompe M (1997) Serial transplantation reveals the stem-cell-like regenerative

potential of adult mouse hepatocytes. Am J Pathol 151:1273–1280
Overturf K, Al-Dhalimy M, Finegold M, Grompe M (1999) The repopulation potential of hepatocyte populations differing in size and prior mitotic expansion. Am J Pathol 155:2135–2143
Paku S, Schnur J, Nagy P, Thorgeirsson SS (2001) Origin and structural evolution of the early proliferating oval cells in rat liver. Am J Pathol 158:1313–1323
Paku S, Dezso K, Kopper L, Nagy P (2005) Immunohistochemical analysis of cytokeratin 7 expression in resting and proliferating biliary structures of rat liver. Hepatology 42:863–870
Paradis V, Perlemuter G, Bonvoust F, Dargere D, Parfait B, Vidaud M, Conti M, Huet S, Ba N, Buffet C, Bedossa P (2001) High glucose and hyperinsulinemia stimulate connective tissue growth factor expression: a potential mechanism involved in progression to fibrosis in nonalcoholic steatohepatitis. Hepatology 34:738–744
Park DY, Suh KS (1999) Transforming growth factor-beta1 protein, proliferation and apoptosis of oval cells in acetylaminofluorene-induced rat liver regeneration. J Korean Med Sci 14:531–538
Pellegrini L (2001) Role of heparan sulfate in fibroblast growth factor signalling: a structural view. Curr Opin Struct Biol 11:629–634
Petersen BE, Bowen WC, Patrene KD, Mars WM, Sullivan AK, Murase N, Boggs SS, Greenberger JS, Goff JP (1999) Bone marrow as a potential source of hepatic oval cells. Science 284:1168–1170
Petersen BE, Grossbard B, Hatch H, Pi L, Deng J, Scott EW (2003) Mouse A6-positive hepatic oval cells also express several hematopoietic stem cell markers. Hepatology 37:632–640
Pi L, Oh SH, Shupe T, Petersen BE (2005) Role of connective tissue growth factor in oval cell response during liver regeneration after 2-AAF/PHx in rats. Gastroenterology 128:2077–2088
Preisegger KH, Factor VM, Fuchsbichler A, Stumptner C, Denk H, Thorgeirsson SS (1999) Atypical ductular proliferation and its inhibition by transforming growth factor beta1 in the 3,5-diethoxycarbonyl-1,4-dihydrocollidine mouse model for chronic alcoholic liver disease. Lab Invest 79:103–109
Rhim JA, Sandgren EP, Degen JL, Palmiter RD, Brinster RL (1994) Replacement of diseased mouse liver by hepatic cell transplantation. Science 263:1149–1152
Rosenberg D, Ilic Z, Yin L, Sell S (2000) Proliferation of hepatic lineage cells of normal C57BL and interleukin-6 knockout mice after cocaine-induced periportal injury. Hepatology 31:948–955
Roskams T (2003) Progenitor cell involvement in cirrhotic human liver diseases: from controversy to consensus. J Hepatol 39:431–434
Roskams T (2006) Liver stem cells and their implication in hepatocellular and cholangiocarcinoma. Oncogene 25:3818–3822
Roskams T, De Vos R, Oord JJ van den, Desmet V (1991) Cells with neuroendocrine features in regenerating human liver. APMIS Suppl 23:32–39
Roskams T, Yang SQ, Koteish A, Durnez A, DeVos R, Huang X, Achten R, Verslype C, Diehl AM (2003a) Oxidative stress and oval cell accumulation in mice and humans with alcoholic and nonalcoholic fatty liver disease. Am J Pathol 163:1301–1311
Roskams TA, Libbrecht L, Desmet VJ (2003b) Progenitor cells in diseased human liver. Semin Liver Dis 23:385–396
Russo FP, Alison MR, Bigger BW, Amofah E, Florou A, Amin F, Bou-Gharios G, Jeffery R, Iredale JP, Forbes SJ (2006) The bone marrow functionally contributes to liver fibrosis. Gastroenterology 130:1807–1821
Sanchez A, Factor VM, Schroeder IS, Nagy P, Thorgeirsson SS (2004) Activation of NF-kappaB and STAT3 in rat oval cells during 2-acetylaminofluorene/partial hepatectomy-induced liver regeneration. Hepatology 39:376–385
Santoni-Rugiu E, Jelnes P, Thorgeirsson SS, Bisgaard HC (2005) Progenitor cells in liver regeneration: molecular responses controlling their activation and expansion. APMIS 113:876–902
Saxena R, Theise ND, Crawford JM (1999) Microanatomy of the human liver-exploring the hidden interfaces. Hepatology 30:1339–1346
Schwartz RE, Reyes M, Koodie L, Jiang Y, Blackstad M, Lund T, Lenvik T, Johnson S, Hu WS, Verfaillie CM (2002) Multipotent adult progenitor cells from bone marrow differentiate into functional hepatocyte-like cells. J Clin Invest 109:1291–1302
Shafritz DA, Oertel M, Menthena A, Nierhoff D, Dabeva MD (2006) Liver stem cells and prospects for liver reconstitution by transplanted cells. Hepatology 43:S89–S98
Shiojiri N, Lemire JM, Fausto N (1991) Cell lineages and oval cell progenitors in rat liver development. Cancer Res 51:2611–2620
Shiota G, Okano J, Kawasaki H, Kawamoto T, Nakamura T (1995) Serum hepatocyte growth factor levels in liver diseases: clinical implications. Hepatology 21:106–112
Solt D, Farber E (1976) New principle for the analysis of chemical carcinogenesis. Nature 263:701–703
Streetz KL, Tacke F, Leifeld L, Wustefeld T, Graw A, Klein C, Kamino K, Spengler U, Kreipe H, Kubicka S, Muller W, Manns MP, Trautwein C (2003) Interleukin 6/gp130-dependent pathways are protective during chronic liver diseases. Hepatology 38:218–229
Subrata LS, Lowes KN, Olynyk JK, Yeoh GC, Quail EA, Abraham LJ (2005) Hepatic expression of the tumor necrosis factor family member lymphotoxin-beta is regulated by interleukin (IL)-6 and IL-1beta: transcriptional control mechanisms in oval cells and hepatoma cell lines. Liver Int 25:633–646
Suzuki A, Iwama A, Miyashita H, Nakauchi H, Taniguchi H (2003) Role for growth factors and extracellular matrix in controlling differentiation of prospectively isolated hepatic stem cells. Development 130:2513–2524
Taniguchi E, Kin M, Torimura T, Nakamura T, Kumemura H, Hanada S, Hisamoto T, Yoshida T, Kawaguchi T, Baba S, Maeyama M, Koga H, Harada M, Kumashiro R, Ueno T, Mizuno S, Ikeda H, Imaizumi T, Murohara T, Sata M (2006) Endothelial progenitor cell transplantation improves the survival following liver injury in mice. Gastroenterology 130:521–531
Tee LB, Smith PG, Yeoh GC (1992) Expression of alpha, mu and pi class glutathione S-transferases in oval and ductal cells in liver of rats placed on a choline-deficient, ethionine-supplemented diet. Carcinogenesis 13:1879–1885
Terada R, Yamamoto K, Hakoda T, Shimada N, Okano N, Baba N, Ninomiya Y, Gershwin ME, Shiratori Y (2003) Stromal cell-derived factor-1 from biliary epithelial cells recruits CXCR4-positive cells: implications for inflammatory liver diseases. Lab Invest 83:665–672
Terai S, Ishikawa T, Omori K, Aoyama K, Marumoto Y, Urata Y, Yokoyama Y, Uchida K, Yamasaki T, Fujii Y, Okita K, Sakaida I (2006) Improved liver function in patients with liver cirrhosis after autologous bone marrow cell infusion therapy. Stem Cells 24:2292–2298
Theise ND, Saxena R, Portmann BC, Thung SN, Yee H, Chiriboga L, Kumar A, Crawford JM (1999) The canals of Hering and hepatic stem cells in humans. Hepatology 30:1425–1433
Theise ND, Nimmakayalu M, Gardner R, Illei PB, Morgan G, Teperman L, Henegariu O, Krause DS (2000) Liver from bone marrow in humans. Hepatology 32:11–16
Theocharis SE, Margeli AP, Skaltsas SD, Skopelitou AS, Mykoniatis MG, Kittas CN (1997) Effect of interferon-alpha2b administration on rat liver regeneration after partial hepatectomy. Dig Dis Sci 42:1981–1986

Thorgeirsson SS, Grisham JW (2006) Hematopoietic cells as hepatocyte stem cells: a critical review of the evidence. Hepatology 43:2–8

Tian YW, Smith PG, Yeoh GC (1997) The oval-shaped cell as a candidate for a liver stem cell in embryonic, neonatal and precancerous liver: identification based on morphology and immunohistochemical staining for albumin and pyruvate kinase isoenzyme expression. Histochem Cell Biol 107:243–250

Tilg H, Wilmer A, Vogel W, Herold M, Nolchen B, Judmaier G, Huber C (1992) Serum levels of cytokines in chronic liver diseases. Gastroenterology 103:264–274

Toyonaga T, Hino O, Sugai S, Wakasugi S, Abe K, Shichiri M, Yamamura K (1994) Chronic active hepatitis in transgenic mice expressing interferon-gamma in the liver. Proc Natl Acad Sci USA 91:614–618

Tsamandas AC, Syrokosta I, Thomopoulos K, Zolota V, Dimitropoulou D, Liava A, Coupoulou AA, Siagris D, Petsas T, Karatza C, Gogos CA (2006) Potential role of hepatic progenitor cells expression in cases of chronic hepatitis C and their relation to response to therapy: a clinicopathologic study. Liver Int 26:817–826

Tsuchiya A, Heike T, Fujino H, Shiota M, Umeda K, Yoshimoto M, Matsuda Y, Ichida T, Aoyagi Y, Nakahata T (2005) Long-term extensive expansion of mouse hepatic stem/progenitor cells in a novel serum-free culture system. Gastroenterology 128:2089–2104

Vassilopoulos G, Wang PR, Russell DW (2003) Transplanted bone marrow regenerates liver by cell fusion. Nature 422:901–904

Vig P, Russo FP, Edwards RJ, Tadrous PJ, Wright NA, Thomas HC, Alison MR, Forbes SJ (2006) The sources of parenchymal regeneration after chronic hepatocellular liver injury in mice. Hepatology 43:316–324

Vivier I, Marguet D, Naquet P, Bonicel J, Black D, Li CX, Bernard AM, Gorvel JP, Pierres M (1991) Evidence that thymocyte-activating molecule is mouse CD26 (dipeptidyl peptidase IV). J Immunol 147:447–454

Wang X, Montini E, Al-Dhalimy M, Lagasse E, Finegold M, Grompe M (2002) Kinetics of liver repopulation after bone marrow transplantation. Am J Pathol 161:565–574

Wang X, Foster M, Al-Dhalimy M, Lagasse E, Finegold M, Grompe M (2003a) The origin and liver repopulating capacity of murine oval cells. Proc Natl Acad Sci USA 100 Suppl 1:11881–11888

Wang X, Willenbring H, Akkari Y, Torimaru Y, Foster M, Al-Dhalimy M, Lagasse E, Finegold M, Olson S, Grompe M (2003b) Cell fusion is the principal source of bone-marrow-derived hepatocytes. Nature 422:897–901

Wege H, Muller A, Muller L, Petri S, Petersen J, Hillert C (2007) Regeneration in pig livers by compensatory hyperplasia induces high levels of telomerase activity. Comp Hepatol 6:6

Wiemann SU, Satyanarayana A, Tsahuridu M, Tillmann HL, Zender L, Klempnauer J, Flemming P, Franco S, Blasco MA, Manns MP, Rudolph KL (2002) Hepatocyte telomere shortening and senescence are general markers of human liver cirrhosis. FASEB J 16:935–942

Willenbring H, Bailey AS, Foster M, Akkari Y, Dorrell C, Olson S, Finegold M, Fleming WH, Grompe M (2004) Myelomonocytic cells are sufficient for therapeutic cell fusion in liver. Nat Med 10:744–748

Wong S, Gauthier T, Kaita KD, Minuk GY (1995) The differential effects of three forms of interferon alfa on hepatic regeneration after partial hepatectomy in the rat. Hepatology 22:883–886

Yamada Y, Nishimoto E, Mitsuya H, Yonemura Y (2006) In vitro transdifferentiation of adult bone marrow Sca-1+ cKit- cells cocultured with fetal liver cells into hepatic-like cells without fusion. Exp Hematol 34:97–106

Yamazaki S, Miki K, Hasegawa K, Sata M, Takayama T, Makuuchi M (2003) Sera from liver failure patients and a demethylating agent stimulate transdifferentiation of murine bone marrow cells into hepatocytes in coculture with nonparenchymal liver cells. J Hepatol 39:17–23

Yannaki E, Athanasiou E, Xagorari A, Constantinou V, Batsis I, Kaloyannidis P, Proya E, Anagnostopoulos A, Fassas A (2005) G-CSF-primed hematopoietic stem cells or G-CSF per se accelerate recovery and improve survival after liver injury, predominantly by promoting endogenous repair programs. Exp Hematol 33:108–119

Yasui O, Miura N, Terada K, Kawarada Y, Koyama K, Sugiyama T (1997) Isolation of oval cells from Long-Evans Cinnamon rats and their transformation into hepatocytes in vivo in the rat liver. Hepatology 25:329–334

Yeoh GC, Ernst M, Rose-John S, Akhurst B, Payne C, Long S, Alexander W, Croker B, Grail D, Matthews VB (2007) Opposing roles of gp130-mediated STAT-3 and ERK-1/ 2 signaling in liver progenitor cell migration and proliferation. Hepatology 45:486–494

Yin L, Lynch D, Sell S (1999) Participation of different cell types in the restitutive response of the rat liver to periportal injury induced by allyl alcohol. J Hepatol 31:497–507

Yin L, Sun M, Ilic Z, Leffert HL, Sell S (2002) Derivation, characterization, and phenotypic variation of hepatic progenitor cell lines isolated from adult rats. Hepatology 35:315–324

Yovchev MI, Grozdanov PN, Joseph B, Gupta S, Dabeva MD (2007) Novel hepatic progenitor cell surface markers in the adult rat liver. Hepatology 45:139–149

Zhang M, Thorgeirsson SS (1994) Modulation of connexins during differentiation of oval cells into hepatocytes. Exp Cell Res 213:37–42

Zheng D, Oh SH, Jung Y, Petersen BE (2006) Oval cell response in 2-acetylaminofluorene/partial hepatectomy rat is attenuated by short interfering RNA targeted to stromal cell-derived factor-1. Am J Pathol 169:2066–2074

Znoyko I, Sohara N, Spicer SS, Trojanowska M, Reuben A (2005) Expression of oncostatin M and its receptors in normal and cirrhotic human liver. J Hepatol 43:893–900

Characterisation of a stereotypical cellular and extracellular adult liver progenitor cell niche in rodents and diseased human liver

Stefania Lorenzini,[1,2] Thomas G Bird,[1,3] Luke Boulter,[1,3] Christopher Bellamy,[4] Kay Samuel,[3] Rebecca Aucott,[1] Elizabeth Clayton,[1,3] Pietro Andreone,[2] Mauro Bernardi,[2] Mathew Golding,[5] Malcolm R Alison,[6] John P Iredale,[1] Stuart J Forbes[1,3]

► Additional figures are published online only. To view these files please visit the journal online (http://gut.bmj.com).

[1]MRC Centre for Inflammation Research, The Queen's Medical Research Institute, University of Edinburgh, Edinburgh, UK
[2]Department of Clinical Medicine, University of Bologna, Bologna, Italy
[3]MRC Centre for Regenerative Medicine, Chancellor's Building, University of Edinburgh, Edinburgh, UK
[4]Pathology Unit, the Royal Infirmary of Edinburgh, Edinburgh, UK
[5]Cancer Research UK, London, UK
[6]Centre for Diabetes and Metabolic Medicine, Barts and the London School of Medicine and Dentistry, Institute of Cell and Molecular Science, London, UK

Correspondence to
Professor Stuart J Forbes, MRC/University of Edinburgh Centre for Inflammation Research, The Queen's Medical Research Institute, 47 Little France Crescent, Edinburgh EH16 4TJ, UK;
stuart.forbes@ed.ac.uk

Revised 11 December 2009
Accepted 16 December 2009

ABSTRACT

Background Stem/progenitor cell niches in tissues regulate stem/progenitor cell differentiation and proliferation through local signalling.

Objective To examine the composition and formation of stem progenitor cell niches.

Methods The composition of the hepatic progenitor cell niche in independent models of liver injury and hepatic progenitor cell activation in rodents and humans was studied. To identify the origin of the progenitor and niche cells, sex-mismatched bone marrow transplants in mice, who had received the choline—ethionine-deficient-diet to induce liver injury and progenitor cell activation, were used. The matrix surrounding the progenitor cells was described by immunohistochemical staining and its functional role controlling progenitor cell behaviour was studied in cell culture experiments using different matrix layers.

Results The progenitor cell response in liver injury is intimately surrounded by myofibroblasts and macrophages, and to a lesser extent by endothelial cells. Hepatic progenitor cells are not of bone marrow origin; however, bone marrow-derived cells associate intimately with these cells and are macrophages. Laminin always surrounds the progenitor cells. In vitro studies showed that laminin aids maintenance of progenitor and biliary cell phenotype and promotes their gene expression (Dlk1, Aquaporin 1, γGT) while inhibiting hepatocyte differentiation and gene expression (CEPB/α).

Conclusions During liver damage in rodents and humans a stereotypical cellular and laminin niche forms around hepatic progenitor cells. Laminin helps maintenance of undifferentiated progenitor cells. The niche links the intrahepatic progenitor cells with bone marrow-derived cells and links tissue damage with progenitor cell-mediated tissue repair.

Significance of this study

What is already known about this subject?
- Hepatic progenitor cells are activated in chronic liver injury and contribute to liver regeneration.
- Hepatic progenitor cells are bipotential and can give rise to hepatocytic and biliary epithelial cells.

What are the new findings?
- A stereotypical progenitor cell niche, composed principally of macrophages, myofibroblasts and laminin matrix, develops in many types of chronic liver injury.
- This niche can develop rapidly in fibrosing cholestatic hepatitis and may contribute to the rapid development of fibrosis seen in this condition.
- The laminin matrix enables hepatic progenitor cells to remain in an undifferentiated phenotype.

How might it impact on clinical practice in the foreseeable future?
- Novel targets to control progenitor cell behaviour may be identified.
- The targeting of progenitor cells using drugs or other techniques may influence both liver regeneration and fibrosis.

INTRODUCTION

A stem cell niche is the restricted compartment in a tissue that maintains and regulates stem cell behaviour, supporting self-renewal and maintaining the balance between quiescence, proliferation and differentiation required in response to injury.[1 2] The existence of a niche structure was first proposed for haematopoietic stem cells in the bone marrow (BM)[3] and in gonads in invertebrate models.[4 5] In humans, the intestinal mucosa crypt has been extensively studied as a model of adult stem cell niche.[6]

In 1958, Wilson and Leduc[7] described a cell population in the distal biliary ducts of the liver capable of both hepatocyte and cholangiocyte differentiation. Subsequent studies[8 9] suggested that hepatocytes and bile duct epithelial cells were of common embryonic origin deriving from a common bipotential progenitor. The canals of Hering, the terminal branches of the intrahepatic biliary system, have been proposed as the source of those bipotential liver cells, termed oval cells (OCs) in rodents and hepatic progenitor cells (HPCs) in humans.[10] OCs are widely considered to be putative liver stem cells that can regenerate the parenchyma when hepatocyte proliferation is overwhelmed by persistent or severe liver injury. Recent studies have also suggested that deregulated OCs might be a potential source of liver cancer (eg, hepatocellular carcinoma and cholangiocarcinoma).[11]

Non-parenchymal cells (NPCs) in the liver include stellate cells/myofibroblasts, which are the main producers of collagen; macrophages, which are involved in tissue remodelling and fibrosis resolution after extensive damage[12]; endothelial cells, which are able to form new vessels[13]; and other leucocytes recruited by local inflammation. NPCs produce cytokines and growth factors, like transforming growth factor β, that influence OC/HPC and hepatocyte proliferation,[14] but most of the signals they exchange with the OC/HPC compartment and their role in regulating OC/HPC behaviour has yet to be fully elucidated.[15] Moreover, studies have demonstrated that in liver injury a proportion of myofibroblasts and macrophages are recruited from the BM.[16 17] It has been claimed that OCs are of BM origin[18 19]; however, other studies have found that OCs are intrinsic to the liver and not of BM origin.[20] We have used a dietary means of OC induction in BM transplanted mice to track which cells within the niche are of BM origin.

Cell—cell interaction and also cell—matrix interplay are likely to be important in regulating stem cell behaviour within niches.[2] In the liver, the extracellular matrix and basement membrane of the bile ducts, where OCs/HPCs reside, is mainly composed of laminin and type IV collagen.[21 22] Interestingly, laminin gene expression has been documented in NPCs in the liver and, in particular, in hepatic stellate cells and endothelial cells.[23 24] In the 2-acetylaminofluorene model of liver injury in rats, a laminin-rich basement membrane has been shown to be intimately associated with the OC response.[25] However, whether this is a general phenomenon in liver progenitor activation and the functional significance of the laminin matrix—progenitor cell interaction is not known.

To determine whether a stereotypical OC/HPC niche forms during liver regeneration, we deliberately analysed the liver tissue from a wide variety of liver injury models in rodent and human tissue and compared it with undamaged tissue. Having determined that a laminin matrix always surrounds the OC/HPC response, we studied the functional consequences of the laminin-rich basement membrane upon OC behaviour. Culturing OCs on various matrices we demonstrated that laminin allows maintenance of OCs in a progenitor/biliary phenotype, and inhibits hepatocyte differentiation. This is consistent with the hypothesis that the adult liver progenitor cell niche is a specialised environment where progenitor cells can remain undifferentiated and proliferate in response to injury, and upon leaving the laminin niche the cells differentiate into a hepatocyte phenotype.

Although progenitor cells are important for regenerating the liver in severe damage, deregulated OC/HPC proliferation might be a source of liver cancer.[11 26 27] Understanding how the niche influences OC/HPC behaviour is therefore likely to be of scientific and clinical importance if novel strategies are to be developed that can promote liver regeneration in the setting of chronic liver injury. Finally, while it is now accepted that niches are important for controlling stem/progenitor cell behaviour in several stem cell systems, the progenitor cells themselves may also influence the niche environment, including that of the liver.[28] Clearly, this could be important in diseases such as fibrosing cholestatic hepatitis where very rapid fibrosis is characteristic and ductular reactions/HPC responses are seen.

MATERIAL AND METHODS

Animal models

All animal work was carried out under procedural and ethical guidelines of the Home Office (UK). Three independent rodent models of OC activation were used to assess the cellular constituents of the liver tissue niche: (*a*) Male Fischer rats weighing 200 g were treated with 2-acetylaminofluorene and subsequent partial hepatectomy as previously described.[29] Livers were analysed from 3 to 13 days after partial hepatectomy. Livers from normal rats were used as controls. (2) Twenty-six-week-old female mice, transgenic for the hepatitis B surface antigen (HBsAg) were used. These mice have hepatocyte-specific expression of the hepatitis B virus BgIII-A fragment and develop hepatocellular injury. To induce OC proliferation animals were treated with the pyrrolizidine alkaloid, retrorsine, (70 mg/kg intraperitoneally, Sigma-Aldrich, Dorset, UK) with a further injection 2 weeks later. Liver tissue was analysed 6 months later. Liver from age-matched C57/B6 animals was used as control. (*c*) In a dietary protocol of OC induction C57/B6 mice were fed a diet composed of powdered choline-deficient chow (MP Biomedicals, Cambridge, UK) mixed in a 1:1 ratio with normal powdered chow (called the 50% CDE diet) supplemented with DL-ethionine (Sigma) at 0.15% in sweetened water (to improve animal tolerance to ethionine). To enable BM tracking, 6-week-old female mice were irradiated with whole-body gamma irradiation (10.5 Gray) followed by injection with 1×10^7 BM cells extracted from 6-week-old male femurs. Mice were allowed to reconstitute for 6 weeks and then started the diet or at 2 weeks before tissue analysis. Mice were treated for 1 week before and for 4 weeks after BM transplantation with Baytril antibiotics (W&J Dunlops, Dumfries, UK).

Human liver tissue

The human tissue analysed belonged to one of the following categories: (*a*) control liver tissue obtained from a pre-perfusion liver biopsy specimen (n=1); (*b*) tissue from patients with hepatitis C virus-related chronic hepatitis (n=10); (*c*) tissue from patients with hepatitis B virus chronic hepatitis (n=10); (*d*) tissue obtained from biopsies performed from 0 to 6 months after liver transplant in a patient who received a liver transplant for hepatitis C and developed recurrent fibrosing cholestatic hepatitis after transplant (n=1).

Immunohistochemistry (IHC)

Paraffin-embedded sections (3—5 μm) were dewaxed and rehydrated before IHC, which was performed using a standard avidin/biotin method. OCs (rodent tissue) and HPCs (human tissue) were identified using antibodies against either cytokeratin 19 (rat tissue; dilution 1:50, Novocastra, Newcastle-upon-Tyne, UK), wide-spectrum cytokeratin (mouse tissue; dilution 1:200, Dako, Cambridge, UK) or cytokeratin 7 (human tissue; dilution 1:100, Dako).

ED1 (rat tissue; dilution 1:400, Serotec), F4/80 (mouse tissue; dilution 1:10, eBioscience, Hatfield, UK) or CD68 (human tissue, dilution 1:200, Dako) were used to identify macrophages. Myofibroblasts were immunostained using an antibody to α smooth muscle actin (αSMA) (dilution 1:4000 (or 1:2000 for immunofluorescence), Sigma). Endothelial cells were detected using a von Willebrand factor (vWF) antibody (dilution 1:50, Dako). Laminin was detected using a rabbit polyclonal antibody to laminin (dilution 1:25, Dako). Clone numbers of primary antibodies are specified in table 1. For immunofluorescence goat anti-rabbit Alexa-488 (Invitrogen, Paisley, UK) conjugated, streptavidin Alexa-555 (Invitrogen) conjugated goat anti-mouse Cy5-labelled (Abcam, Cambridge, UK) secondary antibodies were used.

Fluorescent in situ hybridisation (FISH)

After IHC, sections were washed in phosphate-buffered saline (PBS) and incubated in 1 M sodium thiocyanate in distilled water for 10 min at 80°C, washed in PBS and digested in 0.4% w/v pepsin in 0.1 M HCl at 37°C for 4 min, quenched in 0.2%

Gut 2010;**59**:645—654. doi:10.1136/gut.2009.182345

Table 1 Clone numbers of primary antibodies

Primary antibodies	Manufacturers	Clone
α Smooth muscle actin (mouse, monoclonal)	Sigma	1A4
Cytokeratin 19 (mouse, monoclonal)	Novocastra	b170
CD68 (mouse anti-rat, monoclonal)	AbdSerotec	ED1
Laminin (rabbit, polyclonal)	Dako	-
F4/80 (rat, monoclonal)	eBioscience	BM8
Polyclonal rabbit anti-cytokeratin, wide spectrum screening	Dako	-
Cytokeratin 7 (mouse, monoclonal)	Dako	OV-TL 12/30
CD68 (mouse, monoclonal)	Dako	PG-M1
von Willebrand factor (rabbit, polyclonal)	Dako	-
CD45 (rat, monoclonal)	BD Pharmingen	30F11
Ki-67 (rabbit, polyclonal)	Novocastra	

glycine in double concentration PBS for 2 min, post-fixed in 4% paraformaldehyde for 2 min, dehydrated through graded alcohols and air dried. A fluorescein isothiocyanate-labelled Y chromosome paint (Star-FISH, Cambio, Cambridge, UK) was added to sections, sealed under a glass cover slip and heated to 60°C for 10 min before overnight incubation in a 37°C water bath. Slides were then washed in formamide (50% w/v)/2× saline sodium citrate (SSC) at 37°C, then with 2× SSC and, finally, with 4× SSC/Tween-20 (0.05% w/v) at 37°C. The slides were rinsed in 0.5× SSC at 37°C, then PBS before being mounted with 4′,6-diamidino-2-phenylindole containing mounting media (Vector Laboratories, Peterborough, UK).

Oval cell induction, progenitor cell isolation, culture and analysis

Eight-week-old C57/Bl6 mice were fed the CDE diet for 12 days, excised livers were minced and digested using 200 ng/ml DNAse1 (Roche, Hertfordshire, UK) and 1.25 mg/ml (=125 collagen-digesting units/mg solid) collagenase B (Sigma) in Leibovitz-15 media (Gibco, Paisley, UK). Digested liver was passed through a 40 µm cell strainer (BD Falcon, BD Biosciences, Oxford, UK) and the resulting suspension was spun over a 20%/50% discontinuous Percoll gradient (Sigma). Cells isolated from the 20%/50% boundary were resuspended in BD iMag buffer (BD Biosciences) and labelled with anti-CD45R beads (BD Biosciences), according to the manufacturer's instructions. Labelled cells were separated from other cells using a BD magnet. Those cells remaining after magnetic separation were used in culture. Cells were plated on plastic at a density of 3×10^{-4} cells/cm^2 and cultured for 7 days in Dulbecco's modified Eagle's medium (PAA Laboratories, Yeovil, UK) and Hams-F10 (Gibco). This was supplemented with 10% fetal calf serum (50 ng/ml insulin (Sigma) and 20 ng/ml hydrocortisone (Sigma). Sodium Pyruvate (PAA Laboratories), L-glutamine (PAA) and gentamicin (Gibco). Cells were then trypsinised and plated on 12-well tissue culture plates at 1×10^4 cells/cm^2 coated with laminin, collagen I, collagen IV or fibronectin, according to the manufacturer's instructions (all Sigma) with culture medium as before. The following day culture medium was supplemented with 5% fetal calf serum and 50 ng/ml epidermal growth factor (Sigma) and left for 5 days to differentiate, with media and epidermal growth factor being replaced every 2 days.

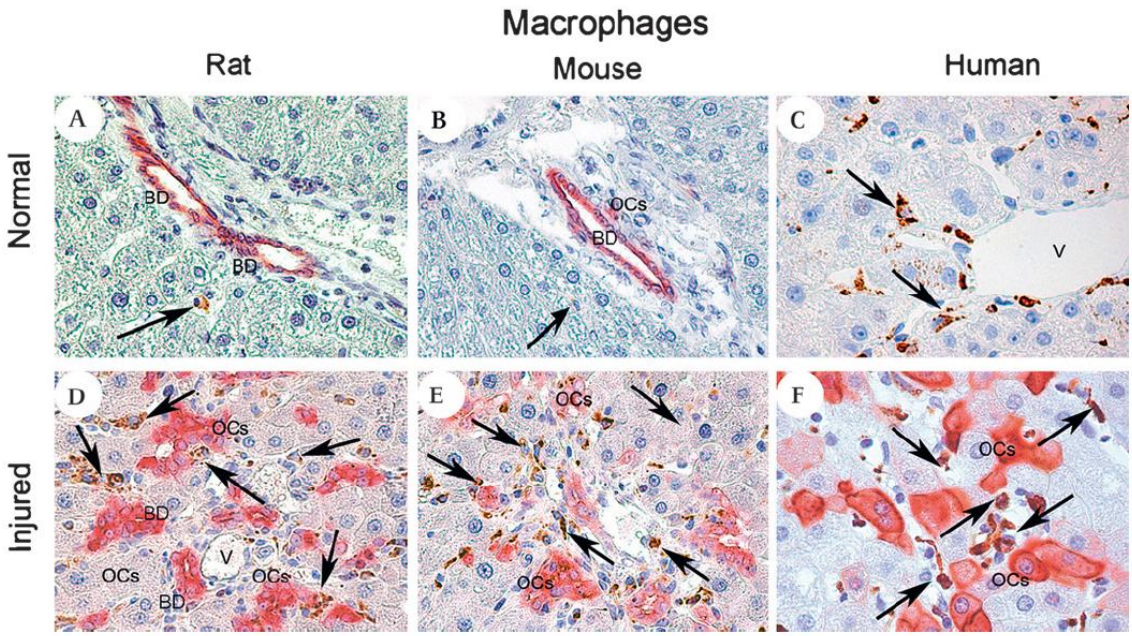

Figure 1 Macrophages. Photomicrographs illustrating rodent and human liver tissue to visualise the partner cells of the hepatic stem cell niche. In control liver tissue (A—C) the macrophage-specific staining shows only a few macrophages (black arrows) scattered near the portal areas but without any specific relationship with the bile ducts. (A) Normal rat liver, double staining for ED1 (brown) and CK19 (red); (B) normal mouse liver, F4/80 (brown); (C) biopsy specimen from control pre-perfusion donor liver, CD68 (brown). In damaged liver tissue (D—F), macrophages (black arrows) increase in number around the oval cells (OCs)/hepatic progenitor cells. (D) 2-Acetylaminofluorene and subsequent partial hepatectomy (2-AAF/PH) rat, day 9 after the PH—double staining for cytokeratin 19 (red) and ED1 (brown); (E) hepatitis B surface antigen-tg/retrorsine-treated mouse—F4/80 (brown); (F) hepatitis C virus-related cirrhotic human liver—double staining for CK7 (red) and CD68 (brown). Magnification (A—E) ×40; (F) ×60.

For gene expression analysis total mRNA was isolated from cells using the Qiagen RNeasy Mini kit (Qiagen, Crawley, UK) and reverse transcribed using the Quantitect Reverse Transcription kit (Qiagen), according to the manufacturer's instructions. Gene expression analysis was conduced using an Applied Biosystems 7500 thermocycler (Applied Biosystems, Warrington, UK), QuantiFast SYBR assay (Qiagen) and QuantiTect (Qiagen). All samples were run in triplicate. Statistical analysis using a two-tailed Student t test was performed using Prism software (GraphPad Software).

RESULTS

Composition of the OC/HPC niche

Consistent with previous reports, our models of rodent liver injury and injured human liver displayed a prominent expansion of the cytokeratin-positive OC/HPC compartment compared with control tissue (online supplementary figure 1).

Only diffusely spread macrophages (black arrows, brown) were seen in uninjured rodents and human liver and no clear spatial proximity to the bile ducts was discernible (figure 1A–C). In injured liver tissue (figure 1D–F), macrophages were found both clustered in areas where the OC/HPC reaction was evident, and distributed in tissue outside the site of the progenitor cell response. Close contact between macrophages and OCs/HPCs can be seen in double-stained images.

In normal liver tissue, αSMA+ myofibroblasts were seen only in very low number throughout the hepatic lobule, adjacent to bile ducts and in vessels walls (figure 2A–C). In both human and rodent injured liver an expanded population of αSMA+ myofibroblasts were seen periportally. Double staining confirmed an intimate association between myofibroblasts and the extending cords of OCs/HPCs (figure 2D–F), with myofibroblasts seen to line the columns of OCs/HPCs. Of note, the myofibroblasts formed a virtually continuous lining of the OC/HPC compartment, whereas macrophage association was more intermittent.

As expected, vWF+ staining was demonstrated in the sinusoids and vessel walls of uninjured liver (figure 3A–C), In contrast, vWF+ vessels were seen periportally adjacent to OCs/HPCs in the injured tissue (figure 3D–F). A rich inflammatory infiltrate was seen, particularly in human chronic viral hepatitis where lymphoid follicles were surrounded by myofibroblasts and HPCs (figure 4A). Double staining showed that inflammatory infiltrate surrounding HPC was mainly composed of T (figure 4B) and B (figure 4C) lymphocytes.

The niche in the HPC response during human liver disease: recurrent fibrosing cholestatic hepatitis and chronic viral hepatitis

We wished to study the cells associated with HPCs throughout the natural history of human liver disease, so we analysed liver tissue from a patient who had fibrosing cholestatic hepatitis due to hepatitis C recurrence after a liver transplant. Here, a pre-perfusion biopsy gave a baseline status (figure 5A). Over the next 6 months a marked ductular reaction developed owing to fibrosing cholestatic hepatitis (figure 5B). Sections serial to the HPCs were stained for macrophages (figure 5D) and myofibroblasts (figure 5E). These non-parenchymal cells were closely localised to the HPCs at both 1 (supplementary figure 2) and 6 months (figure 5C–E) after transplant. False colouring (figure 5F) of the three cell types from the 6-month serial sections with geographical

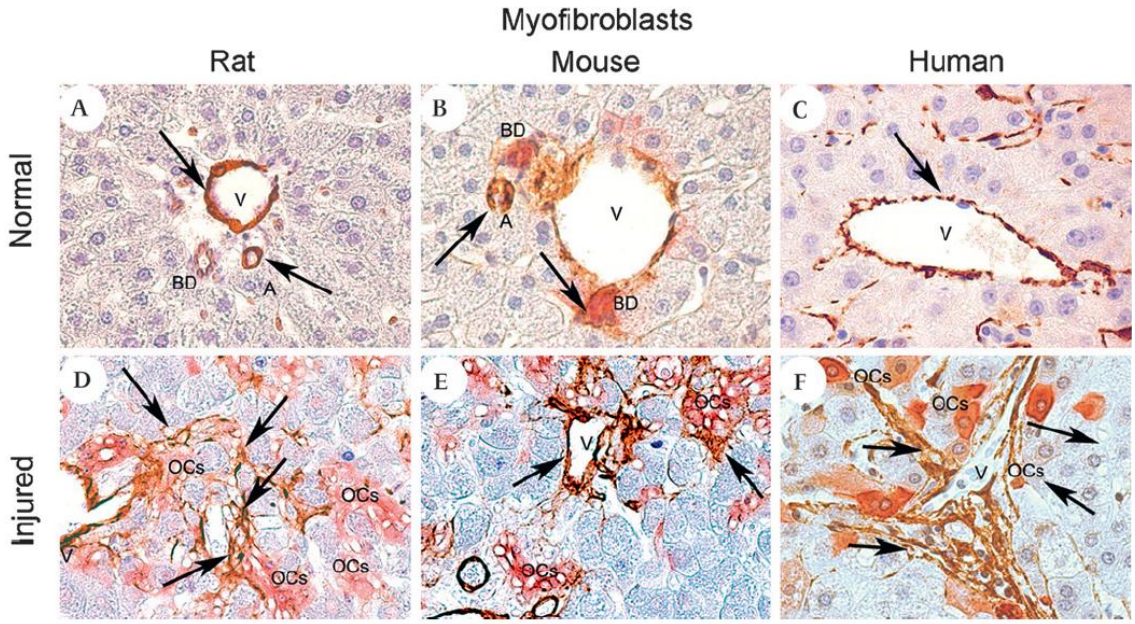

Figure 2 Myofibroblasts. Photomicrographs illustrating rodent and human liver tissue to visualise the partner cells of the hepatic stem cell niche. In control liver tissue (A–C) myofibroblast staining is localised mainly around the vessels (veins and arteries). (A) Normal rat liver, double staining for CK19 (red) and αSMA (brown); (B) normal mouse liver—double staining for panCK (red) and αSMA (brown); (C) control donor liver, αSMA (brown). In the injured liver (D–F) myofibroblasts form intimate contact with the bile ducts and the oval cells (OCs). (D) 2-Acetylaminofluorene and subsequent partial hepatectomy (2-AAF/PH) rat, day 9 after the PH—double staining for CK19 (red) and αSMA (brown); (E) hepatitis B surface antigen-tg-tg/retrorsine treated mouse—αSMA staining (brown); (F) hepatitis C virus-related cirrhotic liver—double staining for CK7 (red) and αSMA (brown). Magnification (A–E) ×40; (F) ×100.

Gut 2010;**59**:645–654. doi:10.1136/gut.2009.182345

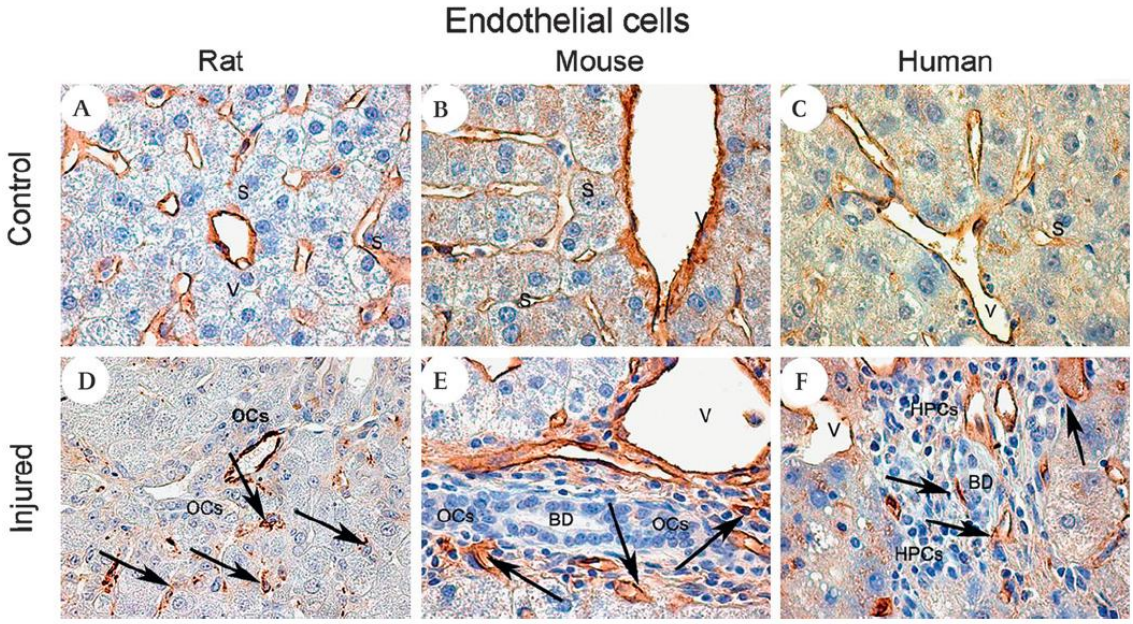

Figure 3 Endothelial cells. Photomicrographs illustrating rodent and human liver tissue to visualise the partner cells of the hepatic stem cell niche. In control liver tissue (A—C) the endothelial cell-specific marker von Willebrand factor (vWF; brown) highlights veins and sinusoids. (A) Normal rat liver; (B) normal mouse liver; (C) control human donor liver. In the injured liver (D—F) endothelial cells (black arrows) appear in close contact with the bile ducts and the oval cells (OCs). (D) 2-Acetylaminofluorene and subsequent partial hepatectomy (2AAF/PH) rat, day 9 after the PH—vWF (brown); (E) hepatitis B surface antigen-tg/retrorsine treated mouse—vWF (brown); (F) biopsy specimen from hepatitis C virus cirrhotic liver—vWF (brown). Magnification (A—F) ×40.

alignment and overlay demonstrated the spatial co-localisation of the macrophages and myofibroblasts with the HPC. To confirm this observation, we performed double immunostaining as above in 10 further patients with chronic hepatitis C and 10 patients with chronic hepatitis B (figure 6). In both type of hepatitis, we confirmed the existence of a close contact between HPCs and myofibroblasts (figure 6A,D), HPCs and macrophages (figure 6B,E) and HPCs and laminin (figure 6C,F).

Origin of the hepatic niche cells

To investigate the BM origin of the OCs and the associated non-parenchymal niche cells, we performed sex-mismatched BM transplants in mice to allow BM cell tracking using in situ hybridisation for the Y chromosome. Previous studies suggesting that OCs do not have a BM origin have been criticised owing to the possibility that hepatotoxins (eg, retrorsine) used in the OC induction experimental protocol may inhibit the BM stem cell response. In this study, we therefore decided to use a dietary regimen, the choline-deficient ethionine-supplemented diet (CDE) alone to induce the OC response in mice (figure 7A). Our current results agree with our previous findings that OCs are not of BM origin[20]; however, immediately adjacent to the OCs we frequently observed BM-derived cells (figure 7B). Dual immunostaining for OC (panCK) and macrophage (F4/80) markers in this model demonstrated their immediate proximity (figure 7C). Confocal analysis of serial sections immunostained for NPC

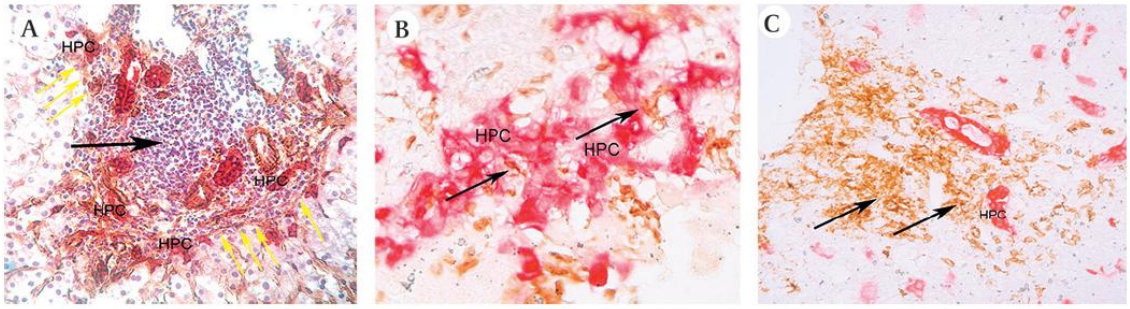

Figure 4 Inflammatory infiltrate and hepatic progenitor cells (HPC) niche in humans with chronic hepatitis C. (A) Photomicrograph showing small inflammatory cells (black arrow) surrounded by HPC (red, CK7) and myofibroblast (brown, αSMA, yellow arrows) proliferation in the liver biopsy specimen of a patient affected by severe chronic hepatitis C. Specific lymphocyte marker showed that the inflammatory cells were mainly B lymphocytes (C, CD20, brown) while T lymphocytes (B, CD3, brown, black arrows) were less common (magnification ×40).

markers demonstrated that the F4/80+ macrophages are the predominant BM-derived cell population in the niche (figure 8E). In contrast to previous work looking at the origin of stellate cells and myofibroblasts in models of chronic liver fibrosis,[17] although we did find Y-chromosome-positive stellate cells scattered throughout the parenchyma, we discovered that they did not co-localise with OCs in the present model of liver injury. It is possible that a longer period of injury would have produced a higher recruitment of myofibroblasts from the BM; however, this phenomenon appears to be injury dependent.

The matrix associated with the OC/HPC response is laminin rich

In rodent liver we found no relationship between collagen I and IV and the OCs (data not shown) but did find a striking relationship between laminin and the OCs in all rodent models of OC activation and human liver tissue studied. Laminin has previously been reported to be present in the basement membrane sheathing OCs. We found that laminin was present prominently around the portal vessels with weak staining in the hepatic sinusoids in the control liver (figure 9A–C). During liver injury, however, laminin was heavily deposited in a sheath which closely surrounds the OCs/HPCs (figure 9D–F), the OCs only extend as far as the laminin sheath (online supplementary figure 3A). Dual staining for laminin with OC and myofibroblast markers demonstrated that the laminin surrounded the OCs but co-localised with the myofibroblasts (supplementary figure 3D). However, in vitro cultures of isolated rat stellate cells and a rat OC line (LE6) confirmed that both cell types could produce laminin (supplementary figure 3E).

Laminin maintains a liver progenitor cell phenotype and aids biliary specification

We found that the extracellular matrix (ECM) strongly influenced the specification of OCs in vitro (figure 10). At baseline OCs were small rounded cells with high nuclear to cytoplasmic ratio which were panCK+. These cells were capable of proliferating for over 2 weeks in culture and increased in numbers (more than fourfold) between days 7 and 11. Isolated primary mouse OCs were cultured on plastic before switching to various ECMs. On plastic, initial cultures showed clusters of panCK+ HPCs (figure 10A). After replating on the matrices for 7 days no panCK + cells persisted on collagen I and IV (figure 10B). Only cells on laminin maintained panCK+ cells (figure 10C), and these cells kept their original morphology. Only on the fibronectin matrix did we see cells of a hepatocyte morphology which were positive for the differentiated hepatocyte marker Cyp2D6 (figure 10D). Gene expression was strongly influenced by the matrices (figure 10E–H). Compared with the control starting cell population

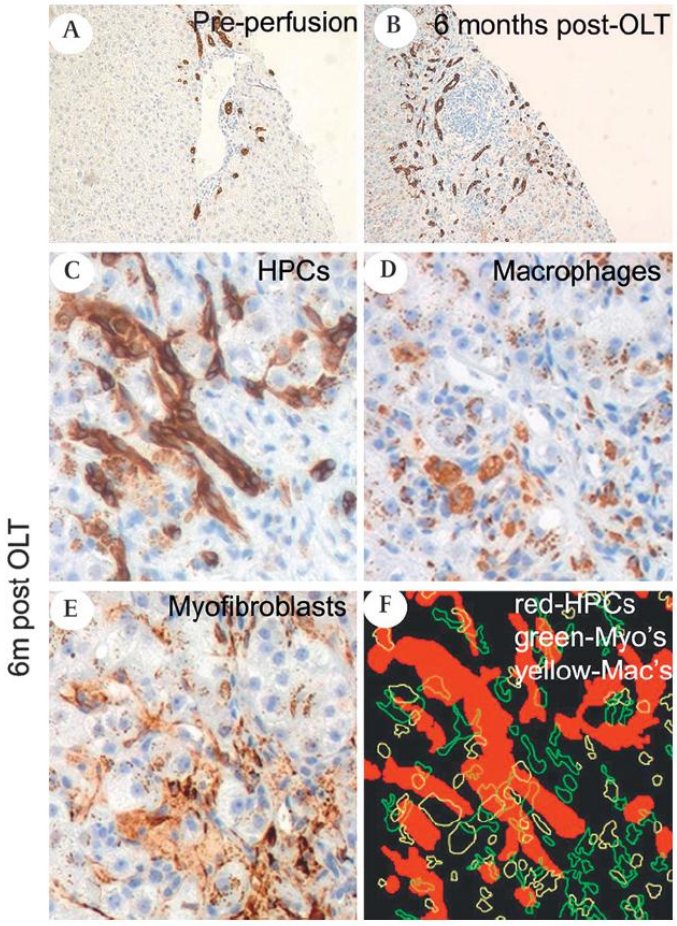

Figure 5 Liver progenitor cells rapidly expand in the human liver disease fibrosing cholestatic hepatitis. (A,B) Photomicrographs showing bile duct and hepatic progenitor cell (HPC) activation (CK7, brown) that has progressed rapidly in the liver of a patient who received a liver transplant for hepatitis C cirrhosis and developed fibrosing cholestatic hepatitis. (C–E) Serial sections from the 6-month biopsy reveal co-localisation of HPCs (CK7, brown), macrophages (CD68, brown) and myofibroblasts (αSMA). (F) In a composite image from the aligned sections, HPCs, macrophages and myofibroblasts are highlighted in red, yellow and green, respectively, and can be seen closely localised (magnification ×200). OLT, orthotopic liver transplantation.

Gut 2010;**59**:645–654. doi:10.1136/gut.2009.182345

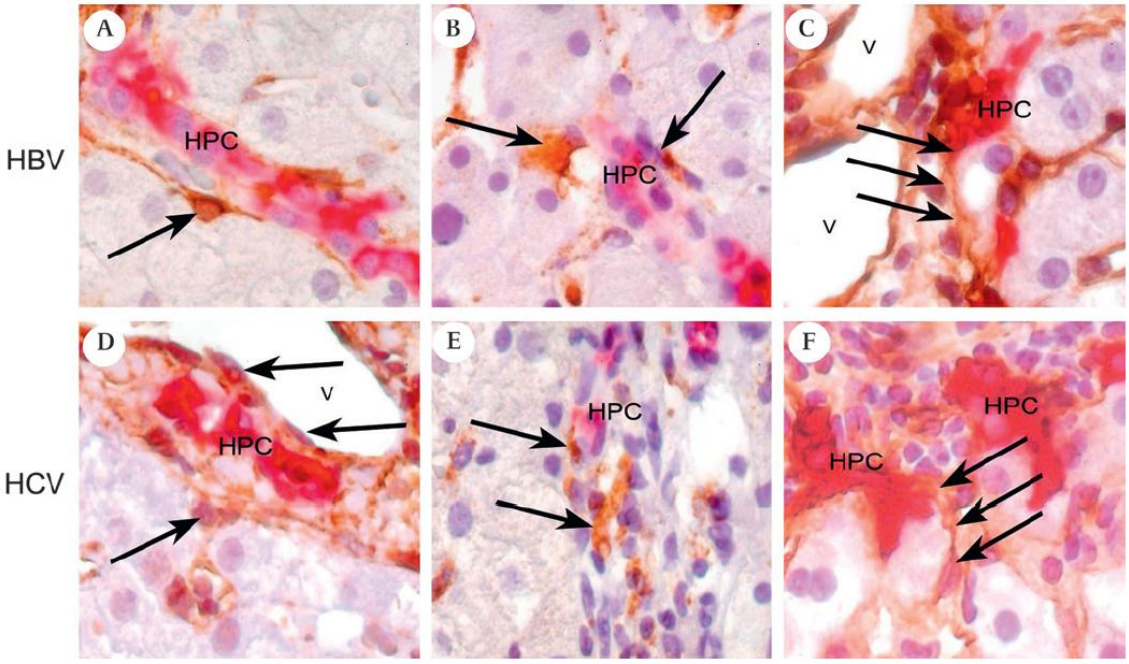

Figure 6 A cellular niche consistently forms round progenitor cells in chronic viral hepatitis. Photomicrographs showing co-localisation of hepatic progenitor cells (HPC) with myofibroblasts (A,D), macrophages (B,E), and laminin (C,F) in chronic hepatitis B (HBV) and C (HCV) in humans. (A,D) CK7—red, αSMA—brown, black arrows indicating a myofibroblast lying HPC; (B,E) CK7—red; CD68—brown, black arrows indicating macrophages; (C,F) CK7—red, laminin—brown, black arrows indicating the laminin sheath (magnification ×100). These pictures are representative of the 10 patients with hepatitis C and of the 10 patients with hepatitis B whose liver biopsies were analysed.

laminin profoundly upregulated progenitor (DLK1) and biliary (GGT, Aquaporin 1) genes while significantly inhibiting the early hepatocyte genes CEBP/a. In contrast, collagen I and IV and fibronectin inhibited or did not influence these progenitor and biliary genes but fibronectin strongly promoted CEPB/a gene expression. These results show that OCs have an ability to form hepatocytes and biliary epithelial cells that is influenced by the ECM.

DISCUSSION

Liver regeneration usually occurs through hepatocyte division but in advanced or severe chronic liver disease, hepatocytes are unable to replicate efficiently and progenitor cells can regenerate the parenchyma.[15 20] These OCs/HPCs have been well characterised but there is little data on their surrounding environment (or 'niche'). In this study, we have systematically examined OC/HPC reactions in both rodent models of OC activation and in human liver disease. We elected to identify OCs/HPCs using cytokeratins as these are already widely accepted HPCs markers and as we have demonstrated, in accordance with previous studies, are analogous between species and models.[10 27] Furthermore here we demonstrate that these cells represent a progenitor cell population which, while potentially heterogeneous, contains cells with the ability to form both hepatic epithelial lineages.

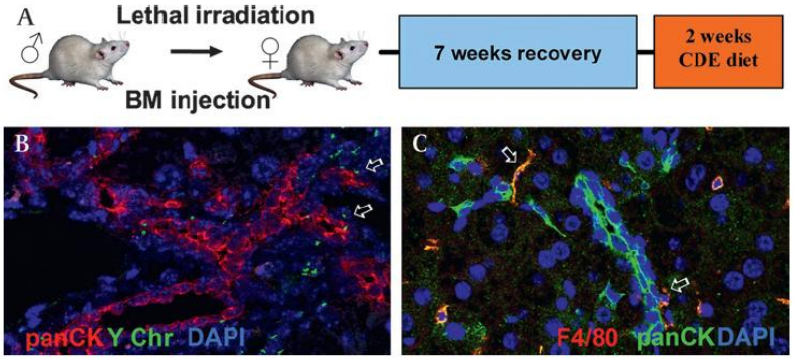

Figure 7 The origin of the oval cells in a mouse model of oval cell activation (choline-deficient ethionine-supplemented diet (CDE diet)). (A) Female mice were irradiated followed by injection of BM cells from a male donor. Seven weeks later the mice were treated with the ½ CDE diet for 2 weeks before tissue analysis. (B) Representative region of staining for oval cells (panCK, red) and in situ hybridisation for mouse Y chromosome (Y Chr, green). Arrows indicate Y chromosome-positive cells adjacent to panCK+ cells. (C) Double immunofluorescence for F4/80 (red) and panCK (green) in a mouse treated with the CDE diet for 2 weeks. Arrows indicate F4/80+ cells adjacent to panCK+ cells (magnification (B) ×10; (C) ×20).

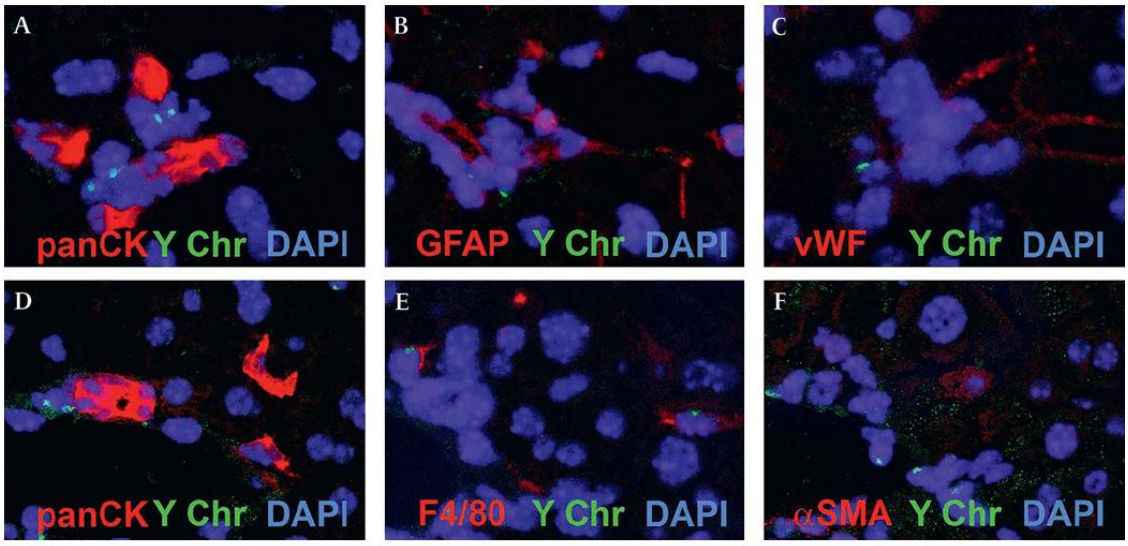

Figure 8 The origin of the oval cell (OC)-associated niche cells in a mouse model of OC activation (choline-deficient ethionine-supplemented diet (CDE diet)). (A—C) and (D—F) Confocal analysis of serial sections of sex-mismatched mice treated with the CDE diet. Staining with panCK (A,D) demonstrated closely localised cells positive for GFAP (B), vWF (C), F4/80 (E) and αSMA (F). F4/80 but not GFAP, αSMA or panCK cells are Y chromosome positive (magnification ×400).

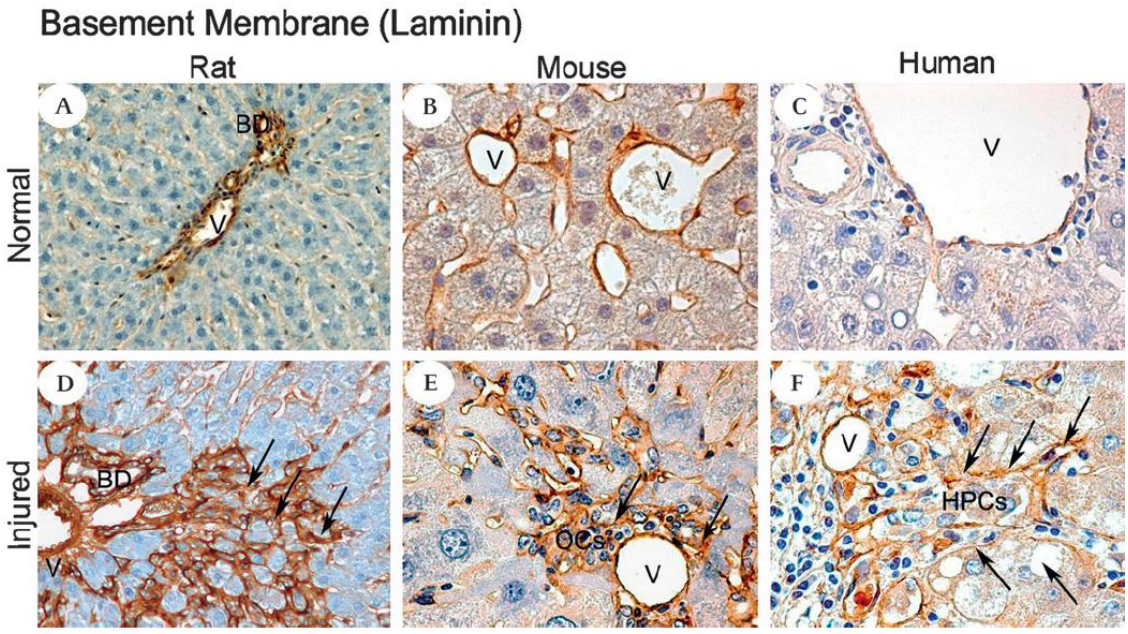

Figure 9 Laminin consistently surrounds liver progenitor cells in a variety of liver injury models and human disease. Photomicrographs illustrating laminin in the control liver (A, B, C) Normal rat, mouse and human pre-perfusion donor liver, respectively. A thin laminin layer (brown) is localised mainly around the bile ducts and the vessels. In the injured liver (D,E,F) laminin staining shows the appearance of a thicker membrane that spreads from the portal tract and builds a network-like structure intimately surrounding the oval cells /hepatic progenitor cells. (D) 2-Acetylaminofluorene and subsequent partial hepatectomy (2-AAF/PH) rat day 9 after the PH - laminin (brown, arrows); (E) hepatitis B surface antigen-tg/retrorsine treated mouse—laminin (brown, arrows); (F) hepatitis C virus-related cirrhotic liver—laminin (brown, arrows). (See also online supplementary figure 2.) Magnification (A,D) ×10; (B,C,E,F) ×40.

Gut 2010;**59**:645—654. doi:10.1136/gut.2009.182345

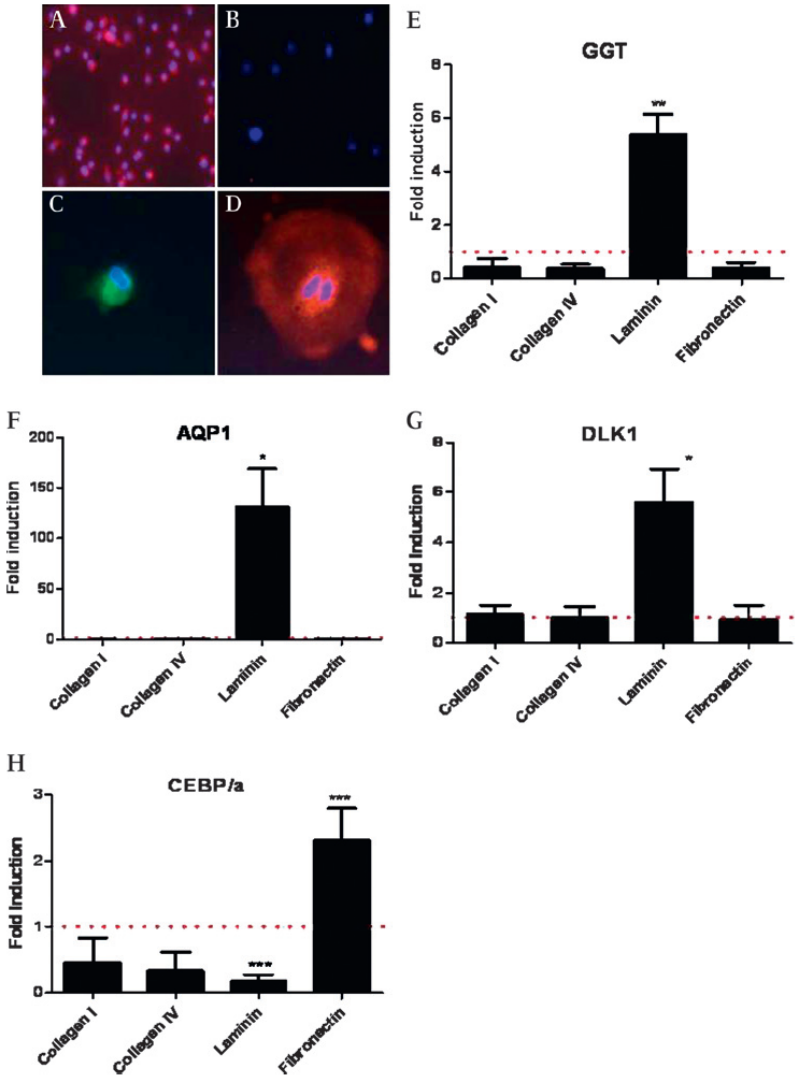

Figure 10 The extracellular matrix determines oval cell (OC) cell behaviour. (A) Freshly isolated murine OCs showed high expression of panCK (red, nuclei blue). (B) After 1 weeks culture on collagen I or IV, no panCK+ cells persisted; (C) however, on laminin, panCK+ cells (panCK green, nuclei blue) were seen. No hepatocytes were differentiated from OCs on laminin. (D) Cells with a hepatocyte morphology (here binuclear and Cyp2D6+, red) were seen on the fibronectin matrix. (E, F,G) Laminin strongly promoted the gene expression of the biliary markers Aquaporin 1 (AQP1) ($n=6$, $p<0.05$) and GGT ($n=6$, $p<0.005$), and the liver progenitor marker DLK1 ($n=6$, $p<0.05$). (H) The early hepatocyte gene CEBP/a is found upregulated on fibronectin ($n=6$, $p<0.0005$); however, there is a significant reduction in CEBP/a gene expression when cells are cultured in the presence of laminin ($n=6$, $p<0.0005$). Values are relative to control cells grown on plastic just before replating onto the matrices (red dotted line).

We found that the OCs/HPCs are closely accompanied by a cellular niche composed of myofibroblasts, macrophages and endothelial cells throughout the progenitor cell response, which remains consistent throughout a range of diverse rodent models of OC activation and also in human liver disease. We sought to identify the origin of the niche cells using genetic tracking techniques in a dietary model of OC activation. This confirmed that in a dietary model of OC activation, without retrorsine administration, OCs/HPCs are definitely of intrahepatic origin; they are, however, intimately surrounded by macrophages of BM origin. This provides a potential link between the BM and the intrahepatic stem/progenitor cells during injury, whereby the BM does not directly contribute to these cells but may influence their behaviour. In contrast with our previously published study,[17] only a few scattered myofibroblasts were found to be of BM origin in the CDE diet model of liver injury and these cells did not localise with the OCs. It may be that longer injury would increase the recruitment of cells from the BM or, alternatively, the mode of liver injury may influence the magnitude of recruitment.

The exact role of these progenitor-associated macrophages and myofibroblasts is unknown; however, these NPCs may act as a link between tissue injury and progenitor cell activation. Indeed, hepatic macrophages and myofibroblasts can express a variety of signals critical for controlling liver development and hepatic stem/progenitor cell behaviour.[27] Macrophages can also remodel the ECM through the production of metalloproteinases,[30] a process that may be necessary for the extension of the OC/HPC response.

In addition to signals passing from the niche cells to the progenitor cells, there may also be signalling from the progenitor cells to the niche cells. We hypothesise that the profound progenitor cell response seen in severe chronic liver disease, such as fibrosing cholestatic hepatitis after transplantation may account for the local activation of

myofibroblasts and macrophages and thus may help to explain the extremely rapid fibrosis in this condition; however, this hypothesis will require further evaluation.

Little is known about the influence of the ECM upon OC function but the uniform presence of laminin around OCs suggests an important role. We hypothesised that laminin was influencing the progenitors and allowing maintenance of the undifferentiated phenotype. Indeed our previous studies have found that laminin matrix promotes the proliferation and expansion of OCs in vitro.[31] We sought to investigate this in a controlled in vitro system. Using isolated primary murine OCs, we found that laminin, unlike the other matrices tested, permitted the culture of OCs in an undifferentiated phenotype. Laminin also promoted gene expression of biliary/OC genes and significantly inhibited expression of the early hepatocyte gene CEBP/a. These findings are consistent with a key role for laminin in controlling liver progenitor cell fate.

In summary, we have shown using independent rodent models of severe liver injury and human disease that a niche composed of myofibroblasts, macrophages and laminin always surrounds the progenitor cells. The OCs are definitively of intrahepatic origin and do not derive from the BM, but macrophages of BM origin intimately associate with the OCs. The signalling pathways linking OCs/HPCs and the cells in the niche are likely to be bidirectional. Simultaneous alteration in matrix composition, activation of resident non-parenchymal cells and activation of intrahepatic progenitor cells are features of liver regeneration. Future work will therefore focus on these matrix–progenitor cell and niche–progenitor cell interactions in order to develop therapeutic interventions in chronic liver diseases.

Acknowledgements SJF is supported by the Medical Research Council, Wellcome Trust and Jules Thorn Trust. SL is supported by European Association for the Study of the Liver (EASL) Sheila Sherlock Post-Doc Fellowship and by "Ordine dei Medici Chirurghi ed Odontoiatri di Bologna". TGB is supported by a Wellcome Trust Clinical Training Fellowship. The authors wish to thank Professor Roland Wolfe for the kind provision of the Cyp2D6 antibody and Professor Nelson Fausto for kindly supplying the LE/6 cell lines used in this study.

Funding Medical Research Council. Other Funders: Wellcome Trust.

Competing interests None to declare.

Patient consent Obtained.

Contributors SL and TGB have contributed equally to this work.

Provenance and peer review Not commissioned; externally peer reviewed.

REFERENCES

1. **Fuchs E,** Tumbar T, Guasch G. Socializing with the neighbors: stem cells and their niche. *Cell* 2004;**116**:769–78.
2. **Spradling A,** Drummonf-Barboda D, Kai T. Stem cells find their niche. *Nature* 2001;**414**:98–104.
3. **Schofield R.** The relationship between the spleen colony-forming cell and the haematopoietic stem cell. *Blood Cells* 1978;**4**:7–25.
4. **Xie T,** Spradling AC. A niche maintaining germ line stem cells in the Drosophila ovary. *Science* 2000;**290**:328–30.
5. **Crittenden S,** Bernstein DS, Bachorik JL, *et al*. A conserved RNA-binding proteins controls germline stem cells in Caenorhabditis elegans. *Nature* 2002;**417**:660–3.
6. **Leedham SJ,** Brittan M, McDonald SAC, *et al*. Intestinal Stem Cells. *J Cell Mol Med* 2005;**9**:11–24.
7. **Wilson JW,** Leduc EH. Roles of cholangioles in restoration of the liver of the mouse after dietary injury. *J Pathol Bacteriol* 1958;**76**:441–9.
8. **Wilson JW,** Groat CS, Leduc EH. Histogenesis of the liver. *Ann N Y Acad Sci* 1963;**111**:8–22.
9. **Theise ND,** Saxena R, Portmann BC, *et al*. The canals of Hering and hepatic stem cells in humans. *Hepatology* 1999;**30**:1425–33.
10. **Roskams TA,** Theise ND, Balabaud C, *et al*. Nomenclature of the finer branches of the biliary tree: canals, ductules, and ductular reactions in human livers. *Hepatology* 2004;**39**:1739–45.
11. **Lee JS,** Heo J, Libbrecht L, *et al*. A novel prognostic subtype of human hepatocellular carcinoma derived from hepatic progenitor cells. *Nat Med* 2006;**12**:410–6.
12. **Duffield JS,** Forbes SJ, Constandinou CM, *et al*. Selective depletion of macrophages reveals distinct, opposing roles during liver injury and repair. *J Clin Invest* 2005;**115**:56–65.
13. **Bockhorn M,** Goralski M, Prokofiev D, *et al*. VEGF is important for early liver regeneration after partial hepatectomy. *J Surg Res* 2007;**138**:291–9.
14. **Nguyen LN,** Furuya MH, Wolfraim LA, *et al*. Transforming growth factor-beta differentially regulates oval cell and hepatocyte proliferation. *Hepatology* 2007;**45**:31–41.
15. **Roskams TA,** Libbrecht L, Desmet VJ. Progenitor cells in diseased human liver. *Semin Liver Dis* 2003;**23**:385–96.
16. **Forbes SJ,** Russo F, Rey V, *et al*. A significant proportion of myofibroblasts are of bone marrow origin in human liver fibrosis. *Gastroenterology* 2004;**126**:955–63.
17. **Russo FP,** Alison MR, Bigger BW, *et al*. The bone marrow functionally contributes to liver fibrosis. *Gastroenterology* 2006;**130**:1807–21.
18. **Petersen BE,** Bowen WC, Patrene KD, *et al*. Bone marrow as a potential source of hepatic oval cells. *Science* 1999;**284**:1168–70.
19. **Oh SH,** Witek RP, Bae S, *et al*. Bone marrow-derived hepatic oval cells differentiate into hepatocytes in 2-acetylaminofluorene/partial hepatectomy-induced liver regeneration. *Gastroenterology* 2007;**132**:1077–87.
20. **Vig P,** Russo FP, Edwards RJ, *et al*. The sources of parenchymal regeneration after chronic hepatocellular liver injury in mice. *Hepatology* 2006;**43**:316–24.
21. **Terada T,** Nakanuma Y. Expression of tenascin, type IV collagen and laminin during human intrahepatic bile duct development and in intrahepatic cholangiocarcinoma. *Histopathology* 1994;**25**:143–50.
22. **Yasoshima M,** Tsuneyama K, Harada K, *et al*. Immunohistochemical analysis of cell-matrix adhesion molecules and their ligands in the portal tracts of primary biliary cirrhosis. *J Pathol* 2000;**190**:93–9.
23. **Knittel T,** Janneck T, Muller L, *et al*. Transforming growth factor B1-regulated gene expression in Ito cells. *Hepatology* 1996;**24**:352–60.
24. **Nikolova G,** Strilic B, Lammert E. The vascular niches and its basement membrane. *Trends Cell Biol* 2006;**17**:19–25.
25. **Paku S,** Nagy P, Kopper L, *et al*. 2-Acetylaminofluorene dose-dependent differentiation of rat oval cells into hepatocytes: confocal and electron microscopic studies. *Hepatology* 2004;**39**:1353–61.
26. **Chiba T,** Kita K, Zheng YW, *et al*. Side population purified from hepatocellular carcinoma cells harbors cancer stem cell-like properties. *Hepatology* 2006;**44**:240–51.
27. **Bird TG,** Lorenzini S, Forbes SJ. Activation of stem cells in hepatic disease. *Cell Tissue Res* 2008;**331**:283–300.
28. **Knight B,** Akhurst B, Matthews VB, *et al*. Attenuated liver progenitor (oval) cell and fibrogenic responses to the choline deficient, ethionine supplemented diet in the BALB/c inbred strain of mice. *J Hepatol* 2007;**46**:134–41.
29. **Alison MR,** Golding M, Lalani EN, *et al*. Wholesale hepatocyte differentiation in the rat from ductular oval cells, the progeny of biliary stem cells. *J Hepatol* 1997;**26**:343–52.
30. **Fallowfield JA,** Mizuno M, Kendall TJ, *et al*. Scar-associated macrophages are a major source of hepatic matrix metalloproteinase-13 and facilitate the resolution of murine hepatic fibrosis. *J Immunol* 2007;**178**:5288–95.
31. **Clayton E,** Forbes SJ. The isolation and in vitro expansion of hepatic Sca-1 progenitor cells. *Biochem Biophys Res Commun* 2009;**381**:549–53.

Appendix 2 Wnt pathway array data (whole liver)

		CDE diet vs control					C57Bl6 control vs S129P2 control		DDC diet vs control				
		AVG ΔC_t		Fold Change		p-value	Fold Change		AVG ΔC_t		Fold Change		p-value
Gene Symbol	Gene Name	CDE diet	C57Bl6 control	CDE diet/ Control	95% CI	P Value	C57Bl control/ S129P2 control	95% CI	DDC diet	S129P2 control	DDC diet/ Control	95% CI	P Value
Aes	Amino-terminal enhancer of split	2.34	2.03	0.81	(0.64, 0.98)	0.112722	0.93	(0.74, 1.12)	3.34	2.14	0.43	(0.38, 0.48)	0.000462
Apc	Adenomatosis polyposis coli	4.03	3.74	0.82	(0.65, 0.99)	0.124535	0.86	(0.77, 0.95)	4.17	3.96	0.86	(0.79, 0.93)	0.020845
Axin1	Axin 1	6.39	6.38	1	(0.69, 1.31)	0.907623	1.75	(0.90, 2.60)	6.68	5.57	0.46	(0.28, 0.64)	0.038327
Bcl9	B-cell CLL/lymphoma 9	9.02	8.74	0.82	(0.67, 0.97)	0.088077	1.64	(1.02, 2.26)	7.94	8.03	1.06	(0.63, 1.49)	0.864282
Btrc	Beta-transducin repeat containing protein	7.22	6.98	0.85	(0.70, 1.00)	0.167281	2.52	(2.02, 3.02)	6.57	5.65	0.53	(0.46, 0.60)	0.001117
Ctnnbip1	Catenin beta interacting protein 1	6.21	6.31	1.07	(0.81, 1.33)	0.542976	1.35	(1.21, 1.49)	7.15	5.88	0.42	(0.30, 0.54)	0.000956
Ccnd1	Cyclin D1	2.31	3.81	2.82	(1.24, 4.40)	0.017252	0.36	(0.15, 0.57)	1.49	5.28	13.85	(8.91, 18.79)	0.000809
Ccnd2	Cyclin D2	4.54	4.79	1.19	(0.88, 1.50)	0.278204	1.16	(0.66, 1.66)	4.39	4.58	1.14	(0.66, 1.62)	0.617147
Ccnd3	Cyclin D3	4.41	4.14	0.83	(0.69, 0.97)	0.119461	1.16	(0.82, 1.50)	4.8	3.93	0.55	(0.37, 0.73)	0.024087
Csnk1a1	Casein kinase 1, alpha 1	2.51	2.27	0.85	(0.77, 0.93)	0.034352	0.79	(0.69, 0.89)	2.66	2.6	0.96	(0.82, 1.10)	0.622054
Csnk1d	Casein kinase 1, delta	3.15	2.88	0.83	(0.72, 0.94)	0.052220	1.13	(1.01, 1.25)	3.28	2.7	0.67	(0.57, 0.77)	0.002496
Csnk2a1	Casein kinase 2, alpha 1 polypeptide	1.69	1.11	0.67	(0.62, 0.72)	0.000459	0.99	(0.89, 1.09)	2.26	1.13	0.46	(0.41, 0.51)	0.000412
Ctbp1	C-terminal binding protein 1	5.4	5.51	1.08	(0.98, 1.18)	0.192623	1.63	(1.17, 2.09)	5.5	4.8	0.62	(0.44, 0.80)	0.045162
Ctbp2	C-terminal binding protein 2	6.11	6	0.93	(0.60, 1.26)	0.760007	1.06	(0.88, 1.24)	5.33	5.91	1.5	(1.05, 1.95)	0.068561
Ctnnb1	Catenin (cadherin associated protein), beta 1	2.41	2.51	1.07	(0.93, 1.21)	0.331378	1.33	(1.17, 1.49)	2.32	2.1	0.86	(0.76, 0.96)	0.064442
Daam1	Dishevelled associated activator of morphogenesis 1	2.87	2.51	0.78	(0.63, 0.93)	0.062387	0.82	(0.62, 1.02)	3.42	2.8	0.65	(0.50, 0.80)	0.034486
Dixdc1	DIX domain containing 1	7.35	5.63	0.3	(0.15, 0.45)	0.001214	0.81	(0.57, 1.05)	6.72	5.94	0.58	(0.28, 0.88)	0.101937
Dkk1	Dickkopf homolog 1 (Xenopus laevis)	15.61	14.75	0.55	(0.37, 0.73)	0.050572	1.25	(0.80, 1.70)	15.79	14.43	0.39	(0.30, 0.48)	0.003817

		CDE diet vs control					C57Bl6 control vs S129P2 control		DDC diet vs control				
		AVG ΔC_t		Fold Change		p-value	Fold Change		AVG ΔC_t		Fold Change		p-value
Gene Symbol	Gene Name	CDE diet	C57Bl6 control	CDE diet/ Control	95% CI	P Value	C57Bl control/ S129P2 control	95% CI	DDC diet	S129P2 control	DDC diet/ Control	95% CI	P Value
Dvl1	Dishevelled, dsh homolog 1 (Drosophila)	5.53	5.1	0.74	(0.65, 0.83)	0.012325	2.29	(1.64, 2.94)	4.6	3.91	0.62	(0.44, 0.80)	0.041396
Dvl2	Dishevelled 2, dsh homolog (Drosophila)	9.19	8.95	0.85	(0.52, 1.18)	0.375331	1.64	(0.91, 2.37)	8.58	8.24	0.79	(0.46, 1.12)	0.347301
Ep300	E1A binding protein p300	5.19	5.07	0.92	(0.66, 1.18)	0.534600	1.03	(0.72, 1.34)	5.59	5.03	0.68	(0.24, 1.12)	0.272692
Fbxw11	F-box and WD-40 domain protein 11	4.32	4.37	1.04	(0.84, 1.24)	0.714881	0.85	(0.63, 1.07)	3.92	4.61	1.61	(0.63, 2.59)	0.237300
Fbxw2	F-box and WD-40 domain protein 2	3.26	3.04	0.86	(0.77, 0.95)	0.044806	0.99	(0.83, 1.15)	3.68	3.05	0.65	(0.53, 0.77)	0.014219
Fbxw4	F-box and WD-40 domain protein 4	7.85	7.6	0.84	(0.45, 1.23)	0.452855	1.26	(0.69, 1.83)	7.81	7.27	0.69	(0.53, 0.85)	0.023534
Fgf4	Fibroblast growth factor 4	15.03	14.71	0.8	(0.48, 1.12)	0.346761	1.71	(0.40, 3.02)	15	13.94	0.48	(0.05, 0.91)	0.244313
Fosl1	Fos-like antigen 1	10.29	11.07	1.71	(0.52, 2.90)	0.219832	0.76	(0.13, 1.39)	8.86	11.47	6.09	(1.00, 11.18)	0.002054
Foxn1	Forkhead box N1	14.3	14.75	1.37	(0.32, 2.42)	0.404344	1.25	(0.80, 1.70)	13.34	14.43	2.13	(1.34, 2.92)	0.029182
Frat1	Frequently rearranged in advanced T-cell lymphomas	9.57	9.28	0.82	(0.37, 1.27)	0.435996	1.5	(0.33, 2.67)	9.41	8.7	0.61	(0.20, 1.02)	0.192832
Frzb	Frizzled-related protein	6.34	6.86	1.44	(0.65, 2.23)	0.319453	0.32	(0.15, 0.49)	5.76	8.52	6.78	(3.08, 10.48)	0.031135
Fshb	Follicle stimulating hormone beta	14.71	14.75	1.03	(0.25, 1.81)	0.748968	2.5	(0.00001, 5.53)	14.23	13.43	0.58	(0.00001, 1.27)	0.388381
Fzd1	Frizzled homolog 1 (Drosophila)	6.94	6.13	0.57	(0.44, 0.70)	0.008243	0.96	(0.53, 1.39)	6.18	6.19	1.01	(0.42, 1.60)	0.985177
Fzd2	Frizzled homolog 2 (Drosophila)	11.61	11.76	1.11	(0.60, 1.62)	0.748321	0.45	(0.23, 0.67)	11.79	12.93	2.19	(1.53, 2.85)	0.004694
Fzd3	Frizzled homolog 3 (Drosophila)	11.66	11.78	1.08	(0.29, 1.87)	0.946706	1.85	(0.62, 3.08)	10.18	10.89	1.64	(0.59, 2.69)	0.228337
Fzd4	Frizzled homolog 4 (Drosophila)	4.14	3.85	0.81	(0.56, 1.06)	0.240311	0.47	(0.32, 0.62)	4.76	4.93	1.13	(0.92, 1.34)	0.273184
Fzd5	Frizzled homolog 5 (Drosophila)	6.14	5.39	0.59	(0.42, 0.76)	0.019782	1.36	(1.16, 1.56)	5.83	4.95	0.54	(0.42, 0.66)	0.002364

		CDE diet vs control					C57Bl6 control vs S129P2 control		DDC diet vs control				
		AVG ΔC_t		Fold Change		p-value	Fold Change		AVG ΔC_t		Fold Change		p-value
Gene Symbol	Gene Name	CDE diet	C57Bl6 control	CDE diet/ Control	95% CI	P Value	C57Bl control/ S129P2 control	95% CI	DDC diet	S129P2 control	DDC diet/ Control	95% CI	P Value
Fzd6	Frizzled homolog 6 (Drosophila)	7.61	7.33	0.83	(0.58, 1.08)	0.295008	0.14	(0.06, 0.22)	9.46	10.22	1.69	(0.85, 2.53)	0.061504
Fzd7	Frizzled homolog 7 (Drosophila)	10.02	10.21	1.14	(0.53, 1.75)	0.811514	2.54	(1.13, 3.95)	10.73	8.86	0.27	(0.13, 0.41)	0.004520
Fzd8	Frizzled homolog 8 (Drosophila)	11.55	11.14	0.76	(0.47, 1.05)	0.200206	2.15	(1.61, 2.69)	11.51	10.04	0.36	(0.19, 0.53)	0.006669
Gsk3b	Glycogen synthase kinase 3 beta	6.64	7.44	1.75	(1.43, 2.07)	0.001829	0.93	(0.67, 1.19)	7.44	7.55	1.08	(0.85, 1.31)	0.542355
Jun	Jun oncogene	4.4	5.77	2.59	(2.16, 3.02)	0.000440	0.88	(0.50, 1.26)	3.55	5.95	5.26	(2.91, 7.61)	0.001263
Kremen1	Kringle containing transmembrane protein 1	6.18	5.62	0.68	(0.54, 0.82)	0.023501	1.1	(0.80, 1.40)	6.08	5.48	0.66	(0.46, 0.86)	0.070231
Lef1	Lymphoid enhancer binding factor 1	14.15	14.19	1.03	(0.21, 1.85)	0.900015	2.67	(0.69, 4.65)	13.11	12.77	0.79	(0.29, 1.29)	0.435241
Lrp5	Low density lipoprotein receptor-related protein 5	5.35	5.15	0.87	(0.57, 1.17)	0.431998	3.2	(1.78, 4.62)	4.77	3.47	0.41	(0.27, 0.55)	0.019623
Lrp6	Low density lipoprotein receptor-related protein 6	3.17	2.63	0.69	(0.55, 0.83)	0.018041	0.94	(0.74, 1.14)	3.4	2.72	0.62	(0.48, 0.76)	0.021726
Myc	Myelocytomatosis oncogene	3.59	5.6	4.02	(0.00001, 8.64)	0.071275	1.01	(0.00001, 2.85)	4.12	5.58	2.77	(0.00001, 7.10)	0.541898
Nkd1	Naked cuticle 1 homolog (Drosophila)	7.17	7.04	0.92	(0.70, 1.14)	0.491942	1.39	(0.59, 2.19)	7.05	6.57	0.72	(0.29, 1.15)	0.290880
Nlk	Nemo like kinase	6.11	6.13	1.01	(0.83, 1.19)	0.905628	1.48	(1.16, 1.80)	6.01	5.56	0.73	(0.61, 0.85)	0.029672
Pitx2	Paired-like homeodomain transcription factor 2	14.41	14.28	0.92	(0.04, 1.80)	0.906068	1.13	(0.50, 1.76)	14.95	14.11	0.56	(0.05, 1.07)	0.379364
Porcn	Porcupine homolog (Drosophila)	9.89	8.55	0.39	(0.29, 0.49)	0.003220	1.6	(0.97, 2.23)	9.53	7.87	0.32	(0.16, 0.48)	0.025190
Ppp2ca	Protein phosphatase 2 (formerly 2A), catalytic subunit, alpha isoform	0.58	0.48	0.93	(0.92, 0.94)	0.000907	1.05	(0.98, 1.12)	0.95	0.41	0.69	(0.59, 0.79)	0.005120
Ppp2r1a	Protein phosphatase 2 (formerly 2A), regulatory subunit A (PR 65), alpha isoform	2.61	2.55	0.96	(0.82, 1.10)	0.624666	1.22	(1.04, 1.40)	2.47	2.27	0.87	(0.76, 0.98)	0.096653
Ppp2r5d	Protein phosphatase 2, regulatory subunit B (B56), delta isoform	5.41	4.8	0.66	(0.57, 0.75)	0.002312	0	(0.00, 0.00)	15.8	14.43	0.39	(0.30, 0.48)	0.003771
Pygo1	Pygopus 1	11.28	10.78	0.71	(0.34, 1.08)	0.276176	1.09	(0.52, 1.66)	10.83	10.66	0.89	(0.39, 1.39)	0.874325

		CDE diet vs control					C57Bl6 control vs S129P2 control		DDC diet vs control				
		AVG ΔC_t		Fold Change		p-value	Fold Change		AVG ΔC_t		Fold Change		p-value
Gene Symbol	Gene Name	CDE diet	C57Bl6 control	CDE diet/ Control	95% CI	P Value	C57Bl control/ S129P2 control	95% CI	DDC diet	S129P2 control	DDC diet/ Control	95% CI	P Value
Rhou	Ras homolog gene family, member U	3.22	4.04	1.76	(1.53, 1.99)	0.000648	0.98	(0.80, 1.16)	3.52	4.07	1.46	(1.20, 1.72)	0.013238
Senp2	SUMO/sentrin specific peptidase 2	4.99	4.67	0.8	(0.76, 0.84)	0.001450	0.78	(0.66, 0.90)	5.19	5.04	0.9	(0.73, 1.07)	0.317245
Sfrp1	Secreted frizzled-related protein 1	11.11	10.92	0.88	(0.34, 1.42)	0.659303	2.8	(1.30, 4.30)	7.16	9.43	4.84	(2.92, 6.76)	0.009988
Sfrp2	Secreted frizzled-related protein 2	13.84	14.26	1.34	(0.50, 2.18)	0.475493	1.67	(0.21, 3.13)	13.6	13.52	0.95	(0.00001, 1.92)	0.961245
Sfrp4	Secreted frizzled-related protein 4	15.47	13.65	0.28	(0.18, 0.38)	0.009177	0.58	(0.37, 0.79)	15.02	14.43	0.66	(0.32, 1.00)	0.159411
Slc9a3r1	Solute carrier family 9 (sodium/hydrogen exchanger), member 3 regulator 1	1.07	0.96	0.92	(0.76, 1.08)	0.460959	0.15	(0.13, 0.17)	3.97	3.73	0.85	(0.72, 0.98)	0.107547
Sox17	SRY-box containing gene 17	13.28	13.71	1.35	(0.55, 2.15)	0.352527	2.86	(1.77, 3.95)	12.36	12.2	0.89	(0.54, 1.24)	0.639505
T	Brachyury	15.61	14.75	0.55	(0.37, 0.73)	0.050572	1.64	(0.89, 2.39)	14.59	14.04	0.68	(0.32, 1.04)	0.254555
Tcf3	Transcription factor 3	8.26	8.06	0.87	(0.50, 1.24)	0.490429	1.65	(0.94, 2.36)	7.8	7.34	0.73	(0.51, 0.95)	0.092606
Tcf7	Transcription factor 7, T-cell specific	6.75	5.64	0.46	(0.33, 0.59)	0.003398	1	(0.82, 1.18)	5.8	5.63	0.89	(0.67, 1.11)	0.406529
Tle1	Transducin-like enhancer of split 1, homolog of Drosophila E(spl)	3.73	3.3	0.74	(0.50, 0.98)	0.152192	1.27	(0.78, 1.76)	4.38	2.95	0.37	(0.28, 0.46)	0.007004
Tle2	Transducin-like enhancer of split 2, homolog of Drosophila E(spl)	13.34	13.28	0.96	(0.23, 1.69)	0.941344	4.66	(1.23, 8.09)	12.68	11.06	0.32	(0.14, 0.50)	0.068097
Wif1	Wnt inhibitory factor 1	14.15	12.72	0.37	(0.07, 0.67)	0.080500	6.05	(1.79, 10.31)	13.45	10.13	0.1	(0.04, 0.16)	0.012897
Wisp1	WNT1 inducible signaling pathway protein 1	7.6	7.6	1	(0.57, 1.43)	0.860073	2.1	(1.22, 2.98)	6.71	6.53	0.88	(0.42, 1.34)	0.769791
Wnt1	Wingless-related MMTV integration site 1	15.01	14.75	0.83	(0.15, 1.51)	0.923943	2.22	(0.13, 4.31)	13.69	13.6	0.94	(0.00001, 2.21)	0.925625
Wnt10a	Wingless related MMTV integration site 10a	15.46	14.75	0.61	(0.40, 0.82)	0.078898	1.74	(0.72, 2.76)	13.65	13.95	1.23	(0.48, 1.98)	0.533690
Wnt11	Wingless-related MMTV integration site 11	13.62	11.51	0.23	(0.06, 0.40)	0.067082	0.35	(0.09, 0.61)	9.53	13	11.09	(2.05, 20.13)	0.031816
Wnt16	Wingless-related MMTV integration site 16	12.33	13.63	2.47	(0.00001, 5.59)	0.206740	8.82	(0.00001, 18.03)	10.61	10.49	0.92	(0.49, 1.35)	0.651352

		CDE diet vs control					C57Bl6 control vs S129P2 control		DDC diet vs control				
		AVG ΔC_t		Fold Change		p-value	Fold Change		AVG ΔC_t		Fold Change		p-value
Gene Symbol	Gene Name	CDE diet	C57Bl6 control	CDE diet/ Control	95% CI	P Value	C57Bl control/ S129P2 control	95% CI	DDC diet	S129P2 control	DDC diet/ Control	95% CI	P Value
Wnt2	Wingless-related MMTV integration site 2	8.73	9.57	1.8	(1.36, 2.24)	0.008454	1.79	(0.80, 2.78)	10.45	8.74	0.3	(0.10, 0.50)	0.066085
Wnt2b	Wingless related MMTV integration site 2b	9.32	9.15	0.89	(0.48, 1.30)	0.652071	2.27	(1.07, 3.47)	9.09	7.97	0.46	(0.23, 0.69)	0.053854
Wnt3	Wingless-related MMTV integration site 3	15.61	14.75	0.55	(0.37, 0.73)	0.050572	1.25	(0.80, 1.70)	15.8	14.43	0.39	(0.30, 0.48)	0.003771
Wnt3a	Wingless-related MMTV integration site 3A	14.54	14.39	0.9	(0.32, 1.48)	0.727133	1.64	(0.75, 2.53)	13.43	13.67	1.18	(0.25, 2.11)	0.506291
Wnt4	Wingless-related MMTV integration site 4	10.08	10.72	1.56	(1.16, 1.96)	0.023505	1.45	(1.11, 1.79)	9.7	10.19	1.4	(1.00, 1.80)	0.088004
Wnt5a	Wingless-related MMTV integration site 5A	14.1	14.58	1.4	(0.00001, 3.11)	0.402589	7.65	(4.35, 10.95)	12.51	11.65	0.55	(0.29, 0.81)	0.071018
Wnt5b	Wingless-related MMTV integration site 5B	5.38	4.92	0.73	(0.48, 0.98)	0.160886	0.76	(0.61, 0.91)	5.58	5.31	0.83	(0.77, 0.89)	0.006508
Wnt6	Wingless-related MMTV integration site 6	14.64	14.27	0.78	(0.00001, 1.60)	0.926742	1.06	(0.50, 1.62)	13.76	14.19	1.35	(0.00001, 3.36)	0.332070
Wnt7a	Wingless-related MMTV integration site 7A	15.43	14.75	0.63	(0.43, 0.83)	0.078959	1.82	(0.69, 2.95)	11.01	13.89	7.37	(2.52, 12.22)	0.008132
Wnt7b	Wingless-related MMTV integration site 7B	15.61	14.75	0.55	(0.37, 0.73)	0.050572	1.25	(0.80, 1.70)	14.3	14.43	1.1	(0.00001, 2.32)	0.510059
Wnt8a	Wingless-related MMTV integration site 8A	15.61	14.75	0.55	(0.37, 0.73)	0.050572	1.25	(0.80, 1.70)	15.8	14.43	0.39	(0.30, 0.48)	0.003771
Wnt8b	Wingless related MMTV integration site 8b	14.83	14.75	0.95	(0.31, 1.59)	0.989827	1.89	(0.66, 3.12)	14.84	13.84	0.5	(0.17, 0.83)	0.110988
Wnt9a	Wingless-type MMTV integration site 9A	13.75	13.64	0.93	(0.39, 1.47)	0.685818	0.88	(0.19, 1.57)	13.3	13.83	1.45	(0.55, 2.35)	0.395735
Gusb	Glucuronidase, beta	3.35	3.43	1.06	(0.91, 1.21)	0.412742	0.79	(0.61, 0.97)	2.67	3.78	2.16	(1.61, 2.71)	0.002801
Hprt1	Hypoxanthine guanine phosphoribosyl transferase 1	1.04	0.79	0.84	(0.65, 1.03)	0.207237	0.91	(0.78, 1.04)	1.35	0.92	0.74	(0.68, 0.80)	0.001811
Hsp90ab1	Heat shock protein 90 alpha (cytosolic), class B member 1	-0.78	-0.92	0.91	(0.80, 1.02)	0.204167	1.16	(1.04, 1.28)	-0.92	-1.13	0.86	(0.81, 0.91)	0.004713
Gapdh	Glyceraldehyde-3-phosphate dehydrogenase	-1.59	-1.91	0.8	(0.73, 0.87)	0.007116	0.74	(0.65, 0.83)	-1.02	-1.47	0.73	(0.62, 0.84)	0.016204
Actb	Actin, beta	-2.02	-1.4	1.53	(1.33, 1.73)	0.002420	1.63	(1.36, 1.90)	-2.08	-2.1	0.99	(0.83, 1.15)	0.872544

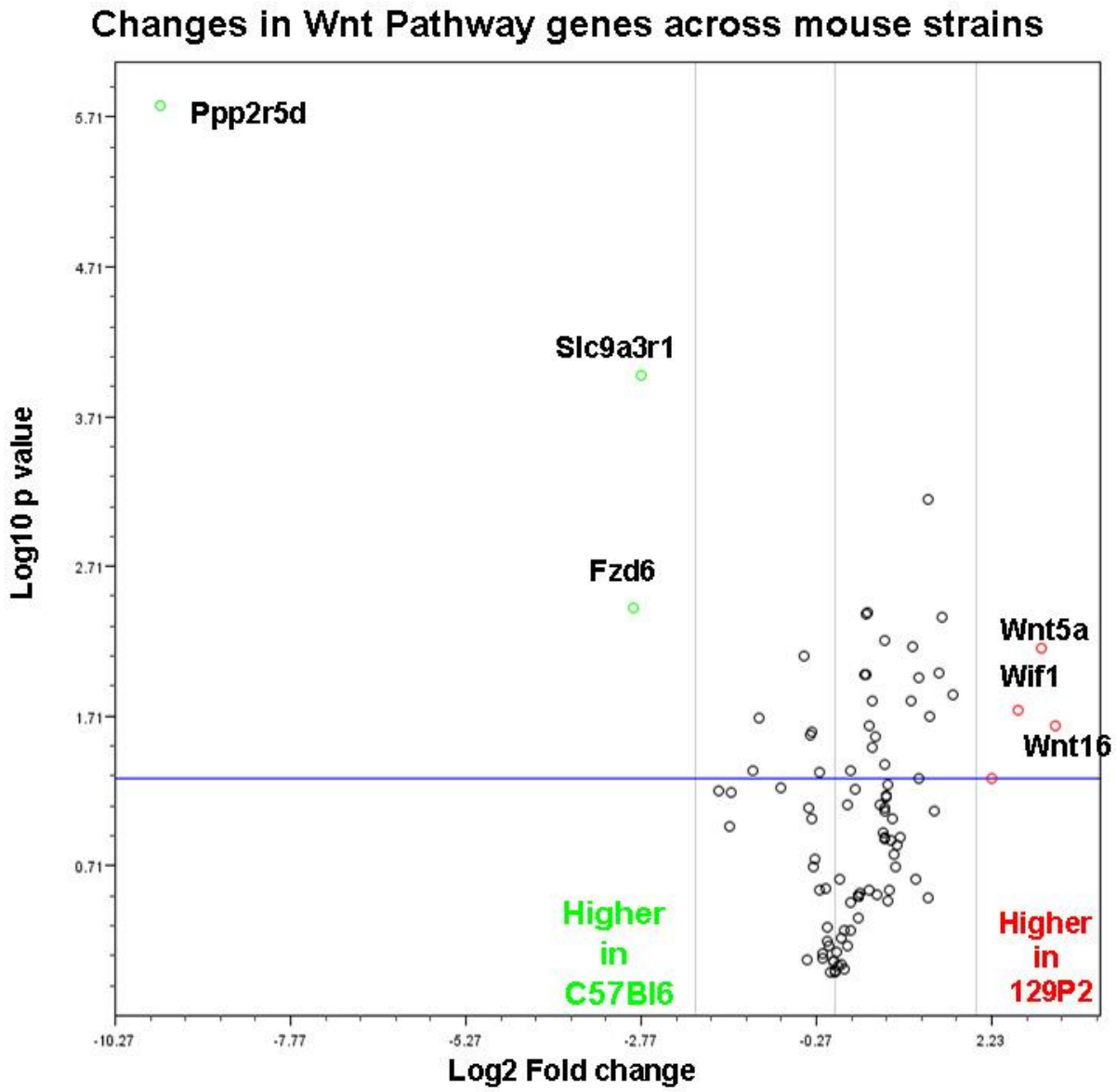
Changes in Wnt Pathway genes across mouse strains
Ppp2r5d
Slc9a3r1
Fzd6
Wnt5a
Wif1
Wnt16
Higher in C57Bl6
Higher in 129P2
Log10 p value
5.71
4.71
3.71
2.71
1.71
0.71
-10.27
-7.77
-5.27
-2.77
-0.27
2.23
Log2 Fold change

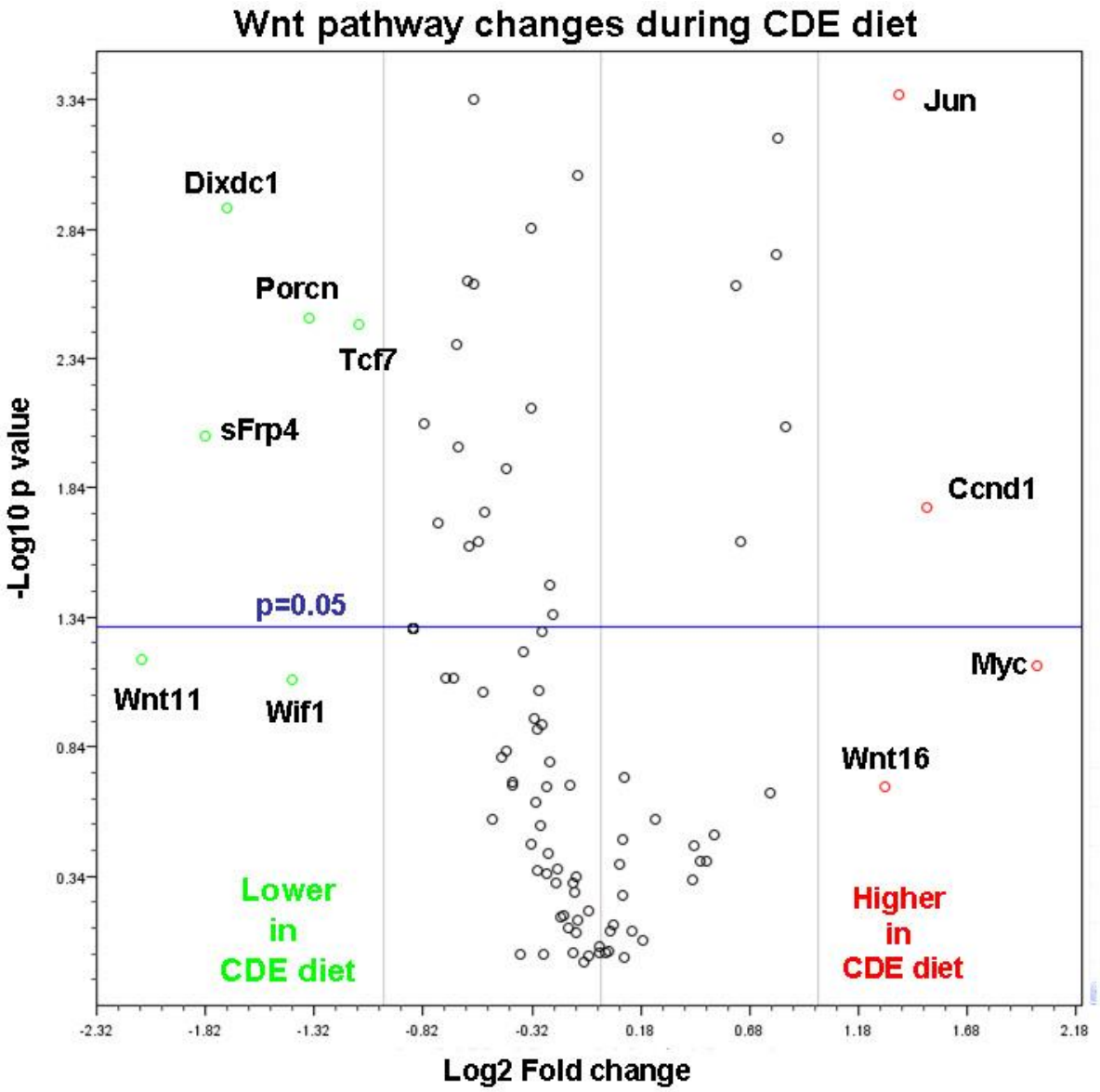
Wnt pathway changes during CDE diet
-Log10 p value
3.34
2.84
2.34
1.84
1.34
0.84
0.34
p=0.05
Jun
Dixdc1
Porcn
Tcf7
sFrp4
Ccnd1
Myc
Wnt11
Wif1
Wnt16
Lower
in
CDE diet
Higher
in
CDE diet
-2.32
-1.82
-1.32
-0.82
-0.32
0.18
0.68
1.18
1.68
2.18
Log2 Fold change

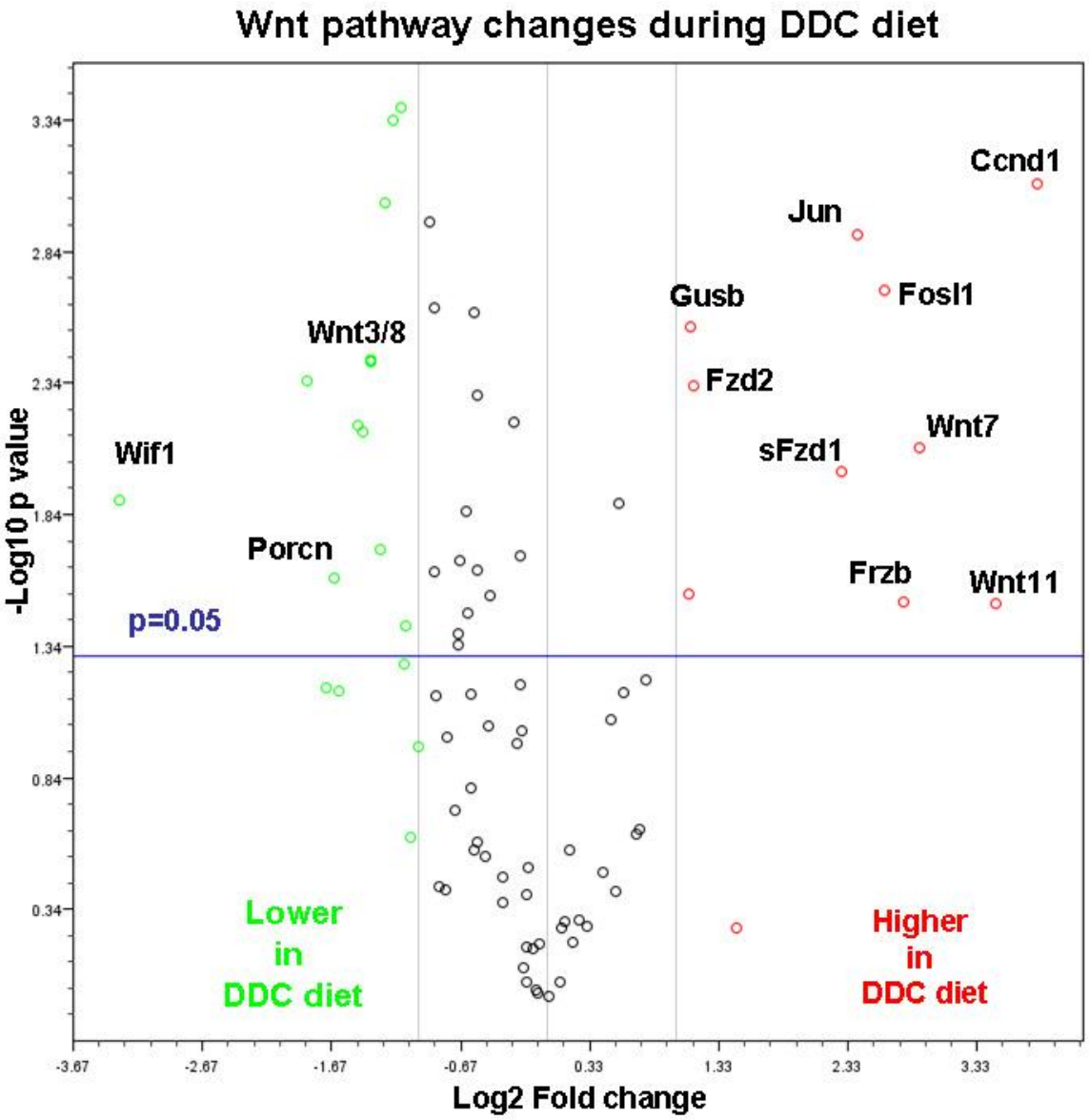
Wnt pathway changes during DDC diet
-Log10 p value
3.34
2.84
2.34
1.84
1.34
0.84
0.34
Ccnd1
Jun
Gusb
Fosl1
Wnt3/8
Fzd2
Wnt7
Wif1
sFzd1
Porcn
Frzb
Wnt11
p=0.05
Lower
in
DDC diet
Higher
in
DDC diet
-3.67
-2.67
-1.67
-0.67
0.33
1.33
2.33
3.33
Log2 Fold change